Investigation of the modification enzymes and the impact of mutations within the lantibiotic nisin

Inaugural-Dissertation

For the attainment of the title of doctor in the Faculty of Mathematics and Natural Sciences at the Heinrich Heine University Duesseldorf

Presented by

Jens Reiners

from Heinsberg

Duesseldorf, November 2022

From the Institute of Biochemistry
At the Heinrich Heine University Duesseldorf

Published by permission of the
Faculty of Mathematics and Natural Science
At Heinrich Heine University Duesseldorf

Supervisor: Prof. Dr. Lutz Schmitt
Co-supervisor: Prof. Dr. Georg Groth

Date of oral examination: 22.12.2022

„Die Frage ist so gut, dass ich sie nicht durch meine Antwort verderben möchte“

(Robert Koch)

Abstract

Nisin A is the model system for lantibiotics. Since its discovery nearly 100 years ago, new naturally occurring variants have been discovered. Nisin A is expressed as a pre-peptide and is post-translationally modified. These modifications are performed by the modification enzymes NisB, which is responsible for the dehydration of serine and threonine residues in the core peptide; and the cyclase NisC, which forms the lanthionine rings via Michael-condensation. These lanthionine rings are responsible for the stability and the antimicrobial activity of nisin A. The modified pre-peptide is secreted via the ABC transporter NisT into the extracellular space, where the protease NisP cleaves off the leader peptide from the core peptide. This results in active nisin A, which is antimicrobial in nanomolar concentrations.

In this thesis, the stoichiometry of the modification complex was determined to be a dimer of NisB and a monomer of NisC in complex with one molecule of nisin A. The visualization of the assembled complex was done with small-angle X-ray scattering (SAXS). Furthermore, the lanthionine ring E was found to be a trigger factor for the modification complex, inducing its dissociation.

The next focus was to analyze the effect of the different nisin mutations on the secretion and modification machinery. The purified nisin variants were cleaved with a purified soluble version of NisP and the cleavage efficiency was determined.

The antimicrobial activity of all variants was tested and benchmarked against the immunity system NisFEG and NisI from *Lactococcus lactis* as well as the nisin resistance system NSR and *Sa*NsrFP from *Streptococcus agalactiae*. Here, it was shown that all nisin variants were secreted and post-translationally modified. Only one variant, in which isoleucine at position one was changed to a proline, was not cleaved by NisP. Furthermore, variants with an aromatic residue at position one showed higher antimicrobial activity than other mutations. This even holds true in comparison to the natural nisin H, with a phenylalanine at position one. Intriguingly, the recognition of the variant $Cys_{29}Pro$ by NSR was drastically reduced, resulting in a bypass of this resistance protein. Furthermore, a variant in which an isoleucine and valine were introduced after the hinge region was less recognized by all the tested immunity and resistance proteins.

Zusammenfassung

Nisin A ist das Model Peptid für Lantibiotika. Seit seiner Entdeckung vor fast 100 Jahren wurden viele Nisin Varianten identifiziert und untersucht. Nisin A wird als Pre-peptid exprimiert und posttranslational modifiziert. Dies geschieht über die Modifikationsenzyme NisB, verantwortlich für die Dehydratisierung der Serin und Threonin Reste im Kernpeptide, und der Zyklase NisC die mittels einer Michael-Addition die namensgebenden Lanthioninringe ausbildet. Diese Lanthioninringe sorgen für eine hohe Stabilität und die antimikrobielle Aktivität von Nisin A. Das modifizierte Pre-peptid wird mittels des ABC-Transporters NisT in den extrazellulären Raum sekretiert und dort von der Protease NisP in seine biologisch aktive Form überführt, indem das Signal-peptid des Kernpeptids abgeschnitten wird. Das resultierende Nisin A ist gegen bestimmte Bakterienstämme in nanomolare Konzentration wirksam.

In dieser Arbeit wurde die Stöchiometrie des Modifikationskomplexes von Nisin A untersucht und eine Stöchiometrie von einem NisB Dimer, zu einem Monomer NisC und einem Nisin A Molekül ermittelt. Ebenso konnte mittels Kleinwinkelstreuung (SAXS) der Modifikationskomplex visualisiert werden. Weiterführend konnte der letzte Lanthioninring E als Faktor identifiziert werden, der den Modifikationskomplex destabilisiert und somit seinen Zerfall einleitet. Des Weiteren, wurden diverse Mutationsstudien von Nisin A und natürlich vorkommenden Nisin-varianten durchgeführt. Ziel war es dabei herauszufinden wie sich die einzelnen Mutationen auf die Expression, den Modifikationsstatus der nisin varianten und auch auf die Sekretion auswirken. Die aufgereinigten Varianten wurden dann mittels einer gereinigten NisP Protease in ihre biologisch aktive form überführet. Die Auswirkungen auf die Schneideeffizienz konnten ebenfalls bestimmt werden. Danach war ein wesentlicher Schritt die Untersuchung der biologischen Aktivität auf das Immunitäts-System NisFEG und NisI von *Lactococcus lactis,* als auch auf das bekannte Resistenz-System NSR und *Sa*NsrFP von *Streptococcus agalactiae*. Es konnte gezeigt werden, dass alle genutzten Varianten sekretiert und auch posttranslational modifiziert wurden. Eine Variation der Position eins im Kernpeptid, an der ein Isoleucin gegen ein Prolin getauscht wurde, konnte von NisP jedoch nicht mehr geschnitten werden. Es konnte gezeigt werden, dass Mutationen der Position eins im Kernpeptid einen großen Effekt auf die antimikrobielle Aktivität hatten. Insbesondere aromatische Aminosäuren konnten die Aktivität von Nisin A steigern, was ebenfalls mit dem natürlich vorkommenden Nisin H validiert werden konnte, da hier bereits ein Phenylalanin an

Position eins vorliegt. Im Rahmen der Untersuchungen konnte ebenfalls gezeigt werden, dass die Nisin variante $Cys_{29}Pro$ von NSR nicht mehr effektiv erkannt wird und somit den Resistenzmechanismus außer Kraft setzten kann. Ebenso zeigte eine Mutante in der Isoleucin und Valin hinter der *hinge*-Region eingefügt wurden, eine verminderte Erkennung durch alle getesteten Immunitäts- oder Resistenz-Proteine.

Table of Contents

List of Figures

Abbreviations

ATP	Adenosine-5-triphosphate
Å	Angström
AMP	antimicrobial peptide
ABC	ATP-binding cassette
B. subtilis 168	*Bacillus subtilis* 168
B. obeum A2-162	*Blautia obeum* A2-162
CP	Core peptide
Dha	2,3-di-dehydroalanine
Dhb	2,3-di-dehydrobutyrine
DNA	desoxyribonucleic acid
E. faecalis ATCC 29212	*Enterococcus faecalis* ATCC 29212
E. faecalis ATCC 51299	*Enterococcus faecalis* ATCC 51299 (VRE)
E. faecium ATCC 35667	*Enterococcus faecium* ATCC 35667
E. faecium ATCC 700221	*Enterococcus faecium* ATCC 700221 (VRE)
ECD	extracellular domain
HPLC	high pressure liquid chromatography
ITC	Isothermal Titration Calorimetry
kDa	kilo dalton
L. lactis	*Lactococcus lactis*
Lan	lanthionine
LP	Leader peptide
mRNA	messenger ribonucleic acid
MeLan	methyl-lanthionine
µM	micromolar
mM	millimolar
MALS	Multi-angle Light Scattering
nm	nanometer
nM	nanomolar
NRP	Non-ribosomally synthesized peptides
NSR	nisin resistance protein
NBD	nucleotide binding domain
NMR	nulear magnetic resonance
mg	milligram
min	minute
ml	milliliter
PAGE	polyacrylamide gel electrophoresis
PTM	post-translational modification
RiPP	ribosomally synthesized and post-translationally modified peptide
RP	reverse phase

RNA	ribonucleic acid
Sa	*Streptococcus agalactiae*
SAXS	small-angle X-ray scattering
S. aureus ATCC 29213	*Staphylococcus aureus* ATCC 29213 (MSSA)
S. aureus ATCC 700699	*Staphylococcus aureus* ATCC 700699 (MRSA)
S. agalactiae	*Streptococcus agalactiae*
S. hyointestinalis	*Streptococcus hyointestinalis*
SPR	Surface Plasmon Resonance
SDS	sodium dodecyl sulfate
TSP	tail specific protease
TMD	transmembrane domain
TMH	transmembrane helix
tRNA	transfer ribonucleic acid
TCS	two-component system

Amino acid	Three letter code	One letter code
Alanine	Ala	A
Arginine	Arg	R
Asparagine	Asn	N
Aspartic acid	Asp	D
Cysteine	Cys	C
Glutamic acid	Glu	E
Glutamine	Gln	Q
Glycine	Gly	G
Histidine	His	H
Isoleucine	Ile	I
Lysine	Lys	K
Methionine	Met	M
Phenylalanine	Phe	F
Proline	Pro	P
Serine	Ser	S
Threonine	Thr	T
Tryptophan	Trp	W
Tyrosine	Tyr	Y
Valine	Val	V

1 Introduction

1.1 Antibiotics

Bacterial infections are responsible for millions of deaths in the history of mankind and there was no effective treatment for it before the 20th century. In 1928, Alexander Flemming discovered the first antimicrobial substance and named it penicillin (Fleming, 1929). This started a revolution as the treatment of infections was now possible and eventually lead to the discovery of more antimicrobial substances in the following years (Powers, 2004; van Hoek et al., 2011). Antibiotics can be classified based on their mode of action and their different targets, including bacterial cellular enzymes, bacterial cellular metabolism, nucleic acids, ribosomes and the cell wall/membrane, respectivly (Bbosa et al., 2014).

One group of antibiotics, which has become more prominent are antimicrobial peptides (AMP) (Bahar & Ren, 2013; Hancock & Lehrer, 1998; Malmsten, 2014). Based on the synthesis of these AMPs, they are grouped into two superfamilies; the ribosomally synthesized and post-translationally modified peptides (RiPPs) and the non-ribosomally synthesized peptides (NRPs) (Arnison et al., 2013; McIntosh et al., 2009; Montalban-Lopez et al., 2021; Rodnina et al., 2007; Schwarzer et al., 2003; Strieker et al., 2010).

As the name suggest, the biosynthesis of NRPs is not based on a mRNA template. It has the advantage of implementing non-proteinogenic amino acids such as ornithine, or the use of fatty acids (McIntosh et al., 2009). One famous member of the NRP family is the antibiotic vancomycin, discovered in 1950 (van Wageningen et al., 1998).

In contrast, RiPPs depend on mRNA templates and thereby, uses proteinogenic amino acids. To extend the spectra of diversity, RiPPs also share the feature of post-translational modifications (PTM) of amino acids (Arnison et al., 2013; Montalban-Lopez et al., 2021). RiPPs are synthesized by the ribosome as a precursor peptide. This precursor peptide can be divided in an N-terminal leader peptide and a C-terminal core peptide (Arnison et al., 2013; Montalban-Lopez et al., 2021). The leader peptide serves as recognition motif for the modification enzymes as well as the transporting protein and keeps the peptide in an inactive state within the cell (Abts et al., 2013; Burkhart et al., 2015; Burkhart et al., 2017; Furgerson Ihnken et al., 2008; Mavaro et al., 2011; Oman & van der Donk, 2010; Patton et al., 2008; Plat et al., 2013; Rink et al., 2005; Trabi et al., 2009; van der Meer et al., 1994). Furthermore, the PTM modifications only occur in the core peptide and not in the leader peptide (Arnison et al.,

2013; Plat et al., 2013). One frequently observed PTM is the formation of (methyl-) lanthionine rings, which are a characteristic feature of the new superfamily of lanthipeptides (Figure 1). Within this new superfamily, lanthipeptides with antimicrobial activity are called lantibiotic (lanthionine-containing antibiotic) (Ingram, 1969; Kellner et al., 1988; Knerr & van der Donk, 2012; Newton et al., 1953; Schnell et al., 1988; Xie & van der Donk, 2004).

1.1.1 Lantibiotics

Lantibiotics are promising candidates for treatment of pathogenic strains (Dischinger et al., 2014) and are mainly produced by Gram-positive bacteria (Klaenhammer, 1993; Sahl & Bierbaum, 1998). A huge number (>50) of lantibiotics have been already identified. Due to advancements in the computational field, new tools like BAGEL4 (van Heel et al., 2018), RiPPMiner (Agrawal et al., 2017) and antiSMASH (Blin et al., 2017), can identify new members of the lantibiotic family and thereby, increase this number (Tracanna et al., 2017). Today, the highly resistant strains like methicillin-resistant *Staphylococcus aureus* (MRSA) or vancomycin-resistant enterococci (VRE) have become a common source of hospital infections. Lantibiotics could counteract on such pathogenic and resistant bacteria, they are highly efficient against these strains and pre-clinical trials are already in progress for the same (Brunati et al., 2018; Crowther et al., 2013; Dawson & Scott, 2012; Dischinger et al., 2014; Jabes et al., 2011; Mota-Meira et al., 2000; Ongey et al., 2017; Sandiford, 2019).

Lantibiotics are synthesized as a precursor peptide with a size of 30-60 amino acids. After the release of the precursor peptide from the ribosome, several modification enzymes are involved in maturation of the precursor peptide to become biologically active. One feature of maturation is PTMs and these modifications take place in the core peptide only (Arnison et al., 2013; Plat et al., 2013; Schnell et al., 1988). The leader peptide is responsible for the recognition of the modification enzymes and maintain the peptide in an inactive state prior to its translocation (Abts et al., 2013; Khusainov & Kuipers, 2012; Kuipers et al., 2004; Kuipers et al., 1993; Mavaro et al., 2011; Plat et al., 2013; van der Meer et al., 1994). The leader peptide is cleaved off before or after the secretion across the membrane via an ABC transporter (Nishie et al., 2011; Ortega et al., 2014; van der Meer et al., 1993; van der Meer et al., 1994).

Usually, PTMs occur in two step, in the first step, serine and threonine residues within the core peptide are dehydrated to 2,3-di-dehydroalanine (Dha from serine) and 2,3-didehydrobutyrine (Dhb from threonine) (Figure 1, PTM 1) (Gross & Morell, 1967, 1971; Gross et al., 1969;

Newton et al., 1953). During the second step, these dehydrated amino acids (Dhb and Dha) form (methyl-) lanthionine rings with a cysteine residue in a Michael-type condensation reaction (Figure 1, PTM 2) (Barber et al., 1988; Gross & Morell, 1967, 1971; Gross et al., 1969). These (methyl-) lanthionine rings are responsible for the high thermostability, antimicrobial activity and resistance of a lantibiotics against proteolytic digestions (Chan et al., 1996; Gross & Morell, 1967; Lu et al., 2010; Oppedijk et al., 2016).

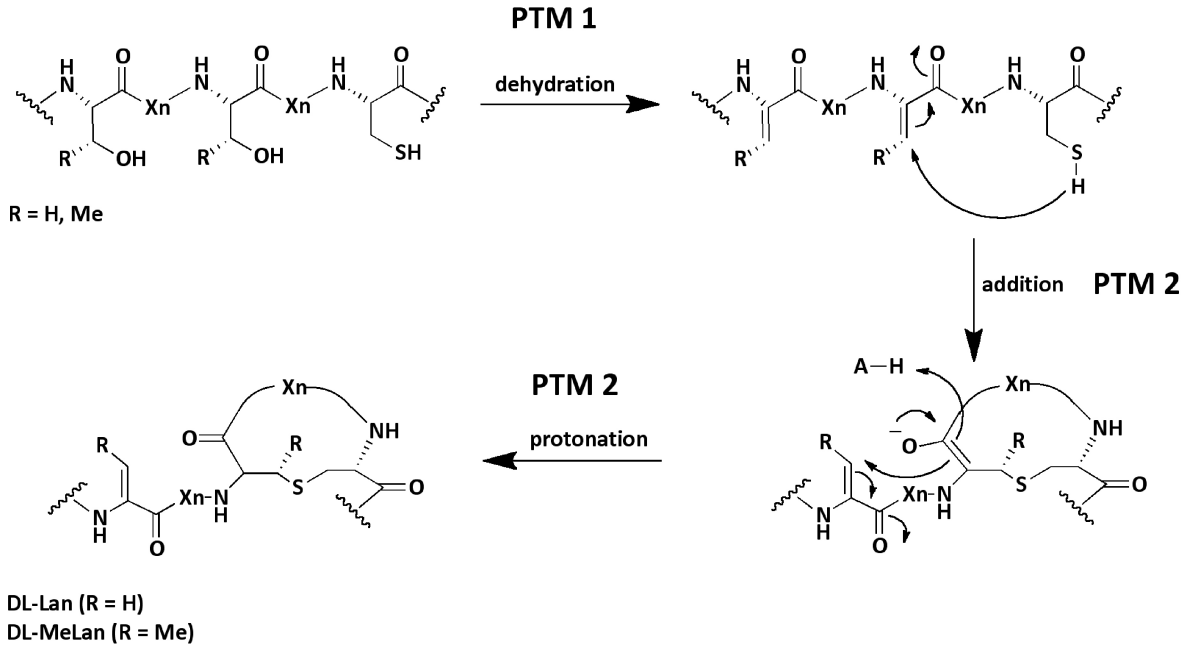

Figure 1: PTM reactions in common lanthipeptides. The first modification (PTM 1) is the dehydration of the serine and threonine residues within the core peptide via a dehydratase. The second step (PTM 2) is the cyclisation of the dehydrated amino acids Dha and Dhb via a Michael-type condensation with a cysteine residue, catalyzed by a cyclase resulting in (methyl-) lanthionine ring formation. The acronym X_n stands for n-quantity amino acids. Based and modified from (Lagedroste et al., 2020; Repka et al., 2017)

1.1.2 Different lanthipeptide classes

Originally, bacteriocins were subdivided into four classes based on their structural diversity and properties (Chatterjee et al., 2005; Heng & Tagg, 2006; Jung, 1991; Klaenhammer, 1993; McAuliffe et al., 2001; Sahl & Bierbaum, 1998). This classification also included antimicrobial peptides without (methyl-) lanthionine rings and was not specific for lantibiotics. Thus, a new classification system was established in 2013 (see Figure 2) (Knerr & van der Donk, 2012; Willey & van der Donk, 2007). The new classification is based on the modification enzymes

which are involved in the maturation of the lantibiotics (Knerr & van der Donk, 2012; Lee & van der Donk, 2022; Pei et al., 2022; Willey & van der Donk, 2007; Xu et al., 2020).

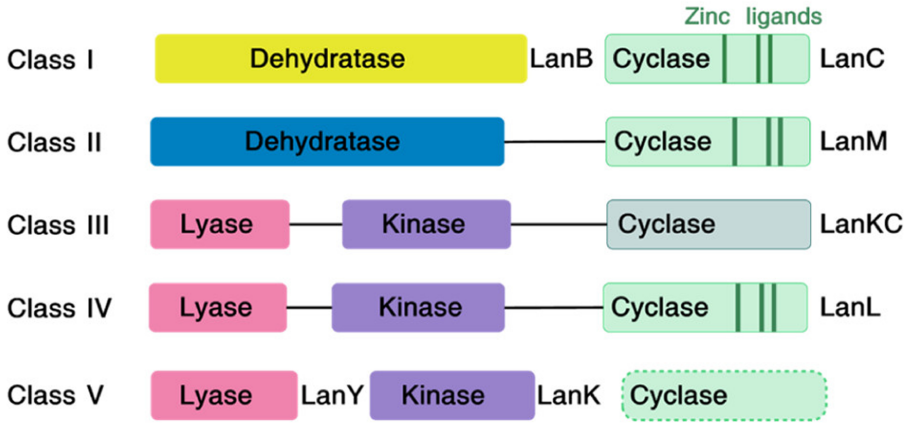

Figure 2: Classification of the different Lanthipeptides. Organization of the enzymes involved for the PTM installation in lanthipeptides from classes I – V. In class I lantibiotics the dehydration of the Ser/Thr residues is done via glutamylation followed by an elimination reaction. The other classes use a NDP-dependent phosphorylation reaction for the dehydration of the Ser/Thr residues instead of a glutamylation reaction. The following cyclisation reaction is catalyzed via a zinc dependent or independent cyclase (zinc ligands are indicated as dark lines). Taken and modified from (Pei et al., 2022).

The first major difference between the classes is the organization of the involved modification enzymes. class I lantibiotics were modified by two discrete enzymes (e.g. LanB and LanC) for the dehydration and the cyclase reaction, respectively. However, these steps are done in classes II-IV lantibiotics via multifunctional single enzymes (LanM, LanKC, and LanL), catalyzing the dehydration via a dehydratase in class II; and lyase and kinases in class III-V, followed via a cyclase reaction from a zinc dependent or independent cyclase (Figure 2) (Arnison et al., 2013; Chatterjee et al., 2005; Knerr & van der Donk, 2012; Koponen et al., 2002; Lee & van der Donk, 2022; Okeley et al., 2003; Ortega et al., 2016; Ortega et al., 2015; Pei et al., 2022; Repka et al., 2017; Zhang et al., 2012). The second major difference between the classes is the dehydration process itself. In class I lantibiotics, the dehydration of the Ser/Thr residues is done via glutamylation followed by an elimination reaction. This step is catalyzed via a glutamyl-tRNA-dependent LanB dehydratase. The other classes use a NDP-dependent phosphorylation reaction for the dehydration of the Ser/Thr residues instead of a glutamylation (Arnison et al., 2013; Chatterjee et al., 2005; Goto et al., 2010; Knerr & van der Donk, 2012; Lee & van der Donk, 2022; Ortega et al., 2016; Ortega et al., 2015; Pei et al., 2022; Repka et al., 2017; Willey & van der Donk, 2007; Zhang et al., 2012). The newly discovered class V lantibiotics differ

from other previously known classes as they combine the usage of the phosphorylation reaction from the classes II-IV, but with separate enzymes like class I (Figure 2) (Lee & van der Donk, 2022; Pei et al., 2022).

1.2 Nisin and its variants

Nearly one century ago, nisin A from *Lactococcus lactis* was discovered as the first natural nisin variant (Rogers, 1928; Rogers & Whittier, 1928) and belongs to the class I family of lantibiotics. With the increased need of highly active antimicrobial peptides, other natural nisin variants were also found and so far, nine natural variants of nisin are known (Figure 3). Nisin Z was discovered from *Lactococcus lactis* NIZO 221 86 strain in 1991, almost 60 years after the discovery of nisin A (Mulders et al., 1991). Due to advanced data-mining tools, the other nisin variants were found in a shorter time span. Nisin Q from *Lactococcus lactis* 61-14 in 2003 (Zendo et al., 2003), nisin U and U2 from *Streptococcus uberis* 42 and D536, respectively, in 2006 (Wirawan et al., 2006), nisin F from *Lactococcus lactis* F10 in 2008 (de Kwaadsteniet et al., 2008), nisin P from *Streptococcus gallolyticus* subsp. *Pasteurianus* in 2012 (Wu et al., 2014; Zhang et al., 2012), nisin H from *Streptococcus hyointestinalis* DPC 6484 in 2015 (O'Connor et al., 2015), nisin O1 to O4 from *Blautia obeum* A2-162 in 2017 (Hatziioanou et al., 2017) and nisin J from *Staphylococcus capitis* APC 2923 in 2020 (O'Sullivan et al., 2020).

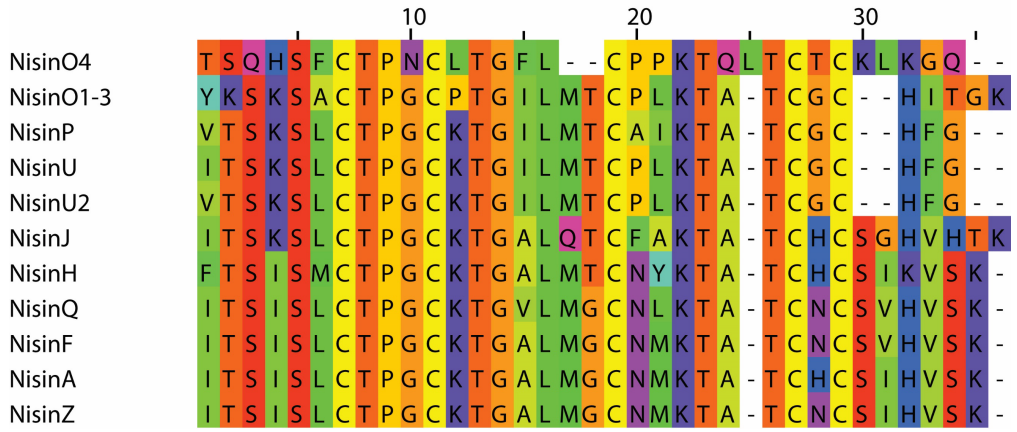

Figure 3: Natural nisin variants. Sequence alignment of the natural nisin variants: nisin O_{1-4}, nisin P, nisin U and U2, nisin J, nisin H, nisin Q, nisin F, nisin A and nisin Z. Alignment was performed with Clustal Omega and the figure was created with Jalview 2.11.0 using the Taylor colour code (Sievers et al., 2011; Taylor, 1997; Waterhouse et al., 2009)

All natural nisin variants contain the characteristic five Cys residues and thereby have the ability to form five (methyl-) lanthionine rings (Figure 3, yellow highlighted Cys residues).

Compared to nisin A, several variations in the amino acid sequence were found in the other natural variants. With just a single change in position 27, in which His is changed to Asn, nisin Z in the most identical natural variant (Mulders et al., 1991). In addition to the $His_{27}Asn$ exchanged (also found in nisin Z), nisin F also has an $Ile_{30}Val$ variation in the core peptide (de Kwaadsteniet et al., 2008). These variations are in the C-terminal part of the core peptide. The other natural nisin variants vary in the amino acid sequence spanning the whole core peptide. Nisin Q, for example, shares the same $His_{27}Asn$ and $Ile_{30}Val$ modification as mentioned before, but has additional $Ala_{15}Val$ and $Met_{21}Leu$ substitutions (Zendo et al., 2003). Compared to nisin A, nisin H has substitutions in five positions (Ile_1Phe, Leu_6Met, $Gly_{18}Thr$, $Met_{21}Gln$ and $His_{31}Tyr$) (O'Connor et al., 2015). In addition to the diversity in the amino acid sequence of the core peptide, the other natural nisin variants (O_{1-4}, U, U2, P and J) also differ in the length of the core peptide. Nisin U, U2, and P are 31 amino acids in length, nisin O_{1-3} 33 consists of amino acids, O_4 32 comprises of amino acids, whereas nisin J is the longest variant with 35 amino acids (Figure 3) (Hatziioanou et al., 2017; O'Sullivan et al., 2020; Wirawan et al., 2006; Wu et al., 2014; Zhang et al., 2012).

1.3 The nisin operon

The nisin operon of the class I lantibiotic nisin A (visualized in Figure 4) from *L. lactis* contains eleven genes which have different function: regulation (*nisR, nisK*), synthesis (*nisA*), PTM (*nisB, nisC*), transport (*nisT*), cleavage (*nisP*), as well as the self-immunity system (*nisI* and *nisFEG*) (Buchman et al., 1988; Kuipers et al., 1993; Qiao et al., 1996; van der Meer et al., 1993). The two-component system comprising of NisR (respone regulator) and NisK (histidine kinase) is responsible for quorum sensing of nisin and induces the expression of all genes of the nisin A operon (de Ruyter et al., 1996; Kuipers et al., 1995).

Figure 4: The nisin operon. The nisin operon consists of 11 genes. The lantibiotic *nisA* (grey), the modification enzymes *nisB* (blue) and *nisC* (yellow). The transporter *nisT* (black) and the protease *nisP* (green). The immunity genes *nisI* (red) and *nisFEG* (orange) and the regulation genes *nisR* (cyan) and *nisK* (light blue). Black arrows indicate promotors.

1.3.1 Nisin A

Nisin A is the best studied model of the class I lantibiotics. It is produced by *L. lactis* strains and was discovered in 1928 (Rogers, 1928; Rogers & Whittier, 1928). Nisin A is used in food industry since 1953 and received the status as 'generally recognized as safe' (GRAS) from the Food and Drug Administration (FDA) in 1988 (Delves-Broughton et al., 1996). As a class I lantibiotic, the PTMs (dehydration and (methyl-) lanthionine rings A-E) are installed via two modification enzymes, NisB (dehydratase) and NisC (cyclase), respectively (Koponen et al., 2002). The serine at position 29 is not dehydrated like the other Ser/Thr residues, due to steric hindrance of the (methyl-) lanthionine rings D and E (Figure 5, lower part) (Lubelski et al., 2009). The transport across the membrane is done via the ABC transporter NisT and the leader is cleaved off via the protease NisP (Kuipers et al., 2004; van der Meer et al., 1993). Nisin A has a 23 amino acid long leader peptide fused to a 34 amino acid long core peptide (Kaletta & Entian, 1989). The leader peptide (Figure 5, upper part) contains a conserved motif, the FNLD-box, which is responsible for the recognition of the modification enzymes NisB and NisC (Abts et al., 2013; Khusainov et al., 2013; Mavaro et al., 2011; Plat et al., 2011). The structure of nisin A was solved via NMR spectroscopy in 1991 (Van de Ven et al., 1991).

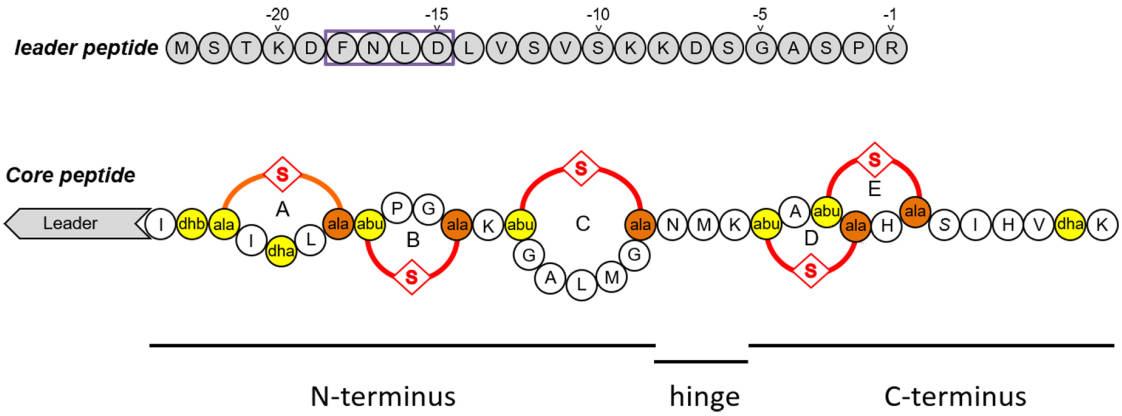

Figure 5: Nisin A with all PTMs installed. The nisin A leader peptide is shown in the upper part. The recognition motif -FLND-box for the modification enzymes is highlighted. In the lower part the core peptide with the attached leader peptide is shown. The (methyl-) lanthionine rings A-E are highlighted in red and orange and the dehydrated amino acids (Dha, Dhb), as well as the cysteine residues are highlighted in yellow and orange, respectively. The serine at position 29 is not dehydrated like the other Ser/Thr residues, due to steric hindrance of the (methyl-) lanthionine rings D and E. Taken and modified from (Mavaro et al., 2011).

The core peptide of nisin A is composed of three different parts. The N-terminal part with the (methyl-) lanthionine rings A, B and C, is responsible for the binding of nisin A to the cell wall precursor lipid II (Figure 6, a-b) (Hsu et al., 2004). A flexible hinge region in between provides

flexibility to the C-terminal part to reorient and insert into the membrane. It forms a stable pore with rings D and E comprising of eight nisin and four lipid II molecules which leads to leakage of cell contents and eventually to cell death (Figure 6, c-d) (AlKhatib et al., 2014a; Hasper et al., 2004; Medeiros-Silva et al., 2018; van Heusden et al., 2002; Wiedemann et al., 2004). This dual mode of action (binding and thereby, blocking lipid II and pore formation) are the reason behind the nanomolar range antimicrobial activity of lantibiotics (Abts et al., 2011; Chan et al., 1996; Gross & Morell, 1967; Oppedijk et al., 2016).

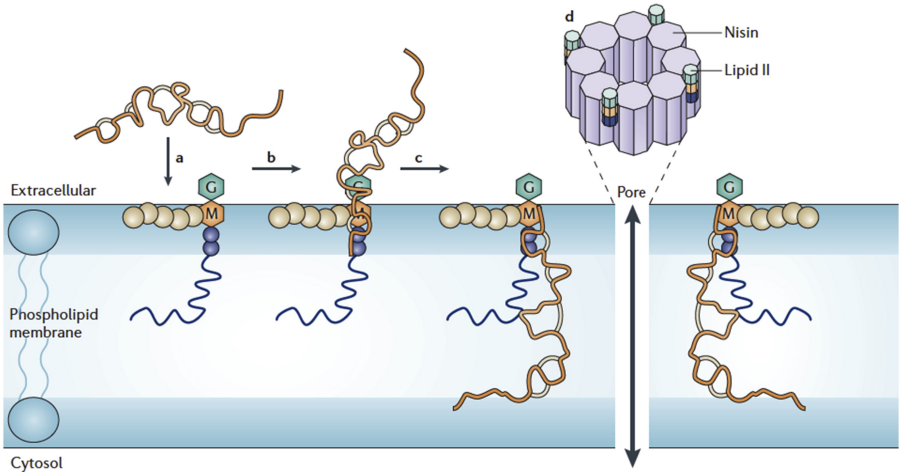

Figure 6: Pore-formation mechanism of nisin. (**a**) Nisin from the extracellular space reaches the bacterial plasma membrane. (**b**) Nisin binds to Lipid II via the (methyl-) lanthionine rings A, B. (**c**) After the binding to Lipid II, the C-terminal part of nisin is inserted into the membrane. (**d**) The pore forming complex consists of eight nisin and four Lipid II molecules, leading to cell death. Taken from (Breukink & de Kruijff, 2006)

1.3.2 NisB

NisB is the dehydratase of the nisin modification machinery (Koponen et al., 2002). The gene of the dehydratase, *nisB* was identified in the 1992, but due to experimental challenges, the mechanistic aspects of the dehydration reaction remained unclear (Engelke et al., 1992). Sequence analysis, in which an amphipathic α-helix was identified lead to the expectation that NisB is membrane associated (Engelke et al., 1992). Deletion mutations of NisB on a plasmid-based expression system, resulted in an unmodified nisin A precursor peptide, indicating the function of NisB within dehydration reaction (Karakas Sen et al., 1999; Koponen et al., 2002; van den Berg van Saparoea et al., 2008). By 2011, it was possible to purify NisB in high and stable amounts and analysis of the oligomeric state via multi-angle-light scattering (MALS) showed that NisB is a dimer in solution (Mavaro et al., 2011). Substrate binding studies via Surface Plasmon Resonance (SPR) with NisB and different nisin A precursor variants were

conducted and an affinity in the micromolar range could be determined (Mavaro et al., 2011). The mechanism of the dehydration process and the involved components were solved nearly 20 years after the identification of the gene, revealing that the dehydration process uses a glutamylation step followed by an elimination step (Garg et al., 2013; Ortega et al., 2015). For the dehydration reaction, NisB utilizes glutamyl-tRNA^{Glu} to transfer the glutamyl-group onto the hydroxyl group of a Ser or Thr side chain, followed by a β-elimination to convert these residues in Dha or Dhb, respectively (Ortega et al., 2015).The structure of NisB dimer was solved in 2015 (shown in Figure 7) and showed that these steps are organized in separate domains, the N-terminal for glutamylation domain (Figure 7, cyan and blue domains) and the C-terminal for elimination domain (Figure 7, orange and light orange domains) (Ortega et al., 2015).

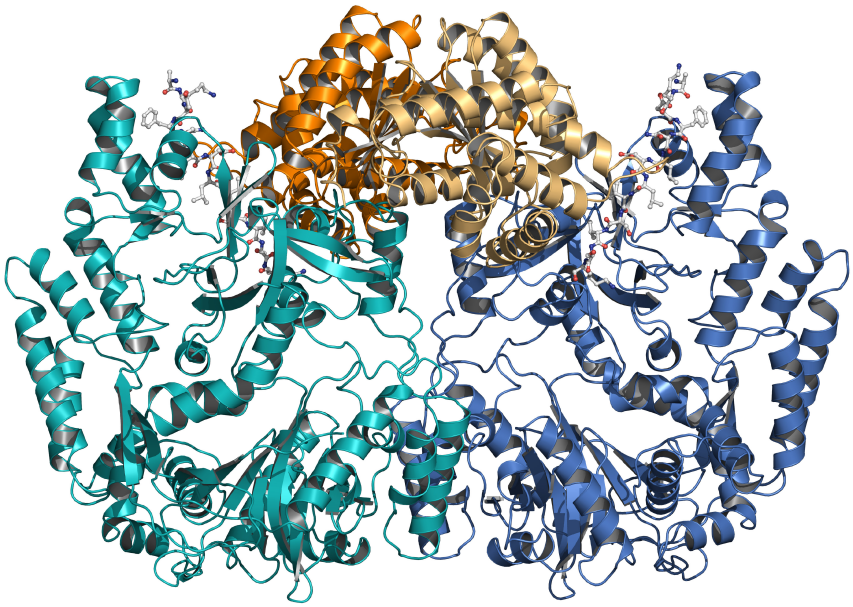

Figure 7: Crystal structure of dimeric NisB (PDB ID: 4WD9). The glutamylation domain of the first protomer is highlighted in cyan and the elimination domain in light orange. The corresponding protomer is highlighted in blue (glutamylation domain) and orange (elimination domain). The visible part of the leader peptide of nisin A is shown in a ball-and-stick representation. Taken and modified from (Lagedroste et al., 2020) and created with PyMOL 2.5 (Schrodinger, 2022).

Mutation analysis identified several critical amino acid residues in these domains (Garg et al., 2013; Khusainov et al., 2015; Ortega et al., 2015; Repka et al., 2017; Rink et al., 2005). Within the glutamylation domain, residues Arg_{14}, Tyr_{80} Arg_{83}, Arg_{87}, Thr_{89}, Asp_{121}, Asp_{299}, and Arg_{464} are important and in the elimination domain Arg_{786}, Arg_{826}, and His_{961} result in poly-glutamylated products (Garg et al., 2013; Khusainov et al., 2015; Ortega et al., 2015; Repka et

al., 2017; Rink et al., 2005). Also, mutations within the leader, especially in the -FNLD- which is responsible for the recognition, drastically influences the dehydration process (Khusainov et al., 2013; Khusainov et al., 2015; Mavaro et al., 2011; Plat et al., 2011; Plat et al., 2013).

1.3.3 NisC

NisC is a zinc ion-dependent cyclase of the nisin modification machinery, guiding the (methyl-) lanthionine ring formation (Koponen et al., 2002; Li et al., 2006; Okeley et al., 2003). Its structure was solved in 2006 and revealed two domains: an α-toroid core and a SH2-like domain (Figure 8) (Li et al., 2006). Within the α-toroid core, a zinc ion is coordinating in a tetrahedral orientation via three important residues, His_{331}, Cys_{330} and Cys_{284} and a water molecule (Li et al., 2006). The residues His_{212} and Arg_{280} support the correct (methyl-) lanthionine ring formation (Figure 8) (Li & van der Donk, 2007).

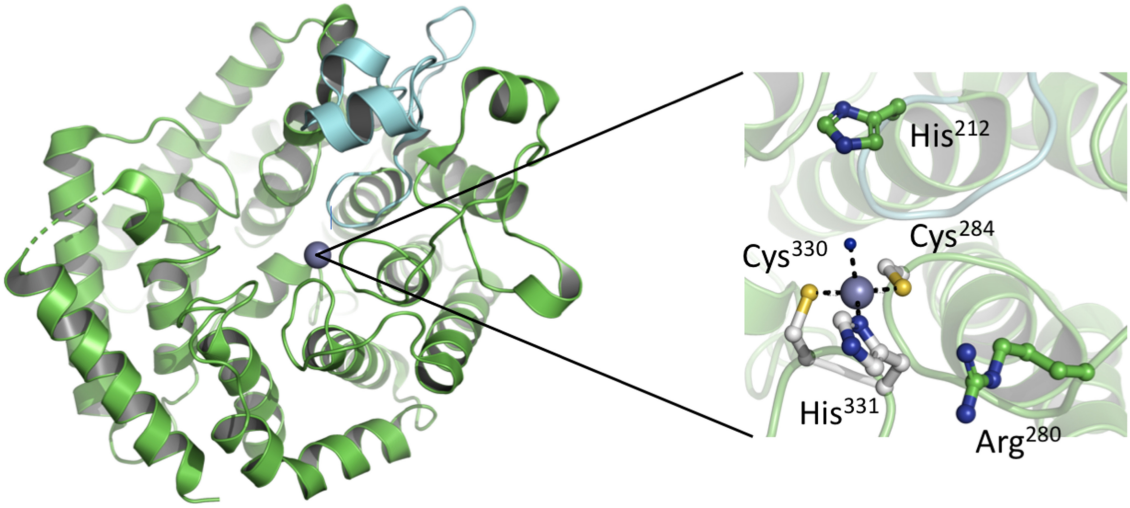

Figure 8: Crystal structure of NisC (PDB ID: 2G0D). On the left side, the overall structure of NisC is shown. The α-toroid core is shown in green, the SH2-like domain in cyan and the zinc ion as grey sphere. On the right side is a zoom-in of the active center. The important residues for the zinc coordination (His_{331}, Cys_{330} and Cys_{284}) and for function (His_{212} and Arg_{280}) are shown in ball-and stick representation. Taken from (Lagedroste et al., 2020) and created with PyMOL 2.5 (Schrodinger, 2022).

The (methyl-) lanthionine ring formation can occur spontaneous at high pH values (>7.5) in an uncontrolled way, resulting in erroneous stereochemistry or ring topology (Burrage et al., 2000; Okeley et al., 2000). NisC catalyses this reaction in a regio- and stereo-specific manner (Koponen et al., 2002; Okeley et al., 2003). The zinc ion in the active center reduces the pKa value of the sulphur atom of a cysteine residue and the resulting deprotonated thiolate attacks

a Dha or Dhb residue via Michael condensation and forms a (methyl-) lanthionine ring (Okeley et al., 2003). An affinity of ~2 µM for nisin A precursor was determined via Isothermal Titration Calorimetry (ITC) experiments (Abts et al., 2013). Although the function of the SH2 domain is still unclear, an interaction with the substrate is postulated but so far, no experimental evidence supports this hypothesis (Bradshaw & Waksman, 2002; Li et al., 2006).

1.3.4 NisT

NisT is an ABC transporter, responsible for the export of nisin A precursor peptide (Qiao & Saris, 1996; Ra et al., 1999). NisT is a half size transporter, containing a transmembrane domain (TMD) with six transmembrane helixes (TMH) and a nucleotide binding domain (NBD) and is functional as a dimer (Figure 9) (Siegers et al., 1996).

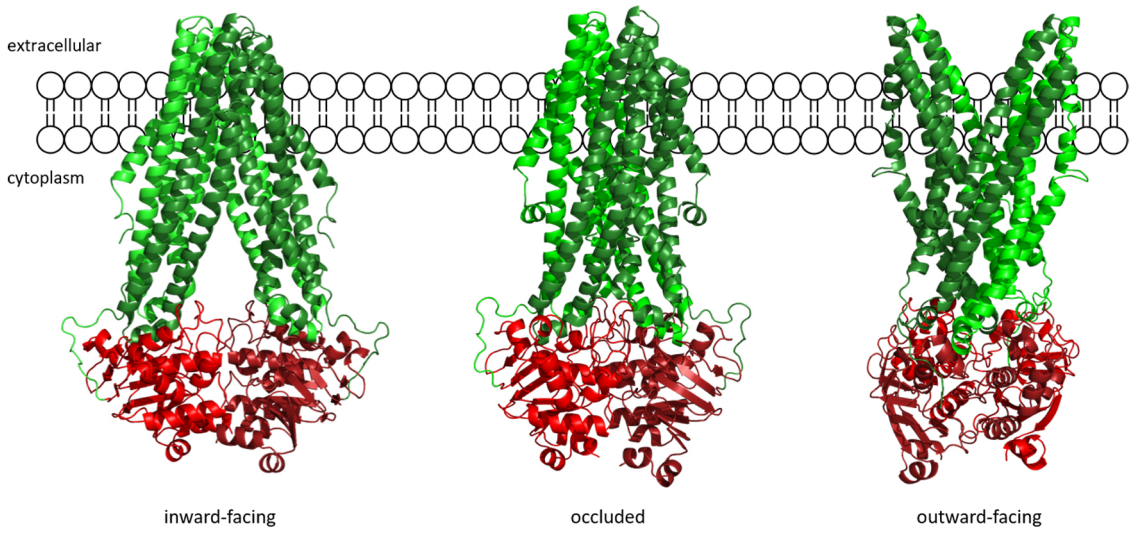

Figure 9: Homology model of the ABC transporter NisT. The TMDs are colored in green and dark green while the NBDs are in red and dark red for each protomer. The different conformations: inward-facing (left), occluded (middle) and outward-facing (right) are shown. Created with PyMOL 2.5 (Schrodinger, 2022), based on conformation homology models of Tm287 (PDB ID: 3QF4), McjD (PDB ID: 5EG1) and Sav1866 (PDB ID: 2ONJ). NisT model was created using AlphaFold2 (Jumper et al., 2021).

It was shown that NisT is able to transport the precursor peptide independent of the modification state of the core peptide, but in the presence of NisB and NisC, no transport of partly modified precursor peptides was observed (Kuipers et al., 2004). This core peptide independent transport even holds true if the core peptide is completely substituted against a non-lantibiotic core, like angiotensin, which makes NisT interesting for the secretion of different types of proteins, as long as they contain the nisin A leader peptide (Kluskens et al.,

2009; Kuipers et al., 2004; Rink et al., 2005). Nevertheless, the translocation efficiency for nisin A precursor is dependent on the presence of the modification enzymes NisB and NisC. Without both modification enzymes the secretion drops to ~2 %, while when only NisC is absent, the secretion is 30 %. This leads to the conclusion that NisB and NisC have a channeling function for NisT and they act as a multimeric lanthionine synthetase complex, such as SpaBTC (Kiesau et al., 1997; Lubelski et al., 2009; Siegers et al., 1996; van den Berg van Saparoea et al., 2008). The structure of NisT as well as the entire multimeric lanthionine synthetase complex is lacking, which is required to shed some light on the interplay of these enzymes.

1.3.5 NisP

NisP is a serine protease, responsible for the cleavage of the nisin A precursor peptide, yielding mature and biologically active nisin A. It belongs to the subtilisin-like proteases (Rawlings & Barrett, 1993; van der Meer et al., 1993) and is ribosomally synthesized as a pro-protein with an N-terminal signal sequence for the Sec-dependent translocation (Schneewind & Missiakas, 2014; van der Meer et al., 1993). After secretion, NisP processes an auto cleavage reaction to remove the pro-sequences, thereby, becoming a functional protease (Siezen et al., 1995; van der Meer et al., 1993).

Additionally, NisP contains a -LPxTG-motif at the C-terminus, which is recognized by a sortase A and anchors NisP in the cell wall via lipidation of Thr_{655} (Dieye et al., 2010; Schneewind et al., 1995; Schneewind & Missiakas, 2014; van der Meer et al., 1993).

The structure of NisP was solved in 2014 (Figure 10) and consist of 16 β-sheets and 11 α-helixes (Xu et al., 2014). The catalytic triad with Asp_{259}, His_{306} and Ser_{512} which are located on β-sheet 1 and α-helixes 3 and 9, respectively (Xu et al., 2014). NisP cleaves off the leader peptide from the nisin A core peptide after the sequence -GASPR- and releases biologically active nisin A, which constitutes the last step of the nisin A maturation pathway (Figure 10) (van der Meer et al., 1993). Initial experiments stated that the cleavage of the nisin A precursor is dependent on at least one (methyl-) lanthionine ring, but recent experiments showed that although NisP is independent but its catalytic activity is dependent on the modification state (Kuipers et al., 2004; Lagedroste et al., 2017; Montalban-Lopez et al., 2018; Plat et al., 2011; van der Meer et al., 1993).

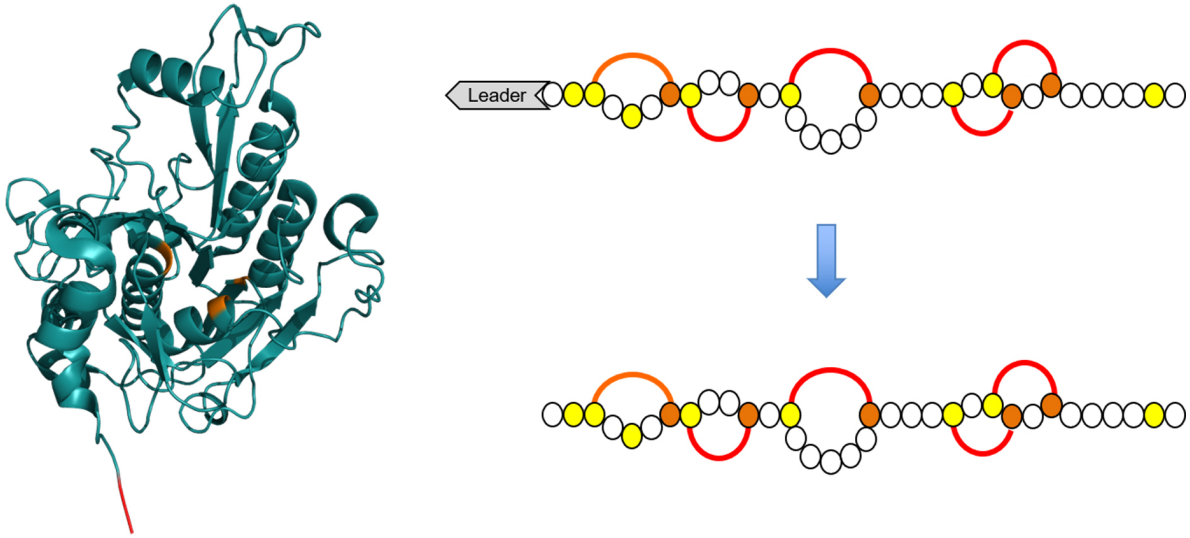

Figure 10: The protease NisP (PDB ID: 4MZD). On the left side, the protease NisP is shown after the auto cleavage reaction. The anchor for its binding to the peptidoglycan is shown in red, the residues from the active center (Ser_{512}, His_{306} and Asp_{259}) are highlighted in orange. On the right side, the cleavage reaction from the precursor peptide nisin A to the mature and biologically active nisin A is shown. The (methyl-) lanthionine rings A-E are highlighted in red and orange and the dehydrated amino acids (Dha, Dhb), as well as the cysteine residues are highlighted in yellow and orange. Created with PyMOL 2.5 (Schrodinger, 2022).

1.4 Nisin immunity system

Nisin producer strains need a system to survive against the antimicrobial activity of their self-produced lantibiotic. This so-called immunity system contains the lipoprotein NisI and the ABC transporter NisFEG, both located in the nisin operon and under control of the two-component system NisRK (de Ruyter et al., 1996; Engelke et al., 1994; Kuipers et al., 1993; Siegers & Entian, 1995). Both proteins work in a cooperative manner to provide full immunity (Ra et al., 1999; Takala et al., 2004; Takala & Saris, 2006).

1.4.1 NisI

NisI is a lipoprotein anchored in the membrane and act as the first line of defense against nisin. The structure was solved in 2015, consists of two domains which are structurally similar to each other but differ in their surface charge (Figure 11) (Hacker et al., 2015). The positively charged N-terminal domain contains a signal sequence with a sequence motif which is responsible for membrane anchoring (16-GLSGCY-21) where Cys_{20} is linked to a diacylglycerol in the membrane (Hacker et al., 2015; Jeong & Ha, 2018; Qiao et al., 1995; Takala et al., 2004). The highly negative charged C-terminal domain is important for the

binding of nisin and modulates the membrane affinity of the N-terminal domains, as shown by various studies (AlKhatib et al., 2014a; Hacker et al., 2015; Jeong & Ha, 2018; Takala & Saris, 2006). The two domains are connected via a linker which gives the domains a high flexibility as shown in SAXS experiments (Hacker et al., 2015). The evaluated K_D values from NMR titration experiments of the nisin binding to NisI shows an affinity in the micromolar range, which is surprisingly high because nisin is active in the nanomolar range (Hacker et al., 2015; Takala et al., 2004). This suggests that the mode of action from NisI is more complex than just simply binding to nisin. Later studies concluded that in the presence of nisin, the expression of NisI changes the morphology of *L. lactis* cells. The cells cluster in long chains of up to 30 cells, thereby reducing the available surface for the nisin interaction (AlKhatib et al., 2014a). Thus, NisI exhibits immunity against nisin through two functions: first is its binding to nisin, thereby protecting the nisin producing bacteria and secondly by clustering the cells. Furthermore, NisI doesn't modify or degrade nisin (AlKhatib et al., 2014a; Geiger et al., 2019; Koponen et al., 2004; Qiao et al., 1995; Ra et al., 1999; Stein et al., 2003; Takala et al., 2004).

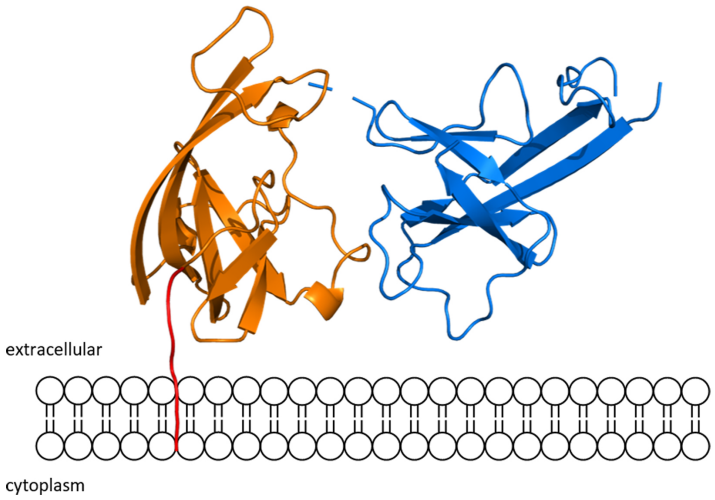

Figure 11: The lipoprotein NisI (PDB ID:5XHB). The N-terminal domain is shown in orange with the membrane anchor in red. The C-terminal domain, responsible for the binding of nisin is shown in blue. Created with PyMOL 2.5 (Schrodinger, 2022).

1.4.2 NisFEG

The ABC transporter NisFEG is the second line of defense against nisin (Stein et al., 2003). The functional transporter contains two different transmembrane domains, NisE and NisG and two copies of the NBD called NisF, with a stoichiometry of $NisF_2EG$ (see Figure 12) (Siegers & Entian, 1995). NisE and NisG, functional as a heterodimer, are responsible for the nisin

binding and for the export out of the membrane and powered by NisF (AlKhatib et al., 2014b; Okuda et al., 2010; Stein et al., 2003). The ABC transporter NisFEG confers immunity against nisin by extruding the substrate (nisin) out of the membrane and exporting it back into the extracellular space (AlKhatib et al., 2014b; Stein et al., 2003). This export prevents pore formation, within a concentration range of up to 60 nM, as shown for nisin A (AlKhatib et al., 2014b). Mutants of nisin where the (methyl-) lanthionine rings D and E (CCCCA and CCCAA) were missing or the truncation variants ($nisin_{1-22}$ and $nisin_{1-28}$), showed a drastic reduction in the immunity provided by NisFEG, clearly indicating that NisFEG recognizes the C-terminal part of nisin (ring D/E) (AlKhatib et al., 2014b). Although the ABC transporter NisFEG works independently but in order to achieve full immunity against nisin A, it works in a cooperative manner with the lipoprotein NisI as sown for SpaFEG (Ra et al., 1999; Siegers & Entian, 1995; Stein et al., 2005; Stein et al., 2003).

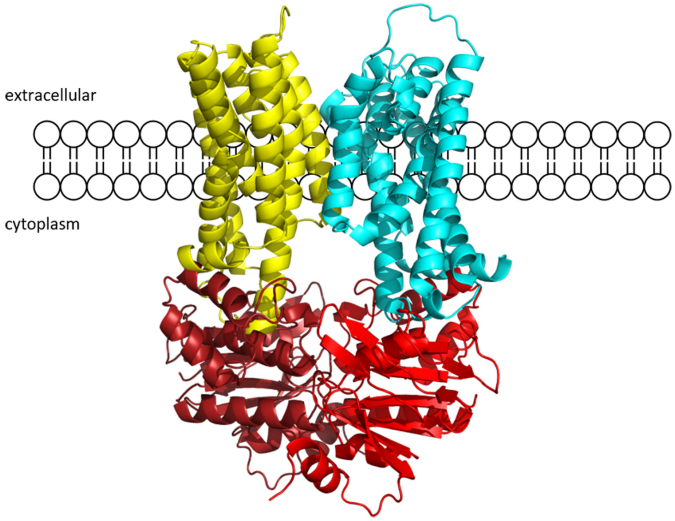

Figure 12: The ABC transporter NisFEG. The TMDs domains NisE and NisG are shown in yellow and cyan and the two NBDs NisF in red and dark red, respectively. Created with PyMOL 2.5 (Schrodinger, 2022), NisFEG models were created using AlphaFold2 (Jumper et al., 2021).

1.5 Nisin resistance operon

Although lantibiotics are highly effective against various bacteria, however, some lantibiotic non-producer strains established a resistance mechanism against lantibiotics (Draper et al., 2015). These resistance systems can either be unspecific such as changes in bacterial cell wall and membrane or more specific through ATP-mediated efflux pumps or two-component

system regulation or proteolytic degradation of the lantibiotic itself (Bastos Mdo et al., 2015; Draper et al., 2015; Nawrocki et al., 2014; Sun et al., 2009). One such example for specific resistance system is the Nisin resistance system from *S. agalactiae* COH1, containing *Sa*NsrFP which encodes for a BceAB-type ABC transporter and a nisin resistance protein NSR. Both genes are located on an operon together with the genes encoding the two-component system (TCS) NsrK and NsrR, and together these five genes constitute the nisin resistance operon (see Figure 13) (Khosa et al., 2013; Khosa, Frieg, et al., 2016; Khosa, Hoeppner, et al., 2016; Khosa, Lagedroste, et al., 2016). NsrK belongs to the intermembrane sensing kinase (IMSK) family, with a characteristic short loop domain responsible for sensing and thus, unable to sense the extracellular space (Mascher, 2006). An external trigger is required for the activation of the histidine kinase, which is postulated to be the extracellular domain of the BceAB-type ABC transporter *Sa*NsrFP (Clemens et al., 2017; Khosa et al., 2013). The response regulator NsrR consists of the classic helix-turn-helix motif, with the putative residues for DNA binding, but the distinct promoter regions on the nisin resistance operon remain unclear (Khosa, Hoeppner, et al., 2016).

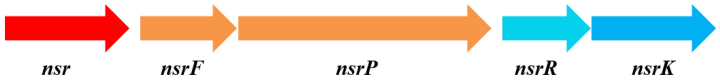

Figure 13: The nisin resistance operon. The nisin operon consists of five genes. The nisin resistance protein *nsr* (red) and the BceAB-type ABC transporter *nsrFP* (orange) and the regulation genes *nsrR* (cyan) and *nsrK* (light blue). Promoter regions are unknown so far (Khosa, Hoeppner, et al., 2016).

1.5.1 NSR

The nisin resistance protein NSR from *S. agalactiae* COH1 is a membrane-anchored endopeptidase with a high hydrophobicity (Khosa et al., 2013). The membrane-anchoring occurs through a 21 amino acid residues long transmembrane sequence at the N-terminus (Froseth & McKay, 1991). NSR belongs to the S41 family of peptidases, specifically the C-terminal processing peptidases (CTPs). NSR confers resistance against nisin through a degradation reaction, cleaving nisin between (methyl-) lanthionine ring E (position 28) and Ser_{29}, resulting in a nisin molecule, $nisin_{1\text{-}28}$, which has 100-fold less antimicrobial activity and reduced affinity towards the cell membrane (Figure 14, right part) (Khosa et al., 2013; Khosa, Frieg, et al., 2016; Liang et al., 2010; Sun et al., 2009). When NSR is expressed in *L. lactis* strain, it confers 18-20 fold resistance against nisin (Khosa et al., 2013). The structure of NSR (Figure 14) was solved in 2016, and consists of eleven β-strands and eleven α-helixes organized

in three domains: a N-terminal helical bundle, the protease cap and a core domain (Khosa, Frieg, et al., 2016). These domains form a hydrophobic tunnel with a width of 10 Å. The active center is formed by a dyad of two residues, His_{98} and Ser_{236} (Khosa, Frieg, et al., 2016). With simulations and molecular docking studies, it was demonstrated that the nisin molecule is trapped within the tunnel near the catalytic dyad by the (methyl-) lanthionine rings D and E (Khosa, Frieg, et al., 2016). It was further confirmed though cell growth assays that NSR recognizes the C-terminus of nisin and the last two rings of nisin are important for the interaction between nisin and NSR (Khosa, Frieg, et al., 2016).

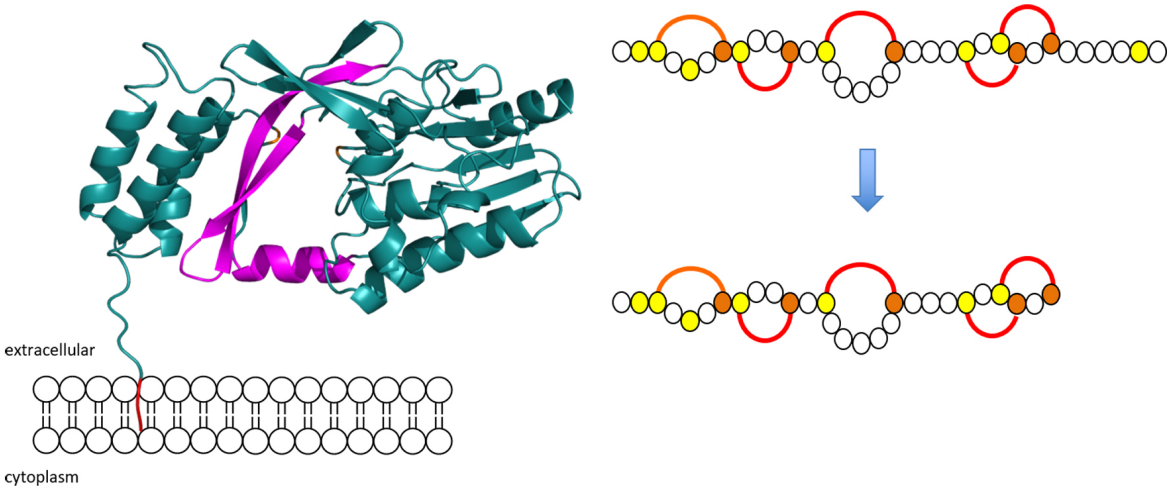

Figure 14: The nisin resistance protein NSR (PDB ID: 4Y68). On the left side, the structure of the protease NSR is shown. The anchor for the membrane binding is shown in red, the residues from the active center dyad (His_{98} and Ser_{236}) are highlighted in orange and the protease cap in magenta. On the right side, the NSR cleavage reaction from the mature biological active nisin to a less efficient variant, $nisin_{1-28}$, missing the last six amino acids is shown. The (methyl-) lanthionine rings A-E are highlighted in red and orange and the dehydrated amino acids (Dha, Dhb), as well as the cysteine residues are highlighted in yellow and orange. Created with PyMOL 2.5 (Schrodinger, 2022).

1.5.2 *Sa*NsrFP

The ABC transporter *Sa*NsrFP from *Streptococcus agalactiae*, belongs to the BceAB-type ABC transporter and consists of nucleotide binding domain *Sa*NsrF and a transmembrane domain *Sa*NsrP in a 2:1 stoichiometry (Khosa et al., 2013). *Sa*NsrP is 69.4 kDa in size and comprises ten TMHs (Figure 15, cyan) with a large ECD of 220 amino acids between helices VII and VII (Figure 15, orange). On the contrary, *Sa*NsrF is only 28.3 kDa in size and is composed of 250 amino acids containing all the signature motifs of the ABC transporters (Figure 15, red and dark red)(Khosa et al., 2013). BceAB-type ABC transporters are putatively

involved in the removal of AMPs from the membrane, functioning as an exporter, or as flippase of undecaprenyl pyrophosphate (UPP) (Gebhard & Mascher, 2011; Kingston et al., 2014; Kobras et al., 2020) and have been named after the BceAB transporter system from *Bacillus subtilis* that confer resistance against bacitracin (Ohki et al., 2003; Rietkotter et al., 2008). Interestingly, the TMD (containing ten TMHs) is encoded by a single protein and contains an extracellular domain (ECD), which is in contrast to other resistance or immunity ABC transporters. This ECD appears to be the hallmark of BceAB-type ABC transporters, because it is involved in the substrate binding and sensing (Clemens et al., 2017; George et al., 2022; Khosa et al., 2013; Ohki et al., 2003; Rietkotter et al., 2008). Normally, in other resistance or immunity operons, sensing is performed via its designated TCS system. However, in BceAB-type operons, the histidine kinase has only a short loop, normally only responsible for substrate sensing. This short loop is almost entirely located in the cytoplasmic membrane and thus, cannot sense the extracellular substrate (Mascher, 2006). It is proposed, that the substrate binding of the ECD also triggers the histidine kinase, which, in combination with the regulator protein upregulates the operon (Bernard et al., 2007; Dintner et al., 2014; Gebhard, 2012). The BceAB transporter from *B. subtilis* has been shown to form a multicomponent complex with its designated TCS BceRS upon binding of bacitracin (Dintner et al., 2014; Dintner et al., 2011; George et al., 2022). Such a detailed information is lacking so far for the ABC transporter *Sa*NsrFP and its TCS system NsrRK.

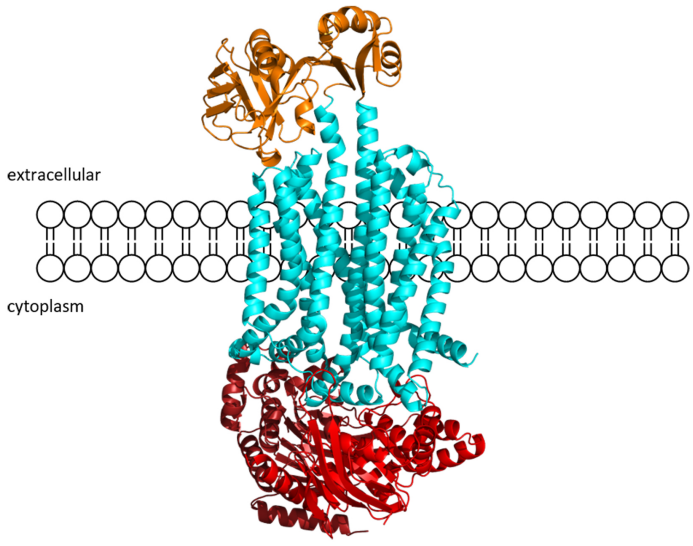

Figure 15: The BceAB-type ABC transporter *Sa*NsrFP. The TMD domain is shown in cyan and the characteristic ECD in orange. The NBDs *Sa*NsrF are highlighted in red and dark red, respectively. Created with PyMOL 2.5 (Schrodinger, 2022), *Sa*NsrFP model was created using AlphaFold2 (Jumper et al., 2021) and is in line with the previously solved structure of the first BceAB-type ABC transporter from *Bacillus subtilis* (George et al., 2022).

2 Aims

Since its discovery, nisin A is the best studied class I lantibiotic so far. Most of these studies were performed mainly on isolated enzymes, for example binding of the leader peptide to one of the modification enzymes. One major breakthrough was the structure of the dehydratase NisB and the identification of the mechanism of dehydration, the glutamylation reaction. But information about the entire modification complex or the effect of mutations on the whole system are still lacking.

One focus of this work was to analyze the interplay between the modification enzymes NisB and NisC depending on the substrate; determining the stoichiometry of the assembled modification complex and identifying the trigger factor(s) for the assembly and the disassembly of the complex. Although the structures of both, NisB and NisC, were already solved but structural information of the assembled complex were missing. Using small-angle X-ray scattering (SAXS), one should be able to visualize the whole assembled complex.

Furthermore, all protein of the nisin biosynthesis machinery will be tested with different nisin variants to get further insights about the secretion and modification levels of the mutated substrates. The purified nisin variants still contained the leader peptide, which had to be cleaved off yield biologically active substrates. Thus, the effect of the mutations on the efficiency of the protease NisP was also determined.

Finally, the analysis of the antimicrobial activity of the variants against the known immunity system NisI and NisFEG as well as the resistance system NSR and *Sa*NsrFP was one major goal of this thesis.

3 Publications

Chapter I	A Structural View on the Maturation of Lanthipeptides
Chapter II	Stoichiometry and structure of a lantibiotic maturation complex
Chapter III	Impact of the nisin modification machinery on the transport kinetics of NisT
Chapter IV	Systematic characterization of position one variants within the lantibiotic nisin
Chapter V	Insights in the Antimicrobial Potential of the Natural Nisin Variant Nisin H
Chapter VI	Bypassing lantibiotic resistance by an effective nisin derivative
Chapter VII	Influence of nisin hinge-region variants on lantibiotic immunity and resistance proteins
Chapter VIII	Characterization of the nucleotide-binding domain NsrF from the BceAB-type ABC-transporter NsrFP from the human pathogen *Streptococcus agalactiae*
Chapter IX	The N-terminal Region of Nisin Is Important for the BceAB-Type ABC Transporter NsrFP from *Streptococcus agalactiae* COH1

3.1 Chapter I

Title: A Structural View on the Maturation of Lanthipeptides

Authors: Marcel Lagedroste[#], **Jens Reiners[#]**, C. Vivien Knospe, Sander H. J. Smits and Lutz Schmitt

[#]Authors contributed equally

Published in: Frontiers in Microbiology (2020)

Impact factor: 5.26

Own proportion of this work: 25%

- Writing the manuscript
- Bioinformatic analysis

frontiers in Microbiology

REVIEW
published: 09 June 2020
doi: 10.3389/fmicb.2020.01183

A Structural View on the Maturation of Lanthipeptides

Marcel Lagedroste[1†], Jens Reiners[1,2†], C. Vivien Knospe[1], Sander H. J. Smits[1,2] and Lutz Schmitt[1*]*

[1] Institute of Biochemistry, Heinrich Heine University Düsseldorf, Düsseldorf, Germany, [2] Center for Structural Studies, Heinrich Heine University Düsseldorf, Düsseldorf, Germany

Lanthipeptides are ribosomally synthesized and posttranslationally modified peptides, which display diverse bioactivities (e.g., antifungal, antimicrobial, and antiviral). One characteristic of these lanthipeptides is the presence of thioether bonds, which are termed (methyl-) lanthionine rings. These modifications are installed by corresponding modification enzymes in a two-step modality. First, serine and threonine residues are dehydrated followed by a subsequent catalyzed cyclization reaction, in which the dehydrated serine and threonine residues are undergoing a Michael-type addition with cysteine residues. The dedicated enzymes are encoded by one or two genes and the classification of lanthipeptides is pending on this. The modification steps form the basis of distinguishing the different classes of lanthipeptides and furthermore reflect also important mechanistic differences. Here, we will summarize recent insights into the mechanisms and the structures of the participating enzymes, focusing on the two core modification steps – dehydration and cyclization.

Keywords: structural biology, biochemistry, lanthionine, enzymes, protein–protein interaction

OPEN ACCESS

Edited by:
Des Field,
University College Cork, Ireland

Reviewed by:
Manuel Montalban-Lopez,
University of Granada, Spain
Yuki Goto,
The University of Tokyo, Japan

****Correspondence:***
Sander H. J. Smits
Sander.Smits@hhu.de
Lutz Schmitt
lutz.schmitt@hhu.de

[†] These authors have contributed equally to this work

Specialty section:
This article was submitted to Antimicrobials, Resistance and Chemotherapy, a section of the journal Frontiers in Microbiology

Received: *30 March 2020*
Accepted: *08 May 2020*
Published: *09 June 2020*

Citation:
Lagedroste M, Reiners J, Knospe CV, Smits SHJ and Schmitt L (2020) A Structural View on the Maturation of Lanthipeptides. Front. Microbiol. 11:1183. doi: 10.3389/fmicb.2020.01183

INTRODUCTION

Ribosomally synthesized and posttranslationally modified peptides (RiPPs) are a large family of natural compounds of diverse biological functions (Arnison et al., 2013). Among the RiPPs, lanthipeptides form the largest sub-family (Skinnider et al., 2016), which is characterized by the presence of multiple lanthionine (Lan) or (methyl-) lanthionine rings ((Me)Lan)-, that restrict the conformational flexibility of the peptides and give rise to their high biological stability (Bierbaum et al., 1996). Common to lanthipeptides is the ribosomal biosynthesis of a precursor peptide that is composed of an N-terminal leader peptide (LP) and a C-terminal core peptide (CP), termed LanA (Oman and van der Donk, 2010; Arnison et al., 2013). While all posttranslational modifications (PTMs) are introduced only in the CP, the LP increases the efficiency of the PTMs to the lanthipeptide by its PTM machinery and keeps the peptide in an inactive state prior to translocation (van der Meer et al., 1994; Kuipers et al., 1993, 2004; Khusainov and Kuipers, 2012). The fully modified lanthipeptide is termed mLanA (Arnison et al., 2013). Subsequently, the LP is proteolytically removed either before or after secretion to the extracellular space via its cognate ABC transporter and the active lanthipeptide is released into the extracellular space (van der Meer et al., 1993, 1994; Nishie et al., 2011; Ortega et al., 2014). In general, all lanthipeptides share at least two common PTMs. The first one is the dehydration of serine and threonine residues, resulting in the formation of 2,3-didehydroalanine (Dha from serine) and 2,3-didehydrobutyrine (Dhb from threonine) (**Figure 1**; Gross and Morell, 1967, 1971; Gross et al., 1969). This reaction is catalyzed by

the dehydratase LanB or dehydratase domains depending on the classification of the lanthipeptide (see next section) (Gilmore et al., 1994; Gutowskieckel et al., 1994; Peschel et al., 1996; Karakas Sen et al., 1999). The second common PTM is the Michael-type addition of a cysteine side chain with the previously dehydrated amino acids yielding *meso*-lanthionine (from Dha) or (3-methyl-) lanthionine (from Dhb) (**Figure 1**) introduced by the cyclase LanC (Gross and Morell, 1967, 1971; Gross et al., 1969; Barber et al., 1988). Additionally to these two PTMs that are the foundation of lanthipeptides, a range of further modifications such as labionin (Lab) ring formation (**Figure 1**; Meindl et al., 2010; Iorio et al., 2014) or tailoring reactions such as halogenation of tryptophan residues, decarboxylation or acylation have been observed (Mortvedt et al., 1991; Kupke et al., 1992; Skaugen et al., 1994; van de Kamp et al., 1995; Heidrich et al., 1998; Ekkelenkamp et al., 2005; Castiglione et al., 2008; He et al., 2008; Velasquez et al., 2011; Huang and Yousef, 2015). However, these reactions are not further discussed in this review and the reader is referred to excellent reviews covering these aspects (Mortvedt et al., 1991; Kupke et al., 1992; Skaugen et al., 1994; van de Kamp et al., 1995; Heidrich et al., 1998; Ekkelenkamp et al., 2005; Castiglione et al., 2008; He et al., 2008; McIntosh et al., 2009; Meindl et al., 2010; Velasquez et al., 2011; Arnison et al., 2013; Dunbar and Mitchell, 2013; Iorio et al., 2014; Walsh, 2014; Huang and Yousef, 2015; Ortega and van der Donk, 2016; Repka et al., 2017).

In 2013, a new nomenclature was suggested that subdivides lanthipeptides based on their modification machinery in four families, termed class I–IV (**Figure 2**; Arnison et al., 2013) that are described in greater detail in the following sections. In this review, we will follow this new nomenclature. Furthermore, we will restrict ourselves to the two common maturation steps that occur in the cytosol of lanthipeptide producing strains.

LANTIBIOTICS – SPECIALIZED LANTHIPEPTIDES

The hallmark of lanthipeptides is the presence lanthionine or (methyl-) lanthionine rings. In cases that lanthipeptides possess antimicrobial activity they are called lantibiotics (Schnell et al., 1988; Arnison et al., 2013). However, other activities, such as antifungal, antiviral, morphogenetic, or antinociceptive have been described (Kodani et al., 2004, 2005; Ferir et al., 2013; Iorio et al., 2014; Mohr et al., 2015). The antimicrobial activity, which is mainly directed against Gram-positive bacteria where the target of most lantibiotics is the membrane and/or a specific receptor. A prominent example, nisin, a lantibiotic produced by *Lactococcus lactis*, targets the peptidoglycan precursor lipid II. Nisin contains five (Me)Lan rings, where the first two bind to the pyrophosphate moiety of lipid II and directly inhibit the cell wall synthesis. Additionally, nisin and lipid II molecules form pores in the cell membrane of the target cell in a stoichiometry of eight nisin and four lipid II molecules (Severina et al., 1998; Breukink et al., 1999; Wiedemann et al., 2001; Brumfitt et al., 2002; van Heusden et al., 2002; Hasper et al., 2004, 2006; Hsu et al., 2004; Chatterjee et al., 2005b; Breukink and de Kruijff, 2006; Lubelski et al., 2008; Bierbaum and Sahl, 2009; Schneider and Sahl, 2010; Islam et al., 2012). Despite its usage in the food industry for almost 50 years (Cotter et al., 2005) this dual mode of action explains why hardly any acquired resistances have been described in the literature.

THE FIRST MATURATION STEP – THE DEHYDRATION REACTION

The major discriminators among the four classes of lanthipeptides are the lanthipeptide modification enzymes. Here, four different routes corresponding to the four subfamilies (LanB, LanM, LanKC, and LanL) have evolved, which mainly differ in the mechanism of dehydrating serine and threonine residues (**Figure 2**).

Class I family dehydratases (LanB) contain the well-studied enzymes NisB or SpaB that dehydrate their substrates nisin (NisA) or subtilin (SpaA), respectively (Gross and Morell, 1967; Gross et al., 1969). NisB adopts a dimeric state in solution and interestingly interacts with the different maturation states of NisA and not only with its cognate substrate (unmodified NisA) in the low micromolar range (Mavaro et al., 2011). *In vivo* co-expression studies of NisB and the cyclase NisC without purification resulted in dehydration and cyclization of NisA indicating functional enzymes (Karakas Sen et al., 1999; Kluskens et al., 2005; Rink et al., 2005; Rink et al., 2007a). In 2013, Garg et al. (2013) demonstrated *in vitro* activity of purified NisB by using extracts of *Escherichia coli* and subsequently identified the cytosolic extract to be the key element for glutamylation of NisA. Finally, the addition of glutamyl-tRNA ($tRNA^{Glu}$), derived from glutamyl-tRNA synthetase, and glutamate to purified recombinant NisB restored the *in vitro* activity and consequently, polyglutamylated intermediates were identified by MS analysis (Ortega et al., 2015). This highlighted that the hydroxyl groups of serine and threonine in the CP of NisA were esterified with the alpha-carboxyl group of glutamate, where a cognate tRNA is the glutamyl-donor. Subsequently, the elimination of these activated residues resulted in the dehydrated residues Dha and Dhb. Of course, this reconstitution allowed a detailed study of the catalytic activity and the identification of essential amino acids of this LanB dehydratase (Garg et al., 2013; Bothwell et al., 2019). In 2015, the fruitful collaboration of the Wilfred van der Donk and Satish K. Nair groups also reported the crystal structure of NisB (**Figure 3A**). Similar to *in vitro* observations, NisB crystallized as a dimer (Ortega et al., 2015; Reiners et al., 2017). Importantly, NisB was co-expressed with NisA and parts of the LP including the FNLD box, which is pivotal for the interaction with NisB, were visible in the final electron density (shown in ball-and-stick representation in **Figure 3A**). In the crystal structure, the LP interacts with a twisted ß-strand resulting in an antiparallel, four-stranded ß-sheet. This resulted in a 2:2 stoichiometry of NisB:NisA, which is in contradiction to the *in vitro* data, which determined a 2:1 ratio of NisB:NisA using surface plasmon resonance (Mavaro et al., 2011). In 2019, a co-crystallization approach with a non-reactive substrate mimic also revealed a 2:2 stoichiometry of NisB-Val169Cys:NisA-Ser3Dap^{Glu}-Ser(-12)Cys

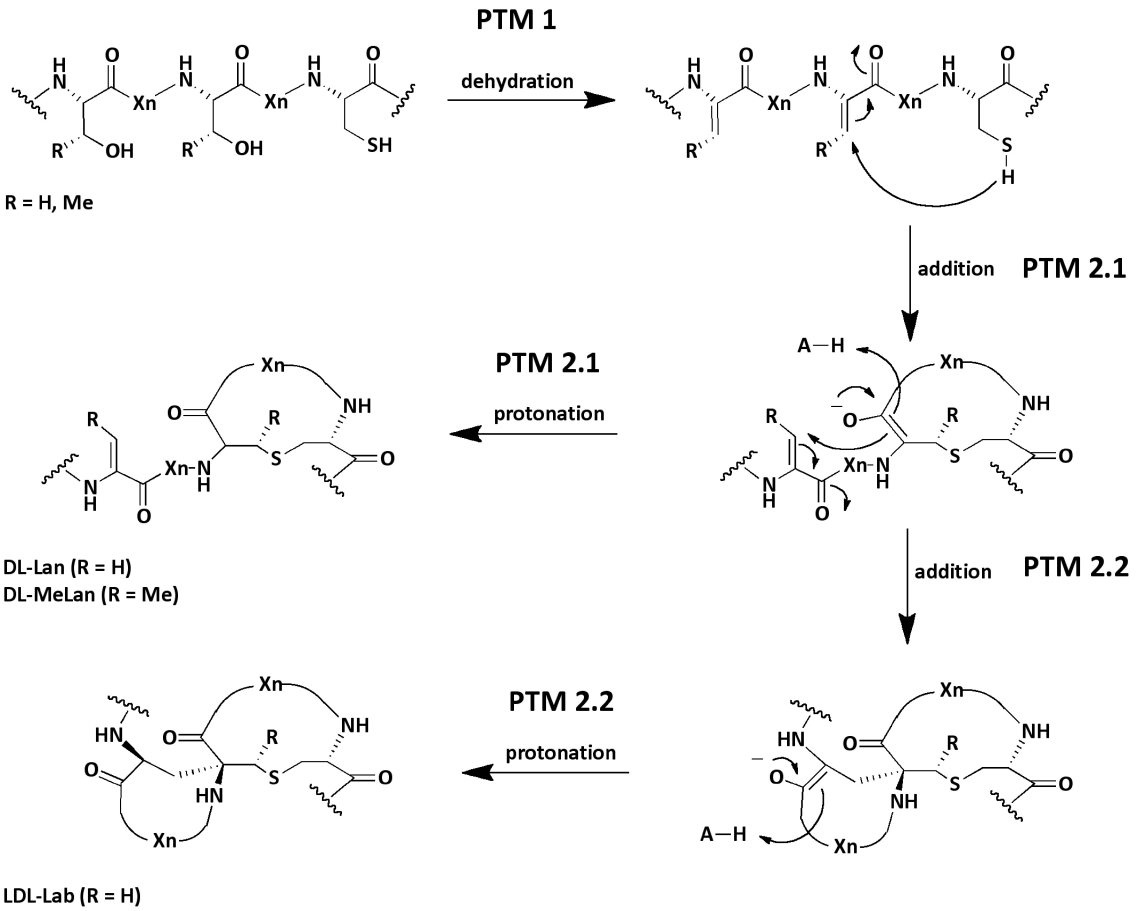

FIGURE 1 | Reaction and structure of common PTMs in lanthipeptides. During a first modification step (PTM 1) a dehydratase catalyzes the dehydration of serine and threonine residues (Dha, Dhb). In a second step (PTM 2.1) a cyclase catalyzes the Michael-type addition of a cysteine residue to a dehydrated amino acid. Within the active center an acid (H-A, e.g., His) protonates the enolate. Finally, the Lan or MeLan rings are formed. In some lanthipeptides an additional Michael-type addition reaction (PTM 2.2) is catalyzed by the cyclase yielding a Lab amino acid. In the scheme the stereochemistry of the chiral center in the final products are exemplary (e.g., DL-Lan; but LL-Lan is also possible). The acronym X_n stands for n-quantity amino acids. The scheme is modified and based on (Repka et al., 2017).

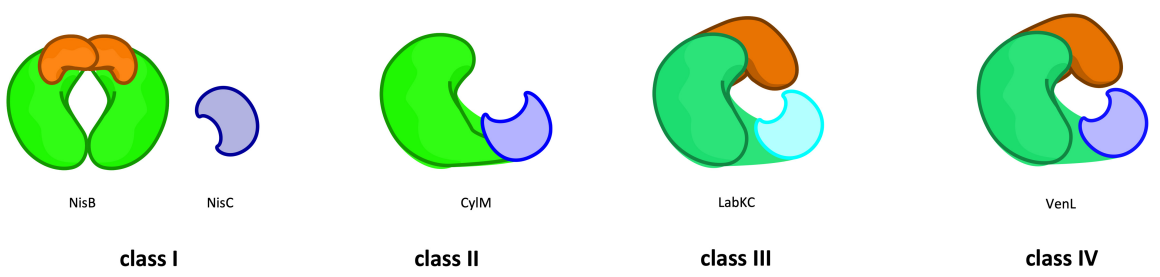

FIGURE 2 | Classes of lanthipeptides based on the modification machineries. The classification of lanthipeptides depends on their modification enzymes and their domain organization as well as those PTM mechanisms. In class I (e.g., NisB) the first PTM (dehydration) is catalyzed by a glutamylation/elimination-domain (green/orange). The dehydration in class II (e.g., CylM) take place in a kinase-domain (green). In class III (LabKC) and IV (VenL) this modification is catalyzed by a lyase/kinase-domain (dark green/dark orange). The second PTM (cyclization) is catalyzed by the zinc-dependent LanC enzyme (e.g., NisC; blue) or LanC-like domain (light blue), whereas in class III the LanC-like domain is independent from a zinc-ion (cyan). For further details see text.

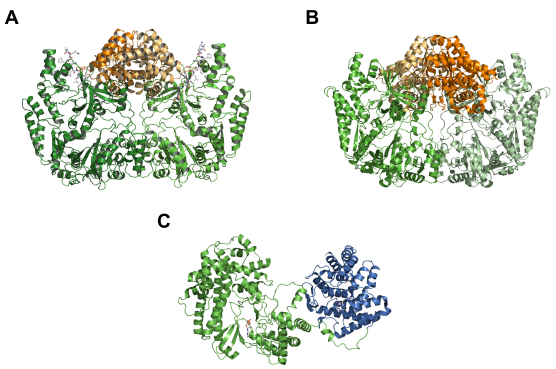

FIGURE 3 | Comparison of LanB and LanM crystal structures. **(A)** Crystal structure of dimeric NisB (PDB ID: 4WD; Ortega et al., 2015), representing the first example of a class I LanB dehydratase. The glutamylation domain is highlighted in green and light green, the elimination domain in orange and light orange. The part of the LP of NisA is shown in ball-and-stick representation. **(B)** Crystal structure of dimeric MibB (PBD ID: 5EHK; Ortega et al., 2016). Color-coding is as in panel **(A)**. **(C)** Crystal structure of CylM (PBD ID 5DZT; Dong et al., 2015), the first example of a LanM enzyme of class II lanthipeptides. The kinase-domain is shown in green and the cyclase-domain in blue. A bond AMP molecule within the kinase-domain is displayed as a ball-and-stick representation. Cartoons were generated using PyMol (www.pymol.org).

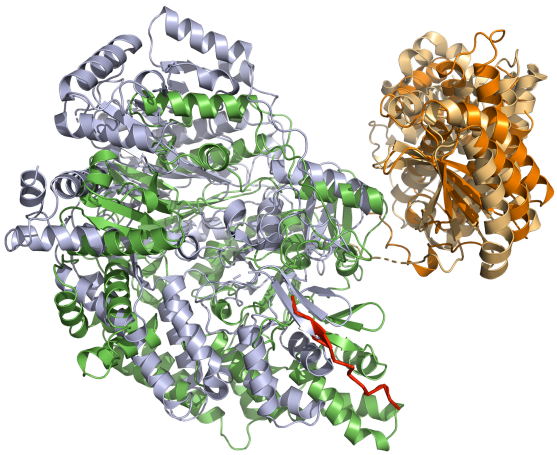

FIGURE 4 | Superimposition of NisB and MibB crystal structures. The superimposition is based on the elimination domain (residues 713–961 of NisB and 800–1048 for MibB with a RSMD of 3.6 Å over 618 Ca atoms). The glutamylation domain is shown in green (NisB) and gray (MibB), while the elimination domain is shown in light orange (NisB) and orange (MibB). For simplicity only monomers of NisB and MibB are shown. The bound LP of NisA in NisB is shown in red. Cartoons were generated using PyMol (www.pymol.org).

(Bothwell et al., 2019). Thus, the reason for this difference is still an open question.

NisB can be sub-divided into an N-terminal glutamylation domain (green and light green cartoons in **Figure 3A** of approximately 800 amino acid residues) and a C-terminal elimination domain (orange and light orange cartoons in **Figure 3A** of approximately 350 amino acid residues). This two-domain structural architecture was also found within MibB (**Figure 3B**), the class I LanB enzyme of NAI-107 (Ortega et al., 2016). Equally important, MibB like NisB requires $tRNA^{Glu}$ to catalyze the dehydration reaction. Three further examples of related LanB enzymes use so-called split LanB, where one protein is involved in aminoacylation and the other protein in the elimination of activated amino acid (aa) residues (Hudson et al., 2015; Mohr et al., 2015; Ozaki et al., 2016), also depend on the presence of $tRNA^{Glu}$ for dehydration. This clearly demonstrates that class I LanB enzymes use this rather unexpected mechanism to dehydrate serine and threonine residues in the CP of lanthipeptides.

In contrast to NisB (Ortega et al., 2015), MibB (Ortega et al., 2016) was crystallized in the absence of a substrate and displayed the same overall dimeric architecture composed of an approximately 800 amino acids large N-terminal glutamylation domain (green and light green in **Figure 3B**) and an approximately 350 amino acid large C-terminal elimination domain (orange and light orange in **Figure 3B**). The absence of the natural substrate allows the comparison with NisB to highlight structural changes that occur concomitant with substrate binding (**Figure 4**). As evident from the structural superimposition of both proteins using the C-terminal elimination domain as an anchor point, the glutamylation domain undergoes a translational and rotational motion resulting in a more compact shape of the LanB enzyme (**Figure 4**). This transition might be reminiscent of the conformational selection proposed for class II LanM enzymes. Here, the LanM enzyme is in equilibrium between an inactive and an active conformation. In the absence of substrate, more precise the LP, the equilibrium is shifted toward the inactive state, while binding of the LP shifts it toward the catalysis-competent state. This model is supported by experiments, in which the LP was added *in trans* or fused to the LanM enzyme (Levengood et al., 2007; Oman et al., 2012; Thibodeaux et al., 2015). In both cases, the isolated CP was modified although the fusion of the LP resulted in a more efficient system. Khusainov and Kuipers performed *in vivo* studies with separately expressed LP (NisA (1-23) and CP of nisin (NisA(24-57)-H_6), leaderless nisin (NisA(24-57)-H_6), and full-size nisin with a C-terminal extension and a His-tag (NisA(1-57)-H_6). These studies revealed partially modifications in spite of missing or in *trans* expressed LP, which led to the conclusion that the LP is not crucial for PTMs but increases the efficiency. However, only the fused LP led to complete modification (Khusainov and Kuipers, 2012). All in all, a mostly similar scenario could be suggested for class I LanB enzymes. In contrast, the LP of class III lanthipeptides seems to be crucial for PTMs (Müller et al., 2011; Wang and van der Donk, 2012).

Structural information is available for class II LanM enzymes (Siezen et al., 1996; Zhang et al., 2012) that encode the dehydration, elimination and cyclization domains on a single gene (**Figure 3C**). In clear contrast to LanB enzymes, these dehydratases require ATP and Mg^{2+} as cofactors as shown

experimentally for LctM in 2005 (Chatterjee et al., 2005a). The crystal structure of CylM (Dong et al., 2015) revealed the expected two-domain organization, an N-terminal dehydration domain (green in **Figure 3C**) and a C-terminal cyclization domain (blue in **Figure 3C**), which resemble the structure of NisC (Li et al., 2006), a class I LanC enzyme (see below). Not anticipated, the N-terminal domain displays structural similarities to eukaryotic lipid kinase domains bearing a novel, secondary structure topology. The activation loops of serine/threonine kinases including the P-loop are present as well as characteristic helices. Nevertheless, also a novel kinase activation domain is present, whose function was determined by mutational studies, explaining the dependence of LanM enzymes on ATP and Mg^{2+}. Here, in contrast to LanB enzymes (Garg et al., 2013), the dehydration relies on phosphorylation of serine and threonine residues of the substrate, the presence of phosphorylated instead of glutamylated intermediates and subsequent the elimination of inorganic phosphate (Chatterjee et al., 2005a). However, only AMP was observed in the structure and conclusions on the molecular mechanism of LanM function are not available at the moment.

The only recently discovered Class III (LanKC) and class IV (LanL) lanthipeptide modification enzymes, display a three-domain organization composed of a lyase, kinase and a C-terminal cyclase domain, which differs among the two classes (**Figure 2**; Goto et al., 2010; Meindl et al., 2010; Zhang et al., 2015). While the cyclase domain of LanL is apparently similar to the C-terminal domain of LanM enzymes or LanC and its activity also clearly relies on Zn^{2+}. On the contrary, the cyclase domain of LanKC is apparently not Zn^{2+}-dependent as it does not contain the highly conserved residues that are required for the coordination of this ion. Thus, two classes depending on the ability to coordinate Zn^{2+} or not were defined and the generic names LanKC (Class III) or LanL (class IV) were introduced (Kodani et al., 2004; Goto et al., 2010). Structural information is so far not available and insights into these lanthipeptide modification enzymes depend solely on genetic and functional data. Sequence analysis revealed similarities to serine/threonine kinases and effector proteins from Gram-negative and Gram-positive bacteria that catalyze the elimination of phosphorylated serine and threonine residues (phospholyases) in the N-terminal part of the protein (Young et al., 2003; Zhu et al., 2007; Chen et al., 2008). In contrast to class II LanM enzymes that are strictly ATP dependent, the kinase domains of LanKC and LanL have no real specificity for a phospho-donor. Depending on the enzyme under investigation, specificities for GTP/dGTP, ATP, ATP/GTP/CTP/TTP or any NTP/dNTP were discovered (Muller et al., 2010; Krawczyk et al., 2012b; Voller et al., 2012; Wang and van der Donk, 2012; Jungmann et al., 2016). However, based on the sequence similarities of the lyase and kinase domains, it can be assumed that the mechanisms of phosphorylation and elimination are shared between LanKC and LanL enzymes.

We have now a fairly detailed understanding of how the dehydration reactions are catalyzed in the different classes of lanthipeptides synthetases. Nevertheless, class I enzymes represent a special case as the dehydratase LanB and the cyclase LanC are separately expressed enzymes that can act on their own (Kluskens et al., 2005; Li et al., 2006; Li and van der Donk, 2007; Rink et al., 2007a; Garg et al., 2013). However, *in vivo* both enzymes are present. An elegant set of experiments using plasmid-based expression of the possible combinations of maturation enzymes demonstrated an astonishing inter-dependence between the dehydratase NisB and the cyclase NisC. Here, ring formation and dehydration acted in concert, which resulted in the protection of potential dehydration positions during ring formation (Karakas Sen et al., 1999; Koponen et al., 2002; Kluskens et al., 2005; Li et al., 2006; Li and van der Donk, 2007; Rink et al., 2007a,b; Lubelski et al., 2009; Oman and van der Donk, 2010; Plat et al., 2011, 2013; Khusainov and Kuipers, 2012; Khusainov et al., 2013; Garg et al., 2013; Ortega et al., 2015). This resulted in the proposal, that a strict N- to C-terminal directionality is operational in NisA maturation, suggesting that dehydration and ring formation is an intertwined process (Ortega et al., 2015). Consequently, such a directionality would also suggested a sort of channeling of the substrate that is bound to a LanB/LanC complex forcing the PTM reactions to start at the N-terminus and proceed all the way to the C-terminus before finalizing the maturation reactions. In 2014, Zhang et al. (2014) confirmed for NisB by mass-spectrometry (more precisely via HSEE analysis) an overall dehydration process from N- to- C- terminus, but a closer view revealed no strict directionality. In clear contrast, *in vitro* studies of the lanthipeptide NAI-107 (MibA, class I), suggest the absence of a N- to C-directionality, rather a C- to N-directionality, after dehydration of the N-terminus was observed (Ortega et al., 2016). The same C- to N-directionality was found for class III LanKC enzymes via single-mutation-studies (AciKC) and isotope labeling studies (LabKC) (Krawczyk et al., 2012a; Wang and van der Donk, 2012). Contrary to this, the synthetases of class II LctM and HalM2 revealed the opposite modification direction from N- to C-terminus (Lee et al., 2009). Surprisingly, the directionality of ProcM, also a class II synthetase, is distinct from the previous mentioned LacM enzymes. Zhang et al. (2012) investigated beside NisB also the dehydration directionality of ProcM, which revealed a generally C- to N-terminal direction of the dehydration process via mass-spectrometry. The difference regarding the directionality of the modification process within one class (i.e., ProcM and HalM2) may indicate that different binding modes are present. ProcM and HalM2 are not phylogenetically closely related, which could have led to distinct binding modes for the lanthipeptides (Zhang et al., 2012). This obviously raises the question whether a unique mechanism is operational and what the molecular ruler underlying these mechanisms actually is. Further structural studies of synthetases (LanM, LanKC, and LanL) with the lanthipeptide LanA or LP are undoubtly necessary to clear up the remaining questions before conclusions can be drawn. All in all, the directionality of the dehydration process is non-uniform among the class I dehydratases (LanBs) and class II synthetases. Consequential, the directionality can not be assumed based on the class of the lanthipeptide and each modification enzyme needs to be investigated.

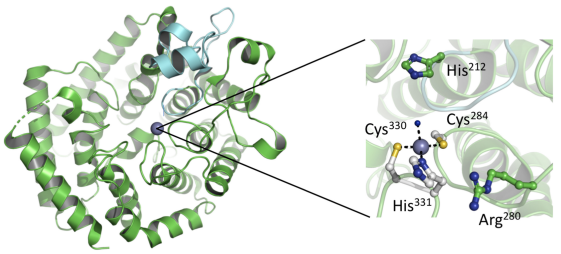

FIGURE 5 | Crystal structure of NisC. **(Left)** The overall crystal structure comprises an a,a toroidal fold (green) and a domain extension. This extension a SH2-like domain (cyan) is located close to the catalytic center. Within the active site a Zn^{2+} ion, shown as a gray sphere, is bound. **(Right)** Zoom-in into the active site of NisC. Residues important for the coordination of the Zn^{2+} ion (Cys284, His330, and Cys331) or function (His212 and Arg280) are shown in ball-and-stick representation. Cartoons were generated using PyMol (www.pymol.org).

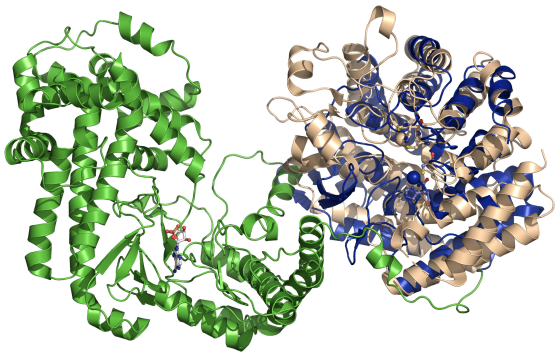

FIGURE 6 | Superimposition of NisC and CylM crystal structures. The superimposition is based on the cyclase domain of CylM (residues 641–992 of CylM). NisC is shown in blue and CylM in green (dehydratase domain) and light brown (cyclase domain). The bound AMP of CylM is shown in ball-and-stick representation. The two Zn^{2+} ions and the coordination amino acids are shown as blue sphere (NisC) and light brown sphere (CylM). The coordination amino acid residues are highlighted in ball-and-stick representation in blue (NisC) and light brown (CylM). Cartoons were generated using PyMol (www.pymol.org).

THE SECOND MATURATION STEP – THE CYCLIZATION REACTION

LanC enzymes and the cyclization domain of classes II–IV enzymes catalyze the nucleophilic attack of a thiolate (from Cys) to dehydrated amino acid (aa), where they facilitating the regio- and stereoselectivity to form thioether rings with the correct ring topology. Although, the lanthionine ring formation can occur spontaneously at basic pH values (pH > 7.5), however, leading to an erroneous stereochemistry of the Lan or (Me)Lan rings (Burrage et al., 2000; Okeley et al., 2000; Kuipers et al., 2004). Due to missing stereochemistry investigations of Lan and MeLan residues of lanthipeptides and the assumption that all Lan and (Me)Lan rings in lanthipeptides have the same "DL"-stereochemistry as previously shown for selected lantibiotics (Chatterjee et al., 2005b), the discovery that CylM can catalyze different stereochemistry within one single polypeptide was surprising. Furthermore, the studies of Tang and van der Donk (2013) revealed that the sequence of the lanthipeptide could be crucial for the stereoselectivity of ring formation.

The analysis of purified LanC enzymes (NisC and SpaC) revealed the presence of equal stoichiometric amounts of Zn^{2+} suggesting that the metal ion plays an essential role in deprotonating the thiol group of the cysteine residue, presumably by decreasing the pK_a value of the cysteine side chain (Okeley et al., 2003). Such a deprotonation or at least polarization accelerates the rate of Michael-type additions during the formation of the (Me)Lan rings. A detailed glimpse on the mechanism was possible, as the crystal structure of NisC was reported in 2006 (Li et al., 2006). The protein displays an a,a toroid consisting of six helices each, a SH2-like domain and one Zn^{2+} ion (**Figure 5**). The Zn^{2+} ion is coordinated by two highly conserved cysteine residues (Cys284 and Cys330) and one histidine residue (His331). Additionally, the tetragonal coordination sphere is complemented by a water molecule (inset of **Figure 5**). The presence of the SH2-like domain suggests that this domain interacts with dehydrated NisA, however there are no experimental evidence supporting this hypothesis and the functional role of this domain remains elusive. Based on the crystal structure of NisC, some residues conserved among LanC proteins were mutated (Li and van der Donk, 2007). There, the mutations of Cys284, Cys330, and His331 lead to inactive NisA. Interestingly, the ability to bind Zn^{2+} was preserved by mutating other active site residues (e.g., mutation H212N, H212F, and D141N) but no cyclization was detected. Thus, we slowly obtain a mechanistic picture of how NisC, but also LanC proteins in general, guide the formation of lanthionine rings. These insights will likely also hold for the cyclization domains of class II and class IV enzymes due to the structural conservation [**Figure 6** – comparison of CylM (LanM) and NisC (LanC)] or the conservation of residues identified to be essential for Zn^{2+} coordination or enzyme function. Noteworthy, an SH2-like domain (Mayer and Gupta, 1998; Li et al., 2006), which is found in NisC and might be involved in substrate binding, is not present in CylM. There, an additional subdomain is included in the cyclization domain, that seem to be important for substrate binding (Dong et al., 2015). Nevertheless, we still do not have structural information of the LanA–LanC complex and only this information will result in a final and complete picture. In contrast, the putative cyclization domain of class III enzymes (LanKC, i.e., AciKC) do not contain the conserved Zn^{2+} coordinating residues, which raises the question how cyclization takes place (Wang and van der Donk, 2012). Another important aspect of class III lanthipeptides is the presence of another type of cyclization, Lab or methyllabionin (MeLab; Meindl et al., 2010; Iorio et al., 2014). After the initial Michael-type addition of a cysteine residue and Dha, the system undergoes another Michael-type addition reaction with a second Dha residue, resulting in the formation of a methylene moiety based ring, a (Me)Lab ring.

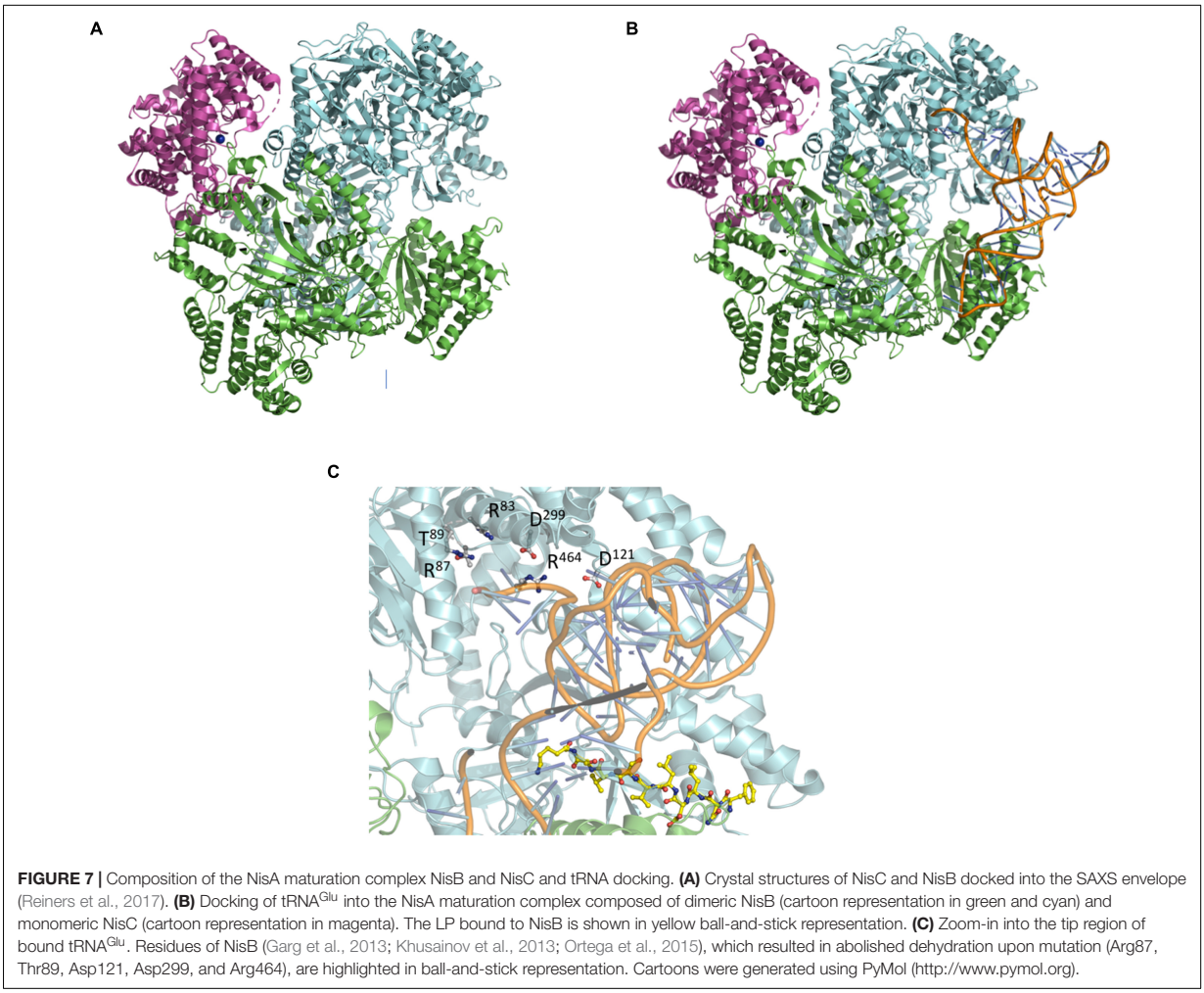

FIGURE 7 | Composition of the NisA maturation complex NisB and NisC and tRNA docking. **(A)** Crystal structures of NisC and NisB docked into the SAXS envelope (Reiners et al., 2017). **(B)** Docking of $tRNA^{Glu}$ into the NisA maturation complex composed of dimeric NisB (cartoon representation in green and cyan) and monomeric NisC (cartoon representation in magenta). The LP bound to NisB is shown in yellow ball-and-stick representation. **(C)** Zoom-in into the tip region of bound $tRNA^{Glu}$. Residues of NisB (Garg et al., 2013; Khusainov et al., 2013; Ortega et al., 2015), which resulted in abolished dehydration upon mutation (Arg87, Thr89, Asp121, Asp299, and Arg464), are highlighted in ball-and-stick representation. Cartoons were generated using PyMol (http://www.pymol.org).

However, one has to wait for structural insights into the LanKC family before further mechanistic conclusions can be drawn.

A CONCERTED ACTION DURING MATURATION

The individual domains of LanKC (class III) and LanL (class IV) enzymes are capable of catalyzing their individual reactions also in the absence of the other domains (Goto et al., 2011). This especially holds true for class I enzymes. However, early on, functional studies based on co-immunoprecipitation, yeast two hybrid approaches or mutational studies demonstrated that at least LanB and LanC act synergistically (Siegers et al., 1996; Kiesau et al., 1997; Lubelski et al., 2009). Moreover, a maturation complex consisting of not only NisB and NisC but also the ABC transporter NisT apparently exists during the modification of NisA (Siegers et al., 1996). Further support of a concerted action came from studies of subtilin, which suggested also the presence of such a complex composed of the dehydratase SpaB, the cyclase SpaC and the ABC transporter SpaT (Kiesau et al., 1997).

First insights into the assembly and architecture of a full class I lanthipeptide maturation complex was obtained for the lanthipeptide nisin. Reiners et al. (2017) used purified components to assemble the NisB/NisC/NisA maturation complex *in vitro*. Using size exclusion chromatography combined with multi-angle light scattering (SEC–MALS), they demonstrated that the complex was composed of a dimer of the dehydratase NisB, a monomer of the cyclase NisC and one molecule of the substrate, NisA resulting in a stoichiometry of 2:1:1 and a molecular weight of approximately 291 kDa. Importantly, the formation of the maturation complex was strictly dependent on the presence of the FNLD box within the LP as shown previously by *in vivo* and *in vitro* studies. Mutation of the four amino acids of the FNLD to AAAA completely prevented complex assembly (Khusainov et al., 2011, 2013; Mavaro et al., 2011; Plat et al., 2011, 2013; Abts et al., 2013).

From a mechanistic point of view, it was also important that a molecular signal was identified in this study that triggered disassembly of the maturation complex. Using a series of (Me)Lan ring mutants, e.g., Cys–Ala exchanges that prevented ring formation at the corresponding position, proved that the presence of the last, C-terminal (Me)Lan ring represented the 'disassembly signal'. This obviously goes nicely in hand with the *in vivo* situation, where a maturation complex should continue the PTM reaction and only release the fully modified product. In other words, the maturation complex is capable of reading out the stage of modifications and only the terminal modification state, the fully modified product is released, ready to be secreted by the cognate ABC transporter. Of course the exact molecular role of the ABC transporter within such a maturation complex is currently completely unknown and requires further investigations addressing its precise role.

Moving one step further, small-angle X-ray scattering (SAXS) was used to produce a low resolution envelope of the NisB/NisC/NisA complex allowing to determine the orientation of the individual high resolution crystal structures of NisB and NisC into the SAXS envelope (**Figure 7A**; Reiners et al., 2017). A comparison of apo-NisB and NisA-saturated NisB suggested the presence of a tunnel and therefore provided an idea for the actual substrate-binding site within the complex. This allowed therefore a first molecular glimpse on the molecular architecture of a maturation complex of a class I lanthipeptide (**Figure 7A**).

Following the protocol of Ortega et al. (2015) the crystal structure of $tRNA^{Glu}$ (extracted from pdb entry 1N78) was docked into the complex using the HDOCK server[1] employing standard settings (Yan et al., 2017). The proposed tertiary complex is shown in **Figure 7B**. Interestingly, the $tRNA^{Glu}$ binding sites are similar in the isolated NisB dimer and the maturation complex. Mapping residues, which result in impaired functionality, cluster around the potential $tRNA^{Glu}$-binding site (**Figure 7C**) suggesting that the model is of functional significance. Additional residues that were identified in mutational studies were also mapped on the proposed complex (Garg et al., 2013; Khusainov et al., 2013; Ortega et al., 2015). Noteworthy, the mutation of arginine and aspartate residues leading to a complete loss of dehydratase activity in NisB mapped in the close vicinity of the bound $tRNA^{Glu}$ (**Figure 7C**). Obviously, this *in silico* complex requires experimental verification. Nevertheless, it represents a starting point to design such experiments, which might help to understand the molecular mechanism by which the nisin maturation complex and eventually other maturation complexes of class I lanthipeptides operate.

[1] http://hdock.phys.hust.edu.cn

CONCLUSION AND OUTLOOK

Over the past years, we have seen tremendous advances in our understanding of lanthipeptides, especially class I lanthipeptides (lantibiotics) on the genetic, functional and structural level. Here, we have focused mainly on the mechanistic and structural insights of the modification process and the corresponding enzymes. The presented findings have answered many questions, but some questions are still open and even new questions arose. Considerably more work will need to be done to understand in detail the molecular coordination and timing of the maturation enzymes and their interplay with the exporter proteins. Only then, the fundamental question of why maturation intermediates of the substrates are not secreted can be answered. Even though literature exhibits great results using lanthipeptide modification enzymes (i.e., synthesis of an analog of angiotensin and an analog of the opioid dermorphin) without full knowledge regarding the mechanisms, a very detailed mechanistic understanding will facilitate higher efficiency regarding drug engineering and design (Luskens et al., 2008; Huo and van der Donk, 2016).

AUTHOR CONTRIBUTIONS

All authors wrote the manuscript.

FUNDING

The Center for Structural Studies is funded by the Deutsche Forschungsgemeinschaft DFG grant number 417919780. Research on Nisin was funded by the Deutsche Forschungsgemeinschaft DFG through grant Schm1279/13-1 to LS.

ACKNOWLEDGMENTS

We thank members of the Institute of Biochemistry for fruitfull discussions.

REFERENCES

Arnison, P. G., Bibb, M. J., Bierbaum, G., Bowers, A. A., Bugni, T. S., Bulaj, G., et al. (2013). Ribosomally synthesized and post-translationally modified peptide natural products: overview and recommendations for a universal nomenclature. *Nat. Prod. Rep* 30, 108–160. doi: 10.1039/c2np20085f

Skinnider, M. A., Johnston, C. W., Edgar, R. E., Dejong, C. A., Merwin, N. J., Rees, P. N., et al. (2016). Genomic charting of ribosomally synthesized natural product chemical space facilitates targeted mining. *Proc Natl Acad Sci U S A* 113, E6343–E6351.

Bierbaum, G., Szekat, C., Josten, M., Heidrich, C., Kempter, C., Jung, G., et al. (1996). Engineering of a novel thioether bridge and role of modified residues in the lantibiotic Pep5. *Appl Environ Microbiol* 62, 385–392.

Oman, T. J., and van der Donk, W. A. (2010). Follow the leader: the use of leader peptides to guide natural product biosynthesis. *Nat Chem Biol* 6, 9–18. doi: 10.1038/nchembio.286

Kuipers, O. P., Beerthuyzen, M. M., Siezen, R. J., and De Vos, W. M. (1993). Characterization of the nisin gene cluster nisABTCIPR of *Lactococcus lactis*. Requirement of expression of the nisA and nisI genes for development of immunity. *Eur. J. Biochem* 216, 281–291.

van der Meer, J. R., Rollema, H. S., Siezen, R. J., Beerthuyzen, M. M., Kuipers, O. P., and de Vos, W. M. (1994). Influence of amino acid substitutions in the nisin leader peptide on biosynthesis and secretion of nisin by *Lactococcus lactis*. *J. Biol. Chem* 269, 3555–3562.

Kuipers, A., de Boef, E., Rink, R., Fekken, S., Kluskens, L. D., Driessen, A. J., et al. (2004). NisT, the transporter of the lantibiotic nisin, can transport fully modified, dehydrated, and unmodified prenisin and fusions of the leader peptide with non-lantibiotic peptides. *J. Biol. Chem* 279, 22176–22182.

Khusainov, R., and Kuipers, O. P. (2012). When the leader gets loose: in vivo biosynthesis of a leaderless prenisin is stimulated by a trans-acting leader peptide. *Chembiochem* 13, 2433–2438. doi: 10.1002/cbic.201200437

Nishie, M., Sasaki, M., Nagao, J., Zendo, T., Nakayama, J., and Sonomoto, K. (2011). Lantibiotic transporter requires cooperative functioning of the peptidase domain and the ATP binding domain. *J Biol Chem* 286, 11163–11169. doi: 10.1074/jbc.M110.212704

Ortega, M. A., Velasquez, J. E., Garg, N., Zhang, Q., Joyce, R. E., Nair, S. K., et al. (2014). Substrate specificity of the lanthipeptide peptidase ElxP and the oxidoreductase ElxO. *ACS Chem. Biol.* 9, 1718–1725. doi: 10.1021/cb5002526

van der Meer, J. R., Polman, J., Beerthuyzen, M. M., Siezen, R. J., Kuipers, O. P., and De Vos, W. M. (1993). Characterization of the *Lactococcus lactis* nisin A operon genes nisP, encoding a subtilisin-like serine protease involved in precursor processing, and nisR, encoding a regulatory protein involved in nisin biosynthesis. *J Bacteriol* 175, 2578–2588.

Gross, E., and Morell, J. L. (1967). The presence of dehydroalanine in the antibiotic nisin and its relationship to activity. *J Am Chem Soc* 89, 2791–2792.

Gross, E., Morell, J. L., and Craig, L. C. (1969). Dehydroalanyllysine: identical COOH-terminal structures in the peptide antibiotics nisin and subtilin. *Proc Natl Acad Sci U S A* 62, 952–956.

Gross, E., and Morell, J. L. (1971). The structure of nisin. *J Am Chem Soc* 93, 4634–4635.

Karakas Sen, A., Narbad, A., Horn, N., Dodd, H. M., Parr, A. J., Colquhoun, I., et al. (1999). Post-translational modification of nisin. The involvement of NisB in the dehydration process. *Eur. J. Biochem.* 261, 524–532.

Gutowskieckel, Z., Klein, C., Siegers, K., Bohm, K., Hammelmann, M., and Entian, K. D. (1994). Growth Phase-Dependent Regulation and Membrane Localization of SpaB, a Protein Involved in Biosynthesis of the Lantibiotic Subtilin. *Applied and Environmental Microbiology* 60, 1–11.

Peschel, A., Ottenwalder, B., and Gotz, F. (1996). Inducible production and cellular location of the epidermin biosynthetic enzyme EpiB using an improved staphylococcal expression system. *Fems Microbiology Letters* 137, 279–284.

Gilmore, M. S., Segarra, R. A., Booth, M. C., Bogie, C. P., Hall, L. R., and Clewell, D. B. (1994). Genetic structure of the *Enterococcus faecalis* plasmid pAD1-encoded cytolytic toxin system and its relationship to lantibiotic determinants. *J Bacteriol* 176, 7335–7344.

Barber, M., Elliot, G. J., Bordoli, R. S., Green, B. N., and Bycroft, B. W. (1988). Confirmation of the structure of nisin and its major degradation product by FAB-MS and FAB-MS/MS. *Experientia* 44, 266–270.

Meindl, K., Schmiederer, T., Schneider, K., Reicke, A., Butz, D., Keller, S., et al. (2010). Labyrinthopeptins: a new class of carbacyclic lantibiotics. *Angew Chem Int Ed Engl* 49, 1151–1154.

Iorio, M., Sasso, O., Maffioli, I., Bertorelli, R., Monciardini, P., Sosio, M., et al. (2014). A glycosylated, labionin-containing lanthipeptide with marked antinociceptive activity. *ACS Chem Biol* 9, 398–404. doi: 10.1021/cb400692w

Mortvedt, C. I., Nissen-Meyer, J., Sletten, K., and Nes, I. F. (1991). Purification and amino acid sequence of lactocin S, a bacteriocin produced by *Lactobacillus sake* L45. *Appl Environ Microbiol* 57, 1829–1834.

Kupke, T., Stevanovic, S., Sahl, H. G., and Gotz, F. (1992). Purification and characterization of EpiD, a flavoprotein involved in the biosynthesis of the lantibiotic epidermin. *J Bacteriol* 174, 5354–5361.

Skaugen, M., Nissen-Meyer, J., Jung, G., Stevanovic, S., Sletten, K., Inger, C., et al. (1994). *In vivo* conversion of L-serine to D-alanine in a ribosomally synthesized polypeptide. *J Biol Chem* 269, 27183–27185.

van de Kamp, M., van den Hooven, H. W., Konings, R. N., Bierbaum, G., Sahl, H. G., Kuipers, O. P., et al. (1995). Elucidation of the primary structure of the lantibiotic epilancin K7 from *Staphylococcus epidermidis* K7. Cloning and characterisation of the epilancin-K7-encoding gene and NMR analysis of mature epilancin K7. *Eur J Biochem* 230, 587–600.

Heidrich, C., Pag, U., Josten, M., Metzger, J., Jack, R. W., Bierbaum, G., et al. (1998). Isolation, Characterization, and Heterologous Expression of the Novel Lantibiotic Epicidin 280 and Analysis of Its Biosynthetic Gene Cluster. *Appl Environ Microbiol* 64, 3140–3146.

Ekkelenkamp, M. B., Hanssen, M., Danny Hsu, S. T., de Jong, A., Milatovic, D., Verhoef, J., et al. (2005). Isolation and structural characterization of epilancin 15X, a novel lantibiotic from a clinical strain of *Staphylococcus epidermidis*. *FEBS Lett* 579, 1917–1922.

Castiglione, F., Lazzarini, A., Carrano, L., Corti, E., Ciciliato, I., Gastaldo, L., et al. (2008). Determining the structure and mode of action of microbisporicin, a potent lantibiotic active against multiresistant pathogens. *Chem Biol* 15, 22–31. doi: 10.1016/j.chembiol.2007.11.009

He, Z., Yuan, C., Zhang, L., and Yousef, A. E. (2008). N-terminal acetylation in paenibacillin, a novel lantibiotic. *FEBS Lett* 582, 2787–2792. doi: 10.1016/j.febslet.2008.07.008

Velasquez, J. E., Zhang, X., and van der Donk, W. A. (2011). Biosynthesis of the antimicrobial peptide epilancin 15X and its N-terminal lactate. *Chem Biol* 18, 857–867. doi: 10.1016/j.chembiol.2011.05.007

Huang, E., and Yousef, A. E. (2015). Biosynthesis of paenibacillin, a lantibiotic with N-terminal acetylation, by *Paenibacillus polymyxa*. *Microbiol Res* 181, 15–21. doi: 10.1016/j.micres.2015.08.001

McIntosh, J. A., Donia, M. S., and Schmidt, E. W. (2009). Ribosomal peptide natural products: bridging the ribosomal and nonribosomal worlds. *Nat Prod Rep* 26, 537–559.

Dunbar, K. L., and Mitchell, D. A. (2013). Revealing nature's synthetic potential through the study of ribosomal natural product biosynthesis. *ACS Chem Biol* 8, 473–487. doi: 10.1021/cb3005325

Walsh, C. T. (2014). Blurring the lines between ribosomal and nonribosomal peptide scaffolds. *ACS Chem Biol* 9, 1653–1661. doi: 10.1021/cb500 3587

Ortega, M. A., and van der Donk, W. A. (2016). New Insights into the Biosynthetic Logic of Ribosomally Synthesized and Post-translationally Modified Peptide Natural Products. *Cell Chem Biol* 23, 31–44. doi: 10.1016/j.chembiol.2015. 11.012

Repka, L. M., Chekan, J. R., Nair, S. K., and van der Donk, W. A. (2017). Mechanistic Understanding of Lanthipeptide Biosynthetic Enzymes. *Chem Rev* 117, 5457–5520. doi: 10.1021/acs.chemrev.6b00591

Schnell, N., Entian, K. D., Schneider, U., Gotz, F., Zahner, H., Kellner, R., et al. (1988). Prepeptide sequence of epidermin, a ribosomally synthesized antibiotic with four sulphide-rings. *Nature* 333, 276–278.

Kodani, S., Hudson, M. E., Durrant, M. C., Buttner, M. J., Nodwell, J. R., and Willey, J. M. (2004). The SapB morphogen is a lantibiotic-like peptide derived from the product of the developmental gene ramS in *Streptomyces coelicolor*. *Proc Natl Acad Sci U S A* 101, 11448–11453.

Kodani, S., Lodato, M. A., Durrant, M. C., Picart, F., and Willey, J. M. (2005). SapT, a lanthionine-containing peptide involved in aerial hyphae formation in the streptomycetes. *Mol Microbiol* 58, 1368–1380.

Ferir, G., Petrova, I., Andrei, G., Huskens, D., Hoorelbeke, B., Snoeck, R., et al. (2013). The lantibiotic peptide labyrinthopeptin A1 demonstrates broad anti-HIV and anti-HSV activity with potential for microbicidal applications. *PLoS One* 8:e64010. doi: 10.1371/journal.pone.0064010

Mohr, K. I., Volz, C., Jansen, R., Wray, V., Hoffmann, J., Bernecker, S., et al. (2015). Pinensins: the first antifungal lantibiotics. *Angew Chem Int Ed Engl* 54, 11254–11258. doi: 10.1002/anie.201500927

Chatterjee, C., Paul, M., Xie, L., and van der Donk, W. A. (2005b). Biosynthesis and mode of action of lantibiotics. *Chem Rev* 105, 633–684.

Breukink, E., and de Kruijff, B. (2006). Lipid II as a target for antibiotics. *Nature Reviews Drug Discovery* 5, 321–332.

Lubelski, J., Rink, R., Khusainov, R., Moll, G. N., and Kuipers, O. P. (2008). Biosynthesis, immunity, regulation, mode of action and engineering of the model lantibiotic nisin. *Cell Mol Life Sci* 65, 455–476.

Bierbaum, G., and Sahl, H. G. (2009). Lantibiotics: mode of action, biosynthesis and bioengineering. *Curr Pharm Biotechnol* 10, 2–18.

Schneider, T., and Sahl, H. G. (2010). Lipid II and other bactoprenol-bound cell wall precursors as drug targets. *Curr Opin Investig Drugs* 11, 157–164.

Islam, M. R., Nagao, J., Zendo, T., and Sonomoto, K. (2012). Antimicrobial mechanism of lantibiotics. *Biochem Soc Trans* 40, 1528–1533. doi: 10.1042/BST20120190

Severina, E., Severin, A., and Tomasz, A. (1998). Antibacterial efficacy of nisin against multidrug-resistant Gram-positive pathogens. *J Antimicrob Chemother* 41, 341–347.

Breukink, E., Wiedemann, I., van Kraaij, C., Kuipers, O. P., Sahl, H. G., and de Kruijff, B. (1999). Use of the cell wall precursor lipid II by a pore-forming peptide antibiotic. *Science* 286, 2361–2364.

Wiedemann, I., Breukink, E., van Kraaij, C., Kuipers, O. P., Bierbaum, G., de Kruijff, B., et al. (2001). Specific binding of nisin to the peptidoglycan precursor lipid II combines pore formation and inhibition of cell wall biosynthesis for potent antibiotic activity. *J Biol Chem* 276, 1772–1779.

Brumfitt, W., Salton, M. R., and Hamilton-Miller, J. M. (2002). Nisin, alone and combined with peptidoglycan-modulating antibiotics: activity against methicillin-resistant *Staphylococcus aureus* and vancomycin-resistant enterococci. *J Antimicrob Chemother* 50, 731–734.

van Heusden, H. E., de Kruijff, B., and Breukink, E. (2002). Lipid II induces a transmembrane orientation of the pore-forming peptide lantibiotic nisin. *Biochemistry* 41, 12171–12178.

Hasper, H. E., de Kruijff, B., and Breukink, E. (2004). Assembly and stability of nisin-lipid II pores. *Biochemistry* 43, 11567–11575.

Hsu, S. T. D., Breukink, E., Tischenko, E., Lutters, M. A. G., de Kruijff, B., Kaptein, R., et al. (2004). The nisin-lipid II complex reveals a pyrophosphate cage that provides a blueprint for novel antibiotics. *Nature Structural & Molecular Biology* 11, 963–967.

Hasper, H. E., Kramer, N. E., Smith, J. L., Hillman, J. D., Zachariah, C., Kuipers, O. P., et al. (2006). An Alternative Bactericidal Mechanism of Action for Lantibiotic Peptides That Target Lipid II. *Science* 313, 1636–1637.

Cotter, P. D., Hill, C., and Ross, R. P. (2005). Bacteriocins: developing innate immunity for food. *Nat Rev Microbiol* 3, 777–788.

Mavaro, A., Abts, A., Bakkes, P. J., Moll, G. N., Driessen, A. J., Smits, S. H., et al. (2011). Substrate recognition and specificity of the NisB protein, the lantibiotic dehydratase involved in nisin biosynthesis. *J Biol Chem* 286, 30552–30560. doi: 10.1074/jbc.M111.263210

Rink, R., Kuipers, A., de Boef, E., Leenhouts, K. J., Driessen, A. J., Moll, G. N., et al. (2005). Lantibiotic structures as guidelines for the design of peptides that can be modified by lantibiotic enzymes. *Biochemistry* 44, 8873–8882.

Kluskens, L. D., Kuipers, A., Rink, R., de Boef, E., Fekken, S., Driessen, A. J., et al. (2005). Post-translational modification of therapeutic peptides by NisB, the dehydratase of the lantibiotic nisin. *Biochemistry* 44, 12827–12834.

Rink, R., Kluskens, L. D., Kuipers, A., Driessen, A. J., Kuipers, O. P., and Moll, G. N. (2007a). NisC, the cyclase of the lantibiotic nisin, can catalyze cyclization of designed nonlantibiotic peptides. *Biochemistry* 46, 13179–13189.

Garg, N., Salazar-Ocampo, L. M., and van der Donk, W. A. (2013). In vitro activity of the nisin dehydratase NisB. *Proc Natl Acad Sci U S A* 110, 7258–7263. doi: 10.1073/pnas.1222488110

Ortega, M. A., Hao, Y., Zhang, Q., Walker, M. C., van der Donk, W. A., and Nair, S. K. (2015). Structure and mechanism of the tRNA-dependent lantibiotic dehydratase NisB. *Nature* 517, 509–512. doi: 10.1038/nature13888

Bothwell, I. R., Cogan, D. P., Kim, T., Reinhardt, C. J., van der Donk, W. A., and Nair, S. K. (2019). Characterization of glutamyl-tRNA-dependent dehydratases using nonreactive substrate mimics. *PNAS* 116, 17245–17250. doi: 10.1073/pnas.1905240116

Reiners, J., Abts, A., Clemens, R., Smits, S. H., and Schmitt, L. (2017). Stoichiometry and structure of a lantibiotic maturation complex. *Sci Rep* 7, 42163. doi: 10.1038/srep42163

Ortega, M. A., Hao, Y., Walker, M. C., Donadio, S., Sosio, M., Nair, S. K., et al. (2016). Structure and tRNA Specificity of MibB, a Lantibiotic Dehydratase from Actinobacteria Involved in NAI-107 Biosynthesis. *Cell Chem Biol* 23, 370–380. doi: 10.1016/j.chembiol.2015.11.017

Ozaki, T., Kurokawa, Y., Hayashi, S., Oku, N., Asamizu, S., Igarashi, Y., et al. (2016). Insights into the Biosynthesis of Dehydroalanines in Goadsporin. *Chembiochem* 17, 218–223. doi: 10.1002/cbic.201500541

Hudson, G. A., Zhang, Z., Tietz, I., Mitchell, D. A., and van der Donk, W. A. (2015). In Vitro Biosynthesis of the Core Scaffold of the Thiopeptide Thiomuracin. *J. Am. Chem. Soc.* 137, 16012–16015. doi: 10.1021/jacs.5b10194

Thibodeaux, G. N., McClerren, A. L., Ma, Y., Gancayco, M. R., and van der Donk, W. A. (2015). Synergistic binding of the leader and core peptides by the lantibiotic synthetase HalM2. *ACS Chem Biol* 10, 970–977. doi: 10.1021/cb5009876

Levengood, M. R., Patton, G. C., and van der Donk, W. A. D. (2007). The leader peptide is not required for post-translational modification by lacticin 481 synthetase. *Journal of the American Chemical Society* 129, 10314.

Oman, T. J., Knerr, P. J., Bindman, N. A., Velasquez, J. E., and van der Donk, W. A. (2012). An engineered lantibiotic synthetase that does not require a leader peptide on its substrate. *J Am Chem Soc* 134, 6952–6955. doi: 10.1021/ja3017297

Müller, W. M., Ensle, P., Krawczyk, B., and Süssmuth, R. D. (2011). Leader Peptide-Directed Processing of Labyrinthopeptin A2 Precursor Peptide by the Modifying Enzyme LabKC. *Biochemistry* 50, 8362–8373. doi: 10.1021/bi200526q

Wang, H., and van der Donk, W. A. (2012). Biosynthesis of the class III lantipeptide catenulipeptin. *ACS Chem Biol* 7, 1529–1535.

Siezen, R. J., Kuipers, O. P., and de Vos, W. M. (1996). Comparison of lantibiotic gene clusters and encoded proteins. *Antonie Van Leeuwenhoek* 69, 171–184.

Zhang, Q., Yu, Y., Velasquez, J. E., and van der Donk, W. A. (2012). Evolution of lanthipeptide synthetases. *Proc Natl Acad Sci U S A* 109, 18361–18366. doi: 10.1073/pnas.1210393109

Chatterjee, C., Miller, L. M., Leung, Y. L., Xie, L., Yi, M., Kelleher, N. L., et al. (2005a). Lacticin 481 synthetase phosphorylates its substrate during lantibiotic production. *J Am Chem Soc* 127, 15332–15333.

Dong, S. H., Tang, W. X., Lukk, T., Yu, Y., Nair, S. K., and van der Donk, W. A. (2015). The enterococcal cytolysin synthetase has an unanticipated lipid kinase fold. *Elife* 4, e07607. doi: 10.7554/eLife.07607

Li, B., Yu, J. P., Brunzelle, J. S., Moll, G. N., van der Donk, W. A., and Nair, S. K. (2006). Structure and mechanism of the lantibiotic cyclase involved in nisin biosynthesis. *Science* 311, 1464–1467.

Goto, Y., Li, B., Claesen, J., Shi, Y., Bibb, M. J., and van der Donk, W. A. (2010). Discovery of unique lanthionine synthetases reveals new mechanistic and evolutionary insights. *PLoS Biol* 8:e1000339. doi: 10.1371/journal.pbio.1000339

Zhang, Q., Doroghazi, J. R., Zhao, X., Walker, M. C., and van der Donk, W. A. (2015). Expanded natural product diversity revealed by analysis of lanthipeptide-like gene clusters in actinobacteria. *Appl Environ Microbiol* 81, 4339–4350. doi: 10.1128/AEM.00635-15

Chen, L., Wang, H., Zhang, J., Gu, L., Huang, N., Zhou, J. M., et al. (2008). Structural basis for the catalytic mechanism of phosphothreonine lyase. *Nat Struct Mol Biol* 15, 101–102.

Young, T. A., Delagoutte, B., Endrizzi, J. A., Falick, A. M., and Alber, T. (2003). Structure of Mycobacterium tuberculosis PknB supports a universal activation mechanism for Ser/Thr protein kinases. *Nat Struct Biol* 10, 168–174.

Zhu, Y., Li, H., Long, C., Hu, L., Xu, H., Liu, L., et al. (2007). Structural insights into the enzymatic mechanism of the pathogenic MAPK phosphothreonine lyase. *Mol Cell* 28, 899–913.

Muller, W. M., Schmiederer, T., Ensle, P., and Sussmuth, R. D. (2010). In vitro biosynthesis of the prepeptide of type-III lantibiotic labyrinthopeptin A2 including formation of a C-C bond as a post-translational modification. *Angew Chem Int Ed Engl* 49, 2436–2440.

Krawczyk, B., Voller, G. H., Voller, J., Ensle, P., and Sussmuth, R. D. (2012b). Curvopeptin: a new lanthionine-containing class III lantibiotic and its co-substrate promiscuous synthetase. *Chembiochem* 13, 2065–2071. doi: 10.1002/cbic.201200417

Voller, G. H., Krawczyk, J. M., Pesic, A., Krawczyk, B., Nachtigall, J., and Sussmuth, R. D. (2012). Characterization of new class III lantibiotics–erythreapeptin, avermipeptin and griseopeptin from *Saccharopolyspora erythraea*, *Streptomyces avermitilis* and *Streptomyces griseus* demonstrates stepwise N-terminal leader processing. *Chembiochem* 13, 1174–1183. doi: 10.1002/cbic.201200118

Jungmann, N. A., van Herwerden, E. F., Hugelland, M., and Sussmuth, R. D. (2016). The Supersized Class III Lanthipeptide Stackepeptin Displays Motif Multiplication in the Core Peptide. *ACS Chem Biol* 11, 69–76. doi: 10.1021/acschembio.5b00651

Li, B., and van der Donk, W. A. (2007). Identification of essential catalytic residues of the cyclase NisC involved in the biosynthesis of nisin. *J Biol Chem* 282, 21169–21175.

Rink, R., Wierenga, J., Kuipers, A., Kluskens, L. D., Driessen, A. J. M., Kuipers, O. P., et al. (2007b). Dissection and modulation of the four distinct activities of nisin by mutagenesis of rings A and B and by C-terminal truncation. *Applied and Environmental Microbiology* 73, 5809–5816.

Lubelski, J., Khusainov, R., and Kuipers, O. P. (2009). Directionality and coordination of dehydration and ring formation during biosynthesis of the lantibiotic nisin. *J Biol Chem* 284, 25962–25972. doi: 10.1074/jbc.M109.026690

Plat, A., Kluskens, L. D., Kuipers, A., Rink, R., and Moll, G. N. (2011). Requirements of the engineered leader peptide of nisin for inducing modification, export, and cleavage. *Appl Environ Microbiol* 77, 604–611. doi: 10.1128/AEM.01503-10

Khusainov, R., Moll, G. N., and Kuipers, O. P. (2013). Identification of distinct nisin leader peptide regions that determine interactions with the modification enzymes NisB and NisC. *FEBS Open Bio* 3, 237–242. doi: 10.1016/j.fob.2013.05.001

Plat, A., Kuipers, A., Rink, R., and Moll, G. N. (2013). Mechanistic aspects of lanthipeptide leaders. *Curr Protein Pept Sci* 14, 85–96.

Koponen, O., Tolonen, M., Qiao, M., Wahlstrom, G., Helin, J., and Saris, P. E. (2002). NisB is required for the dehydration and NisC for the lanthionine formation in the post-translational modification of nisin. *Microbiology* 148(Pt 11), 3561–3568. doi: 10.1099/00221287-148-11-3561

Zhang, Q., Ortega, M., Shi, Y., Wang, H., Melby, J. O., Tang, W., et al. (2014). Structural investigation of ribosomally synthesized natural products by hypothetical structure enumeration and evaluation using tandem MS. *PNAS* 111, 12031–12036. doi: 10.1073/pnas.1406418111

Krawczyk, B., Ensle, P., Müller, W. M., and Süssmuth, R. D. (2012a). Deuterium Labeled Peprides Give Insights into the Directionality of Class III Lantibiotic synthetase LabKC. *J. Am. Chem. Soc.* 134, 9922–9925. doi: 10.1021/ja3040224

Lee, M. V., Ihnken, L. A., You, Y. O., McClerren, A. L., van, der Donk WA, and Kelleher, N. L. (2009). Distributive and Directional Behavior of Lantibiotic Synthetases Revealed by High-Resolution Tandem Mass Spectrometry. *J. Am. Chem. Soc.* 131, 12258–12264. doi: 10.1021/ja9033507

Burrage, S., Raynham, T., Williams, G., Essex, J. W., Allen, C., Cardno, M., et al. (2000). Biomimetic synthesis of lantibiotics. *Chem-Eur J* 6, 1455–1466.

Okeley, N. M., Zhu, Y. T., and van der Donk, W. A. (2000). Facile chemoselective synthesis of dehydroalanine-containing peptides. *Org Lett* 2, 3603–3606.

Tang, W., and van der Donk, W. A. (2013). The Sequence of the Enterococcal Cytolysin Imparts Unusual Lanthionine Stereochemistry. *Nat. Chem. Biol.* 9, 157–159. doi: 10.1038/nchembio.1162

Okeley, N. M., Paul, M., Stasser, J. P., Blackburn, N., and van der Donk, W. A. (2003). SpaC and NisC, the cyclases involved in subtilin and nisin biosynthesis, are zinc proteins. *Biochemistry* 42, 13613–13624.

Mayer, B. J., and Gupta, R. (1998). Functions of SH2 and SH3 domains. *Curr Top Microbiol Immunol* 228, 1–22.

Goto, Y., Okesli, A., and van der Donk, W. A. (2011). Mechanistic studies of Ser/Thr dehydration catalyzed by a member of the LanL lanthionine synthetase family. *Biochemistry* 50, 891–898. doi: 10.1021/bi101750r

Siegers, K., Heinzmann, S., and Entian, K. D. (1996). Biosynthesis of lantibiotic nisin. Posttranslational modification of its prepeptide occurs at a multimeric membrane-associated lanthionine synthetase complex. *J. Biol. Chem.* 271, 12294–12301.

Kiesau, P., Eikmanns, U., Gutowski-Eckel, Z., Weber, S., Hammelmann, M., and Entian, K. D. (1997). Evidence for a multimeric subtilin synthetase complex. *J Bacteriol* 179, 1475–1481.

Abts, A., Montalban-Lopez, M., Kuipers, O. P., Smits, S. H., and Schmitt, L. (2013). NisC binds the FxLx motif of the nisin leader peptide. *Biochemistry* 52, 5387–5395. doi: 10.1021/bi4008116

Khusainov, R., Heils, R., Lubelski, J., Moll, G. N., and Kuipers, O. P. (2011). Determining sites of interaction between prenisin and its modification enzymes NisB and NisC. *Mol Microbiol* 82, 706–718. doi: 10.1111/j.1365-2958.2011.07846.x

Yan, Y., Zhang, D., Zhou, P., Li, B., and Huang, S. Y. (2017). HDOCK: a web server for protein-protein and protein-DNA/RNA docking based on a hybrid strategy. *Nucleic Acids Res* 45, W365–W373. doi: 10.1093/nar/gkx407

Luskens, L. D., Nelemans, S. A., Rink, R., de Vries, L., Meter-Arkema, A., Wang, Y., et al. (2008). Angiotensin-(1-7) with Thioether Bridge: An Angiotensin-Converting Enzyme-resistant, Potent Angiotensin-(1-7) Analog. *JPET* 328, 849–855. doi: 10.1124/jpet.108.146431

Huo, L., and van der Donk, W. A. (2016). Discovery and Characterization of Bicereucin, an Unusual D-Amino Acid-Containing Mixed Two-Component Lantibiotic. *J. Am. Chem. Soc.* 138, 5254–5257. doi: 10.1021/jacs.6b02513

Conflict of Interest: The authors declare that the research was conducted in the absence of any commercial or financial relationships that could be construed as a potential conflict of interest.

3.2 Chapter II

Title: Stoichiometry and structure of a lantibiotic maturation complex

Authors: **Jens Reiners,** André Abts, Rebecca Clemens, Sander H. J. Smits & Lutz Schmitt

Published in: Scientific Reports (2017)
Impact factor: 4.85

Own proportion of this work: 60%

- Protein purification of NisB and NisC and pre-nisin A variants
- Interaction studies with nisin A ring mutations
- MALS & SAXS analysis
- Writing the manuscript

SCIENTIFIC REPORTS

OPEN

Stoichiometry and structure of a lantibiotic maturation complex

Jens Reiners, André Abts, Rebecca Clemens, Sander H. J. Smits & Lutz Schmitt

Received: 24 June 2016
Accepted: 06 January 2017
Published: 07 February 2017

Lantibiotics are ribosomally synthesized antimicrobial peptides secreted by mainly Gram-positive bacteria. Class 1 lantibiotics mature via two modification steps introduced by a modification LanBC complex. For the lantibiotic nisin, the dehydratase NisB catalyzes the dehydration of serine and threonine residues in the so-called core peptide. Second, five (methyl)-lanthionine rings are introduced in a regio- and stereospecific manner by the cyclase NisC. Here, we characterized the assembly of the NisBC complex *in vitro*, which is only formed in the presence of the substrate. The complex is composed of a NisB dimer, a monomer of NisC and one prenisin molecule. Interestingly, the presence of the last lanthionine ring prevented complex formation. This stoichiometry was verified by small-angle X-ray scattering measurements, which revealed the first structural glimpse of a LanBC complex in solution.

Bacteriocins are a group of antimicrobial peptides produced by Gram-positive as well as Gram-negative bacteria and some of them undergo posttranslational modifications (PTM(s))[1,2]. Within bacteria they mostly remain inactive and are secreted via dedicated transport systems. So far, more than 750 different bacteriocins have been isolated from natural sources[1] and the number constantly rises. Within the group of bacteriocins, a subfamily consists of ribosomally synthesized and posttranslational modified peptides, which are called lantibiotics. Here, non-natural amino acids and specific structures, which have an essential role on activity (e.g. lanthionine rings, dehydrated amino acids, heterocycles or head to tail cyclization of the peptide) are posttranslationally introduced. Common to all class I lantibiotics is a N-terminal leader sequence, which is crucial for the recognition by the PTM enzymes, secretion and for keeping the peptide in an inactive state within the cell. This leader sequence, which is often also called leader peptide, is fused to the so-called core peptide, in which all modifications occur.

Lanthipeptides contain the non-natural amino acids lanthionine or (methyl)-lanthionine and in case that they also display antimicrobial activity, these peptides are consequently called lantibiotics[3,4]. They are classified in four different classes (Type I-IV) depending on the enzymes involved in the PTM(s)[3,4]. Up to now, however, antimicrobial activities have only been reported for members of class I and II. Type I lantibiotics are modified by two different PTM enzymes, a lantibiotic dehydratase, LanB, and a lantibiotic cyclase, LanC. The enzyme LanB dehydrates specifically serine or threonine residues, whereas LanC catalyzes the thioether ring formation of the dehydrated amino acid and a C-terminally located cysteine residue within the core peptide via a Michael addition reaction[5]. This results in the formation of lanthionine (from Ser) or (methyl)-lanthionine (from Thr) rings, which are crucial for the activity as well as stability[6–12]. Type II lantibiotics are modified by a single enzyme called LanM, which catalyzes both, the dehydration and cyclization reaction, respectively[13]. In all cases the genes encoding the lantibiotic as well as the PTM enzymes are localized within in a single gene cluster and are valuable probes to identify lantibiotic operons in newly sequenced genomes[14].

Nisin is a class I lantibiotic produced by several *Lactococcus lactis* (*L. lactis*) strains[15–17]. It contains characteristic dehydrated amino acids and five (methyl)-lanthionine rings, named rings A to E[18,19]. These rings are essential for the antimicrobial activity displayed against numerous Gram-positive bacteria[8,20,21]. The leader peptide as elaborated above is responsible for the recognition by the PTM enzymes, here called NisB and NisC, and furthermore is essential for the subsequent secretion by the ABC transporter, here called NisT[22–28].

In detail, NisB dehydrates serine and threonine residues in the core peptide after ribosomal synthesis of nisin[29–32]. Seminal work on the mechanism of the dehydration reaction has demonstrated that a glutamate is transferred from glutamyl-tRNA^{Glu} to specific Ser/Thr side chains within the nisin core peptide introducing glutamylated intermediates[29,33]. After glutamate elimination, these Ser/Thr residues are converted to dehydroalanine and dehydrobutyrine with absolute stereoselectivity. Subsequently, NisC catalyzes a Michael addition of a C-terminal cysteine residue with the corresponding dehydrated amino acids to form thioether rings, the characteristic (methyl)-lanthionine rings[5,30,34,35]. The entire maturation process is schematically summarized in

Institute of Biochemistry, Heinrich-Heine-University Duesseldorf, Universitaetsstraße 1, 40225 Duesseldorf, Germany. Correspondence and requests for materials should be addressed to L.S. (email: Lutz.Schmitt@hhu.de)

Supplementary Fig. 1. Although the activity of the single enzymes, NisB and NisC, has been demonstrated[29,33–35], the assembly of a lantibiotic PTM complex has so far not been described *in vitro*.

In 1996, the first study revealed an interaction between NisC and NisB as well as between NisC and the ABC transporter NisT[36]. Furthermore, information about the directionality of the modification reaction was obtained suggesting a N- to C-terminal modification mechanism[9]. This is apparently in contrast to the PTM complex involved in NAI-107 maturation where an opposite directionality (C- to N-terminal) was discussed, which still is not fully understood[37].

The PTM complex consisting of NisB-NisC-NisA was observed using a system that employed a His-tag fused to prenisin[38]. This allowed the isolation of the PTM complex from the cytosol of *L. lactis*. These associated proteins were identified as NisB and NisC, although in sub-stoichiometric amounts[38].

Structural information is available for both PTM enzymes, NisB and NisC. However, this information is restricted to the isolated states of both enzymes. Two structures of lantibiotic dehydratases have been published[33,37]. The structure of NisB in complex with its substrate from *L. lactis*[33] as well as the apo structure of MibB involved in NAI-107 biosynthesis from *Actinobacteria*[37] were reported. Despite the low sequence homology (approximately 20%), the topology and fold of both proteins were very similar[37]. Interestingly, the amino acids involved in glutamylation and glutamate elimination are structurally highly conserved in both enzymes, which obviously suggests a fundamental similar mechanism of dehydration. The structure of NisC in the apo state has been solved with the catalytically important Zn^{2+} ion[34,35].

Despite our increased knowledge of the nisin maturation reaction, little if any information about the complex stoichiometry of the PTM NisBC complex is available. Furthermore, the complex assembling process remains unclear. The nisin maturation machinery has been successfully explored to install PTMs in therapeutic peptides[39–41]. This substrate spectrum can be even further extended if the PTM complex could be employed *in vitro*.

Here, we describe for the first time an *in vitro* study revealing the formation of the nisin maturation complex composed of NisB, NisC and either unmodified or dehydrated prenisin peptide. Prenisin presents the essential trigger to initiate the *in vitro* formation of the maturation complex. Here, the -FNLD- box located within the leader sequence was identified as the crucial part in triggering complex assembly. Furthermore, our data demonstrated that the nisin PTM machinery consists of a functional dimer of NisB, a monomer of NisC and a single prenisin peptide. Once all rings are installed, as in fully modified prenisin peptide, the complex cannot assemble anymore suggesting a releasing factor upon formation of the last ring. Finally, structural information of the nisin modification complex was obtained by small-angle X-ray scattering (SAXS). Here, the same stoichiometry of the PTM complex was determined and revealed a tunnel located at the interface of NisB and NisC harboring the prenisin substrate. This result supports our *in vitro* studies and provides the first molecular picture of a class I lantibiotic maturation complex.

Results

Characterization of the modification enzymes NisB, NisC and the prenisin variants. Nisin contains several PTMs introduced by a proposed complex of NisB and NisC in an alternating manner[9]. To investigate the assembly of such a complex, we purified NisB and NisC to homogeneity. Previously, it was shown for NisC that the N-terminal His_6-tag interfered with substrate binding and was therefore removed by thrombine cleavage prior to complex formation[22]. Both proteins were purified to a highly pure state as judged from SDS-PAGE analysis (Supplementary Fig. 2A and B). The oligomeric state of isolated NisB or NisC was analyzed via a combination of multi-angle light scattering and size exclusion chromatography (MALS-SEC)[22,25]. NisB is a dimer with a molecular weight of 237.5 ± 0.3 kDa (Supplementary Fig. 2C) and NisC is a monomer with a molecular weight of 48.1 ± 0.5 kDa. (Supplementary Fig. 2D) as previously reported[22,25]. The prenisin peptide and its variants were expressed and secreted by *L. lactis* NZ9000 and isolated via cation exchange chromatography as described[22,25] (Supplementary Fig. 3).

Prior to the complex formation studies, the ability of the single proteins to bind prenisin was tested using MALS-SEC. Here, a dimer of NisB binds one unmodified prenisin molecule[25] and the monomer of NisC binds also one unmodified prenisin molecule[22] (Supplementary Fig. 4A and B) resulting in an increase of the observed molecular masses to 54.5 ± 0.6 kDa for NisC and 241.9 ± 0.4 kDa for NisB, respectively. Thus, purified NisB and NisC are capable to binding unmodified prenisin peptide. Higher amounts of prenisin did not result in higher molecular masses suggesting that both protein can only bind one prenisin molecule.

PTM complex assembly. To assemble the nisin PTM complex *in vitro* we incubated NisB and NisC in different molar ratios ranging from 1:1 to 1:8 for 1 h at 25 °C and analyzed a potential complex formation by MALS-SEC. This resulted in two clearly separated elution peaks occurring at 7.4 min and 9.0 min. The first peak contained dimeric NisB with a theoretical molecular mass of 236.6 kDa (Fig. 1, black dashed line) and the second peak contained only NisC with a theoretical molecular weight of 48.5 kDa (not shown). To analyze this further we subjected single elution fractions of the SEC experiment to SDS-PAGE analysis (Supplementary Fig. 5) combined with Western blotting (Fig. 2A) using polyclonal antibodies against NisB and NisC, respectively. This revealed that NisB, even in the presence of a high excess of NisC, formed no complex with NisC (Fig. 1, black dashed line, Fig. 2A).

Next PTM complex formation was analyzed under conditions, in which either of the two enzymes, NisB or NisC, was preloaded with unmodified prenisin peptide. Upon saturation of NisB with unmodified prenisin peptide and subsequent incubation with 20 μM NisC prior to complex formation, a molecular mass of 263.8 ± 0.3 kDa was observed. This indicated formation of a NisB-NisC-NisA complex. When NisC was first saturated with unmodified prenisin peptide and subsequently incubated with 20 μM NisB, a molecular weight of 247.1 ± 0.4 kDa was observed for NisB (Supplementary Fig. 6).

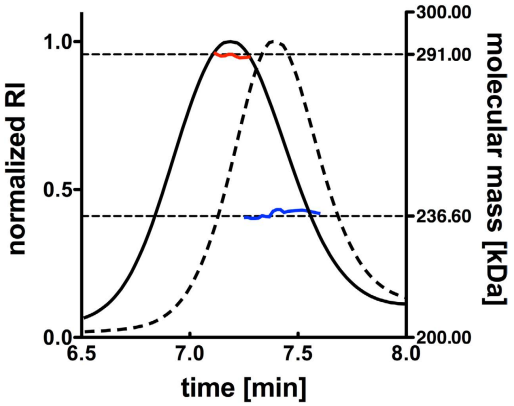

Figure 1. MALS-SEC analysis of the mixed protein samples consisting of NisB and NisC, in the presence or absence of the dehydrated prenisin peptide. The dashed black graph shows the elution profile of a mixture of 20 μM NisB and 160 μM NisC resulting in a molecular weight of 237.5 ± 0.3 kDa (blue line). The analysis of 20 μM NisB, 160 μM NisC and 200 μM dehydrated prenisin peptide is shown by the black graph, revealing an apparent molecular weight of 291.2 ± 0.9 kDa (red line) of the formed complex. The two black dotted lines indicate the theoretical molecular weight of an isolated NisB (236.6 kDa) dimer and of a complex consisting of a NisB dimer, a monomer of NisC and one prenisin peptide molecule (291 kDa).

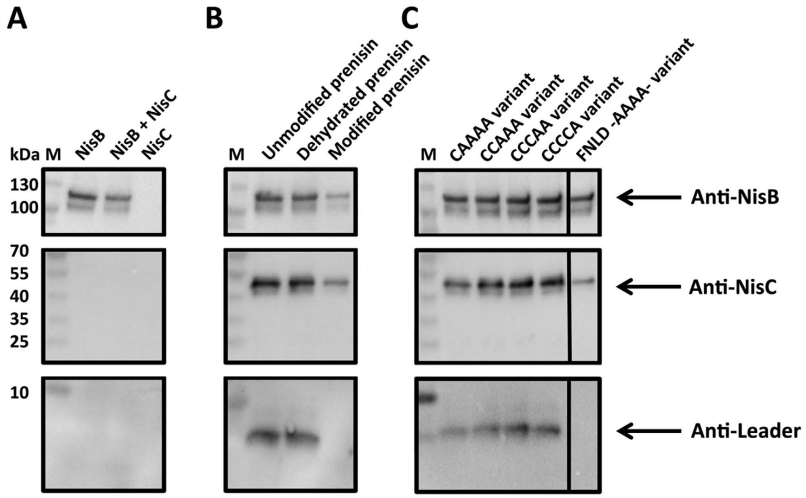

Figure 2. Western blot analysis of the PTM complex containing fraction. Elution fractions marked with a red box in the corresponding SDS-PAGE gels (Supplementary Figs 5, 7 and 8) were used for further analysis. The antibodies used are indicated with an arrow. (**A**) **M**: protein marker. **NisB**: The fraction resulting of the analytical SEC of 20 μM NisB. NisB and NisC: This sample represents the interaction analysis of 20 μM NisB and 160 μM NisC. **NisC**: The fraction resulting of the analytical SEC of 160 μM NisC. (**B**,**C**) In the following lanes the results of the complex formation for the different prenisin peptide variants are shown. PTM complex is formed and consists of NisB, NisC and prenisin peptide.

This demonstrates that the presence of unmodified prenisin peptide triggers complex formation. However, the molecular mass determined in both experiments did not fit to any theoretically combination of the three components (1: 1: 1 or 2: 1: 1 or 2: 2: 2 or any other ratio) (Supplementary Table 2). This suggested that a fully assembled NisB-NisC-NisA complex with equimolar concentrations of NisB and NisC and an excess of unmodified prenisin peptide was not obtained under these experimental conditions.

To obtain a fully assembled complex, we kept the concentration of NisB constant at 20 μM as well as the 10 fold-excess of unmodified prenisin peptide (200 μM). We increased the concentration of NisC stepwise from 10 μM to 160 μM and analyzed the molecular weights of the formed complexes via MALS-SEC. Here, we observed a gradual increase of the molecular weight at NisC concentrations of up to 80 μM (Fig. 3 and Supplementary Table 1). Further increase of the NisC concentrations to 160 μM did not change the observed molecular weight of 293.6 ± 1.2 kDa any further (Fig. 3, Table 1 and for a detailed view Supplementary Table 1). This suggested the presence of a stable complex of NisC/NisB/unmodified prenisin peptide at NisC

NisB	NisC	NisA variants	Molekular weight [kDa]
+	−	—	237.5 ± 0.3
+	−	unmodified	241.9 ± 0.4
−	+	—	48.1 ± 0.5
−	+	unmodified	54.5 ± 0.6
+	+	unmodified	293.6 ± 1.2
+	+	dehydrated	291.2 ± 0.9
+	+	modified	250.4 ± 0.7
+	+	FNLD-Box	248.0 ± 0.9

Table 1. MALS-SEC data summarizing the molecular weight of the complex forming analysis for the different prenisin peptide variants and without any prenisin peptide. The theoretical molecular weight of a NisB dimer is calculated to 236.6 kDa, 48.5 kDa for a cleaved NisC monomer and 5.9 kDa for the unmodified prenisin peptide.

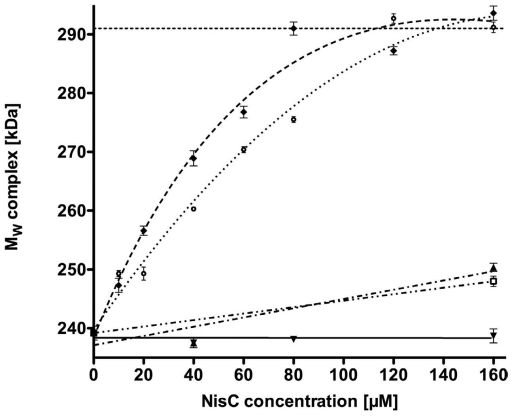

Figure 3. Assembly of the nisin maturation complex visualized via MALS-SEC. The molecular weight of the protein within the elution fraction was determined using MALS-SEC. The concentration of NisB (20 μM) and the different prenisin peptide variants (200 μM) were kept constant and the NisC concentration was varied (indicated on the X-axis). The upper dotted line shows the molecular weight of the theoretical PTM complex of 291 kDa. The molecular weight of NisB incubated with NisC is shown in ▼. With ♦, the molecular weight dependency of the complex with the unmodified prenisin peptide is shown. The dehydrated prenisin peptide profile corresponds to ○. The molecular weight of the complex in the presence of the modified prenisin peptide is indicated by ▲. □ represents the dependency of the molecular weight of the complex in the presence of the -FNLD- box (-AAAA-) variant.

concentrations of 80 μM or higher. The corresponding SDS-PAGE and Western blot analysis demonstrated the presence of both NisB and NisC in the elution fraction, together with the unmodified prenisin peptide (Fig. 2B and Supplementary Fig. 7A). After calculation of all possible stoichiometry's, the nisin PTM machinery possessed a stoichiometry of 2:1:1 (see Supplementary Table 2).

The modification state of nisin dictates complex formation. The unmodified prenisin peptide initiated complex formation between NisB and NisC (Figs 2 and 3). This raised the question whether the modification state within the prenisin core peptide modulates complex formation? We therefore repeated the experiment employing dehydrated or fully modified prenisin peptide. In the latter case, all (methyl)-lanthionine rings are present, while in the dehydrated prenisin core peptide all serine residues and threonine residues are dehydrated[31], but due to the lack of NisC during expression of prenisin, no (methyl)-lanthionine rings were introduced. We incubated the dehydrated and the fully modified prenisin peptide (200 μM) with 20 μM NisB and up to 160 μM NisC. We observed a complex of the PTM machinery after incubation of NisB and NisC with dehydrated prenisin peptide resulting in a molecular weight of 291.2 ± 0.9 kDa employing MALS-SEC analysis (Fig. 1 black line; Figs 2B and 3). This mass is identical within experimental error with the molecular weight determined for the unmodified prenisin peptide PTM enzyme complex. Importantly, an increase of the NisC concentration above 120 μM did not result in higher molecular weights indicating that no higher molecular weight PTM complex was formed (Figs 2B and 3, Table 1 and Supplementary Table 1). The corresponding SDS-PAGE analysis revealed the presence of NisB, NisC and dehydrated prenisin peptide in the elution fraction of the PTM enzyme complex (Supplementary Fig. 7B).

Incubating the fully modified prenisin peptide with NisB and NisC, resulted only in a small shift in the elution profile indicating that the modified prenisin peptide did not trigger complex formation (Figs 2B and 3, Table 1 and Supplementary Table 1 and Supplementary Fig. 7C). In MALS-SEC, a molecular weight of 250.4 ± 0.7 kDa was determined, which supported the idea of a weak interaction and reflects the lack of a stable PTM complex. Altogether, this demonstrated that fully modified prenisin peptide is not capable of inducing the formation of the completely assembled PTM complex, while unmodified and dehydrated prenisin peptide can do.

The role of the (methyl)-lanthionine rings in complex formation. Only the presence of unmodified and dehydrated prenisin peptide triggered complex formation (see above). To investigate whether one or more of the five rings inhibits complex formation, four prenisin peptide variants were produced only differing in the number of (methyl)-lanthionine rings within the core peptide. The native prenisin core peptide contains five cysteine residues giving rise to the five (methyl)-lanthionine rings A-E after modification (Supplementary Fig. 1). By exchanging these cysteine residues subsequently to alanine, prenisin peptide variants were created which vary in the number of (methyl)-lanthionine rings. The CAAAA variant contains only ring A, CCAAA rings A and B, CCCAA rings A-C and CCCCA rings A-D. Here the variants are expressed in the presence of NisB and NisC, which ensures that these variants are dehydrated and the lanthionine rings are present when a cysteine residue is still available. After purification, we incubated 20 μM NisB, 160 μM NisC and 200 μM of these different ring variants of the prenisin peptide for 1 h at 25 °C and analyzed the reaction mixtures by analytical SEC. The corresponding SDS-PAGE analysis is shown in Supplementary Fig. 8A–D. The analysis demonstrated that all ring deficient prenisin peptide variants are capable to form the PTM complex. In all cases, a co-elution of NisB, NisC and the prenisin peptide was observed. The co-elution fraction was furthermore analyzed by Western blot (Fig. 2C) to visualize the presence of NisB, NisC and the prenisin peptide variant used. This result demonstrates that the PTM complex is obtained, in the presence of at least one up to four (methyl)-lanthionine rings. Only when the last (methyl)-lanthionine ring (ring E) was present, i.e. fully modified prenisin peptide, no complex formation was detected. This suggests that coming to the last ring or dehydratable residue at the C-terminus might stimulate the dissociation of the entire PTM complex.

The recognition motive within the leader peptide: the -FNLD- box. We showed above that the modification state of the core peptide has a profound influence on complex formation. Next, we concentrated on the role of the N-terminal leader peptide in the assembly of the modification complex. The single NisB and NisC enzymes recognize the highly conserved -FNLD- box motif within the leader peptide[22,25]. MALS-SEC analysis using the -FNLD- to -AAAA- mutant resulted in a molecular weight of 248.0 ± 0.9 kDa, which indicated low efficiency of PTM complex formation (Figs 2C and 3, Table 1 and Supplementary Fig. 7D). The SDS-PAGE analysis of the analytical SEC revealed a minor shift of NisC and only low amounts of NisC co-eluted with NisB (Supplementary Fig. 7D). This suggests that the -FNLD- box has an important role during complex formation and demonstrated that both, the leader and the core peptide, are essential for the assembly of the nisin PTM complex. This is in line with the observations that this prenisin peptide variant is poorly modified *in vivo*[23,26,27,38].

Visualization of the nisin modification complex with small-angle x-ray scattering (SAXS). We used SAXS to obtain a structural glimpse of the fully assembled PTM complex. Here, we applied 200 μl of each enzyme, NisB (200 μM) and NisC (470 μM), respectively, on a Superdex 200 column and measured the X-ray scatter (Supplementary Fig. 9). We estimated the molecular weight from the POROD volumes[42] (Supplementary Table 3). This resulted in a molecular mass of 239.26 kDa for the NisB sample corresponding to a dimer, and in a molecular mass of 51.56 kDa for NisC, which corresponds to the monomeric state. These results fitted to the theoretically calculated masses deduced from the corresponding sequences (Supplementary Table 3) and were in-line with our MALS-SEC results (Table 1). Next we applied the same method to a NisB sample saturated with dehydrated prenisin peptide (200 μM NisB, 2 mM prenisin). Here, we incubated NisB with prenisin peptide, which should result in saturation of the enzyme. The calculated molecular weight of 256.54 kDa indicated that dehydrated prenisin peptide bound to NisB. The volumetric envelope was calculated from the background-subtracted scattering curves using DAMMIF[43] (Fig. 4).

The structure of NisB (PDB code 4WD9) and NisC (PDB code 2GOD), which were solved previously by X-ray crystallography, were superimposed into the volumetric envelopes using the program SUPCOMB[44] (Fig. 4), demonstrating that the envelope of the enzymes in solution nicely fitted to the published X-ray structures (Fig. 4). Interestingly in the map of the apo-NisB a tunnel on only one site of the envelope was observed (Fig. 5A), which might serve as an entrance to the binding site of prenisin. The leader sequence was visible in the X-ray structure of NisB and after fitting the model into the volumetric envelope obtained by SAXS, it was localized in close vicinity of the observed tunnel (highlighted in red in Fig. 5A). This further strengthens the suggestion that the tunnel might be the binding site for the prenisin molecule. This tunnel however appears to be closed in the volumetric envelope derived from our SAXS measurements of NisB saturated with dehydrated prenisin peptide. An overlay of both envelopes revealed that the tunnel is blocked in the NisB-dehydrated prenisin peptide map (Fig. 5B). Please note that the measurement of both samples were performed at similar concentrations and resulted in volumetric envelopes of comparable resolution. This suggests that the tunnel represents an opening for prenisin, which is blocked once prenisin is bound. Furthermore, this tunnel points into the active site of NisB and to the residues involved in the dehydration reaction as well as glutamylation[23,33,38].

Next we also measured the fully assembled PTM complex. This revealed a molecular weight of 275.1 kDa as deduced from the POROD volume indicating that the PTM complex was not fully assembled, which is likely due to the dilution effect occurring during SEC. Even after increasing the concentration of the PTM complex, the amount of formed complex did not increase. The different molecular weights from the POROD Volume were

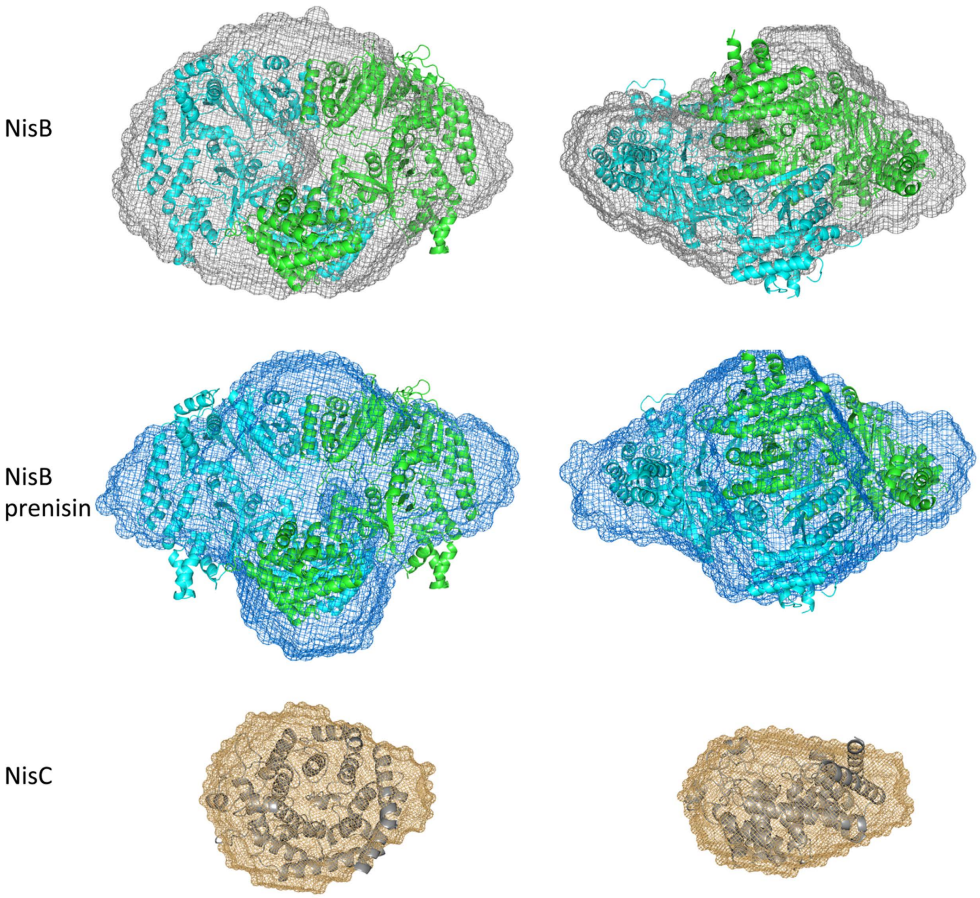

Figure 4. SAXS analysis of apo-NisB, NisB-prenisin and NisC. The volumetric envelopes are shown for NisB (grey mesh), NisB-prenisin (blue mesh) and NisC (orange mesh) as calculated from the scattering data using DAMMIF[43]. The structure of NisB (PDB code: 4WD9) and NisC (PDB code: 2GOD) were docked into the volumetric envelopes using SUPCOMB[44].

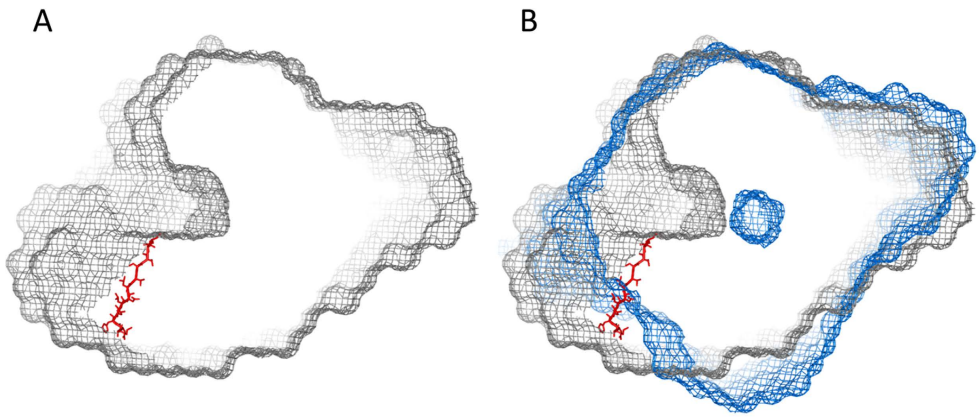

Figure 5. Comparison of the NisB and NisB-prenisin peptide volumetric envelopes as obtained by SAXS. (**A**) The volumetric envelope of NisB is shown as a grey mesh. A 30 Å clip was calculated around the leader peptide as derived from the fitted NisB structure (highlighted in red stick representation) (**B**) An overlay of the NisB envelope (grey mesh) and the NisB-dehydrated prenisin peptide envelope (blue mesh) highlighted that the observed tunnel is closed once dehydrated prenisin peptide is bound to NisB.

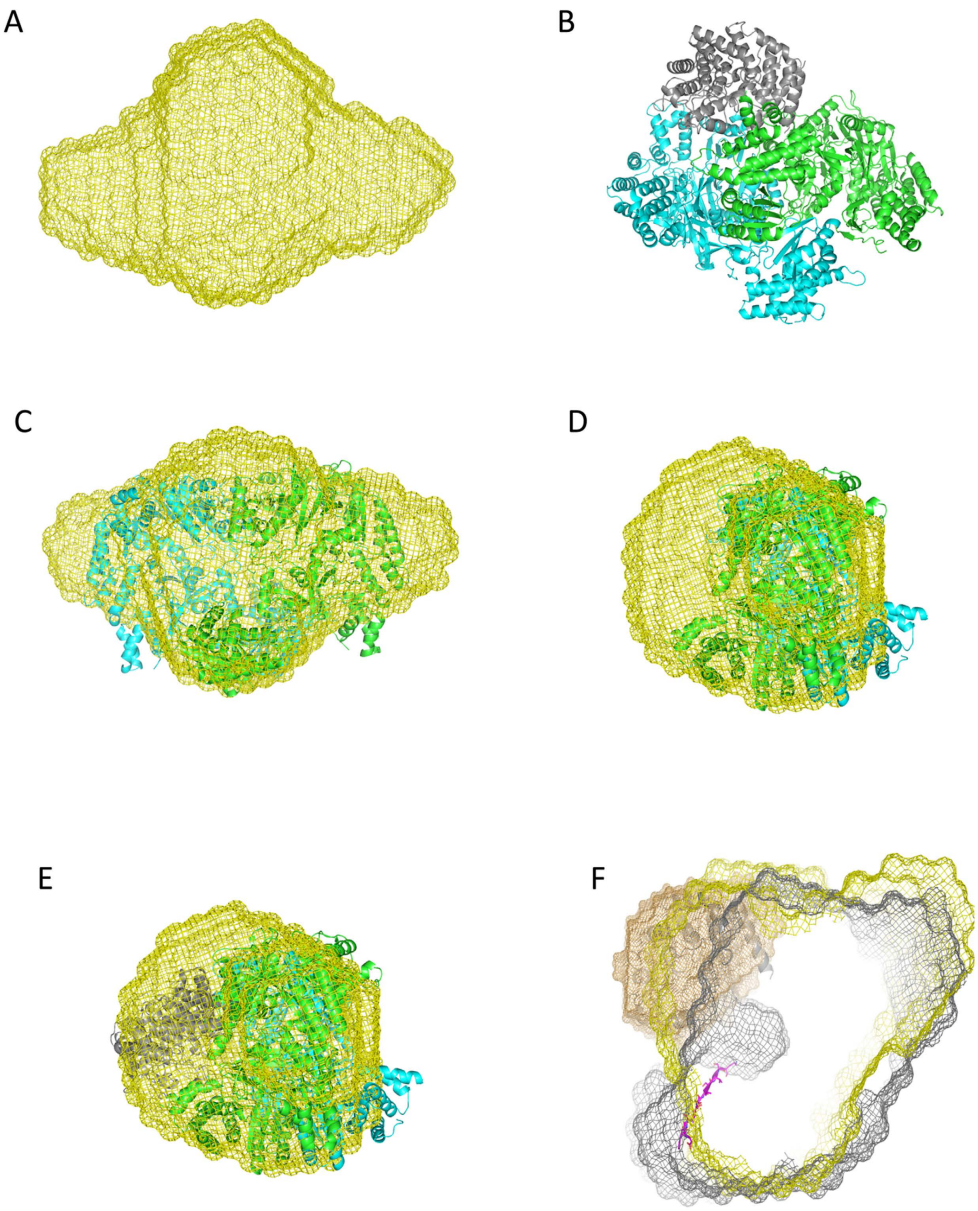

Figure 6. SAXS analysis of the fully assembled PTM complex. (**A**) The volumetric envelope of the fully assembled complex is shown as a yellow mesh. (**B**) The assembled PTM complex as deduced from the program SASREF[54] (The monomers of NisB are colored in blue and green, NisC in dark orange). (**C**) Front view of the PTM complex with only NisB highlighted, (**D**) side view of the PTM complex with only NisB highlighted, (**E**) fully assembled PTM complex with the complex aligned to the volumetric envelope. (**F**) Zoom in into the PTM complex identical to Fig. 5. The observed tunnel in NisB is occupied by dehydrated prenisin peptide and also NisC is located at the same interface of the protein.

also supported by the calculated Radius of Gyration (R_g) as well as estimated D_{max}. We could observe an increase for the PTM complex in comparison to isolated NisB (Supplementary Table 3). The overall shape of the obtained volumetric envelope revealed additional density on top of the NisB volume near the tunnel observed in the NisB experiment (Fig. 6A–D), suggesting that NisC is localized at that position. Furthermore, no additional volume large enough to accommodate another NisC molecule was observed. This demonstrates that the stoichiometry obtained by SAXS was identical to the stoichiometry deduced by SEC-MALS. Independently, we used the program SASREF to calculate the shape of the PTM complex using the structures of NisB and NisC and the experimental scattering data. Here a similar location of NisC was observed. NisC is again localized on top of the tunnel suggesting that this represents the stable conformation of the PTM complex *in vitro* (Fig. 6D–F). NisC has a bowl

like structure and the active site points again towards the tunnel (Fig. 6F). This suggests that NisC is localized next to the prenisin binding site observed for NisB within the PTM complex.

Discussion

Bacteriocins are peptides produced by bacteria and there is one specific class, called lanthipeptides, contains PTMs introduced by specific enzymes, which can be either a single protein (LanM) or two proteins (LanB and LanC, respectively)[3,13,16,17]. In the case of systems containing LanB and LanC, a complex of both enzymes is proposed to be the catalytically active species, but direct experimental evidence of its existence is rare. Here, we provide the first *in vitro* data on the assembly of the nisin PTM complex consisting of the dehydratase NisB and the cyclase NisC. The enzyme NisB and NisC are proposed to work in an alternating fashion to introduce the PTMs in the core section of the prenisin peptide[9]. We only observe the assembly of the PTM complex in the presence of unmodified and dehydrated prenisin peptide (Figs 2 and 3). This is in line with *in vivo* and *in vitro* data, in which direct interaction(s) between NisB and NisC was never observed without the presence of the substrate[3,17,36,38,45]. Purification of the prenisin peptide via an affinity tag directly from the cytosol of *L. lactis* resulted in elution fractions containing both, NisB as well as NisC[38]. This strongly suggested that a fully assembled maturation complex was present within the cytosol. The data presented here provides the first *in vitro* reconstitution of a lantibiotic PTM complex using the three separately purified components.

The stoichiometry of the PTM complex was determined to be 2:1:1 (NisB: NisC: prenisin peptide) by two independent approaches, SEC-MALS as well as SAXS.

The structure of NisB also revealed a dimeric organization with prenisin bound although electron density only for the region surrounding the -FNLD-box within the leader peptide was clearly visible[33]. Within this NisB structure the leader was detected in both monomers, which might be due to the simultaneous overexpression of both, NisB and prenisin, respectively, in combination with the lack of NisC. In the recently published structure of MibB, no substrate was observed[37]. While comparing the binding site of both enzymes, it became obvious that this particular region is rather flexible. This suggests that upon substrate binding NisB undergoes a conformational change as observed in the SAXS experiment. The differences are however subtle.

Interaction between NisB, NisC and the prenisin core peptide. Here, we demonstrated that complex formation between NisB and NisC strictly relies on the presence of prenisin, i.e. either the unmodified or the dehydrated peptide variant. When the cyclization reactions are completed and five (methyl)-lanthionine rings are present in the prenisin peptide, only a very minor amount of PTM complex can be obtained. This might reflect the *in vivo* situation, in which fully modified prenisin peptide is released from the PTM complex as soon as the (methyl)-lanthionine rings are formed and handed over to the dedicated transport system NisT. Since all three components were apparently localized at the membrane of *L. lactis*[36], it seems plausible that an even larger complex consisting of the PTM enzymes and the ABC transporter exists within the bacterial cell. Installing the lantibiotic PTMs and the subsequent secretion benefits from an efficient coupling of lantibiotic biosynthesis, maturation and secretion.

Within the leader peptide of class I lantibiotics, the -FNLD- box is highly conserved[26] and was identified as the recognition motif for the isolated enzymes NisB and NisC, respectively[22,25,38]. With the exchange of the -FNLD- motif against four alanines (-AAAA-), the formation of the PTM complex was drastically reduced (Figs 2 and 3 and Table 1). This is in contrast to *in vitro* results with isolated proteins, where no binding was observed[22,25]. But we have to stress that in these *in vitro* studies only low concentrations of the -AAAA- mutant of prenisin peptide were used and that the concentrations used in this study were several times higher. Nevertheless, our result clearly support that this highly conserved motif possesses a strong effect on complex formation as exemplified by the -AAAA- mutant. This was previously also highlighted by *in vivo* studies, which demonstrated that this variant is poorly modified and contains almost no dehydrations or cyclisation within its core peptide[23,26,27,38].

SAXS analysis revealed that in the apo-NisB structure a tunnel is present in close proximity of the binding site of the leader sequence. This tunnel is not observed within the NisB-dehydrated prenisin peptide complex. This suggested that the dehydrated prenisin peptide occupies this space. Interestingly, only one tunnel is observed indicating that one prenisin molecule can bind to NisB in solution. The other possible binding site appears to be closed. Furthermore, we observed that NisC is localized next to this tunnel with its active site pointing towards the prenisin binding site as well as the region of NisB, which contains the residues important for the dehydration and glutamylation reactions[29,33].

Taken all data together the dehydration reaction within the core peptide likely changes the conformation of prenisin such that the active site of NisC becomes accessible, which is capable to cyclize the first ring. This would be inline with the model proposed that nisin is modified via a ping-pong mechanism[9,46] were dehydration and cyclization occur in an alternate fashion. Due to (methyl)-lanthionine ring formation, the peptide shifts forward and the second dehydration step can occur. It remains unclear whether the position of the leader peptide is also shifted during this process and consequently moves out of the PTM complex. *In vivo* this might be favorable since the leader sequence needs to be recruited by the ABC transporter NisT. Finally, the presence of ring E prevented complex formation, or stimulate the dissociation. Apparently, the conformation of the core peptide is different in comparison to the conformation of nisin that contains rings A-D. This likely is ensured by the more bulky intertwined conformation of ring D and E[19].

In summary, the data obtained in this study identified two factors influencing complex formation of the maturation enzymes NisB and NisC, respectively. First the core peptide, it can be dehydrated and also particular modified. *In vitro* the presence of the last (methyl)-lanthionine ring, ring E, abolished complex formation. Second, the N-terminal leader peptide plays an important role. The highly conserved -FNLD- box is an essential recognition factor for the modification enzymes NisB and NisC. Finally, the MALS-SEC analysis revealed the first quantitative

data elucidating the stoichiometry of the nisin maturation complex. This complex revealed a molecular weight of approximately 291 kDa corresponding to a stoichiometry of 2:1:1 (NisB/NisC/prenisin peptide) *in vitro*.

Materials and Methods

Cloning the prenisin ring deficient variants. For producing ring deficient prenisin peptides, a shuttle vector accessible for the bacteria *L. lactis* and *E. coli* was created[47]. The correctness of the obtained plasmids was successfully verified by sequencing.

Purification of NisB, NisC and the prenisin peptide variants. NisB was expressed in *L. lactis* and purified as previously described[25]. The expression and purification of NisC was performed as described in ref. 22. Briefly, the dehydratase NisB was homologously expressed in *L. lactis* NZ9000 and purified to homogeneity via immobilized metal ion affinity chromatography (IMAC) followed by SEC. NisC was heterologously expressed in *E. coli* BL21 and isolated via a three-step purification strategy. The first step was again IMAC chromatography using a TALON® Superflow Cartage Colum, followed by a SEC purification step. The N-terminal His_6-tag of NisC was cleaved off by thrombin treatment. Non-digested NisC was removed via a second IMAC step.

The prenisin peptide purification was performed as described in ref. 22. For the determination of the prenisin concentration and the variants a RP-18 HPLC column was used[22]. In general prenisin is expressed via a two plasmid system. On the first plasmid wildtype prenisin or the cysteine variants of core nisin or the FNLD variants of the leader part of nisin is expressed. The second plasmid contains the PTM complex consisting of NisB, NisC and NisT. By varying the latter plasmid, the modification status of prenisin can be varied. Here, the deletion of NisC leads to a prenisin peptide variant, which is dehydrated but no lanthionine rings are installed. Similarly, the deletion of both, NisB and NisC, on the plasmid results in a prenisin peptide varians where no dehydration and no cyclization are present. The differences in modification are highlighted in Supplementary Figure S1.

Analysis of complex formation. To determine the molecular weight and stoichiometry of the NisB/NisC/prenisin peptide complex, a combination of multi-angle light scattering and size exclusion (MALS-SEC) was used to visualize complex formation. The analyses were performed on an Agilent 1260 HPLC System in combination with a triple-angle light scatter detector (miniDAWN TREOS) and a differential refractive index detector (Optilab rEX – both Wyatt Technology Europe).

Analysis of isolated NisB and NisC were performed by injection of 200 μL of a 20 μM solution of each protein. The second step was the analysis of prenisin peptide bound proteins. We used 20 μM NisC, respectively 20 μM NisB and incubate it with 200 μM prenisin peptide for 1 h at 25 °C.

For the initial complex analysis we saturated NisB with the unmodified prenisin peptide and analyzed the mixture by MALS-SEC. Here, we used 20 μM unmodified prenisin peptide saturated NisB and incubate it with 20 μM NisC for 1 h at 25 °C. The same analysis was performed with 20 μM unmodified prenisin peptide saturated NisC and subsequent incubation with 20 μM NisB. A Volume of 200 μL was applied on an Agilent BioSEC-5 colum (300 Å, 7.8 × 300 mm) pre-equilibrated with MALS buffer (50 mM HEPES-NaOH, pH 7.5, 500 mM NaCl) at a flow rate of 1.0 mL/min or on a Superdex 200 10/300 increase colum (GE Healthcare) at a flow rate of 0.75 mL/min. Data-analysis was performed with the ASTRA software package (Astra V 5.3.4.20) (Wyatt Technology).

To visualize complex formation, we kept the concentrations of NisB (20 μM) and of the prenisin peptide variants (200 μM) constant in the different samples. We used only different concentrations of NisC from 10 μM to 160 μM.

Analytical co-elution studies. The co-elution studies were performed on a Äkta Micro system using a Superdex 200 PC 3.2 column (GE Healthcare) equilibrated with 50 mM HEPES-NaOH, pH 7.5, 500 mM NaCl with a flow rate of 0.05 mL/min.

A 50 μL reaction mixture consisting of 20 μM NisB, 160 μM NisC and 200 μM prenisin peptide variant was incubated for 1 h at 25 °C and subsequently applied to SEC analysis. Elution was observed at 280 nm. After co-elution, the corresponding fractions were analyzed by a 4–20% gradient Tris-Glycine SDS-PAGE (Biorad) gel stained with Page-Blue (Thermo Fisher).

Immunoblotting and SDS-PAGE analysis. All SDS-PAGE and Western blotting experiments were performed with standard laboratory techniques[48–50]. The antibodies for NisB[38], NisC[38] and the nisin leader peptide[26] were kindly provided by Dr. Moll, LanthioPharma, Groningen (Netherlands).

Visualization of the nisin modification complex by small-angle X-ray scattering (SAXS). SAXS data were collected at ESRF Grenoble on beamline BM29 equipped with a PILATUS 1 M detector (Dectris). The sample to detector distance was kept fixed at 2.867 m. The achievable q-range under these conditions was 0.025–5 nm^{-1}. The maximum measurable R_g (radius of gyration) of the investigated particles were 20 nm. All measurements were performed at 4 °C and the system was coupled to a size exclusion chromatography.

For analysis of the nisin modification complex, a mixture of 40 μM NisB, 320 μM NisC and 400 μM dehydrated prenisin peptide was incubated for 1 h at 25 °C. Analysis of isolated NisB was performed with a 200 μM solution and for NisC with a 470 μM solution. A volume of 200 μL was applied on a Superdex 200 10/300 increase colum (GE Healthcare) pre-equilibrated with SAXS-buffer (50 mM HEPES-NaOH, pH 7.5, 500 mM NaCl, 5% Glycerol) at a flow rate of 0.75 mL/min. For data processing we used the ATSAS Software package (Version 2.7.1)[51]. Primary data reduction were performed using the program PRIMUS[42]. The forward scattering $I(0)$ as well as the radius of gyration (R_g) were calculated with the Guinier approximation[52], which is implemented in PRIMUS[42]. We calculated the pair-distribution function $p(r)$ and estimate the maximum particle dimension (D_{max}) employing the program GNOM[53]. The low resultion *ab initio* models were calculated with DAMMIF[43] (10 runs for each sample)

and used to perform the docking of the NisB-NisC dehydrated prenisin peptide complex, which was calculated with SASREF[54]. For superimposing of the models, we used SUPCOMB[44]. These programs are all part of the ATSAS program package available on the EMBL website (http://www.embl-hamburg.de/biosaxs/software.html).

References

1. Alvarez-Sieiro, P., Montalban-Lopez, M., Mu, D. D. & Kuipers, O. P. Bacteriocins of lactic acid bacteria: extending the family. *Appl. Microbiol. Biot.* **100,** 2939–2951 (2016).
2. Cotter, P. D., Hill, C. & Ross, R. P. Bacteriocins: developing innate immunity for food. *Nature Rev. Microbiol.* **3,** 777–88 (2005).
3. Chatterjee, C., Paul, M., Xie, L. & van der Donk, W. A. Biosynthesis and mode of action of lantibiotics. *Chem. Rev.* **105,** 633–84 (2005).
4. Zhang, Q., Yu, Y., Velasquez, J. E. & van der Donk, W. A. Evolution of lanthipeptide synthetases. *Proc. Natl. Acad. Sci. USA* **109,** 18361–6 (2012).
5. Okeley, N. M., Paul, M., Stasser, J. P., Blackburn, N. & van der Donk, W. A. SpaC and NisC, the cyclases involved in subtilin and nisin biosynthesis, are zinc proteins. *Biochemistry* **42,** 13613–24 (2003).
6. AlKhatib, Z. *et al.* The C-terminus of nisin is important for the ABC transporter NisFEG to confer immunity in *Lactococcus lactis*. *Microbiology open* **3,** 752–63 (2014).
7. Chan, W. C. *et al.* Structure-activity relationships in the peptide antibiotic nisin: Antibacterial activity of fragments of nisin. *Febs Letters* **390,** 129–132 (1996).
8. Hasper, H. E., de Kruijff, B. & Breukink, E. Assembly and stability of nisin-lipid II pores. *Biochemistry* **43,** 11567–75 (2004).
9. Lubelski, J., Khusainov, R. & Kuipers, O. P. Directionality and coordination of dehydration and ring formation during biosynthesis of the lantibiotic nisin. *J. Biol. Chem.* **284,** 25962–72 (2009).
10. Rink, R. *et al.* Dissection and modulation of the four distinct activities of nisin by mutagenesis of rings A and B and by C-terminal truncation. *Appl. Environ. Microbiol.* **73,** 5809–5816 (2007).
11. van Heusden, H. E., de Kruijff, B. & Breukink, E. Lipid II induces a transmembrane orientation of the pore-forming peptide lantibiotic nisin. *Biochemistry* **41,** 12171–12178 (2002).
12. Wiedemann, I. *et al.* Specific binding of nisin to the peptidoglycan precursor lipid II combines pore formation and inhibition of cell wall biosynthesis for potent antibiotic activity. *J. Biol. Chem.* **276,** 1772–1779 (2001).
13. Knerr, P. J. & van der Donk, W. A. Discovery, Biosynthesis, and Engineering of Lantipeptides. *Annu. Rev. Biochem.* **81,** 479–505 (2012).
14. van Heel, A. J., de Jong, A., Montalban-Lopez, M., Kok, J. & Kuipers, O. P. BAGEL3: automated identification of genes encoding bacteriocins and (non-)bactericidal posttranslationally modified peptides. *Nucleic Acids Res.* **41,** W448–W453 (2013).
15. Breukink, E. *et al.* Use of the cell wall precursor lipid II by a pore-forming peptide antibiotic. *Science* **286,** 2361–4 (1999).
16. Lubelski, J., Rink, R., Khusainov, R., Moll, G. N. & Kuipers, O. P. Biosynthesis, immunity, regulation, mode of action and engineering of the model lantibiotic nisin. *Cell. Mol. Life Sci.* **65,** 455–76 (2008).
17. Arnison, P. G. *et al.* Ribosomally synthesized and post-translationally modified peptide natural products: overview and recommendations for a universal nomenclature. *Nat. Prod. Rep.* **30,** 108–60 (2013).
18. Rogers, L. A. The Inhibiting Effect of *Streptococcus Lactis* on *Lactobacillus Bulgaricus*. *J. Bacteriol.* **16,** 321–5 (1928).
19. Van de Ven, F. J., Van den Hooven, H. W., Konings, R. N.& Hilbers, C. W. NMR studies of lantibiotics. The structure of nisin in aqueous solution. *Eur. J. Biochem.* **202,** 1181–8 (1991).
20. Severina, E., Severin, A. & Tomasz, A. Antibacterial efficacy of nisin against multidrug-resistant Gram-positive pathogens. *J. Antimicrob. Chemother.* **41,** 341–7 (1998).
21. Brumfitt, W., Salton, M. R. & Hamilton-Miller, J. M. Nisin, alone and combined with peptidoglycan-modulating antibiotics: activity against methicillin-resistant *Staphylococcus aureus* and vancomycin-resistant *enterococci*. *J. Antimicrob. Chemother.* **50,** 731–4 (2002).
22. Abts, A., Montalban-Lopez, M., Kuipers, O. P., Smits, S. H. & Schmitt, L. NisC binds the FxLx motif of the nisin leader peptide. *Biochemistry* **52,** 5387–95 (2013).
23. Khusainov, R., Moll, G. N. & Kuipers, O. P. Identification of distinct nisin leader peptide regions that determine interactions with the modification enzymes NisB and NisC. *FEBS Open Bio* **3,** 237–42 (2013).
24. Kuipers, A. *et al.* NisT, the transporter of the lantibiotic nisin, can transport fully modified, dehydrated, and unmodified prenisin and fusions of the leader peptide with non-lantibiotic peptides. *J. Biol. Chem.* **279,** 22176–82 (2004).
25. Mavaro, A. *et al.* Substrate recognition and specificity of the NisB protein, the lantibiotic dehydratase involved in nisin biosynthesis. *J. Biol. Chem.* **286,** 30552–60 (2011).
26. Plat, A., Kluskens, L. D., Kuipers, A., Rink, R. & Moll, G. N. Requirements of the engineered leader peptide of nisin for inducing modification, export, and cleavage. *Appl. Environ. Microbiol.* **77,** 604–11 (2011).
27. Plat, A., Kuipers, A., Rink, R. & Moll, G. N. Mechanistic aspects of lanthipeptide leaders. *Curr. Protein Pept Sci.* **14,** 85–96 (2013).
28. Qiao, M. & Saris, P. E. Evidence for a role of NisT in transport of the lantibiotic nisin produced by *Lactococcus lactis N8*. *FEMS Microbiol. Lett.* **144,** 89–93 (1996).
29. Garg, N., Salazar-Ocampo, L. M. & van der Donk, W. A. *In vitro* activity of the nisin dehydratase NisB. *Proc. Natl. Acad. Sci. USA* **110,** 7258–63 (2013).
30. Koponen, O. *et al.* NisB is required for the dehydration and NisC for the lanthionine formation in the post-translational modification of nisin. *Microbiology* **148,** 3561–8 (2002).
31. Karakas Sen, A. *et al.* Post-translational modification of nisin. The involvement of NisB in the dehydration process. *Eur. J. Biochem.* **261,** 524–32 (1999).
32. Qiao, M. *et al.* Regulation of the nisin operons in *Lactococcus lactis N8*. *J. Appl. Bacteriol.* **80,** 626–34 (1996).
33. Ortega, M. A. *et al.* Structure and mechanism of the tRNA-dependent lantibiotic dehydratase NisB. *Nature* **517,** 509–12 (2015).
34. Li, B. & van der Donk, W. A. Identification of essential catalytic residues of the cyclase NisC involved in the biosynthesis of nisin. *J. Biol. Chem.* **282,** 21169–75 (2007).
35. Li, B. *et al.* Structure and mechanism of the lantibiotic cyclase involved in nisin biosynthesis. *Science* **311,** 1464–7 (2006).
36. Siegers, K., Heinzmann, S. & Entian, K. D. Biosynthesis of lantibiotic nisin. Posttranslational modification of its prepeptide occurs at a multimeric membrane-associated lanthionine synthetase complex. *J. Biol. Chem.* **271,** 12294–301 (1996).
37. Ortega, M. A. *et al.* Structure and tRNA Specificity of MibB, a Lantibiotic Dehydratase from Actinobacteria Involved in NAI-107 Biosynthesis. *Cell. chemical. biology* **23,** 370–80 (2016).
38. Khusainov, R., Heils, R., Lubelski, J., Moll, G. N. & Kuipers, O. P. Determining sites of interaction between prenisin and its modification enzymes NisB and NisC. *Mol. Microbiol.* **82,** 706–18 (2011).
39. Kluskens, L. D. *et al.* Post-translational modification of therapeutic peptides by NisB, the dehydratase of the lantibiotic nisin. *Biochemistry* **44,** 12827–34 (2005).
40. Rink, R. *et al.* NisC, the cyclase of the lantibiotic nisin, can catalyze cyclization of designed nonlantibiotic peptides. *Biochemistry* **46,** 13179–89 (2007).
41. Rink, R. *et al.* Lantibiotic structures as guidelines for the design of peptides that can be modified by lantibiotic enzymes. *Biochemistry* **44,** 8873–82 (2005).

42. Konarev, P. V., Volkov, V. V., Sokolova, A. V., Koch, M. H. J. & Svergun, D. I. PRIMUS: a Windows PC-based system for small-angle scattering data analysis. *J. Appl. Crystallogr.* **36,** 1277–1282 (2003).
43. Franke, D. & Svergun, D. I. DAMMIF, a program for rapid *ab-initio* shape determination in small-angle scattering. *J. Appl. Crystallogr.* **42,** 342–346 (2009).
44. Kozin, M. B. & Svergun, D. I. Automated matching of high- and low-resolution structural models. *J. Appl. Crystallogr.* **34,** 33–41 (2001).
45. Khusainov, R. & Kuipers, O. P. When the leader gets loose: *in vivo* biosynthesis of a leaderless prenisin is stimulated by a trans-acting leader peptide. *Chembiochem* **13,** 2433–8 (2012).
46. Kuipers, A., Meijer-Wierenga, J., Rink, R., Kluskens, L. D. & Moll, G. N. Mechanistic dissection of the enzyme complexes involved in biosynthesis of lacticin 3147 and nisin. *Appl. Environ. Microbiol.* **74,** 6591–7 (2008).
47. AlKhatib, Z. *et al.* Lantibiotic immunity: inhibition of nisin mediated pore formation by NisI. *PLoS One* **9,** e102246 (2014).
48. Laemmli, U. K. Cleavage of structural proteins during the assembly of the head of bacteriophage *T4. Nature* **227,** 680–5 (1970).
49. Towbin, H., Staehelin, T. & Gordon, J. Electrophoretic transfer of proteins from polyacrylamide gels to nitrocellulose sheets: procedure and some applications. *Proc. Natl. Acad. Sci. USA* **76,** 4350–4 (1979).
50. Burnette, W. N. "Western blotting": electrophoretic transfer of proteins from sodium dodecyl sulfate–polyacrylamide gels to unmodified nitrocellulose and radiographic detection with antibody and radioiodinated protein A. *Anal. Biochem.* **112,** 195–203 (1981).
51. Petoukhov, M. V. *et al.* New developments in the ATSAS program package for small-angle scattering data analysis. *J. Appl. Crystallogr.* **45,** 342–350 (2012).
52. Guinier, A. Diffraction of x-rays of very small angles-application to the study of ultramicroscopic phenomenon. *Annales de Physique* **12,** 161–237 (1939).
53. Svergun, D. I. Determination of the Regularization Parameter in Indirect-Transform Methods Using Perceptual Criteria. *J. Appl. Crystallogr.* **25,** 495–503 (1992).
54. Petoukhov, M. V. & Svergun, D. I. Global rigid body modeling of macromolecular complexes against small-angle scattering data. *Biophys. J.* **89,** 1237–1250 (2005).

Acknowledgements

We thank the EMBL-Lab Outstation Grenoble for the local support as well as the whole team of BM-29 beamline at the ESRF (Grenoble). We also thank Christine Tölzer (Institute of Biochemistry, University of Cologne, Germany) for helping with the SAXS evaluation and Dr. Gert Moll (Lanthiopharma, Groningen, The Netherlands) for his kind gift of antibodies. The Crystal and X-ray facility of the Heinrich Heine University is acknowledged for their support throughout the project. This work was supported by the DFG (grant Schm1279/13-1) to L.S.

Author Contributions

J.R., A.A. and R.C. performed the experiments, J.R., A.A., S.H.J.S. and L.S. designed the experiments, J.R., S.H.J.S. and L.S. evaluated the data and J.R., S.H.J.S. and L.S. wrote the manuscript.

Additional Information

Supplementary information accompanies this paper at http://www.nature.com/srep

Competing financial interests: The authors declare no competing financial interests.

How to cite this article: Reiners, J. *et al.* Stoichiometry and structure of a lantibiotic maturation complex. *Sci. Rep.* **7**, 42163; doi: 10.1038/srep42163 (2017).

Publisher's note: Springer Nature remains neutral with regard to jurisdictional claims in published maps and institutional affiliations.

Supplementary material

Stoichiometry and structure of a lantibiotic maturation complex

Jens Reiners, André Abts, Rebecca Clemens, Sander H. J. Smits and Lutz Schmitt*

Institute of Biochemistry, Heinrich-Heine-University Duesseldorf, Universitaetsstraße 1, 40225 Duesseldorf, Germany

Figure S1: **Schematic overview of the nisin maturation process**. **I)** The leader peptide is shown on the top and the highly conserved -FNLD- box is highlighted by a red box. The unmodified prenisin peptide represents the ribosomally synthesized peptide. **II)** NisB dehydrates specific serine and threonine residues (grey) in the core peptide. The final peptide is called dehydrated prenisin peptide, which contains the dehydrated amino acids dehydroalanine (dha) and dehydrobutyrine (dhb). **III)** These dehydrated amino acid residues get linked via NisC to C-terminal located cysteine residues (brown), resulting in the modified prenisin peptide. In the core peptide one lanthionine ring A (orange) and four (methyl)-lanthionine rings B-E (red) are present. **IV)** After introduction of the post-translational modifications the modified prenisin peptide is secreted via NisT across the cytoplasmic membrane and processed by the serine protease NisP. The modified prenisin peptide is cleaved into the leader peptide and mature nisin. Modified from [1].

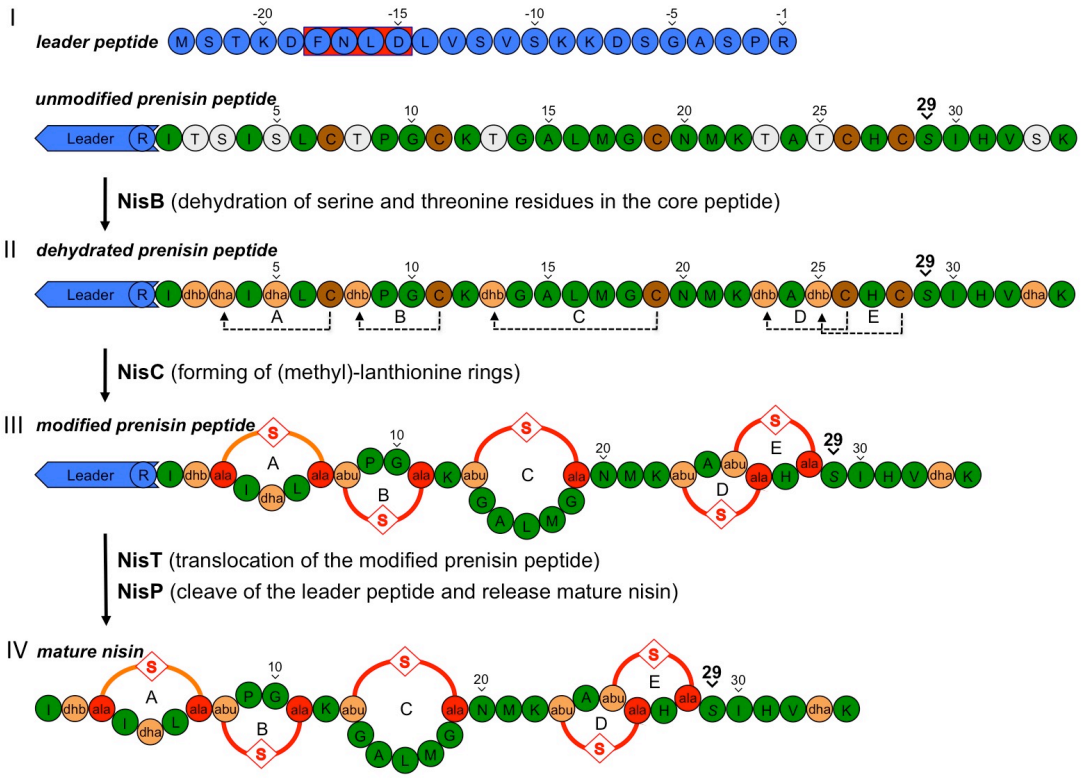

Figure S2: **SDS-PAGE analysis of the purification process of NisC and NisB, respectively**. **(A) NisB purification:** Lane M: protein marker. Lane 1: Crude extract of *L. lactis* cells expressing NisB-His_6. Lane 2: Flow through of the IMAC column. Lane 3: Combined IMAC elution fractions containing NisB-His_6. Lane 4: NisB-His_6 elution fraction after SEC. **(B) NisC purification:** Lane M: protein marker. Lane 1: Crude extract of His_6-NisC expressing *E. coli* cells. Lane 2: IMAC flow through. Lane 3: Combined His_6-NisC IMAC elution fractions. Lane 4: His_6-NisC elution fraction after SEC. Lane 5: Tag-free NisC after thrombin treatment. **(C)** Molecular weight determination of NisB using MALS-SEC: In black the elution profile of a purified NisB sample analyzed with MALS-SEC is shown. The observed molecular weight of 237.5 ± 0.3 kDa fits very well with the theoretical molecular weight of a NisB dimer 236.6 kDa (www.expasy.org). **(D)** The black elution profile represents the MALS-SEC analysis of a purified NisC sample. A molecular weight of 48.1 ± 0.5 kDa was determined, which is in-line with the theoretical calculated molecular weight of a cleaved NisC monomer of 48.5 kDa (www.expasy.org).

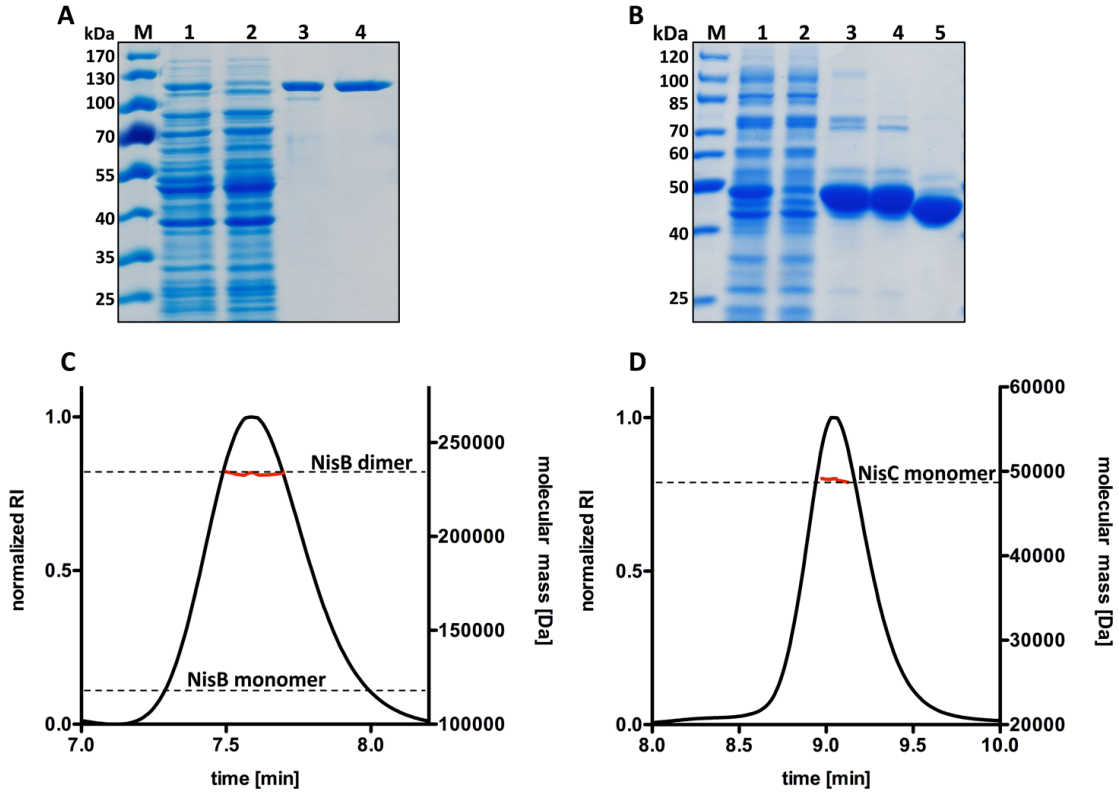

Figure S3: **Page-Blue (Thermo Fischer) stained Tricine SDS-PAGE [2] analysis of the purified prenisin peptide variants**: All variants were purified using cation exchange chromatography as previously described [1,3]. The final concentration of the purified peptide variants was determined by subjecting the prenisin peptide variants to HPLC analysis [3]. Due to space limitation several gels have been made, which are indicated by black boxes and vertical lines.

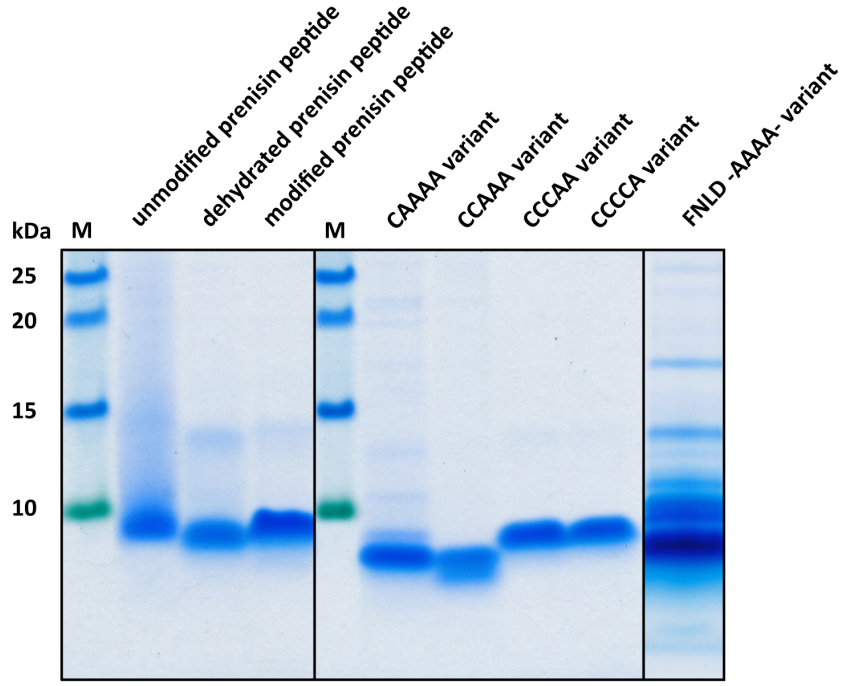

NisB and NisC substrate binding

With the MALS-SEC analysis we could show the substrate binding from NisB and NisC. The prenisin binding to NisC resulted in a changes elution time due to a change in the hydrodynamic radius (Figure S4 A, black line) in comparison to ligand-free NisC (Figure S4 A, dashed line). The observed molecular weight of ligand-free NisC was 48.1 ± 0.5 kDa. After incubation of unmodified prenisin peptide with NisC, we observed a molecular weight of 54.5 ± 0.6 kDa, which fits to NisC with one prenisin bound (theoretical molecular weight of 54.3 kDa). NisB showed no difference in the elution profile, but MALS-SEC analysis highlighted a molecular weight of 237.5 ± 0.3 kDa (Figure S4 B, blue line) for NisB and 241.9 ± 0.4 kDa for the NisB-NisA bound complex. This indicated that one unmodified prenisin peptide molecule was bound to a NisB dimer (theoretical molecular weight of 242.2 kDa). Thus, these results demonstrate a 1:1 stoichiometry for a monomer of NisC with one prenisin molecule, and also that a dimer of NisB binds one prenisin molecule. The results are in-line with previous *in vitro* studies [1,3], but in contrast to the NisB structure [4], which showed two leader peptide fragments bound within the NisB dimer.

Figure S4: **MALS-SEC analysis of the mixed protein samples consisting of NisB or NisC, in the presence and absence of prenisin peptide**. **(A)** The dashed black graph shows the elution profile of 20 µM NisC resulting in a molecular weight of 48.1 ± 0.5 kDa (blue line). The analysis of 20 µM NisC and 200 µM unmodified prenisin peptide is shown as the black graph, revealing an apparent molecular weight of 54.5 ± 0.6 kDa (red line) of the formed complex. **(B)** The dashed black graph represents the elution profile of 20 µM NisB resulting in a molecular weight of 237.5 ± 0.3 kDa (blue line). The analysis of 20 µM NisB and 200 µM unmodified prenisin peptide is shown as the black graph revealing an apparent molecular weight of 241.9 ± 0.4 kDa (red line) of the formed complex.

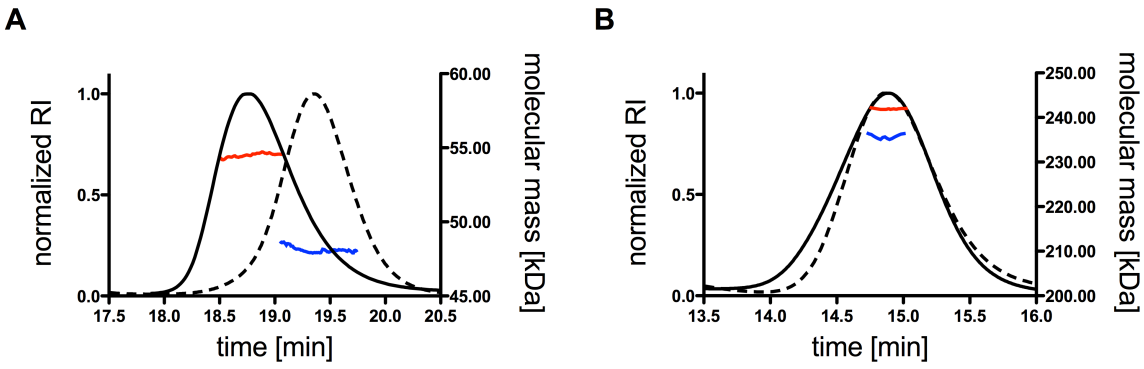

Figure S5**: SDS-PAGE analysis of fractions of size exclusion chromatograms of NisB or NisC sample as well as a NisB / NisC sample**.

The corresponding SDS gels from the size exclusion chromatography (Superdex 200 PC 3.2) fractions are shown in **(A)** 20 µM NisB (blue profile). **(B)** 160 µM NisC (red profile) **(C)** 20 µM NisB and 160 µM NisC (black profile). As observed, NisB and NisC are detected in different fractions of the SEC elution profile. The elution profiles of NisB and NisC remain unchanged in the case of the simultaneous injection of both proteins (C) indicating no complex formation. For the analysis of complex formation the fraction highlighted by a red box was used in SDS page analysis and subsequent Western blot analysis (Figure 2a).

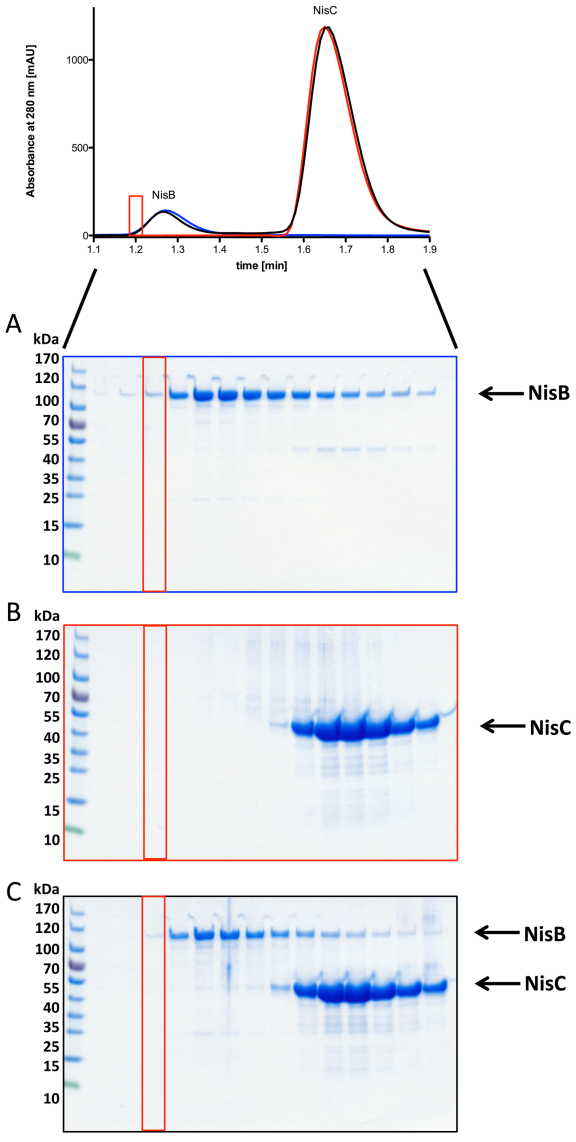

Figure S6: **MALS-SEC analysis of the pre-saturated protein samples consisting of NisB or NisC, in the presence of prenisin peptide**. **(A)** The black graph shows the elution profile of 20 µM NisB saturated with unmodified prenisin peptide and incubated with 20 µM NisC, Resulting in a molecular weight of 263.8 ± 0.3 kDa (red line). **(B)** The analysis of 20 µM NisC saturated with unmodified prenisin peptide and incubated with 20 µM NisB is shown with the black graph, revealing an apparent molecular weight of 247.1 ± 0.4 kDa (red line).

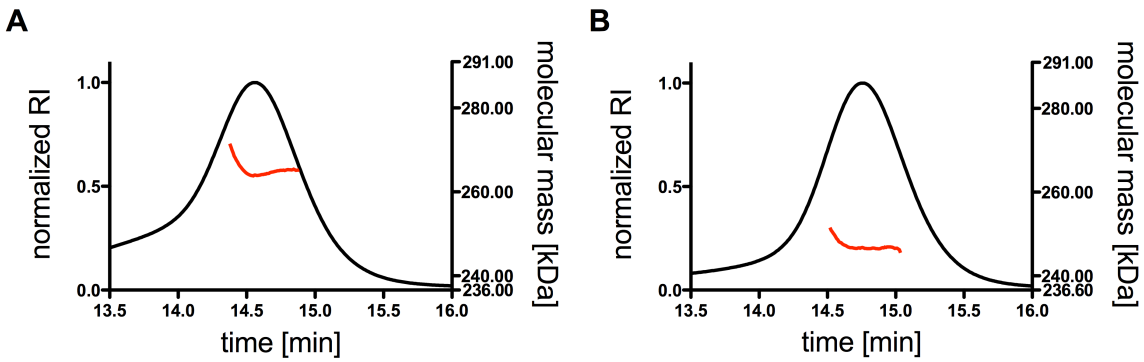

Figure S7: **SDS-PAGE analysis showing the results of the dependency of the leader and core peptides on complex formation**. The corresponding SDS gels from the size exclusion chromatography (Superdex 200 PC 3.2) fractions are shown. **(A)** 20 µM NisB and 160 µM NisC in the presence of 200 µM of the unmodified prenisin peptide. **(B)** 20 µM NisB and 160 µM NisC in the presence of 200 µM of the dehydrated prenisin peptide. **(C)** 20 µM NisB and 160 µM NisC in the presence of 200 µM of the modified prenisin peptide. **(D)** 20 µM NisB and 160 µM NisC in the presence of 200 µM of the –FNLD- box variant (-AAAA-) mutant prenisin. Red-boxed elution fractions were used for Western blot analysis (Fig. 2b-c).

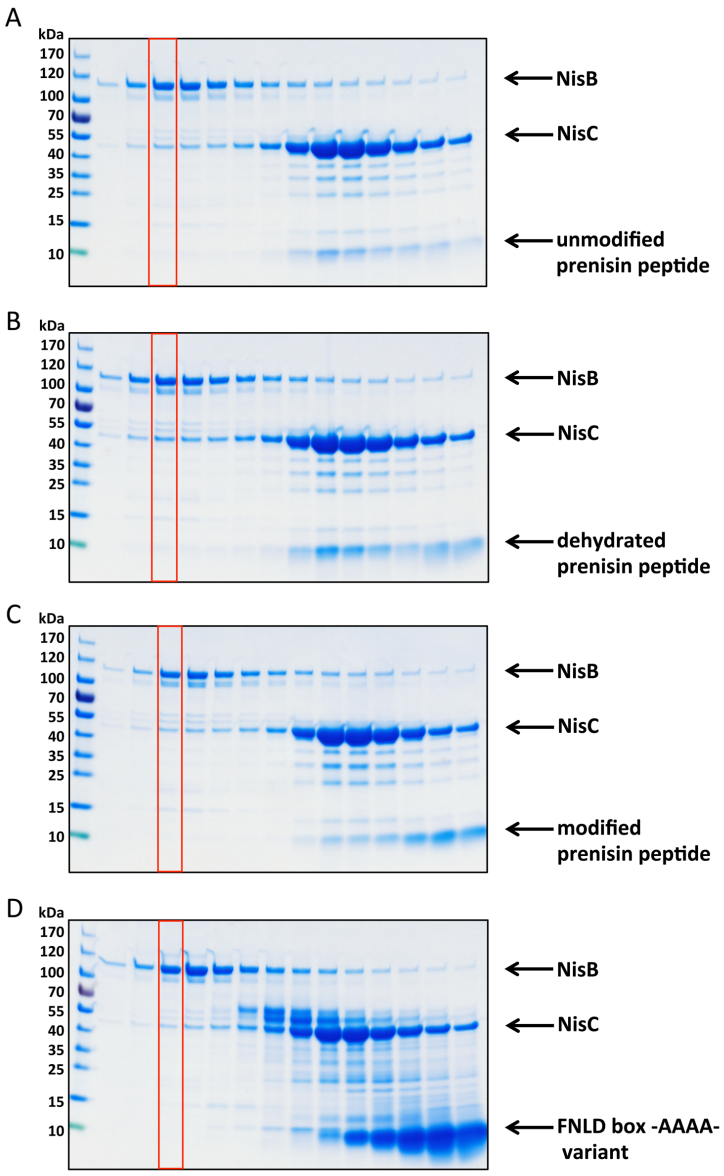

Figure S8: **SDS-PAGE analysis showing the influence in varying the number of installed (methyl)-lanthionine rings**. The corresponding SDS gels from the size exclusion chromatography (Superdex 200 PC 3.2) fractions are shown. **(A)** 20 µM NisB and 160 µM NisC in the presence of 200 µM of the CAAAA variant. **(B)** 20 µM NisB and 160 µM NisC in the presence of 200 µM of the CCAAA variant. **(C)** 20 µM NisB and 160 µM NisC in the presence of 200 µM of the CCCAA variant. **(D)** 20 µM NisB and 160 µM NisC in the presence of 200 µM of the CCCCA variant. Red-boxed elution fractions were used for the Western blot analysis (Fig. 2c).

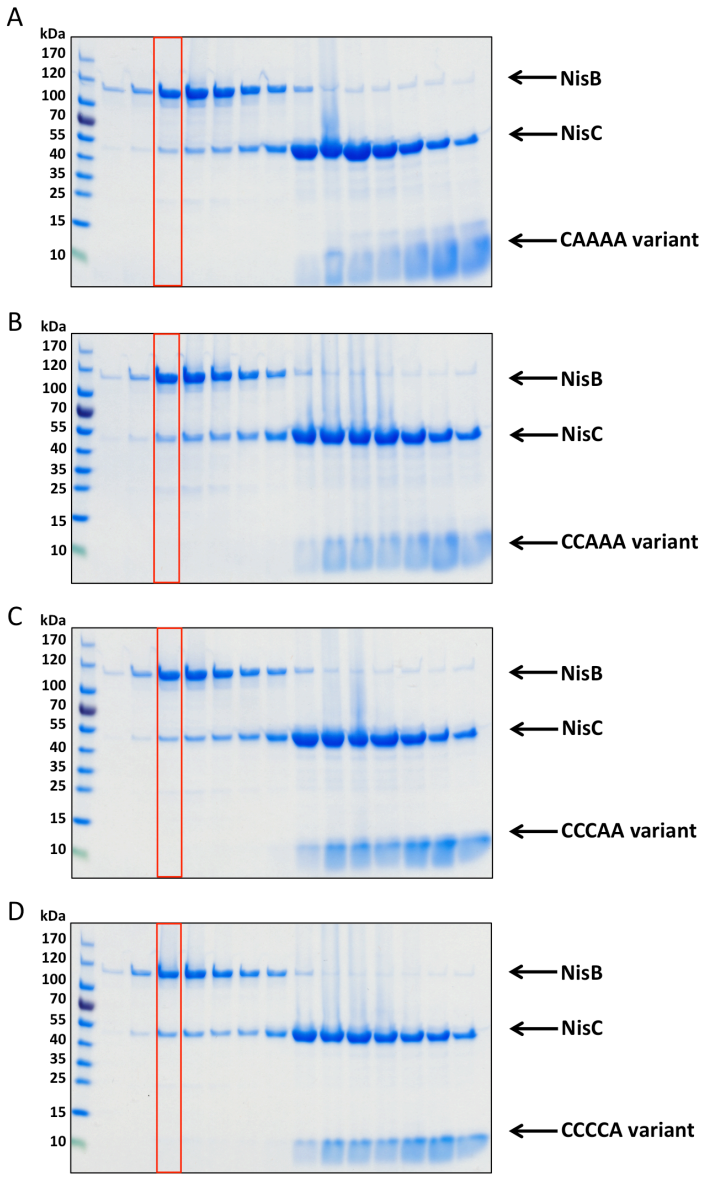

Figure S9: **SAXS plots of the different Proteins.** Experimental curves are shown in black dots and the *ab-initio* model fit as red line. Displayed is the intensity as a function of momentum transfer s. **(A)** Plot NisB, DAMMIF fit. **(B)** NisB saturated with dehydrated prenisin peptide, DAMMIF fit. **(C)** NisC, DAMMIF fit. **(D)** NisBCA complex, DAMMIF fit. **(E)** NisBCA complex, SASREF fit.

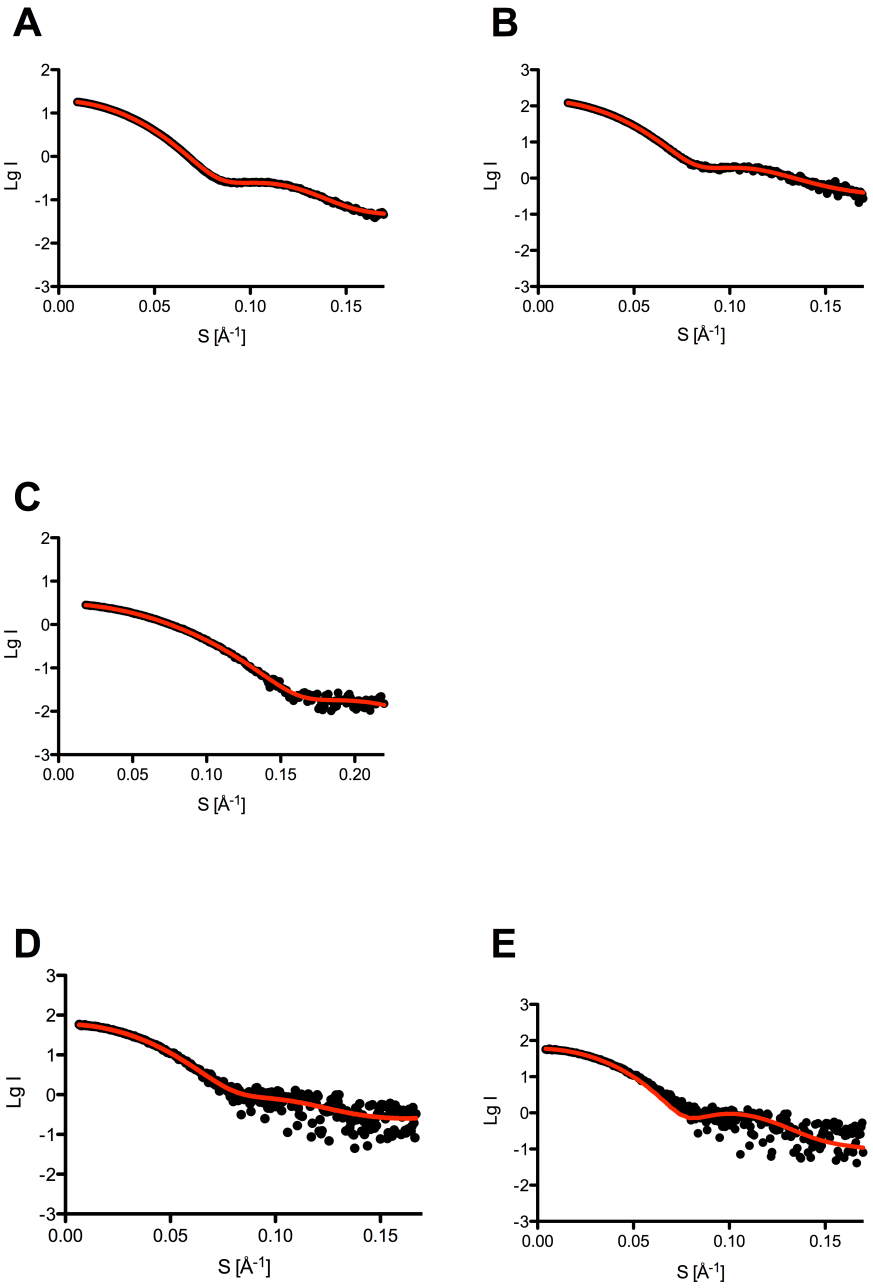

Table S1: **MALS-SEC data summarizing the molecular weight (M_w) of the analysis of complex forming for the different prenisin peptide variants.** For the analysis, we kept the concentration of NisB (20 µM) and the different prenisin peptides (200µM) constant. We only changed the concentration of NisC from 0 µM up to 160 µM. The theoretical molecular weight of a NisB dimer is calculated to 236.6 kDa, 48.5 kDa for a tag-free NisC monomer and 5.9 kDa for the unmodified prenisin peptide. All measurements were done at least in triplicate. n.d. = not determined.

NisC concentration [µM]	without prenisin peptide	M_W nisin maturation complex [kDa]			
		unmodified	dehydrated	modified	FNLD Variant
0	236.4 ± 0.3	n. d.	241.9 ± 0.4	n.d.	n.d.
10	n.d.	247.3 ± 1.2	249.3 ± 0.5	n.d.	n.d.
20	n.d.	256.6 ± 0.8	249.3 ± 1.1	n.d.	n.d.
40	237.5 ± 0.3	268.9 ± 1.3	260.3 ± 0.3	237.5 ± 0.8	n.d.
60	n.d.	276.8 ± 1.0	270.4 ± 0.5	n.d.	n.d.
80	238.1 ± 0.3	291.2 ± 1.1	275.5 ± 0.5	n.d.	n.d.
120	n.d.	287.2 ± 0.7	292.7 ± 0.8	n.d.	n.d.
160	238.7 ± 1.2	293.6 ± 1.2	291.2 ± 0.9	250.4 ± 0.7	248.0 ± 0.9

Table S2: **Theoretical Molecular weight from different ratios of NisB, NisC and NisA.**

The theoretical molecular weight of a NisB dimer is calculated to 236.6 kDa, 48.5 kDa for a tag-free NisC monomer and 5.9 kDa for the unmodified prenisin peptide

Ratio			
NisB	NisC	NisA	Molecular weight [kDa]
1	1	1	172.7
1	2	1	221.2
1	1	2	178.6
1	2	2	227.1
2	1	2	296.9
2	1	1	291.0
2	2	1	339.5
2	2	2	345.4

Table S3: **Overall SAXS Data**

Data collection parameters				
Detector	PILATUS 1 M			
Detector distance (m)	2.867			
Beam size (µm x µm)	700 x 700			
Wavelength (Å)	0.99			
Sample environment	Quartz glass capillary, 1 mm ø			
s range (nm^{-1})‡	0.025–5.0			
Temperature (°C)	4			
Exposure time per frame (s)	1.5 s continuously*			
Mode of measurement	online SEC			
Sample	**NisB**	**NisBA**	**NisC**	**NisBCA**
Structural parameters				
I(0) from P(r)	19.07	141.10	3.0	58.79
R_g (real-space from P(r)) (nm)	4.29	4.33	2.41	4.42
I(0) from Guinier fit	19.20	142.14	3.00	58.94
s-range for Guinier fit (nm^{-1})	0.12 - 0.30	0.16 - 0.33	0.21 - 0.54	0.14 - 0.32
R_g (from Guinier fit, AutoR_g) (nm)	4.37	4.39	2.42	4.45
D_{max} (nm)	13.44	15.06	8.16	15.66
POROD volume estimate (nm^3)	382.82	410.47	82.5	440.17
Molecular mass (kDa)				
From POROD volume [kDa]	239.26	256.54	51.56	275.1
From I(0)	n.a.			
From sequence	236.6	242.4	48.5	291
Software				
Primary data reduction	PRIMUS [5]			
Data processing	GNOM [6]			
Ab initio modelling	DAMMIF [7]			DAMMIF[7]/SASREF[8]
Evaluation, averaging of models	DAMAVER [9]			
Superimposing	SUPCOMB [10]			
Model visualization	PyMOL			

‡s = $4\pi\sin(\theta)/\lambda$, 2θ – scattering angle, λ – Xray-wavelength.* 0.5 s dead time between frames, n.a. not applicable.

Literature

1. Mavaro, A. et al. Substrate recognition and specificity of the NisB protein, the lantibiotic dehydratase involved in nisin biosynthesis. *J. Biol. Chem.* **286**, 30552-60 (2011).
2. Schagger, H. Tricine-SDS-PAGE. *Nat Protoc.* **1**, 16-22 (2006).
3. Abts, A., Montalban-Lopez, M., Kuipers, O.P., Smits, S.H. & Schmitt, L. NisC binds the FxLx motif of the nisin leader peptide. *Biochemistry* **52**, 5387-95 (2013).
4. Ortega, M.A. et al. Structure and mechanism of the tRNA-dependent lantibiotic dehydratase NisB. *Nature* **517**, 509-12 (2015).
5. Konarev, P.V., Volkov, V.V., Sokolova, A.V., Koch, M.H.J. & Svergun, D.I. PRIMUS: a Windows PC-based system for small-angle scattering data analysis. *J. Appl. Crystallogr.* **36**, 1277-1282 (2003).
6. Svergun, D.I. Determination of the Regularization Parameter in Indirect-Transform Methods Using Perceptual Criteria. *J. Appl. Crystallogr.* **25**, 495-503 (1992).
7. Franke, D. & Svergun, D.I. DAMMIF, a program for rapid *ab-initio* shape determination in small-angle scattering. *J. Appl. Crystallogr.* **42**, 342-346 (2009).
8. Petoukhov, M.V. & Svergun, D.I. Global rigid body modeling of macromolecular complexes against small-angle scattering data. *Biophys. J.* **89**, 1237-1250 (2005).
9. Volkov, V.V. & Svergun, D.I. Uniqueness of ab initio shape determination in small-angle scattering. *J. Appl. Crystallogr.* **36**, 860-864 (2003).
10. Kozin, M.B. & Svergun, D.I. Automated matching of high- and low-resolution structural models. *J. Appl. Crystallogr.* **34**, 33-41 (2001).

3.3 Chapter III

Title: Impact of the nisin modification machinery on the transport kinetics of NisT

Authors: Marcel Lagedroste, **Jens Reiners**, Sander H. J. Smits & Lutz Schmitt

Published in: Scientific Reports (2020)
Impact factor: 4.38

Own proportion of this work: 15%

- Purification of NisB, NisB and pre-nisin A variants

SCIENTIFIC REPORTS
nature research

OPEN

Impact of the nisin modification machinery on the transport kinetics of NisT

Marcel Lagedroste[1], Jens Reiners[1,2], Sander H. J. Smits[1] & Lutz Schmitt[1]✉

Lanthipeptides are ribosomally synthesized and post-translationally modified peptides containing dehydrated amino acids and (methyl-)lanthionine rings. One of the best-studied examples is nisin produced by *Lactococcus lactis*. Nisin is synthesized as a precursor peptide comprising of an N-terminal leader peptide and a C-terminal core peptide. Amongst others, the leader peptide is crucial for enzyme recognition and acts as a secretion signal for the ABC transporter NisT that secretes nisin in a proposed channeling mechanism. Here, we present an in vivo secretion analysis of this process in the presence and absence of the nisin maturation machinery, consisting of the dehydratase NisB and the cyclase NisC. Our determined apparent secretion rates of NisT show how NisB and NisC modulate the transport kinetics of NisA. Additional in vitro studies of the detergent-solubilized NisT revealed how these enzymes and the substrates again influence the activity of transporter. In summary, this study highlights the pivotal role of NisB for NisT in the secretion process.

Abbreviations

ABC transporter	ATP binding cassette transporter
CP	Core peptide
Dha	Didehydroalanine
Dhb	Didehydrobutyrine
Lan	Lanthionine
LP	Leader peptide
MeLan	Methyl-lanthionine
MS	Mass spectrometry
NBD	Nucleotide-binding domain
NisA	Precursor peptide of nisin
NisB	Dehydratase of nisin precursor peptide
NisC	Cyclase of nisin precursor peptide
NisT	Transporter of nisin precursor peptide
PTM	Post-translational modificationn
RP-HPLC	Reverse-phase HPLC
SEC	Size-exclusion chromatography

Many natural products (NP) produced as secondary metabolites by microorganisms can be used as pharmaceuticals (e.g. as anticancer, antibacterial or antiviral drugs)[1]. One class of these NPs are ribosomally synthesized and post-translationally modified peptides (RiPPs). The RiPP family of lanthipeptides, especially those with antimicrobial activity (lantibiotics), is gaining interest as a potential alternative for antibiotics to treat harmful multidrug resistance strains such as methicillin-resistant *Staphylococcus aureus* or vancomycin-resistant *Enterococci*[2,3].

Lanthipeptides (LanA) are produced as precursor peptides with an N-terminal leader peptide (LP) and a C-terminal core peptide (CP)[4]. The LP serves as a signal sequence and recognition site for the modification enzymes and the export protein[5–8]. Furthermore, the LP keeps the modified peptide (mLanA) inactive in the cytosol[9], while the post-translational modifications (PTM) are installed within the CP and not found in the LP[10].

[1]Institute of Biochemistry, Heinrich Heine University Düsseldorf, Universitätsstr. 1, 40225 Düsseldorf, Germany. [2]Present address: Center for Structural Studies, Heinrich Heine University Düsseldorf, Universitätsstr. 1, 40225 Düsseldorf, Germany. ✉email: lutz.schmitt@hhu.de

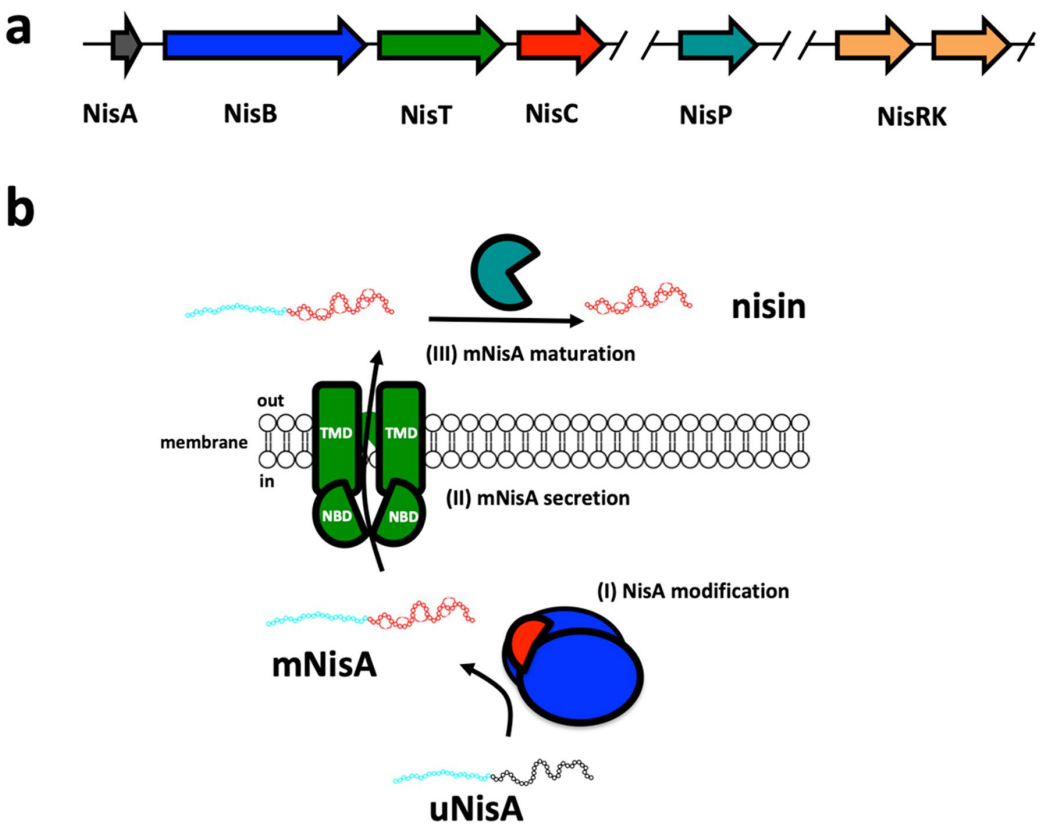

Figure 1. Scheme of nisin modification and secretion system. (**a**) The lanthipeptide nisin (NisA, grey) operon encodes for the modification and secretion enzymes. (**b**) The enzyme NisB (blue) catalyzes the dehydration reaction of unmodified NisA (uNisA), whereas NisC (red) catalyzes the thioether ring formation resulting in modified NisA (mNisA). The ABC transporter NisT (green) translocates mNisA across the membrane to the exterior. Finally, the mature peptide is processed by the serine protease NisP (turquoise) and active nisin is released. The two-component system (TCS) consisting of NisR and NisK (orange) is controlling the expression of these proteins. Please note, that the operon is partial represented and shows only proteins responsible for nisin maturation and secretion.

These PTM's are unusual amino acids such as didehydroalanine (Dha), didehydrobutyrine (Dhb) or (methyl-) lanthionine ((Me)Lan)[11,12].

Nisin is produced by the Gram-positive bacterium *Lactococcus lactis* as a precursor peptide (NisA), where the genes for modification, secretion and maturation enzymes are located on one operon (Fig. 1a)[8]. First, the ribosomally synthesized NisA is modified by the modification enzymes NisB and NisC (Fig. 1b, I). Within the unmodified NisA serine and threonine residues are dehydrated by the dehydratase NisB via a tRNA-depended glutamylation and elimination reaction to Dha and Dhb residues[13–15]. Subsequently, the dehydrated amino acid are coupled to neighboring cysteine residues via a Michael-like addition catalyzed stereo- and regio-specifically by the cyclase NisC[16–18]. The reaction of both enzymes follows an alternating mode with a N- to C-terminus directionality yielding (Me)Lan residues[19,20]. Next, the exporter protein NisT secretes the modified NisA (mNisA) to the exterior (Fig. 1b, II)[21]. Finally, the LP is cleaved by the extracellularly located serine protease NisP and active nisin is released (Fig. 1b, III)[10].

The lanthipeptide exporters (LanT) belong to the superfamily of ABC transporters, which are found in all kingdoms of life[22]. Bacterial ABC transporters are composed of mainly two domains[23]. One domain is the transmembrane domain (TMD) important for substrate translocation. The other domain is the nucleotide-binding domain (NBD), which binds and hydrolyses ATP to energize conformational changes used for substrate translocation. Some lanthipeptide exporters harbor an additional domain, a C39 peptidase domain. This domain is classified as a bacteriocin-processing endopeptidase[24] and we term this subfamily of transporters $LanT_{C39P}$.

All known lanthipeptide exporters function as dimers and translocation of the lanthipeptide is LP-dependent[5,25–27]. For some LanT/ $Lan_{C39P}T$ proteins it is proposed that the exporter and modification proteins assemble a multimeric enzyme complex at the membrane, which translocate the substrate to the exterior (e.g. nisin, subtilin and nukacin ISK-1)[28–30].

In 2004, it was shown that the secretion of nisin without the modification enzymes NisB, NisC and the protease NisP was possible[5]. In vivo studies on the secretion process expanded the knowledge on the nisin

modification and secretion system[31–34]. According to these studies the observed high secretion efficiency of NisA by NisBTC was explained by a 'channeling mechanism'[19,35]. Other studies focused on the application of the nisin modification machinery to produce nisin variants or lantibiotics and secrete them by NisT[36–39]. Despite the in vivo analysis of NisA secretion, a first analysis with labeled precursor peptides was performed and gave first insights into the kinetics of secretion[35]. Nevertheless, a systematic and quantitative analysis of the secretion mechanism by determining kinetic parameters for NisA translocation by NisT is still required.

In our study, we performed an in vivo and in vitro characterization of NisT to shed light on the secretion mechanism of NisA. We determined the kinetic parameters of NisA secretion by analyzing the supernatant of NisA secreting *L. lactis* strains via reverse-phase (RP-)HPLC. The resulting apparent secretion rate ($NisA \cdot NisT^{-1} \cdot min^{-1}$) of NisT was compared with the rate of the NisBTC system and demonstrated a large enhancement in the presence of the nisin modification machinery. The in vitro characterization of NisT is the first study revealing insights into the specific activity of a LanT lanthipeptide transporter and its modification enzymes as well as its substrate. In conclusion, we could demonstrate a direct enhancement of the secretion by the maturation enzymes and a bridging function of the dehydratase NisB for the interaction of NisC and NisT.

Results

In vivo secretion assay of NisA. To obtain further insights into the mechanism of lanthipeptide secretion, the NisA secretion level of the *L. lactis* strain NZ9000 was investigated in the presence and absence of the modification machinery. Here, the well-known nisin secretion and maturation system[19,31,35,37] was used to establish an in vivo secretion assay, where the supernatants were employed to determine the secretion level of NisA peptide via RP-HPLC analysis. In our study, we used the strain *L. lactis* NZ9000BTC (Table S1) producing fully modified NisA (mNisA) that is secreted by NisT. The secretion of other modification states of NisA can be analyzed by deletions of one of the modification enzymes or by creating inactive mutants. The mutation $NisC_{H331A}$ (strain $NZ9000BTC_{H331A}$) or the deletion of NisC (strain NZ9000BT) resulted in the secretion of dehydrated NisA (dNisA). Deletion of NisB (strain NZ9000TC) or NisB and NisC (strain NZ9000T) resulted in the secretion of unmodified NisA (uNisA). The deletion of NisT (strain NZ9000BC) or the mutation of the histidine of the H-loop in the NBD of NisT (strain $NZ9000BT_{H551A}C$) totally abolished NisA secretion (Fig. 2). The latter two strains were defined as the background of the secretion analysis, in which NisA is expressed but not secreted. For the secretion analysis, all *L. lactis* strains were grown in minimal medium at 30 °C and after induction samples of supernatants were analyzed every hour (0–6 h). Subsequently, the supernatant was analyzed by RP-HPLC (Fig. 2, Figure S1) and the peak area of NisA peptides was determined to calculate the amount of peptide. The amount of secreted peptide was plotted against time and a non-linear fitting was applied to determine V_{max} (maximal amount of peptide; in nmol) and $K_{0.5}$ (time point of 50% secreted peptide in min). These kinetic parameters allowed a direct comparison of the secretion efficiency of the different *L. lactis* strains employed in this study.

Strain NZ9000BTC had a V_{max} value of 534 ± 44 nmol and a $K_{0.5}$ of 134 ± 12 min. It secreted NisA most efficiently in comparison to the other strains (Fig. 2, Table S3). In the cytoplasmic fraction of this strain only a small amount of mNisA was detected by Western blot at hours 2, 3 and 4 after induction (Figure S2a). This finding is similar to the previously published data for the nisin secretion and modification system[35].

Mutation of the H-loop at position 551 to alanine in the NBD of the ABC transporter NisT abolished the secretion of mNisA and no peptide was detected in the supernatant (Fig. 2, Figure S2c). The same result was observed for the strain NZ9000BC (Figure S2g). Here, high amounts of mNisA were detected in the cytoplasmic fraction of the strains $NZ9000BT_{H551A}C$ and NZ9000BC (Figure S1c/g). Thus, *nisT* deletion and the H-loop mutation both abolished mNisA secretion.

Deletion of *nisC* (strain NZ9000BT) resulted in a lower secretion efficiency of dNisA and the V_{max} value of 247 ± 15 nmol and a $K_{0.5}$ of 152 ± 9 min (Fig. 2, Table S3). The amount of secreted dNisA was reduced by a factor of 2.2 in comparison to mNisA (strain NZ9000BTC). Interestingly, the mutation of the catalytic histidine residue (H331) to alanine[40] reduced the V_{max} value (168 ± 16 nmol) by factor of 3.2. The $K_{0.5}$ value increased to 200 ± 16 min (Fig. 2). The analysis of the cytoplasmic fraction of the strain $NZ9000BTC_{H331A}$ showed a higher amount of dNisA inside the cell, which only slowly decreased over the time (Figure S2b). Slightly lower amounts of dNisA were observed in the cytoplasmic fraction of NZ9000BT (Figure S2d).

Strain NZ9000T, which was obtained after the deletion of *nisB* and *nisC*, had a slightly reduced V_{max} value of 137 ± 30 nmol with a $K_{0.5}$ of 144 ± 41 min (Fig. 2, Table S3). The secretion of uNisA was reduced by a factor of 3.9 compared to strain NZ9000BTC. The lowest amount of secreted peptide was determined in the supernatant of strain NZ9000TC with a V_{max} value of 38 ± 8 nmol. Here, a higher amount of uNisA was detected in the cytoplasmic fraction, whereas no peptide was observed in strain NZ9000T.

In all strains, NisB, NisC and NisT were detected in their corresponding fraction (cytoplasmic or membrane) (Figure S2a–g). The proteins NisB, NisC/$NisC_{H331A}$ and NisA were observed in the cytoplasmic fractions (except uNisA from the cytoplasm of NZ9000T). NisT was detected by Western blot in the membrane fraction of all strains (Figure S2a–g). In the case of mNisA expressing strains (NZ9000BTC, $NZ9000BT_{H551A}C$, and NZ9000BC) all proteins were detected by Western blot even at time point zero.

Determination of the apparent secretion rate of mNisA. We measured the apparent secretion rate ($V_{S\ app.}$) by an in vivo secretion assay. First, the amount of secreted mNisA at different time points was determined and plotted as nmol mNisA against time (Fig. 2). Second, the amount of the ABC transporter NisT was obtained by analyzing the membrane fraction of strains NZ9000BTC and NZ9000T at each time point by Western blot (Figure S3a,b). Here, known concentrations of purified NBD protein were used as a standard to determine the amount of NisT in pmol. Combining these data, the secretion rate of NisA molecules per NisT

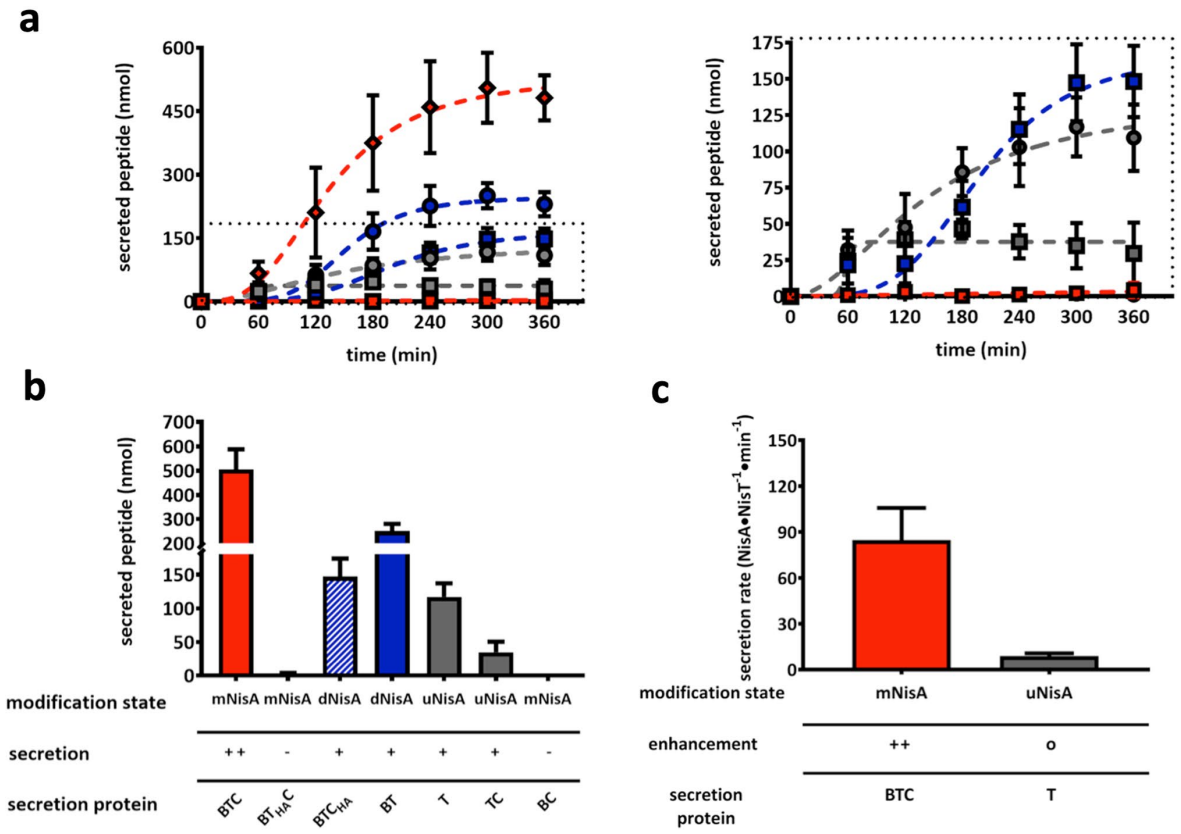

Figure 2. In vivo secretion assay of different *L. lactis* NZ9000 strains. (**a**) The supernatants of NisA secreting *L. lactis* NZ9000 strains was analyzed by RP-HPLC and the amount of NisA were determined. Amounts of secreted peptides (nmol) are plotted against time (min) and the resulting curves were fitted by an allosteric sigmoidal fit. Modified NisA (mNisA, red) was secreted by strain NZ9000BTC (red rhomb) and can be precluded by *nisT* deletion (strain NZ9000BC, clear dot) or an ATPase deficient mutant (NZ9000BT$_{H551A}$C, red square). Dehydrated NisA (dNisA, blue) was secreted by strains NZ9000BTC$_{H331A}$ (blue square) and NZ9000BT (blue dots), whereas unmodified NisA (uNisA, grey) was secreted by the strains NZ9000T (grey dots) and NZ9000TC (grey square). Dashed square shows a zoom-in on strains with lower secretion level. (**b**) The kinetic parameter of V_{max} (nmol) of secreted peptides was plotted as bars against the various secretion systems. (**c**) The secretion rate of NisA molecules per NisT molecule was plotted against time (min) and fitted by linear regression. The slope represented the secretion rate of NisA·NisT^{-1}·min^{-1} for the strains NZ9000BTC and NZ9000T. All data represent secretion experiments from at least five different transformants and are represented as means ± s.d. (n = 5). ++: WT secretion; o: low secretion; −: no secretion.

molecules was calculated. The plot of nmol·NisA·NisT^{-1} against time (min) was fitted by linear regression (Figure S3c). The slope of the linear regression corresponds to $V_{S\ app.}$ of NisA·NisT^{-1}·min^{-1}, which is 84.8 ± 21 for the strain NZ9000BTC (Fig. 2c, Figure S3c). A strongly reduced secretion rate was determined for the strain NZ9000T (8.8 ± 1.8) as described qualitatively previously[35]. The determined secretion rate thus clearly demonstrated an enhancement in the presence of the modification enzymes NisB and NisC.

Purification and basal ATPase activity of NisT, a class I lanthipeptide transporter. In order to determine the in vitro activity of a lanthipeptide ABC transporter, we purified NisT the exporter of the class I lanthipeptide nisin as a deca-histidine tagged protein variant (10HNisT). 10HNisT was homologously expressed in *L. lactis* NZ9000 and purified (Fig. 3a) after solubilization with the lipid-like surfactant Fos-choline-16 (FC-16, Anatrace) by immobilized metal ion affinity (IMAC) and size-exclusion chromatography (SEC). Similar to other membrane proteins, 10HNisT (72.5 kDa) showed a higher mobility on the SDS-PAGE gel and migrated at approximately 60 kDa. 10HNisT eluted as a homogeneous peak from SEC (Fig. 3a), subsequently the main elution fractions were further concentrated to 50 µM and used for ATPase activity assay.

For the ATPase activity assay, the detergent was exchanged to CYMAL5 (Anatrace) and the ATPase rate was expressed as specific ATPase rate (nmol·min^{-1}·mg^{-1}). The kinetic parameters of 10HNisT in detergent solution were determined and resulted in V_{max}, K_m and k_{cat} values for the transporter without its substrate (basal ATPase activity). The concentration of 10HNisT was kept constant (1 µM), whereas the concentration of ATP was varied

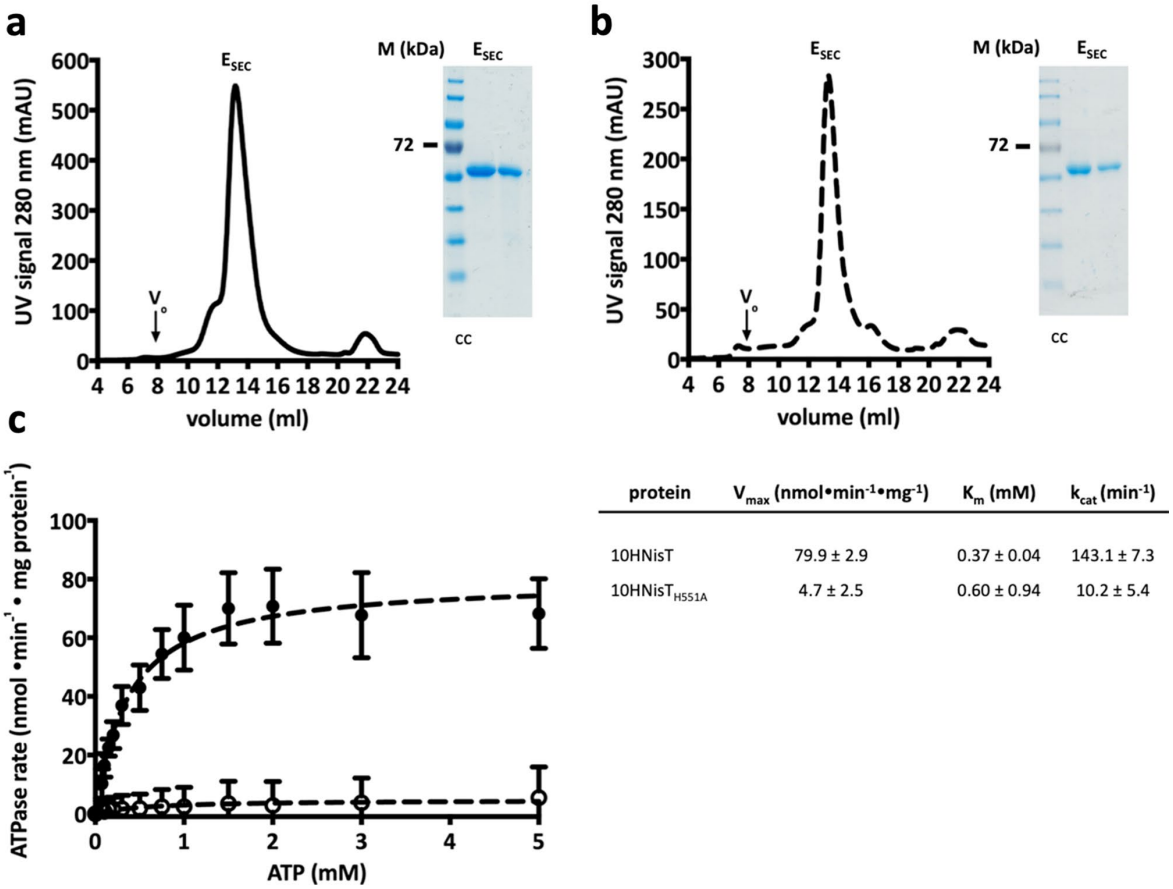

protein	V_{max} (nmol•min^{-1}•mg^{-1})	K_m (mM)	k_{cat} (min^{-1})
10HNisT	79.9 ± 2.9	0.37 ± 0.04	143.1 ± 7.3
10HNisT$_{H551A}$	4.7 ± 2.5	0.60 ± 0.94	10.2 ± 5.4

Figure 3. Purification and ATPase activity assay of NisT. (**a**) SEC chromatogram of 10HNisT (WT, black line) displayed a homogeneous peak (E_{SEC}) at 13 ml on a Superose 6 10/300 GL column (V_0: void volume of the column). Inset: A typical colloidal Coomassie (cc) stained SDS-PAGE gel shows a protein band between 55 and 72 kDa marker protein bands (M). (**b**) Purification of the H-loop mutant 10HNisT$_{H551A}$ (HA, dashed line) showed comparable results for SEC profile and SDS-PAGE gel (inset). (**c**) The specific ATPase rate (nmol·min^{-1}·mg protein^{-1}) of purified WT (black dot) and HA mutant (unfilled circle) was plotted against ATP concentration (mM) to determine kinetic parameters. The ATPase rate was fitted by Michaelis–Menten equation to determine V_{max} (nmol·min^{-1}·mg protein^{-1}), K_m (mM) and k_{cat} (min^{-1}). Activity assays were performed from five independent experiments with three replicates and are represented as means ± s.d. (n = 5).

from 0 to 5 mM and the reaction was stopped after 30 min. The basal ATPase rate of 10HTNisT had a V_{max} value of 79.9 ± 2.9 nmol·min^{-1}·mg^{-1}, a K_m value of 0.37 ± 0.04 mM resulting in a k_{cat} value of 143.1 ± 7.3 min^{-1} (Fig. 3c). As a control the H-loop mutant of 10HNisT (10HNisT$_{H551A}$; HA-mutant) was also purified following the same protocol and used in the ATPase activity assay (Fig. 3b). The ATPase rate of the HA-mutant was reduced by a factor of 17 (V_{max} value 4.7 ± 2.5 nmol·min^{-1}·mg^{-1}). The K_m value increased by a factor of 1.62 (0.60 ± 0.94 mM), whereas the k_{cat} value was 10.2 ± 5.4 min^{-1} (14-fold lower than WT 10HNisT) (Fig. 3c).

In vitro ATPase activity with NisA variants. To investigate the effect of substrate on the ATPase rate of 10HNisT, we added different NisA variants. First, the NisA peptides in different modification states (uNisA, dNisA and mNisA, respectively) were purified (Figure S4). Additionally, the leader peptide of NisA (NisA$_{LP}$) was used in the ATPase assay to evaluate whether the isolated LP is sufficient for recognition by NisT.

For the activity assay the ATP concentration was kept constant at 5 mM, while the substrate concentration was varied from 0 to 40 µM. 10HNisT was pre-incubated with the peptides prior to the activity assay. The basal activity of 10HNisT was set to 100% and the ATPase rate with substrates was expressed as normalized ATPase rate. The ATPase rate of 10HNisT was slightly increased for all peptides. However, a concentration dependent stimulation of the transporter was not observed for all the different tested peptides (Fig. 4a,b) suggesting that the ATPase is not modulated by the NisA variants under the experimental conditions.

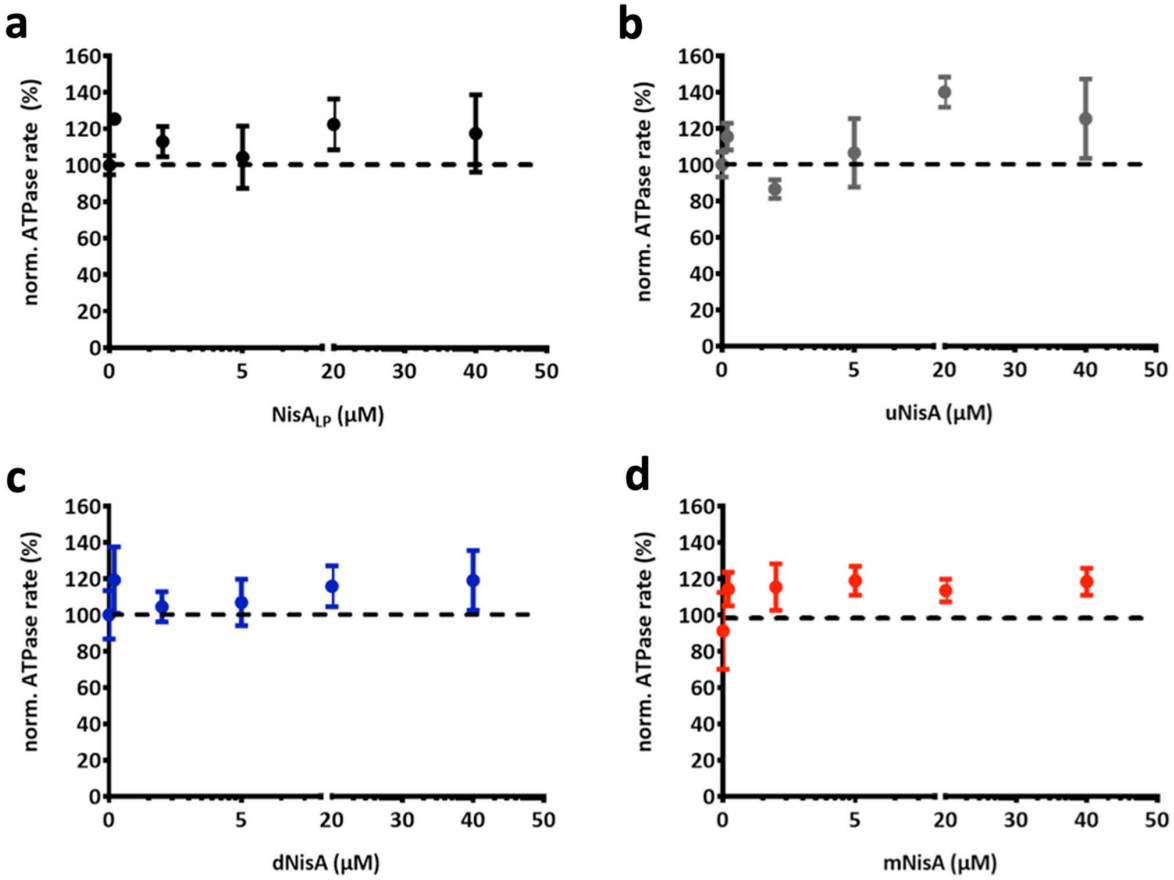

Figure 4. Dependence of NisT ATPase rate on different substrates. The ATPase rate of purified 10HNisT was analyzed in the presence of different substrates. (**a**) The leader peptide of NisA (NisA$_{LP}$, black dots), (**b**) uNisA (grey dots), (**c**) dNisA (blue dots) and (**d**) mNisA (red dots) was used in various concentrations (µM) and the ATPase rate is shown as normalized ATPase rate (%). The basal ATPase rate (from 10HNisT without any substrate; compare Fig. 3) was set as 100% (dashed line) and further values were normalized accordingly. The assays were performed in at least four independent experiments and are represented as means ± s.d. (n = 4). The means were analyzed by a one-way ANOVA and the differences were not significant (p-value: ≥ 0.05). ns: not significant.

In vitro ATPase activity in presence of NisBC and mNisA. Previous studies[35] and our data demonstrated that the secretion of NisA is strongly enhanced by the modification proteins NisB and NisC (see in vivo secretion assay) and therefore the ATPase rate of NisT might also be influenced by these interaction partner. To investigate the effect of NisB and NisC on the ATPase rate of 10HNisT the ATPase activity assay was repeated under the same conditions (ATP concentration constant, various concentration of interaction partners). We observed that the ATPase rate of NisT was independent of the various concentrations of NisB or NisC. Thus, only fixed molar ratio of 10HNisT to the interaction partner was used (NisT:NisB/NisC 1:2; in the case of NisT:NisBC 1:2:2) (Fig. 5a). The basal ATPase rate of NisT was 62.5 ± 9.4 nmol·min^{-1}·mg^{-1} and was not changed within the experimental error in the presence of NisB or NisC (54.7 ± 4.5 nmol·min^{-1}·mg^{-1}, 59.3 ± 4.9 nmol·min^{-1}·mg^{-1}). If both proteins were used in the assay (NisBC), the ATPase rate of 10HNisT was reduced by a factor of 1.3 (49.3 ± 4.4 nmol·min^{-1}·mg^{-1}), but the difference was not significant (Fig. 5a).

Next, the ATPase rate of NisT with NisBC was investigated in presence of NisA$_{LP}$ and mNisA, at concentrations ranging from 0 to 40 µM. The ATPase rate with the substrate NisA$_{LP}$ was slightly increased but not in a concentration dependent manner (Fig. 5b), while a decreasing effect on the ATPase rate was observed in presence of mNisA. However, a concentration dependent is not observed and the change is within the experimental error (Fig. 5c).

Interaction of NisT with NisBC. In 2017 the assembly of the nisin modification complex consisting of NisB$_2$C and NisA was published and shed light on the stoichiometry and structure of the complex in solution[41]. Additionally, an influence of the last ring on complex disassembly was determined. The next step would be

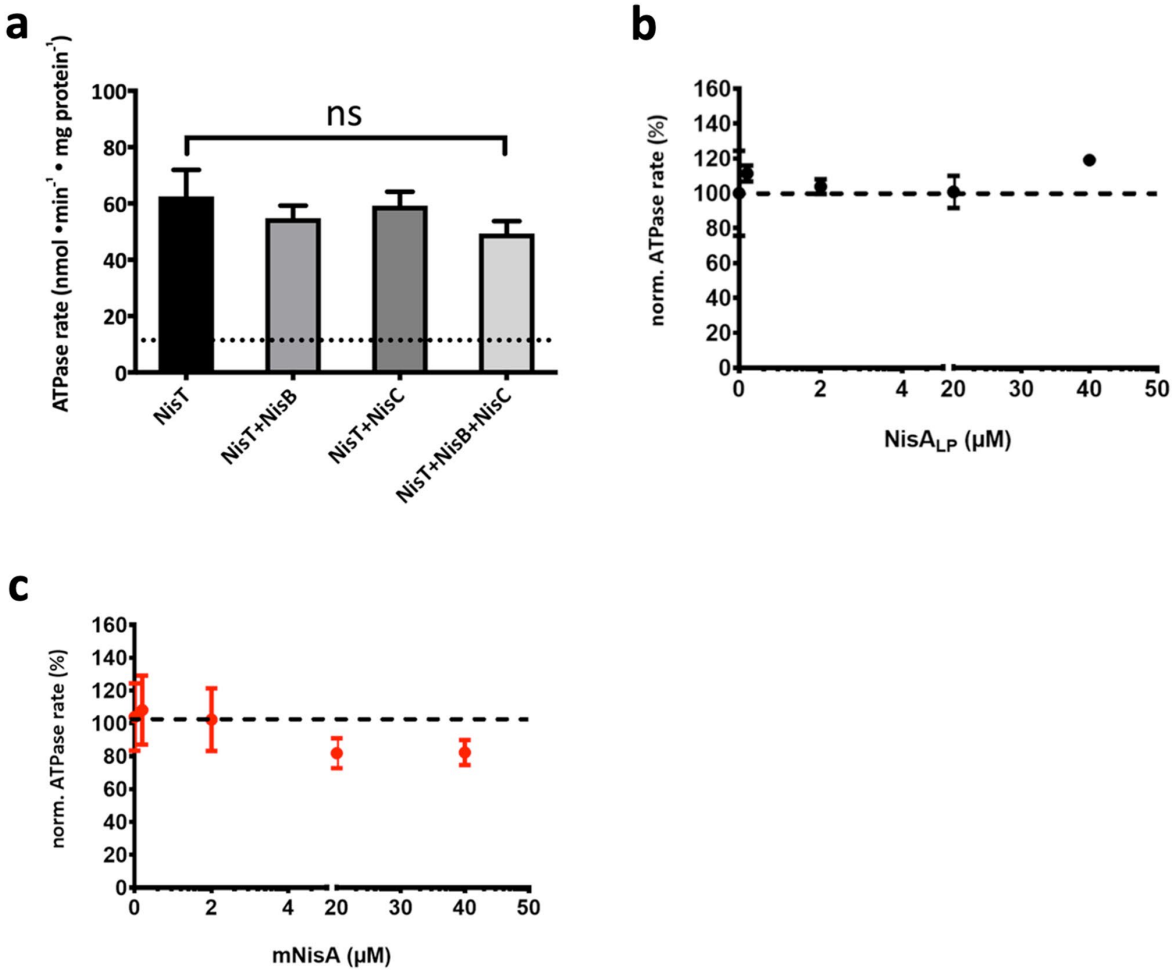

Figure 5. Influence of NisBC on the ATPase rate of NisT. The ATPase rate of purified 10HNisT was analyzed in the presence of the modification enzymes NisB and NisC, respectively. (**a**) ATPase rate of 10HNisT was plotted against variation of 10HNisT with the modification enzymes NisB, NisC and NisBC. It showed the normalized ATPase rate, in which the ATPase rate of 10HNisT was set to 100% (dashed line). (**b**) The substrate $NisA_{LP}$ (black dots) and (**c**) mNisA (red dots) were used in the assay with 10HNisT in presence of NisBC. The normalized ATPase rate was plotted against various concentrations (µM), where the ATPase rate of 10HNisT plus NisBC was set to 100% (dashed line). All assay assays were performed in at least four independent experiments and are represented as means ± s.d. (n = 4). The means were analyzed by a one-way ANOVA and the differences were not significant (p-value: ≥ 0.05).

the interaction with NisT prior to secretion, as a proposed transient multimeric nisin modification/secretion complex[28], but detailed information about the interaction with the ABC transporter NisT is still missing.

Therefore, the interaction of NisT with NisB and NisC was investigated by a pull-down assay, in which 10HNisT was immobilized on Ni-NTA-magnetic beads (Qiagen). Initially, the interaction of NisT was tested with 10 µM NisB, NisC or NisBC. Interestingly, in all cases the interaction partner of NisT were observed in the elution fractions. This clearly shows a specific interaction of NisB and NisC with NisT independent of NisA (Fig. 6a). The controls, in which the Ni-NTA-magnetic beads were incubated with NisB and NisC without immobilized 10HNisT, revealed no protein in the elution fractions (Figure S5).

The same set up was used in the presence of the substrate $mNisA_{CCCCA}$, which lacks the last lanthionine-ring (ring E) and stabilizes the maturation complex of NisBC[41]. This substrate showed no additional effect on the interaction of NisB with NisT. However, the interaction of NisT and NisC was affected and the amount of co-eluted NisC was strongly reduced (Fig. 6b). After addition of NisB, the interaction of NisB and NisC with NisT was restored (Fig. 6b). Noteworthy, the addition of mNisA instead of the ring-mutant shows an identical result on complex formation. Unfortunately, the analysis of all elution fractions with an antibody against the LP gave no signals for the substrates mNisA/$mNisA_{CCCCA}$. This might be due to low concentrations of the peptides in the elution fractions.

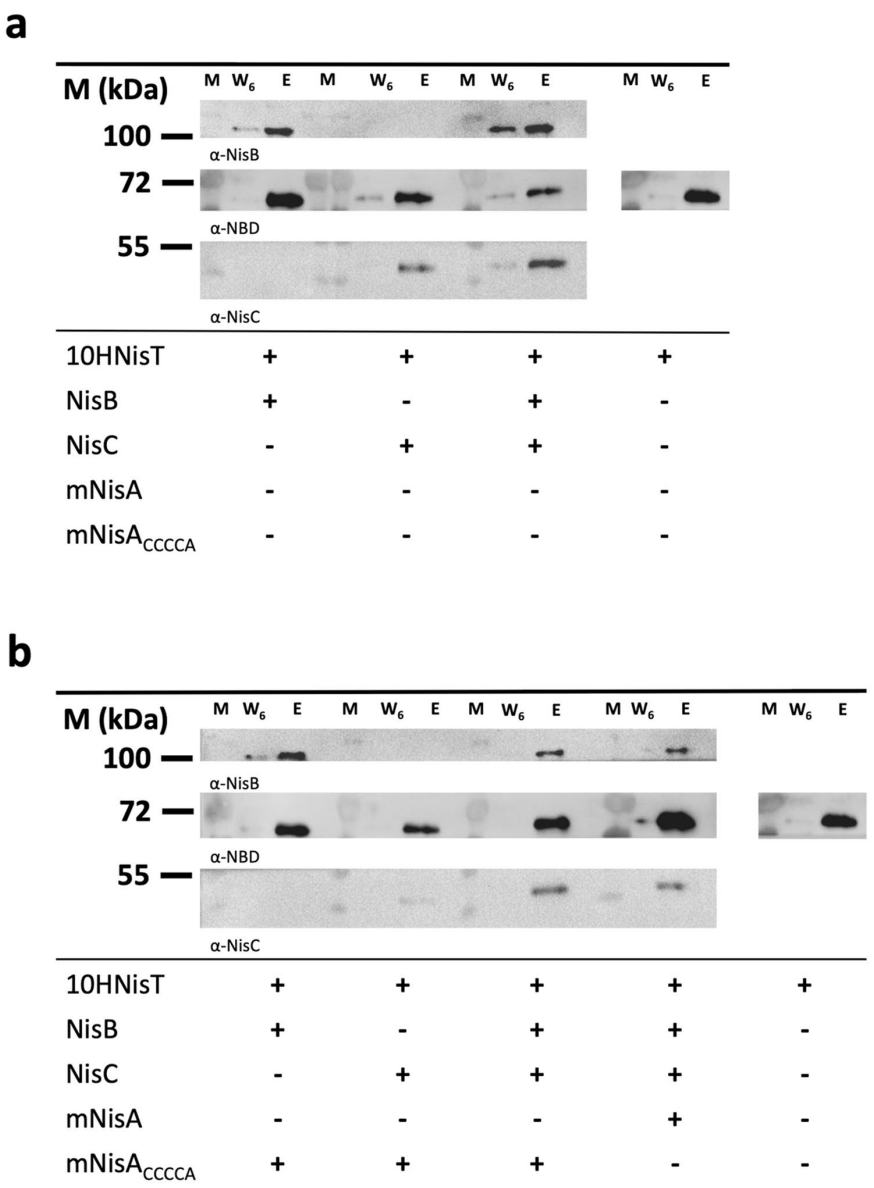

Figure 6. Pull-down assay of NisT with NisB and NisC. The interaction of 10HNisT with NisB and NisC was studied by a pull-down assay. The ABC transporter was immobilized on NTA-magnetic beads, the specific interaction partner were added and incubated. After six washing steps, the last washing step (W_6) and the EDTA elution fraction (E) were analyzed by Western blot with the specific antibodies (α-NDB, α-NisB or α-NisC). Western blots displayed the eluted bands for NisB, NisT and NisC without substrate (**a**) and with substrates mNisA or $mNisA_{CCCCA}$ (**b**). The pull-down assay was repeated three times and showed similar results. M: marker protein bands; +: protein was used in assay; −: protein was not used in assay.

In summary, this is the first time that beside the interaction of NisT and NisC, an interaction of NisT with NisB was shown. Even the co-elution of NisB and NisC with NisT as a complex in the presence of the substrates mNisA and the ring-mutant $mNisA_{CCCCA}$ was observed. Although no enhancement of the interaction between NisT and NisBC in presence of substrates mNisA/ $mNisA_{CCCCA}$ was detected, NisB seems to have a pivotal role for complex formation.

Discussion

The mechanism of lanthipeptide modifications was subject to many studies, but still only little is known about the secretion process of class I lanthipeptide ABC transporters (LanT). Only a few in vivo studies investigated the translocation of lanthipeptides nisin, subtilin, Pep5 or epidermin[5,25,42–44]. Amongst these systems, the nisin modification and secretion system (NisBTC) is the best studied one and is commonly employed to secrete nisin variants, lanthipeptides or non-lanthionine containing peptides[5,31,37]. It is commonly established, that nisin is ribosomally synthesized as a precursor peptide NisA which undergoes special post-translational modifications (e.g. Dha, Dhb, Lan and MeLan)[11,45,46]. The PTM of the CP are installed in a coordinated manner by the nisin modification complex $NisB_2C$[41,47].

Not only is the modification is a tightly coupled process, but also the secretion of mNisA by NisT. A proposed channeling mechanism through interaction with NisB/NisC might explain mNisA translocation. Here, mNisA can be detected in the medium within the first minute after induction[35]. We characterized the LanT-type transporter NisT with respect to the secretion process and its specific ATPase activity. To study the mechanism of nisin secretion, we focused on two main topics: (I) In vivo secretion rate of NisA by NisT and (II) in vitro activity of NisT with and without substrate.

In 2008 van den Berg van Saparoea et al. conducted a kinetic analysis of nisin production with the strains NZ9700 and NZ9000 transformed with a two plasmid system[35]. They demonstrated distinct contributions of the modification enzymes NisB and NisC with respect to lanthipeptide secretion and proposed that the secretion process of NisT occurred via a channeling mechanism. This hypothesis was supported by further in vivo studies, in which some mechanistic aspects of NisB and NisC modification were investigated[19,47,48]. Although these studies clearly demonstrated the dependence of NisA secretion on the modification enzymes, they did not include a determination of the underlying kinetic parameters. To determine these kinetic parameters, we quantified the amount of secreted peptide via HPLC from different time points of various NZ9000 strains.

The first two kinetic parameters were V_{max} and $K_{0.5}$, which were obtained by an allosteric sigmoidal analysis (Fig. 2). Generally, our results are consistent with the aforementioned studies, in which strain NZ9000BTC had the highest V_{max} and the lowest $K_{0.5}$ value reflecting a high secretion efficiency. The strains, which secreted uNisA (NZ9000T and NZ9000TC), show lower V_{max} and higher $K_{0.5}$ values. Interestingly, we observed in our secretion assay some aberrations with respect to dNisA secretion. The expression of a catalytic-inactive NisC (H331A mutant) in the NisBTC system (strain $NZ9000BTC_{H331A}$) did not restore the secretion level of dNisA to the WT level. This is in contrast to Lubelski et al., where a recovery of the NisA secretion to WT level was observed[19]. The secretion of dNisA by NZ9000BT has a higher V_{max} level and a lower $K_{0.5}$ value. However, one has to consider the time scale of the secretion assays, which might explain this difference. In our assay, the early kinetics of apparent secretion (also see[35]) might pronounce the differences between the strains more clearly as an end-point determination after an overnight secretion. The precise determination of the apparent secretion efficiency revealed a descending order of the NisA secreting strains (NZ9000BTC > NZ9000BT > NZ9000BT C_{H331A} > NZ9000T > NZ9000TC). The secretion efficiency clearly shows, that mNisA is secreted at high rates by strain NZ9000BTC and every aberration of the secretion system reduced the rate at least by a factor of 2.2 (see strain NZ9000BT). The third kinetic parameter was the apparent secretion rate $V_{S\ app.}$ ($NisA{\cdot}NisT^{-1}{\cdot}min^{-1}$), which we determined for the strains NZ9000BTC and NZ9000NisT, in which the secretion efficiency was the highest for NisBTC system (84.8 ± 21 $NisA{\cdot}NisT^{-1}{\cdot}min^{-1}$; Fig. 2). This is 9.6-fold higher than with the transporter NisT alone (8.8 ± 1.68 $NisA{\cdot}NisT^{-1}{\cdot}min^{-1}$).

We observed similar results like other ABC transporter depended secretion system (e.g. HlyA T1SS[49]) that ATP hydrolysis is essential for the secretion process. As the H551A mutant of NisT (strain $NZ9000BT_{H551A}C$) did not secrete mNisA. This mutant enables ATP binding and NBD dimerization but not ATP hydrolysis[50].

Thus, ATP hydrolysis is clearly important for ABC transporter mediated substrate translocation, we determined the in vitro activity of NisT in terms of ATPase rate without and with substrate. Here, the basal ATPase activity had a value of 79.9 ± 2.9 $nmol{\cdot}min^{-1}{\cdot}mg^{-1}$ with a K_m value of 0.37 ± 0.04 mM, which is in the range of other ABC transporters[51–54] (Fig. 3). In comparison to NisT, the $Lan_{C39P}T$ transporter NukT has a low V_{max} value of 12.6 $nmol{\cdot}min^{-1}{\cdot}mg^{-1}$, but it is stimulated by mNukA up to max. 500% (at 50 µM substrate). The cleaved substrate stimulates up to 200% (at 25 µM substrate) and the unmodified substrate does not stimulate at all[55]. In the case of NisT, we did not observe a substrate concentration dependent stimulation in the presence of $NisA_{LP}$, uNisA, dNisA and mNisA (Fig. 4). Next, we extended the ATPase activity by addition of NisB and NisC to simulate NisBTC, in which the secretion of NisA is the most efficient (Fig. 5). The addition of Nis_{LP} had no effect on the ATPase rate. However, the addition of mNisA revealed an inhibiting effect on the ATPase rate with increasing substrate concentration, although it was within the experimental error. Interestingly, a similar behavior was observed for PCAT1[52]. Another study on an ABC transporter homologue to PrtD from *Aquifex aeolicus* also noticed an inhibitory effect on ATPase activity after substrate addition[56]. The open question is now, if NisT uses an equivalent mechanism, in which the interaction of the modification/ secretion complex inhibits the ATPase rate prior to translocation.

In 1996 a multimeric enzyme complex of NisBTC was proposed, but the isolation of such a complex was not successful[28]. Therefore, we choose to study the specific interaction of NisT with NisB and NisC via a pull-down assay. Such a pull-down assay was performed with His-tagged NisA, where NisB and NisC were co-eluted from cytoplasmic fraction[47,57]. In our study, we expanded this set up and used purified NisT, NisB, NisC and NisA (Fig. 6). We observed a specific interaction of NisT with NisC, which is in line with previously observed interaction of NisT with NisC via co-immunoprecipitation and yeast two-hybrid assay[28]. Another specific interaction of the modification enzyme with the ABC transporter was shown for NukM and NukT. Here, the C-terminal domain of LanM (LanC-like domain; amino acids 480–917) interacts with TMD and NBD of NukT, but not with the C39 peptidase domain[30]. Besides the interaction of NisT with NisC, we also noticed an interaction

of NisT with NisB, which was not observed in the above-mentioned study, but for SpaT and SpaB in a similar experiment[29]. Since secretion of dNisA by NZ9000BT was observed[5], an interaction of NisT and NisB was also proposed. Furthermore, we observed for the first time the co-elution of NisBC with NisT in the proposed lanthionine synthetase complex. Remarkably, the co-elution of transporter with the modification enzymes is not increased by addition of the substrates mNisA or $mNisA_{CCCCA}$. Similar amounts of the enzymes were co-eluted and we conclude that the interaction of NisT with NisB and NisC is independent of substrate. One exception was the addition of $mNisA_{CCCCA}$ to NisT/NisC, in which the amount of co-elute NisC was reduced. Only the addition of NisB to the sample increased the co-elution of NisC. It is now commonly accepted that NisB represents the main component of the NisBTC modification/secretion complex[19,35] and based on our data, NisB stabilizes the NisBTC complex.

In summary, we have determined the kinetic parameters for the in vivo secretion of nisin peptides by the modification and secretion complex NisBTC. We demonstrated that alterations in the NisBTC system lead to impaired secretion of NisA or even to no secretion, when an ATP hydrolysis deficient mutant of NisT was used. For an efficient secretion by NisT the modification enzymes NisB and NisC are prerequisite and their interaction with NisT enhances the secretion process directly by the proposed channeling mechanism[35]. Interestingly, it is the function not the mere presence of NisC that is required, as the secretion of NisBTC with the catalytically inactive mutant of NisC did not restore the secretion. Additionally, the in vitro activity data of NisT demonstrate that the lanthipeptide exporter is not stimulated by the interaction partner and substrate, respectively. The observed complex formation of NisB and NisC with NisT hint to the proposed lanthionine synthetase complex, in which NisT under goes a transition to a transport competent exporter in presence of only NisB, NisC and the substrate mNisA.

Methods

Bacterial strains and growth conditions. Strains of *Escherichia coli* and *Lactococcus lactis* and plasmids used in this study are listed in Table S1. The strains *E. coli* DH5α or BL21 were grown in LB medium at 37 °C under aerobic conditions with appropriate antibiotics (30 µg/ml kanamycin or 100 µg/ml ampicillin). The transformation of *E. coli* strains was performed following standard procedures.

The strain *L. lactis* NZ9000 (and its variants) was grown in M17[58] or minimal medium (MM)[31,59] at 30 °C under semi aerobic conditions supplemented with 0.5% glucose (GM17/ GMM) and appropriate antibiotics (erythromycin or/and chloramphenicol at a final concentration of 5 µg/ml). To MM a vitamin mix (100 × stock solution, 1 × final) was added[31].

For transformation of *L. lactis* NZ9000 with the expression plasmids a standard procedure for preparation of competent cells and electroporation was used[60].

Cloning of nisT and nisT variants. A nucleotide sequence for a MCS with 10H nucleotide sequence (5′–3′: CAAAATAAATTATAAGGAGGCACTCAATGCATCATCATCATCATCATCATCATCATCATGATT ATGATATTCCGACCACCGAAAACCTGTATTTTCAGGGCCCATGGCATATGCATATGTCTAGACACC ACCACCACCACCACTGAGATCCG) was ordered as a codon-optimized, synthetic gene fragment from Life Technologies to insert it into the pNZ-SV plasmid[61]. The synthetic gene fragment were amplified by Phusion DNA polymerase (NEB) with the primer pair 10Hfor and 10Hrev (Table S4) for Gibson assembly. The plasmid pNZ-SV was amplified by Phusion DNA polymerase (NEB) with the primer pair infupNZ-SVfor and infupNZ-SVrev (Table S4) to linearize the vector. The gene fragment and the vector pNZ-SV were employed in the Gibson assembly by following the manufactures instructions (NEB). The Gibson assembly reactions were transformed into *E. coli* DH5α. The sequence of the construct pNZ-SV10H (Table S5) was verified by DNA sequencing (Microsynth Seqlab).

The *nisT* gene (accession number: Q03203) was amplified using genomic DNA from *L. lactis* NZ9700[8] as a template. Phusion DNA polymerase (NEB) with the primer pair infunisTfor and infunisTrev (Table S4) was used to create overhang sequences for Gibson assembly. The plasmid pNZ-SV10H was amplified by Phusion DNA polymerase (NEB) with the primer pair linpNZ-SVfor and linpNZ-SVrev (Table S4) to linearize the vector. Subsequently, the gene and the linearized vector pNZ-SV10H were employed in the Gibson assembly and the reactions were transformed into *E. coli* DH5α. The sequence of the construct pNZ-SV10HnisT (Table S5) was verified by DNA sequencing (Microsynth Seqlab).

To generate the plasmid pIL-SVnisT the *nisT* gene from pNZ-SV10HnisT was amplified by Phusion DNA polymerase (NEB) with the primer pair infupIL-SVfor and infupIL-SVrev (Table S4) to create overhanging sequences. The plasmid pIL-SV[62] was linearized by Phusion DNA polymerase (NEB) with the primer pair termpNZfor and pnisArev (Table S4). The gene with overhang sequences and the vector was employed in Gibson assembly. The Gibson assembly reactions were transformed into *E. coli* DH5α. Additionally, the 10H nucleotide sequence was deleted by Phusion DNA polymerase (NEB) with the primer pair 10Hfor and infupNZ-SVrev (Table S4). The sequence of the construct pIL-SVnisT (Table S5) was verified by DNA sequencing (Microsynth Seqlab).

To generate the $nisT_{H551A}$ mutant, a polymerase chain reaction using Pfu DNA polymerase (Thermo Fischer Scientific) or Pfu DNA polymerase (Promega), the template pNZ-SV10HnisT or pIL-SVnisT and the primer pair $nisT_{H551A}$for and $nisT_{H551A}$rev (Table S4) was performed according to standard procedures. The sequence of the constructs (Table S5) was verified by DNA sequencing (Microsynth Seqlab).

The plasmid pNZ-SVnisTNBD$_{H348}$ was obtained by the deletion of the TMD sequence (1–347) from the plasmid pNV-SV10HnisT. The plasmid was amplified with Phusion DNA polymerase (NEB) with the primer pair $\Delta nisT_{TMD}$for and $\Delta nisT_{TMD}$rev (Table S4). The linear vector was ligated with T4-ligase (NEB) and transformed

into *E. coli* DH5α. The sequence of the construct pNZ-SVnisTNBD$_{H348}$ (Table S5) was verified by DNA sequencing (Microsynth Seqlab).

Cloning of nisBTC and nisBTC variants. The plasmid pIL-SVnisBTC was generated from pIL-SV and pIL3BTC[31]. The plasmid pIL3BTC was digested with the restriction enzymes NotI (NEB) and BstXI (NEB) to receive a fragment BTC containing the genes *nisB*, *nisT* and *nisC*. Next, pIL-SV[62] was also digested with NotI and BstXI (pIL-SV**). The fragment BTC and pIL-SV** were ligated with T4-ligase (NEB) and transformed into *E. coli* DH5α. The sequence of the construct pIL-SVnisBTC (Table S5) was verified by DNA sequencing (Microsynth Seqlab).

By using Phusion DNA polymerase (NEB) with the appropriate primer pairs (Table S4) the gene deletions of *nisB*, *nisC* or *nisT* were performed to generate pIL-SVnisBTC derivatives. Subsequently, the linearized vectors were ligated with T4-ligase (NEB) and transformed into *E. coli* DH5α. The sequence of the constructs (Table S5) were verified by DNA sequencing (Microsynth Seqlab).

To generate *nisT*$_{H551A}$ and nisC$_{H331A}$ mutants, a polymerase chain reaction using PfuUltra II Fusion DNA polymerase (Agilent Technologies), the template pIL-SVnisBTC and the appropriate pair of oligonucleotides (Table S4) was performed according to standard procedures. The sequence of the new constructs (Table S5) were verified by DNA sequencing (Microsynth Seqlab).

In vivo secretion assay: expression and secretion of NisA. Strain *L. lactis* NZ9000 harboring the plasmids pIL-SVnisBTC and pNZ-SVnisA hereupon termed NZ9000BTC (Table S1) was used to investigate the in vivo secretion activity of the nisin modification and secretion system (NisBTC). The use of pIL-SVnisBTC derivatives and pNZ-SVnisA for transformation into *L. lactis* NZ9000 led to strains described in detail in Table S1. For each secretion experiment new transformants were prepared and used to inoculate GM17 (Erm + Cm) with one colony. The overnight culture was centrifuged at 4,000×*g* for 20 min and cells were resuspended in GMM. Subsequently, 0.5 l GMM (Erm + Cm) were inoculated to OD_{600} of 0.3 and incubated at 30 °C. After 60–90 min the culture (OD_{600} of 0.4–0.5) was induced with 10 ng/ml nisin (powder from Sigma-Aldrich dissolved in 50 mM lactic acid). A 50 ml sample before induction (0 h) and every other hour (1–6 h) was taken. For each sample the cell were harvested by centrifugation at 4,000×*g* for 20 min. Subsequently, the cells were resuspended in R-buffer (50 mM Na-Phosphate buffer, pH 8, 100 mM KCl, 20% glycerol) to an OD_{600} of 200, flash frozen in liquid nitrogen (N_2) and stored at − 80 °C until further use. The supernatant was additionally centrifuged at 17,000×*g* for 20 min at 8 °C. Supernatants were kept on ice before the RP-HPLC analysis. Furthermore, 2 ml or 10 ml of the supernatant were precipitated by 1/10 volume (10%) TCA. TCA samples were incubated at 8 °C overnight. The TCA-precipitated peptide was centrifuged at 17,000×*g* for 20 min at 8 °C and consecutively washed three-times with ice-cold acetone. The pellets were vacuum-dried and resuspended in 60 µl per OD_{600} 1 of 1 × SDS-PAGE loading dye containing 5 mM β-mercaptoethanol (β-ME). These resuspended TCA-pellets were analyzed by Tricine-SDS-PAGE and Western blot.

In vivo secretion assay: analysis of cell pellets. The resuspended cell pellets were thawed on ice and 1/3 (w/v) glass beads (0.3 mm diameter) were added. Cells were disrupted on a vortex-shaker (Disrutor Genie, Scientific Industries). A cycle of 2 min disruption and 1 min incubation on ice was repeated five times. A low spin step at 17,000×g for 30 min at 8 °C and subsequently a high spin step at 100,000×g for 120 min at 8 °C was performed. The supernatant of the latter centrifugation step represents the cytoplasmic fraction and the pellet corresponds to the membrane fraction. The SDS-PAGE samples of cytoplasmic and membrane fractions were prepared by adding 4 × SDS-PAGE loading dye containing 5 mM β-ME and used for SDS-PAGE as well as Western blot analysis.

In vivo secretion assay: analysis of culture supernatant. The culture supernatants containing NisA variants were analyzed by RP-HPLC (Agilent Technologies 1260 Infinity II). A LiChrospher WP 300 RP-18 end-capped column and an acetonitrile/water solvent system were used as described previously[7]. In the case of modified NisA 300 µl and for all other variants (dehydrated/unmodified) 500 µl sample were injected. Prior to the gradient (20–50% acetonitrile) a washing step of 20% acetonitrile was used to remove most of the casein peptides. The peptide amount or NisA in the supernatant was determined using the peak area integration analyzed with the Agilent Lab Advisor software. In the case of the unmodified peptide (uNisA) a retention time from 29 to 33 min, for dehydrated peptide (dNisA) from 31 to 38 min and for modified peptide (mNisA) from 33 to 38 min was used for peak integration peak. A calibration with known amounts of nisin or insulin chain B was used to obtain a linear regression line. Unknown amounts in the in vivo secretion assay samples were calculated as nmol or µM based on this linear regression line.

In vivo secretion assay: determination of kinetic parameter. The amount of secreted NisA of the different *L. lactis* NZ9000 strains were plotted against time and fitted using an allosteric sigmoidal fit (1). Note that y is the amount of secreted peptide (nmol), V_{max} the maximal secreted amount, x is time (min), $K_{0.5}$ the time point at which 50% of V_{max} is present and h is the Hill slope indicating cooperativity. The analysis was performed using Prism 7.0c (GraphPad).

$$y = V_{max}\frac{X^h}{{K_{0.5}}^h + X^h} \quad (1)$$

The apparent secretion rate ($V_{s\,app}$) was determined by plotting the amount of NisA and NisT against time (min). The values were fitted using a linear regression (2). Note that y is the amount of NisA molecules per NisT molecules (NisA·NisT^{-1}), m is the slope $V_{s\,app}$ (NisA·NisT^{-1}·min^{-1}), x is the time (min), and b the y-axis interception. The analysis was performed using Prism 7.0c (GraphPad).

$$y = mx + b \tag{2}$$

Expression and purification of NisT. *L. lactis* NZ9000 strain was transformed with pNZ-SV10HnisT and placed on SGM17 (0.5 M sucrose, 0.5% glucose, 22 g/l agarose in M17 medium) agar plates containing 5 µg/ml erythromycin. A GM17 (Erm) overnight culture was inoculated with one colony and incubated at 30 °C. A GM17 (Erm) main culture was inoculated to an OD_{600} of 0.1 with the overnight culture. After 3 h incubation, expression was induced by adding 10 ng/ml nisin (powder from Sigma-Aldrich dissolved in 50 mM lactic acid) and further grown for additional 3 h. Cells were harvested by centrifugation at 4,000×g for 20 min at 8 °C and resuspended in R-buffer (50 mM Na-Phosphate buffer, pH 8, 100 mM KCl, 20% glycerol) to an OD_{600} of 200. To the resuspended cells 10 mg/ml lysozyme was added and incubated at 30 °C for 30 min. Prior to cell disruption, cells were incubated on ice for 15 min. The cell suspension was passed through a homogenizer (M-110P, Microfluidics System) at 1.5 kbar at least four times. The homogenized cell suspension was centrifuged at 12,000×g for 30 min at 8 °C. Subsequently, the supernatant was centrifuged at 100,000×g for 120 min at 4 °C to collect the membrane fraction. Membranes were resuspended with R-buffer containing 10 mM imidazole and 0.5 mM AEBSF. The total membrane protein concentration was measured by BCA assay (Thermo Fischer Scientific) and the concentration was adjusted to 5–7.5 mg/ml. Membranes were solubilized with 1% (w/v) of the lipid-like detergents FC-16 (Anatrace) for 1 h at 8 °C. Insoluble material was removed by centrifugation at 100,000×g for 30 min at 4 °C. The supernatant was applied to a 5 ml IMAC (Immobilized Metal-Ion-Affinity Chromatography) HiTrap Chelating column (GE Healthcare) preloaded with 100 mM zinc sulphate and equilibrated with low IMAC1 buffer (50 mM Na-Phosphate buffer, pH 8, 100 mM KCl, 20% glycerol and 10 mM imidazole) containing 0.5 mM AEBSF and 0.005% FC-16. Consecutively, non-bound protein was washed and the buffer was exchanged to low IMAC2 buffer (50 mM Tris–HCl pH 8, 100 mM KCl, 10% glycerol, 10 mM imidazole, 0.5 mM AEBSF and 0.005% FC-16). After an additional washing step with 30% high IMAC buffer (50 mM Tris–HCl pH 8, 100 mM KCl, 10% glycerol, 150 mM histidine, 0.5 mM AEBSF and 0.005% FC-16), 10HNisT was eluted with 100% high IMAC buffer. The elution fractions containing NisT were pooled, 10 mM DTT was added and further concentrated with a Vivaspin20 100 kDa molecular weight cut off (MWCO) centrifugal concentrator (Sartorius AG). Next, a size exclusion chromatography (SEC) was performed, where the concentrated protein sample was applied onto a Superose 6 10/300 GL column (GE Healthcare) equilibrated with SEC buffer (25 mM Tris–HCl pH 8, 50 mM KCl, 10% glycerol, 0.5 mM AEBSF, 2 mM DTT and 0.0015% FC-16). The main peak fractions were analyzed via SDS-PAGE and further concentrated via a Vivaspin6 100 kDa MWCO centrifugal concentrator (Sartorius AG) until a concentration of 50 µM was reached. The protein concentration was determined by NanoDrop spectrophotometer (Thermo Fischer Scientific) using a molar extinction coefficient of 86,180 M^{-1} cm^{-1} and the molecular mass of 72.6 kDa. Aliquots of 50 µM 10HNisT were flash frozen in liquid N_2 and stored at − 80 °C until further use. The NisT variants $10HNisT_{H551A}$ was expressed following the same protocol.

In vitro ATPase activity assay. The ATPase activity of NisT was determined with the malachite green assay as described previously with experimental alterations[63]. In this assay the release of inorganic orthophosphate after ATP hydrolysis was colorimetrically quantified based on a Na_2HPO_4 standard curve.

All reactions were performed at 30 °C in a total volume of 30 µl in activity assay buffer containing 0.4% CYMAL5 and 10 mM $MgCl_2$.

In each reaction ~ 2 µg of detergent-solubilized and purified NisT was used and the reaction was started by adding ATP (0–5 mM). The background of the reaction was a sample without $MgCl_2$. After 30 min the reaction was stopped by transferring 25 µl of each reaction into a 96-well plate containing 175 µl stop-solution (20 mM sulphuric acid). Consecutively, 50 µl of a staining solution (0.096% (w/v) malachite green, 1.48% (w/v) ammonium heptamolybdate and 0.173% (w/v) Tween-20 in 2.36 M sulphuric acid) was added. After 10 min the amount of free inorganic orthophosphate was quantified by measuring the absorption at 595 nm using an iMark microplate reader (Bio-Rad).

The specific ATPase activity of NisT was plotted against ATP concentrations and fitted using the Michaelis–Menten Eq. (3). Note that y is the reaction velocity, V_{max} the maximal reaction velocity, x is the substrate concentration and K_m the Michaelis–Menten constant. The analysis was performed using Prism 7.0c (GraphPad).

$$y = V_{max}\frac{X}{K_m + X} \tag{3}$$

For the reactions with substrates (NisA variants) or interaction partner (NisB and NisC) NisT was pre-incubated at 30 °C for 10 min before ATP was added to start the reaction. All reactions were performed at 30 °C in a total volume of 30 µl in activity assay buffer containing 0.4% CYMAL5, 400 mM glutamate and 10 mM $MgCl_2$. In each reaction ~ 2 µg of detergent-solubilized and purified NisT was used and the reaction was started by adding 5 mM ATP and stopped after 15 min following the procedure described above. In this reaction the concentration of the different substrates (0–40 µM) and/or interaction partner was varied and the ATPase activity was normalized to the specific ATPase activity of NisT without substrate/interaction partner. In these cases, the background was subtracted prior to normalization.

In vitro pull-down assay. The immobilization of 10HNisT to Ni-NTA magnetic beads (Quiagen) was performed as described in the manufacturer's manual. In brief, ~15 µg 10HNisT was incubated with Ni-NTA magnetic beads for 30 min at 30 °C. Excess of protein was removed by three washing steps with activity assay buffer containing 0.4% CYMAL5 and 400 mM glutamate. 10 µM of the interaction partners NisC and NisB were incubated in 1:1 molar ratio (but > 10 × molar excess to NisT) separately with or without mNisA/ $mNisA_{CCCCA}$ (20 × molar excess to NisT) in activity assay buffer containing 0.4% CYMAL5, 400 mM glutamate and 5 mM MgATP for 15 min on ice. Next, interaction partner were added to 10HNisT immobilized to Ni-NTA magnetic beads and incubated for 1 h at 30 °C. Positive control (only 10HNisT) and negative control (NisB, NisC samples were prepared by incubating the proteins with Ni-NTA magnetic beads separately. After binding the Ni-NTA magnetic beads were washed six times with activity assay buffer. Finally, 10HNisT was eluted by adding activity assay buffer containing 50 mM EDTA. The SDS-PAGE samples of pull-down assay fractions were prepared by adding 4 × SDS-PAGE loading dye containing 5 mM β-ME and used for Western blot analysis.

Received: 26 March 2020; Accepted: 6 July 2020
Published online: 23 July 2020

References

1. Newman, D. J. & Cragg, G. M. Natural products as sources of new drugs from 1981 to 2014. *J. Nat. Prod.* **79**, 629–661. https://doi.org/10.1021/acs.jnatprod.5b01055 (2016).
2. Hudson, G. A. & Mitchell, D. A. RiPP antibiotics: biosynthesis and engineering potential. *Curr. Opin. Microbiol.* **45**, 61–69. https://doi.org/10.1016/j.mib.2018.02.010 (2018).
3. Dischinger, J., Basi Chipalu, S. & Bierbaum, G. Lantibiotics: promising candidates for future applications in health care. *Int. J. Med. Microbiol.* **304**, 51–62. https://doi.org/10.1016/j.ijmm.2013.09.003 (2014).
4. Arnison, P. G. *et al.* Ribosomally synthesized and post-translationally modified peptide natural products: overview and recommendations for a universal nomenclature. *Nat. Prod. Rep.* **30**, 108–160. https://doi.org/10.1039/c2np20085f (2013).
5. Kuipers, A. *et al.* NisT, the transporter of the lantibiotic nisin, can transport fully modified, dehydrated, and unmodified prenisin and fusions of the leader peptide with non-lantibiotic peptides. *J. Biol. Chem.* **279**, 22176–22182. https://doi.org/10.1074/jbc.M312789200 (2004).
6. Mavaro, A. *et al.* Substrate recognition and specificity of the NisB protein, the lantibiotic dehydratase involved in nisin biosynthesis. *J. Biol. Chem.* **286**, 30552–30560. https://doi.org/10.1074/jbc.M111.263210 (2011).
7. Abts, A., Montalban-Lopez, M., Kuipers, O. P., Smits, S. H. & Schmitt, L. NisC binds the FxLx motif of the nisin leader peptide. *Biochemistry* **52**, 5387–5395. https://doi.org/10.1021/bi4008116 (2013).
8. Kuipers, O. P., Beerthuyzen, M. M., Siezen, R. J. & De Vos, W. M. Characterization of the nisin gene cluster nisABTCIPR of *Lactococcus lactis*. Requirement of expression of the nisA and nisI genes for development of immunity. *Eur. J. Biochem.* **216**, 281–291 (1993).
9. Van der Meer, J. R. *et al.* Influence of amino acid substitutions in the nisin leader peptide on biosynthesis and secretion of nisin by *Lactococcus lactis*. *J. Biol. Chem.* **269**, 3555–3562 (1994).
10. van der Meer, J. R. *et al.* Characterization of the *Lactococcus lactis* nisin A operon genes nisP, encoding a subtilisin-like serine protease involved in precursor processing, and nisR, encoding a regulatory protein involved in nisin biosynthesis. *J. Bacteriol.* **175**, 2578–2588 (1993).
11. Newton, G. G., Abraham, E. P. & Berridge, N. J. Sulphur-containing amino-acids of nisin. *Nature* **171**, 606 (1953).
12. Gross, E. & Morell, J. L. The number and nature of alpha, beta-unsaturated amino acids in nisin. *FEBS Lett* **2**, 61–64 (1968).
13. Karakas Sen, A. *et al.* Post-translational modification of nisin. The involvement of NisB in the dehydration process. *Eur. J. Biochem.* **261**, 524–532 (1999).
14. Garg, N., Salazar-Ocampo, L. M. & van der Donk, W. A. In vitro activity of the nisin dehydratase NisB. *Proc. Natl. Acad. Sci. U. S. A.* **110**, 7258–7263. https://doi.org/10.1073/pnas.1222488110 (2013).
15. Ortega, M. A. *et al.* Structure and mechanism of the tRNA-dependent lantibiotic dehydratase NisB. *Nature* **517**, 509–512. https://doi.org/10.1038/nature13888 (2015).
16. Koponen, O. *et al.* NisB is required for the dehydration and NisC for the lanthionine formation in the post-translational modification of nisin. *Microbiology* **148**, 3561–3568. https://doi.org/10.1099/00221287-148-11-3561 (2002).
17. Okeley, N. M., Paul, M., Stasser, J. P., Blackburn, N. & van der Donk, W. A. SpaC and NisC, the cyclases involved in subtilin and nisin biosynthesis, are zinc proteins. *Biochemistry* **42**, 13613–13624. https://doi.org/10.1021/bi0354942 (2003).
18. Li, B. & van der Donk, W. A. Identification of essential catalytic residues of the cyclase NisC involved in the biosynthesis of nisin. *J. Biol. Chem.* **282**, 21169–21175. https://doi.org/10.1074/jbc.M701802200 (2007).
19. Lubelski, J., Khusainov, R. & Kuipers, O. P. Directionality and coordination of dehydration and ring formation during biosynthesis of the lantibiotic nisin. *J. Biol. Chem.* **284**, 25962–25972. https://doi.org/10.1074/jbc.M109.026690 (2009).
20. Repka, L. M., Hetrick, K. J., Chee, S. H. & van der Donk, W. A. Characterization of leader peptide binding during catalysis by the nisin dehydratase NisB. *J. Am. Chem. Soc.* **140**, 4200–4203. https://doi.org/10.1021/jacs.7b13506 (2018).
21. Quiao, M. & Saris, P. E. Evidence for a role of NisT in transport of the lantibiotic nisin produced by *Lactococcus lactis* N8. *FEMS Microbiol. Lett.* **144**, 89–93 (1996).
22. Higgins, C. F. ABC transporters: from microorganisms to man. *Annu. Rev. Cell Biol.* **8**, 67–113. https://doi.org/10.1146/annurev.cb.08.110192.000435 (1992).
23. Fath, M. J. & Kolter, R. ABC transporters: bacterial exporters. *Microbiol. Rev.* **57**, 995–1017 (1993).
24. Håvarstein, L. S., Diep, D. B. & Nes, I. F. A family of bacteriocin ABC transporters carry out proteolytic processing of their substrates concomitant with export. *Mol. Microbiol.* **16**, 229–240 (1995).
25. Schnell, N. *et al.* Analysis of genes involved in the biosynthesis of lantibiotic epidermin. *Eur. J. Biochem.* **204**, 57–68 (1992).
26. Klein, C., Kaletta, C., Schnell, N. & Entian, K. D. Analysis of genes involved in biosynthesis of the lantibiotic subtilin. *Appl. Environ. Microbiol.* **58**, 132–142 (1992).
27. Bierbaum, G., Brotz, H., Koller, K. P. & Sahl, H. G. Cloning, sequencing and production of the lantibiotic mersacidin. *FEMS Microbiol. Lett.* **127**, 121–126. https://doi.org/10.1111/j.1574-6968.1995.tb07460.x (1995).
28. Siegers, K., Heinzmann, S. & Entian, K. D. Biosynthesis of lantibiotic nisin. Posttranslational modification of its prepeptide occurs at a multimeric membrane-associated lanthionine synthetase complex. *J. Biol. Chem.* **271**, 12294–12301 (1996).
29. Kiesau, P. *et al.* Evidence for a multimeric subtilin synthetase complex. *J. Bacteriol.* **179**, 1475–1481 (1997).
30. Nagao, J. *et al.* Localization and interaction of the biosynthetic proteins for the lantibiotic, Nukacin ISK-1. *Biosci. Biotechnol. Biochem.* **69**, 1341–1347. https://doi.org/10.1271/bbb.69.1341 (2005).

31. Rink, R. *et al.* Lantibiotic structures as guidelines for the design of peptides that can be modified by lantibiotic enzymes. *Biochemistry* **44**, 8873–8882. https://doi.org/10.1021/bi050081h (2005).
32. Kluskens, L. D. *et al.* Post-translational modification of therapeutic peptides by NisB, the dehydratase of the lantibiotic nisin. *Biochemistry* **44**, 12827–12834. https://doi.org/10.1021/bi050805p (2005).
33. Rink, R. *et al.* NisC, the cyclase of the lantibiotic nisin, can catalyze cyclization of designed nonlantibiotic peptides. *Biochemistry* **46**, 13179–13189. https://doi.org/10.1021/bi700106z (2007).
34. Kuipers, A., Meijer-Wierenga, J., Rink, R., Kluskens, L. D. & Moll, G. N. Mechanistic dissection of the enzyme complexes involved in biosynthesis of lacticin 3147 and nisin. *Appl. Environ. Microbiol.* **74**, 6591–6597. https://doi.org/10.1128/AEM.01334-08 (2008).
35. van den Berg van Saparoea, H. B., Bakkes, P. J., Moll, G. N. & Driessen, A. J. Distinct contributions of the nisin biosynthesis enzymes NisB and NisC and transporter NisT to prenisin production by *Lactococcus lactis*. *Appl. Environ. Microbiol.* **74**, 5541–5548. https://doi.org/10.1128/AEM.00342-08 (2008).
36. Zhou, L., van Heel, A. J. & Kuipers, O. P. The length of a lantibiotic hinge region has profound influence on antimicrobial activity and host specificity. *Front. Microbiol.* **6**, 11. https://doi.org/10.3389/fmicb.2015.00011 (2015).
37. van Heel, A. J. *et al.* Discovery, production and modification of five novel lantibiotics using the promiscuous nisin modification machinery. *ACS Synth. Biol.* **5**, 1146–1154. https://doi.org/10.1021/acssynbio.6b00033 (2016).
38. Zhou, L., van Heel, A. J., Montalban-Lopez, M. & Kuipers, O. P. Potentiating the activity of nisin against *Escherichia coli*. *Front. Cell Dev. Biol.* **4**, 7. https://doi.org/10.3389/fcell.2016.00007 (2016).
39. Lagedroste, M., Reiners, J., Smits, S. H. J. & Schmitt, L. Systematic characterization of position one variants within the lantibiotic nisin. *Sci. Rep.* **9**, 935. https://doi.org/10.1038/s41598-018-37532-4 (2019).
40. Li, B. *et al.* Structure and mechanism of the lantibiotic cyclase involved in nisin biosynthesis. *Science* **311**, 1464–1467. https://doi.org/10.1126/science.1121422 (2006).
41. Reiners, J., Abts, A., Clemens, R., Smits, S. H. & Schmitt, L. Stoichiometry and structure of a lantibiotic maturation complex. *Sci. Rep.* **7**, 42163. https://doi.org/10.1038/srep42163 (2017).
42. Ra, S. R., Qiao, M., Immonen, T., Pujana, I. & Saris, E. J. Genes responsible for nisin synthesis, regulation and immunity form a regulon of two operons and are induced by nisin in *Lactoccocus lactis* N8. *Microbiology* **142**(Pt 5), 1281–1288. https://doi.org/10.1099/13500872-142-5-1281 (1996).
43. Izaguirre, G. & Hansen, J. N. Use of alkaline phosphatase as a reporter polypeptide to study the role of the subtilin leader segment and the SpaT transporter in the posttranslational modifications and secretion of subtilin in *Bacillus subtilis* 168. *Appl. Environ. Microbio.l* **63**, 3965–3971 (1997).
44. Meyer, C. *et al.* Nucleotide sequence of the lantibiotic Pep5 biosynthetic gene cluster and functional analysis of PepP and PepC. Evidence for a role of PepC in thioether formation. *Eur. J. Biochem.* **232**, 478–489 (1995).
45. Gross, E. & Morell, J. L. The presence of dehydroalanine in the antibiotic nisin and its relationship to activity. *J. Am. Chem. Soc.* **89**, 2791–2792 (1967).
46. Ingram, L. A ribosomal mechanism for synthesis of peptides related to nisin. *Biochim. Biophys. Acta* **224**, 263–265 (1970).
47. Khusainov, R., Heils, R., Lubelski, J., Moll, G. N. & Kuipers, O. P. Determining sites of interaction between prenisin and its modification enzymes NisB and NisC. *Mol. Microbiol.* **82**, 706–718. https://doi.org/10.1111/j.1365-2958.2011.07846.x (2011).
48. Khusainov, R. & Kuipers, O. P. The presence of modifiable residues in the core peptide part of precursor nisin is not crucial for precursor nisin interactions with NisB- and NisC. *PLoS ONE* **8**, e74890. https://doi.org/10.1371/journal.pone.0074890 (2013).
49. Lenders, M. H., Beer, T., Smits, S. H. & Schmitt, L. In vivo quantification of the secretion rates of the hemolysin A Type I secretion system. *Sci. Rep.* **6**, 33275. https://doi.org/10.1038/srep33275 (2016).
50. Zaitseva, J., Jenewein, S., Jumpertz, T., Holland, I. B. & Schmitt, L. H662 is the linchpin of ATP hydrolysis in the nucleotide-binding domain of the ABC transporter HlyB. *EMBO J* **24**, 1901–1910. https://doi.org/10.1038/sj.emboj.7600657 (2005).
51. Choudhury, H. G. *et al.* Structure of an antibacterial peptide ATP-binding cassette transporter in a novel outward occluded state. *Proc. Natl. Acad. Sci. U. S. A.* **111**, 9145–9150. https://doi.org/10.1073/pnas.1320506111 (2014).
52. Lin, D. Y., Huang, S. & Chen, J. Crystal structures of a polypeptide processing and secretion transporter. *Nature* **523**, 425–430. https://doi.org/10.1038/nature14623 (2015).
53. Reimann, S. *et al.* Interdomain regulation of the ATPase activity of the ABC transporter haemolysin B from *Escherichia coli*. *Biochem. J.* **473**, 2471–2483. https://doi.org/10.1042/BCJ20160154 (2016).
54. Bock, C., Zollmann, T., Lindt, K.-A., Tampé, R. & Abele, R. Peptide translocation by the lysosomal ABC transporter TAPL is regulated by coupling efficiency and activation energy. *Sci. Rep.* **9**, 11884. https://doi.org/10.1038/s41598-019-48343-6 (2019).
55. Zheng, S., Nagao, J. I., Nishie, M., Zendo, T. & Sonomoto, K. ATPase activity regulation by leader peptide processing of ABC transporter maturation and secretion protein, NukT, for lantibiotic nukacin ISK-1. *Appl. Microbiol. Biotechnol.* https://doi.org/10.1007/s00253-017-8645-2 (2017).
56. Morgan, J. L. W., Acheson, J. F. & Zimmer, J. Structure of a Type-1 secretion system ABC transporter. *Structure* **25**, 522–529. https://doi.org/10.1016/j.str.2017.01.010 (2017).
57. Khusainov, R., Moll, G. N. & Kuipers, O. P. Identification of distinct nisin leader peptide regions that determine interactions with the modification enzymes NisB and NisC. *FEBS Open Bio* **3**, 237–242. https://doi.org/10.1016/j.fob.2013.05.001 (2013).
58. Terzaghi, B. E. & Sandine, W. E. Improved medium for lactic streptococci and their bacteriophages. *Appl. Microbiol.* **29**, 807–813 (1975).
59. Jensen, P. R. & Hammer, K. Minimal requirements for exponential growth of *Lactococcus lactis*. *Appl. Environ. Microbiol.* **59**, 4363–4366 (1993).
60. Holo, H. & Nes, I. F. High-frequency transformation, by electroporation, of *Lactococcus lactis* subsp. *cremoris* grown with glycine in osmotically stabilized media. *Appl. Environ. Microbiol.* **55**, 3119–3123 (1989).
61. AlKhatib, Z. *et al.* Lantibiotic immunity: inhibition of nisin mediated pore formation by NisI. *PLoS ONE* **9**, e102246. https://doi.org/10.1371/journal.pone.0102246 (2014).
62. AlKhatib, Z. *et al.* The C-terminus of nisin is important for the ABC transporter NisFEG to confer immunity in *Lactococcus lactis*. *Microbiol. Open* **3**, 752–763. https://doi.org/10.1002/mbo3.205 (2014).
63. Infed, N., Hanekop, N., Driessen, A. J., Smits, S. H. & Schmitt, L. Influence of detergents on the activity of the ABC transporter LmrA. *Biochim. Biophys. Acta* **2313–2321**, 2011. https://doi.org/10.1016/j.bbamem.2011.05.016 (1808).

Acknowledgements

We thank Peter Tommes for support and analysis of MALDI-TOF–MS experiments. We are greatly obliged to Diana Kleinschrodt and Iris Fey (former Protein Production Facility of HH) for their support of cloning the constructs. We also thank Olivia Spitz, Ioannis Panetas and Didem Kaya for their support during the early stages of the project. We are indebted to all members of the Institute of Biochemistry for stimulating discussions and support during the project. This work was suported by the Deutsche Forschungsgemeinschaft (DFG Grant Schm1279/13-1 to L.S.

Author contributions

M.L., S.H.J.S. and L.S. designed the experiments, M.L. performed the experiments, J.R. purified NisB and NisC, M.L., S.H.J.S. and L.S. analyzed and interpreted the data, M.L., S.H.J.S. and L.S. wrote and revised the manuscript.

Competing interests

The authors declare no competing interests.

Additional information

Supplementary information is available for this paper at https://doi.org/10.1038/s41598-020-69225-2.

Correspondence and requests for materials should be addressed to L.S.

Reprints and permissions information is available at www.nature.com/reprints.

Publisher's note Springer Nature remains neutral with regard to jurisdictional claims in published maps and institutional affiliations.

Supplemental information

Impact of the nisin modification machinery on the transport kinetics of NisT

Marcel Lagedroste[1], Jens Reiners[1], Sander H.J. Smits[1] and Lutz Schmitt[1]*

[1]:Institute of Biochemistry, Heinrich Heine University Düsseldorf

*: To whom correspondence should be addressed

Lutz Schmitt
Institute of Biochemistry
Heinrich Heine University Düsseldorf
Universitätsstr. 1
40225 Düsseldorf, Germany
Phone: +49(0)211-81-10773
Fax: +49(0)211-81-15310
Email: lutz.schmitt@hhu.de

Methods

Chemicals and Antibodies

Fos-choline 16 (FC-16) and CYMAL5 (C5) were obtained from Anatrace. Lyophilized nisin powder (2.5% nisin content) and insulin chain B were obtained from Sigma-Aldrich. The leader peptide of NisA was synthesized and obtained from JPT peptide technologies. Antibodies for $NisT_{NBD}$, NisC and $NisA_{LP}$ peptide were purchased from Davids Biotechnology (Germany) as polyclonal antibodies. NisB antibody was kindly provided by Dr. G. Moll (Lanthio Pharma; Groningen, Netherlands). All standard chemicals were purchased from Sigma-Aldrich or VWR.

Expression and purification of $NisT_{NBD}$

L. lactis NZ9000 was transformed with pNZ-SVnisTNBD$_{H348}$ and placed on SMGG17 agar plates containing 5 µg/ml erythromycin. A GM17 (Erm) overnight culture was inoculated with one colony and incubated at 30°C. A GM17 (Erm) main culture was inoculated to an OD_{600} of 0.1 with the overnight culture. After 90 min incubation the culture was incubated on ice. Then expression was induced by adding 10 ng/ml nisin (powder from Sigma-Aldrich dissolved in 50 mM lactic acid) and further grown for additional 3 h at 20 °C. Cells were harvested by centrifugation at 4000 xg for 20 min at 8°C and resuspended in R-buffer (50 mM Na-Phosphate buffer, pH 8, 100 mM KCl, 20% glycerol) to an OD_{600} of 200. Then 10 mg/ml lysozyme was added and incubated at 30°C for 30 min. Prior to cell disruption, cells were incubated on ice for 15 min. Then the cell suspension was passed through a homogenizer (M-110P, Microfluidics System) at 1.5 kbar at least four times. The homogenized cell suspension was centrifuged at 12,000 xg for 30 min at 8°C. Subsequently, the supernatant was centrifuged at 100,000 xg for 120 min at 4°C. The supernatant was applied to a 5ml IMAC HiTrap Chelating column (GE Healthcare) preloaded with 100 mM zinc sulphate and equilibrated with low IMAC1 buffer (50 mM Na-Phosphate buffer, pH 8, 100 mM KCl, 20% glycerol and 10 mM imidazole). Consecutively, non-bound protein was washed by a 30% step with high IMAC buffer (50 mM Na-Phosphate buffer, pH 8, 100 mM KCl, 20% glycerol, 500 mM imidazole). The protein 10H$NisT_{NBDH348}$ was eluted by a gradient of 30 to 100% high IMAC buffer. The elution fractions containing $NisT_{NBDH348}$ (T_{NBD}) were pooled, 10 mM DTT was added and further concentrated with an Amicon 10 kDa MWCO centrifugal concentrator (Millipore). Next, the concentrated protein sample was applied onto a HiLoad Superdex 200 16/60 prep grade column (GE Healthcare) equilibrated with SEC buffer (25 mM CAPS pH 10, 20% glycerol, 2 mM DTT). The main peak fractions are analyzed via SDS-PAGE and further concentrated with an Amicon 10 kDa MWCO centrifugal concentrator (Millipore). The protein concentration was determined by NanoDrop spectrophotometer (Thermo

Fischer Scientific) using a molar extinction coefficient of 45,840 $M^{-1} \bullet cm^{-1}$ and the molecular mass of 32.2 kDa. Aliquots of 30 µM T_{NBD} were flash frozen in liquid N_2 and stored at −80 °C until further use.

Expression and purification of nisin modification enzymes NisB and NisC

NisB and NisC were expressed and purified as described previously [1-3]. Aliquots of concentrated proteins (90 µM (NisB) or 110 µM (NisC)) were flash frozen in liquid nitrogen and stored at −80 °C until further use. For the *in vitro* ATPase activity assay and pull-down assay the buffer of the proteins was exchanged via a PD SpinTrap G-25 spin columns (GE Healthcare) to activity assay buffer (25mM Tris-HCl pH 7.5, 50 mM KCl) containing 400 mM glutamate and 0.4% CYMAL5 (3 x cmc). Proteins were stored on ice and directly used for the *in vitro* assays. The protein concentration was determined by NanoDrop spectrophotometer (Thermo Fischer Scientific) by using the theoretical molar extinction coefficient and the molecular mass of the proteins.

Expression and purification of NisA variants

All NisA variants used in this study were expressed and purified as described previously with modifications [1,4]. Briefly, NisA variants were purified after 5 h expression in MM from 2 l (0.5 l in the case of the secretion experiments) culture supernatant via cation-exchange chromatography (cIEX). The cell-free supernatant was diluted 1:1 with LA buffer (50 mM lactic acid, pH 3) and applied to a 5 ml HiTrap SP Sepharose column (GE Healthcare). The column was washed by applying a pH gradient from 100 % LA buffer to 100% H buffer (50 mM HEPES-NaOH, pH 7). Finally, the peptides were eluted with H buffer containing 1 M NaCl. The fractions containing the peptides were pooled and concentrated with an Amicon (Millipore) centrifugal concentrator. First, the flow through (FT) fraction of a 30 kDa molecular weight cut off (MWCO) concentrator was collect. Then a 3 kDa MWCO filter was used to concentrate the peptides of the FT fraction. Aliquots of concentrated peptides were flash frozen in liquid N_2 and stored at −80 °C until further use. For concentration determination the NisA variants were analyzed by RP-HPLC (Agilent Technologies 1260 Infinity II) with a LiChrospher WP 300 RP-18 end-capped column and an acetonitrile/water solvent system as described previously [2].

SDS-PAGE and immunoblotting for protein/ peptide analysis

In general the sodium dodecyl sulfate−polyacrylamide gel electrophoresis (SDS-PAGE) experiments were performed using standard procedures [5]. In the SDS-PAGE gels the acrylamide portion was 10% to have a separation range from 30 to 120 kDa for the proteins NisC (~48 kDa), NisT (~69 kDa) and NisB (~117 kDa).

All peptides (NisA variants) from secretion experiments or from cIEX purification were analyzed by Tricine-SDS−PAGE [6]. For Tricine-SDS-PAGE gels (12%) a Mini-Protean system (Bio-Rad) was used. Tricine-SDS−PAGE and SDS−PAGE gels were stained with colloidal Coomassie (cc) [7].

All immunoblotting experiments were conducted following standard procedures. For the quantification of NisT in the membrane fractions (*in vivo* secretion assay) various amounts of a T_{NBD} standard (stock solution 12.5 µg/ml) was added to create a calibration curve. The band intensities on the Western blots were processed and determined by ImageJ [8]. Then the amount of NisT was determined as pmol protein of the different membrane fractions of the time points 2-6 h.

Mass spectrometry analysis

NisA variants were either desalted via ZipTip (C18 resin) purification accordingly to the manufacture manual (Merk-Millipore) or by RP-HPLC and vacuum dried.

For the MALDI-TOF-MS analysis the vacuum dried pellet was dissolved in 50% acetonitrile solution containing 0.1% TFA and analyzed as described elsewhere [9].

Results (supporting results section of main manuscript)

In vivo secretion assay

The supernatants of the *in vivo* secretion assay were analyzed by RP-HPLC. The secreted peptides were separated by an acetonitrile/water gradient after a 20% washing step on a C-18 RP-HPLC column. The eluted peptides were monitored via UV signal at 205 nm and collected fractions of 1 ml were collected and used for MALDI-TOF-MS analysis. The MS analysis confirmed the correct masses for NisA peptides (uNisA, dNisA or mNisA) in fractions 30-36 min of the chromatogram (Figure S1). The modified peptide mNisA with eight (-Met: 5689 Da) or seven (-Met: 5707 Da) dehydrations from strain NZ9000BTC was detected in fractions 34-36 min (Figure S1A, Table S2). Furthermore, the modified peptides (dNisA) from strains NZ9000BTC$_{H331A}$ and NZ9000BT with eight dehydrations (-Met: 5689 Da) were found in fractions 33-36 min (Figure S1B/D, Table S2). In the case of the peptide from strains NZ9000T and NZ9000TC the retention time was shifted and the unmodified peptide was eluted in fractions 30-32 min (Figure S1E/F). The corresponding molecular mass for unmodified NisA (+Met: 5951 Da; -Met: 5834 Da) was verified (Table S2).

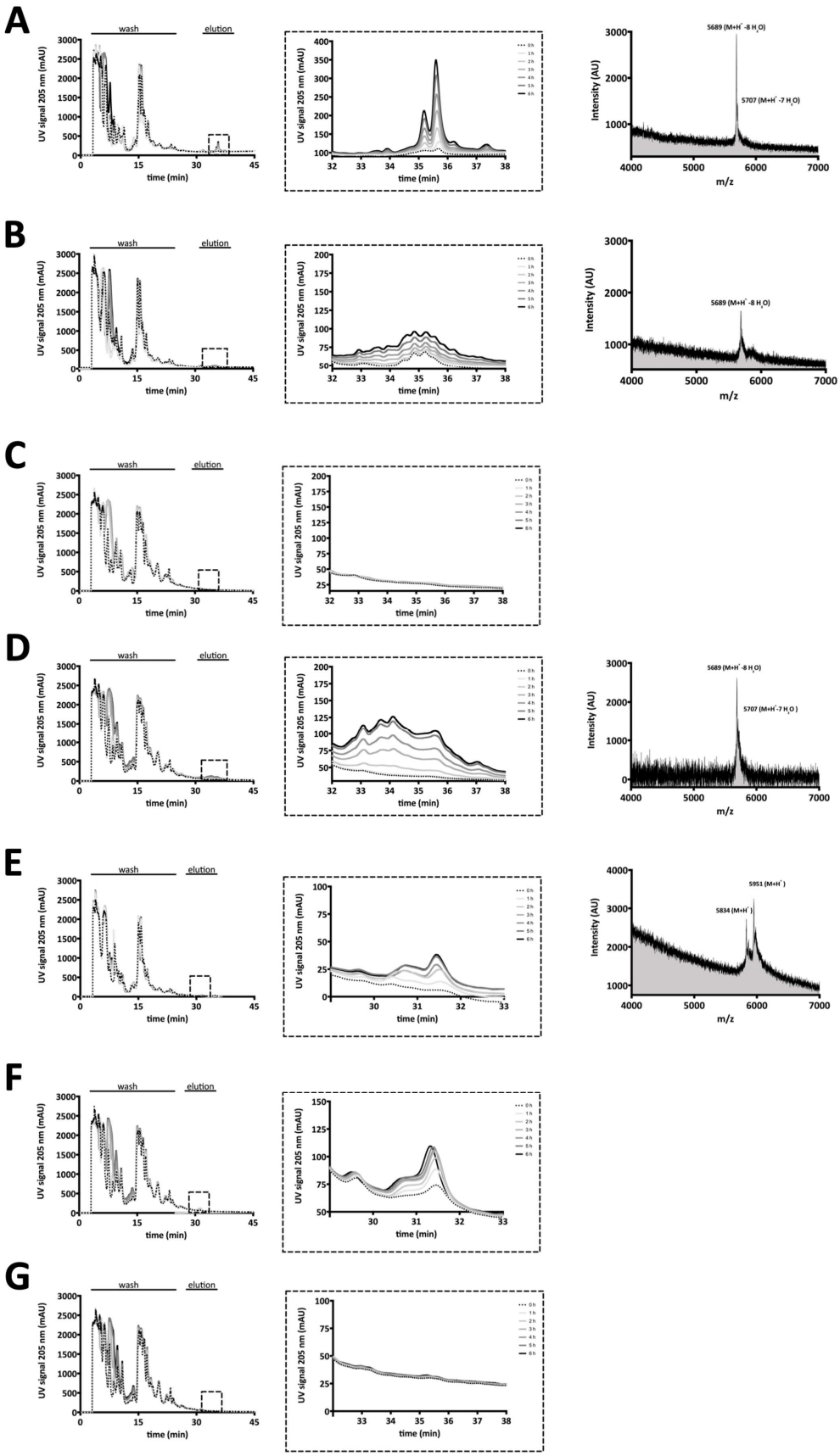

Figure S1: RP-HPLC chromatograms and MALDI-TOF-MS spectra of *in vivo* secretion assay.

The supernatants of NisA secreting *L. lactis* NZ9000 strains were employed for an RP-HPLC analysis. The NisA variants (mNisA, dNisA and uNisA) were separated from other peptides in the supernatant by an acetonitrile/water gradient on a C-18 RP-HPLC column (left panel). The elution fractions (dashed square; middle panel) were further analyzed by MALDI-TOF-MS (right panel) to verify the correct mass. Integration of the corresponding peaks enables the determination of peptide amounts (nmol). Supernatant analysis of *L. lactis* strains (**A**) NZ9000BTC, (**B**) NZ9000BTC$_{H331A}$, (**C**) NZ9000BT$_{H551A}$C, (**D**) NZ9000BT, (**E**) NZ9000T, (**F**) NZ9000TC and (**G**) NZ9000BC.

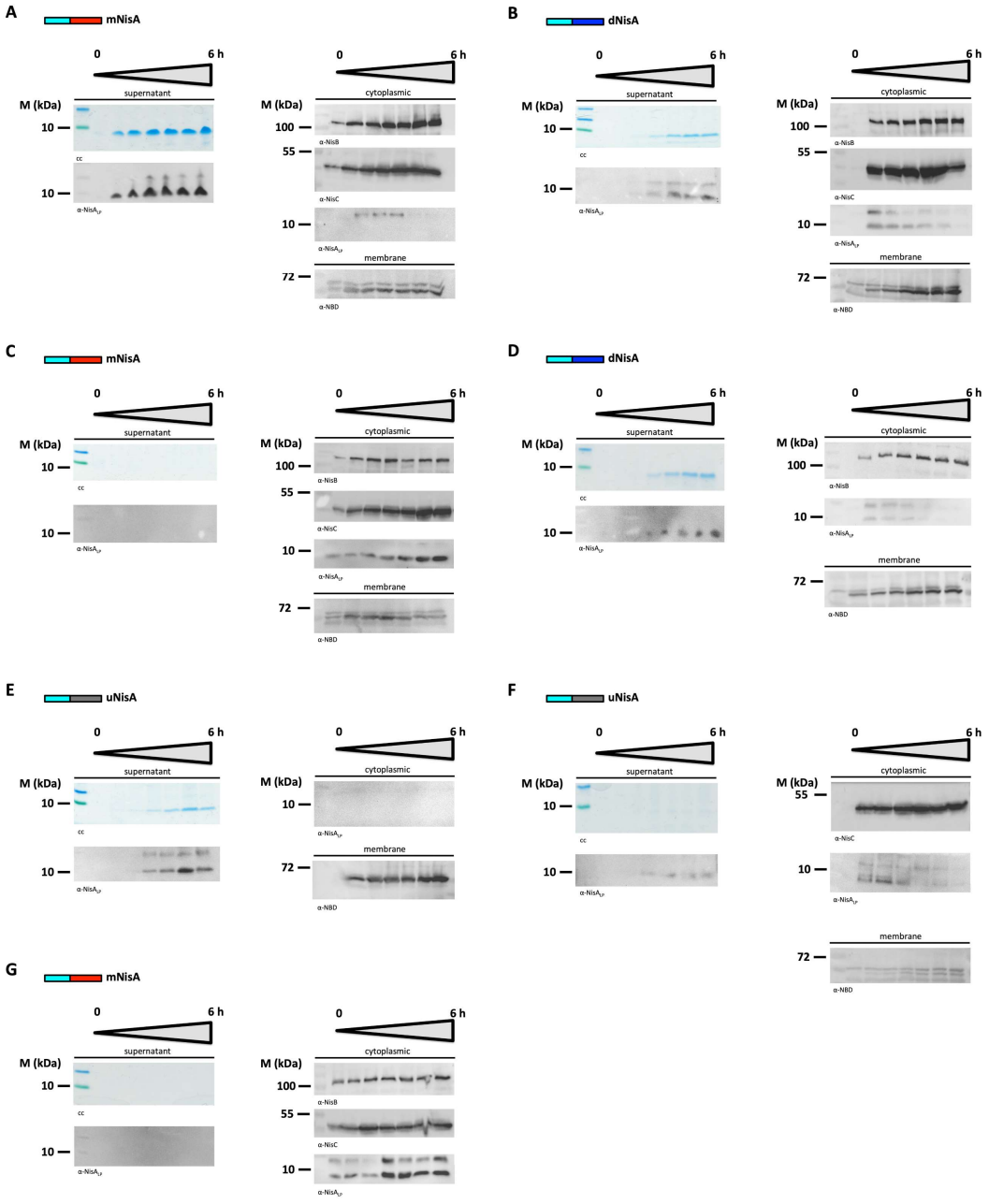

Figure S2: Tricine-SDS-PAGE and Western blot analysis of *in vivo* secretion assay.
The supernatants of NisA secreting *L. lactis* NZ9000 strains from different time points were TCA-precipitated and the pellets were analyzed by Tricine-SDS-PAGE and Western blot using an α-NisA$_{LP}$ antibody (left panel). The Tricine-SDS-PAGE gels were stained by colloidal Coomassie (cc). The cytoplasmic and membrane fractions of the cell from different time points were analyzed by Western blot (right panel) with the specific antibodies

(α-NisB, α-NisA$_{LP}$, α-NisC and α-NBD). Sample analysis of *L. lactis* strains **A**) NZ9000BTC, (**B**) NZ9000BTC$_{H331A}$, (**C**) NZ9000BT$_{H551A}$C, (**D**) NZ9000BT, (**E**) NZ9000T, (**F**) NZ9000TC and (**G**) NZ9000BC.
M: marker protein bands

Determination of NisT amount for NisA secretion rate

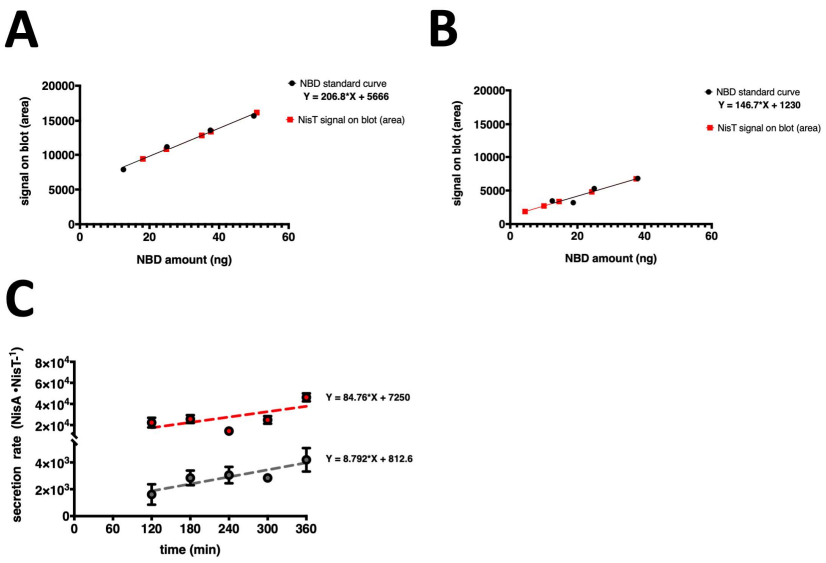

Figure S3: Determination of NisT amount of *in vivo* secretion assay samples.
Calibration curves after Western blot analysis of membrane fractions from strains (**A**) NZ9000T (grey square) and (**B**) NZ9000BTC (red square) with an antibody raised against the NBD (α-NBD). Standard of known amount of T_{NBD} (black dots) was used to determine the amount of NisT (ng) in the membrane for time points 2-5 h. (**C)** A linear regression of plotted values of nmol NisA per nmol NisT against the time (min) results in a slope, which is the apparent secretion rate ($V_{s\ app}$). Here, the molecular weight of NisT (~ 69 kDa; per monomer) and the correction factors, due to volume reduction at each time point (50 ml of the starting volume of 500 ml) were taken into account.

Purification of NisA variants

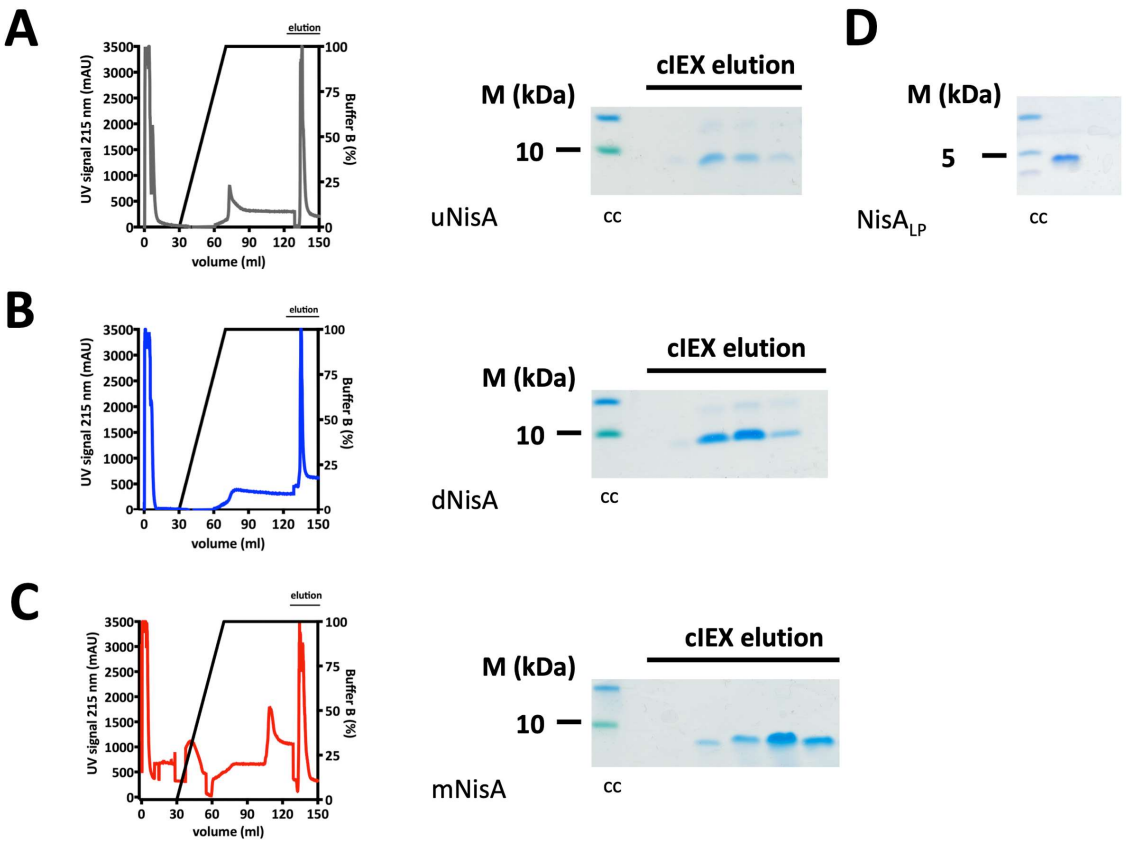

Figure S4: Chromatograms of cIEX from uNisA, dNIsA and mNisA.
The cIEX chromatograms and Tricine-SDS-PAGE of NisA variants (**A**) uNisA (grey), (B) dNisA (blue) and (C) mNisA (red). (**D**) The purity of the NisA leader peptide (NisA$_{LP}$) was controlled by Tricine-SDS-PAGE. The Tricine-SDS-PAGE gels were stained by colloidal Coomassie (cc).
M: marker protein bands

Pull-down assay

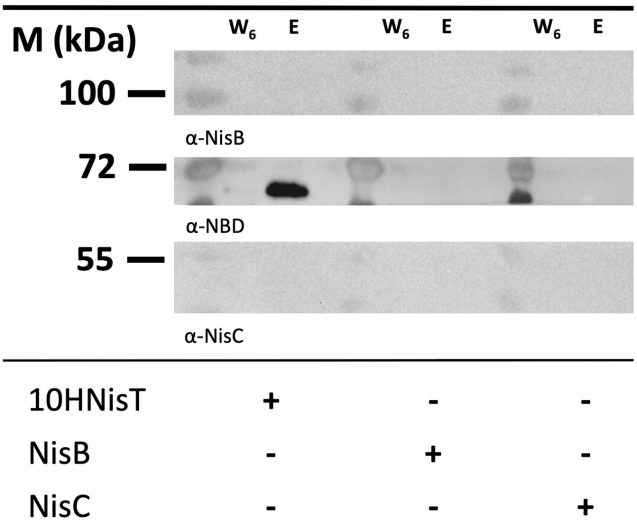

Figure S5: Western blot of pull-down assay with 10HNisT, NisB and NisC.
Controls of the pull-down assay were blotted and analyzed with the specific antibodies of α-NisB, α-NBD and α-NisC. Samples of the sixth washing step (W_6) and the elution fractions (E) were used to detect 10HNisT, NisB or NisC in the samples.
M: marker protein bands; +: addition of protein; -: no protein added

Table supplemental information

Table S1: Strains and plasmids used in this study.

strain	plasmid	name	properties	reference
Escherichia coli DH5α		DH5α	F– Φ80*lac*ZΔM15 Δ(*lac*ZYA-*arg*F) U169 *rec*A1 *end*A1 *hsd*R17 (rK–, mK+) *pho*A *sup*E44 λ– *thi*-1 *gyr*A96 *rel*A1	[10]
Lactococcus lactis NZ9000	-	NZ9000	expression strain; *nisR* and *nisK* on the chromosome (*pepN*::*nisRnisK*)	[11]
L. lactis NZ9000	pIL-SV nisBTC pNZ-SV nisA	NZ9000BTC	mNisA secreting strain	This study
L. lactis NZ9000	pIL-SV nisBTC$_{H331A}$ pNZ-SV nisA	NZ9000BTC$_{H331A}$	dNisA secreting strain	This study
L. lactis NZ9000	pIL-SV nisBT$_{H551A}$C pNZ-SV nisA	NZ9000BT$_{H551A}$C	non NisA secreting strain	This study
L. lactis NZ9000	pIL-SV nisBT pNZ-SV nisA	NZ9000BT	dNisA secreting strain	This study
L. lactis NZ9000	pIL-SV nisT pNZ-SV nisA	NZ9000T	uNisA secreting strain	This study
L. lactis NZ9000	pIL-SV nisT$_{H551A}$ pNZ-SV nisA	NZ9000T$_{H551A}$	non NisA secreting strain	This study
L. lactis NZ9000	pIL-SV nisTC pNZ-SV nisA	NZ9000TC	uNisA secreting strain	This study
L. lactis NZ9000	pIL-SV nisBC pNZ-SV nisA	NZ9000BC	non NisA secreting strain	This study

Table S2: MALDI-TOF-MS analysis of RP-HPLC fractions from *in vivo* secretion assay.
The fractions of RP-HPLC were analyzed by MALDI-TOF-MS and are displayed as masses ($M+H^+$) without or with start methionine. The modified peptides display eight or seven dehydrations and are expected for normally modified NisA by the nisin modification system.

peptide	sample	calc. mass (Da)	observ. mass (+Met*) (Da)
mNisA	RP-HPLC run Fr. 33 from BTC+A supernatant	5688 5706#	5689 5707#
dNisA	RP-HPLC run Fr. 33 from BTC_{H331A}+A supernatant	5688 5706#	5689#
dNisA	RP-HPLC run Fr. 33 from BT+A supernatant	5688 5706#	5689 5707#
uNisA	RP-HPLC run Fr. 31 From T+A supernatant	5832	5834 (5951)
uNisA	RP-HPLC run Fr. 31 From TC+A supernatant	5832	n.d.

8x /7x dehydration
* plus start-methionine
n.d.: not determined

Table S3: The determined kinetic parameter of the in vivo secretion assay.
The supernatant of NisA secreting *L. lactis* strains was analyzed by RP-HPLC. The amount of NisA (nmol) plotted against time (min) was fitted with an allosteric sigmoidal fit and kinetic parameter were determined. Here, V_{max} is the maximal amount of secreted NisA, h is the Hill-coefficient and $K_{0.5}$ is the time point, where half of the NisA is secreted. By determine the amount of NisT an apparent secretion rate ($V_{s\ app}$) NisA•NisT^{-1}•min^{-1} was calculated.

strain	V_{max} (nmol)	$K_{0.5}$ (min)	h	$V_{s\ app}$ (NisA•NisT^{-1}•min^{-1})
NZ9000BTC	534 ± 44	134 ± 12	2.9 ± 0.7	100.3 ± 35.2
NZ9000BT$_{H551A}$C	n.d.	n.d.	n.d.	n.d.
NZ9000BTC$_{H331A}$	168 ± 16	200 ± 16	4.1 ± 0.9	n.d.
NZ9000BT	247 ± 15	152 ± 9	4.8 ± 1.2	n.d.
NZ9000T	137 ± 30	144 ± 41	1.9 ± 0.8	7.4 ± 1.6
NZ9000TC	38 ± 4	n.d.	n.d.	n.d.
NZ9000BC	n.d.	n.d.	n.d.	n.d.

n.d.: not determined

Table S4: Oligonucleotides used in this study.
The forward (for) and reverse (rev) oligonucleotides/primers used for the cloning are displayed in 5'-3' direction. Mutated codons are underlined.

Name	Sequence (5'-3')
10Hfor	CAAAATAAATTATAAGGAGGCAC
10Hrev	CGGATCTCAGTGGTA
infupNZ-SVfor	CACCACCACCACCACTGAGATC
infupNZ-SVrev	TGAGTGCCTCCTTATAATTTATTTTGTAG
infunisTfor	TTTCAGGGCCCATGGATGGATGAAGTGAAAGAATTCA
infunisTrev	GTGGTGGTGTCTAGATTATTCATCATTATCCTCATATTGC
linpNZ-SVfor	TCTAGACACCACCACCACCACCACTG
linpNZ-SVrev	CCATGGGCCCTGAAAATACAGGTTTTCGG
infupIL-SVfor	CGCGAGCATAATAAACGGCTCTGATTAAATTCTGAAGTTTG
infupIL-SVrev	CGTTTCAAGCCTTGGTTTTCTAATTTTGGTTCAAAGAAAG
Δ10Hfor	ATGGATGAAGTGAAAGAATTCACATCAAAAC
Δnis$T_{TMD}$for	CATATAGGAACTGTTAAAGTAATTAATTTATCATATG
ΔnisT_{TMD}rev	CCATGGGCCCTGAAAATACAGGTTTTCGG
ΔnisTfor	CTTTATTATTCAGAGCAATATGAGGATAATGATG
ΔnisTrev	GTTTTGATGTGAATTCTTTCACTTCATCCATC
ΔnisBfor	GACTAATAGATGGATGAAGTGAAAGAATTCAC
ΔnisBrev	GTTTTTTCCTCTCTTTATTTTTATAAGCTATTTAGCAAC
ΔnisCfor	GACCCAGCTTTCTTGTACAAAG
ΔnisCrev	CCCATTGAGCAATAATTTTTTC
nisT_{H551A}_for	CAATTTTCATTTCTGCAAGTTTGAATGCTG
nisT_{H551A}_rev	CAGCATTCAAACTTGCAGAAATGAAAATTG
nis$C_{H331A}$for	CATATATGATTTGCGCAGGCTATTCTGGTTTAATAG
nisC_{H331A}rev	CTATTAAACCAGAATAGCCTGCGCAAATCATATATG
termpNZfor	GAAAACCAAGGCTTGAAACG
pnisArev	CAGAGCCGTTTATTATGCTCGCG

Table S5: Additional plasmids used in this study.

name	properties	reference
pNZ-SV	*E. coli* /*L. lactis* shuttle vector; ErmR; pnisA promoter; empty vector for cloning	[12]
pNZ-SVnisA	NisA expression	[13]
pNZ-SV10HnisT	NisT expression, deca-histidine tag at N-terminus; single alanine substitution at pos. H551 in the T_{NBD}: ATP hydrolysis deficient mutant	This study
pNZ-SV10HnisT_{H551A}	NisT expression, deca-histidine tag at N-terminus	This study
pIL-SV	*E. coli* /*L. lactis* shuttle vector; CmR; pnisA promoter; empty vector for cloning	[13]
pIL-SVnisT	NisT expression	This study, [14]
pIL-SVnisT_{H551A}	NisT expression; single alanine substitution at pos. H551 in the T_{NBD}: ATP hydrolysis deficient mutant	This study
pIL-SVnisBTC	NisBTC expression	This study, [15]
pIL-SVnisBTC_{H331A}	NisBTC expression; single alanine substitution at pos. H331 in the NisC; catalytically inactive NisC	This study, [4]
pIL-SVnisBT_{H551A}C	NisBTC expression; single alanine substitution at pos. H551 in the T_{NBD}: ATP hydrolysis deficient mutant	This study
pIL-SVnisBT	NisBT expression	This study, [14]
pIL-SVnisTC	NisTC expression	This study, [14]
pIL-SVnisBC	NisBC expression	This study, [14]
pNGnisB6His	*L. lactis* expression vector; CmR; NisB expression; hexa-histidine tag and TEV-protease cleavage site at C-terminus	[1,3]
pET28b-AA-nisC	*E. coli* expression vector; KanR; NisC expression; hexa-histidine tag and thrombin cleavage site at N-terminus	[2]

ErmR: erythromycin resistance; CmR: chloramphenicol resistance; KanR: kanamycin resistance ; T_{NBD}: nucleotide binding domain of NisT

References

1 Mavaro, A. *et al.* Substrate recognition and specificity of the NisB protein, the lantibiotic dehydratase involved in nisin biosynthesis. *J Biol Chem* **286**, 30552-30560, doi:10.1074/jbc.M111.263210 (2011).

2 Abts, A., Montalban-Lopez, M., Kuipers, O. P., Smits, S. H. & Schmitt, L. NisC binds the FxLx motif of the nisin leader peptide. *Biochemistry* **52**, 5387-5395, doi:10.1021/bi4008116 (2013).

3 Reiners, J., Abts, A., Clemens, R., Smits, S. H. & Schmitt, L. Stoichiometry and structure of a lantibiotic maturation complex. *Sci Rep* **7**, 42163, doi:10.1038/srep42163 (2017).

4 Lubelski, J., Khusainov, R. & Kuipers, O. P. Directionality and coordination of dehydration and ring formation during biosynthesis of the lantibiotic nisin. *J Biol Chem* **284**, 25962-25972, doi:10.1074/jbc.M109.026690 (2009).

5 Laemmli, U. K. Cleavage of structural proteins during the assembly of the head of bacteriophage T4. *Nature* **227**, 680-685 (1970).

6 Schagger, H. Tricine-SDS-PAGE. *Nat. Protoc.* **1**, 16-22, doi:10.1038/nprot.2006.4 (2006).

7 Dyballa, N. & Metzger, S. Fast and sensitive colloidal coomassie G-250 staining for proteins in polyacrylamide gels. *J Vis Exp*, doi:10.3791/1431 (2009).

8 Schneider, C. A., Rasband, W. S. & Eliceiri, K. W. NIH Image to ImageJ: 25 years of image analysis. *Nat Methods* **9**, 671-675 (2012).

9 Lagedroste, M., Reiners, J., Smits, S. H. J. & Schmitt, L. Systematic characterization of position one variants within the lantibiotic nisin. *Sci Rep* **9**, 935, doi:10.1038/s41598-018-37532-4 (2019).

10 Grant, S. G., Jessee, J., Bloom, F. R. & Hanahan, D. Differential plasmid rescue from transgenic mouse DNAs into Escherichia coli methylation-restriction mutants. *Proceedings of the National Academy of Sciences of the United States of America* **87**, 4645-4649 (1990).

11 Kuipers, O. P., de Ruyter, P. G. G. A., Kleerebezem, M. & de Vos, W. M. Controlled overproduction of proteins by lactic acid bacteria. *Trends Biotechnol* **15**, 135-140, doi:10.1016/S0167-7799(97)01029-9 (1997).

12 AlKhatib, Z. *et al.* Lantibiotic immunity: inhibition of nisin mediated pore formation by NisI. *PLoS One* **9**, e102246, doi:10.1371/journal.pone.0102246 (2014).

13 AlKhatib, Z. *et al.* The C-terminus of nisin is important for the ABC transporter NisFEG to confer immunity in Lactococcus lactis. *Microbiologyopen* **3**, 752-763, doi:10.1002/mbo3.205 (2014).

14 van den Berg van Saparoea, H. B., Bakkes, P. J., Moll, G. N. & Driessen, A. J. Distinct contributions of the nisin biosynthesis enzymes NisB and NisC and transporter NisT to prenisin production by Lactococcus lactis. *Appl Environ Microbiol* **74**, 5541-5548, doi:10.1128/AEM.00342-08 (2008).

15 Rink, R. *et al.* Lantibiotic structures as guidelines for the design of peptides that can be modified by lantibiotic enzymes. *Biochemistry* **44**, 8873-8882, doi:10.1021/bi050081h (2005).

3.4 Chapter IV

Title: Systematic characterization of position one variants within the lantibiotic nisin

Authors: Marcel Lagedroste[#], **Jens Reiners[#]**, Sander H. J. Smits & Lutz Schmitt
[#]Authors contributed equally

Published in: Scientific Reports (2019)
Impact factor: 4.12

Own proportion of this work: 40%

- Cloning of the nisin A variants
- Purification of the pre-nisin A variants
- Performing biological and biochemical assays
- HPLC & MS data analysis
- Writing the manuscript

SCIENTIFIC REPORTS

OPEN

Systematic characterization of position one variants within the lantibiotic nisin

Received: 28 September 2018
Accepted: 4 December 2018
Published online: 30 January 2019

Marcel Lagedroste, Jens Reiners, Sander H. J. Smits & Lutz Schmitt

Lantibiotics are a growing class of natural compounds, which possess antimicrobial activity against a broad range of Gram-positive bacteria. Their high potency against human pathogenic strains such as MRSA and VRE makes them excellent candidates as substitutes for classic antibiotics in times of increasing multidrug resistance of bacterial strains. New lantibiotics are detected in genomes and can be heterologously expressed. The functionality of these novel lantibiotics requires a systematic purification and characterization to benchmark them against for example the well-known lantibiotic nisin. Here, we used a standardized workflow to characterize lantibiotics consisting of six individual steps. The expression and secretion of the lantibiotic was performed employing the promiscuous nisin modification machinery. We mutated the first amino acid of nisin into all proteinaceous amino acids and compared their bactericidal potency against sensitive strains as well as strains expressing nisin resistance proteins. Interestingly, we can highlight four distinct groups based on the residual activity of nisin against sensitive as well as resistant *L. lactis* strains.

Since the last decade the exponential increase of the number of antibiotic resistant strains steadily alarms the world health organization, which is reflected in their annually reports regarding the surveillance of antimicrobial and antibiotic resistance (WHO, GLASS report 2016–2017). Therefore, the urgent need for antimicrobial compounds, which can be used as alternatives to the classic antibiotic treatment, has dramatically increased. Some classes of antibiotic such as cephalosporins, macrolides, carbapenems or penicillin derivatives are vital for human medicine and the treatment of microbial infections. However, observed resistance to important antibiotic classes makes it necessary to explore new classes of natural or synthetic antimicrobial compounds[1].

One possible class are antimicrobial peptides (AMP). Within this class especially lanthipeptides possessing antimicrobial activity, which are called lantibiotics (lanthionine containing antibiotics), are considered as possible lead compounds[2]. Lantibiotics are ribosomally synthesized as a precursor peptide (LanA), between 30–60 amino acids in size and undergo specific post-translational modifications (PTM)[3,4]. They are furthermore dissected into an N-terminal leader peptide and a C-terminal core peptide, in which the PTMs are installed by specialized modification enzymes. Upon leader peptide cleavage, the lantibiotic becomes activated and exhibits antimicrobial activity with efficiencies in the low nanomolar to millimolar range. Lantibiotics like NAI-107 or NVB302 are already subjected to pre-clinical trails and might be good candidates in the treatment of multidrug-resistant strains like MRSA or similar Gram-positive strains[5–7].

Up to now >50 different lantibiotics with a similar set of PTMs have been described (for more details see review[8]). One specific PTM within the core peptide of lantibiotics is the dehydration of serine and threonine residues resulting in the formation of dehydroalanine and dehydrobutyrine residues. This reaction is catalysed by a specific dehydratase called LanB (dehydratase of class I lantibiotics)[9]. The hallmark of lantibiotics is the second modification, which leads to the formation of lanthionine (Lan) and/or methyl-lanthionine (MeLan) rings. The reaction proceeds via a Michael-type condensation of the dehydrated serine or threonine residues with the thiol group of a cysteine residue, which is introduced regio- and stereospecifically by the cyclase LanC (cylcase of class I lantibiotics)[10]. This ring formation results in a thioether bond giving rise to high thermostability and more profound resistance against proteolytic degradation. Furthermore, antimicrobial activity strictly depends on the presence of the Lan/MeLan rings[11].

Institute of Biochemistry, Heinrich-Heine-University Duesseldorf, Universitaetsstrasse 1, 40225, Duesseldorf, Germany. Marcel Lagedroste and Jens Reiners contributed equally. Correspondence and requests for materials should be addressed to S.H.J.S. (email: sander.smits@hhu.de) or L.S. (email: lutz.schmitt@hhu.de)

In general, lantibiotics exercise their antimicrobial activity through different modes of action. One prominent mode is the binding to the pyrophosphate moiety of lipid II molecules concomitant with the inhibition of peptidoglycan biosynthesis[12]. Another mode of action is the perturbation of bacterial cell membranes. Nisin or subtilin build a pore-forming complex with its receptor lipid II thereby sequestering lipid II within the membrane[13,14] (for a review about lipid II binding peptides see[11]). In the case of nisin, which is active in the low nM range, this process occurs on the ms time scale[15,16]. Some lantibiotics such as for example Pep5 however, directly penetrate the target membrane[17].

In comparison to other cationic AMPs, cytotoxicity against human cells is rarely observed, since lipid II, the main target of lantibiotics, is absent in eukaryotic membranes (except the two-peptide lantibiotic cytolysin S/L[18]). Thus, the efficient activity and the low cytotoxicity combined with few examples of known inherent resistances (see[19–21]) constitute these peptides as excellent lead structures for new antibiotics.

Nevertheless, the bottleneck of lantibiotic research is the identification and characterization of these compounds. With respect to the first, lantibiotics can be detected in genome sequences by data-mining approaches using bioinformatic tools such as BAGEL4[22], antiSMASH[23], RiPPquest[24] and RiPPMiner[25]. Such tools either detect open reading frames encoding lantibiotics within a genome based on neighbouring PTM-enzymes or combine specific sequences of PTM-enzymes and the cleavage motifs within the leader peptides.

However, every newly identified lantibiotic requires a detailed experimental characterization with respect to its antimicrobial properties. Therefore, the isolation of a native sample or heterologously expressed samples in Gram-negative bacteria (*E. coli*)[26,27] or Gram-positive bacteria (*L. lactis* or *B. subtilis*)[28–30] is a prerequisite. Several reports indicate that the nisin modification and secretion system can be employed to modify and secrete other lantibiotics. Apparently, the nisin PTM system provides sufficient promiscuity to produce for example bagelicin from *Streptococcus suis* R61, flavucin from *Corynebacterium lipophiloflavum* and others peptides, if their core peptide is fused to the nisin leader peptide[29,31,32]. Nisin, produced by the Gram-positive *Lactococcus lactis* (*L. lactis*) bacterium and modified by the nisin PTM machinery is one, if not the best characterized lantibiotic and may therefore be used as a standardized lantibiotic for benchmarking.

Since the number of novel lanthipeptides/lantibiotics increases due to genome mining, design of hybrid-peptides (by coupling different lanthipeptides to a certain leader peptide), simple mutations or even chemical synthesis, a general pipeline to characterize the potential antimicrobial activity and thereby potency of a lantibiotic is urgently required to ensure appropriate benchmarking of such lantibiotics[1,33,34].

Here, we used a standardized workflow for the characterization of lantibiotics, containing up to six steps depending on the availability of the lantibiotic (Fig. 1a). We exchanged the isoleucine at position one (I_1) of nisin to all other 20 natural occurring amino acids (aa) (Fig. 1b) and determined the impact on the expression, modification and antimicrobial properties of these nisin variants and benchmarked it against wild type nisin.

Results

General characterisation of nisin I1 mutants. The nisin A core peptide was a target of many former studies aiming to alter the antimicrobial activity of nisin or to broaden its spectrum against microbial targets. Position 1 in the nisin core peptide received our attention since some mutations were described that lacked in our opinion a complete and quantitative characterization. For example, the substitutions of tryptophan-analogues[35] as well as the mutants I_1W, I_1K, I_1D[36], I_1G and I_1Q (described in[37]). Accordingly, we characterized all mutants at I_1 of nisin A using our standardized protocol, which is based on six individual steps (Fig. 1a; I-VI).

The first steps (I-III) concerning expression, secretion and purification of the nisin variants gave no major variation compared to wild type nisin, which were all expressed as a leader-containing variant (pre-nisin). The yield of pre-nisin was 6.0 ± 0.3 mg/ L culture supernatant (Supplementary Fig. S1) with a purity >95% based on Tricine-SDS-PAGE (Supplementary Fig. S2). The yield of most I_1 mutants decreased to 40–60% of wild type nisin (Supplementary Fig. S1). The mutants I_1C and I_1W had an even lower yield of approximately 35%. This lower yield however did not affect our purification protocol and all pre-nisin variants were purified using the same protocol and resulted in comparable purity (Supplementary Fig. S2)[29,32].

Step IV concerns leader peptide cleavage and thereby activation of the purified pre-nisin variants. Here, we used the secreted variant of the natural leader peptidase NisP, by which the leader peptide is cleaved *in vitro* and the cleavage efficiency (%) can be calculated as recently shown[38]. We used an RP-HPLC set-up to monitor product formation, in which the appearance of the leader peptide in the chromatograms was used to determine the concentration of activated nisin (Supplementary Fig. S3). Pre-nisin (Supplementary Fig. S3) had a retention time (RT) between 19 to 21 min, whereas the leader peptide eluted as two peaks corresponding to the variants with and without the N-terminal methionine between 14 to 16 min, respectively. The nisin core peptide eluted at a later retention time of approximately 23 min (Supplementary Fig. S3). In some cases, the nisin I_1 mutants resulted in separated peaks of pre-peptide and core peptide after the activation by NisP (compare mutants I_1M, I_1L, I_1V, I_1W, I_1Y, I_1F and I_1C in Supplementary Fig. S4). However, in the case of the I_1 mutants I_1A, I_1G, I_1T, I_1S, I_1K, I_1R, I_1H, I_1Q, I_1E, I_1N and I_1D) the formation of a core peptide peak in terms of a new and separated peak in the chromatogram was not observed (Supplementary Fig. S4). Rather, the peaks with a retention time between 18–21 min contained both species, the cleaved and non-cleaved lantibiotic, and can therefore not be deconvoluted for proper determination of the amount of activated nisin. Hence, only the two peaks of the leader peptide were used and the area was integrated for the determination of the concentration of activated nisin and its I_1 mutants. The concentration was calculated based on a standard calibration curve (Supplementary Fig. S5), where we precisely determined the concentration of the activated nisin or I_1 mutants. We used this concentration determination instead of the colorimetric protein concentration determination as for example Bradford or the BCA-assay since the latter two assays cannot differentiate between the activated and non-activated form of the secreted variants. Since nisin is not active unless the leader is cleaved off, the determination of the area of the leader peak to calculate the

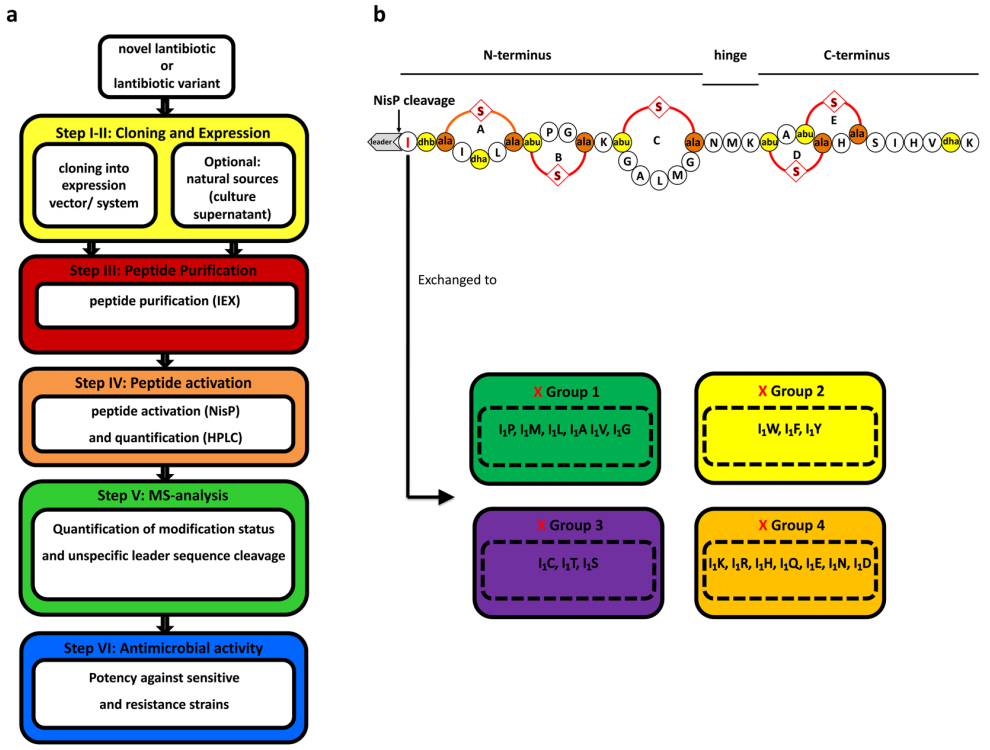

Figure 1. Scheme of lantibiotic characterization (**a**) the lantibiotic nisin and its I_1 mutants (**b**). The characterization of novel lantibiotics or variants is based on a six steps protocol (**a**). I-II are cloning and expression steps (yellow box). Step III covers peptide purification (red box). Step IV represents the activation of the peptide (orange box). Step V is the MS-analysis (green box), while step VI represents the antimicrobial activity of the lantibiotic (blue box). The lantibiotic nisin (NisA) can be dissected into an N-terminal region (with lanthionine ring A and the methyl-lanthionine rings B and C), a hinge region and a C-terminal region (with the intertwined methyl-lanthionine rings D and E) (**b**). The dehydrated amino acids dehydroalanine (dha) and dehydrobutyrine (dhb) (former serines and threonines) are highlighted in yellow. The coupled cysteine residues to dehydrated amino acids are highlighted in orange. The thioether bonds between the (methyl-) lanthionine are marked with a red S. The position one isoleucine is highlighted in red and exchanged to X amino acid from the four different groups of natural amino acids.

amount of the activated lantibiotic directly relates to the antimicrobial activity without need to further purify the peptide after cleavage.

All I_1 mutations were subjected to NisP cleavage and most of the variants were cleaved, but a strong influence of the nature of the I_1 substitutions with respect to cleavage efficiency was observed (Supplementary Fig. S6). The cleavage efficiency for wild type pre-nisin A was $94.3 \pm 1.7\%$ but lower for the mutants I_1M, I_1L, I_1A and I_1V ($72.3 \pm 1.4\%$, $72.4 \pm 1.3\%$, $81.0 \pm 1.8\%$ and $58.1 \pm 2.8\%$, respectively). All other variants displayed efficiency below 50% (Supplementary Fig. S6). This holds especially in those cases, where the amino acid at position one was exchanged to a charged amino acid (e.g. I_1K $9.2 \pm 1.3\%$; I_1E $9.5 \pm 0.7\%$) or contained a bulky hydrophobic side chain (e.g. I_1F $12.9 \pm 0.8\%$; I_1W $5.7 \pm 0.2\%$; I_1Y $22.6 \pm 2.3\%$) (Supplementary Fig. S6). To highlight two examples, NisP was only able to cleave $5.7 \pm 0.2\%$ of the I_1W variant, which was significantly lower as the cleavage efficiency previously reported[35,39]. Interestingly, the I_1P mutant was not cleaved at all by NisP (Supplementary Figs S4 and S6). Even after an extensive prolongation of the incubation time, no leader peptide peak was detected in the RP-HPLC chromatogram (Supplementary Fig. S4). It is important to stress in this context that the cleavage efficiencies cannot be determined from Tricine-SDS gels (20%). Here, the leader peptide as well as the core peptide would co-migrate, which obviously will falsify the staining results.

As previously reported[37,38], a prerequisite for high cleavage efficiency by NisP is the presence of at least one (methyl-)lanthionine ring. Therefore, we wondered whether some of the nisin variants with low cleavage efficiencies were altered in their modification status (step V). To detect possible ring formation(s) we incubated the lantibiotic prior to MS analysis with the thiol-reactive agent 1-cyano-4-dimethylaminopyridinium tetrafluoroborate (CDAP), which binds to free cysteines and results in a mass shift of 25 Da per covalently attached CDAP. When no mass shift occurs, all cysteine residues are part of thioether rings, while for every mass shift of 25 Da one cysteine is not part of a (Me)Lan thioether ring. As controls, we also used the unmodified version of pre-nisin (Supplementary Fig. S7a), in which no rings are present and five CDAP adducts were identified indicating that five cysteine side

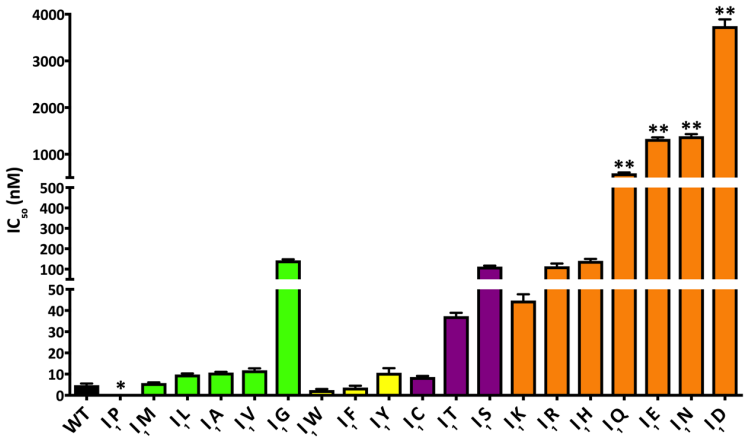

Figure 2. Growth inhibition assay of strain NZ9000-Cm in the presence of nisin and the corresponding I_1 variants. The lantibiotic nisin A (WT) and its I_1 mutants were used for growth inhibition (IC_{50}) against strain NZ9000-Cm. IC_{50} values were grouped in four different sub-groups (group 1: aa M-G, green; group 2: aa W-Y, yellow; group 3: aa C-S, magenta; group 4: aa K-D, orange), Values represents the average of at least five independent measurements and the errors report the standard deviation of the mean (SDM). The nisin variant I_1P was not cleaved by NisP (*) and no growth inhibition assay was conducted. The nisin variants within the forth group marked with (**) showed less antimicrobial activity ($IC_{50} > 500$ nM).

chains were available for a simultaneous labelling reaction and the fully modified pre-nisin, showing no coupling products (Supplementary Fig. S7b). This highlights the quantitative nature of the CDAP assay[31].

For most analysed I_1 mutants no CDAP attachment was observed (Supplementary Figs S8, S9, S10 and Supplementary Table S1). Exceptions of this observation are the mutants I_1L, I_1A, I_1V, I_1G, I_1F, I_1Y, I_1R, I_1H, I_1Q, I_1N, where small amounts of coupling products were observed with variations from 7x dehydrations (dh) to 5x dh with one coupling product (Supplementary Figs S8, S9, S10 and Table S1). These amounts are very small, in comparison to the main species and the MS analysis showed clearly, that the I_1 mutants primary containing all lanthionine rings. In the case of nisin I_1C, where one additional cysteine residue was introduced also one coupling product was observed (Supplementary Fig. S9) In summary, although the analysis of the cleavage reaction revealed I_1 mutants with lower cleavage efficiency, the modifications of the core peptide within these variants were not altered.

Impact of mutations at position I_1 on antimicrobial activity of nisin. Growth inhibition assays (step VI) were used to determine the potency of the activated I_1 mutants. First, this assay was performed against the sensitive strain NZ9000-Cm harbouring an empty plasmid pIL-SV (the strain NZ9000-Erm gave identical results) to determine the value, at which 50% of the cells were inhibited in growth (IC_{50} value).

The nisin A wild type (WT) had an IC_{50} value of 4.8 ± 0.7 nM, which is in a similar range as previous reported values determined with strains NZ9000-Cm/NZ9000-Erm[40–42] (Fig. 2 and Supplementary Table S2). The I_1P mutant was used in very high concentrations (>1 mM) in the growth inhibition assay but displayed no antimicrobial activity (Fig. 2; IC_{50} value is marked with a star symbol). This indicated that this variant was not activated by NisP, in line with our observations described above.

All other variants were used and displayed IC_{50} values ranging from wild type level to 100 nM or even to lower µM values. Based on the measured activities, the variants can be grouped into four classes depending on the amino acid property.

The first group contains mainly aliphatic amino acids (except M)(Fig. 2, green bars and Supplementary Table S2). The mutation to methionine gave similar IC_{50} values to WT (5.8 ± 0.3 nM), but the exchange to the amino acids leucine, alanine and valine lead to a two-fold decrease in activity (9.8 ± 0.5 nM, 10.7 ± 0.4 nM and 11.8 ± 0.9 nM, respectively). The mutation to glycine lead to an even further decrease in activity and the IC_{50} value was determined to 143.0 ± 5.1 nM.

The second group (Fig. 2, yellow bars and Supplementary Table S2) contained aromatic amino acids (except histidine, which belongs to the fourth group) and displayed a high antimicrobial activity against the sensitive strain. Especially, the mutants I_1W and I_1F displayed lower IC_{50} values (2.5 ± 0.2 nM and 3.7 ± 0.8 nM) than WT, indicating an increased antimicrobial activity. The mutant I_1Y showed a lower activity and displayed an IC_{50} value of 10.6 ± 0.9 nM.

The third group (Fig. 2, magenta bars and Supplementary Table S2) displayed IC_{50} values ranging from 8.6 to 112 nM. The mutation I_1C lead to antimicrobial activity of WT (below 10 nM) with an IC_{50} value of 8.6 ± 0.5 nM, whereas the mutation to I_1T or I_1S displayed a considerable reduction of the antimicrobial activity with IC_{50} values of 37.3 ± 1.6 nM and 112.4 ± 5.0 nM, respectively. Interestingly, these substitutions are all amino acids, which are potential targets of the PTM machinery. Since the mutation I_1C introduced an additional cysteine residue, we carefully analysed for the presence of an additional (Me)Lan ring. However, the coupling assay clearly

demonstrated the presence of one accessible cysteine suggesting that this nisin variant still harbours five (Me) Lan rings (Supplementary Fig. S9). Unfortunately, this assay cannot determine which ring(s) are formed. Since the IC_{50} value is not altered, we propose that this mutant follows normal ring formation and the additional introduced cysteine at position one was labelled with CDAP.

The mutations I_1T and I_1S, containing an additional dehydration position. Based on our MS analysis, we saw mainly no additional dehydration, which leads to the conclusion that this position is not well recognized by NisB (Supplementary Fig. S9). But we clearly observed that the possible higher number of dehydrations of the peptide at the N-terminus of the core peptide decreased antimicrobial activity (IC_{50} values > 30 nM). Here, mutation to the polar residue serine had a larger impact on the antimicrobial activity of the core peptide compared to the threonine substitution.

The fourth group (Fig. 2, orange bars and Supplementary Table S2) contained charged amino acids and the amide side chains of glutamate and aspartate. In general, a strong negative effect on the antimicrobial activity was observed within this group. The IC_{50} values were higher compared to the other groups and ranged from 44 nM to 3746 nM. The substitutions at position 1 to the amino acids lysine, arginine or histidine lead to 10-fold or even 20-fold higher IC_{50} values (I_1K: 44.7 ± 3.0 nM, I_1R: 113.9 ± 13.6 nM and I_1H: 140.0 ± 5.0 nM) compared to the WT IC_{50} value. A major alteration in antimicrobial activity was observed in the case of an exchange I_1Q and I_1E, respectively. Here, the IC_{50} values were 592.0 ± 17.8 nM for I_1Q and 1328.0 ± 32.7 nM for I_1E. An even more dramatic effect was observed upon introduction of I_1N or I_1D. Here, IC_{50} values of 1386.0 ± 46.3 nM and 3746.0 ± 144.1 nM were determined. These variants displayed such high IC_{50} values (marked by two star symbols (**)) that these mutations were not analysed in further growth inhibition assays using resistant strains.

In summary, the antimicrobial activity of the different I_1 mutants towards the sensitive strain NZ9000-Cm correlated with the physico-chemical properties of amino acid at position one. Although this substitution was only one amino acid and the modification state of the core peptide was not altered, the active lantibiotics showed drastic variations in antimicrobial activities. Based on the growth inhibition assay, these I_1 mutants were divided into four groups, where aromatic amino acids at position one lead to higher activity but an introduction of polar, charged amino acids or its amidated counterparts decreased the potency of the corresponding variant to the sensitive strain.

The influence of I_1 mutants on immunity and resistance proteins. Lantibiotics are regarded as potential antibiotic candidates, which might have the potential to replace classic antibiotics and thereby overcome the increasing resistances against major antibiotic classes. One potential drawback of lantibiotics is highlighted by the few reported resistance mechanisms against for example nisin[43]. Therefore, it is critical, to screen for strains, which might be resistant against the new lantibiotic, if a new lantibiotic is characterized and its potency is determined. In our protocol, we implemented first the screen against a sensitive strain (see above), but more importantly we included four strains expressing immunity or resistance proteins against nisin. The immunity proteins NisI (lipoprotein) and NisFEG (ABC transporter) from L. *lactis* are the first and second line of defence of the nisin producer strain[44]. Upon expression in the sensitive strain NZ9000, these proteins might provide immunity and one can study the activity of the lantibiotic in the presence of immunity proteins. Additionally, we screened the effect of the I_1 variants on the nisin resistance proteins *Sa*NSR (lipoprotein) and *Sa*NsrFP (ABC transporter) to fully consider the potency of the newly lantibiotic/lantibiotic variant. If these proteins are expressed in the sensitive strain, they confer resistance against the nisin and likely to nisin variants.

The nisin variants were analysed according to the above provided classification of four groups. The first group of I_1 mutants showed a similar tendency in activity towards the strains for immunity and resistance as for the sensitive strain (Supplementary Table S2). The substitutions of isoleucine to methionine, leucine, valine and alanine gave IC_{50} values for strain NZ9000-NisI in a range of 35–65 nM and were comparable to nisin A WT (46.0 ± 6.0 nM) (Fig. 3a). Only the substitution to glycine gave a higher value of 785.7 ± 9.7 nM reflecting the low activity of this variant. The IC_{50} values of the first group for the strain NZ9000-NisFEG were also in the range of 34–50 nM (nisin A WT: 53.0 ± 4.5 nM). Again, a higher IC_{50} value of 557.8 ± 28.3 nM was determined for the I_1G mutant.

When analysing the results of the resistance strains two major changes were observed. In general, the IC_{50} values of the I_1 mutants for strain NZ9000-*Sa*NSR were similar (53–84 nM) to the WT (73.1 ± 3.6 nM). The IC_{50} value for the I_1G mutant was 278.5 ± 13.3 nM and lower in comparison to the IC_{50} values of the other strains (Fig. 3a). The IC_{50} values for strain NZ9000-*Sa*NsrFP changed only for the mutants I_1A (166.1 ± 5.1 nM) and I_1G (2257.0 ± 53.4 nM), respectively, reflecting the lower activity of these variants towards the strain.

The second group of I_1 mutants included the aromatic amino acids, for which a higher activity against the immunity and resistance strains was observed (Supplementary Table S2). The higher activity was determined for all strains ($I_1W > I_1F >$ wild type $> I_1Y$). The exception is the mutant I_1Y and strain NZ9000-NisFEG. Here, the IC_{50} value was lower than the one of nisin A WT (53.0 ± 4.5 nM) (Fig. 3b). Interestingly, the mutant I_1W showed high potency for the strains NZ9000-NisI, NZ9000-NisFEG and NZ9000-*Sa*NSR with IC_{50} values below 25 nM. A higher IC_{50} value of 46.6 ± 1.1 nM was only determined against strain NZ9000-*Sa*NsrFP (Fig. 3b).

The third group of I_1 mutants showed opposing results concerning immunity and resistance (Supplementary Table S2). Here, mutants I_1T and I_1S had lower antimicrobial activity than wild type reflected by IC_{50} value even above 100 nM (Fig. 3c). Especially, the more than five-fold lower activity against strains NZ9000-NisI and NZ9000-*Sa*NsrFP is surprising as the IC_{50} values were determined to be above 500 nM. For the mutant I_1T the values are 653.3 ± 5.1 nM and 716.1 ± 28.6 nM, whereas for the mutant I_1S the values are two-fold higher (1898.0 ± 62.3 nM and 2893.0 ± 34.8 nM) (Fig. 3c). The exception is the mutant I_1C, which showed a similar activity towards the strains as nisin A WT with IC_{50} value in the range of 41 to 101 nM. Based on the MS analysis only one free cysteine was present, we cannot conclude which of the cysteines is not part of a thioether bridge. As this variant showed a similar antimicrobial activity, we however suggest no alteration in ring pattern (Supplementary Fig. S9).

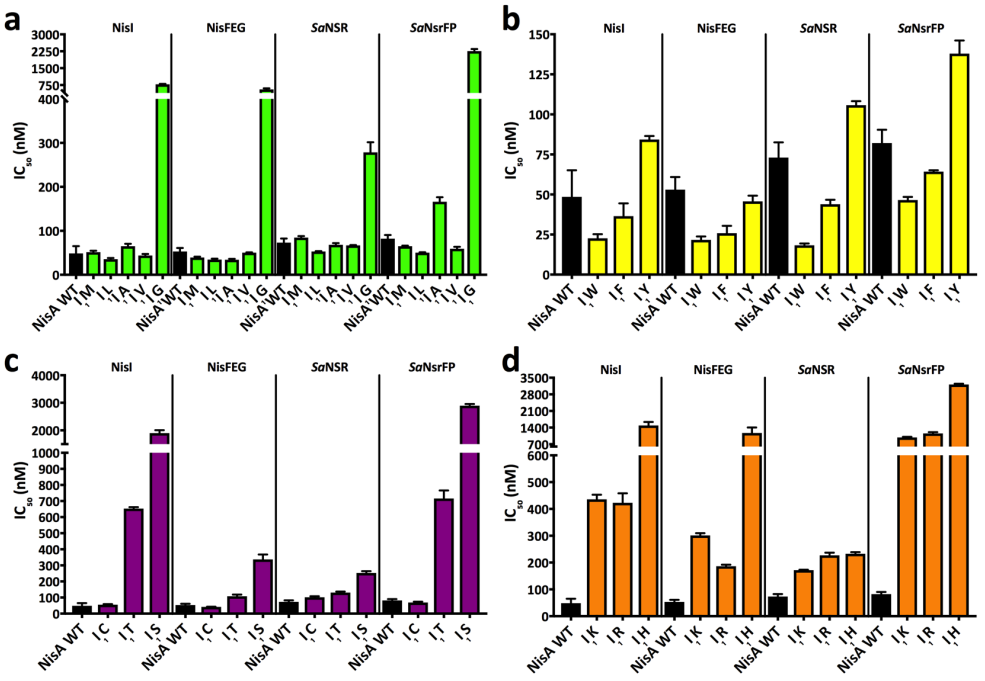

Figure 3. Growth inhibition assay of strains NZ9000-NisI, NZ9000-NisFEG, NZ9000-*Sa*NSR and NZ9000-*Sa*NsrFP in the presence of nisin and the corresponding I_1 variants. The lantibiotic nisin A (WT) and its I_1 mutants were used for growth inhibition (IC_{50}) with strains NZ9000-NisI, NZ9000-NisFEG, NZ9000-*Sa*NSR and NZ9000-*Sa*NsrFP. The IC_{50} values were grouped in sub-groups of the I_1 mutants. The group 1 with the aa M-G (**a**), group 2 with the aa W-Y (**b**), group 3 with the aa C-S (**c**) and group 4 with the aa K-H (**d**). Values represent the average of at least five independent measurements and the errors report the standard deviation of the mean (SDM).

In the last group of I_1 mutants, all variants showed lower antimicrobial activity towards the strains of immunity and resistance (Supplementary Table S2). The IC_{50} values were above 400 nM (Fig. 3d) except for mutants I_1R and I_1K, which had IC_{50} values of 186.4 ± 3.1 and 301.2 ± 4.7 nM, respectively, against strain NZ9000-NisFEG. Similar to this, mutants I_1R, I_1K and I_1H showed a higher antimicrobial activity against strain NZ9000-*Sa*NSR (Fig. 3d).

In summary, I_1 mutations clearly influenced the efficiency of the immunity and resistance proteins. The IC_{50} values of the sensitive strain and resistance strains for the different I_1 mutations can be used to calculate a fold of resistance (Fig. 4). Here, the effect of certain mutations is even less pronounced (e.g. I_1S or I_1T on NZ9000-NisI) but still show the reduced activity. The reasons for this reduction might be that these variants are better ligand and/or substrates for the immunity and resistance proteins. Another explanation might be, that the variants have an altered interaction with the membrane (I_1K; I_1R, I_1W, I_1F). The same is true for the opposite case, in which the mutants are more active. Here, the mutants are either worse substrates or showed a loss in membrane attraction due to charge repulsion (I_1E/D mutants) or reduced hydrophobicity (I_1G mutant).

Discussion

The increased detection of antibiotic resistances of human pathogenic strains urgently calls for the identification of novel lead structures, which can be used to develop long lasting antibiotics. One promising family of candidates are the antimicrobial peptide subfamily of lantibiotics. They are small ribosomally synthesized and post-translational modified peptides[45,46], which possess a potent antimicrobial activity generally in the nM range. Their antimicrobial activity makes them excellent candidates to treat MDR-strains such as MRSA or VRE[47]. Recently, numerous new lantibiotics were discovered by "*in silico* genome mining" approaches, using available bacterial genome sequence data[48]. Here, BAGEL4 and its predecessor BAGEL3 are powerful algorisms to detect lantibiotics sequences within bacterial genome sequences[22]. Novel lantibiotic such as flavucin, bagelicin and agalacticin were found and their antimicrobial properties were determined[29]. In the study by Heel *et al.* 2016 the potency of many new lantibiotics were screen against a set of Gram-positive and Gram-negative strains to show their antimicrobial potencies. Till now, however, it is not possible to deduce the potency solely on sequence information and every lantibiotic needs to be expressed and purified for subsequent characterization of its antimicrobial activity. To ensure comparability of the determined activities and the potencies derived from these experiments a standardized protocol needs to be established, which allows benchmarking novel against already characterized lantibiotics (e.g. nisin). This should also include mutations designed or natural variants of previously characterized lantibiotics.

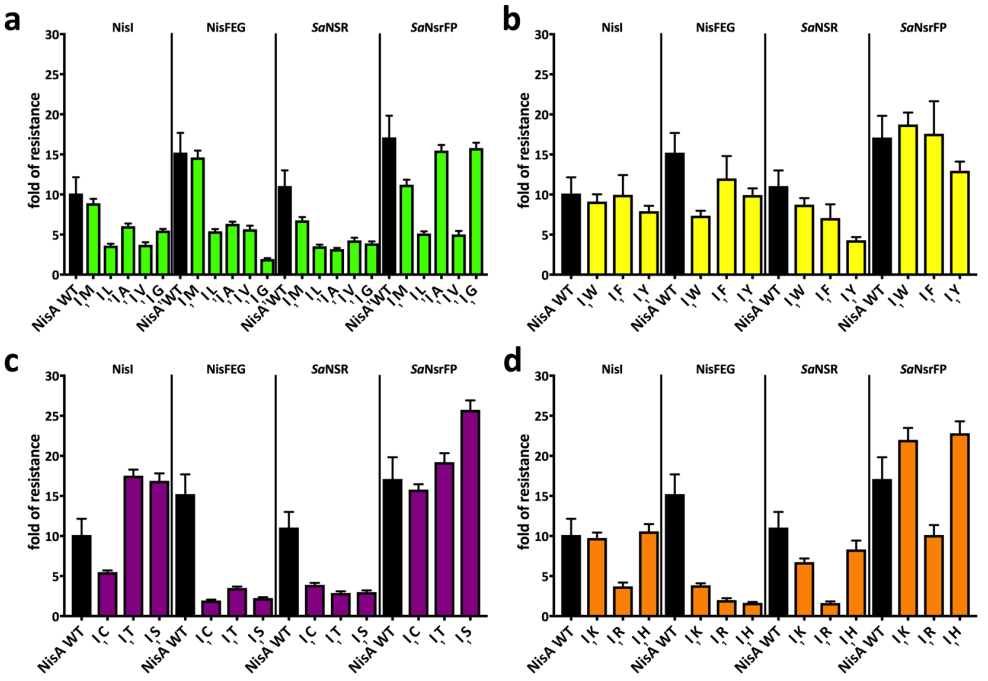

Figure 4. Fold of resistance of strains NZ9000-NisI, NZ9000-NisFEG, NZ9000-*Sa*NSR and NZ9000-*Sa*NsrFP in comparison to NZ9000-Cm. The resistance of the strains NZ9000-NisI, NZ9000-NisFEG, NZ9000-*Sa*NSR and NZ9000-*Sa*NsrFP towards the lantibiotic nisin A (WT) and its I_1 mutants are presented as fold of resistance. The fold of resistance values were grouped in sub-groups of the I_1 mutants. The group 1 with the aa M-G (**a**), group 2 with the aa W-Y (**b**), group 3 with the aa C-S (**c**) and group 4 with the aa K-H (**d**). Values represent the average of at least five independent measurements and the errors report the standard deviation of the mean (SDM).

In this study, we used a standardized protocol based on six individual steps (I-VI). Some of these steps have been previously (partly) published, but not as a combined robust protocol[29,32,40,42,49]. By replacing I_1 of nisin A against any other amino acid, the complete influence of the exchange on expression, purification and/or activity was monitored to provide a quantitative characterisation.

The characterisation of a novel lantibiotic starts with the expression system and the choice of homologous or heterologous expression. Homologous expression of a lantibiotic is often associated with its isolation from supernatants of lantibiotic producer strains (examples are epidermin[50], mutacin 1140[51], NAI-107 and related lantibiotics[52] or pinensins[53]). The yield of this strategy can be limited, especially if the producer is hardly cultivable under lab conditions or induction of the lantibiotic is not trigged (e.g. geobacillin I[54], salivaricin 9[55] and staphylococcin Au-26,[56]).

Therefore, for some lantibiotics such as lichenicidin from *Bacillus licheniformis* ATCCC 14580[26], or prochlorosins from *Prochlorococcus* MIT 9313[57] a heterologous expression in *E. coli* is the preferential strategy to obtain higher yields of the pre-lantibiotic. Alternatively, the expression via the NICE-system in *L. lactis*[58] is a possibility. Here, the pre-lantibiotic is modified after induction with the lantibiotic nisin by the PTM system (NisB/NisC) and secreted by the ABC transporter NisT[32].

The nisin PTM system was shown to be of sufficient promiscuity to modify and secrete lantibiotics as well as non-lantibiotic peptides[29,32]. As an advantage any lantibiotic can be produced as a pre-lantibiotic. This results in higher yields, as the lantibiotic is not antimicrobial active and is not limiting the growth of the producer strain. Furthermore, the pre-lantibiotic (as pre-nisin) shows higher pH stability in contrast to nisin (low solubility at $pH > 7$)[59]. Normally, we observed yields for the pre-nisin and its variants of 3–6 mg per liter cell culture supernatant after purification (Supplementary Fig. S1). Considering these yields further down-streaming steps are employed to characterize the lantibiotic.

Although NisB and NisC are promiscuous in modifying their substrate, it is crucial that both enzymes fully modify the core peptide similar to pre-nisin. Otherwise, the steps III (cleavage by NisP) and VI (antimicrobial assay) might be less informative. Thus, even new mutants of nisin, like mutants in the hinge region[60,61] or in the leader peptide[37], required a full characterisation with respect to their modification and antimicrobial activity.

The purified pre-lantibiotics need to be analysed by RP-HPLC before and after activation by proteolytic cleavage of the leader peptide. In this study, we activated pre-nisin and the I_1 mutants *in vitro* by purified leader peptidase NisP (Supplementary Figs S3 and S4; described in[38,49]). The cleavage efficiency and also the exact concentration of the active lantibiotic were determined via RP-HPLC (Supplementary Fig. S6). Hence, every activation of the pre-lantibiotic can be monitored and quantified by integrating the leader peptide peaks, which are used for calculation of the amount of activated lantibiotic. We observed for some I_1 mutants, that the properties

during the RP-HPLC runs of the pre-lantibiotics and activated lantibiotics made it impossible to distinguish between both peaks (Supplementary Fig. S4). Consequently, the areas of leader peptide peaks were used for quantification. One other aspect that has to be taken in consideration is the fact that for nisin mutants, such as I_1A or I_1K, the core peptide cannot be purified by means of preparative RP-HPLC from the supernatant. In general, the analytic RP-HPLC is needed to quantify the lantibiotic and as a quality control for the purification and the cleavage reaction.

The major advantage of RP-HPLC compared to other technics is the more accurate determination of the concentration of the activated lantibiotic, which is a prerequisite for a reliable determination of the biological activity of the lantibiotic. In comparison to methods determining the total amount of peptide/protein (e.g. BCA-assay and other colorimetric assays) the determination via HPLC minimizes the error. For example, if only 15% of a pre-lantibiotic is cleaved, but the total amount of pre-lantibiotic is used for the calculations, the determined IC_{50} value would be six to seven-fold larger, which obviously indicates a falsely lower antimicrobial activity.

Sometimes a lower cleavage efficiency of the leader peptidase and later a lower antimicrobial activity might reflect incomplete modification of the peptide (e.g. dehydrations or the lack of lanthionine rings) or disrupted recognition by the leader peptidase. As an example, the mutation of I_1 in nisin Z to tryptophan leads to the production of two variants. The I_1W mutant as a main product and a small amount of I1W/Dh2T, where the threonine residue escape the dehydration and an altered activity is proposed[62]. Therefore, a proper determination of dehydration and the formation of lanthionine rings by MS-analysis is required. MS-analysis provides information about the dehydration reaction of NisB[63] by the loss of water (−18 Da), but cannot indicate the formation of the (methyl-)lanthionine rings. Furthermore, it is not possible to distinguish between the position of the dehydration within the nisin core peptide, which might have escaped modification like threonine position 2 or serine position 33[64]. Thus, it is inevitable to use at least one orthogonal method to determine the presence of lanthionine ring(s). Either the use of an alkylation agent (e.g. CDAP to couple the free thiol group from cysteine residues) or tandem MS-MS analysis to determine the alternate fragmentation pattern between WT pre-lantibiotic and potential mutant variants is necessary.

In our protocol we choose the CDAP-coupling assay to detect nisin I_1 mutants, which might still possess free thiol groups. The advantage of the CDAP-coupling assay is the additional mass shift in the MS spectra. Here, a mass shift of 25 Da per thiol-conjugated easily indicates incomplete ring-formation.

The activated lantibiotic was used for antimicrobial activity assays (step VI), in which different indicator strains were employed. Here, the assay for antimicrobial activity needs to be suitable for the characterisation of the lantibiotic. The broth dilution with 2-fold dilution series of lantibiotics in a MIC assay is generally used to determine the antimicrobial activity[65]. However, if only one stock concentration is used, one obvious limitation is the factor two in serial dilutions, which will detect only changes larger than two. Therefore, we suggest to use the IC_{50} assay with a high diversity of stock concentrations to screen every data point. Still, both methods have their limit as no information about the mode of action of the lantibiotic can be acquired.

The active lantibiotic were screened against a sensitive strain to determine the IC_{50} value by growth inhibition assay (described with modifications in[41]). We used the *L. lactis* strain NZ9000 with the corresponding empty vector systems pNZ-SV or pIL-SV, termed NZ9000-Erm and NZ9000-Cm, respectively. Generally, we would like to propose that the strain *L. lactis* NZ9000 is used as a standard strain, in order to have comparable values from antimicrobial activity assay.

The full potential of a lantibiotic or lantibiotic variants can be shrouded if the screen is only performed against sensitive strains. Therefore, based on the IC_{50} value from the sensitive strains, a second screen against strains, which express immunity or resistance proteins should be performed[66]. We used the strains NZ9000-NisI and NZ9000-NisFEG to study the effect of the immunity proteins from *L. lactis* as they confer immunity via different mechanisms[67,68]. To analyse the effect of a lantibiotic on resistance potency, strains NZ9000-*Sa*NSR and NZ9000-*Sa*NsrFP expressing proteins involved the nisin resistance from *Streptococcus agalactiae* were used[42,66]. Importantly, the ratio of the IC_{50} values (fold of resistance) of these strains to the sensitive strain describes the alteration of substrate specificity on the immunity or resistance proteins (described in[40]).

As final remark, the production of lantibiotics, especially if they are heterologously expressed, has to be benchmarked against a standardized lantibiotic. Here, the well-studied lantibiotic nisin can be used again to benchmark against novel and unknown lantibiotics.

In summary, our analysis and the suggested roadmap demonstrate that a detailed and multifaceted investigation of the antimicrobial potency of lantibiotic is necessary to uncover the full potential of novel lantibiotics, but also to quantitatively compare the efficiency of different members of this promising family of antimicrobial peptides.

Materials and Methods

Microorganisms and culture conditions. Strains and the plasmids used in this study are listed in Table S3. Cultures of *L. lactis* NZ9000 were grown in M17 medium at 30 °C supplemented with 0.5% glucose (GM17 and the appropriate antibiotics (final concentrations 5 µg/ml). In the case of pre-lantibiotic secretion, the *L. lactis* strain NZ9000 was grown in minimal medium at 30 °C supplemented with 0.5% glucose and the appropriate antibiotics (final concentrations 5 µg/ml).

The cultures of the *E. coli* strain DH5α were grown in Luria-Bertani (LB) medium at 37 °C under aerobic conditions with the appropriate antibiotic (100 µg/ml ampicillin or 30 µg/ml kanamycin final concentration).

Cloning of nisin variants. The substitution of amino acids in the *nisA* gene was performed by standard site-directed mutagenesis. Here, the vector pNZ-SV-nisA was used as a template to introduce mutations by Pfu-DNA polymerase (Thermo-Scientific) following standard protocol of the manufacture. Used oligonucleotides are listed elsewhere (Supplementary Table S4). Sequence analysis verified the correctness of the nisin variants

and plasmids were transformed into electro-competent *L. lactis* NZ9000 strain, already containing the pIL3-BTC vector for expression.

Expression and purification of NisP. The soluble variant of NisP was expressed by *L. lactis* NZ9000 harbouring the plasmid pNGnisP8His and subsequently purified as previously described[38].

Expression purification and activation of pre-nisin variants. Pre-nisin and its variants were expressed and purified as previously described[41,49,69]. The purity of pre-nisin and its variants was controlled by Tricine-SDS-PAGE (20%)[70]. The activation of all variants was performed by NisP cleavage overnight at 8 °C. Pre-nisin cleavage and its variants was monitored by RP-HPLC[49,69].

Determination of active nisin by HPLC analysis. Pre-nisin and the activated nisin variants were analysed by RP-HPLC (Agilent Technologies 1260 Infinity II) with a LiChrospher WP 300 RP-18 end-capped column and an acetonitrile/water solvent system. The cleavage efficiency and the concentration of active lantibiotic was calculated as described previously[49,69].

Cloning and expression of immunity and resistance proteins. The cloning of plasmids encoding for immunity and resistance proteins used in this study were previously described[40–42,71]. A nomenclature of the strains used for antimicrobial activity assay is shown elsewhere (Supplementary Table S3).

Determination antimicrobial activity by growth inhibition assay. The growth inhibition assay with the NZ9000 strains was conducted as described in[41]. There, the inhibitory concentration (IC_{50}), where only 50% of the cells survive can be calculated for the different lantibiotics.

The fold of immunity/resistance was calculated by dividing the IC_{50} values of strains expressing the immunity or resistance proteins from the IC_{50} value of the control strain harbouring the empty plasmid[40,42].

MALD-TOF analysis: Dehydration and lanthionine ring analysis. Prior to MS analysis the activated nisin variant were desalted via C_{18} ZipTip purification according to the manufactory manual (Merk-Millipore). The vacuum dried pellet was directly used for MALDI-TOF analysis or coupled with an organic coupling agent for free cysteine residues[72]. For coupling, the pellet was dissolved in 9 µl citrate buffer (25 mM, pH 3) and incubated with 2 µl TCEP (Tris[2- carboxyethyl]phosphine) (100 nmol) for 20 min at 29 °C. After the incubation, the coupling agent CDAP (1-cyano-4 dimethylaminopyridinium tetrafluoroborate) (140 nmol) was added and incubated for 15 min at 29 °C.

For MALDI-TOF analysis the vacuum dried pellet was dissolved with 50 µL 50% acetonitrile solution containing 0.1% TFA. From the soluble sample, 1 µl was mixed with 10 µl matrix solution (10 mg/ml alpha-cyano-4-hydroxycinnamic acid, dissolved in 50% acetonitrile containing 0.1% (v/v) trifluoroacetic acid) and 1 µl of the mixture was spotted on the target. The sample was analysed with MALDI-TOF (UltrafleXtreme, Bruker Daltonics, Bremen, Software: Compass 1.4) in positive mode.

References

1. Tracanna, V., de Jong, A., Medema, M. H. & Kuipers, O. P. Mining prokaryotes for antimicrobial compounds: from diversity to function. *FEMS Microbiol Rev* **41**, 417–429, https://doi.org/10.1093/femsre/fux014 (2017).
2. Dischinger, J., Basi Chipalu, S. & Bierbaum, G. Lantibiotics: promising candidates for future applications in health care. *Int J Med Microbiol* **304**, 51–62, https://doi.org/10.1016/j.ijmm.2013.09.003 (2014).
3. Schnell, N. *et al*. Prepeptide sequence of epidermin, a ribosomally synthesized antibiotic with four sulphide-rings. *Nature* **333**, 276–278, https://doi.org/10.1038/333276a0 (1988).
4. Arnison, P. G. *et al*. Ribosomally synthesized and post-translationally modified peptide natural products: overview and recommendations for a universal nomenclature. *Nat. Prod. Rep.* **30**, 108–160, https://doi.org/10.1039/c2np20085f (2013).
5. Brunati, C. *et al*. Expanding the potential of NAI-107 for treating serious ESKAPE pathogens: synergistic combinations against Gram-negatives and bactericidal activity against non-dividing cells. *J Antimicrob Chemoth* **73**, 414–424, https://doi.org/10.1093/jac/dkx395 (2018).
6. Jabes, D. *et al*. Efficacy of the New Lantibiotic NAI-107 in Experimental Infections Induced by Multidrug-Resistant Gram-Positive Pathogens. *Antimicrobial Agents and Chemotherapy* **55**, 1671–1676, https://doi.org/10.1128/Aac.01288-10 (2011).
7. Crowther, G. S. *et al*. Evaluation of NVB302 versus vancomycin activity in an *in vitro* human gut model of Clostridium difficile infection. *J Antimicrob Chemoth* **68**, 168–176, https://doi.org/10.1093/jac/dks359 (2013).
8. Repka, L. M., Chekan, J. R., Nair, S. K. & van der Donk, W. A. Mechanistic Understanding of Lanthipeptide Biosynthetic Enzymes. *Chem Rev* **117**, 5457–5520, https://doi.org/10.1021/acs.chemrev.6b00591 (2017).
9. Koponen, O. *et al*. NisB is required for the dehydration and NisC for the lanthionine formation in the post-translational modification of nisin. *Microbiology* **148**, 3561–3568, https://doi.org/10.1099/00221287-148-11-3561 (2002).
10. Li, B. & van der Donk, W. A. Identification of essential catalytic residues of the cyclase NisC involved in the biosynthesis of nisin. *J Biol Chem* **282**, 21169–21175, https://doi.org/10.1074/jbc.M701802200 (2007).
11. Oppedijk, S. F., Martin, N. I. & Breukink, E. Hit 'em where it hurts: The growing and structurally diverse family of peptides that target lipid-II. *Biochim Biophys Acta* **1858**, 947–957, https://doi.org/10.1016/j.bbamem.2015.10.024 (2016).
12. Hsu, S. T. *et al*. The nisin-lipid II complex reveals a pyrophosphate cage that provides a blueprint for novel antibiotics. *Nat Struct Mol Biol* **11**, 963–967, https://doi.org/10.1038/nsmb830 (2004).
13. Hart, P., Oppedijk, S. F., Breukink, E. & Martin, N. I. New Insights into Nisin's Antibacterial Mechanism Revealed by Binding Studies with Synthetic Lipid II Analogues. *Biochemistry* **55**, 232–237, https://doi.org/10.1021/acs.biochem.5b01173 (2016).
14. Hasper, H. E., de Kruijff, B. & Breukink, E. Assembly and stability of nisin-lipid II pores. *Biochemistry* **43**, 11567–11575, https://doi.org/10.1021/bi049476b (2004).
15. Wiedemann, I., Benz, R. & Sahl, H. G. Lipid II-mediated pore formation by the peptide antibiotic nisin: a black lipid membrane study. *J Bacteriol* **186**, 3259–3261 (2004).
16. Breukink, E. Use of the Cell Wall Precursor Lipid II by a Pore-Forming Peptide Antibiotic. *Science* **286**, 2361–2364, https://doi.org/10.1126/science.286.5448.2361 (1999).
17. Brötz, H. *et al*. Role of lipid-bound peptidoglycan precursors in the formation of pores by nisin, epidermin and other lantibiotics. *Molecular Microbiology* **30**, 317–327, https://doi.org/10.1046/j.1365-2958.1998.01065.x (1998).

18. Cox, C. R., Coburn, P. S. & Gilmore, M. S. Enterococcal cytolysin: A novel two component peptide system that serves as a bacterial defense against eukaryotic and prokaryotic cells. *Curr Protein Pept Sc* **6**, 77–84, https://doi.org/10.2174/1389203053027557 (2005).
19. Draper, L. A., Cotter, P. D., Hill, C. & Ross, R. P. Lantibiotic resistance. *Microbiol Mol Biol Rev* **79**, 171–191, https://doi.org/10.1128/MMBR.00051-14 (2015).
20. Khosa, S., Hoeppner, A., Gohlke, H., Schmitt, L. & Smits, S. H. Structure of the Response Regulator NsrR from Streptococcus agalactiae, Which Is Involved in Lantibiotic Resistance. *PLoS One* **11**, e0149903, https://doi.org/10.1371/journal.pone.0149903 (2016).
21. Revilla-Guarinos, A., Gebhard, S., Mascher, T. & Zuniga, M. Defence against antimicrobial peptides: different strategies in Firmicutes. *Environ Microbiol* **16**, 1225–1237, https://doi.org/10.1111/1462-2920.12400 (2014).
22. van Heel, A. J. *et al*. BAGEL4: a user-friendly web server to thoroughly mine RiPPs and bacteriocins. *Nucleic Acids Res*, https://doi.org/10.1093/nar/gky383 (2018).
23. Blin, K., Medema, M. H., Kottmann, R., Lee, S. Y. & Weber, T. The antiSMASH database, a comprehensive database of microbial secondary metabolite biosynthetic gene clusters. *Nucleic Acids Res* **45**, D555–D559, https://doi.org/10.1093/nar/gkw960 (2017).
24. Mohimani, H. *et al*. Automated Genome Mining of Ribosomal Peptide Natural Products. *ACS Chemical Biology* **9**, 1545–1551, https://doi.org/10.1021/cb500199h (2014).
25. Agrawal, P., Khater, S., Gupta, M., Sain, N. & Mohanty, D. RiPPMiner: a bioinformatics resource for deciphering chemical structures of RiPPs based on prediction of cleavage and cross-links. *Nucleic Acids Res*, https://doi.org/10.1093/nar/gkx408 (2017).
26. Caetano, T., Krawczyk, J. M., Mosker, E., Sussmuth, R. D. & Mendo, S. Heterologous expression, biosynthesis, and mutagenesis of type II lantibiotics from Bacillus licheniformis in Escherichia coli. *Chem Biol* **18**, 90–100, https://doi.org/10.1016/j.chembiol.2010.11.010 (2011).
27. Tang, W. & van der Donk, W. A. Structural characterization of four prochlorosins: a novel class of lantipeptides produced by planktonic marine cyanobacteria. *Biochemistry* **51**, 4271–4279, https://doi.org/10.1021/bi300255s (2012).
28. Sherwood, E. J., Hesketh, A. R. & Bibb, M. J. Cloning and analysis of the planosporicin lantibiotic biosynthetic gene cluster of Planomonospora alba. *J Bacteriol* **195**, 2309–2321, https://doi.org/10.1128/JB.02291-12 (2013).
29. van Heel, A. J. *et al*. Discovery, Production and Modification of Five Novel Lantibiotics Using the Promiscuous Nisin Modification Machinery. *ACS Synth Biol* **5**, 1146–1154, https://doi.org/10.1021/acssynbio.6b00033 (2016).
30. Chakicherla, A. & Hansen, J. N. Role of the leader and structural regions of prelantibiotic peptides as assessed by expressing nisin-subtilin chimeras in Bacillus subtilis 168, and characterization of their physical, chemical, and antimicrobial properties. *J Biol Chem* **270**, 23533–23539 (1995).
31. Kluskens, L. D. *et al*. Post-translational modification of therapeutic peptides by NisB, the dehydratase of the lantibiotic nisin. *Biochemistry* **44**, 12827–12834, https://doi.org/10.1021/bi050805p (2005).
32. Rink, R. *et al*. Lantibiotic structures as guidelines for the design of peptides that can be modified by lantibiotic enzymes. *Biochemistry* **44**, 8873–8882, https://doi.org/10.1021/bi050081h (2005).
33. Ongey, E. L. & Neubauer, P. Lanthipeptides: chemical synthesis versus *in vivo* biosynthesis as tools for pharmaceutical production. *Microb Cell Fact* **15**, 97, https://doi.org/10.1186/s12934-016-0502-y (2016).
34. Burkhart, B. J., Kakkar, N., Hudson, G. A., van der Donk, W. A. & Mitchell, D. A. Chimeric Leader Peptides for the Generation of Non-Natural Hybrid RiPP Products. *ACS Cent Sci* **3**, 629–638, https://doi.org/10.1021/acscentsci.7b00141 (2017).
35. Zhou, L. *et al*. Incorporation of tryptophan analogues into the lantibiotic nisin. *Amino Acids* **48**, 1309–1318, https://doi.org/10.1007/s00726-016-2186-3 (2016).
36. Montalban-Lopez, M., Deng, J., van Heel, A. J. & Kuipers, O. P. Specificity and Application of the Lantibiotic Protease NisP. *Front Microbiol* **9**, 160, https://doi.org/10.3389/fmicb.2018.00160 (2018).
37. Plat, A., Kluskens, L. D., Kuipers, A., Rink, R. & Moll, G. N. Requirements of the engineered leader peptide of nisin for inducing modification, export, and cleavage. *Appl Environ Microbiol* **77**, 604–611, https://doi.org/10.1128/AEM.01503-10 (2011).
38. Lagedroste, M., Smits, S. H. J. & Schmitt, L. Substrate Specificity of the Secreted Nisin Leader Peptidase NisP. *Biochemistry*, https://doi.org/10.1021/acs.biochem.7b00524 (2017).
39. Kuipers, O. P., Rollema, H. S., Beerthuyzen, M. M., Siezen, R. J. & de Vos, W. M. Protein engineering and biosynthesis of nisin and regulation of transcription of the structural nisA gene. *International Dairy Journal* **5**, 785–795, https://doi.org/10.1016/0958-6946(95)00032-1 (1995).
40. AlKhatib, Z. *et al*. The C-terminus of nisin is important for the ABC transporter NisFEG to confer immunity in Lactococcus lactis. *Microbiologyopen* **3**, 752–763, https://doi.org/10.1002/mbo3.205 (2014).
41. AlKhatib, Z. *et al*. Lantibiotic immunity: inhibition of nisin mediated pore formation by NisI. *PLoS One* **9**, e102246, https://doi.org/10.1371/journal.pone.0102246 (2014).
42. Reiners, J. *et al*. The N-terminal Region of Nisin Is Important for the BceAB-Type ABC Transporter NsrFP from Streptococcus agalactiae COH1. *Front Microbiol* **8**, 1643, https://doi.org/10.3389/fmicb.2017.01643 (2017).
43. Khosa, S., AlKhatib, Z. & Smits, S. H. NSR from Streptococcus agalactiae confers resistance against nisin and is encoded by a conserved nsr operon. *Biol Chem* **394**, 1543–1549, https://doi.org/10.1515/hsz-2013-0167 (2013).
44. Alkhatib, Z., Abts, A., Mavaro, A., Schmitt, L. & Smits, S. H. Lantibiotics: how do producers become self-protected? *J Biotechnol* **159**, 145–154, https://doi.org/10.1016/j.jbiotec.2012.01.032 (2012).
45. Alvarez-Sieiro, P., Montalban-Lopez, M., Mu, D. D. & Kuipers, O. P. Bacteriocins of lactic acid bacteria: extending the family. *Appl Microbiol Biot* **100**, 2939–2951, https://doi.org/10.1007/s00253-016-7343-9 (2016).
46. Cotter, P. D., Hill, C. & Ross, R. P. Bacteriocins: developing innate immunity for food. *Nat Rev Microbiol* **3**, 777–788, https://doi.org/10.1038/nrmicro1273 (2005).
47. Piper, C., Cotter, P. D., Ross, R. P. & Hill, C. Discovery of medically significant lantibiotics. *Curr Drug Discov Technol* **6**, 1–18 (2009).
48. van Heel, A. J., de Jong, A., Montalban-Lopez, M., Kok, J. & Kuipers, O. P. BAGEL3: automated identification of genes encoding bacteriocins and (non-)bactericidal posttranslationally modified peptides. *Nucleic Acids Res* **41**, W448–W453, https://doi.org/10.1093/nar/gkt391 (2013).
49. Abts, A., Montalban-Lopez, M., Kuipers, O. P., Smits, S. H. & Schmitt, L. NisC binds the FxLx motif of the nisin leader peptide. *Biochemistry* **52**, 5387–5395, https://doi.org/10.1021/bi4008116 (2013).
50. Bonelli, R. R., Schneider, T., Sahl, H. G. & Wiedemann, I. Insights into *in vivo* activities of lantibiotics from gallidermin and epidermin mode-of-action studies. *Antimicrob Agents Chemother* **50**, 1449–1457, https://doi.org/10.1128/AAC.50.4.1449-1457.2006 (2006).
51. Escano, J., Stauffer, B., Brennan, J., Bullock, M. & Smith, L. The leader peptide of mutacin 1140 has distinct structural components compared to related class I lantibiotics. *Microbiologyopen* **3**, 961–972, https://doi.org/10.1002/mbo3.222 (2014).
52. Maffioli, S. I. *et al*. Family of class I lantibiotics from actinomycetes and improvement of their antibacterial activities. *ACS Chem Biol* **10**, 1034–1042, https://doi.org/10.1021/cb500878h (2015).
53. Mohr, K. I. *et al*. Pinensins: the first antifungal lantibiotics. *Angew Chem Int Ed Engl* **54**, 11254–11258, https://doi.org/10.1002/anie.201500927 (2015).
54. Garg, N., Tang, W., Goto, Y., Nair, S. K. & van der Donk, W. A. Lantibiotics from Geobacillus thermodenitrificans. *Proc Natl Acad Sci USA* **109**, 5241–5246, https://doi.org/10.1073/pnas.1116815109 (2012).
55. Wescombe, P. A. *et al*. Salivaricin 9, a new lantibiotic produced by Streptococcus salivarius. *Microbiology* **157**, 1290–1299, https://doi.org/10.1099/mic.0.044719-0 (2011).

56. Daly, K. M. *et al*. Production of the Bsa lantibiotic by community-acquired Staphylococcus aureus strains. *J Bacteriol* **192**, 1131–1142, https://doi.org/10.1128/JB.01375-09 (2010).
57. Shi, Y., Yang, X., Garg, N. & van der Donk, W. A. Production of lantipeptides in Escherichia coli. *J Am Chem Soc* **133**, 2338–2341, https://doi.org/10.1021/ja109044r (2011).
58. Eichenbaum, Z. *et al*. Use of the *lactococcal* nisA promoter to regulate gene expression in gram-positive bacteria: comparison of induction level and promoter strength. *Appl Environ Microbiol* **64**, 2763–2769 (1998).
59. Rollema, H. S., Kuipers, O. P., Both, P., de Vos, W. M. & Siezen, R. J. Improvement of solubility and stability of the antimicrobial peptide nisin by protein engineering. *Appl Environ Microbiol* **61**, 2873–2878 (1995).
60. Healy, B. *et al*. Intensive mutagenesis of the nisin hinge leads to the rational design of enhanced derivatives. *PLoS One* **8**, e79563, https://doi.org/10.1371/journal.pone.0079563 (2013).
61. Zhou, L., van Heel, A. J. & Kuipers, O. P. The length of a lantibiotic hinge region has profound influence on antimicrobial activity and host specificity. *Front Microbiol* **6**, 11, https://doi.org/10.3389/fmicb.2015.00011 (2015).
62. Breukink, E. *et al*. The orientation of nisin in membranes. *Biochemistry* **37**, 8153–8162, https://doi.org/10.1021/bi972797l (1998).
63. Lubelski, J., Khusainov, R. & Kuipers, O. P. Directionality and coordination of dehydration and ring formation during biosynthesis of the lantibiotic nisin. *J Biol Chem* **284**, 25962–25972, https://doi.org/10.1074/jbc.M109.026690 (2009).
64. Karakas Sen, A. *et al*. Post-translational modification of nisin. The involvement of NisB in the dehydration process. *Eur. J. Biochem.* **261**, 524–532 (1999).
65. Wiegand, I., Hilpert, K. & Hancock, R. E. W. Agar and broth dilution methods to determine the minimal inhibitory concentration (MIC) of antimicrobial substances. *Nature Protocols* **3**, 163, https://doi.org/10.1038/nprot.2007.521 (2008).
66. Khosa, S. *et al*. Structural basis of lantibiotic recognition by the nisin resistance protein from Streptococcus agalactiae. *Sci Rep* **6**, 18679, https://doi.org/10.1038/srep18679 (2016).
67. Stein, T., Heinzmann, S., Solovieva, I. & Entian, K. D. Function of Lactococcus lactis nisin immunity genes nisI and nisFEG after coordinated expression in the surrogate host Bacillus subtilis. *J Biol Chem* **278**, 89–94, https://doi.org/10.1074/jbc.M207237200 (2003).
68. Hacker, C. *et al*. The Solution Structure of the Lantibiotic Immunity Protein NisI and Its Interactions with Nisin. *J Biol Chem* **290**, 28869–28886, https://doi.org/10.1074/jbc.M115.679969 (2015).
69. Lagedroste, M., Smits, S. H. J. & Schmitt, L. Substrate Specificity of the Secreted Nisin Leader Peptidase NisP. *Biochemistry* **56**, 4005–4014, https://doi.org/10.1021/acs.biochem.7b00524 (2017).
70. Schagger, H. Tricine-SDS-PAGE. *Nat. Protoc.* **1**, 16–22, https://doi.org/10.1038/nprot.2006.4 (2006).
71. Khosa, S., Lagedroste, M. & Smits, S. H. Protein Defense Systems against the Lantibiotic Nisin: Function of the Immunity Protein NisI and the Resistance Protein NSR. *Front Microbiol* **7**, 504, https://doi.org/10.3389/fmicb.2016.00504 (2016).
72. Wu, J. & Watson, J. T. Optimization of the cleavage reaction for cyanylated cysteinyl proteins for efficient and simplified mass mapping. *Anal Biochem* **258**, 268–276, https://doi.org/10.1006/abio.1998.2596 (1998).

Acknowledgements

We thank Oscar P. Kuipers and Manuel Montalbán-López (University of Groningen) for the pIL3-BTC and the pNGnisP8His plasmids prior to their own publication. We thank Silke Mavaro for technical assistance during the cloning of the I_1 mutations. We thank all members of the Institute of Biochemistry for fruitful discussions. We especially thank Dr. Peter Tommes (Heinrich Heine University Düsseldorf) for performing the MALDI-TOF measurements. This work was supported by the Deutsche Forschungsgemeinschaft (DFG, grant Schm1279/13-1 to L.S.).

Author Contributions

L.S. and S.H.J.S. conceived and directed this study. M.L. and J.R. conducted the experiments. M.L., J.R., S.H.J.S. and L.S. wrote the manuscript. All authors read and approved the manuscript.

Additional Information

Supplementary information accompanies this paper at https://doi.org/10.1038/s41598-018-37532-4.

Competing Interests: The authors declare no competing interests.

Publisher's note: Springer Nature remains neutral with regard to jurisdictional claims in published maps and institutional affiliations.

Supplemental information

Systematic characterization of position one variants within the lantibiotic nisin

Marcel Lagedroste*, Jens Reiners*, Sander H.J. Smits#

and Lutz Schmitt #

Institute of Biochemistry, Heinrich-Heine-University Duesseldorf, Universitaetsstrasse 1, 40225, Duesseldorf, Germany.

*Contributed equally

#Address correspondence to Lutz Schmitt: lutz.schmitt@hhu.de and Sander H.J. Smits: sander.smits@hhu.de

Key words: lantibiotic, nisin, MS analysis, antimicrobial activity

Figures of supplemental information:

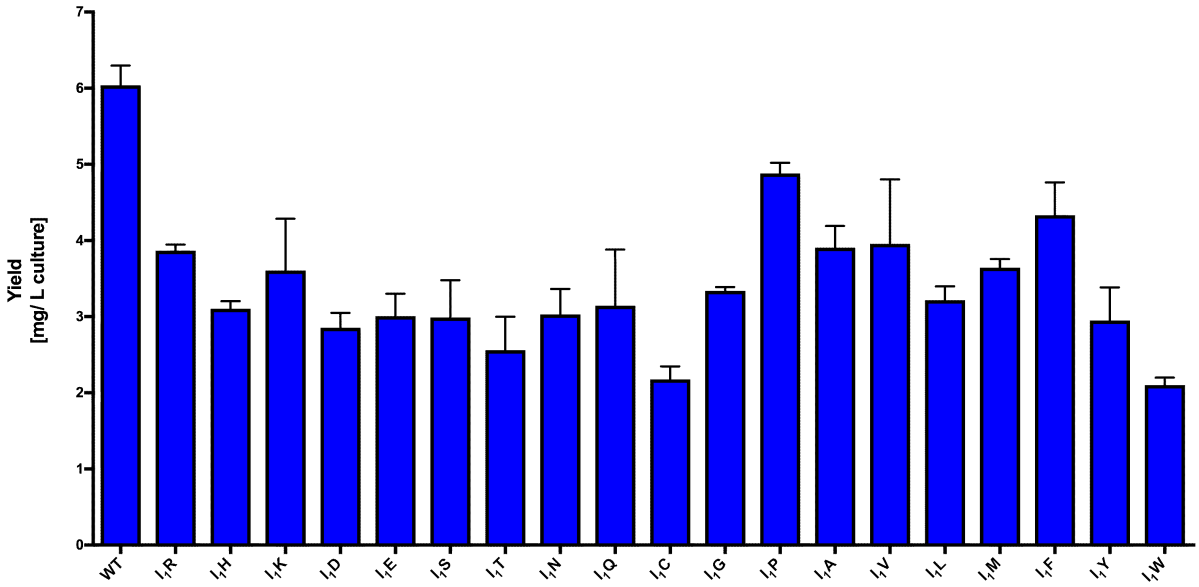

Figure S1: The yield per liter cell culture of pre-nisin variants
Summary of the yields per liter cell culture supernatant after cation-exchange chromatography of nisin A and their corresponding I_1 mutants. The purified peptides were quantified via RP-HPLC. Error bars represent the standard deviation of at least three biological replicates.

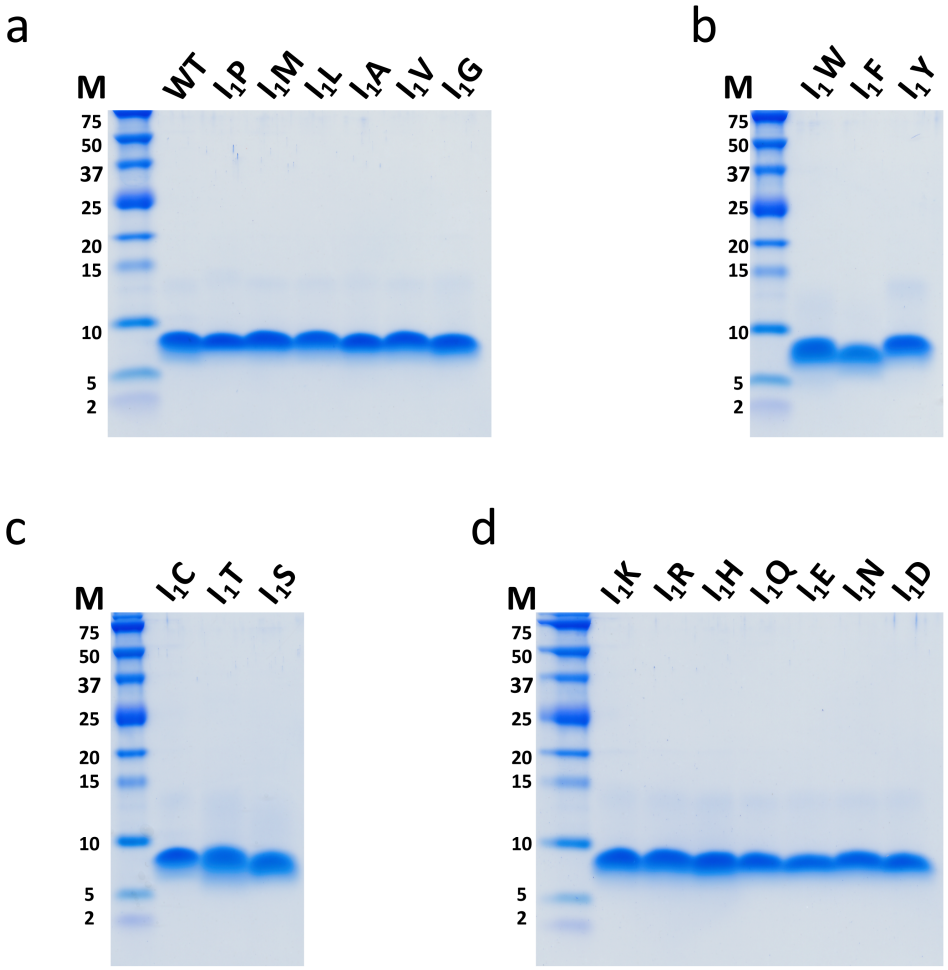

Figure S2: Tricine-SDS-Gels of pre-nisin, I_1 mutants.
Group 1 contained amino acids M-G (**a**), group 2 amino acids W-Y (**a**), group 3 with the amino acids C-S (**a**) and group 4 the amino acids K-H (**a**).

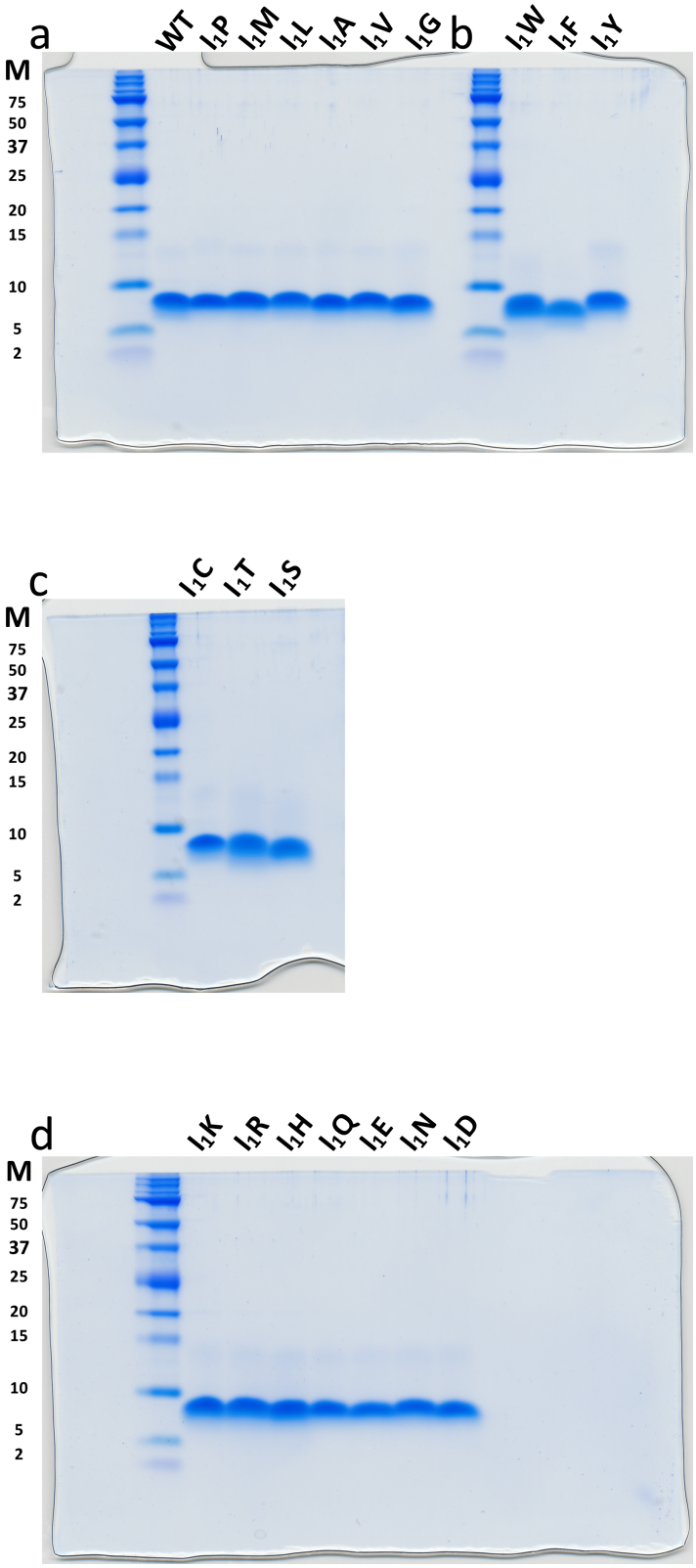

Figure S2: Original Tricine-SDS-Gels of pre-nisin, I_1 mutants.

Group 1 contained amino acids M-G (**a**), group 2 amino acids W-Y (**a**), group 3 with the amino acids C-S (**a**) and group 4 the amino acids K-H (**d**).

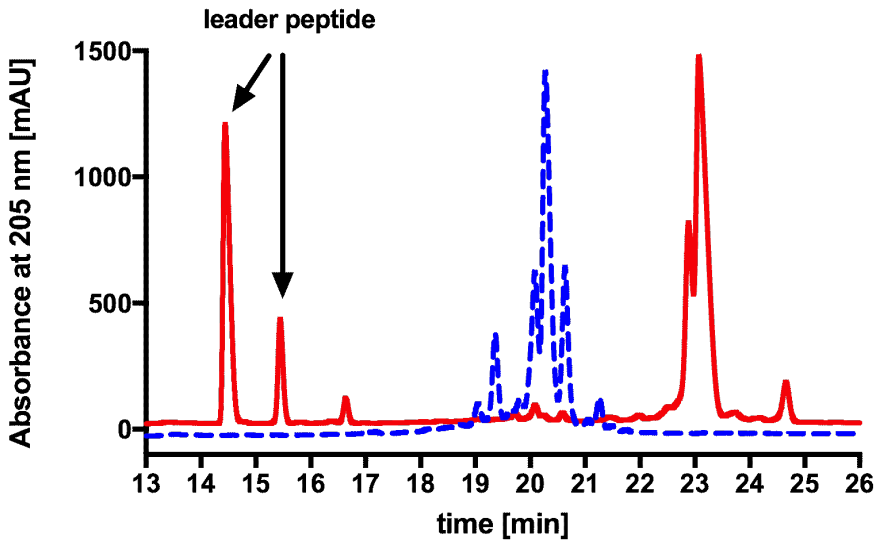

Figure S3: RP-HPLC chromatogram of pre-nisin and nisin.
The retention profile (min) of pre-nisin WT is shown in blue and the product of the cleavage reaction is shown in red. The black arrows indicate the leader peptide peaks (± N-terminal methionine) of cleaved pre-nisin, which is used for quantification.

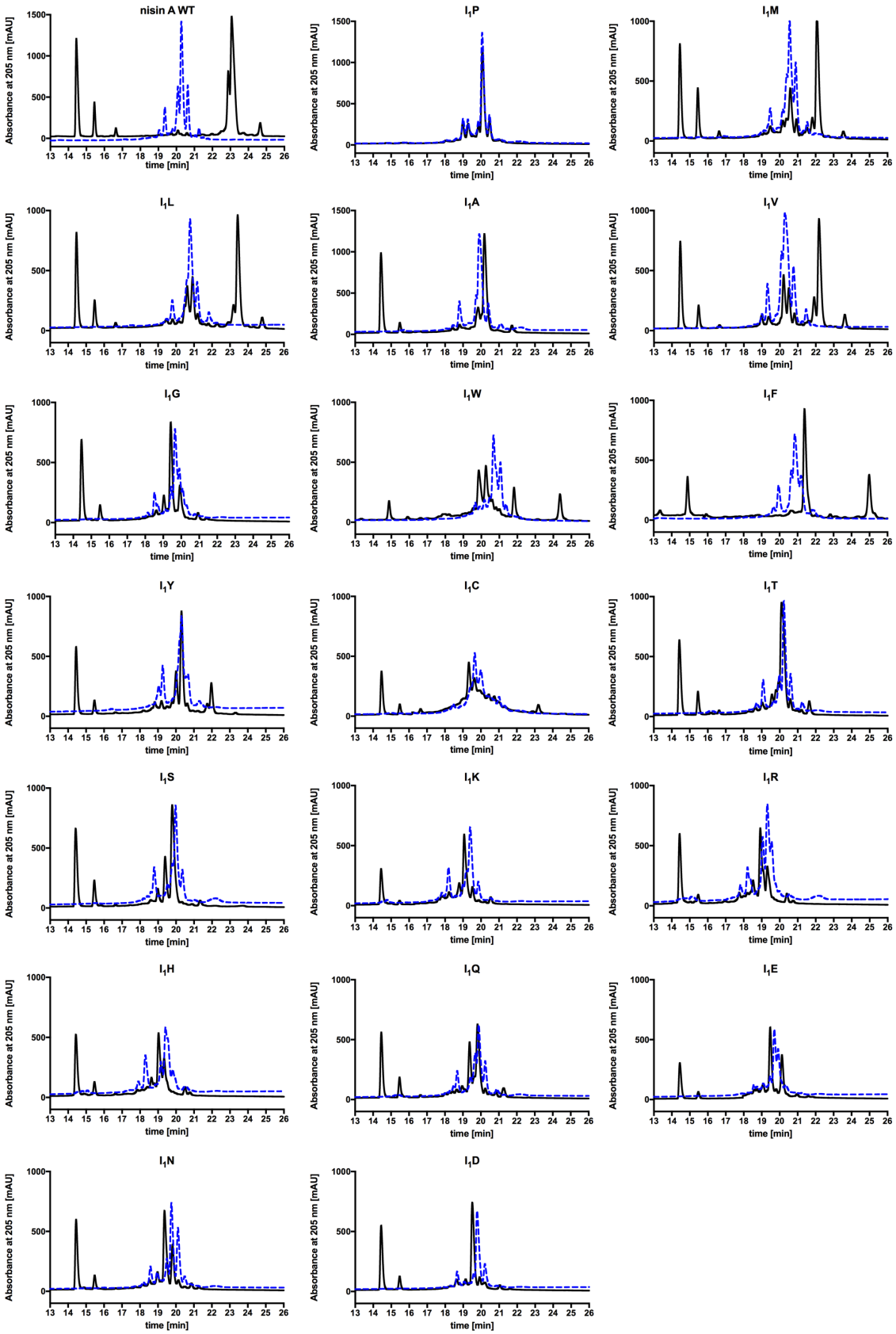

Figure S4: RP-HPLC chromatograms of the cleaved pre-nisin and I_1 mutants
The RP-HPLC chromatogram summaries all pre-nisin and I_1 mutants, which were used in this study. The pre-nisin variants were analysed before cleavage (blue dotted line) and after NisP cleavage (black line). Please note that the scaling of the y axis is different for nisin A WT, I_1P and I_1A.

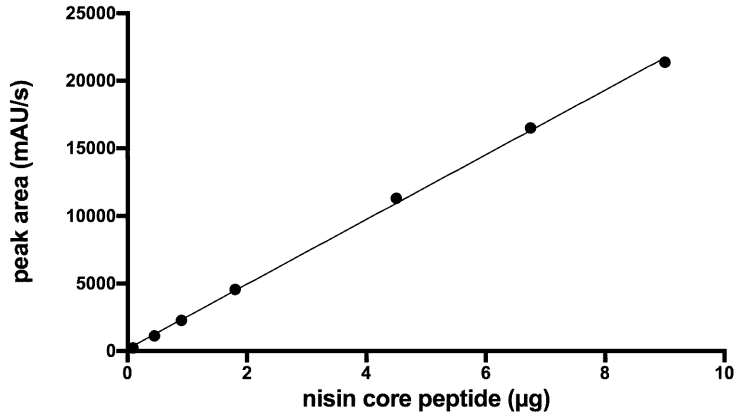

Figure S5: Calibration line of the nisin core peptide.
The slope of the calibration line makes it possible to quantify the total yield and the cleavage efficiency of NisP. Slope: 2392 ± 30.16, R^2: 0.9992

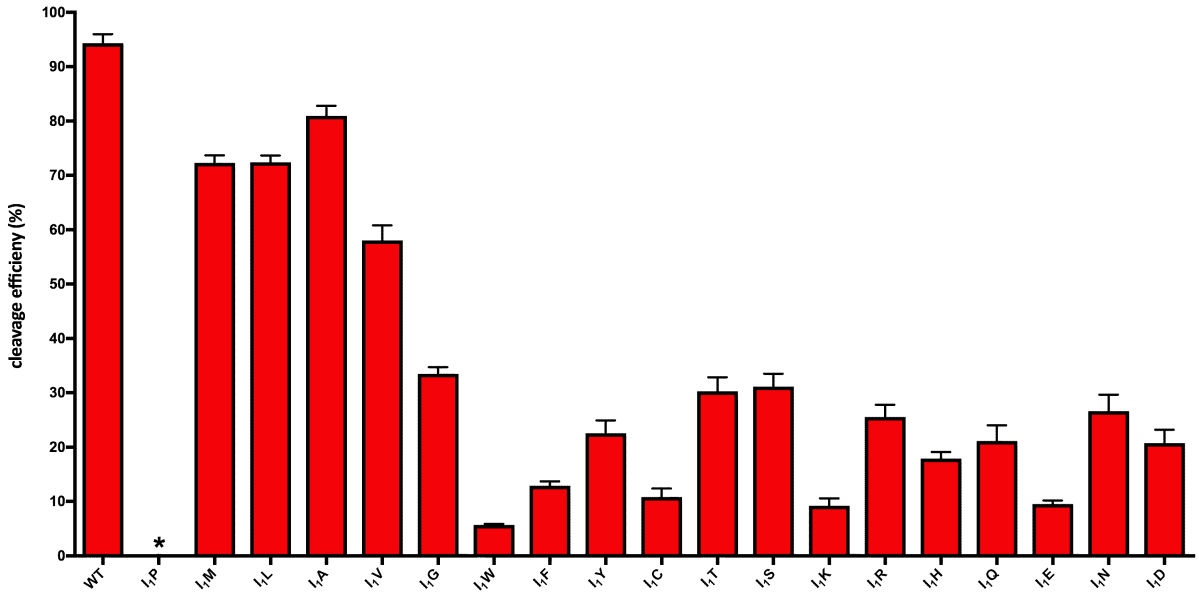

Figure S6: Quantification of the cleavage efficiency of NisP by RP-HPLC.
The leader peptide peak areas were used to determine the final concentration of the activated species and to calculate the efficiency (example see Supplementary Fig. S3, red line). The nisin mutant I_1P was not cleaved by NisP (*). Error bars represent the standard deviation of at least three biological replicates.

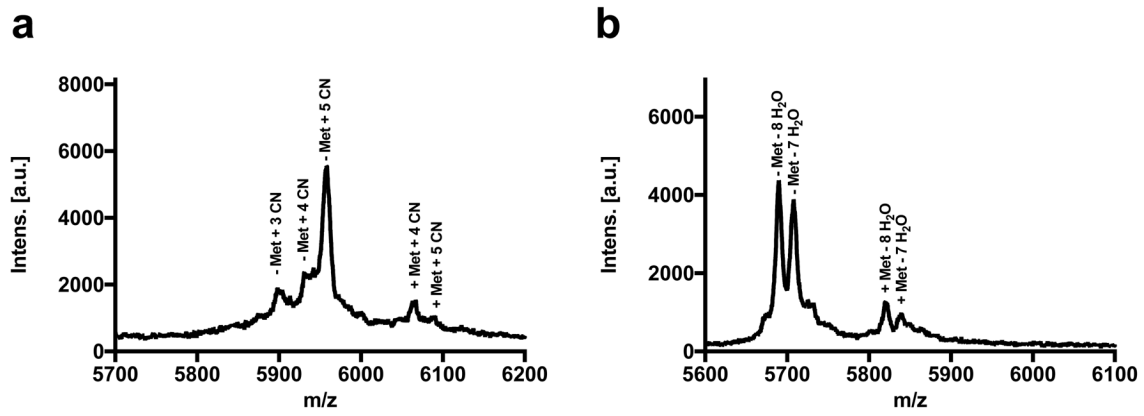

Figure S7: MALDI-TOF analysis to determine the level of dehydrations and ring formations

To demonstrate the specificity of the CDAP coupling, we threated unmodified pre-nisin and fully modified pre-nisin. **a**: unmodified pre-nisin with a maximum number of five coupling products, which demonstrated the accessibility of all five cysteine residues. The fully modified pre-nisin showed no coupling products indicating that all cysteine residues were involved in lanthionine rings (**b**).

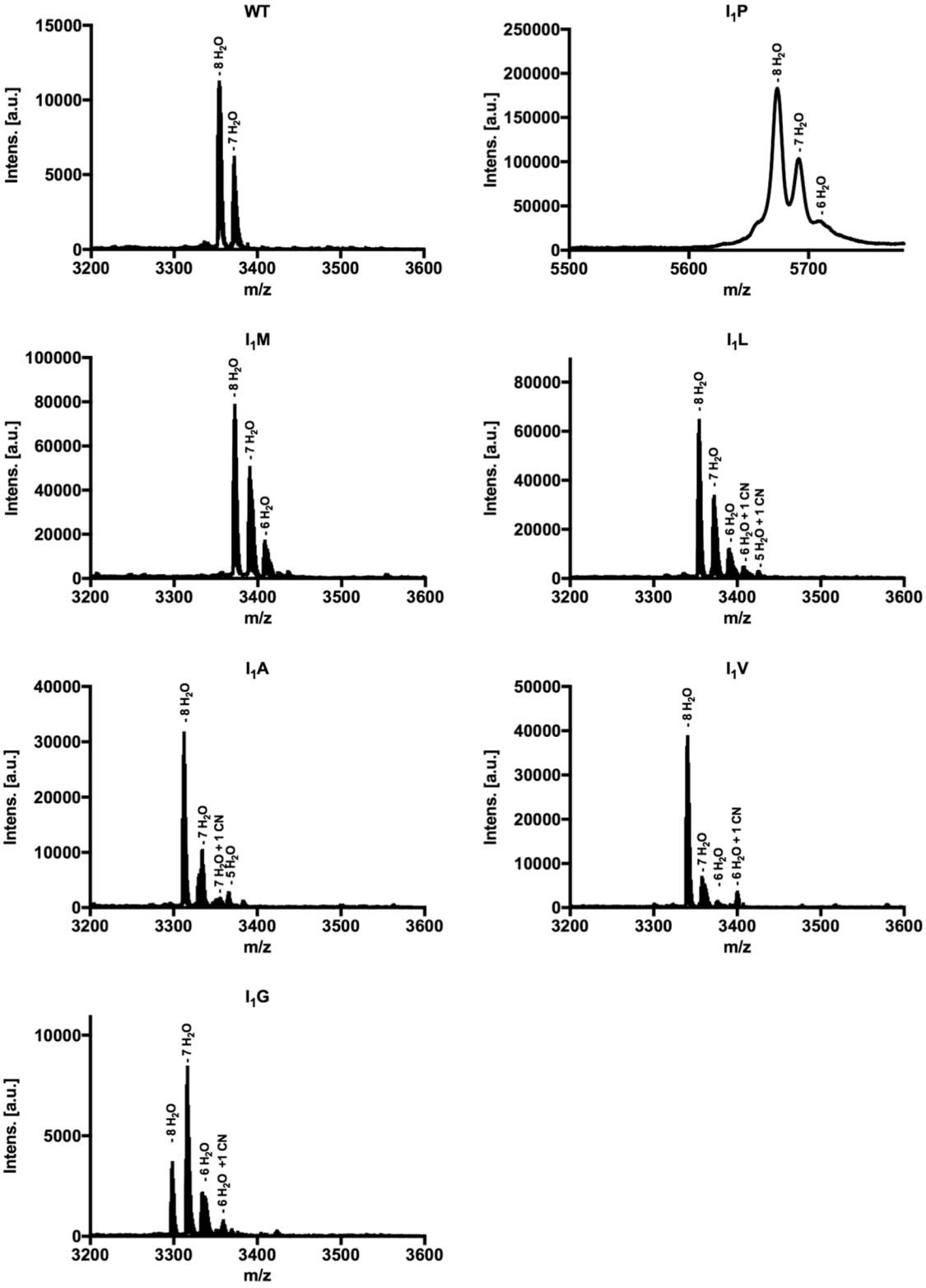

Figure S8: MALDI-TOF analysis to determine the level of dehydrations and ring formations for the nisin A variant group 1.

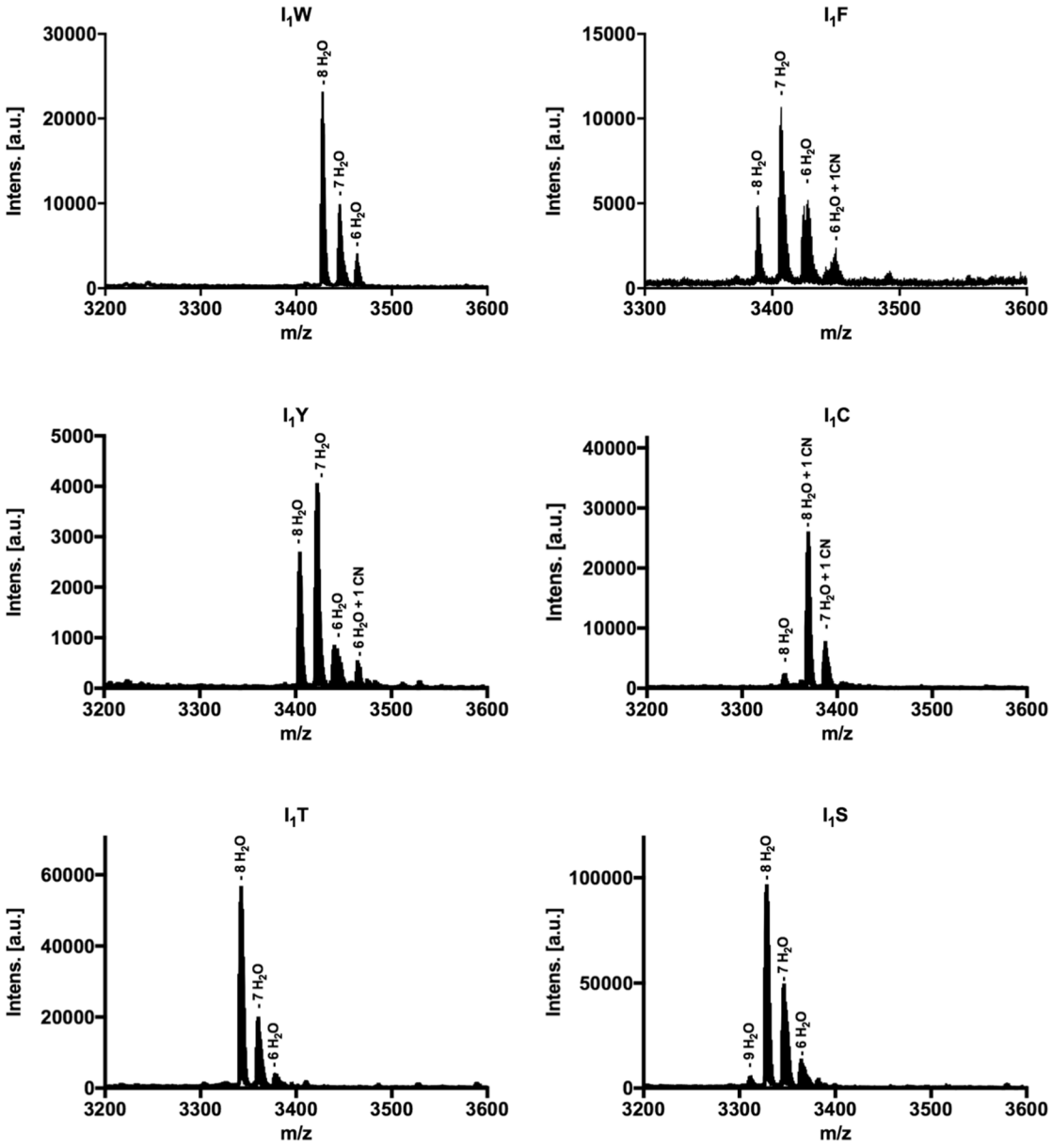

Figure S9: MALDI-TOF analysis to determine the level of dehydrations and ring formations for the nisin A variant group 2 and 3.

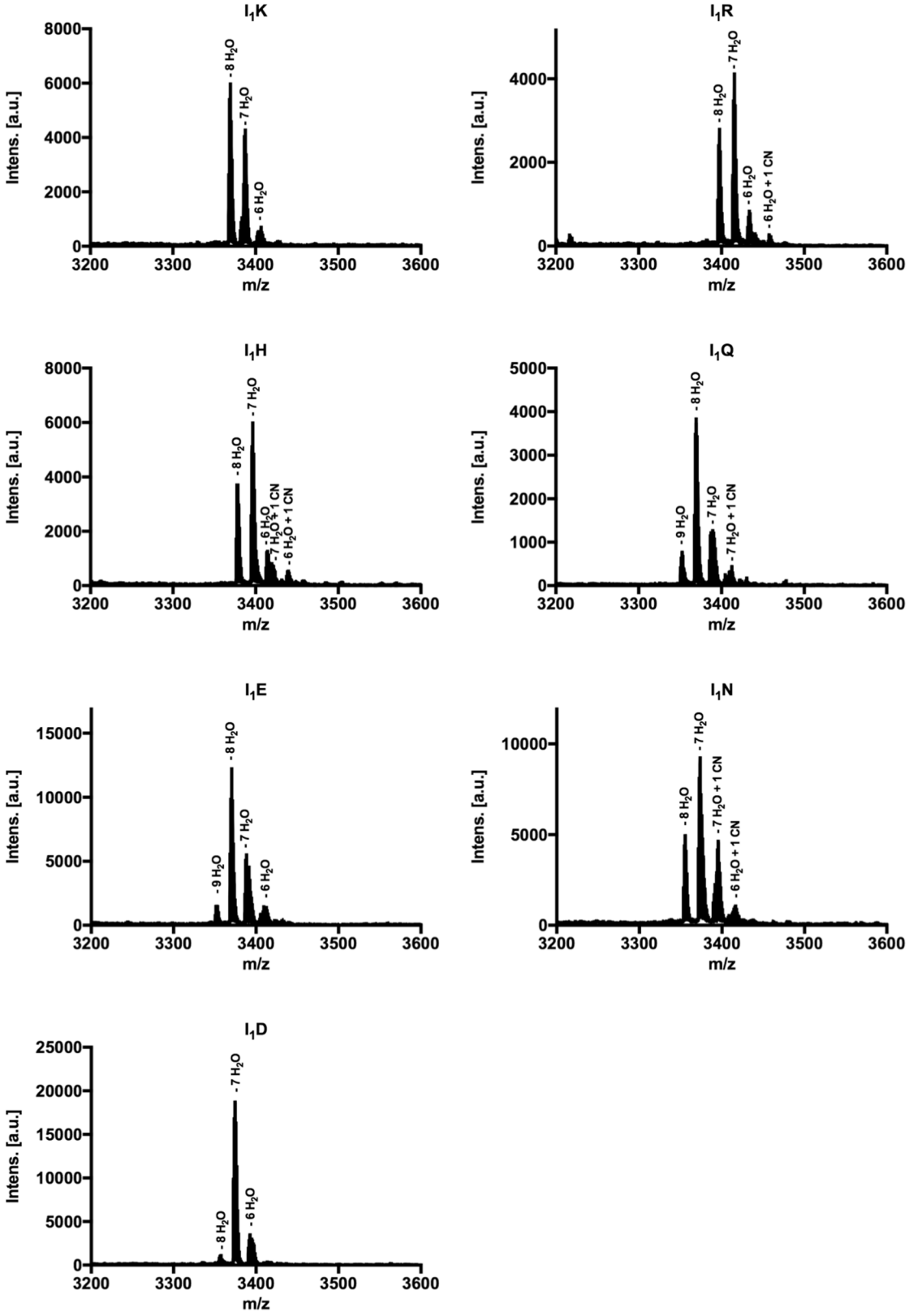

Figure S10: MALDI-TOF analysis to determine the level of dehydrations and ring formations for the nisin A variant group 4.

Tables of supplemental information:

Table S1: Overall data from the MS analysis of nisin A variants

	Variant	Observed masses [Da]	Modification
Group 1	WT	3354	- 8 H_2O
		3372	- 7 H_2O
	I_1P	5672	Uncleaved + Met - 8 H_2O
		5690	Uncleaved + Met - 7 H_2O
		5708	Uncleaved + Met - 6 H_2O
	I_1M	3372	- 8 H_2O
		3390	- 7 H_2O
		3408	- 6 H_2O
	I_1L	3354	- 8 H_2O
		3372	- 7 H_2O
		3390	- 6 H_2O
		3415	- 6 H_2O + 1 CN
		3433	- 5 H_2O + 1 CN
	I_1A	3312	- 8 H_2O
		3330	- 7 H_2O
		3355	- 7 H_2O + 1 CN
		3366	- 5 H_2O
	I_1V	3340	- 8 H_2O
		3358	- 7 H_2O
		3376	- 6 H_2O
		3401	- 6 H_2O + 1 CN
	I_1G	3298	- 8 H_2O
		3316	- 7 H_2O
		3334	- 6 H_2O
		3359	- 6 H_2O + 1 CN
Group 2	I_1W	3427	- 8 H_2O
		3445	- 7 H_2O
		3463	- 6 H_2O
	I_1F	3388	- 8 H_2O
		3406	- 7 H_2O
		3424	- 6 H_2O
		3449	- 6 H_2O + 1 CN
	I_1Y	3404	- 8 H_2O
		3422	- 7 H_2O
		3440	- 6 H_2O
		3465	- 6 H_2O + 1 CN
Group 3	I_1C	3344	- 8 H_2O
		3369	- 8 H_2O + 1 CN
		3387	- 7 H_2O + 1 CN
	I_1T	3342	- 8 H_2O
		3360	- 7 H_2O
		3378	- 6 H_2O
	I_1S	3310	- 9 H_2O
		3328	- 8 H_2O
		3346	- 7 H_2O
		3364	- 6 H_2O
Group 4	I_1K	3369	- 8 H_2O
		3387	- 7 H_2O
		3405	- 6 H_2O
	I_1R	3397	- 8 H_2O
		3415	- 7 H_2O
		3433	- 6 H_2O
		3458	- 6 H_2O + 1 CN
	I_1H	3378	- 8 H_2O
		3396	- 7 H_2O

		3414 **3421** **3439**	**- 6 H_2O** **- 7 H_2O + 1 CN** **- 6 H_2O + 1 CN**
	I_1Q	**3351** **3369** **3387** **3412**	**- 9 H_2O** **- 8 H_2O** **- 7 H_2O** **- 7 H_2O + 1 CN**
	I_1E	**3352** **3370** **3388** **3406**	**- 9 H_2O** **- 8 H_2O** **- 7 H_2O** **- 6 H_2O**
	I_1N	**3355** **3373** **3398** **3416**	**- 8 H_2O** **- 7 H_2O** **- 7 H_2O + 1 CN** **- 6 H_2O + 1 CN**
	I_1D	**3356** **3374** **3392**	**- 8 H_2O** **- 7 H_2O** **- 6 H_2O**

Table S2: IC_{50} values of nisin A and variants

IC_{50} values were determined against the sensitive strain NZ9000-Cm and against strain NZ9000 expressing the immunity/resistance proteins NisI, NisFEG, *Sa*NSR and *Sa*NsrFP.

	NZ9000-Cm	NZ9000-NisI	NZ9000-NisFEG	NZ9000-*Sa*NSR	NZ9000-*Sa*NsrFP
	IC_{50} [nM]	IC_{50} [nM]	IC_{50} [nM]	IC_{50} [nM]	IC_{50} [nM]
WT	4.8 ± 0.7	46.0 ± 6.0	53.0 ± 4.5	73.1 ± 3.6	82.1 ± 3.7
I_1P			not cleavable		
I_1M	5.8 ± 0.3	51.5 ± 1.6	39.2 ± 1.0	84.5 ± 1.7	64.9 ± 0.7
I_1L	9.8 ± 0.5	35.5 ± 1.5	34.6 ± 1.2	53.0 ± 0.4	50.4 ± 0.6
I_1A	10.7 ± 0.4	65.0 ± 2.8	34.2 ± 1.0	68.0 ± 1.9	166.1 ± 5.1
I_1V	11.8 ± 0.9	43.8 ± 1.7	50.4 ± 0.3	66.8 ± 0.34	59.2 ± 2.2
I_1G	143.0 ± 5.1	785.7 ± 9.7	557.8 ± 28.3	278.5 ± 13.3	2257.0 ± 53.4
I_1W	2.5 ± 0.2	22.7 ± 1.5	21.7 ± 1.2	18.3 ± 0.7	46.6 ± 1.1
I_1F	3.7 ± 0.8	36.5 ± 3.3	25.9 ± 1.9	43.9 ± 1.2	64.3 ± 0.4
I_1Y	10.6 ± 0.9	84.3 ± 1.1	45.7 ± 1.8	105.7 ± 1.3	137.9 ± 4.1
I_1C	8.6 ± 0.5	55.1 ± 2.3	41.7 ± 0.7	101.4 ± 3.8	68.8 ± 3.2
I_1T	37.3 ± 1.6	653.3 ± 5.1	107.7 ± 6.2	130.8 ± 3.4	716.1 ± 28.6
I_1S	112.4 ± 5.0	1898.0 ± 62.3	337.3 ± 17.5	253.1 ± 6.2	2893.0 ± 34.8
I_1K	44.7 ± 3.0	435.7 ± 9.9	301.2 ± 4.7	171.7 ± 0.8	983.6 ± 16.2
I_1R	113.9 ± 13.6	422.9 ± 20.4	186.4 ± 3.1	227.0 ± 5.6	1153.0 ± 31.0
I_1H	140.0 ± 5.0	1488.0 ± 85.1	1172.0 ± 134.3	232.9 ± 3.4	3213.0 ± 19.1
I_1Q	592.0 ± 17.8				
I_1E	1328.0 ± 32.7			n.d.	
I_1N	1386.0 ± 46.3				
I_1D	3746.0 ± 144.1				

n.d.: not determined.

Table S3: Nomenclature of the strain NZ9000 expressing immunity (NisI and NisFEG) and resistance proteins (*Sa*NSR and *Sa*NsrFP)

Strain name	plasmid	Expressed protein	properties	Ref.
NZ9000	-	-	sensitive *Lactococcus lactis* strain lacking the gens for *NisABTCPIFEG*	1
NZ9000-Erm	pNZ-SV Erm	-	erythromycin resistance; sensitiv strain	2
NZ9000-Cm	pIL-SV Cm	-	chloramphenicol resistance; sensitiv strain	3
NZ9000-NisP	pNG-nisP8His	NisP	chloramphenicol resistance; sensitive strain expressing the peptidase NisP from *Lactococcus lactis*	4
NZ9000-NisBTC	pIL3-BTC	NisBTC	chloramphenicol resistance; sensitive strain expressing the modification proteins NisB, NisC and the ABC transporter NisT from *Lactococcus lactis*	5
NZ9000-NisI	pNZ-SV-nisI	NisI	erythromycin resistance; immunity strain expressing the lipoprotein NisI from *Lactococcus lactis*	2
NZ9000-NisFEG	pIL-SV-nisFEG	NisFEG	chloramphenicol resistance; immunity strain expressing the ABC transporter NisFEG from *Lactococcus lactis*	3
NZ9000-*Sa*NSR	pNZ-SV-nsr	*Sa*NSR	erythromycin resistance; resistance strain expressing the nisin peptidase NSR from *Streptococcus agalactiae*	6
NZ9000-*Sa*NsrFP	pIL-SV-nsrFP	*Sa*NsrFP	chloramphenicol resistance; resistance strain expressing the BceAB-type ABC transporter NsrFP from *Streptococcus agalactiae*	7

Table S4: Primer sequences used for site-directed mutagenesis

The primer pairs were used for the point mutations at position 1 in the core peptide of nisin A. The exchanged codon is labelled red within the forward (fw) and reversed (rw) primer sequences.

Oligonucleotide name	Sequence (5'-3')
I-K fw	GTGCATCACCACGCAAAACAAGTATTTCGC
I-K rw	GCGAAATACTTGTTTTGCGTGGTGATGCAC
I-M fw	GTGCATCACCACGCATGACAAGTATTTCGC
I-M rw	GCGAAATACTTGTCATGCGTGGTGATGCAC
I-N fw	GTGCATCACCACGCAATACAAGTATTTCGC
I-N rw	GCGAAATACTTGTATTGCGTGGTGATGCAC
I-R fw	GTGCATCACCACGCAGAACAAGTATTTCGC
I-R rw	GCGAAATACTTGTTCTGCGTGGTGATGCAC
I-S fw	GTGCATCACCACGCAGTACAAGTATTTCGC
I-S rw	GCGAAATACTTGTACTGCGTGGTGATGCAC
I-T fw	GTGCATCACCACGCACAACAAGTATTTCGC
I-T rw	GCGAAATACTTGTTGTGCGTGGTGATGCAC
I-V fw	GTGCATCACCACGCGTTACAAGTATTTCGC
I-V rw	GCGAAATACTTGTAACGCGTGGTGATGCAC
I-A fw	GTGCATCACCACGCGCTACAAGTATTTCGC
I-A rw	GCGAAATACTTGTAGCGCGTGGTGATGCAC
I-D fw	GTGCATCACCACGCGATACAAGTATTTCGC
I-D rw	GCGAAATACTTGTATCGCGTGGTGATGCAC
I-E fw	GTGCATCACCACGCGAAACAAGTATTTCGC
I-E rw	GCGAAATACTTGTTTCGCGTGGTGATGCAC
I-G fw	GTGCATCACCACGCGGTACAAGTATTTCGC
I-G rw	GCGAAATACTTGTACCGCGTGGTGATGCAC
I-L fw	GTGCATCACCACGCTTAACAAGTATTTCGC
I-L rw	GCGAAATACTTGTTAAGCGTGGTGATGCAC
I-Y fw	GTGCATCACCACGCTATACAAGTATTTCGC
I-Y rw	GCGAAATACTTGTATAGCGTGGTGATGCAC

I-C fw	GTGCATCACCACGCTGTACAAGTATTTCGC
I-C rw	GCGAAATACTTGTACAGCGTGGTGATGCAC
I-W fw	GTGCATCACCACGCTGGACAAGTATTTCGC
I-W rw	GCGAAATACTTGTCCAGCGTGGTGATGCAC
I-P fw	GTGCATCACCACGCCCAACAAGTATTTCGC
I-P rw	GCGAAATACTTGTTGGGCGTGGTGATGCAC
I-H fw	GTGCATCACCACGCCATACAAGTATTTCGC
I-H rw	GCGAAATACTTGTATGGCGTGGTGATGCAC
I-Q fw	GTGCATCACCACGCCAAACAAGTATTTCGC
I-Q rw	GCGAAATACTTGTTTGGCGTGGTGATGCAC
I-F fw	CATCACCACGCTTTACAAGTATTTCGC
I-F rw	GCGAAATACTTGTAAAGCGTGGTGATG

References:

1. de Ruyter, P.G., Kuipers, O.P. & de Vos, W.M. Controlled gene expression systems for Lactococcus lactis with the food-grade inducer nisin. *Appl Environ Microbiol* **62**, 3662-7 (1996).
2. AlKhatib, Z. et al. Lantibiotic immunity: inhibition of nisin mediated pore formation by NisI. *PLoS One* **9**, e102246 (2014).
3. AlKhatib, Z. et al. The C-terminus of nisin is important for the ABC transporter NisFEG to confer immunity in Lactococcus lactis. *Microbiologyopen* **3**, 752-63 (2014).
4. Abts, A., Montalban-Lopez, M., Kuipers, O.P., Smits, S.H. & Schmitt, L. NisC binds the FxLx motif of the nisin leader peptide. *Biochemistry* **52**, 5387-95 (2013).
5. Rink, R. et al. Lantibiotic structures as guidelines for the design of peptides that can be modified by lantibiotic enzymes. *Biochemistry* **44**, 8873-82 (2005).
6. Khosa, S. et al. Structural basis of lantibiotic recognition by the nisin resistance protein from Streptococcus agalactiae. *Sci Rep* **6**, 18679 (2016).
7. Reiners, J., Abts, A., Clemens, R., Smits, S.H. & Schmitt, L. Stoichiometry and structure of a lantibiotic maturation complex. *Sci Rep* **7**, 42163 (2017).

3.5 Chapter V

Title: Insights in the Antimicrobial Potential of the Natural Nisin Variant Nisin H

Authors: **Jens Reiners**[#], Marcel Lagedroste[#], Julia Gottstein, Emmanuel T. Adeniyi, Rainer Kalscheuer, Gereon Poschmann, Kai Stühler, Sander H. J. Smits and Lutz Schmitt

[#]Authors contributed equally

Published in: Frontiers in Microbiology (2020)

Impact factor: 5.26

Own proportion of this work: 40%

- Cloning of the nisin H variants
- Purification of the pre-nisin H variants
- Performing biological and biochemical assays
- HPLC & MS data analysis
- Writing the manuscript

frontiers in Microbiology

ORIGINAL RESEARCH
published: 20 October 2020
doi: 10.3389/fmicb.2020.573614

Insights in the Antimicrobial Potential of the Natural Nisin Variant Nisin H

Jens Reiners[1,2†], Marcel Lagedroste[1†], Julia Gottstein[1], Emmanuel T. Adeniyi[3], Rainer Kalscheuer[3], Gereon Poschmann[4], Kai Stühler[4,5], Sander H. J. Smits[1,2] and Lutz Schmitt[1*]*

[1] Institute of Biochemistry, Heinrich-Heine-University Düsseldorf, Düsseldorf, Germany, [2] Center for Structural Studies, Heinrich-Heine-University Düsseldorf, Düsseldorf, Germany, [3] Institute of Pharmaceutical Biology and Biotechnology, Heinrich-Heine-University Düsseldorf, Düsseldorf, Germany, [4] Institute for Molecular Medicine, Medical Faculty, Heinrich-Heine-University Düsseldorf, Düsseldorf, Germany, [5] Molecular Proteomics Laboratory, BMFZ, Heinrich-Heine-University-Düsseldorf, Düsseldorf, Germany

OPEN ACCESS

Edited by:
Des Field,
University College Cork, Ireland

Reviewed by:
Oscar P. Kuipers,
University of Groningen, Netherlands
Stefano Donadio,
Naicons Srl, Italy

***Correspondence:**
Lutz Schmitt
lutz.schmitt@hhu.de
Sander H. J. Smits
sander.smits@hhu.de

[†]These authors have contributed equally to this work

Specialty section:
This article was submitted to Antimicrobials, Resistance and Chemotherapy, a section of the journal Frontiers in Microbiology

Received: *17 June 2020*
Accepted: *25 September 2020*
Published: *20 October 2020*

Citation:
Reiners J, Lagedroste M, Gottstein J, Adeniyi ET, Kalscheuer R, Poschmann G, Stühler K, Smits SHJ and Schmitt L (2020) Insights in the Antimicrobial Potential of the Natural Nisin Variant Nisin H. Front. Microbiol. 11:573614. doi: 10.3389/fmicb.2020.573614

Lantibiotics are a growing class of antimicrobial peptides, which possess antimicrobial activity against mainly Gram-positive bacteria including the highly resistant strains such as methicillin-resistant *Staphylococcus aureus* or vancomycin-resistant enterococci. In the last decades numerous lantibiotics were discovered in natural habitats or designed with bioengineering tools. In this study, we present an insight in the antimicrobial potential of the natural occurring lantibiotic nisin H from *Streptococcus hyointestinalis* as well as the variant nisin H F_1I. We determined the yield of the heterologously expressed peptide and quantified the cleavage efficiency employing the nisin protease NisP. Furthermore, we analyzed the effect on the modification via mass spectrometry analysis. With standardized growth inhibition assays we benchmarked the activity of pure nisin H and the variant nisin H F_1I, and their influence on the activity of the nisin immunity proteins NisI and NisFEG from *Lactococcus lactis* and the nisin resistance proteins *Sa*NSR and *Sa*NsrFP from *Streptococcus agalactiae* COH1. We further checked the antibacterial activity against clinical isolates of *Staphylococcus aureus*, *Enterococcus faecium* and *Enterococcus faecalis* via microdilution method. In summary, nisin H and the nisin H F_1I variant possessed better antimicrobial potency than the natural nisin A.

Keywords: lantibiotics, nisin, nisin H, MS analysis, antimicrobial activity

INTRODUCTION

Lantibiotics (lanthionine containing antibiotics) are a growing class of antimicrobial peptides (AMPs), which posses antimicrobial activity even against highly resistant strains such as methicillin-resistant *Staphylococcus aureus* (MRSA) or vancomycin-resistant *enterococci* (VRE) and some are already in pre-clinical trials (Mota-Meira et al., 2000; Jabes et al., 2011; Dawson and Scott, 2012; Crowther et al., 2013; Dischinger et al., 2014; Ongey et al., 2017; Brunati et al., 2018; Sandiford, 2019). Lantibiotics are peptides, containing 19–38 amino acids and are mainly produced by Gram-positive bacteria (Klaenhammer, 1993; Sahl and Bierbaum, 1998). In the last decades an increasing number of lantibiotic gene clusters were found by data-mining approaches using tools such as BAGEL4 (van Heel et al., 2018).

The best studied lantibiotic is nisin, which was first discovered in 1928 by Rogers and Whittier and belongs to the class I lantibiotics (Rogers, 1928; Rogers and Whittier, 1928; Arnison et al., 2013). It is used in the food industry since 1953 and obtained the status as generally recognized as safe (GRAS) in 1988 from the Food and Drug Administration (FDA) (Delves-Broughton et al., 1996). The class I lantibiotic nisin contains 34 amino acids and five (methyl)-lanthionine rings. These (methyl)-lanthionine rings require multiple posttranslational modifications (PTMs) which are introduced in the precursor peptide. First, the serine and threonine residues in the core peptide are dehydrated by a specific dehydratase NisB (lantibiotic class I LanB dehydratase) (Kaletta and Entian, 1989; Karakas Sen et al., 1999; Koponen et al., 2002; Ortega et al., 2015; Repka et al., 2017). The next step is a Michael-type condensation of dehydrated residues with the thiol group of a cysteine residue, thereby forming (methyl)-lanthionine rings, guided in a regio- and stereospecific manner by the cyclase NisC (class I lantibiotic cyclase) (Okeley et al., 2003; Li et al., 2006; Li and van der Donk, 2007; Repka et al., 2017). These characteristic (methyl)-lanthionine rings give lantibiotics high heat stability, resistance against proteolytic digestion and are responsible for the nanomolar antimicrobial activity (Gross and Morell, 1967; Rollema et al., 1995; Chan et al., 1996; Lu et al., 2010; Oppedijk et al., 2016).

The sequence of nisin A can be subdivided into three parts (see **Figure 1**). The N-terminal part with ring A, B, and C is responsible for binding to the cell wall precursor lipid II (Hsu et al., 2004). The hinge region is very flexible and allows reorientation of the C-terminal part to insert into the membrane (van Heusden et al., 2002; Hasper et al., 2004; Wiedemann et al., 2004; Medeiros-Silva et al., 2018), while changes in this region have a strong impact on the target antimicrobial activity (Zhou et al., 2015; Zaschke-Kriesche et al., 2019b). After penetrating the membrane, the C-terminal part with ring D and E forms a stable pore with a stoichiometry of eight nisin and four lipid II molecules, which subsequently leads to rapid cell death (Hasper et al., 2004; Wiedemann et al., 2004; Alkhatib et al., 2014a; Medeiros-Silva et al., 2018).

Unfortunately, some bacteria established resistance mechanism against lantibiotics. For instance lantibiotic producing strains express the immunity system LanI and LanFEG (Alkhatib et al., 2014a,b), which prevent a suicidal effect after the lantibiotic is secreted. In the case of nisin A from *Lactococcus lactis* these proteins are called NisI and NisFEG. But also non-lantibiotic producing strains showed resistance against lantibiotics like *Streptococcus agalactiae* COH1, which arises from the expression of the membrane-anchored peptidase *Sa*NSR and the ABC transporter *Sa*NsrFP (Khosa et al., 2013, 2016a,b; Reiners et al., 2017).

Several natural nisin variants have been discovered and up to now eight are known. First of all nisin A from *L. lactis* (Rogers and Whittier, 1928), nisin Z from *L. lactis* NIZO 221 86 (Mulders et al., 1991), nisin F from *L. lactis* F10 (de Kwaadsteniet et al., 2008), nisin Q from *L. lactis* 61-14 (Zendo et al., 2003), nisin O_1 to O_4 from *Blautia obeum* A2-162 (Hatziioanou et al., 2017), nisin U and U2 from *Streptococcus uberis* 42 and D536 (Wirawan et al., 2006), nisin P from *Streptococcus gallolyticus* subsp. *pasteurianus* (Zhang et al., 2012; Wu et al., 2014), nisin J from *Staphylococcus capitis* APC 2923 (O'Sullivan et al., 2020) and nisin H from *Streptococcus hyointestinalis* DPC 6484 (O'Connor et al., 2015).

In this study we focused on the natural nisin H variant (**Figure 1**). We used a standardized workflow for the characterization of lantibiotics, previous described in Lagedroste et al. (2019) to determine the impact on the expression, modification and antimicrobial properties of this nisin variant. We tested further the antimicrobial activity against some pathogen strains from *Staphylococcus aureus*, *Enterococcus faecium,* and *Enterococcus faecalis* using the microdilution method. As a reference we used the wild-type version of nisin A expressed using the same experimental setup. Furthermore, we exchanged the phenylalanine at position one (F_1) of nisin H to isoleucine, which is the natural amino acid of nisin A at this position (**Figure 1**). This position one was previously analyzed in nisin A and showed a major impact on different levels of the characterization (Lagedroste et al., 2019).

MATERIALS AND METHODS

Microorganisms and Culture Conditions

Cultures of *L. lactis* NZ9000 (Kuipers et al., 1997) containing the plasmids for immunity and resistance proteins were grown in M17 medium (Terzaghi and Sandine, 1975) at 30°C supplemented with 0.5% glucose [GM17 and the appropriate antibiotics descripted in Alkhatib et al. (2014a,b), Khosa et al. (2016b), Reiners et al. (2017), Lagedroste et al. (2019)]. For pre-nisin secretion, the *L. lactis* strain NZ9000 was grown in minimal medium (Jensen and Hammer, 1993) at 30°C supplemented with 0.5% glucose and the appropriate antibiotics. All bacteria used for minimum inhibitory concentration (MIC) determination of nisin variants [*Bacillus subtilis* 168; *S. aureus*: MSSA strain ATCC 29213, MRSA/VISA strain ATCC 700699; *E. faecium*: ATCC 35667, ATCC 700221 (vancomycin resistant); *E. faecalis*: ATCC 29212, ATCC 51299 (vancomycin resistant)] were cultivated in Mueller-Hinton broth (MHB) at 37°C and shaking at 150 rpm.

Cloning of Nisin H and the F_1I Variant

Nisin H was created as described in Reiners et al. (2017). The substitution of the phenylalanine at position one (F_1I) to an isoleucine was performed by site-directed mutagenesis. Here, we used the following primers (forward: 5′-GTGCATCACCACGCTTTACAAGTATTTCGC-3′; reverse: 5′-GCGAAATACTTGTAAAGCGTGGTGATGCAC-3′). After sequence analysis a competent *L. lactis* NZ9000 strain was transformed with the resulting plasmid via electroporation (Holo and Nes, 1989). The *L. lactis* NZ9000 strain already contain a vector (pil3-BTC) encoding for the modification and secretion proteins (Rink et al., 2005).

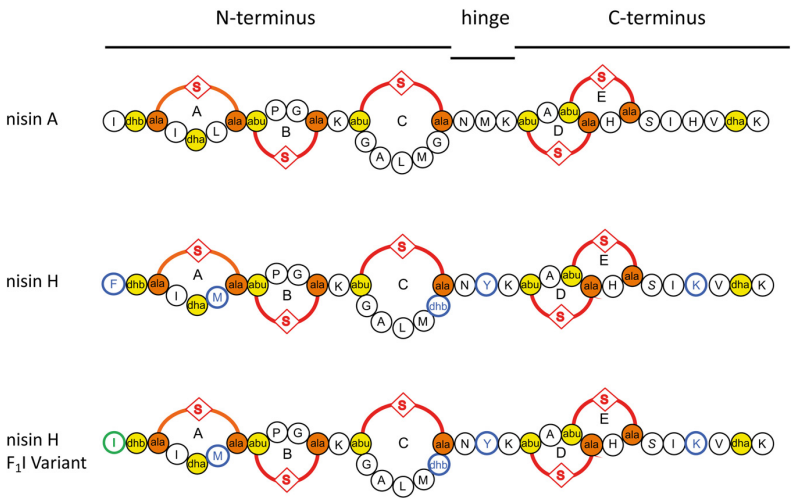

FIGURE 1 | Schematic overview of the used lantibiotics nisin A, nisin H, and the nisin H F_1I variant. Point mutations in nisin H and nisin H F_1I in comparison to nisin A are highlighted in blue. Dehydrated amino acids and cysteine residues involved in (methyl)-lanthionine ring formation (ring A, B, C, D, and E) are labeled in yellow and orange. The mutation of the nisin H F_1I variant is highlighted in green.

Expression, Purification and Activation of Pre-nisin Variants

The precursor of nisin H and its variant were expressed and purified as previously described (Abts et al., 2013; Alkhatib et al., 2014b; Lagedroste et al., 2017, 2019). Briefly, for pre-nisin secretion, the *L. lactis* strain NZ9000 was grown in minimal medium (Jensen and Hammer, 1993) supplemented with 0.5% glucose and 5 μg/ml of each erythromycin and chloramphenicol at 30°C. Cells were induced with 10 ng/ml nisin at an OD_{600} of 0.4 and further grown overnight at 30°C without shaking. After harvesting the cells, the 0.45 μm-filtered supernatant was loaded onto a HiTrap SP HP cation exchange chromatography column. After washing with 50 mM lactic acid, the buffer was changed to 50 mM Hepes pH 7 via gradient and the final elution was done with 50 mM Hepes pH 7, 500 mM NaCl buffer. Elution fractions were concentrated in a 3 kDa cutoff filter. With a soluble version of NisP, the activation of all variants was performed overnight at 8°C (Lagedroste et al., 2017). The yield and cleavage efficiency determination was done by RP-HPLC (Agilent Technologies 1260 Infinity II) with a LiChrospher WP 300 RP-18 end-capped column and an acetonitrile/water solvent system (Abts et al., 2013; Lagedroste et al., 2017, 2019).

MALDI-TOF Analysis: Dehydration and (Methyl)-Lanthionine Ring Analysis

With MALDI-TOF analysis we analyzed the modification state of nisin H and its variant. Dehydrations are directly visible in the spectra, due to the loss of mass (−18 Da). For the determination of the presence of (methyl)-lanthionine rings, we used the organic coupling agent CDAP (1-cyano-4 dimethylaminopyridinium tetrafluoroborate) that binds to free cysteine residues (Wu and Watson, 1998). The reaction of the coupling agent to free cysteine side chains would results in an increased mass in the spectra. The analysis was performed as previously descripted (Lagedroste et al., 2019). The samples were analyzed with MALDI-TOF (UltrafleXtreme, Bruker Daltonics, Bremen, Software: Compass 1.4) in positive mode.

Tandem Mass Spectrometric Analysis of Nisin H and Nisin H F_1I

Nisin H and the nisin H F_1I variant were purified using solid phase extraction (Oasis HLB, Waters) and finally resuspended in 0.1% trifluoroacetic acid. The samples were first subjected to liquid chromatography on a rapid separation liquid chromatography system (Ultimate 3000, Thermo Fisher Scientific) using an 1 h gradient and C18 columns as described (PMID 24646099) and further analyzed by a QExactive Plus mass spectrometer (Thermo Fisher Scientific) coupled via a nano-source electrospray interface. First, a precursor spectrum was acquired at a resolution of 140,000 (advanced gain control target 3E6, maximum ion time 50 ms, scan range 200–2000 m/z, profile data type). Subsequently, up to four 4–6-fold charged precursors were selected by the quadrupole (2 m/z isolation window), fragmented by higher-energy collisional dissociation (normalized collision energy 30) and recorded at a resolution of 35,000 (advanced gain control target 1E5, maximum ion time 50 ms, available scan range 200–2000 m/z, centroid data type).

Recorded spectra were analyzed by the MASCOT search engine (version 2.4.1, Matrix Science) and searches triggered by Proteome Discoverer (version 2.4.0.305, Thermo Fisher Scientific). A database was generated for the searches including 1000 randomly generated sequence entries each 34 amino acid long) and the sequences of nisin H and nisin H F_1I. Methionine oxidation and dehydration of serine and threonine residues were

considered as variable modifications and the precursor mass tolerance set to 10 ppm and the fragment mass tolerance set to 0.02 Da. For peptide validation, the Fixed Value PSM validator was used (1% false discovery rate) and the IMP-ptmRS node for site validation (PMID 22073976). No random sequences were found by the search.

Determination of the Antimicrobial Activity by Growth Inhibition Assay

The determination of the antimicrobial activity of the different nisin variants was tested using a growth inhibition assay. The used strains were described in Alkhatib et al. (2014a,b), Reiners et al. (2017), and Lagedroste et al. (2019).

Briefly, the *L. lactis* NZ9000 strains were grown in M17 medium (Terzaghi and Sandine, 1975) at 30°C supplemented with 0.5% glucose (GM17 and the appropriate antibiotics) overnight with 1 ng/ml nisin. In a 96-well plate, a serial dilution of the nisin variant was applied and incubated with the test strains at a final OD_{600} of 0.1 for 5 h at 30°C. Later on, the optical density was measured at 584 nm via 96-well plate reader BMG. The normalized optical density was plotted against the logarithm of the nisin concentration and the resulting inhibitory concentration (IC_{50}), represents the value where 50% of the cells died in the presence of the different nisin variants. By dividing the IC_{50} values of strains expressing the immunity or resistance proteins from the IC_{50} value of the sensitive strain we calculated the fold of immunity/resistance, which is an indicator for the recognition of nisin H or its variant by the immunity or resistance proteins.

Minimum Inhibitory Concentration Determination of Nisin Variants

Nisin variants were tested for antibacterial capabilities against *B. subtilis* and different strains from *S. aureus*, *E. faecium,* and *E. faecalis* using the microdilution method, according to the recommendations of Clinical and Laboratory Standards Institute (2012). Briefly, fresh cultures prepared from overnight cultures were incubated until exponential phase (OD ∼ 0.6) and seeded at 5×10^4 CFU/well in 96-well round-bottom microplates, in a total volume of 100 μL containing twofold serially diluted test peptides. Moxifloxacin was used as a positive control. Plates were incubated statically and aerobically for 24 h at 37°C. MICs were determined macroscopically by identifying the least concentration of peptides that resulted in complete inhibition of bacterial visual growth.

SYTOX Green Nucleic Acids Binding Assay

The cells of NZ9000Cm were grown overnight in GM17 supplemented with 5 mg/ml chloramphenicol. The overnight culture was diluted to an OD_{600} of 0.1 in fresh media and the cultures were grown until the OD_{600} reaches 0.3. The SYTOX green dye was added at a final concentration of 2.5 mM according to the manual of the manufacturer (Invitrogen). After reaching a stable baseline (∼200 s) we added 100 nM of the nisin variants. The fluorescence signal was measured at an excitation wavelength of 504 nm and emission wavelength of 523 nm, respectively (using a fluorolog Horiba III). After a stable baseline was reached, the nisin variant was added and the fluorescence was monitored over an additional time period. The measurement was performed at 30°C.

RESULTS

O'Connor et al. (2015) described a new natural nisin variant from *S. hyointestinalis* DPC 6484 and named it nisin H. In following, we compared nisin A and its natural variant nisin H, both heterologously produced in *L. lactis*, following the protocol of lantibiotic characterization (Lagedroste et al., 2019). We also included the nisin H F_1I variant.

The characterization starts with the expression, secretion and purification of the lantibiotic and its comparison to nisin A. The heterologously expressed and secreted nisin A and the variants nisin H and nisin H F_1I can be purified with high purity as observed on the Tricine-SDS-PAGE gel (**Figure 2A**). Nisin A was purified with a yield of 6.0 ± 0.3 mg/L of cell culture (Lagedroste et al., 2019), nisin H was expressed and purified with a yield of 5.3 ± 0.6 mg/L of cell culture, which is identical within experimental error. The nisin H F_1I variant displayed a slightly reduced yield of 4.9 ± 0.2 mg/L of cell culture (**Figure 2B** and **Table 1**).

An important step prior to the activity assay is the cleavage of the leader sequence form the pre-nisin variants, resulting in biologically active compounds. For the cleavage reaction, we used the peptidase NisP and monitored the cleavage efficiency via RP-HPLC (**Figures 2C–E**).

Intriguingly, the natural variant nisin H showed only a low cleavage efficiency of 15.6 ± 1.4%, compared to nisin A with 94.6 ± 2.0% (**Figure 2C** and **Table 1**). In comparison to nisin A, nisin H contains a phenylalanine at the first position (O'Connor et al., 2015), which apparently leads to a significant reduction in cleavage efficiency. The first residue of nisin A is an isoleucine, and as demonstrated before (Lagedroste et al., 2019), the introduction of aromatic residues at position one results in a clearly reduced cleavage efficiency. To counteract the lower cleavage efficiency of nisin H by NisP, we created a mutant of nisin H, in which the phenylalanine was substituted by isoleucine and termed it nisin H F_1I. For this variant, nisin H F_1I, the cleavage efficiency of the pre-lantibiotic was restored with an efficiency of 91.8 ± 0.8% (**Figure 2C** and **Table 1**), which corresponds to levels previously observed for nisin A. We monitored the cleavage via RP-HPLC, the pre-nisin elutes normally between 18 and 22 min (shown as blue dashed lines, **Figures 2D,E**). After cleavage by NisP, the leader peptide can be detected at 14.5 and 15.5 min in the chromatogram (shown as black lines, **Figures 2D,E**). For nisin H there was a high amount of uncleaved nisin H visible (eluting from 18 to 21 min) and only a small amount of cleaved product at 23–24 min (black lines, **Figure 2D**). For the nisin H F_1I variant, high amounts of leader peptide and cleaved product could be detected in the chromatogram, indicating high cleavage efficiency (black lines, **Figure 2E**). This efficiency was similar as observed for nisin A and in line with previous results that the position

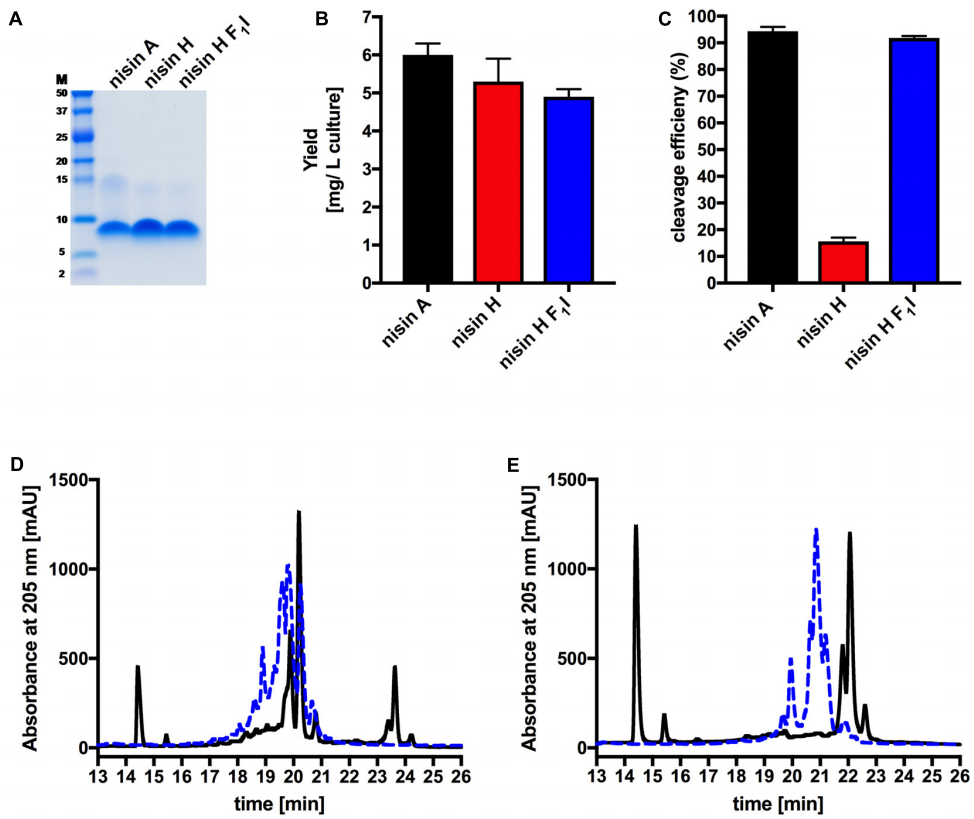

FIGURE 2 | Determination of purity, yield and cleavage efficiency of the pre-nisin variants. **(A)** Purity of the purified nisin A and the variants nisin H and nisin H F_1I (Marker: Precision Plus Protein Dual Xtra standards Bio-Rad). **(B)** Yields after purification of nisin A and their corresponding variants via cation-exchange chromatography. **(C)** Quantification of the cleavage efficiency of NisP. **(D)** Chromatogram of nisin H. **(E)** Chromatogram of the nisin H F_1I variant. The pre-nisin variants before NisP cleavage were shown by blue dashed lines and after NisP cleavage by black lines. Error bars represent the standard deviation of at least three biological replicates.

one is important for the cleavage reaction (Lagedroste et al., 2019). Thus, we assume, that the four other mutations naturally occurring in nisin H (compared to nisin A) do not interfere with cleavage, however the isoleucine at position one does.

The next step was to determine the modification state of the heterologous produced nisin H and its F_1I variant. As the natural variant nisin H contains ten possible residues in the core peptide that can be dehydrated, we were curious to determine if the modification machinery of nisin A was able to modify the peptide as efficiently (O'Connor et al., 2015). In the MALDI-TOF spectra, a dominant species of eightfold dehydrated residues was observed for nisin H, followed by a minor species containing nine- and sevenfold dehydrations. The possible 10-fold dehydrated species however was not observed (**Figure 3A** and **Table 1**). Furthermore no CDAP-coupling products were observed, which indicates that all cysteine residues are linked in (methyl)-lanthionine rings. We proved the functionality of the assay with unmodified pre-nisin A as demonstrated in Lagedroste et al. (2019). Thus, the modification enzymes were able to modify nisin H proving the promiscuity of the nisin modification machinery. Interestingly, the nisin H F_1I variant showed a dominant ninefold dehydrated species in comparison the nisin H wild-type (**Figure 3B** and **Table 1**) and also showed no CDAP-coupling products, indicating that all cysteine residues are closed to (methyl)-lanthionine rings. The difference in the dehydration pattern for the nisin H F_1I variant indicates a different accessibility of the serine and/or threonine residues in the core peptide for at least the dehydratase NisB. To validate which serine or threonine residues is dehydrated, we performed a tandem mass spectrometric

TABLE 1 | Determination of the yield, cleavage efficiency, dehydrations, and (methyl)-lanthionine ring formation for nisin A, nisin H, and nisin H F_1I.

Variant	Yield (mg/L culture)	Cleavage (%)	Dehydrations	Lanthionine rings
Nisin A	6.0 ± 0.3	94.6 ± 2.0	**8**, 7	5
Nisin H	5.3 ± 0.6	15.6 ± 1.4	9, **8**, 7	5
Nisin H F_1I	4.9 ± 0.2	91.8 ± 0.8	**9**, 8, 7, 6	5

Main species found in MALDI-TOF analysis are marked in bold.

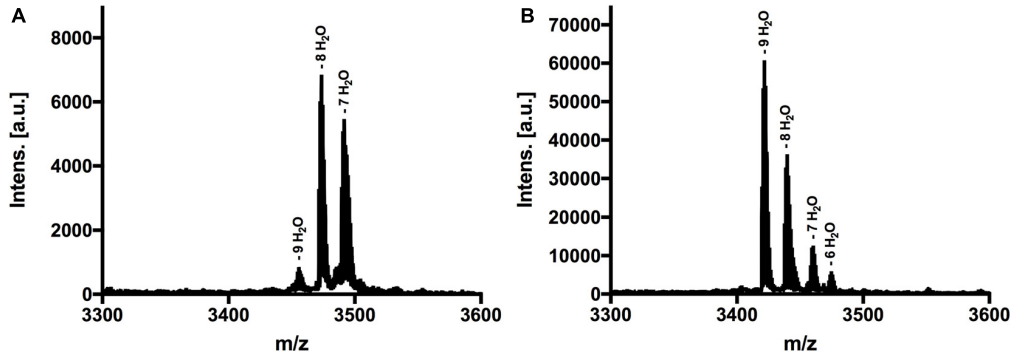

FIGURE 3 | MALDI-TOF analysis to determine dehydrations and (methyl)-lanthionine ring formations. **(A)** MS spectra of nisin H, threated with CDAP. Dominant species was eightfold dehydrated. **(B)** MS spectra of nisin H F_1I variant, threated with CDAP. Dominant species was ninefold dehydrated. Both variants showed no coupling products, indicating that all cysteine residues were involved in (methyl)-lanthionine rings.

analysis of nisin H and the F_1I variant. Here we found that the Thr_2 partially escape the dehydration in nisin H. Only in the small amount of the ninefold dehydrated species the Thr_2 is dehydrated, in all other species we found a mix in the dehydration pattern, where Thr_2 partially escape the dehydration. For example in the eightfold species we have a mix of dehydrated Thr_2 or Ser_{33}. In the nisin H F_1I variant the Thr_2 was in all species dehydrated, which suggests that, the phenylalanine at position one in nisin H is critical for the dehydratase NisB. Ser_{29} was never dehydrated in the found species.

Lantibiotics are very potent and possess an antimicrobial activity in the nanomolar range (Gross and Morell, 1967; Rollema et al., 1995; Chan et al., 1996; Lu et al., 2010; Oppedijk et al., 2016). To verify this potential for nisin H and the nisin H F_1I variant we used a standardized growth inhibition assay and first screened against the nisin sensitive *L. lactis* strain NZ9000Cm. Here, Cm stands for chloramphenicol resistance, which arises from the empty plasmid, which was transformed. In comparison to nisin A (IC_{50} value: 4.8 ± 0.7 nM), the heterologous expressed variant nisin H possessed a comparable IC_{50} value (5.3 ± 1.0 nM) (**Figure 4** and **Table 2**). Both values are in line with previously determined IC_{50} values for the strain NZ9000Cm (Reiners et al., 2017). The effect of the nisin H F_1I variant was more pronounced. For the NZ9000Cm sensitive strain we calculated an IC_{50} value of 14.2 ± 0.2 nM, approximately threefold lower than the wild-type nisin H (**Figure 4** and **Table 2**).

To test the effect of the nisin variants on the immunity proteins NisI (Alkhatib et al., 2014a) and NisFEG (Alkhatib et al., 2014b), as well as the resistance proteins *Sa*NSR (Khosa et al., 2016a) and *Sa*NsrFP (Reiners et al., 2017), we expressed each of them in a plasmid-based system in a *L. lactis* NZ9000 strain. We termed these strains NZ9000NisI, NZ9000NisFEG, NZ9000*Sa*NSR and NZ9000*Sa*NsrFP, respectively.

Nisin A displayed an IC_{50} value of 48.6 ± 6.3 nM against strain NZ9000NisI and 53.0 ± 4.5 nM against strain NZ9000NisFEG. For the resistance strains NZ9000*Sa*NSR and NZ9000*Sa*NsrFP nisin A displayed IC_{50} values of 73.0 ± 3.6 and 82.1 ± 3.1 nM, respectively (**Figure 4** and **Table 2**). By comparing theses values, we calculated the fold of immunity/resistance to 10.1 ± 2.0 for NZ9000NisI, 11.1 ± 1.9 for NZ9000NisFEG, 15.2 ± 2.5 for NZ9000*Sa*NSR and 17.1 ± 2.7 for NZ9000*Sa*NsrFP (**Table 2**). After the first screen against the sensitive strain NZ9000Cm, nisin H and its variant were used to screen against the strains expressing the immunity or resistance proteins.

Nisin H revealed an IC_{50} value of 43.2 ± 8.7 nM against the NZ9000NisI strain, similar to nisin A, and a fold of immunity of 8.1 ± 2.2. Against the NZ9000NisFEG strain we determined an IC_{50} value of 23.4 ± 3.3 nM for nisin H which displayed a fold of resistance of 4.4 ± 1.0. Against the NZ9000*Sa*NSR strain we obtained an IC_{50} value of 52.4 ± 9.9 nM, resulting in a fold of resistance of 9.8 ± 2.6. Nisin H showed an IC_{50} value of 86.4 ± 4.0 nM for the NZ9000*Sa*NsrFP strain, resulting in a fold of resistance of 16.2 ± 3.1 (**Figure 4** and **Table 2**). NZ9000*Sa*NsrFP showed the highest fold of resistance for nisin H [in-line with a previous report (Reiners et al., 2017)]. Intriguingly, strain NZ9000NisFEG showed a reduced immunity and consequently we propose that nisin H is not recognized as efficiently as nisin A. Even NZ9000*Sa*NSR had a reduced resistance. That could be due to the exchange of His_{31} against lysine in the C-terminal part of nisin H (**Figure 1**).

Surprisingly, all strains displayed a reducing resistance/immunity effect for the nisin H F_1I variant in comparison to nisin A and also, with exception of NZ9000FEG for nisin H. Against the NZ9000NisI strain we determined an IC_{50} value of 34.1 ± 0.3 nM for the nisin H F_1I variant, with a fold of resistance 2.4 ± 0.1, which is nearly threefold lower than for nisin A. We obtained an IC_{50} value of 32.1 ± 0.8 nM against the ABC transporter NZ9000NisFEG, with a fold of resistance 2.3 ± 0.1 (**Figure 4** and **Table 2**). Nisin H F_1I showed for the resistance strain NZ9000*Sa*NSR and NZ9000*Sa*NsrFP an IC_{50} value of 44.2 ± 1.3 and 50.2 ± 1.6 nM, respectively. The calculated folds of resistance were 3.1 ± 0.1 and 3.5 ± 0.1, respectively (**Figure 4** and **Table 2**) and both are fivefold less than the observed fold of resistances for nisin A.

Since a similar activity for nisin H and nisin A was observed it became obvious that both exhibit the same mode of action. In

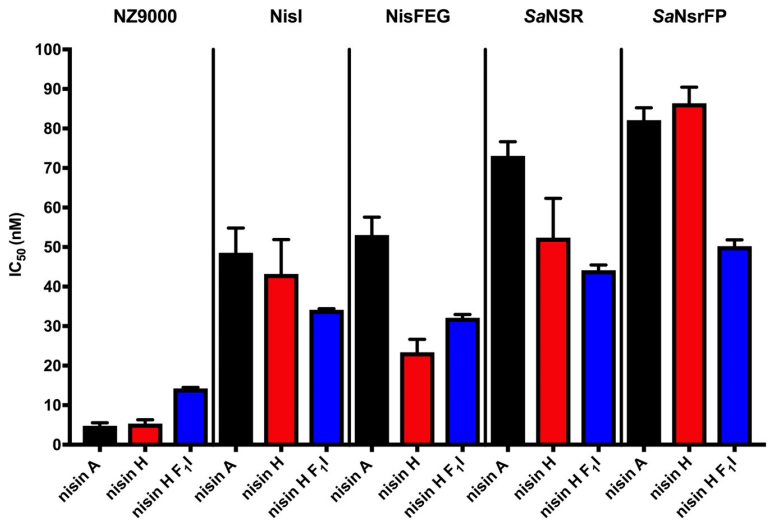

FIGURE 4 | Growth inhibition assays in the presence of nisin A and the nisin H varants. The lantibiotic nisin A (black bars), the heterologous expressed nisin H (red bars) and the position 1 variant of nisin H F_1I (blue bars) were used for growth inhibition (IC_{50}) with the strains NZ9000Cm, NZ9000NisI, NZ9000NisFEG, NZ9000*Sa*NSR, and NZ9000*Sa*NsrFP. Values represent the average of at least five biological independent measurements and the errors report the standard deviation of the mean (SDM).

TABLE 2 | IC_{50} values (nM) for nisin A, nisin H, and nisin H F_1I with the corresponding fold of resistance (FR) against the strains NZ9000Cm, NZ9000NisI, NZ9000NisFEG, NZ9000*Sa*NSR, and NZ9000*Sa*NsrFP.

Variant	NZ9000Cm	NZ9000NisI		NZ9000NisFEG		NZ9000*Sa*NSR		NZ9000*Sa*NsrFP	
		IC_{50}	FR	IC_{50}	FR	IC_{50}	FR	IC_{50}	FR
Nisin A	4.8 ± 0.7	48.6 ± 6.3	10.1 ± 2.0	53.0 ± 4.5	11.1 ± 1.9	73.0 ± 3.6	15.2 ± 2.5	82.1 ± 3.1	17.1 ± 2.7
Nisin H	5.3 ± 1.0	43.2 ± 8.7	8.1 ± 2.2	23.4 ± 3.3	4.4 ± 1.0	52.4 ± 9.9	9.8 ± 2.6	86.4 ± 4.1	16.2 ± 3.1
Nisin H F_1I	14.2 ± 0.2	34.1 ± 0.3	2.4 ± 0.1	32.1 ± 0.8	2.3 ± 0.1	44.2 ± 1.3	3.1 ± 0.1	50.2 ± 1.6	3.5 ± 0.1

the case of nisin A this combines growth inhibition with pore formation in the membrane with subsequent cell death. To test this we performed a SYTOX assay previously used for nisin A (Reiners et al., 2017). Here the SYTOX dye was added to *L. lactis* cells and displayed an increased fluorescence signal upon binding of DNA which is released from the cell upon pore formation (Roth et al., 1997). We use 100 nM of nisin A, nisin H and nisin H F_1I variant respectively and observed an almost instant fluorescence increase similar to the signal increase observed for nisin A (**Figure 5**). This shows that nisin H as well as its F_1I variant form pores in the membrane of *L. lactis* cell.

The nisin variants were further tested for antibacterial capabilities against *B. subtilis* and different pathogenic strains from *S. aureus*, *E. faecium,* and *E. faecalis* using the microdilution method, according to the recommendations of CLSI (2012). Here we found that nisin H and the F_1I variant performed almost identically or in most cases even better than the natural nisin A. Especially against the MSSA and MRSA strains, nisin H had significant lower MIC values of 0.19 and 0.78 μM, in comparison to 0.78 and 6.25 μM for nisin A, respectively (**Table 3**). Also, against *E. faecium* ATCC 35667, *B. subtilis* 168 as well as *E. faecium* ATCC 700221 (VRE), nisin H showed more potency with about two to eightfold lower MIC values than nisin A [0.39, 0.1, and 0.39 μM compared to 1.56, 0.78, and 0.78 μM for nisin A, respectively (**Table 3**)]. While the nisin H F_1I variant and nisin A had similar MIC values against both MSSA and MRSA strains, the nisin H F_1I variant only performed better than nisin A or nisin H against *E. faecalis* ATCC 51299 (VRE) with a MIC value of 0.78 μM compared to 1.56 μM for nisin A and nisin H. Against *E. faecium* ATCC 35667 and *B. subtilis* 168 nisin H F_1I was less efficient than nisin H, but still better than nisin A (**Table 3**).

DISCUSSION

We focused in this study on the natural variant nisin H and the nisin H F_1I mutant. Nisin H was discovered from the gut-derived strain *S. hyointestinalis* DPC6484 in 2015 by O'Connor et al. (2015). Here, we showed the heterologous expression of nisin H and the F_1I variant with the NICE-system in *L. lactis* (Eichenbaum et al., 1998; Mierau and Kleerebezem, 2005; Rink et al., 2005; Zhou et al., 2006; Lagedroste et al., 2019) and extended the characterization in terms of cleavage efficiency by the protease NisP and the antimicrobial activity against

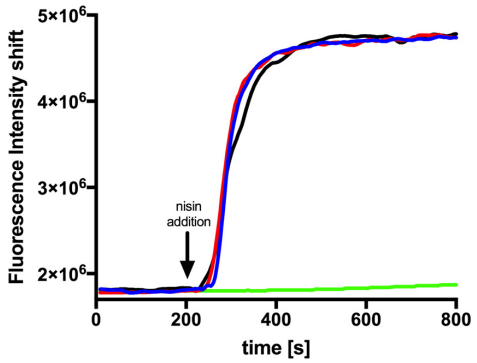

FIGURE 5 | Nisin mediated pore formation, visualized with the SYTOX green assay. The NZ9000Cm strain incubated with the SYTOX dye. After a stable baseline (~200 s), one of the nisin variants (100 nM) was added (indicated with an arrow). The fluorescence signal was measured using a fluorolog (Horiba III). The rapid increase in fluorescence indicates pore formation. The black line represents the addition of nisin A, the red line nisin H, and the blue line nisin H F_1I. As a control we added buffer shown as green line.

the immunity proteins NisFEG (Alkhatib et al., 2014b) and NisI (Alkhatib et al., 2014a), as well as the resistance proteins *Sa*NSR (Khosa et al., 2013; Khosa et al., 2016a,b) and *Sa*NsrFP (Khosa et al., 2016a; Reiners et al., 2017). We further tested for antibacterial capabilities against *B. subtilis* and different pathogenic strains from *S. aureus*, *E. faecium,* and *E. faecalis.*

Both lantibiotics, nisin H and the F_1I variant were purified in high amounts and purity with 5.3 ± 0.6 mg/L of cell culture for nisin H and 4.9 ± 0.2 mg/L of cell culture for nisin H F_1I variant, respectively (**Figure 2B** and **Table 1**). In comparison, the homologous expression of nisin H in *S. hyointestinalis* and nisin A in *L. lactis* NZ9700 results in a very low amount of 0.15 mg/L of cell culture and 0.50 mg/L of cell culture (O'Connor et al., 2015), respectively, which demonstrates the enormous potential of the NICE-system, for lantibiotic and even non-lantibiotic expression (Eichenbaum et al., 1998; Mierau and Kleerebezem, 2005; Rink et al., 2005; Zhou et al., 2006; Lagedroste et al., 2019).

An important step in the maturation of a lantibiotic is the cleavage of the leader peptide to become biological active. The cleavage efficiency of the natural substrate nisin A was determined with 94.6 ± 2.0%. For nisin H the cleaving efficiency was drastically reduced to 15.6 ± 1.4%. The first residue of nisin A is an isoleucine, while the corresponding residue in nisin H is phenylalanine and as demonstrated before (Lagedroste et al., 2019), aromatic residues prevent efficient cleavage likely by interfering with the S1′ binding pocket of NisP. With the nisin H F_1I variant, the cleavage efficiency was restored to 91.8 ± 0.8% (**Figures 1**, **2C** and **Table 1**). This indicated that the other point mutations naturally occurring in nisin H did not affect cleavage by NisP. With respect to other natural nisin variants, NisP cleavage could be a critical step. For example nisin O1 to O4 from *B. obeum* A2-162 (Hatziioanou et al., 2017) has a tyrosine or a threonine, respectively, at position one, which should also result in a low NisP cleavage efficiency. Natural variants such as nisin U (Wirawan et al., 2006), nisin J (O'Sullivan et al., 2019, 2020), nisin Q (Zendo et al., 2003), nisin Z (Mulders et al., 1991) and nisin F (de Kwaadsteniet et al., 2008) have an isoleucine and nisin U2 (Wirawan et al., 2006) and nisin P (Zhang et al., 2012; Wu et al., 2014) a valine at position one, which should result in high NisP cleavage efficiency.

Furthermore, we made a sequence alignment with Clustal Omega (Madeira et al., 2019) for the NshP (the natural protease for the nisin H cleavage) from *S. hyointestinalis* and NisP from *L. lactis* to see if there is any difference in the active site, which could be the reason for the reduced cleavage efficiency (**Figure 6A** and **Supplementary Figure 1**). Here the three important residues His_{306}, Asp_{259}, and Ser_{512} which build up the catalytic triad in NisP are conserved in NshP. We also calculated a homology model of NshP based on the known NisP structure (PDB code 4MZD) using Phyre2 (Kelley et al., 2015; **Figure 6B** and **Supplementary Figure 2**). Here, no significant differences are found within the overall fold as well as the active site which would explain the difference in the cleavage site. This is intriguing since the recognition site within the leader peptide differs between nisin A (sequence is ASPR) and nisin H (sequence is ASTR) (see **Supplementary Figure 3**). This suggests that the proteases NisP and NshP recognize their substrate by small difference in their active site.

Nevertheless, for an efficient cleavage, (methyl)-lanthionine rings have to be present. This even holds true in light of the presence of all (methyl)-lanthionine rings, which is generally assumed as the prerequisite for fast and efficient conversion of the pre-nisin to modified nisin (Plat et al., 2011;

TABLE 3 | MIC values for nisin A, nisin H, and nisin H F_1I against different pathogenic strains.

Organisms	Minimum inhibitory concentration (μM)		
	Nisin A	Nisin H	Nisin H F_1I
Staphylococcus aureus ATCC 29213 (MSSA)	0.78	0.19	0.78
Staphylococcus aureus ATCC 700699 (MRSA)	6.25	0.78	6.25
Enterococcus faecalis ATCC 29212	1.56	1.56	1.56
Enterococcus faecium ATCC 35667	1.56	0.39	0.78
Bacillus subtilis 168	0.78	0.1	0.39
Enterococcus faecalis ATCC 51299 (VRE)	1.56	1.56	0.78
Enterococcus faecium ATCC 700221 (VRE)	0.78	0.39	0.78

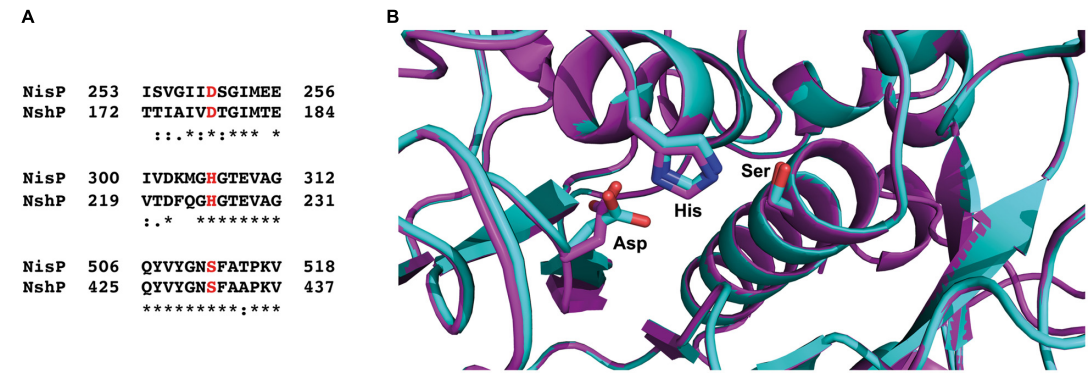

FIGURE 6 | Sequence alignment of NisP from *Lactococcus lactis* and NshP from *Streptococcus hyointestinalis*. **(A)** The important residues from the active site (Asp_{259}, His_{306}, and Ser_{512} for NisP and Asp_{178}, His_{225}, and Ser_{431} for NshP) are marked in red, shown together with the close neighborhood residues. The sequence alignment was done with Clustal Omega (Madeira et al., 2019). **(B)** Zoom-in into the active sites of NshP (magenta) and NisP (cyan). The important residues for the catalytic activity (Asp_{259}, His_{306}, and Ser_{512} for NisP and Asp_{178}, His_{225}, and Ser_{431} for NshP) are shown in stick representation. Figure was generated using Pymol (2015). For a full alignment and a corresponding homology model, please see **Supplementary Material**.

Lagedroste et al., 2017). To check the amount of dehydrations, necessary for (methyl)-lanthionine ring formation we applied MALDI-TOF analysis. The loss of water molecules within the peptide is directly visible in the reduced molecular weight, but not the (methyl)-lanthionine ring formation. Here we used 1-cyano-4 dimethylaminopyridinium tetrafluoroborate (CDAP) (Wu and Watson, 1998), which binds to free cysteine residues, indicating that these cysteines are not involved in a (methyl)-lanthionine ring. For both lantibiotics, nisin H and the nisin H F_1I variant no CDAP coupling products were found, indicating that no (methyl)-lanthionine ring is lacking (**Figure 3** and **Table 1**). Nisin H has 10 possible dehydration sites and is predicated to be ninefold dehydrated when expressed homologous (O'Connor et al., 2015). A minor species of nine dehydrations was found, but the dominant species was eightfold dehydrated. The dehydration pattern of the F_1I variant is changed in comparison to nisin H. Here we determined a dominant ninefold species (**Figure 3** and **Table 1**). This provides a hint, that position two of wild-type nisin H might not have been previously dehydrated, due to steric hindrance of the phenylalanine. To validate which serine or threonine residues is dehydrated, we perform a tandem mass spectrometric analysis of nisin H and the F_1I variant. Here we found that the Thr_2 partially escape the dehydration in nisin H. In the nisin H F_1I variant the Thr_2 was in all species dehydrated, which gives a hint that, the phenylalanine at position one in nisin H is critical for the dehydratase NisB. This is in line with previous data from the I_1F variant of nisin A, where the dominant species was sevenfold dehydrated and not eightfold as wild-type nisin A (Lagedroste et al., 2019). It has also been reported for the natural nisin Z (Mulders et al., 1991), that the I_1W mutation showed a partial inhibition of dehydration of the Thr_2 (Breukink et al., 1998), which could also be the case for nisin H with the aromatic phenylalanine at position one, resulting in eight dehydrations. A dehydration of position Ser_{29} normally goes in line with the lack of ring E (Lubelski et al., 2009), which drastically reduces the antimicrobial activity of nisin A against the sensitive NZ9000Cm strain (Alkhatib et al., 2014b; Khosa et al., 2016a; Reiners et al., 2017). Since the activity was high for nisin H and the F_1I variant, we expected that Ser_{29} was not dehydrated and tandem mass spectrometric analysis supported this.

Nisin H showed nearly the same activity as nisin A against the sensitive NZ9000Cm strain but the nisin H F_1I variant is roughly threefold less active. For the immunity protein NisI, it was revealed that nisin H has an identical activity like nisin A within experimental error. However, the nisin H F_1I variant exhibited a lower IC_{50} value of 34.1 $\pm$ 0.3 nM and due to the weaker wild-type activity more than a threefold lower fold of resistance (2.4 $\pm$ 0.1 compared to 8.1 $\pm$ 2.2) (**Figure 4** and **Table 2**). NisI recognizes the N-terminus of nisin (Wiedemann et al., 2001) and the lower IC_{50} could be due to the fact that Thr_2 is dehydrated in the nisin H F_1I variant in contrast to nisin H. An additional change is the leucine at position 6 against methionine in nisin H and the nisin H F_1I variant, which could be responsible for the better recognition by NisI.

The immunity protein NisFEG, in comparison to nisin A, showed a strong reduction in immunity in the presence of nisin H and the nisin H F_1I variant. NisFEG recognizes the C-terminus of nisin (Alkhatib et al., 2014b), which indicates that the point mutations of nisin H affect NisFEG. So, we suppose that nisin H and the nisin H F_1I variant are not recognized and subsequently transported out of the membrane like nisin A.

The resistance protein *Sa*NSR also recognizes the C-terminus of nisin (Khosa et al., 2016a), and cleaves nisin between the positions 28 and 29. Other studies showed that mutations in this area of the nisin molecule, e.g., $S_{29}P$ or $C_{28}P$ strongly reduce the efficiency of *Sa*NSR (Field et al., 2019; Zaschke-Kriesche et al., 2019a). We assume that the exchange of His_{31} against lysine in nisin H and the nisin H F_1I variant (**Figure 1**) has the same effect on *Sa*NSR thereby lowering the resistance efficiency to an IC_{50} value of 52.4 $\pm$ 2.6 nM for nisin H and 44.2 $\pm$ 1.3 nM for the nisin H F_1I variant, respectively (**Figure 4** and **Table 2**).

For the resistance protein *Sa*NsrFP, we observed an activity for nisin H identical to nisin A. *Sa*NsrFP recognizes the N-terminus of nisin (Reiners et al., 2017), which is affected due to the different dehydration pattern in wild-type nisin H in comparison to the nisin H F_1I variant. The nisin H F_1I variant showed a lower IC_{50} value of 50.2 ± 1.6 nM, compared to 86.4 ± 4.1 nM for nisin H. This effect is even more pronounced when comparing the fold of resistances of 16.2 ± 3.1 for nisin H to 3.5 ± 0.1 for the nisin H F_1I variant, respectively (**Figure 4** and **Table 2**).

This study demonstrated again that only a complete characterization of a lantibiotic reveals the full antimicrobial potential. Based on the IC_{50} value of the sensitive NZ9000Cm strain the F_1I variant might be classified as weakly antimicrobial active, but with respect to the immunity and resistance proteins, it becomes more interesting, due to its high activity even against the immunity proteins NisI and NisFEG from *L. lactis* and the nisin resistance proteins *Sa*NSR and *Sa*NsrFP from *S. agalactiae* COH1. Against the tested pathogenic bacteria, we found that nisin H and the nisin H F_1I variant performed almost identically or in the most cases even better than the natural nisin A. Nisin H displayed high antimicrobial potential against both methicillin-resistant and –susceptible the *S. aureus* strains, both vancomycin-resistant and -susceptible, *E. faecium* strains, as well as *B. subtilis.*

DATA AVAILABILITY STATEMENT

The raw data supporting the conclusions of this article will be made available by the authors, without undue reservation.

AUTHOR CONTRIBUTIONS

LS and SS conceived and directed this study. JR and ML conducted the expression, purification, MS-analysis, and the growth inhibition experiments. JG performed the SYTOX experiments. GP and KS performed the tandem mass spectrometric analysis. EA and RK performed the MIC experiments. JR, ML, SS, and LS wrote the manuscript. All authors read and approved the manuscript.

FUNDING

This work was supported by the Deutsche Forschungsgemeinschaft (DFG, grant Schm1279/13-1 to LS). The Center for Structural studies is funded by the DFG (Grant number 417919780 to SS). Project number 270650915 (Research Training Group GRK2158, TP2a to RK and TP4a to SS).

ACKNOWLEDGMENTS

We thank all members of the Institute of Biochemistry for fruitful discussions.

SUPPLEMENTARY MATERIAL

The Supplementary Material for this article can be found online at: https://www.frontiersin.org/articles/10.3389/fmicb.2020.573614/full#supplementary-material

REFERENCES

Abts, A., Montalban-Lopez, M., Kuipers, O. P., Smits, S. H., and Schmitt, L. (2013). NisC binds the FxLx motif of the nisin leader peptide. *Biochemistry* 52, 5387–5395. doi: 10.1021/bi4008116

Alkhatib, Z., Lagedroste, M., Fey, I., Kleinschrodt, D., Abts, A., and Smits, S. H. (2014a). Lantibiotic immunity: inhibition of nisin mediated pore formation by NisI. *PLoS One* 9:e102246. doi: 10.1371/journal.pone.0102246

Alkhatib, Z., Lagedroste, M., Zaschke, J., Wagner, M., Abts, A., Fey, I., et al. (2014b). The C-terminus of nisin is important for the ABC transporter NisFEG to confer immunity in *Lactococcus lactis*. *Microbiologyopen* 3, 752–763. doi: 10.1002/mbo3.205

Arnison, P. G., Bibb, M. J., Bierbaum, G., Bowers, A. A., Bugni, T. S., Bulaj, G., et al. (2013). Ribosomally synthesized and post-translationally modified peptide natural products: overview and recommendations for a universal nomenclature. *Nat. Prod. Rep.* 30, 108–160.

Breukink, E., Van Kraaij, C., Van Dalen, A., Demel, R. A., Siezen, R. J., De Kruijff, B., et al. (1998). The orientation of nisin in membranes. *Biochemistry* 37, 8153–8162. doi: 10.1021/bi9727971

Brunati, C., Thomsen, T. T., Gaspari, E., Maffioli, S., Sosio, M., Jabes, D., et al. (2018). Expanding the potential of NAI-107 for treating serious ESKAPE pathogens: synergistic combinations against Gram-negatives and bactericidal activity against non-dividing cells. *J. Antimicrob. Chemother.* 73, 414–424. doi: 10.1093/jac/dkx395

Chan, W. C., Leyland, M., Clark, J., Dodd, H. M., Lian, L. Y., Gasson, M. J., et al. (1996). Structure-activity relationships in the peptide antibiotic nisin: antibacterial activity of fragments of nisin. *FEBS Lett.* 390, 129–132. doi: 10.1016/0014-5793(96)00638-2

Clinical and Laboratory Standards Institute (2012). *Methods for Dilution Antimicrobial Susceptibility Tests for Bacteria that Grow Aerobically; Approved Standard*, 9th Edn. Wayne PA: Clinical and Laboratory Standards Institute.

Crowther, G. S., Baines, S. D., Todhunter, S. L., Freeman, J., Chilton, C. H., and Wilcox, M. H. (2013). Evaluation of NVB302 versus vancomycin activity in an in vitro human gut model of Clostridium difficile infection. *J. Antimicrob. Chemother.* 68, 168–176. doi: 10.1093/jac/dks359

Dawson, M. J., and Scott, R. W. (2012). New horizons for host defense peptides and lantibiotics. *Curr. Opin. Pharmacol.* 12, 545–550. doi: 10.1016/j.coph.2012.06.006

de Kwaadsteniet, M., Ten Doeschate, K., and Dicks, L. M. (2008). Characterization of the structural gene encoding nisin F, a new lantibiotic produced by a *Lactococcus lactis* subsp. lactis isolate from freshwater catfish (*Clarias gariepinus*). *Appl. Environ. Microbiol.* 74, 547–549. doi: 10.1128/aem.01862-07

Delves-Broughton, J., Blackburn, P., Evans, R. J., and Hugenholtz, J. (1996). Applications of the bacteriocin, nisin. *Antonie Van Leeuwenhoek* 69, 193–202. doi: 10.1007/bf00399424

Dischinger, J., Basi Chipalu, S., and Bierbaum, G. (2014). Lantibiotics: promising candidates for future applications in health care. *Int. J. Med. Microbiol.* 304, 51–62. doi: 10.1016/j.ijmm.2013.09.003

Eichenbaum, Z., Federle, M. J., Marra, D., De Vos, W. M., Kuipers, O. P., Kleerebezem, M., et al. (1998). Use of the lactococcal nisA promoter to regulate gene expression in gram-positive bacteria: comparison of induction level and promoter strength. *Appl. Environ. Microbiol.* 64, 2763–2769. doi: 10.1128/aem.64.8.2763-2769.1998

Field, D., Blake, T., Mathur, H., Pm, O. C., Cotter, P. D., Paul Ross, R., et al. (2019). Bioengineering nisin to overcome the nisin resistance protein. *Mol. Microbiol.* 111, 717–731.

Gross, E., and Morell, J. L. (1967). The presence of dehydroalanine in the antibiotic nisin and its relationship to activity. *J. Am. Chem. Soc.* 89, 2791–2792. doi: 10.1021/ja00987a084

Hasper, H. E., De Kruijff, B., and Breukink, E. (2004). Assembly and stability of nisin-lipid II pores. *Biochemistry* 43, 11567–11575. doi: 10.1021/bi049476b

Hatziioanou, D., Gherghisan-Filip, C., Saalbach, G., Horn, N., Wegmann, U., Duncan, S. H., et al. (2017). Discovery of a novel lantibiotic nisin O from Blautia obeum A2-162, isolated from the human gastrointestinal tract. *Microbiology* 163, 1292–1305. doi: 10.1099/mic.0.000515

Holo, H., and Nes, I. F. (1989). High-Frequency transformation, by electroporation, of *Lactococcus lactis* subsp. cremoris grown with glycine in osmotically stabilized media. *Appl. Environ. Microbiol.* 55, 3119–3123. doi: 10.1128/aem.55.12.3119-3123.1989

Hsu, S. T. D., Breukink, E., Tischenko, E., Lutters, M. A. G., De Kruijff, B., Kaptein, R., et al. (2004). The nisin-lipid II complex reveals a pyrophosphate cage that provides a blueprint for novel antibiotics. *Nat. Struct. Mol. Biol.* 11, 963–967. doi: 10.1038/nsmb830

Jabes, D., Brunati, C., Candiani, G., Riva, S., Romano, G., and Donadio, S. (2011). Efficacy of the new lantibiotic NAI-107 in experimental infections induced by multidrug-resistant Gram-positive pathogens. *Antimicrob. Agents Chemother.* 55, 1671–1676. doi: 10.1128/aac.01288-10

Jensen, P. R., and Hammer, K. (1993). Minimal requirements for exponential growth of *Lactococcus lactis*. *Appl. Environ. Microbiol.* 59, 4363–4366. doi: 10.1128/aem.59.12.4363-4366.1993

Kaletta, C., and Entian, K. D. (1989). Nisin, a peptide antibiotic: cloning and sequencing of the nisA gene and posttranslational processing of its peptide product. *J. Bacteriol.* 171, 1597–1601. doi: 10.1128/jb.171.3.1597-1601.1989

Karakas Sen, A., Narbad, A., Horn, N., Dodd, H. M., Parr, A. J., Colquhoun, I., et al. (1999). Post-translational modification of nisin. The involvement of NisB in the dehydration process. *Eur. J. Biochem.* 261, 524–532. doi: 10.1046/j.1432-1327.1999.00303.x

Kelley, L. A., Mezulis, S., Yates, C. M., Wass, M. N., and Sternberg, M. J. (2015). The Phyre2 web portal for protein modeling, prediction and analysis. *Nat. Protoc.* 10, 845–858. doi: 10.1038/nprot.2015.053

Khosa, S., Alkhatib, Z., and Smits, S. H. (2013). NSR from Streptococcus agalactiae confers resistance against nisin and is encoded by a conserved nsr operon. *Biol. Chem.* 394, 1543–1549. doi: 10.1515/hsz-2013-0167

Khosa, S., Frieg, B., Mulnaes, D., Kleinschrodt, D., Hoeppner, A., Gohlke, H., et al. (2016a). Structural basis of lantibiotic recognition by the nisin resistance protein from Streptococcus agalactiae. *Sci. Rep.* 6:18679.

Khosa, S., Lagedroste, M., and Smits, S. H. (2016b). Protein defense systems against the lantibiotic nisin: function of the immunity protein NisI and the resistance protein NSR. *Front. Microbiol.* 7:504. doi: 10.3389/fmicb.2016.00504

Klaenhammer, T. R. (1993). Genetics of bacteriocins produced by lactic acid bacteria. *FEMS Microbiol. Rev.* 12, 39–85. doi: 10.1016/0168-6445(93)90057-g

Koponen, O., Tolonen, M., Qiao, M., Wahlstrom, G., Helin, J., and Saris, P. E. J. (2002). NisB is required for the dehydration and NisC for the lanthionine formation in the post-translational modification of nisin. *Microbiology* 148, 3561–3568. doi: 10.1099/00221287-148-11-3561

Kuipers, O. P., De Ruyter, P. G., Kleerebezem, M., and De Vos, W. M. (1997). Controlled overproduction of proteins by lactic acid bacteria. *Trends Biotechnol.* 15, 135–140. doi: 10.1016/s0167-7799(97)01029-9

Lagedroste, M., Reiners, J., Smits, S. H. J., and Schmitt, L. (2019). Systematic characterization of position one variants within the lantibiotic nisin. *Sci. Rep.* 9:935.

Lagedroste, M., Smits, S. H. J., and Schmitt, L. (2017). Substrate specificity of the secreted nisin leader peptidase NisP. *Biochemistry* 56, 4005–4014. doi: 10.1021/acs.biochem.7b00524

Li, B., and van der Donk, W. A. (2007). Identification of essential catalytic residues of the cyclase NisC involved in the biosynthesis of nisin. *J. Biol. Chem.* 282, 21169–21175. doi: 10.1074/jbc.m701802200

Li, B., Yu, J. P., Brunzelle, J. S., Moll, G. N., Van Der Donk, W. A., and Nair, S. K. (2006). Structure and mechanism of the lantibiotic cyclase involved in nisin biosynthesis. *Science* 311, 1464–1467. doi: 10.1126/science.1121422

Lu, Y., Jiang, L., Chen, M., Huan, L., and Zhong, J. (2010). [Improving heat and pH stability of nisin by site-directed mutagenesis]. *Wei Sheng Wu Xue Bao* 50, 1481–1487.

Lubelski, J., Khusainov, R., and Kuipers, O. P. (2009). Directionality and coordination of dehydration and ring formation during biosynthesis of the lantibiotic nisin. *J. Biol. Chem.* 284, 25962–25972. doi: 10.1074/jbc.m109.026690

Madeira, F., Park, Y. M., Lee, J., Buso, N., Gur, T., Madhusoodanan, N., et al. (2019). The EMBL-EBI search and sequence analysis tools APIs in 2019. *Nucleic Acids Res.* 47, W636–W641.

Medeiros-Silva, J., Jekhmane, S., Paioni, A. L., Gawarecka, K., Baldus, M., Swiezewska, E., et al. (2018). High-resolution NMR studies of antibiotics in cellular membranes. *Nat. Commun.* 9:3963.

Mierau, I., and Kleerebezem, M. (2005). 10 years of the nisin-controlled gene expression system (NICE) in *Lactococcus lactis*. *Appl. Microbiol. Biotechnol.* 68, 705–717. doi: 10.1007/s00253-005-0107-6

Mota-Meira, M., Lapointe, G., Lacroix, C., and Lavoie, M. C. (2000). MICs of mutacin B-Ny266, nisin A, vancomycin, and oxacillin against bacterial pathogens. *Antimicrob. Agents Chemother.* 44, 24–29. doi: 10.1128/aac.44.1.24-29.2000

Mulders, J. W., Boerrigter, I. J., Rollema, H. S., Siezen, R. J., and De Vos, W. M. (1991). Identification and characterization of the lantibiotic nisin Z, a natural nisin variant. *Eur. J. Biochem.* 201, 581–584. doi: 10.1111/j.1432-1033.1991.tb16317.x

O'Sullivan, J. N., O'Connor, P. M., Rea, M. C., O'Sullivan, O., Walsh, C. J., Healy, B., et al. (2020). Nisin J, a novel natural nisin variant, is produced by *Staphylococcus capitis* Sourced from the human skin microbiota. *J. Bacteriol* 202. doi: 10.1128/JB.00639-19

O'Connor, P. M., O'Shea, E. F., Guinane, C. M., O'Sullivan, O., Cotter, P. D., Ross, R. P., et al. (2015). Nisin H is a new nisin variant produced by the gut-derived strain *Streptococcus hyointestinalis* DPC6484. *Appl. Environ. Microbiol.* 81, 3953–3960. doi: 10.1128/aem.00212-15

Okeley, N. M., Paul, M., Stasser, J. P., Blackburn, N., and Van Der Donk, W. A. (2003). SpaC and NisC, the cyclases involved in subtilin and nisin biosynthesis, are zinc proteins. *Biochemistry* 42, 13613–13624. doi: 10.1021/bi0354942

Ongey, E. L., Yassi, H., Pflugmacher, S., and Neubauer, P. (2017). Pharmacological and pharmacokinetic properties of lanthipeptides undergoing clinical studies. *Biotechnol. Lett.* 39, 473–482. doi: 10.1007/s10529-016-2279-9

Oppedijk, S. F., Martin, N. I., and Breukink, E. (2016). Hit 'em where it hurts: the growing and structurally diverse family of peptides that target lipid-II. *Biochim. Biophys. Acta* 1858, 947–957. doi: 10.1016/j.bbamem.2015.10.024

Ortega, M. A., Hao, Y., Zhang, Q., Walker, M. C., Van Der Donk, W. A., and Nair, S. K. (2015). Structure and mechanism of the tRNA-dependent lantibiotic dehydratase NisB. *Nature* 517, 509–512. doi: 10.1038/nature13888

O'Sullivan, J. N., Rea, M. C., O'Connor, P. M., Hill, C., and Ross, R. P. (2019). Human skin microbiota is a rich source of bacteriocin-producing staphylococci that kill human pathogens. *FEMS Microbiol. Ecol.* 95:fiy241.

Plat, A., Kluskens, L. D., Kuipers, A., Rink, R., and Moll, G. N. (2011). Requirements of the engineered leader peptide of nisin for inducing modification, export, and cleavage. *Appl. Environ. Microbiol.* 77, 604–611. doi: 10.1128/aem.01503-10

Pymol (2015). *The PyMOL Molecular Graphics System, Version 2.0*. New York, NY: Schrödinger.

Reiners, J., Lagedroste, M., Ehlen, K., Leusch, S., Zaschke-Kriesche, J., and Smits, S. H. J. (2017). The N-terminal region of nisin is important for the BceAB-Type ABC Transporter NsrFP from *Streptococcus agalactiae* COH1. *Front. Microbiol.* 8:1643. doi: 10.3389/fmicb.2017.01643

Repka, L. M., Chekan, J. R., Nair, S. K., and Van Der Donk, W. A. (2017). Mechanistic understanding of lanthipeptide biosynthetic enzymes. *Chem. Rev.* 117, 5457–5520. doi: 10.1021/acs.chemrev.6b00591

Rink, R., Kuipers, A., De Boef, E., Leenhouts, K. J., Driessen, A. J., Moll, G. N., et al. (2005). Lantibiotic structures as guidelines for the design of peptides that can be modified by lantibiotic enzymes. *Biochemistry* 44, 8873–8882. doi: 10.1021/bi050081h

Rogers, L. A. (1928). The inhibiting effect of streptococcus lactis on Lactobacillus Bulgaricus. *J. Bacteriol.* 16, 321–325. doi: 10.1128/jb.16.5.321-325.1928

Rogers, L. A., and Whittier, E. O. (1928). Limiting factors in the lactic fermentation. *J. Bacteriol.* 16, 211–229. doi: 10.1128/jb.16.4.211-229.1928

Rollema, H. S., Kuipers, O. P., Both, P., De Vos, W. M., and Siezen, R. J. (1995). Improvement of solubility and stability of the antimicrobial peptide nisin by

protein engineering. *Appl. Environ. Microbiol.* 61, 2873–2878. doi: 10.1128/aem.61.8.2873-2878.1995

Roth, B. L., Poot, M., Yue, S. T., and Millard, P. J. (1997). Bacterial viability and antibiotic susceptibility testing with SYTOX green nucleic acid stain. *Appl. Environ. Microbiol.* 63, 2421–2431. doi: 10.1128/aem.63.6.2421-2431.1997

Sahl, H. G., and Bierbaum, G. (1998). Lantibiotics: biosynthesis and biological activities of uniquely modified peptides from gram-positive bacteria. *Annu. Rev. Microbiol.* 52, 41–79. doi: 10.1146/annurev.micro.52.1.41

Sandiford, S. K. (2019). Current developments in lantibiotic discovery for treating Clostridium difficile infection. *Expert Opin. Drug. Discov.* 14, 71–79. doi: 10.1080/17460441.2019.1549032

Terzaghi, B. E., and Sandine, W. E. (1975). Improved medium for lactic Streptococci and Their Bacteriophages. *Appl. Microbiol.* 29, 807–813. doi: 10.1128/aem.29.6.807-813.1975

van Heel, A. J., De Jong, A., Song, C., Viel, J. H., Kok, J., and Kuipers, O. P. (2018). BAGEL4: a user-friendly web server to thoroughly mine RiPPs and bacteriocins. *Nucleic Acids Res.* 46, W278–W281.

van Heusden, H. E., De Kruijff, B., and Breukink, E. (2002). Lipid II induces a transmembrane orientation of the pore-forming peptide lantibiotic nisin. *Biochemistry* 41, 12171–12178. doi: 10.1021/bi026090x

Wiedemann, I., Benz, R., and Sahl, H. G. (2004). Lipid II-mediated pore formation by the peptide antibiotic nisin: a black lipid membrane study. *J. Bacteriol.* 186, 3259–3261. doi: 10.1128/jb.186.10.3259-3261.2004

Wiedemann, I., Breukink, E., Van Kraaij, C., Kuipers, O. P., Bierbaum, G., De Kruijff, B., et al. (2001). Specific binding of nisin to the peptidoglycan precursor lipid II combines pore formation and inhibition of cell wall biosynthesis for potent antibiotic activity. *J. Biol. Chem.* 276, 1772–1779. doi: 10.1074/jbc.m006770200

Wirawan, R. E., Klesse, N. A., Jack, R. W., and Tagg, J. R. (2006). Molecular and genetic characterization of a novel nisin variant produced by *Streptococcus uberis*. *Appl. Environ. Microbiol.* 72, 1148–1156. doi: 10.1128/aem.72.2.1148-1156.2006

Wu, J., and Watson, J. T. (1998). Optimization of the cleavage reaction for cyanylated cysteinyl proteins for efficient and simplified mass mapping. *Anal. Biochem.* 258, 268–276. doi: 10.1006/abio.1998.2596

Wu, Z., Wang, W., Tang, M., Shao, J., Dai, C., Zhang, W., et al. (2014). Comparative genomic analysis shows that *Streptococcus suis* meningitis isolate SC070731 contains a unique 105K genomic island. *Gene* 535, 156–164. doi: 10.1016/j.gene.2013.11.044

Zaschke-Kriesche, J., Behrmann, L. V., Reiners, J., Lagedroste, M., Groner, Y., Kalscheuer, R., et al. (2019a). Bypassing lantibiotic resistance by an effective nisin derivative. *Bioorg. Med. Chem.* 27, 3454–3462. doi: 10.1016/j.bmc.2019.06.031

Zaschke-Kriesche, J., Reiners, J., Lagedroste, M., and Smits, S. H. J. (2019b). Influence of nisin hinge-region variants on lantibiotic immunity and resistance proteins. *Bioorg. Med. Chem.* 27, 3947–3953. doi: 10.1016/j.bmc.2019.07.014

Zendo, T., Fukao, M., Ueda, K., Higuchi, T., Nakayama, J., and Sonomoto, K. (2003). Identification of the lantibiotic nisin Q, a new natural nisin variant produced by *Lactococcus lactis* 61-14 isolated from a river in Japan. *Biosci. Biotechnol. Biochem.* 67, 1616–1619. doi: 10.1271/bbb.67.1616

Zhang, Q., Yu, Y., Velasquez, J. E., and Van Der Donk, W. A. (2012). Evolution of lanthipeptide synthetases. *Proc. Natl. Acad. Sci. U.S.A.* 109, 18361–18366. doi: 10.1073/pnas.1210393109

Zhou, L., Van Heel, A. J., and Kuipers, O. P. (2015). The length of a lantibiotic hinge region has profound influence on antimicrobial activity and host specificity. *Front. Microbiol* 6:11. doi: 10.3389/fmicb.2015.00011

Zhou, X. X., Li, W. F., Ma, G. X., and Pan, Y. J. (2006). The nisin-controlled gene expression system: construction, application and improvements. *Biotechnol. Adv.* 24, 285–295. doi: 10.1016/j.biotechadv.2005.11.001

Conflict of Interest: The authors declare that the research was conducted in the absence of any commercial or financial relationships that could be construed as a potential conflict of interest.

Supplementary Material

Insights in the antimicrobial potential of the natural nisin variant nisin H

Jens Reiners[1,2]*, Marcel Lagedroste[1]*, Julia Gottstein[1], Emmanuel T. Adeniyi[3], Rainer Kalscheuer[3], Gereon Poschmann[4], Kai Stühler[4,5], Sander H.J. Smits[1,2 #] and Lutz Schmitt[1 #]

[1]Institute of Biochemistry, Heinrich-Heine-University Düsseldorf, Universitaetsstrasse 1, 40225, Düsseldorf, Germany.

[2]Center for Structural Studies, Heinrich-Heine-University Düsseldorf, Universitaetsstrasse 1, 40225, Düsseldorf, Germany.

[3]Institute of Pharmaceutical Biology and Biotechnology, Heinrich-Heine-University Düsseldorf, Universitaetsstrasse 1, 40225, Düsseldorf, Germany.

[4]Institute for Molecular Medicine, Medical Faculty, Heinrich-Heine-University Düsseldorf, 40225 Düsseldorf, Germany

[5]Molecular Proteomics Laboratory, BMFZ, Heinrich-Heine-University-Düsseldorf, 40225 Düsseldorf, Germany

*Contributed equally

#Address correspondence to Lutz Schmitt: lutz.schmitt@hhu.de or Sander Smits sander.smits@hhu.de

Key words: lantibiotics, nisin, nisin H, MS analysis, antimicrobial activity

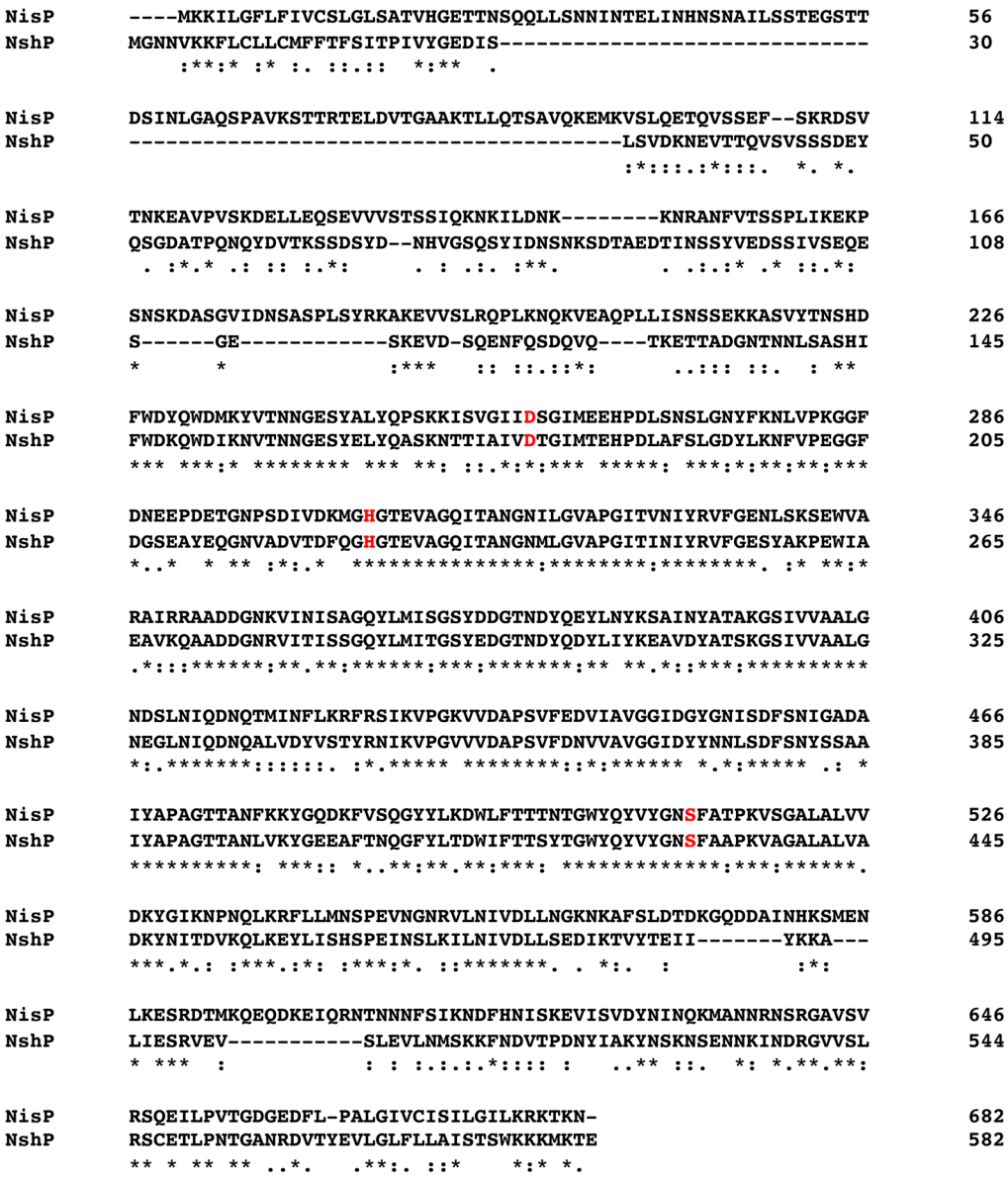

Figure S1: Sequence alignment of NispP from *Lactococcus lactis* and NshP from *Streptococcus hyointestinalis*. The important residues of the active site (Asp_{259}, His_{306}, and Ser_{512} for NisP and Asp_{178}, His_{225}, and Ser_{431} for NshP) are highlighted in red. The sequence alignment was done with Clustal Omega [1].

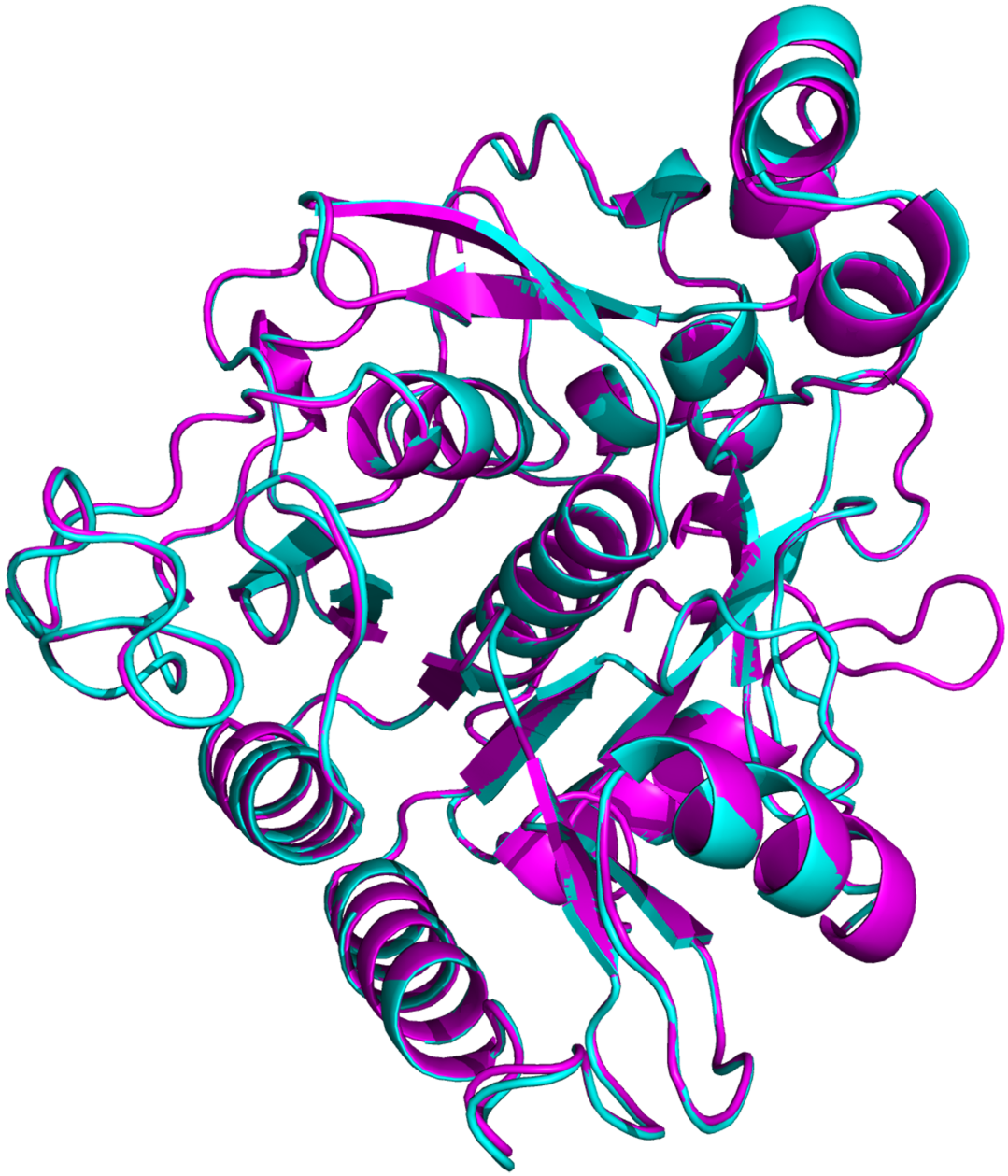

Figure S2: Homology model of NshP from *Streptococcus hyointestinalis*. A homology model of NshP was created using Phyre2 [2]. We used the sequence of the active protein without the self-cleaving part. The NshP model is shown in magenta and NisP (PDB code: 4MZD) in cyan. Figure was generated using PyMol [3].

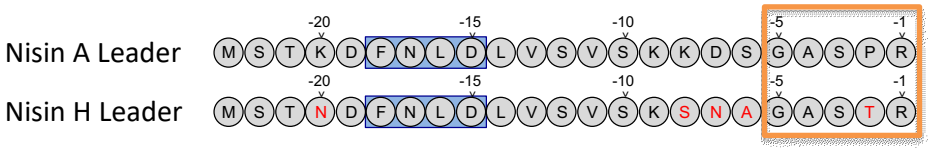

Nisin A Leader MSTKDFNLDLVSVSKKDSGASPR
Nisin H Leader MSTNDFNLDLVSVSKSNAGASTR

Figure S3: Sequence of nisin A and Nisin H leader sequence. Highlighted are the FNLD box (blue box) known to be important for the modification enzymes as well differences in sequence indicated by red letters. The cleavage site within the leader sequence of nisin A and nisin H is highlighted by an orange box.

1. Madeira, F., et al., *The EMBL-EBI search and sequence analysis tools APIs in 2019.* Nucleic Acids Res, 2019. **47**(W1): p. W636-W641.
2. Kelley, L.A., et al., *The Phyre2 web portal for protein modeling, prediction and analysis.* Nat Protoc, 2015. **10**(6): p. 845-58.
3. *The PyMOL Molecular Graphics System, Version 2.0 Schrödinger, LLC.*

3.6 Chapter VI

Title: Bypassing lantibiotic resistance by an effective nisin derivative

Authors: Julia Zaschke-Kriesche, Lara V. Behrmann, **Jens Reiners**, Marcel Lagedroste, Yvonne Gröner, Rainer Kalscheuer, Sander H.J. Smits

Published in: Bioorganic & Medicinal Chemistry (2019)
Impact factor: 2.59

Own proportion of this work: 20%

- Cloning of the nisin A $Cys_{29}Pro$ construct
- Purification of the pre-nisin A $Cys_{29}Pro$ variant
- HPLC & MS data analysis
- Writing the manuscript

Bioorganic & Medicinal Chemistry 27 (2019) 3454–3462

Contents lists available at ScienceDirect

Bioorganic & Medicinal Chemistry

journal homepage: www.elsevier.com/locate/bmc

Bypassing lantibiotic resistance by an effective nisin derivative

Julia Zaschke-Kriesche[a], Lara V. Behrmann[a], Jens Reiners[a], Marcel Lagedroste[a], Yvonne Gröner[b], Rainer Kalscheuer[b], Sander H.J. Smits[a,c,*]

[a] Institute of Biochemistry, Heinrich-Heine-University Duesseldorf, Universitaetsstrasse 1, 40225 Duesseldorf, Germany
[b] Institute of Pharmaceutical Biology and Biotechnology, Heinrich-Heine-University Düsseldorf, Universitaetsstrasse 1, 40225 Duesseldorf, Germany
[c] Center for Structural Studies, Heinrich-Heine-University Duesseldorf, Universitaetsstrasse 1, 40225 Duesseldorf, Germany

ARTICLE INFO

Keywords:
Lantibiotic
Nisin resistance protein
Activity

ABSTRACT

The need for new antibiotic compounds is rising and antimicrobial peptides are excellent candidates to fulfill this object. The bacteriocin subgroup lantibiotics, for example, are active in the nanomolar range and target the membranes of mainly Gram-positive bacteria. They bind to lipid II, inhibit cell growth and in some cases form pores within the bacterial membrane, inducing rapid cell death. Pharmaceutical usage of lantibiotics is however hampered by the presence of gene clusters in human pathogenic strains which, when expressed, confer resistance. The human pathogen *Streptococcus agalactiae* COH1, expresses several lantibiotic resistance proteins resulting in resistance against for example nisin.

This study presents a highly potent, pore forming nisin variant as an alternative lantibiotic which bypasses the *Sa*NSR protein. It is shown that this nisin derivate $nisin_{C28P}$ keeps its nanomolar antibacterial activity against *L. lactis* NZ9000 cells but is not recognized by the nisin resistance protein *Sa*NSR.

$Nisin_{C28P}$ is cleaved by *Sa*NSR *in vitro* with a highly decreased efficiency, as shown by an cleavage assay. Furthermore, we show that $nisin_{C28P}$ is still able to form pores in the membranes of *L. lactis* and is three times more efficient against *Sa*NSR-expressing *L. lactis* cells than wildtype nisin.

1. Introduction

Many efforts are currently taken to combat multi-drug resistant bacterial pathogens, which cause serious problems in hospital and health care settings. New antibiotics or new derivatives are required to fight against these bacteria. The difficulty in developing new antibiotics is that they have to bypass already known resistance systems in order to be highly active and to be considered for treatment. The family of antimicrobial peptides and here especially the subgroup of lantibiotics are very promising.

Lantibiotics are small antimicrobial peptides of 19–38 amino acids in size, ribosomally synthesized as prepeptides and mainly produced by Gram-positive bacteria.[1,2] They mature in the cytosol of these bacteria, where serine and threonine residues within the core peptide are specifically dehydrated and covalently linked with a neighbored cysteine side chain[3] forming so- called (methyl-)lanthionine rings. After maturation the modified prepeptide is secreted into the extracellular space and activated by cleaving off the leader peptide by a specific protease.[4,5] The family of lantibiotics is steadily increasing mainly due to the possibility to detect the encoding gene clusters by bioinformatical tools such as BAGEL4.[6] Most characterized lantibiotics are highly potent and display activities in the nM range,[7–12] and due to their low toxicity and high potency they are considered as potential novel antibiotics for the usage in the mammalian as well as veterinary medical treatment.[13,14] This is reflected by the fact that several lantibiotics like mutacin 1140, microbisporicin (also known as NAI-107) and actagardine have entered the state of clinical trials for the treatment of a variety of life-threatening diseases caused by human pathogenic bacteria.[15–17]

Importantly, lantibiotics are able to inhibit the growth of various multi-drug resistant pathogenic Gram-positive bacteria.[18,19] The mode of action of lantibiotics varies from binding to the bacterial cell wall precursor lipid II inducing growth inhibition to directing pore formation in the bacterial membrane, which leads to immediate cell death.[20–23]

The best characterized lantibiotic is nisin produced by several *Lactococcus lactis* (*L. lactis*) and *Streptococcus uberis* (*S. uberis*) strains and was discovered in 1928 by L. A. Rogers.[24–26] It has a broad antimicrobial spectrum against a wide range of Gram-positive bacteria including staphylococci, streptococci, bacilli and enterococci and has

* Corresponding author at: Institute of Biochemistry, Heinrich-Heine-University Duesseldorf, Universitaetsstrasse 1, 40225 Duesseldorf, Germany.
E-mail address: sander.smits@hhu.de (S.H.J. Smits).

https://doi.org/10.1016/j.bmc.2019.06.031
Received 12 March 2019; Received in revised form 29 May 2019; Accepted 18 June 2019
Available online 20 June 2019
0968-0896/

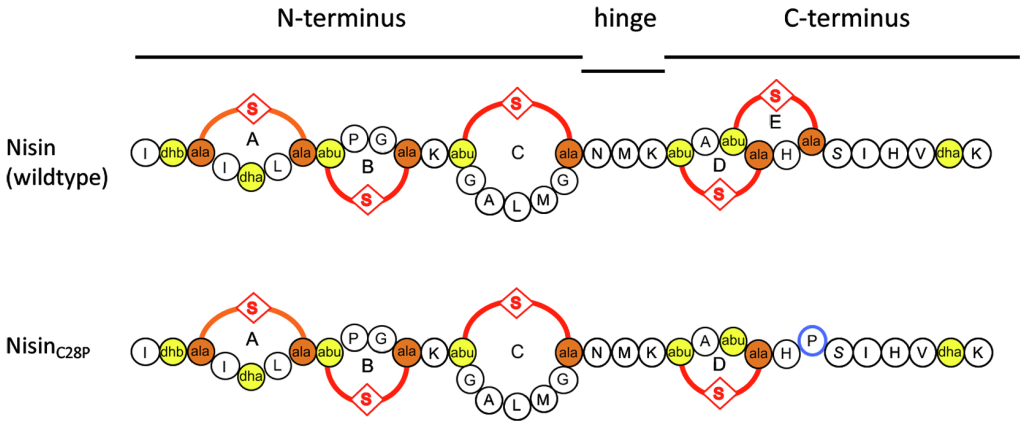

Fig. 1. Schematic view of nisin A wildtype and nisin$_{C28P}$. Introduced mutation at position 28 is highlighted in blue. The (methyl-)lanthionine rings, formed by a cysteine residue sidechain and a dehydrated amino acid residue are highlighted in orange and yellow (rings A, B, C, D and E) (adopted from Reiners et al.[42]).

therefore been used for food preservation for more than 60 years.[27] Nisin is composed of 34 amino acids and contains five (methyl-)lanthionine rings (ring A-E) (Fig. 1). With the *N*-terminal rings A and B it is able to bind to the pyrophosphate moiety of the cell wall precursor lipid II and thereby hampers the cell wall synthesis, which consequently inhibits cell growth.[20,28,29] By binding lipid II, the C-terminal part of nisin is able to flip into the membrane and to form pores composed of eight nisin and four lipid II molecules.[21,29,30] This induces the rapid diffusion of essential ions, causing a collapse of the vital ion gradients across the membrane, thereby leading to cell death.

The modification of the nisin precursor peptide in the cytosol has been very well understood, and numerous variants of nisin have been characterized with respect to their activity and the possibility to act against different species like Gram-negative bacteria.[31–33] Interestingly, although these lantibiotics use two simultaneous modes of action, some targeted bacteria escape the treatment by inducing changes in the cell wall composition, the induction of biofilm formation or by the expression of specific resistance proteins.[34]

In the case of nisin resistance, the latter is mediated by the so-called nisin resistance protein NSR encoded on the *nsr* gene cluster.[35] This gene was originally identified in *Streptococcus lactis* subsp. *diacetylactis* DRC3[36] and encodes a nisin resistance protein (NSR) which is membrane-associated *via* its strongly hydrophobic *N*-terminus.[36] NSR belongs to the S41 family of peptidases, specifically the C-terminal processing peptidases.[35]

An *nsr* gene has also been identified in *S. agalactiae* ATCC 13813, encoding a protein of 320 amino acids and a molecular weight of 36.2 kDa.[37] Heterologous expression of NSR from *S. agalactiae*, termed *Sa*NSR, in *L. lactis* NZ9000 was shown to confer a 20-fold increase in resistance against nisin. Genomic data and comparative sequence analysis using *nsr* from *S. agalactiae* as the query sequence revealed that *nsr* is found within an operon, which contains five different proteins and is very similar to the immunity system present in the producer strains.[38,39] The *nsr* operon consists of NSR and the ABC transporter NsrFP as well as a two-component system consisting of the response regulator NsrR and the histidine kinase NsrK. This operon was identified in different genera, more specifically in various strains of *Corynebacterium*, *Enterococcus*, *Leuconostoc*, *Staphylococcus* and *Streptococcus*.[35]

In vivo and *in vitro* studies have shown that *Sa*NSR proteolytically inactivates nisin by cleaving the peptide bond between MeLan28 and Ser29, i.e. cleaving off the last 6 amino acids of nisin. Sun et al. found that the resulting truncated nisin (nisin$_{1-28}$) displays reduced affinity for the cell membrane, a significantly diminished effectiveness in pore formation and a 100-fold reduction of bactericidal activity against *L. lactis* MG1363 compared to that of intact nisin.[40]

Many studies are known about nisin variants. However, in most cases they display a reduction of the activity and, more importantly, cannot bypass the NSR protein since they comprise modifications at the *N*-terminus of nisin. Recently, a nisin derivative was reported which bypasses the NSR protein by substituting the serine 29 at which cleavage takes place by a proline. However, the activity of this variant also dropped significantly.[41] We chose a different and rational approach for a mutation as we replaced the last cysteine residue by a proline, leading to a variant lacking the last lanthionine ring and thereby introducing a small ring-like structure which sterically is rather rigid (Fig. 1). We termed this variant nisin$_{C28P}$.

Interestingly, nisin$_{C28P}$ is highly active compared to wildtype nisin and is still able to induce pores in the membrane. The nisin resistance protein, however, is not able to cleave this variant efficiently. Altogether, this nisin variant appears to be a good candidate to bypass the known resistance systems while still displaying low nanomolar activity.

2. Material and Methods

2.1. Cloning and purification of the nisin variant nisin$_{C28P}$

Cloning of the nisin variant nisin$_{C28P}$ was performed as described in Reiners et al.[42] The plasmid pNZ-SV-nisA$_{C28P}$ was co-transformed into the *pIL3-BTC*-containing *L. lactis* NZ9000 strain[43] by electroporation as described by Holo and Nes.[44] Briefly, electrocompetent *L. lactis* NZ9000 pIL3-BTC cells were incubated for 30 min on ice with the plasmid pNZ-SV-nisA$_{C28P}$. The cells were exposed to a pulse setting of 1 kV, 25 µF, 200 Ω, for 4.5–5.0 ms and afterwards incubated with 950 µl of M17 medium with 0.5% glucose (GM17) for 3 h at 30 °C. Then cells were plated on SGM17-agar plates (M17 agar, 0.5% glucose, 0.5 M sucrose) with the appropriate antibiotics (5 µg/ml Cm/Erm), and a single colony was used for expression.

The prenisin variant nisin$_{C28P}$ was expressed and purified as described in Alkhatib et al.[45] though the expression time was changed from 24 h to 6 h. After harvesting the cells, lactic acid was added to the supernatant to a final concentration of 50 mM, and it was filtered with 0.45 µm filters. A cation exchange chromatography was performed, and nisin$_{C28P}$ was eluted by adding a buffer containing 1 M NaCl. The prenisin variant was activated by cleavage with purified NisP at 8 °C overnight as described by Abts et al.[46] For this, the endopeptidase NisP was expressed in *L. lactis* NZ9000 cells and purified from the supernatant by an immobilized metal affinity chromatography (IMAC). The pure protein was desalted and stored at −80 °C. The concentration of the active nisin variant was determined by RP-HPLC,[46] using a water/acetonitrile gradient (from 10% to 64% acetonitrile) acidified with 0.1% TFA and Tricine-SDS-PAGE.[47] The activated nisin$_{C28P}$ was directly

used for further assays.

Nisin was purified as previously described[12] with a cation exchange chromatography similar to the nisin$_{C28P}$ purification. The concentration was measured with RP-HPLC as described above and in Abts et al.[46]

The modification status of nisin$_{C28P}$ was analyzed using MALDI-TOF MS analysis, which was performed with an UltrafleXtreme, Bruker Daltonics, Software: Compass 1.4 in positive mode.[31]

2.2. Cloning and purification of the NSR protein

Cloning of the *nsr* gene from *Streptococcus agalactiae* COH1 was done as previously described[35] to obtain the plasmids pNZ-SV-*Sa*NSR and pNZ-SV-*Sa*NSR$_{S236A}$ for studies with recombinant *L. lactis* cells, as well as the plasmid pET-28b-*Sa*NSR30-N8His and pET-28b-*Sa*NSR30$_{S236A}$-N8His accordingly to Khosa et al. (2015) and Khosa et al. (2016) for *in vitro* studies.[37,48]

The plasmids pNZ-SV-*Sa*NSR and pNZ-SV-*Sa*NSR$_{S236A}$ were transformed into electrocompetent *L. lactis* NZ9000 by electroporating[44] the cells, using a pulse setting of 1 kV, 25 µF, 200 Ω, for 4.5–5.0 ms. After pulsing, 950 µl GM17 medium was added, the cells were incubated for 3 h at 30 °C and finally plated on SMGG-agar plates containing 5 µg/ml erythromycin.

The plasmids pET-28b-*Sa*NSR30-N8His and pET-28b-*Sa*NSR30$_{S236A}$-N8His were transformed into chemocompetent *E. coli* BL21 (DE3) cells for expression *via* a heat shock for 60 s at 42 °C. Afterwards 950 µl LB medium was added and the cells were incubated for one hour at 37 °C.

Expression and purification of *Sa*NSR30-N8His and *Sa*NSR30$_{S236A}$-N8His was performed like described in Khosa et al.[48] Briefly, the expression was induced with 1 mM IPTG at an OD_{600} of 0.8–1.0 and grown at 18 °C with 160 rpm shaking overnight. After harvesting the cells and adding buffer containing 10% glycerol (50 mM TRIS, pH 8.0, 50 mM NaCl, 10% glycerol), the cells were disrupted with a homogenizer (Microfluidics) five times at 1.5 kbar. The cell suspension was centrifuged 45 min at 42,000 rpm, and the supernatant was loaded onto a HiTrap Chelating HP 5 ml column with immobilized nickel. The elution was performed with a 1–150 mM histidine gradient, and the concentrated protein fractions were further purified using a Superose 12 10/300 GL column for the size exclusion chromatography (SEC). The purified proteins were directly used for further assays since freezing of the protein resulted in a reduced activity. Further, the SEC buffer (25 mM MES, pH 6, 150 mM NaCl) was used for all *in vitro* assays unless stated otherwise.

2.3. Antimicrobial activity of nisin and nisin$_{C28P}$

The plasmids pNZ-SV-*Sa*NSR and pNZ-SV-*Sa*NSR$_{S236A}$ were transformed into *L. lactis* NZ9000 cells like described above. A plasmid named pNZ-SV-Erm, representing an empty vector, was also transformed into *L. lactis* NZ9000 and used as a control. In the following, these bacterial strains are referred to as NZ9000*Sa*NSR$_{S236A}$, NZ9000*Sa*NSR and NZ9000Erm. Growth inhibition assays with *L. lactis* NZ9000 pNZ-SV-Erm, *L. lactis* NZ9000 pNZ-SV-*Sa*NSR and *L. lactis* NZ9000 pNZ-SV-*Sa*NSR$_{S236A}$ were performed to determine the half maximal inhibitory concentration (IC_{50}) as previously described.[42] The nisin variant was diluted into a 96-well plate and the cells were added. After 5 h of incubation at 30 °C, the optical density was determined and the IC_{50} values were calculated. The fold of resistance was obtained based on the IC_{50} values according to Reiners et al.[42] There, the values from the NSR-expressing strains were compared to the values of the control strain (NZ9000Erm).

For the *in vitro* determination, the cleavage efficiency assay with freshly purified *Sa*NSR30-N8His, diluted in 25 mM MES, pH 6, 150 mM NaCl buffer was performed. The reaction was started by adding nisin or nisin$_{C28P}$, respectively.

The cleavage reaction was performed under varying conditions to obtain the best cleavage efficiency by *Sa*NSR30-N8His. The incubation time was varied from 5 to 30 min, the temperature from 20 °C to 40 °C. Further, the pH of the assay buffer was varied from 5.5 to 7.5.

For determination of the kinetics for the substrates nisin and nisin$_{C28P}$, the assay was performed for 10 min at 30 °C with 1 µM NSR30-N8His at pH 6 and 7.5, respectively.

The cleavage reaction was stopped by adding 0.2% trifluoroacetic acid (TFA) and analyzed by RP-HPLC as modified from Abts et al. (2013).[46] The measurement was performed with solvent A consisting of water/0.1% TFA (v/v) and solvent B acetonitrile/0.1% TFA (v/v). After the sample was injected into the LiChrospher RP-18 HPLC column (Merck), the elution was performed by a linear gradient over 60 min from 90% solvent A and 10% solvent B to 36% solvent A and 64% solvent B at a flow rate of 1 ml/min. The elution of the peptide was monitored by absorption at 205 nm. The cleavage efficiency of *Sa*NSR30-N8His was determined by integrating the peak of the cleaved last 6 amino acids.

Minimal inhibitory concentration (MIC) against nosocomial bacteria *S. aureus* ATCC 29213 and *E. faecalis* ATCC 29212 were determined according to the Clinical and Laboratory Standards Institute (CLSI) guidelines[49] in 96-well round bottom microtiter plates using Mueller Hinton broth. Briefly, precultured cells were seeded at a density of 5×10^4 colony forming units per well in a total volume of 100 µl containing twofold serial diluted compounds nisin or nisin$_{C28P}$, respectively. Protein buffer and Moxifloxacin were used as controls. Plates were incubated aerobically at 37 °C overnight. MIC values were determined macroscopically by identifying the concentration of tested compounds that led to complete inhibition of visual growth.

2.4. Pore formation of nisin and nisin$_{C28P}$

To visualize the pore formation mediated by nisin, the SYTOX green dye was used, which binds nucleic acid but is not membrane permeable.[37] The SYTOX Green Nucleic Acids Binding Assay was performed as described in Reiners et al.[37,42] We used *L. lactis* cells, with one of the described plasmids, at an OD_{600} of 0.3 and added 1 µM SYTOX dye. The fluorescence signal was measured at an excitation and emission wavelength of 504 and 523 nm, respectively. During the whole assay the cell suspension was stirred and heated at 30 °C. After reaching a stable baseline the nisin variant was added and the changing fluorescence intensity could be observed.

3. Results

3.1. Expression and purification of nisin$_{C28P}$

We were interested in the ability to characterize a nisin variant which I) still is highly active like wildtype nisin, II) is able to form pores, and III) most importantly is not recognized by the nisin resistance protein. A nisin variant lacking the last ring (ring E) already showed that any adjustment leads to the result that the NSR protein from *S. agalactiae* is not able to cleave off the last six amino acids.[37] However, also the replacement of cysteine by alanine caused a 13-fold reduced activity. Whereas the IC_{50} of wildtype nisin was determined to be 3.3 ± 0.1 nM, the nisin$_{C28A}$ variant displayed 42.2 ± 0.7 nM. Consequently, by introducing a proline residue, we designed a new variant termed nisin$_{C28P}$ which lacks the last lanthionine ring but still has a ring-like structure at this position.

The nisin variant nisin$_{C28P}$ was expressed in *L. lactis* NZ9000 containing a plasmid with the nisin modification and secretion system NisBTC as previously described for many other nisin variants.[31,37,50] We could express and purify nearly 6 mg nisin$_{C28P}$ per liter of cell culture similar to the yields described for wildtype prenisin expressed via the same procedure [31]. After purification *via* cation exchange chromatography, the prenisin leader peptide was cleaved by the purified leader peptidase NisP[31] resulting in active nisin$_{C28P}$ with a theoretical molecular weight of 3348 Da with eight dehydrations. The analysis of the

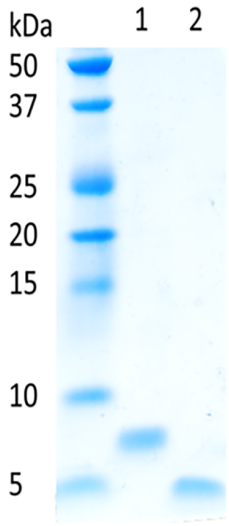

Fig. 2. Prenisin variant nisin$_{C28P}$ (1) and nisin variant nisin$_{C28P}$ (2) analyzed by a 16% Tricine-SDS gel with Precision Plus Protein Dual Xtra Standard (Bio-Rad) (left).

nisin variant with a 16% Tricine-SDS gel (Fig. 2) indicates the cleavage of the leader peptide with a mass difference of approximately 2 kDa. Since the peptidase NisP cleaves off the *N*-terminal leader sequence, no differences were observed in terms of cleavage efficiencies (92%) as determined by RP-HPLC analysis.

In addition, we tested the effect of the mutation on diffusion property *via* agar diffusion assay and could not detect a significant change for nisin$_{C28P}$ compared to wildtype nisin (data not shown).

The nisin$_{C28P}$ prenisin variant eluted between 18 and 21 min (Fig. 3a, blue trace). After cleavage the leader peptide eluted at 14–15 min (Fig. 3a, black trace) and the core peptide eluted between 22 and 24 min.

The nisin$_{C28P}$ core peptide is clearly visible and the concentration can be determined by peak integration using different insulin concentrations as a standard. We used the RP-HPLC measurements to analyze the purity and concentration of the nisin variant, however for further antimicrobial studies we used the total batch of nisin$_{C28P}$.

Furthermore, the nisin$_{C28P}$ core peptide was analyzed with MALDI-TOF MS to identify its modification status (Fig. 3b). Here, we observed that nisin$_{C28P}$ mainly exhibits 7–8 dehydrations as observed for wildtype nisin. Also, some nisin$_{C28P}$ species were present with nine dehydrations, which occurred due to the lack of the last lanthionine ring thereby allowing the dehydration of Ser29, which in the wildtype system is not possible due to sterical hindrance provoked by the lanthionine ring E (as previously described [51]).

3.2. Activity of nisin$_{C28P}$

The activity of nisin$_{C28P}$ was determined by IC$_{50}$ studies against three different recombinant strains derived from *L. lactis* NZ9000, which is intrinsically highly sensitive towards nisin. The NZ9000 strain was transformed with the empty pNZ-Erm vector control or with either the plasmid pNZ-*Sa*NSR or pNZ-*Sa*NSR$_{S236A}$, which, when induced, express the wildtype nisin resistance protein (*Sa*NSR) or an inactive variant (*Sa*NSR$_{S236A}$), respectively.[35] The only difference between the latter strains is therefore the presence or absence of an active *Sa*NSR protein.

The expression of both *Sa*NSR proteins was induced with a sublethal amount of nisin (0.3 nM), which has been shown to not interfere with the IC$_{50}$ determination.[37,42,45,52,53]

To determine the activity of nisin$_{C28P}$ against the NZ9000Erm, NZ9000*Sa*NSR and NZ9000*Sa*NSR$_{S236A}$ strains, cell growth was monitored at different nisin concentrations. From these experiments, growth inhibition of 50% of the cells was calculated, which is reflected in the IC$_{50}$ value.

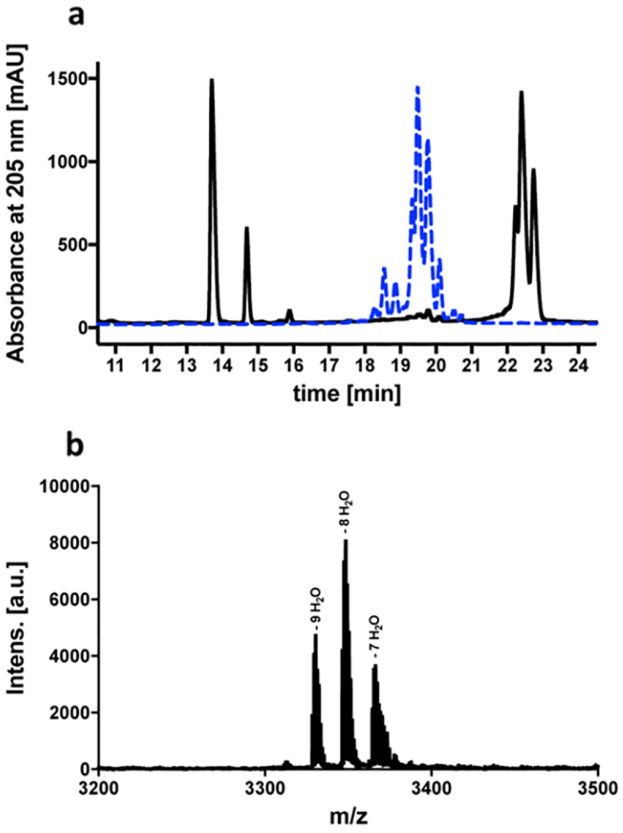

Fig. 3. RP-HPLC chromatogram and MALDI-TOF MS spectrum from nisin$_{C28P}$. RP-HPLC chromatogram of prenisin$_{C28P}$ (blue) and activated nisin variant nisin$_{C28P}$ (black) (a). MALDI-TOF spectrum from activated nisin$_{C28P}$ (b).

Nisin$_{C28P}$ was highly active as displayed by the IC$_{50}$ value against the NZ9000Erm strain of 5.5 ± 0.8 nM (Fig. 4 (black curve) and Table 1). This is comparable with the value obtained by wildtype nisin of 3.3 ± 0.1 nM. Against the *L. lactis* NZ9000*Sa*NSR (Fig. 4, green curve) and NZ9000*Sa*NSR$_{S236A}$ (Fig. 4, red curve) strains, an IC$_{50}$ value

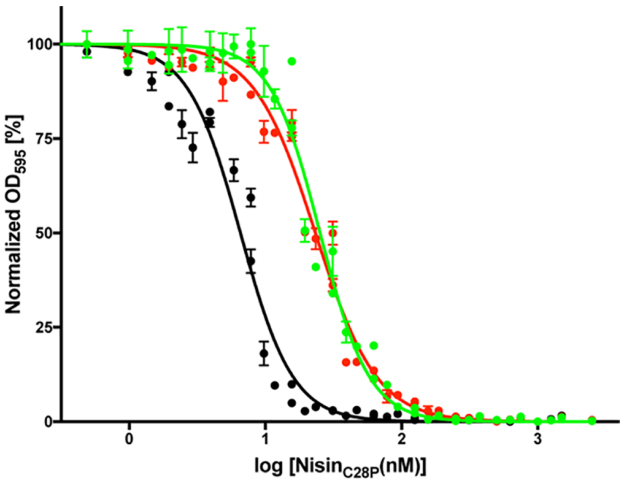

Fig. 4. Determination of the IC$_{50}$ values of nisin$_{C28P}$. The normalized measured OD$_{595}$ in percent against the logarithmic concentration of nisin$_{C28P}$. NZ9000Erm in black, NZ9000*Sa*NSR$_{S236A}$ in red and NZ9000*Sa*NSR in green.

Table 1
IC_{50} values of $nisin_{C28P}$ against NZ9000Erm, NZ9000*Sa*NSR, and NZ9000*Sa*NSR_{S236A} strains. By dividing the IC_{50} values of the NZ9000*Sa*NSR and NZ9000*Sa*NSR_{S236A} strains by the IC_{50} value obtained for the NZ9000Erm strain, the fold of resistance is obtained. *, Data for nisin taken from Khosa et al.[37]

	NZ9000Erm	NZ9000*Sa*NSR	NZ9000*Sa*NSR_{S236A}
IC_{50} $nisin_{C28P}$ [nM] (fold of resistance)	5.5 ± 0.8	22.5 ± 4.2 (3.5)	24.1 ± 2.3 (3.5)
IC_{50} nisin *[nM] (fold of resistance)	3.3 ± 0.1	66.4 ± 2.1 (20.1)	12.6 ± 0.7 (3.8)

Table 2
MIC values of nisin and $nisin_{C28P}$ against *S. aureus* ATCC 29213 and *E. faecalis* ATCC 29212. The MIC data are expressed as the mean (range) obtained from at least three independent repetitions for each strain.

	Nisin [μM]	$Nisin_{C28P}$ [μM]
S. aureus ATCC 29213	1.35 (0.937–1.875)	10.63 (9.375–12.5)
E. faecalis ATCC 29212	1.35 (0.937–1.875)	10.63 (9.375–12.5)

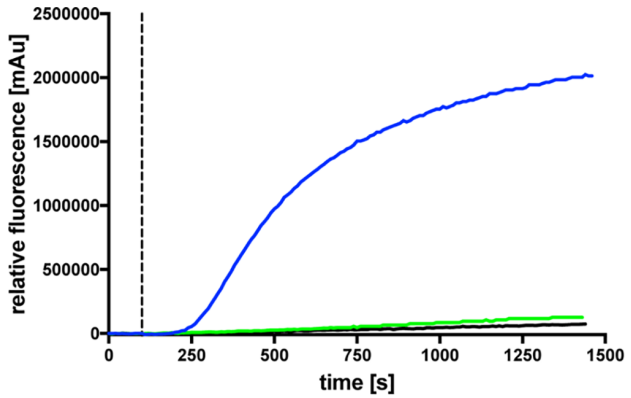

Fig. 5. Detection of pore formation. NZ9000*Sa*NSR strain with SYTOX green nucleic acid dye measured at 30 °C. Buffer (black), 30 nM nisin (green) and 30 nM $nisin_{C28P}$ (blue) added after 100 s (dashed line), respectively.

of 22.5 ± 4.2 nM and 24.1 ± 2.3 nM was determined, respectively.

These IC_{50} values indicate that *Sa*NSR *in vivo* does not properly cleave $nisin_{C28P}$; as a consequence, no resistance against $nisin_{C28P}$ is observed compared to *Sa*NSR_{S236A}. Wildtype nisin displays an IC_{50} value of 66.4 ± 2.1 nM against the NZ9000*Sa*NSR and 12.6 ± 0.7 nM against NZ9000*Sa*NSR_{S236A}.[37]

The fold of resistance values of wildtype nisin against the strains NZ9000*Sa*NSR_{S236A} and NZ9000*Sa*NSR were determined previously.[37] For the *L. lactis* strain NZ9000*Sa*NSR, a fold of resistance of 20 can be observed whereas for the *Sa*NSR_{S236A} mutant, unable to cleave nisin, the value for the fold of resistance is 3.8. Regarding the nisin derivate $nisin_{C28P}$, the fold of resistance value was determined to be 3.5 for both strains, the NZ9000*Sa*NSR and the mutant NZ9000*Sa*NSR_{S236A}, respectively (Table 1).

In addition the minimal inhibitory concentration (MIC) of nisin and $nisin_{C28P}$ were determined, according to the CLSI guidelines, against the nosocomial strains *S. aureus* and *E. faecalis* (Table 2). Wildtype nisin showed the same inhibitory activity (1.35 μM) against *S. aureus* and *E. faecalis* with a range of 0.937–1.875 μM. The assays with $nisin_{C28P}$ resulted in a MIC value of 10.63 μM (range from 9.375 μM to 12.5 μM) for *S. aureus* and *E. faecalis*, respectively, which is 7.8-fold decreased compared to wildtype.

3.3. Pore formation of the $nisin_{C28P}$ variant

Nisin is able to form pores in the membrane of Gram-positive bacteria by binding to lipid II and reorientation of the C-terminal part into the membrane.[21] This leads to membrane leakage, thus pore formation can be monitored using the SYTOX green nucleic acid dye.[54] If pores are formed, the dye is able to bind to the DNA and the fluorescence signal is increased. Since this is a rapid process, pore formation can be monitored in real time using fluorescence. We determined the pore formation capability of the nisin variant $nisin_{C28P}$ against the NZ9000*Sa*NSR strain.

The relative fluorescence is plotted against time and shown for different assay set ups (Fig. 5). First, the fluorescence is monitored until a stable baseline is reached (here 100 s) before $nisin_{C28P}$ was added, which is marked by the dashed line. We monitored the influence of 30 nM $nisin_{C28P}$ on the NZ9000*Sa*NSR strains (blue line). Here, it can be observed that the fluorescence highly increases after adding $nisin_{C28P}$, indicating that $nisin_{C28P}$ is able to form pores. This shows that *Sa*NSR is

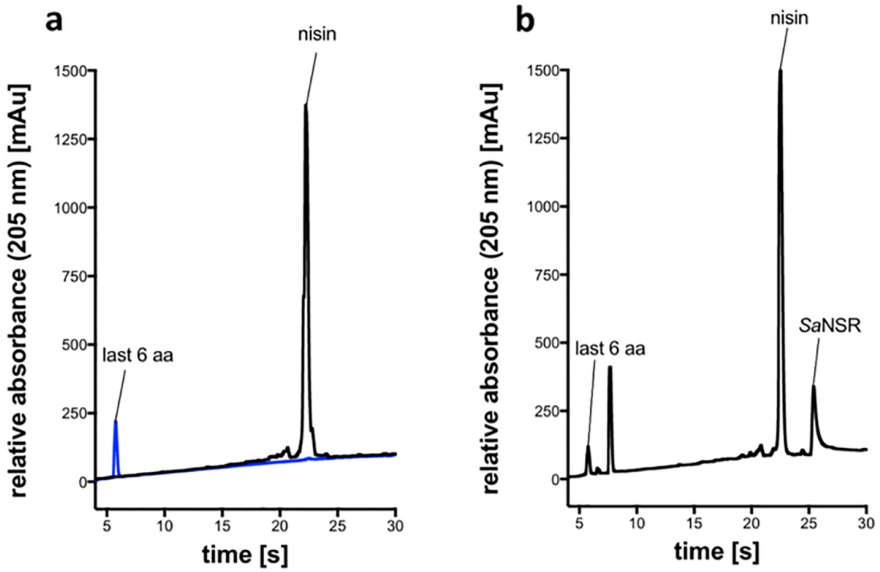

Fig. 6. Detection of nisin cleavage by *Sa*NSR. Analysis of *in vitro* samples *via* RP-HPLC. a) Relative absorbance spectrum of synthetic last 6 amino acids (blue) and pure nisin (black). b) spectrum of performed cleavage efficiency assay with *Sa*NSR and nisin in 1:10 ratio.

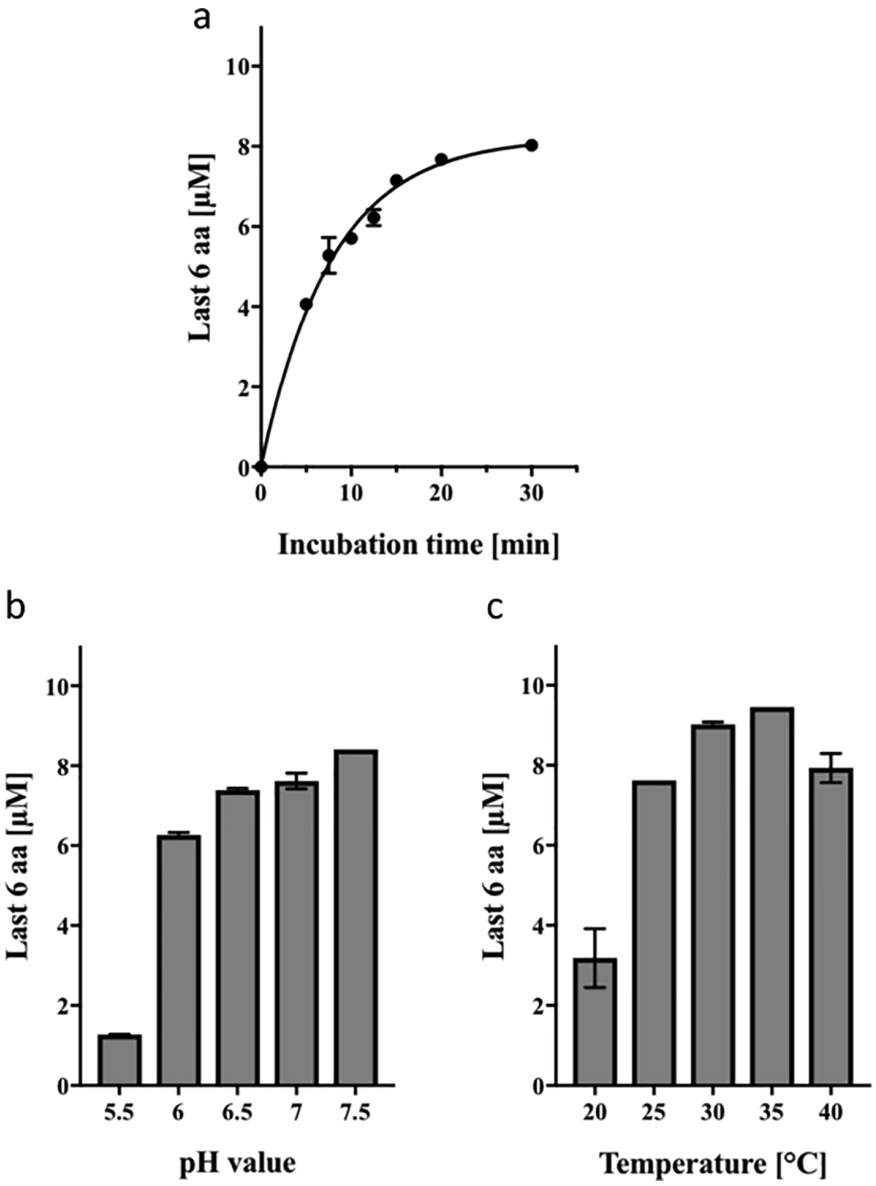

Fig. 7. In vitro characterization of *Sa*NSR. The amount of cleaved off last 6 amino acids of nisin is shown against different conditions. a) Varied incubation times between 5 and 30 min. b) Cleavage efficiency at different pH values from 5.5 to 7.5. c) Effect of different temperatures from 25 to 40 °C on cleavage efficiency (values were determined by at least three independent experiments).

not able to confer resistance and that nisin$_{C28P}$ bypasses the *Sa*NSR protein.

As a control, the assay was performed with buffer to ensure the buffer conditions did not influence the integrity of the *L. lactis* cells (Fig. 5, black line). No increase in fluorescence intensity was observed, indicating that no cells were permeabilized. Additionally, we checked for pore formation by adding 30 nM nisin, which is indicated by the green line. Since *Sa*NSR is able to confer resistance against nisin up to 60–70 nM, no pore formation was observed as previously reported.[55] Importantly, we used the same culture for these experiments so that the expression level of *Sa*NSR was the same, ensuring comparability of the experiments (see Section 2).

3.4. In vitro characterization of SaNSR30

Since we have observed that *Sa*NSR was not able to confer resistance against nisin$_{C28P}$ in recombinant *L. lactis*, we were wondering whether the cleavage of nisin$_{C28P}$ was inhibited and therefore tested *Sa*NSR's *in vitro* activity. To characterize the *Sa*NSR protein of *S. agalactiae,* it was heterologously expressed in *Escherichia coli* and purified *via* an *N*-terminal His-Tag using an immobilized ion metal affinity chromatography (IMAC) column followed by a size exclusion chromatography (SEC).[48] To monitor the cleavage efficiency of the purified protein towards nisin, an *in vitro* assay was performed and analyzed *via* RP-HPLC. Fig. 6 shows a representative chromatogram of the cleavage efficiency experiment.

A synthetic peptide composed of the C-terminal last 6 amino acids of nisin (Fig. 6a, blue spectrum) leads to an elution peak at 6 min, whereas the full-length nisin elutes as a broad peak at 22–23 min (Fig. 6a, black spectrum). The cleavage experiment shows a peak for the *Sa*NSR protein (26 min) as well as for nisin (22–23 min) and the C-terminally cleaved off 6 aa-peptide (6 min) (Fig. 6b). Additionally, two peaks with retention times of 7 and 8 min were detected in the chromatogram (Fig. 6b), those peaks were analyzed via mass spectrometry but could

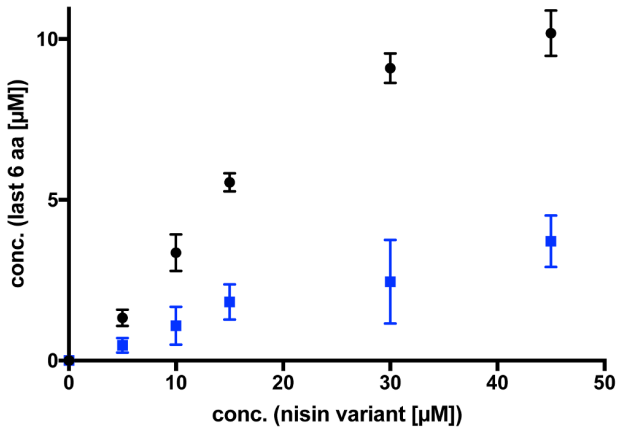

Fig. 8. *Sa*NSR cleavage of nisin and nisin$_{C28P}$. The cleaved off last six amino acids against the used amount of nisin (black) and nisin$_{C28P}$ (blue), respectively.

not be related to our protein or nisin, likely those peaks result from buffer conditions. The amount of the C-terminally cleaved off 6 aa-peptide of nisin was determined by integrating the peak and calculated based on a calibration with insulin.[46]

To establish the cleavage efficiency assay of *Sa*NSR, different conditions were tested. For all assays a protein-to-substrate ratio of 1:10 was used. The cleavage efficiency, indicated by the measured concentration of the cleaved off last 6 amino acids, was plotted against varying incubation times (pH 6, 30 °C) (Fig. 7a). There, the efficiency shows linearity between 10 and 15 min. Thus, for further studies an incubation time of 10 min was chosen to optimize the validity of the measurements. Next, the pH-dependency of nisin-cleavage by *Sa*NSR was investigated (Fig. 7b), using pH values from 5.5 to 7.5 at 30 °C with a 1:10 *Sa*NSR to nisin ratio. The optimal pH value for nisin cleavage seems to be 7.5. Higher pH values were not tested because nisin is unstable at basic pH. Instead of the optimal pH value of 7.5, the following assays were performed at pH 6 due to stability reasons of the substrate. Furthermore, different assay temperatures were tested to find the optimal temperature for the cleavage efficiency (1:10 ration, 30 °C, pH 6) (Fig. 7c). The temperature with the highest *Sa*NSR cleavage efficiency was found to be at 35 °C. The assays performed at 30 °C showed a similar cleavage efficiency. Due to protein stability (*Sa*NSR) the following assays were performed at 30 °C.

Considering these parameters, the cleavage of nisin and nisin$_{C28P}$ at different concentrations was examined. Fig. 8 shows an almost linear increase of cleaved product correlating with the amount of nisin variant. For nisin the highest detected amount of cleaved product is 10 µM (Fig. 8, black dots), for nisin$_{C28P}$ only an amount of 3 µM can be monitored (Fig. 8, blue squares). Further, it can be observed that the slope of the nisin assay is 3 times higher than the one of the nisin$_{C28P}$ assay.

4. Discussion

Antibiotics are essential for the prevention, control and treatment of infectious diseases in humans and animals. However, antibiotic resistance has increased drastically, so that it became crucial to find alternatives.[56] One alternative could be the treatment with lantibiotics, which exhibit antimicrobial activity against different human pathogenic bacteria.[57] Nevertheless, some human pathogens are resistant against lantibiotics, such as *Streptococcus agalactiae*, which expresses two resistance proteins. One is the BceAB-type transporter NsrFP[58] and the other is the nisin resistance protein NSR.[35]

We focused on a rational approach to design a nisin variant which bypasses the latter resistance protein.

The growth inhibition studies with the nisin variant nisin$_{C28P}$ revealed an IC$_{50}$ of 22.5 nM for the NZ9000*Sa*NSR strain, which is almost similar to the IC$_{50}$ value for the mutant NZ9000*Sa*NSR$_{S236A}$ (24.1 nM) (Fig. 4, Table 1).

In comparison to the values for nisin from Khosa et al.[55] (Table 1), the nisin$_{C28P}$ fold of resistance of NZ9000*Sa*NSR as well as of NZ9000*Sa*NSR$_{S236A}$ against the sensitive strain are similar to the nisin fold of resistance of the NZ9000*Sa*NSR$_{S236A}$. Considering that the *Sa*NSR$_{S236A}$ mutant is able to bind nisin but not to cleave off the last six amino acids, it is suggested that *Sa*NSR is also still able to bind the nisin variant *in vivo* but is not able to cleave it. This fits to the molecular dynamic studies which showed the interactions between the catalytic domain in *Sa*NSR and the rings D and E of nisin.[37]

The determination of the minimal inhibitory concentration (MIC) for nisin$_{C28P}$ revealed in a 7.8-fold decreased antimicrobial activity when compared to nisin for both tested strains, *S.aureus* and *E. faecalis* (Table 2).

The nosocomial strain *S. aureus* was found to hold a gene encoding for the BceAB-type transporter VraDE.[59] Besides bacitracin this transporter confers resistance against nisin A.[59,60] One could conclude that the variant nisin$_{C28P}$ is a more efficient identified substrate of VraDE, which would explain the decreased MIC value compared to nisin. Additional to the ABC transporter a small transmembrane protein VraH of *S. aureus* forms a complex with VraD, in the presence of VraE.[60]

The resistance against nisin and bacitracin appears to be independent of VraH, however, gallidermin resistance is based on VraH.[60] As gallidermin and nisin have a structural similar *N*-terminus and only differ at the C-terminal part, it is very likely that nisin$_{C28P}$, with the mutation at the C-terminus, is recognized by the transmembrane protein VraH, whereas wildtype nisin remains unaffected, which would result in a higher MIC value for the nisin variant.

Similar MIC results were obtained for *E. faecalis*, which is bacitracin resistant due to the BcrAB-type transporter BcrAB.[61,62] Till date not

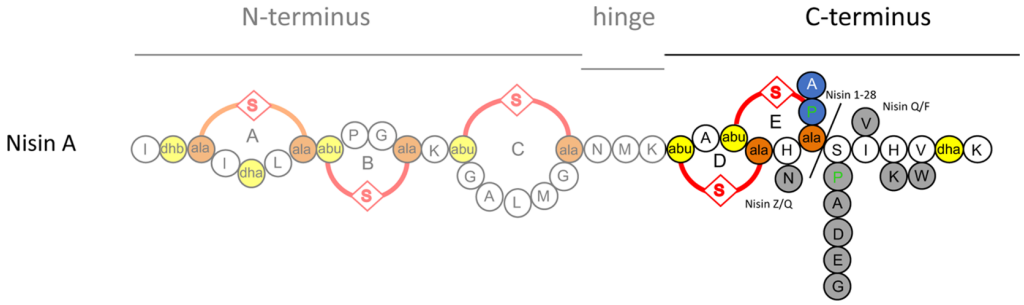

Fig. 9. Schematic view of nisin A with C-terminal variants and mutations. Highlighted view of the C-terminus of nisin A with natural variants and single mutations (grey) as well as ring disrupting mutations (blue). Mutations which result in a diminished *Sa*NSR resistance are highlighted as green letters. The (methyl-)lanthionine rings, formed by a cysteine residue side chain and a dehydrated amino acid residue are highlighted in orange and yellow (rings A, B, C, D and E) (41, 42, 45, 65–69).

much is known about this type of resistance ABC-transporters,[63] nevertheless for bacteriocin resistance associated transporters it is common, that they confer resistance against several bacteriocins.[34,58] Supposable the BcrAB transporter of *E. faecalis* confers resistance against nisin and, in a greater extent, to the nisin variant investigated in this study. Former studies also reported a nisinase activity connected to *E. faecalis*, which is supposed to reduce the C-terminal dehydroalanyllysine of nisin.[34,64] This part of nisin could be more accessible for the enzyme in nisin$_{C28P}$ due to the smaller ring-like structure at the C-terminus.

Summarized for both investigated nosocomial strains knock-out mutants for every potential target protein must be examined to elucidate the reason for different antimicrobial effectiveness of nisin$_{C28P}$ compared to nisin. However, the nisin variant is active against *S. aureus* and *E, faecalis*, although 7.8-fold decreased, leading to the assumption that the modification of the last ring in nisin conserves the overall antimicrobial activity but specifically influences the recognition by *Sa*NSR.

Further, we demonstrated that the nisin variant nisin$_{C28P}$ is still able to form pores in the *L. lactis* cells, even at concentrations (30 nM) were nisin does not affect the *Sa*NSR-expressing cells. In addition, we observed that the increase of fluorescence intensity appears with a delay of about 100 s after addition of nisin$_{C28P}$, indicating that pore formation starts slowly. This result is in line with studies showing that the rings D and E of nisin are, together with the hinge region, responsible for the flipping inside the membrane to form the pores.[21]

The nisin cleavage assay showed a decreased efficiency by *Sa*NSR to cleave the variant nisin$_{C28P}$ compared to nisin (Fig. 8). This cleavage is likely possible since this nisin variant is still able to bind to the *Sa*NSR protein. Although ring E is a major determinant for stable *Sa*NSR binding and cleavage the proline in this variant will allow more flexibility within the binding site, thereby adopting slightly different orientations. Since the exact orientation is needed for cleavage this will ultimately result in less cleavage efficiency.

Previous nisin variant studies showed diverse outcomes of mutations at the C-terminus. On the one hand, mutations of ring E, where the last cysteine residue was substituted by an alanine, resulted in a lack of the last ring E. This led to a clear drop of the activity compared to the wildtype nisin A.[42,45] On the other hand, a mutation within the last ring E from Asn27 to Lys resulted in no change of the activity of nisin.[65] Latter is comparable to the natural nisin variants A and Z, which differ in the position 27 with a histidine residue and an asparagine residue, respectively, and have similar activities as well.[66,67]

The natural variant nisin Q also possesses an asparagine residue at position 27, like nisin Z, and additionally the isoleucine at position 30 is substituted by a valine residue, which leads to a drop of the activity against *L. lactis* cells.[67] Surprisingly, nisin F, another natural nisin variant which differs to nisin A only in position 30 with a valine residue similar to nisin Q, has an activity against *L. lactis* similar to nisin A[67] (Fig. 9).

Previous studies showed that mutations in Ser29, the amino acid directly after ring E, result in activities against *L. lactis* strains that are comparable to nisin A wildtype.[41,68] Interestingly, the substitution of this serine by a proline led to an increased activity of the lantibiotic against the nisin resistance protein NSR.[41] Contradictory, further mutations within the last 6 amino acids after ring E, like His31 and Val32, and the complete deletion of these last 6 amino acids of nisin caused diminished antibacterial activity[42,45,65,69] (Fig. 9).

Comparing those previous results, the only known mutations leading to a decreased resistance of the NSR protein against a nisin variant are the Ser29Pro mutations by Field et al.[41] and the results of the nisin$_{C28P}$ variant depicted here (Fig. 9, green letters).

This study presents a highly potent, pore forming nisin variant as an alternative lantibiotic to bypass the nisin resistance protein of *S. agalactiae*. We showed that *Sa*NSR indeed displayed a decreased cleavage efficiency *in vitro* but conferred no resistance against nisin$_{C28P}$ *in vivo*. Compared to the *Sa*NSR mutant and the previous data for nisin, it can be assumed that *Sa*NSR is still able to bind nisin$_{C28P}$ *in vivo*, which however revealed in low IC_{50} values. In summary, we detected a lantibiotic with a three times higher activity against *Sa*NSR-expressing *L. lactis* cells than nisin.

Funding

This work has been funded by the Deutsche Forschungsgemeinschaft (DFG, German Research Foundation) – Project number 270650915 (Research Training Group GRK2158, TP4a to S.S. and TP2a to R.K.).

Acknowledgments

We thank all members of the Institute of Biochemistry for fruitful discussions. J.Z.-K. and S.S. would like to thank Peter Proksch for his enthusiasm as well as continuous interest in our project.

Appendix A. Supplementary data

Supplementary data to this article can be found online at https://doi.org/10.1016/j.bmc.2019.06.031.

References

1. Sahl HG, Bierbaum G. Lantibiotics: biosynthesis and biological activities of uniquely modified peptides from gram-positive bacteria. *Annu Rev Microbiol.* 1998;52:41–79.
2. Klaenhammer TR. Genetics of bacteriocins produced by lactic acid bacteria. *FEMS Microbiol Rev.* 1993;12(1–3):39–85.
3. Chatterjee C, Paul M, Xie L, van der Donk WA. Biosynthesis and mode of action of lantibiotics. *Chem Rev.* 2005;105(2):633–684.
4. Lagedroste M, Smits SHJ, Schmitt L. Substrate specificity of the secreted nisin leader peptidase NisP. *Biochem.* 2017;56(30):4005–4014.
5. Montalban-Lopez M, Deng J, van Heel AJ, Kuipers OP. Specificity and application of the lantibiotic protease NisP. *Front Microbiol.* 2018;9:160.
6. van Heel AJ, de Jong A, Song C, Viel JH, Kok J, Kuipers OP. BAGEL4: a user-friendly web server to thoroughly mine RiPPs and bacteriocins. *Nucleic Acids Res.* 2018;46(W1):W278–W281.
7. Birri DJ, Brede DA, Nes IF. Salivaricin D, a novel intrinsically trypsin-resistant lantibiotic from *Streptococcus salivarius* 5M6c isolated from a healthy infant. *Appl Environ Microbiol.* 2012;78(2):402–410.
8. Draper LA, Cotter PD, Hill C, Ross RP. The two peptide lantibiotic lacticin 3147 acts synergistically with polymyxin to inhibit Gram negative bacteria. *BMC Microbiol.* 2013;13:212.
9. Brotz H, Bierbaum G, Leopold K, Reynolds PE, Sahl HG. The lantibiotic mersacidin inhibits peptidoglycan synthesis by targeting lipid II. *Antimicrob Agents Chemother.* 1998;42(1):154–160.
10. Ghobrial OG, Derendorf H, Hillman JD. Pharmacodynamic activity of the lantibiotic MU1140. *Int J Antimicrob Agents.* 2009;33(1):70–74.
11. Xin B, Zheng J, Liu H, et al. Thusin, a novel two-component lantibiotic with potent antimicrobial activity against several Gram-positive pathogens. *Front Microbiol.* 2016;7:1115.
12. Abts A, Mavaro A, Stindt J, et al. Easy and rapid purification of highly active nisin. *Int J Pept.* 2011;2011:175145.
13. Cotter PD. Bioengineering: a bacteriocin perspective.F54. *Bioengineered.* 2012;3(6):313–319.
14. Knerr PJ, van der Donk WA. Discovery, biosynthesis, and engineering of lantipeptides. *Annu Rev Biochem.* 2012;81:479–505.
15. Dawson MJ, Scott RW. New horizons for host defense peptides and lantibiotics. *Curr Opin Pharmacol.* 2012;12(5):545–550.
16. Sandiford SK. Current developments in lantibiotic discovery for treating *Clostridium difficile* infection. *Expert Opin Drug Discov.* 2019;14(1):71–79.
17. Ongey EL, Yassi H, Pflugmacher S, Neubauer P. Pharmacological and pharmacokinetic properties of lanthipeptides undergoing clinical studies. *Biotechnol Lett.* 2017;39(4):473–482.
18. Dischinger J, Chipalu SB, Bierbaum G. Lantibiotics: promising candidates for future applications in health care. *Int J Med Microbiol.* 2014;304(1):51–62.
19. Mota-Meira M, Lapointe G, Lacroix C, Lavoie MC. MICs of mutacin B-Ny266, nisin A, vancomycin, and oxacillin against bacterial pathogens. *Antimicrob Agents Chemother.* 2000;44(1):24–29.
20. Brötz H, Josten M, Wiedemann I, et al. Role of lipid-bound peptidoglycan precursors in the formation of pores by nisin, epidermin and other lantibiotics. *Mol Microbiol.* 1998;30(2):317–327.
21. Hasper HE, de Kruijff B, Breukink E. Assembly and stability of nisin-lipid II pores. *Biochem.* 2004;43(36):11567–11575.
22. Hasper HE, Kramer NE, Smith JL, et al. An alternative bactericidal mechanism of action for lantibiotic peptides that target lipid II. *Science.* 2006;313(5793):1636–1637.

23. Roy U, Islam MR, Nagao J, et al. Bactericidal activity of nukacin ISK-1: an alternative mode of action. *Biosci Biotechnol Biochem.* 2014;78(7):1270–1273.
24. Rogers LA. The inhibiting effect of *Streptococcus lactis* on *Lactobacillus bulgaricus*. *J Bacteriol.* 1928;16(5):321–325.
25. Rogers LA, Whittier EO. Limiting factors in the lactic fermentation. *J Bacteriol.* 1928;16(4):211–229.
26. Wirawan RE, Klesse NA, Jack RW, Tagg JR. Molecular and genetic characterization of a novel nisin variant produced by *Streptococcus uberis*. *Appl Environ Microbiol.* 2006;72(2):1148–1156.
27. Delves-Broughton J, Blackburn P, Evans RJ, Hugenholtz J. Applications of the bacteriocin, nisin. *Antonie Van Leeuwenhoek.* 1996;69(2):193–202.
28. Breukink E, Wiedemann I, van Kraaij C, Kuipers OP, Sahl HG, de Kruijff B. Use of the cell wall precursor lipid II by a pore-forming peptide antibiotic. *Science.* 1999;286(5448):2361–2364.
29. Medeiros-Silva J, Jekhmane S, Paioni AL, et al. High-resolution NMR studies of antibiotics in cellular membranes. *Nat Commun.* 2018;9(1):3963.
30. Breukink E, van Heusden HE, Vollmerhaus PJ, et al. Lipid II is an intrinsic component of the pore induced by nisin in bacterial membranes. *J Biol Chem.* 2003;278(22):19898–19903.
31. Lagedroste M, Reiners J, Smits SHJ, Schmitt L. Systematic characterization of position one variants within the lantibiotic nisin. *Sci Rep.* 2019;9(1):935.
32. Li Q, Montalban-Lopez M, Kuipers OP. Increasing the antimicrobial activity of nisin-based lantibiotics against Gram-negative pathogens. *Appl Environ Microbiol.* 2018;84(12).
33. Zhou L, van Heel AJ, Montalban-Lopez M, Kuipers OP. Potentiating the activity of nisin against *Escherichia coli*. *Front Cell Dev Biol.* 2016;4:7.
34. Draper LA, Cotter PD, Hill C, Ross RP. Lantibiotic resistance. *Microbiol Mol Bio Rev.* 2015;79(2):171–191.
35. Khosa S, Alkhatib Z, Smits SH. NSR from *Streptococcus agalactiae* confers resistance against nisin and is encoded by a conserved nsr operon. *J Biol Chem.* 2013;394(11):1543–1549.
36. Froseth BR, McKay LL. Molecular characterization of the nisin resistance region of *Lactococcus lactis subsp. lactis* biovar diacetylactis DRC3. *Appl Environ Microbiol.* 1991;57(3):804–811.
37. Khosa S, Frieg B, Mulnaes D, et al. Structural basis of lantibiotic recognition by the nisin resistance protein from *Streptococcus agalactiae*. *Sci Rep.* 2016;6:18679.
38. Kuipers OP, Beerthuyzen MM, Siezen RJ, De Vos WM. Characterization of the nisin gene cluster nisABTCIPR of *Lactococcus lactis*. Requirement of expression of the nisA and nisI genes for development of immunity. *Eur J Biochem.* 1993;216(1):281–291.
39. Siegers K, Entian KD. Genes involved in immunity to the lantibiotic nisin produced by *Lactococcus lactis* 6F3. *Appl Environ Microbiol.* 1995;61(3):1082–1089.
40. Sun Z, Zhong J, Liang X, Liu J, Chen X, Huan L. Novel mechanism for nisin resistance via proteolytic degradation of nisin by the nisin resistance protein NSR. *Antimicrob Agents Chemother.* 2009;53(5):1964–1973.
41. Field D, Blake T, Mathur H, et al. Bioengineering nisin to overcome the nisin resistance protein. *Mol Microbiol.* 2018.
42. Reiners J, Lagedroste M, Ehlen K, Leusch S, Zaschke-Kriesche J, Smits SHJ. The N-terminal region of nisin is important for the BceAB-Type ABC transporter NsrFP from *Streptococcus agalactiae* COH1. *Front Microbiol.* 2017;8:1643.
43. Rink R, Kuipers A, de Boef E, et al. Lantibiotic structures as guidelines for the design of peptides that can be modified by lantibiotic enzymes. *Biochem.* 2005;44(24):8873–8882.
44. Holo H, Nes IF. High-Frequency Transformation, by electroporation, of *Lactococcus lactis subsp. cremoris* grown with glycine in osmotically stabilized media. *Appl Environ Microbiol.* 1989;55(12):3119–3123.
45. AlKhatib Z, Lagedroste M, Zaschke J, et al. The C-terminus of nisin is important for the ABC transporter NisFEG to confer immunity in *Lactococcus lactis*. *MicrobiologyOpen.* 2014;3(5):752–763.
46. Abts A, Montalban-Lopez M, Kuipers OP, Smits SH, Schmitt L. NisC binds the FxLx motif of the nisin leader peptide. *Biochem.* 2013;52(32):5387–5395.
47. Tricine-SDS-PAGE Schägger H. *Nat Protoc.* 2006;1(1):16–22.
48. Khosa S, Hoeppner A, Kleinschrodt D, Smits SH. Overexpression, purification, crystallization and preliminary X-ray diffraction of the nisin resistance protein from *Streptococcus agalactiae*. *Acta Crystallogr F Struct Biol Commun.* 2015;71(Pt 6):671–675.
49. CLSI. *Methods for Dilution Antimicrobial Susceptibility Tests for Bacteria That Grow Aerobically: Approved Standard.* CLSI; 2012:9.
50. Khusainov R, Kuipers OP. The presence of modifiable residues in the core peptide part of precursor nisin is not crucial for precursor nisin interactions with NisB- and NisC. *PLoS ONE.* 2013;8(9):e74890.
51. Lubelski J, Khusainov R, Kuipers OP. Directionality and coordination of dehydration and ring formation during biosynthesis of the lantibiotic nisin. *J Biol Chem.* 2009;284(38):25962–25972.
52. Plat A, Kluskens LD, Kuipers A, Rink R, Moll GN. Requirements of the engineered leader peptide of nisin for inducing modification, export, and cleavage. *Appl Environ Microbiol.* 2011;77(2):604–611.
53. Kuipers A, de Boef E, Rink R, et al. NisT, the transporter of the lantibiotic nisin, can transport fully modified, dehydrated, and unmodified prenisin and fusions of the leader peptide with non-lantibiotic peptides. *J Biol Chem.* 2004;279(21):22176–22182.
54. Roth BL, Poot M, Yue ST, Millard PJ. Bacterial viability and antibiotic susceptibility testing with SYTOX green nucleic acid stain. *Appl Environ Microbiol.* 1997;63(6):2421–2431.
55. Khosa S, Lagedroste M, Smits SH. Protein Defense Systems against the Lantibiotic Nisin: Function of the Immunity Protein NisI and the Resistance Protein NSR. *Front Microbiol.* 2016;7:504.
56. Cheng G, Hao H, Xie S, et al. Antibiotic alternatives: the substitution of antibiotics in animal husbandry? *Front Microbiol.* 2014;5:217.
57. Piper C, Cotter PD, Ross RP, Hill C. Discovery of medically significant lantibiotics. *Curr Drug Discov Technol.* 2009;6(1):1–18.
58. Clemens R, Zaschke-Kriesche J, Khosa S, Smits SHJ. Insight into Two ABC Transporter Families Involved in Lantibiotic Resistance. *Front Mol Biosci.* 2017;4:91.
59. Hiron A, Falord M, Valle J, Debarbouille M, Msadek T. Bacitracin and nisin resistance in *Staphylococcus aureus*: a novel pathway involving the BraS/BraR two-component system (SA2417/SA2418) and both the BraD/BraE and VraD/VraE ABC transporters. *Mol Microbiol.* 2011;81(3):602–622.
60. Popella P, Krauss S, Ebner P, Nega M, Deibert J, Gotz F. VraH Is the Third Component of the *Staphylococcus aureus* VraDEH System Involved in Gallidermin and Daptomycin Resistance and Pathogenicity. *Antimicrob Agents Chemother.* 2016;60(4):2391–2401.
61. Manson JM, Keis S, Smith JM, Cook GM. Acquired bacitracin resistance in *Enterococcus faecalis* is mediated by an ABC transporter and a novel regulatory protein. *BcrR Antimicrob Agents Chemother.* 2004;48(10):3743–3748.
62. Fang C, Stiegeler E, Cook GM, Mascher T, Gebhard S. *Bacillus subtilis* as a platform for molecular characterisation of regulatory mechanisms of *Enterococcus faecalis* resistance against cell wall antibiotics. *PLoS ONE.* 2014;9(3):e93169.
63. Gebhard S. ABC transporters of antimicrobial peptides in Firmicutes bacteria-phylogeny, function and regulation. *Mol Microb.* 2012;86(6):1295–1317.
64. Jarvis B. Enzymic reduction of the C-terminal dehydroalanyl-lysine sequence in nisin. *Biochem J.* 1970;119(5):56P.
65. Rollema HS, Kuipers OP, Both P, de Vos WM, Siezen RJ. Improvement of solubility and stability of the antimicrobial peptide nisin by protein engineering. *Appl Environ Microbiol.* 1995;61(8):2873–2878.
66. de Vos WM, Mulders JW, Siezen RJ, Hugenholtz J, Kuipers OP. Properties of nisin Z and distribution of its gene, nisZ. *Lactococcus lactis Appl Environ Microbiol.* Jan 1993;59(1):213–218.
67. Piper C, Hill C, Cotter PD, Ross RP. Bioengineering of a Nisin A-producing *Lactococcus lactis* to create isogenic strains producing the natural variants Nisin F. *Q and Z Microb Biotechnol.* 2011;4(3):375–382.
68. Field D, Begley M, O'Connor PM, et al. Bioengineered nisin A derivatives with enhanced activity against both Gram positive and Gram negative pathogens. *PLoS ONE.* 2012;7(10):e46884.
69. Breukink E, van Kraaij C, van Dalen A, et al. The orientation of nisin in membranes. *J Biochem.* 1998;37(22):8153–8162.

3.7 Chapter VII

Title: Influence of nisin hinge-region variants on lantibiotic immunity and resistance proteins

Authors: Julia Zaschke-Kriesche, **Jens Reiners**, Marcel Lagedroste, Sander H.J. Smits

Published in: Bioorganic & Medicinal Chemistry (2019)
Impact factor: 2.59

Own proportion of this work: 35%

- Cloning of the nisin A variants
- Purification of the pre-nisin A variants
- Performing biological and biochemical assays
- HPLC & MS data analysis
- Writing the manuscript

Bioorganic & Medicinal Chemistry 27 (2019) 3947–3953

Contents lists available at ScienceDirect

Bioorganic & Medicinal Chemistry

journal homepage: www.elsevier.com/locate/bmc

Influence of nisin hinge-region variants on lantibiotic immunity and resistance proteins

Julia Zaschke-Kriesche, Jens Reiners, Marcel Lagedroste, Sander H.J. Smits*

Institute of Biochemistry, Heinrich-Heine-University Duesseldorf, Universitaetsstrasse 1, 40225 Duesseldorf, Germany

ARTICLE INFO

Keywords:
Lantibiotic
Nisin immunity
Nisin resistance protein
Antimicrobial activity

ABSTRACT

The rising existence of antimicrobial resistance, confirms the urgent need for new antimicrobial compounds. Lantibiotics are active in a low nanomolar range and represent good compound candidates. The lantibiotic nisin is well studied, thus it is a perfect origin for exploring novel lantibiotics via mutagenesis studies. However, some human pathogens like *Streptococcus agalactiae COH1* already express resistance proteins against lantibiotics like nisin.

This study presents three nisin variants with mutations in the hinge-region and determine their influence on both the growth inhibition as well as the pore-forming activity. Furthermore, we analyzed the effect of these mutants on the nisin immunity proteins NisI and NisFEG from *Lactococcus lactis,* as well as the nisin resistance proteins *Sa*NSR and *Sa*NsrFP from *Streptococcus agalactiae COH1*.

We identified the nisin variant $_{20}$NMKIV$_{24}$ with an extended hinge-region, to be an excellent candidate for further studies to eventually overcome the lantibiotic resistance in human pathogens, since these proteins do not recognize this variant well.

1. Introduction

Antimicrobial resistance (AMR) is a severe danger to human health across the world. Many compounds, which were blockbuster in pharmaceutical sales, are nearly ineffective due to AMR.

Therefore, it is of fundamental importance to explore the wide biological landscape for new compounds, that exploit new antimicrobial mechanism, or to re-design existing compounds such that resistance mechanisms are bypassed. To achieve the latter, an understanding of the exact mode of action of the compound is the first priority, as well as the resistance mechanism, which was developed by the threated bacteria.

One large class of potentially antimicrobial compounds are antimicrobial peptides (AMPs), secreted by bacteria for quorum sensing and surviving purpose. There, one extensively studied class of AMPs are lantibiotics, which are classified in different classes (class I-IV).[1–3] They are expressed and secreted by numerous bacteria and can be discovered in genome sequences by new genome mining tools like for example BAGEL4.[4] Lantibiotics are expressed as a precursor peptide inside the cell and are post-translationally modified by specific enzymes, which are all localized on a single operon.[5–9] The modifications are installed in the core peptide by the modification enzymes LanB and LanC (lantibiotics class I). LanB dehydrates specifically serine and threonine residues, whereas LanC catalyzes the crosslink of cysteine residues to the dehydrated amino acids, to subsequently form (methyl-)lanthionine rings.[10–16] These rings are characteristic for lantibiotics and cause high heat stability, resistance to proteolytic cleavage and are most importantly crucial for their high antimicrobial potency.[17–22]

Nisin is one of the best studied lantibiotics, produced by *Lactococcus lactis* and is considered as a model system for lantibiotics as well as the modification and secretion of lantibiotics. The whole nisin biosynthesis is well understood and the modification enzymes NisB and NisC have been successfully employed to install (methyl-)lanthionine rings in unrelated targets like angiotensin and several unrelated lantibiotics.[23–25]

Nisin consists of 34 amino acids and five (methyl-)lanthionine rings (Fig. 1), which can be subdivided in three parts. An *N*-terminal part harboring ring A, B and C, where it was shown that ring A and B bind to the cell wall precursor lipid II[26] and results in cell growth inhibition.[27] Next is a flexible hinge-region, consisting of three amino acids (NMK), which allow the third part (C-terminal) to reorient after lipid II binding and penetrate into the target cell membrane.[28–30] Once four lipid II molecules and eight nisin molecules come together, the C-terminal part of the nisin molecules form a stable pore in the membrane. This pore induces leakage and efflux of vital ions, vitamins and other substances of the cell, which subsequently leads to rapid cell death.[29,31] There,

* Corresponding author.
E-mail address: sander.smits@hhu.de (S.H.J. Smits).

https://doi.org/10.1016/j.bmc.2019.07.014
Received 2 May 2019; Received in revised form 6 July 2019; Accepted 9 July 2019
Available online 10 July 2019
0968-0896/

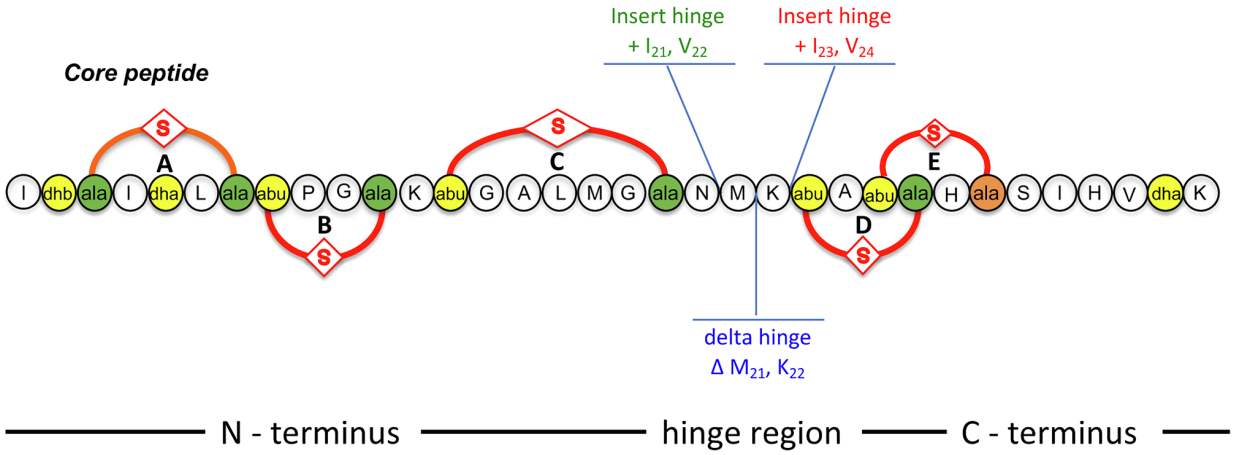

Fig. 1. Schematic representation of nisin. The (methyl-)lanthionine rings, formed by a cysteine residue side chain and a dehydrated amino acid residue are highlighted in yellow and green. The (methyl-)lanthionine rings A, B, C, D and E are depicted in red (adopted from (49)). Introduced mutations are indicated in green (extension inside hinge-region), red (extension after hinge-region) and blue (partially deletion of the hinge-region).

pore formation is a very rapid process and cell lysis occurs already within seconds after addition of nanomolar concentration of nisin to a cell culture.[31,32]

Although impressive progress has been made in to use of lantibiotics as medical treatment compounds there are some drawbacks.[33–35] Lantibiotics are used for decades as food-preservatives (e.g. nisin[36]) and bacterial resistance seldom occurred. Nevertheless, some mechanisms are described, which mainly involve proteins conferring resistance against lantibiotics.[37] First of all, the lantibiotic producing strains express two proteins LanI and LanFEG, which prevent a suicidal effect.[37,38] Secondly, some human pathogenic strains that do not produce lantibiotics express proteins, causing resistance to lantibiotics. This resistance is often conferred by a membrane-anchored peptidase and an ABC transporter belonging to the BceAB-type superfamily.[39,40] Both systems are able to confer resistance even up to high nanomolar concentration.[32,39,41]

Several variants of nisin have been made and characterized.[42–47] Here, we focus on the hinge-region of nisin and made three variants. First a partially deletion in the hinge-region ($\Delta_{21}MK_{22}$) and two extended hinge-regions by introducing extra amino acids either at the C-terminus of the hinge-region, or within the hinge-region, and named them after their sequence ($_{20}NMKIV_{24}$ and $_{20}NIVMK_{24}$). It was shown that the hinge-region of nisin is predicted to be a pharmaceutical hotspot. Some variants of this region were characterized and showed improved activity against used indicator strains.[30,47,48] We characterize these variants with respect to their growth inhibition ability, as well as for their pore forming efficiency.

Furthermore, we extended this study on these variants by analyzing whether the immunity proteins NisI and NisFEG from *L. lactis,* as well as the resistance protein *Sa*NSR and *Sa*NsrFP from *Streptococcus agalactiae COH1* are still able to confer resistance.

2. Material and methods

2.1. Cloning and purification of the nisin hinge-region variants

The insertion of the amino acids IV and the deletion of the amino acids MK were achieved by PCR, using the primer pairs (forward:5′ ATTGTTATGAAAACAGCAACTTGTCATTGTAG3′, reverse 5′GTTACAA CCCATCAGAGCTCC3′) for the hinge-region sequence $_{20}NIVMK_{24}$, the primer pairs (forward: 5′ATTGTTACAGCAACTTGTCATTGTAG3′, reverse 5′TTTCATGTTACAACCCATCAG3′) for the insert $_{20}NMKIV_{24}$ and the primer pairs (forward: 5′ACAGCAACTTGTCATTGTAG3′, reverse 5′ GTTACAACCCATCAGAGC3′) for the partially deleted hinge-region variant, named delta hinge ($\Delta_{21}MK_{22}$). Therefore, oligonucleotides were 5′ phosphorylated. After successful PCR-reaction the template pNZ-SV-nisA was digested with *Dpn*I. The amplified PCR products were gel-extracted, ligated and transformed into *E. coli* DH5α. Sequence analysis verified the new plasmids.

The hinge-region variants were expressed and purified as previously described.[32,50,51] After harvesting the cells, 50 mM lactic acid was added to the supernatant before filtering through 0.45 µm filters. An ion-exchange chromatography was performed and by adding a buffer containing 1 M NaCl the hinge-region variants were eluted. The pre-nisin variants were activated using purified NisP at 8 °C overnight to cleave off the leader peptide, as described.[52] Therefore, the endopeptidase NisP was expressed in *L. lactis* cells and purified by an immobilized metal-ion affinity chromatography (IMAC). After desalting the pure NisP protein was stored at −80 °C upon further usage. The concentration of the active hinge-region variant was determined by RP-HPLC, using a gradient from 90% water and 10% acetonitrile containing 0.1% TFA to 36% water and 64% acetonitrile.[52] The activated variants were directly used for further analysis.

Wild-type nisin was purified as previously described,[53] using an ion-exchange chromatography step. The concentration was measured with RP-HPLC as described above.

The modification state of the nisin hinge-region variants were analyzed using MALDI-TOF analysis, which were performed as described elsewhere.[54]

2.2. Expression of resistance and immunity proteins

The used *L. lactis* strains were previously described.[32,41,49,55] The strains containing the plasmid for the nisin resistance protein (*Sa*NSR) is termed NZ9000NSR, for the ABC transporter NisFEG the strain is called NZ9000NisFEG. The strain containing the lipoprotein NisI is termed NZ9000NisI and with the Bce-AB-type transporter *Sa*NsrFP is called NZ9000NsrFP. A nisin sensitive control strain NZ9000 without any resistance proteins, called NZ9000Cm, is however transformed with an empty plasmid and threatened the same as the other strains used.

2.3. Pore formation of nisin hinge-region variants

The SYTOX Green dye was used to visualize pore formation mediated by wild-type nisin or the variants. This dye binds nucleic acid without crossing intact membranes of living cells.[56] The SYTOX Green Nucleic Acids Binding Assay was performed as described.[32,41,49] Here, we used *L. lactis* cells, containing the described empty plasmid, at an

OD_{600} of 0.3 and added 1 μM SYTOX dye. The fluorescence signal was detected at an excitation and emission wavelength of 504 and 523 nm, respectively. The cell suspension was stirred and heated at 30 °C during the whole assay. After reaching a stable baseline, the nisin variants were added (final concentration was three times the determined IC_{50} value) and the change of fluorescence intensity was monitored online.

2.4. Activity of hinge-region variants against sensitive and resistant strains

As described in Reiners et al. (2017)[49] growth inhibition assays were performed to determine the half-maximal inhibitory concentration (IC_{50}). In a 96-well plate the nisin variants were diluted and the different *L. lactis* NZ9000 cells were added. The plate was incubated at 30 °C for 5 h and afterwards the OD_{595} was measured to finally determine the IC_{50} values.

3. Results

3.1. Expression and purification of nisin hinge-region variants

Here, we cloned and expressed three different variants of nisin inside the hinge-region. We extended the hinge-region (in wild-type nisin the amino acids are NMK) by the amino acids isoleucine and valine in the beginning ($_{20}$NIVMK$_{24}$) and at the end of the hinge-region ($_{20}$NMKIV$_{24}$). Furthermore, we created a mutant where the hinge-region was partially deleted (Δ_{21}MK$_{22}$). These nisin variants were expressed using the *L. lactis* NZ9000 strain transformed with a plasmid with the nisin modification and secretion system NisBTC,[57] as well as the plasmid with the modified nisin gene. As a control we used the same system expressing the wild-type nisin. We could express and purify nearly 4.4 mg of all three nisin variants per liter of cell culture, which is 70% of the yield described for wild-type prenisin plasmid based expression system (Fig. 2D).[54] After purification, the prenisin leader peptide was cleaved off by the purified peptidase NisP[54] resulting in activation of the nisin variants. Although the peptidase NisP cleaves off the *N*-terminal leader peptide sequence, some differences were observed in terms of cleavage efficiencies as determined by RP-HPLC analysis. The core peptide for all three variants was clearly visible and by peak integration the concentration was determined using different insulin (chain B) or nisin concentrations as a standard.[54] Whereas under these experimental conditions the efficiency of wild-type prenisin was nearly 94%,[54] the cleavage efficiency for the $_{20}$NIVMK$_{24}$, $_{20}$NMKIV$_{24}$ and Δ_{21}MK$_{22}$ variants were determined to be 81.2 ± 4.9 %, 74.3 ± 3.8 % and 48.1 ± 3.5 %, respectively (Fig. 2A–C). This indicates that the flexibility of the hinge-region influences the binding to or the cleavage by NisP.

Table 1
Nisin variants with percentage of cleavage by NisP, detected dehydrations with MS, installed lanthionine rings and protein yield per liter culture. Main species found in MS analysis are marked in bold.

Nisin variant	Cleavage [%]	Dehydrations	Lanthionine rings	Yield [mg/L culture]
wild-type nisin	94.0 ± 1.8	**8**; 7	5	6.04 ± 0.26
$_{20}$NIVMK$_{24}$	81.2 ± 4. 9	9; **8**; 7; 6; 5; 4	5; 4; 3	4.38 ± 0.66
$_{20}$NMKIV$_{24}$	74.3 ± 3.8	9; **8**; 7; 6; 5	5; 4	4.42 ± 0.45
Δ_{21}MK$_{22}$	48.1 ± 3.5	9; **8**; 7; 6; 5; 4; 1; 0	5; 4; 3; 2; 1; 0	4.34 ± 0.56

Furthermore, the core peptides of the $_{20}$NIVMK$_{24}$, $_{20}$NMKIV$_{24}$ and Δ_{21}MK$_{22}$ variants were analyzed with MALDI-TOF MS to determine their modification state. Here, we observed that the variants exhibit a wider spectrum of dehydrations then observed for wild-type nisin (Table 1). Whereas wild-type nisin exhibits seven to eight dehydrations and five installed lanthionine rings, the amount of dehydrations found in the nisin variant $_{20}$NIVMK$_{24}$ ranges from four to nine. Similarly, the number of free thiol-groups from cysteine residues, which are not involved in (methyl-) lanthionine rings vary from three to five. In the nisin variant $_{20}$NMKIV$_{24}$ the number of dehydrations is five to nine with

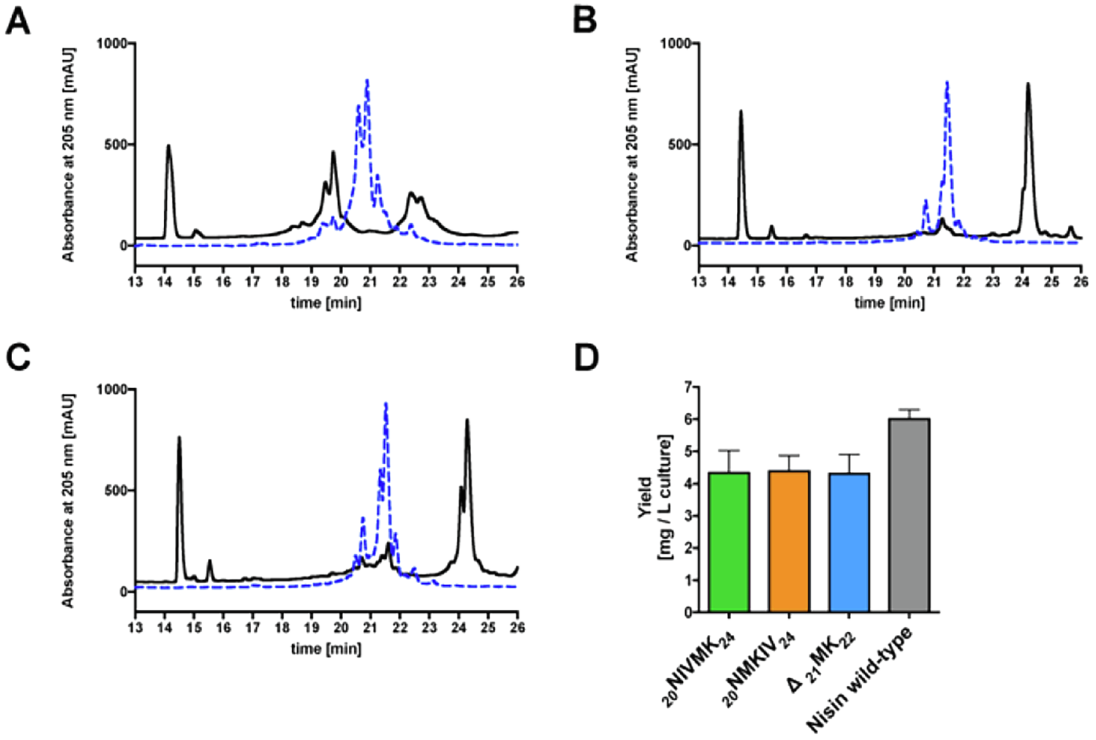

Fig. 2. RP-HPLC chromatogram of the nisin variants. Shown are the elution profiles of the prenisin variants (blue) and the nisin variants after cleavage by NisP (black) A) Δ_{21}MK$_{22}$ B) $_{20}$NIVMK$_{24}$ C) $_{20}$NMKIV$_{24}$. D) Yield of the prenisin variants as determined by HPLC analyses using an insulin chain B standard.

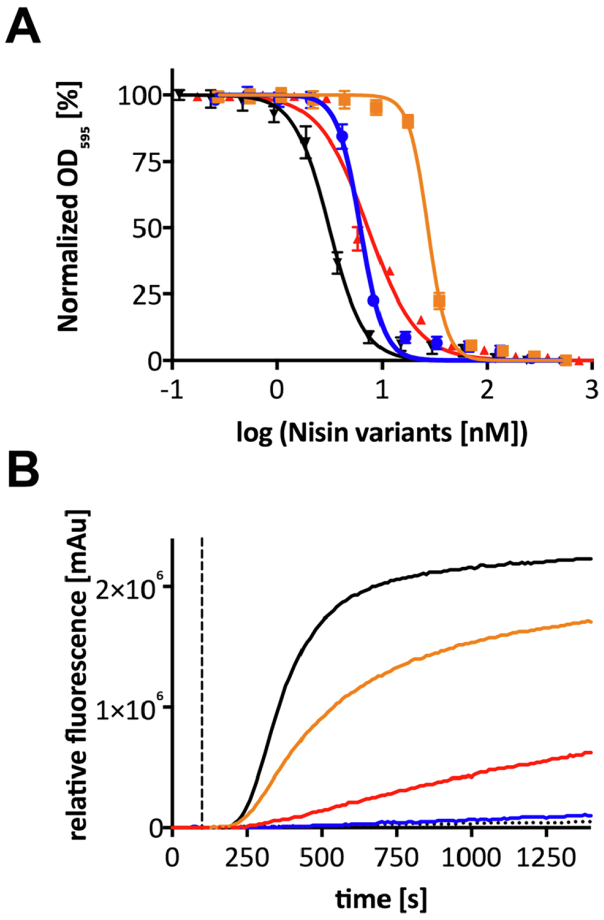

Fig. 3. IC_{50} measurements and SYTOX green assay A) Determination of the IC_{50} values of nisin and the nisin variants. The normalized OD_{595} in percentage was plotted against the logarithmic concentration of nisin variants. The measurements were performed using the sensitive *L. lactis* NZ9000Cm strain. B) NZ9000Cm strain with SYTOX green nucleic acid dye measured at 30 °C. The nisin variants, were added at a final concentration of three times the determined IC_{50} value. The addition of nisin is indicated by the vertical dotted line. Shown are the curves for wild-type nisin (black) $\Delta_{21}MK_{22}$ (blue) $_{20}NIVMK_{24}$ (red) and $_{20}NMKIV_{24}$ (orange) and buffer (black dots).

four to five installed (methyl-) lanthionine rings. The variant $\Delta_{21}MK_{22}$ has zero to eight dehydrations with zero to five installed (methyl-) lanthionine rings. However, the main species contained eight dehydrations, with five installed (methyl-) lanthionine rings. In summary, one can observe that the hinge-region influences the modification machinery, resulting in less dehydrated species. Clearly, the main species in all variants were fully modified (Table 1).

3.2. Activity of nisin hinge-region variants

We tested the activity of the different nisin variants using a growth inhibition assay, resulting in an IC_{50} value against the *L. lactis* NZ9000Cm strain, which is highly sensitive to nisin.[49] As a control we used freshly purified wild-type nisin, which was purified similarly to the nisin variants. Here, wild-type nisin displayed an IC_{50} value of 7.13 ± 0.35 nM, which is in-line with previous studies.[32,41,49,58] The variants displayed a lower antimicrobial activity, which was also observed previously.[47] Here, the variant $\Delta_{21}MK_{22}$ displayed an IC_{50} value of 43.44 ± 13.98 nM (Fig. 3a and Table 2), which leads to a six-fold increase compared to wild-type nisin. The activity of the variant $_{20}NIVMK_{24}$ was the same as wild-type nisin within experimental error and resulted in an IC_{50} value of 8.17 ± 1.23 nM (Fig. 3A and Table 2). This is in contrast to Zhou et al. (2015), where a four-fold decreased antimicrobial activity was determined for this variant.[47] The nisin variant $_{20}NMKIV_{24}$ showed a medium antimicrobial activity with an IC_{50} value of 22.26 ± 5.93 nM, which implies a three-fold reduction (Fig. 3A and Table 2). Summarized, the mutation of the hinge-region influences the antimicrobial activity. Especially, deletions of amino acids in the hinge-region lead to significantly drop in antimicrobial activity.[47]

Further, we tested whether the nisin variants are still able to form pores in the membranes of bacterial cells using the well-established SYTOX Green assay.[32,41,49] Here, we used the *L. lactis* NZ9000Cm strain, where the addition of three times the measured IC_{50} value of wild-type nisin resulted in an almost immediate increase of the fluorescence signal. This indicates a rapid pore formation within the membrane (Fig. 3B black line). As a control, we added buffer to the cells, which resulted in no fluorescence increase over the measured time interval.

For the hinge-region variants, we also used a final concentration of three times the previously determined IC_{50} value. The variant $_{20}NMKIV_{24}$ still displayed the ability to form pores in the membrane of *L. lactis*, nevertheless the pore formation is slower in comparison to wild-type nisin as depicted by a less steep increase of the fluorescence signal (Fig. 3B orange line). For the variant $_{20}NIVMK_{24}$ an even slower pore formation and only 15% of the fluorescence signal increase were observed (Fig. 3B red line).

Interestingly, the variant $\Delta_{21}MK_{22}$ displayed no pore formation under this experimental setup (Fig. 3B blue line), indicating that the flexible hinge-region indeed is crucial for the insertion of nisin into the lipid bilayer as previously shown.[30] The results of the SYTOX green assay in combination with the determined antimicrobial activities (IC_{50} values of the variants) allow the connection of a decreased activity with an altered pore forming ability of the nisin variants.

3.3. Activity against immunity and resistance proteins

LanI and LanFEG are the immunity proteins expressed in some lantibiotic producers, to circumvent a suicidal effect of lantibiotic. For the nisin producer *L. lactis* these proteins are NisI and NisFEG. Whereas NisI seems to recognize the full nisin molecule, the ABC transporter NisFEG recognizes the C-terminus.[41] We tested whether the hinge-region variants effect the immunity system of *L. lactis* by expressing each protein using a plasmid-based system,[32,41] where the strains are termed NZ9000NisI and NZ9000NisFEG. By determining the IC_{50} value and comparison of the IC_{50} with the sensitive strain a fold of resistance (FR) can be calculated. The FR value of wild-type nisin for NZ9000NisI is 6.91 ± 0.65 and 7.43 ± 0.74 for NZ9000NisFEG (Table 2, Figs. 4A and 5).

For the variant $_{20}NIVMK_{24}$ the determined IC_{50} values were 77.35 ± 3.82 nM and 106.73 ± 2.37 nM against NZ9000NisI and NZ9000NisFEG, respectively. This corresponds to FR values of 9.46 ± 0.98 for NZ9000NisI and 13.06 ± 1.72 for NZ9000NisFEG reflecting a better recognition of this variant by the immunity proteins.

For the variant $_{20}NMKIV_{24}$ the IC_{50} values were determined to be 73.16 ± 7.71 nM and 36.89 ± 7.17 against NZ9000NisI and NZ9000NisFEG, respectively. This resulted in FR values of 3.29 ± 0.57 for NZ9000NisI and of 1.66 ± 0.13 for NZ9000NisFEG, which represent a decreased immunity potency against this variant. Thus, this nisin variant, although slightly lower in antimicrobial activity is not recognized by the immunity proteins anymore.

The variant $\Delta_{21}MK_{22}$ displayed IC_{50} values of 108.70 ± 5.77 and 72.11 ± 2.57 against the NZ9000NisI and NZ9000NisFEG, respectively. This results in a reduction of the FR value to 2.50 ± 0.75 for NZ9000NisI and 1.66 ± 0.53 for NZ9000NisFEG. This suggests that the flexible linker needs to be present for the recognition of nisin by the immunity protein (Table 2, Figs. 4B and 5).

Table 2
IC_{50} values of nisin wild-type and hinge-region variants as well as calculated fold of resistance (FR) values for the strains NZ9000Cm, NZ9000NisI, NZ9000NisFEG, NZ9000NSR and NZ9000NsrFP.

Nisin variant	NZ9000Cm	NZ9000NisI		NZ9000NisFEG		NZ9000NSR		NZ9000NsrFP	
	IC50 (nM)	IC50 (nM)	FR	IC50 (nM)	FR	IC50 (nM)	FR	IC50 (nM)	FR
Wild-type nisin	7.13 ± 0.35	49.32 ± 7.02	6.91 ± 0.65	53.03 ± 7.84	7.43 ± 0.74	76.04 ± 5.75	10.66 ± 0.28	82.29 ± 5.11	11.54 ± 0.15
$_{20}$NIVMK$_{24}$	8.17 ± 1.23	77.35 ± 3.82	9.46 ± 0.98	106.73 ± 2.37	13.06 ± 1.72	101.80 ± 1.67	12.45 ± 1.71	121.43 ± 3.06	14.85 ± 1.91
$_{20}$NMKIV$_{24}$	22.26 ± 5.93	73.16 ± 7.71	3.29 ± 0.57	36.89 ± 7.17	1.66 ± 0.13	64.76 ± 3.10	2.91 ± 0.68	44.35 ± 2.15	1.99 ± 0.47
Δ_{21}MK$_{22}$	43.44 ± 13.98	108.70 ± 5.77	2.50 ± 0.75	72.11 ± 2.57	1.66 ± 0.53	221.13 ± 10.95	5.09 ± 1.55	212.80 ± 11.26	4.90 ± 1.47

We also tested the nisin hinge-region variants against strains of *L. lactis*, which are transformed with a plasmid encoding *Sa*NSR and *Sa*NsrFP, respectively. Both proteins originate from an operon in the human pathogen *S. agalactiae* and it has been shown that they confer resistance against nisin when expressed in *L. lactis*.[49,58] The variant $\Delta_{21}MK_{22}$ displayed an IC_{50} value of 221.1 ± 10.95 nM and 212.80 ± 11.26 nM against NZ9000NSR and NZ9000NsrFP, respectively. This represents a lower FR value of 5.09 ± 1.55 for NZ9000NSR and 4.90 ± 1.47 for NZ9000NsrFP when compared to wild-type nisin (see Table 2).

The variant $_{20}NIVMK_{24}$ is in contrast similarly recognized by the resistance proteins as observed by the IC_{50} values of 101.80 ± 1.67 nM (FR of 12.45 ± 1.71) and 121.43 ± 3.06 (FR of 14.85 ± 1.91) for the NZ9000NSR and NZ9000NsrFP strains, respectively (Table 2, Figs. 4C and 5).

However, the highest decrease of FR mediated by the resistance proteins was observed for the variant $_{20}NMKIV_{24}$, which displayed low IC_{50} values. Here, the IC_{50} values were 64.76 ± 3.10 nM (FR of 2.91 ± 0.68) against NZ9000NSR and 44.35 ± 2.15 nM (FR of 1.99 ± 0.47) against NZ9000NsrFP bypasses the resistance mechanism and might be a less suitable substrate for the resistance proteins (Table 2, Figs. 4C and 5).

4. Discussion

In this study, we focused on three nisin hinge-region variants including their property in expression and activation along with investigating their effect on antimicrobial activity. Here, we especially focused on their impact to immunity and resistance proteins compared to wild-type nisin. The two variants $_{20}NIVMK_{24}$ and $_{\Delta 21}MK_{22}$ were previously partly characterized[47] and we extended these studies by the immunity and resistance proteins.

The nisin variant $_{20}NIVMK_{24}$ showed four to nine dehydrations, which leads to the assumption that the dehydratase NisB either has a reduced recognition of this variant or the variant itself somehow hinders the dehydration reaction sterically. The cleavage efficiency of NisP

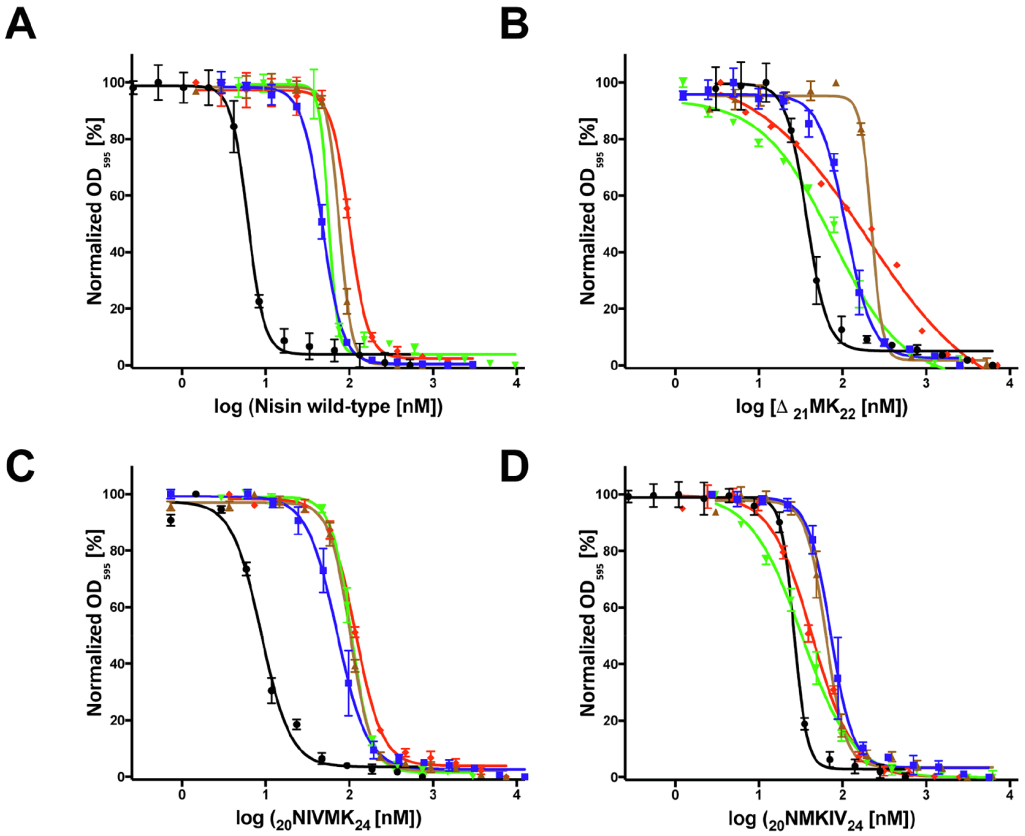

Fig. 4. IC_{50} measurements of the nisin variants against the *L. lactis* NZ9000 strain expressing the immunity and resistance protein respectively. A) nisin wild-type B) nisin $\Delta_{21}MK_{22}$ C) nisin $_{20}NIVMK_{24}$ and D) nisin $_{20}NMKIV_{24}$. L. lactis NZ9000Cm (black), NZ9000NisI (blue), NZ9000NisFEG (green), NZ9000NSR (brown) and NZ9000NsrFP (red).

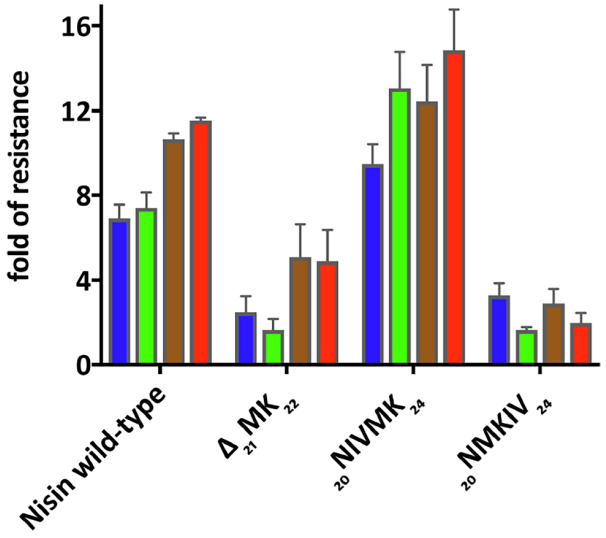

Fig. 5. Calculated fold of resistance values against of NZ9000NisI (blue), NZ9000NisFEG (green), NZ9000NSR (brown) and NZ9000NsrFP (red) against NZ9000Cm for nisin wild-type, nisin $\Delta_{21}MK_{22}$, nisin $_{20}NIVMK_{24}$ and nisin $_{20}NMKIV_{24}$.

for $_{20}NIVMK_{24}$ (81.2 ± 4.9 %) is slightly reduced compared to wild-type nisin, suggesting a reduced binding affinity of NisP. Nevertheless, the extended hinge-region influences the antimicrobial activity against *L. lactis* NZ9000Cm marginal, but strongly inhibits the pore-forming activity. This is in contrast to previous studies, where the same variant showed an highly decreased activity compared to nisin wild-type against *L. lactis*[47].

Higher folds of resistance of $_{20}NIVMK_{24}$ for the immunity proteins NisI (9.46 ± 0.98) and NisFEG (13.06 ± 1.72) compared to wild-type nisin (6.91 ± 0.65 for NisI and 7.43 ± 0.74 for NisFEG) indicate an increased recognition of the nisin variant by the nisin immunity proteins. There, the mutation inside the hinge-region seems not to influence the recognition or affinity of the resistance proteins *Sa*NSR and *Sa*NsrFP. Furthermore, due to the extended flexible hinge-region of the nisin variant $_{20}NIVMK_{24}$ the binding of lipid II seems not influenced but the insertion into the cell membrane and thereby pore formation is malfunctioning.

The nisin variant $_{20}NMKIV_{24}$ has two additional amino acids at the end of the hinge-region, which shows five to nine dehydrations and a cleavage efficiency of NisP of 74%, leading to the assumption that also for this variant the NisB and NisP recognition might be affected.

In view of the antimicrobial activity against NZ9000Cm a drop is observed (22.26 ± 5.93 nM), whereas the fold of resistance for the immunity transporter NisFEG and the resistance transporter *Sa*NsrFP remains very low (Table 2). Besides, the FR values for NisI and *Sa*NSR are reduced, compared to wild-type nisin.

Furthermore, this nisin variant showed an almost similar increase of the fluorescence signal in the SYTOX assay, suggesting it is still able to form pores.

This nisin variant with an extended hinge-region seems not to be recognized by the resistance and immunity proteins, although it exhibits a slightly lower antimicrobial activity. The antimicrobial activity is slightly decreased by this mutation, which can be explained by a broadened dehydration pattern. The pore forming ability seems not to be influenced, compared to the decreased recognition of immunity as well as resistance proteins this implies an improved flexibility of nisin $_{20}NMKIV_{24}$.

Thus, it appears that this variant might be a less suitable substrate for the resistance proteins. This characteristic could be utilized as a new starting point to discover a new lantibiotic derivative, to overcome the nisin resistance in human pathogens such as *S. agalactiae*.

Nisin variant $\Delta_{21}MK_{22}$ with a radical shortened hinge-region shows an extended dehydration pattern and surprisingly a drastically reduced cleavage efficiency (49.6 ± 3.57 %). Additionally, the formation of the lanthionine rings was hindered, resulting in less amount of active nisin variant. Hence, this indicates that the flexibility of the hinge-region not only influences the binding to the dehydratase NisB and the protease NisP but also might hinder the effectiveness of the cyclase NisC. Continuative the antimicrobial activity of nisin $\Delta_{21}MK_{22}$ is six times reduced compared to wild-type nisin, which is in-line with the results of Zhou *et al.* (2015)[47]. This observation is confirmed by the SYTOX assay, which reveals almost no pore formation for the shortened nisin variant.

However, the fold of resistance of the immunity proteins against nisin $\Delta_{21}MK_{22}$ suggests that the flexible linker needs to be present for the recognition of nisin by them. Additionally, the resistance proteins also showed a decreased FR value compared to wild-type nisin, indicating the limited flexibility influences the recognition by *Sa*NSR and *Sa*NsrFP.

The immunity protein NisFEG, as well as the resistance protein *Sa*NSR recognize the C-terminal part of nisin, whereas NisI and *Sa*NsrFP seem to perceive nisin *N*-terminus[27,41,49,58] leading to the assumption, that not a sterically hindrance of the accessibility of one of the termini is responsible for a loss of recognition by the immunity proteins but the restricted flexibility.

Comparing the results for the three nisin hinge-region variants it can be combined that not the extension of the hinge-region in nisin variant $_{20}NIVMK_{24}$ is responsible for the decrease in pore-forming activity but the interruption of the wild-type hinge-region due to the fact that the mutation of nisin variant $_{20}NMKIV_{24}$ does not influence the pore forming process, whereas the nisin variant $_{20}NIVMK_{24}$ showed drastically reduced pore formation.

Moreover, it can be assumed that the wild-type hinge-region of nisin is essential for the recognition by the immunity protein NisI, but especially by NisFEG, as we see a drop in immunity when reducing the length of the hinge-region as well as extending it.

Although, preceding mutagenesis studies showed an enhanced activity of nisin hinge-region variants against *S. agalactiae*[46], this study exhibits a promising nisin variant ($_{20}NMKIV_{24}$), bypassing this lantibiotic resistance of the human pathogen, while showing just a slight decrease of antimicrobial and pore forming activity. These results can be used as a basis for further investigations on the recognition mechanism of the nisin modification enzymes and immunity proteins as well as for profound studies of the nisin resistance proteins of *S. agalactiae*.

Funding

This work has been funded by the Deutsche Forschungsgemeinschaft (DFG, German Research Foundation) – Project number 270,650,915/GRK2158 TP4a to S.S.

Acknowledgment

We thank all members of the Institute of Biochemistry for fruitful discussions.

Appendix A. Supplementary data

Supplementary data to this article can be found online at https://doi.org/10.1016/j.bmc.2019.07.014.

References

1. Kellner R, Jung G, Horner T, et al. Gallidermin: a new lanthionine-containing polypeptide antibiotic. *Eur J Biochem.* 1988;177(1):53–59.
2. Willey JM, van der Donk WA. Lantibiotics: peptides of diverse structure and function.

Annu Rev Microbiol. 2007;61:477–501.
3. Arnison PG, Bibb MJ, Bierbaum G, et al. Ribosomally synthesized and post-translationally modified peptide natural products: overview and recommendations for a universal nomenclature. *Nat Prod Rep.* 2013;30(1):108–160.
4. van Heel AJ, de Jong A, Song C, Viel JH, Kok J, Kuipers OP. BAGEL4: a user-friendly web server to thoroughly mine RiPPs and bacteriocins. *Nucleic Acids Res.* 2018;46(W1):W278–W281.
5. Schnell N, Entian KD, Schneider U, et al. Prepeptide sequence of epidermin, a ribosomally synthesized antibiotic with four sulphide-rings. *Nature.* 1988;333(6170):276–278.
6. Banerjee S, Hansen JN. Structure and expression of a gene encoding the precursor of subtilin, a small protein antibiotic. *J Biol Chem.* 1988;263(19):9508–9514.
7. Buchman GW, Banerjee S, Hansen JN. Structure, expression, and evolution of a gene encoding the precursor of nisin, a small protein antibiotic. *J Biol Chem.* 1988;263(31):16260–16266.
8. Kaletta C, Entian KD. Nisin, a peptide antibiotic: cloning and sequencing of the nisA gene and posttranslational processing of its peptide product. *J Bacteriol.* 1989;171(3):1597–1601.
9. Dodd HM, Horn N, Gasson MJ. Analysis of the genetic determinant for production of the peptide antibiotic nisin. *J Gen Microbiol.* 1990;136(3):555–566.
10. Karakas Sen A, Narbad A, Horn N, et al. Post-translational modification of nisin. The involvement of NisB in the dehydration process. *Eur J Biochem.* 1999;261(2):524–532.
11. Koponen O, Tolonen M, Qiao M, Wahlström G, Helin J, Saris PE. NisB is required for the dehydration and NisC for the lanthionine formation in the post-translational modification of nisin. *Microbiology.* 2002;148(Pt 11):3561–3568.
12. Kluskens LD, Kuipers A, Rink R, et al. Post-translational modification of therapeutic peptides by NisB, the dehydratase of the lantibiotic nisin. *Biochemistry.* 2005;44(38):12827–12834.
13. Weil HP, Beck-Sickinger AG, Metzger J, et al. Biosynthesis of the lantibiotic Pep5. Isolation and characterization of a prepeptide containing dehydroamino acids. *Eur J Biochem.* 1990;194(1):217–223.
14. Gutowski-Eckel Z, Klein C, Siegers K, Bohm K, Hammelmann M, Entian KD. Growth phase-dependent regulation and membrane localization of SpaB, a protein involved in biosynthesis of the lantibiotic subtilin. *Appl Environ Microbiol.* 1994;60(1):1–11.
15. Okeley NM, Paul M, Stasser JP, Blackburn N, van der Donk WA. SpaC and NisC, the cyclases involved in subtilin and nisin biosynthesis, are zinc proteins. *Biochemistry.* 2003;42(46):13613–13624.
16. Rink R, Kluskens LD, Kuipers A, Driessen AJ, Kuipers OP, Moll GN. NisC, the cyclase of the lantibiotic nisin, can catalyze cyclization of designed nonlantibiotic peptides. *Biochemistry.* 2007;46(45):13179–13189.
17. Rollema HS, Kuipers OP, Both P, de Vos WM, Siezen RJ. Improvement of solubility and stability of the antimicrobial peptide nisin by protein engineering. *Appl Environ Microbiol.* 1995;61(8):2873–2878.
18. Lu Y, Jiang L, Chen M, Huan L, Zhong J. Improving heat and pH stability of nisin by site-directed mutagenesis. *Wei Sheng Wu Xue Bao.* 2010;50(11):1481–1487.
19. Rink R, Arkema-Meter A, Baudoin I, et al. To protect peptide pharmaceuticals against peptidases. *J Pharmacol Toxicol Methods.* 2010;61(2):210–218.
20. Gross E, Morell JL. The presence of dehydroalanine in the antibiotic nisin and its relationship to activity. *J Am Chem Soc.* 1967;89(11):2791–2792.
21. Chan WC, Leyland M, Clark J, et al. Structure-activity relationships in the peptide antibiotic nisin: antibacterial activity of fragments of nisin. *FEBS Lett.* 1996;390(2):129–132.
22. Jung G. Lantibiotics—ribosomally synthesized biologically active polypeptides containing sulfide bridges and α,β-didehydroamino acids. *Angew. Chem., Int. Ed.* 1991;30(9):1051–1068.
23. Kuipers A, de Boef E, Rink R, et al. NisT, the transporter of the lantibiotic nisin, can transport fully modified, dehydrated, and unmodified prenisin and fusions of the leader peptide with non-lantibiotic peptides. *J Biol Chem.* 2004;279(21):22176–22182.
24. van Heel AJ, Kloosterman TG, Montalban-Lopez M, et al. Discovery, production and modification of five novel lantibiotics using the promiscuous nisin modification machinery. *ACS Synth Biol.* 2016;5(10):1146–1154.
25. Montalbán-López M, van Heel AJ, Kuipers OP. Employing the promiscuity of lantibiotic biosynthetic machineries to produce novel antimicrobials. *FEMS Microbiol Rev.* 2017;41(1):5–18.
26. Hsu ST, Breukink E, Tischenko E, et al. The nisin-lipid II complex reveals a pyrophosphate cage that provides a blueprint for novel antibiotics. *Nat Struct Mol Biol.* 2004;11(10):963–967.
27. Wiedemann I, Breukink E, van Kraaij C, et al. Specific binding of nisin to the peptidoglycan precursor lipid II combines pore formation and inhibition of cell wall biosynthesis for potent antibiotic activity. *J Biol Chem.* 2001;276(3):1772–1779.
28. van Heusden HE, de Kruijff B, Breukink E. Lipid II induces a transmembrane orientation of the pore-forming peptide lantibiotic nisin. *Biochemistry.* 2002;41(40):12171–12178.
29. Hasper HE, de Kruijff B, Breukink E. Assembly and stability of nisin-lipid II pores. *Biochemistry.* 2004;43(36):11567–11575.
30. Medeiros-Silva J, Jekhmane S, Paioni AL, et al. High-resolution NMR studies of antibiotics in cellular membranes. *Nat Commun.* 2018;9(1):3963.
31. Wiedemann I, Benz R, Sahl HG. Lipid II-mediated pore formation by the peptide antibiotic nisin: a black lipid membrane study. *J Bacteriol.* 2004;186(10):3259–3261.
32. AlKhatib Z, Lagedroste M, Fey I, Kleinschrodt D, Abts A, Smits SH. Lantibiotic immunity: inhibition of nisin mediated pore formation by NisI. *PLoS ONE.* 2014;9(7) e102246.
33. Dischinger J, Basi Chipalu S, Bierbaum G. Lantibiotics: promising candidates for future applications in health care. *Int J Med Microbiol.* 2014;304(1):51–62.
34. Gomes KM, Duarte RS, de Freire Bastos MD. Lantibiotics produced by *Actinobacteria* and their potential applications (a review). *Microbiology.* 2017;163(2):109–121.
35. Sandiford SK. Current developments in lantibiotic discovery for treating *Clostridium difficile* infection. *Expert Opin Drug Discov.* 2019;14(1):71–79.
36. Delves-Broughton J, Blackburn P, Evans RJ, Hugenholtz J. Applications of the bacteriocin, nisin. *Antonie Van Leeuwenhoek.* 1996;69(2):193–202.
37. Draper LA, Cotter PD, Hill C, Ross RP. Lantibiotic resistance. *Microbiol Mol Biol Rev.* 2015;79(2):171–191.
38. Alkhatib Z, Abts A, Mavaro A, Schmitt L, Smits SH. Lantibiotics: how do producers become self-protected? *J Biotechnol.* 2012;159(3):145–154.
39. Khosa S, AlKhatib Z, Smits SH. NSR from *Streptococcus agalactiae* confers resistance against nisin and is encoded by a conserved nsr operon. *Biol Chem.* 2013;394(11):1543–1549.
40. Clemens R, Zaschke-Kriesche J, Khosa S, Smits SHJ. Insight into Two ABC Transporter Families Involved in Lantibiotic Resistance. *Front Mol Biosci.* 2017;4:91.
41. AlKhatib Z, Lagedroste M, Zaschke J, et al. The C-terminus of nisin is important for the ABC transporter NisFEG to confer immunity in *Lactococcus lactis*. *Microbiologyopen.* 2014;3(5):752–763.
42. Plat A, Kuipers A, G De Lange J, N Moll G, Rink R. Activity and Export of Engineered Nisin-(1-22) Analogs; 2011.
43. Rink R, Wierenga J, Kuipers A, et al. Dissection and modulation of the four distinct activities of nisin by mutagenesis of rings A and B and by C-terminal truncation. *Appl Environ Microbiol.* 2007;73(18):5809–5816.
44. Molloy EM, Field D, O' Connor PM, Cotter PD, Hill C, Ross RP. Saturation mutagenesis of lysine 12 leads to the identification of derivatives of nisin A with enhanced antimicrobial activity. *PLoS One.* 2013;8(3) e58530.
45. Zhou L, Shao J, Li Q, et al. Incorporation of tryptophan analogues into the lantibiotic nisin. *Amino Acids.* 2016;48(5):1309–1318.
46. Healy B, Field D, O'Connor PM, Hill C, Cotter PD, Ross RP. Intensive mutagenesis of the nisin hinge leads to the rational design of enhanced derivatives. *PLoS ONE.* 2013;8(11) e79563.
47. Zhou L, van Heel AJ, Kuipers OP. The length of a lantibiotic hinge region has profound influence on antimicrobial activity and host specificity. *Front Microbiol.* 2015;6:11.
48. Piper C, Cotter PD, Ross RP, Hill C. Discovery of medically significant lantibiotics. *Curr Drug Discov Technol.* 2009;6(1):1–18.
49. Reiners J, Lagedroste M, Ehlen K, Leusch S, Zaschke-Kriesche J, Smits SHJ. The N-terminal region of nisin is important for the BceAB-type ABC transporter NsrFP from *Streptococcus agalactiae* COH1. *Front Microbiol.* 2017;8:1643.
50. Mavaro A, Abts A, Bakkes PJ, et al. Substrate recognition and specificity of the NisB protein, the lantibiotic dehydratase involved in nisin biosynthesis. *J Biol Chem.* 2011;286(35):30552–30560.
51. Lubelski J, Overkamp W, Kluskens LD, Moll GN, Kuipers OP. Influence of shifting positions of Ser, Thr, and Cys residues in prenisin on the efficiency of modification reactions and on the antimicrobial activities of the modified prepeptides. *Appl Environ Microbiol.* 2008;74(15):4680–4685.
52. Abts A, Montalban-Lopez M, Kuipers OP, Smits SH, Schmitt L. NisC binds the FxLx motif of the nisin leader peptide. *Biochemistry.* 2013;52(32):5387–5395.
53. Abts A, Mavaro A, Stindt J, et al. Easy and rapid purification of highly active nisin. *Int J Pept.* 2011;2011 175145.
54. Lagedroste M, Reiners J, Smits SHJ, Schmitt L. Systematic characterization of position one variants within the lantibiotic nisin. *Sci Rep.* 2019;9(1):935.
55. Khosa S, Lagedroste M, Smits SH. Protein defense systems against the lantibiotic nisin: function of the immunity protein NisI and the resistance protein NSR. *Front Microbiol.* 2016;7:504.
56. Roth BL, Poot M, Yue ST, Millard PJ. Bacterial viability and antibiotic susceptibility testing with SYTOX green nucleic acid stain. *Appl Environ Microbiol.* 1997;63(6):2421–2431.
57. Rink R, Kuipers A, de Boef E, et al. Lantibiotic structures as guidelines for the design of peptides that can be modified by lantibiotic enzymes. *Biochemistry.* 2005;44(24):8873–8882.
58. Khosa S, Frieg B, Mulnaes D, et al. Structural basis of lantibiotic recognition by the nisin resistance protein from *Streptococcus agalactiae*. *Sci Rep.* 2016;6:18679.

3.8 Chapter VIII

Title: Characterization of the nucleotide-binding domain NsrF from the BceAB-type ABC-transporter NsrFP from the human pathogen *Streptococcus agalactiae*

Authors: Fabia Furtmann, Nicola Porta, Dai Tri Hoang, **Jens Reiners**, Julia Schumacher, Julia Gottstein, Holger Gohlke & Sander H. J. Smits

Published in: Scientific Reports (2020)
Impact factor: 4.38

Own proportion of this work: 15%

- SAXS analysis
- Data analysis
- Writing the manuscript

SCIENTIFIC REPORTS
nature research

Check for updates

OPEN

Characterization of the nucleotide-binding domain NsrF from the BceAB-type ABC-transporter NsrFP from the human pathogen *Streptococcus agalactiae*

Fabia Furtmann[1,5], Nicola Porta[2,5], Dai Tri Hoang[1], Jens Reiners[3], Julia Schumacher[1], Julia Gottstein[1], Holger Gohlke[2,4] & Sander H. J. Smits[1,3]✉

Treatment of bacterial infections is a great challenge of our era due to the various resistance mechanisms against antibiotics. Antimicrobial peptides are considered to be potential novel compound as antibiotic treatment. However, some bacteria, especially many human pathogens, are inherently resistant to these compounds, due to the expression of BceAB-type ABC transporters. This rather new transporter family is not very well studied. Here, we report the first full characterization of the nucleotide binding domain of a BceAB type transporter from *Streptococcus agalactiae*, namely *Sa*NsrF of the transporter *Sa*NsrFP, which confers resistance against nisin and gallidermin. We determined the NTP hydrolysis kinetics and used molecular modeling and simulations in combination with small angle X-ray scattering to obtain structural models of the *Sa*NsrF monomer and dimer. The fact that the *Sa*NsrF$_{H202A}$ variant displayed no ATPase activity was rationalized in terms of changes of the structural dynamics of the dimeric interface. Kinetic data show a clear preference for ATP as a substrate, and the prediction of binding modes allowed us to explain this selectivity over other NTPs.

Therapeutic compounds against bacterial infections are currently one of the biggest needs worldwide. Among antibiotics, antimicrobial peptides (AMP) offer promising potential for the treatment of bacterial infections, alone or in combination with already known molecules[1,2]. An alarming number of pathogenic multidrug resistant strains have evolved under the selective pressure caused by decades of incorrect antibiotic usage. Among them, methicillin-resistant *Staphylococcus aureus* (MRSA) or vancomycin-resistant *Enterococcus* (VRE) pose a high risk to therapeutic regimens[3]. To include new classes of antibiotics in therapy, studies were performed with lantibiotics, a class of AMPs. These ribosomally-synthesized peptides exhibit high potency against several human pathogenic bacterial strains[2–4] and show high stability to chemical and enzymatic degradation due to multiple intramolecular thioether rings and unsaturated amino acids[4–8].

Most known lantibiotics act similar in that they inhibit cell wall synthesis[9]. A common target for AMPs is the peptidoglycan layer, which exists in Gram-positive as well as Gram-negative bacteria. It is built up by altering amino sugars such as *N*-acetylglucosamine (GlcNAc) and *N*-acetylmuramic acid (MurNAc) and stabilized by a cross-linkage of those polymer chains. The inhibition of the cell wall synthesis results in reduced cell growth

[1]Institute of Biochemistry, Heinrich-Heine-Universität Düsseldorf, Universitätsstraße 1, 40225 Düsseldorf, Germany. [2]Institute for Pharmaceutical and Medicinal Chemistry, Heinrich-Heine-Universität Düsseldorf, Universitätsstraße 1, 40225 Düsseldorf, Germany. [3]Center for Structural Studies, Heinrich-Heine-Universität Düsseldorf, Universitätsstraße 1, 40225 Düsseldorf, Germany. [4]John von Neumann Institute for Computing (NIC), Jülich Supercomputing Centre (JSC), Institute of Biological Information Processing (IBI-7: Structural Biochemistry),, Forschungszentrum Jülich GmbH, Wilhelm-Johnen-Straße, 52425 Jülich, Germany. [5]These authors contributed equally: Fabia Furtmann and Nicola Porta. ✉email: sander.smits@hhu.de

and subsequent cell death. The well-known lantibiotic nisin contains five lanthionine rings and primarily targets the cell wall precursor Lipid II. The initial binding of the first two N-terminal lanthionine rings (A and B) of the lantibiotic to Lipid II is followed by a reorientation of the C-terminus into the membrane, resulting in pore formation and subsequently cell lysis[10,11]. Even though lantibiotics are effective in the nanomolar range, their application is hampered by resistance-conferring mechanisms found in human pathogenic bacteria[7,12,13]. The resistance is mediated by a newly discovered class of ATP binding cassette transporters, called Bacitracin efflux ABC transporters (BceAB), named after their first discovery in the bacitracin resistant strain of *Bacillus subtilis*[14,15]. In *Streptococcus agalactiae* such a BceAB-type ABC transporter is also present, as part of an operon that confers resistance against the lantibiotic nisin[16]. This operon consists of the membrane-associated protease *Sa*Nsr[17], the ABC transporter *Sa*NsrFP[8], and the two-component system comprising the response regulator *Sa*NsrR and the histidine kinase *Sa*NsrK[18]. So far, structural information is known only for *Sa*Nsr[17] and *Sa*NsrR[18].

Like all ABC transporters, BceAB-type transporters are composed of a nucleotide-binding domain (NBD) and a transmembrane domain (TMD). The NBD hydrolyses ATP, which drives conformational changes in the TMD, leading to substrate translocation. The TMD of BceAB-type ABC transporters are characterized by ten predicted transmembrane helices and a large extracellular domain (ECD_L) of ~ 220 amino acids that is the hallmark of this transporter family[4,8,16].

Sequences of the TMD domains from various BceAB-type ABC transporters are not very similar, which explains the large variety of substances they are able to translocate[16]. In contrast, NBDs share sequence and distinct motifs which are highly conserved throughout the ABC transporter superfamily[19–22]. NBDs are mainly L-shaped and comprise a helical signaling domain and a catalytic domain built of α-helices and β-strands[23–25]. The catalytic domain contains the Walker A motif that forms the nucleotide-binding site. A glutamate residue in the Walker B motif takes part in proper nucleotide binding; the γ-phosphate of the ATP molecule is sensed by a conserved histidine (H-loop) which when mutated results in an inactive variant[22,23,26]. Signaling and catalytic domains are connected by the Q- and the P-loop. Within the signaling domain the C-loop is located, which is the signature motif of an ABC transporter (for an alignment see Fig. S6 and Table S2)[22,27,28].

Dimerization of two NBD monomers in a head-to-tail conformation, is needed to enable ATP hydrolysis with the nucleotide binding sites located in the dimer interface. Each ATP molecule is sandwiched between the Walker A motif of one monomer and the C-loop of the second one, which results in a closed, stable complex[24,29–31]. An interaction between the NBD and the nucleotide is supposed to occur by π–π-stacking between the aromatic ring system of the nucleotide and an aromatic residue of the protein (F or Y). Hence, no preference towards any nucleotide-triphosphate (NTP) has been assumed[24], as also observed for example for yeast PDR5[32]. The hydrolysis of ATP is coupled to the presence of a cofactor, almost exclusively Mg^{2+}, which is coordinated by the Walker B motif. The divalent cation participates in the hydrolytic attack on the γ-phosphate of the nucleotide[26,28,31].

Here, we report for the first time biochemical and structural characteristics of the BceA nucleotide binding domain *Sa*NsrF, through NTP hydrolysis assays, molecular modeling and simulations. *Sa*NsrF is part of the BceAB-type ABC transporter NsrFP from *Streptococcus agalactiae*[16]. We show that the NBD $SaNsrF_{WT}$ and its hydrolysis-deficient variant $SaNsrF_{H202A}$ are monomeric in solution. Broad-ranging in vitro ATPase screenings delivered detailed information about the protein's properties with regard to its structure and physiology. We show that the preferred substrate of *Sa*NsrF is ATP as demonstrated by its kinetic parameters. Moreover, we built a structural model of the ATP/Mg^{2+}-bound *Sa*NsrF protein in its monomeric and dimeric form by comparative modeling and molecular dynamics simulations. In all, this constitutes the first biochemical characterization of a BceAB-type NBD.

Results

Cloning, expression and purification. For substrate transport BceAB-type ABC transporters depend on energy supply generated by ATP hydrolysis, which is mediated by the NBD. Here, we characterized the NBD NsrF of the BceAB-type ABC transporter NsrFP from *Streptococcus agalactiae*. To heterologously express $SaNsrF_{WT}$ and $SaNsrF_{H202A}$, we constructed expression vectors using a codon-optimized version of *Sa*NsrF for the heterologous expression in *E. coli* (Gen Bank accession number: WP_000923537). These constructs expressed a *Sa*NsrF protein with an N-terminal His10-tag attached for purification using Metal Ion Affinity Chromatography. The corresponding *Sa*NsrF constructs were expressed under the control of the plasmid-based T7-promoter via induction with Isopropyl-β-D-thiogalactopyranoside (IPTG). $SaNsrF_{WT}$ was purified to high homogeneity (Fig. 1A), and was examined by Size Exclusion Chromatography coupled to Multiangle Light Scattering (SEC-MALS)[33], which revealed a molecular mass of 31.9 ± 0.4 kDa for the $SaNsrF_{WT}$ protein (Fig. 1B). This corresponds nicely with the calculated theoretical molecular mass of the recombinant monomer of 30.9 kDa including the His10-tag. Thus, the conducted SEC-MALS analysis revealed that $SaNsrF_{WT}$ exists as a stable monomer in solution, which is in line with previous observations of other NBDs from different ABC transporter families[34–36].

By sequence alignments, His_{202} was identified to be the essential residue of the H-loop[37–39]. As shown for other NBDs, a point mutation to alanine results in a loss of the ATPase activity of the NBD. We generated this variant of *Sa*NsrF ($SaNsrF_{H202A}$), which indeed displayed no NTP hydrolysis (see below). This variant served as a negative control in all our experiments. The lack of NTP hydrolysis for $SaNsrF_{H202A}$ is in line with in vivo studies that show that this variant abolishes the activity of *Sa*NsrFP[8,40].

Activity of $SaNsrF_{WT}$. After successful purification, we functionally characterized $SaNsrF_{WT}$. To do so, we screened the following parameters for their influence on the ATP hydrolysis velocity: (I) pH, (II) salt concentration, (III) nature of the divalent ion and (IV) temperature (see Supporting Information and Fig. S1). As a result, the optimized conditions were found to be 100 mM HEPES at pH 7 with 0 mM NaCl as an assay buffer. The

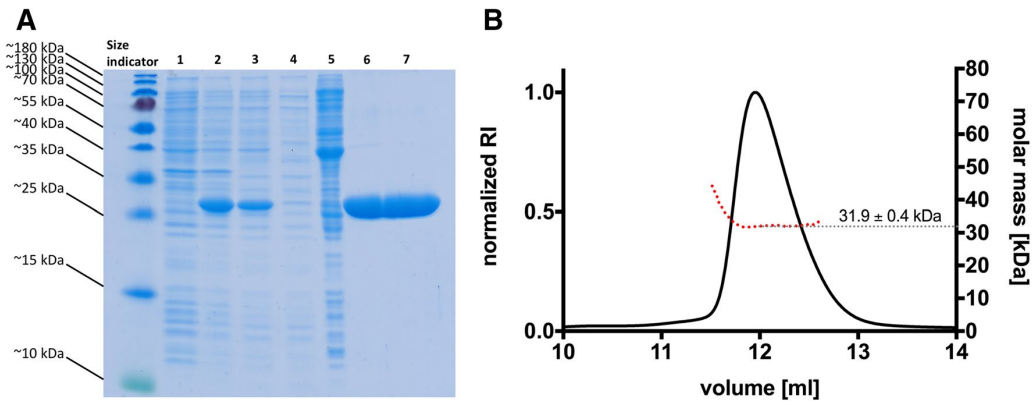

Figure 1. Purification and SEC-MALS of *Sa*NsrF$_{WT}$. (**A**) SDS-PAGE of the *Sa*NsrF$_{WT}$ purification progress. PageRuler Prestained Protein Ladder (size indicator; 10 to 180 kDa), *E. coli* strain before IPTG induction (1), *E. coli* strain after IPTG induction (2), IMAC load (3), IMAC flow-through (4), IMAC wash-fraction (5), IMAC eluate (6), SEC eluate (7). (**B**) Multiangle Light Scattering of *Sa*NsrF$_{WT}$. Freshly purified *Sa*NsrF$_{WT}$ was diluted in MALS-buffer and applied with a concentration of 3 mg mL^{-1} onto a Superdex 75 16/300 increase column. MALS-RI analysis shows that the *Sa*NsrF$_{WT}$ protein elutes with an absolute molecular mass of 31.9 ± 0.4 kDa, consistent with a theoretical monomeric mass in solution.

buffer included 10 mM Mg^{2+} and the reaction was finally performed at 30 °C, with an incubation time of 18 min (Fig S1). These optimized conditions were applied in all following experiments.

Velocity of NTP hydrolysis by SaNsrF$_{WT}$ and SaNsrF$_{H202A}$. Kinetic measurements were performed by quantifying the NTP hydrolysis under increasing concentrations of the respective nucleotide. We determined the NTP hydrolysis behaviour of *Sa*NsrF$_{WT}$ and *Sa*NsrF$_{H202A}$ using increasing amounts of ATP, GTP, CTP or UTP.

As depicted in Fig. 2A, the *Sa*NsrF$_{WT}$ protein demonstrated a nonlinear dependency of ATPase activity over a range of 0–5 mM ATP. The maximal reaction velocity was calculated to be 190.9 ± 10.0 nmol min^{-1} mg^{-1} when using ATP. Moreover, the calculation of the kinetic parameters resulted in a kinetic constant of k_{half} = 0.41 ± 0.05 mM and a Hill coefficient of h = 1.72 ± 0.27 (Fig. 2A and Table 1). A Hill coefficient > 1 demonstrates a cooperative behaviour, and suggests that *Sa*NsrF$_{WT}$ needs to dimerize to hydrolyze ATP, which is in line with other previously characterized NBDs[41–43]. For GTP, the maximal reaction velocity was 221.6 ± 11.1 nmol min^{-1} mg^{-1} with a Hill coefficient of h = 1.82 ± 0.27 and a k_{half} value of 0.69 ± 0.07 mM (Fig. 2B and Table 1). Interestingly, the highest reaction velocity with a value of 339.0 ± 30.4 nmol min^{-1} mg^{-1} was reached using CTP as a substrate with the highest measured k_{half} value of 1.23 ± 0.20 mM and a Hill coefficient of 1.63 ± 0.53 (Fig. 2C and Table 1). The kinetic parameters using UTP as a substrate resulted in comparably high values of v_{max} = 314.8 ± 23.4 nmol min^{-1} mg^{-1}, k_{half} = 0.90 ± 0.13 mM and h = 1.55 ± 0.25 (Fig. 2D and Table 1). The variant *Sa*NsrF$_{H202A}$ displayed no hydrolytic activity for any of the four used NTPs (Fig. 2, dashed lines).

Structural models of SaNsrF monomer and dimer. Since no experimental structure of *Sa*NsrF is available, we generated a structural model of the NBD by comparative modeling. NBDs are the most conserved parts of ABC transporters and in the case of *Sa*NsrF, the templates used for modeling show a sequence identity of ~ 30–40% and a sequence similarity of 84–89% (Table S1). Of these X-ray structures (resolution between 1.7 and 3.4 Å), two constitute NBDs in the functionally active assembly; they were crystallized with the TMD of the macrolide exporter MacAB from *Acinetobacter baumannii* (PDB ID 5GKO[44]) and MacAB-like from *Streptococcus pneumoniae* (PDB ID 5XU1[45]).

The homology model of *Sa*NsrF$_{WT}$ in the monomeric form is of high quality, given the low overall TopScore[46] (TS) value of 0.24 (Fig. 3A). This superimposition-free score evaluates local distance differences[47] of all atoms in a model, and a value closer to zero indicates higher quality. The regions modeled with lower reliability (TS > 0.5), accounting only for ~ 6% of the total sequence, are located at the β-hairpin (residues 15–18) and the two C-terminal helices (residues 229–232, 235–236, 246–250). Both substructures can be found in other NDBs, however, indicating the plausibility of the model. For example, when compared to the structure of ComA from *Streptococcus mutans* (PDB ID 3VX4[48]), the C-terminal helices have a virtually identical fold, with an RMSD of 0.6 Å for the last 50 residues, based on sequence alignment followed by structural superimposition.

The dimeric *Sa*NsrF$_{WT}$ model is structurally similar to other known structures, given RMSD values of ~ 5 Å or lower (RMSD of 3.5 Å, 4.5 Å and 5.2 Å for PDB IDs 1L2T, 5GKO, and 5XU1, respectively), indicating the suitability of the performed protein–protein docking. The reliability of the model is additionally verified by the presence of conserved motifs (Fig. 2B and Table S2), such as the phosphate-binding loop (P-loop or Walker A motif), the cofactor-chelating region (Walker B motif), and a short consensus sequence "LSGGQ" (C-loop or ABC signature motif), which signify ABC transporter family membership at the sequence level. Moreover, the α-helical and RecA-like domains are in the canonical head-to-tail arrangement (Fig. 3C). Interestingly, the

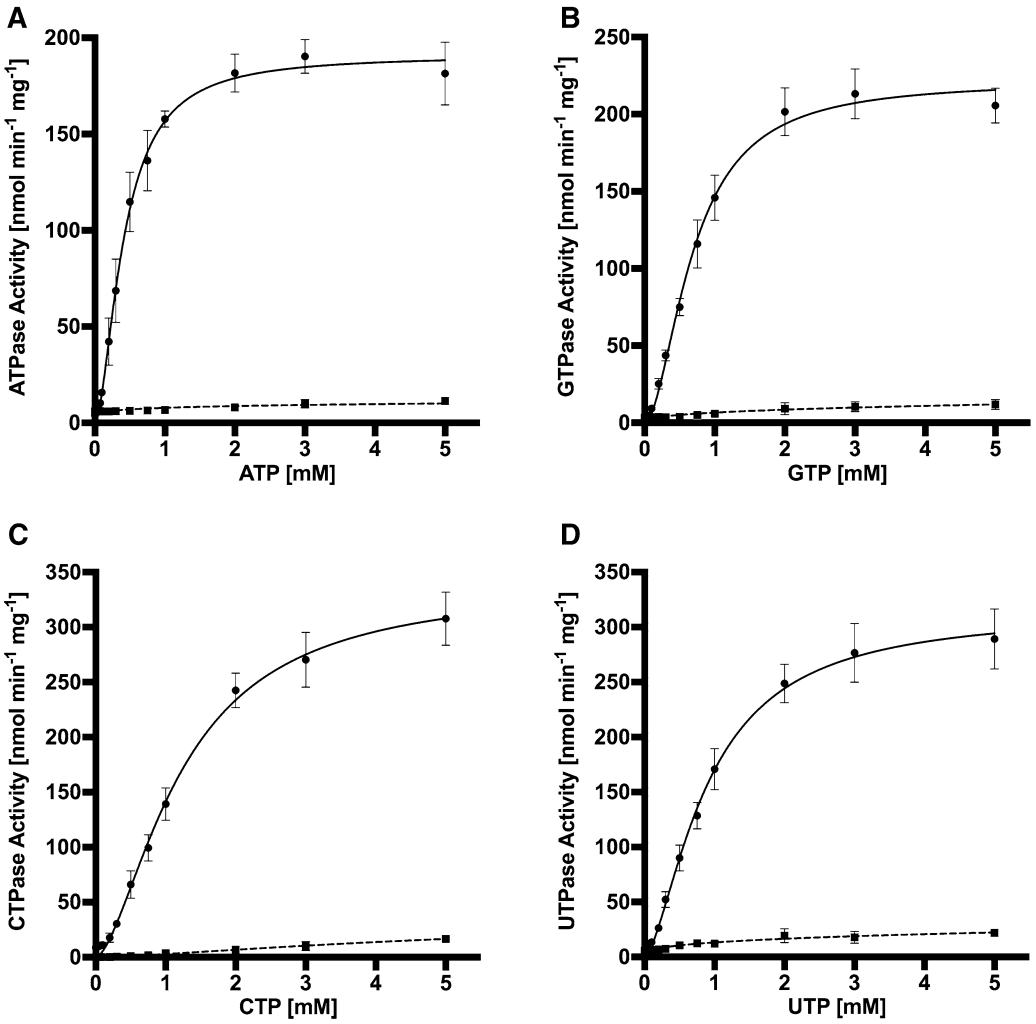

Figure 2. Kinetic measurement of *Sa*NsrF$_{WT}$ (black) and *Sa*NsrF$_{H202A}$ (dashed lines) NTPase Activity [nmol min^{-1} mg^{-1}] after 18 min of incubation. A concentration range of each NTP from 0 to 5 mM was applied on freshly purified *Sa*NsrF or *Sa*NsrF$_{H202A}$ (0.1 mg mL^{-1}; diluted in 100 mM HEPES at pH 7). The reaction was stopped after 18 min and dyed for 7 min. A sigmoidal fit was applied using GraphPad PRISM 8.3.0. (**A**) Kinetic parameters of *Sa*NsrF$_{WT}$ exposed to 0–5 mM ATP: v_{max}: 190.9 ± 10.0 [nmol min^{-1} mg^{-1}], h: 1.72 ± 0.27, k_{half}: 0.41 ± 0.05 [mM]. (**B**) Kinetic parameters of *Sa*NsrF$_{WT}$ exposed to 0–5 mM GTP: v_{max}: 221.6 ± 11.1 [nmol min^{-1} mg^{-1}], h: 1.82 ± 0.27, k_{half}: 0.69 ± 0.07 [mM]. (**C**) Kinetic parameters of *Sa*NsrF$_{WT}$ exposed to 0–5 mM CTP: v_{max}: 339.0 ± 30.4 [nmol min^{-1} mg^{-1}], h: 1.63 ± 0.53, k_{half}: 1.23 ± 0.20 [mM]. (**D**) Kinetic parameters of *Sa*NsrF exposed to 0–5 mM UTP: v_{max}: 314.8 ± 23.4 [nmol min^{-1} mg^{-1}], h: 1.55 ± 0.25, k_{half}: 0.90 ± 0.13 [mM]. All experiments have been performed in at least three biological replicates and are represented as means ± s.d.

NTP	V_{max}	k_{half}	h
ATP	190.9 ± 10.0	0.41 ± 0.05	1.72 ± 0.27
GTP	221.6 ± 11.1	0.69 ± 0.07	1.82 ± 0.27
CTP	339.0 ± 30.4	1.23 ± 0.20	1.63 ± 0.53
UTP	314.8 ± 23.4	0.90 ± 0.13	1.55 ± 0.25

Table 1. Kinetic parameters V_{max} [nmol min^{-1} mg^{-1}], k_{half} [mM] and the Hill-coefficient h resulting from different NTPs as a substrate for *Sa*NsrF$_{WT}$. All experiments have been performed in at least three biological replicates and are represented as means ± s.d.

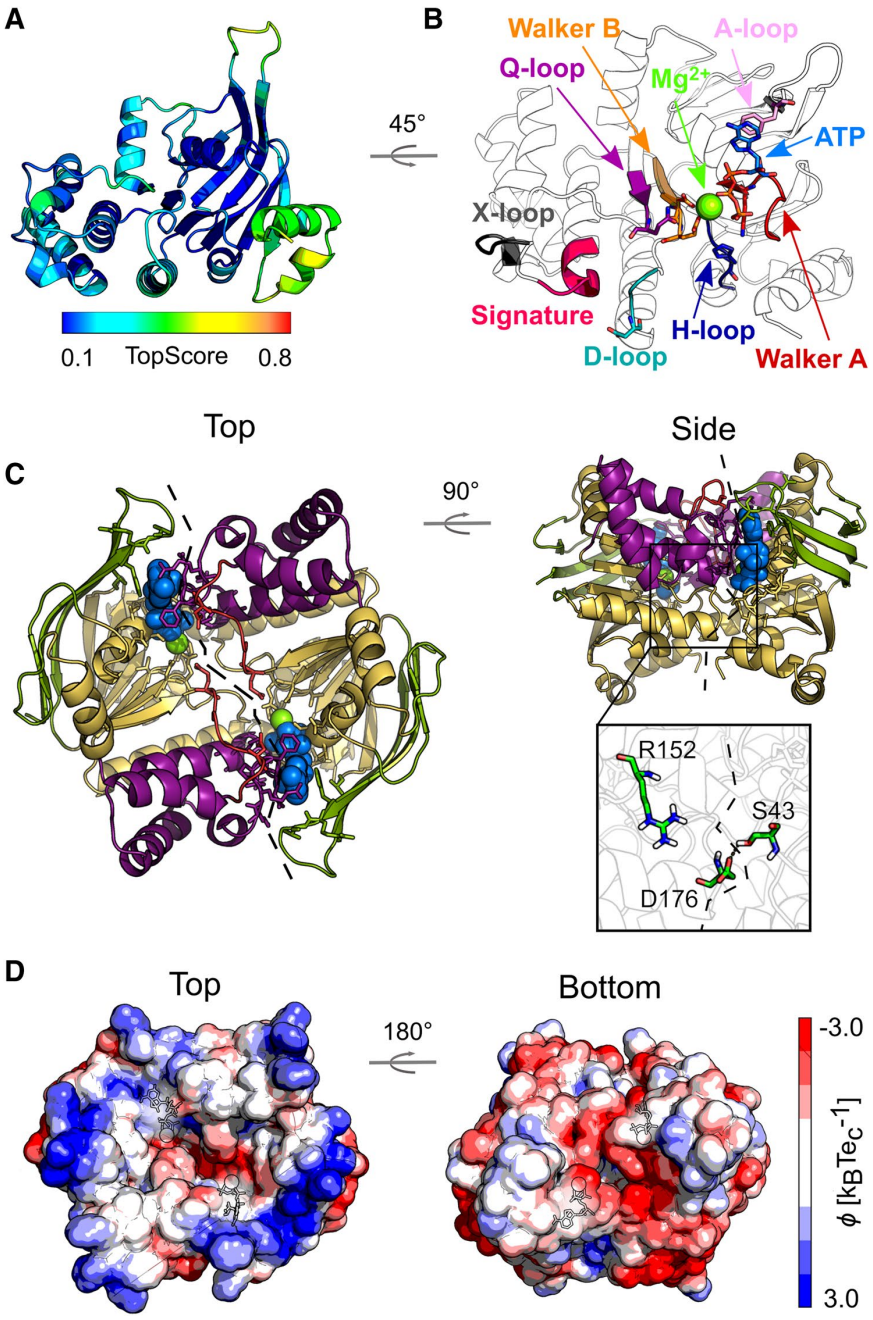

Figure 3. Homology models of *Sa*NsrF$_{WT}$ monomer (**A**, **B**) and dimer (**C**, **D**). (**A**) Structure colored according to the residue-wise TopScore. Green/yellow colors indicate regions with low residue-wise error (< 50%). (**B**) Zoom into the NBD-NBD interface with ATP and Mg^{2+} bound, highlighting the conserved motifs necessary for ATP binding and hydrolysis, and for NBD-NBD and NBD-TM communication. See Table S2 for the location of the conserved motifs in the primary sequence[22]. (**C**) Structure colored according to domain organization and zoom into the NBD–NBD interface, reporting the conserved residues used as restraints for protein–protein docking. The α-helical domain is shown in violet; the RecA-like domain, further subdivided into F1-type ATP binding core, antiparallel β subdomain, and γ-phosphate linker is colored respectively in yellow, green, and red. The bound ATP (blue) and Mg^{2+} (green) are shown in space-filling representation. The dashed line highlights the interface between subunits. (**D**) Electrostatic potential computed for the representative structure of the most populated cluster of conformations obtained by MD simulations. The color scale of the electrostatic potential ranges from − 3.0 (red) to + 3.0 (blue) $k_BTe_c^{-1}$; the potentials were computed with the Adaptive Poisson-Boltzmann Solver (APBS)[49].

calculated electrostatic potential shows a clear polarization (Fig. 3D) with positively charged residues (such as R and K) prevalent on the dimer's side oriented towards the membrane (named "top") and negatively charged residues (such as D and E) on the opposite side (named "bottom") in agreement with the expected topology.

Structural dynamics at the NBD–NBD interface and impact of the $SaNsrF_{H202A}$ substitution. The *Sa*NsrF models were subjected to all-atom MD simulations of in total 10 µs length to investigate the structural dynamics at the NDB-NDB interface and to highlight the impact of the H202A substitution on ATP/Mg^{2+} binding. The RMSD profiles for *Sa*$NsrF_{WT}$ and *Sa*$NsrF_{H202A}$ monomers (Fig. S2) reach almost immediately a plateau at ~ 4 Å, indicating that the overall structure is mostly invariant over simulation times of 0.5 µs for each replica. Additionally, the low variability of ATP/Mg^{2+} coordinates (Fig. S3A,B) suggests that the *Sa*$NsrF_{H202A}$ substitution does not impact ATP/Mg^{2+} binding, at least on the timescale of our simulations.

The RMSD profile for the *Sa*$NsrF_{WT}$ and *Sa*$NsrF_{H202A}$ dimers is mostly invariant (Fig. S4A) when the structures are superimposed onto the two subunits separately (red and blue lines). However, when the superimposition is done with respect to the least mobile regions in the whole dimer (black line), RMSD values reach ~ 6–9 Å in three out of five replicas for *Sa*$NsrF_{WT}$, indicating that the arrangement of the two subunits changes during the simulations. In particular, the interface between the subunits partially opens (Fig. S4B) up to ~ 25 Å (Fig. S5). The change of ATP molecule and Mg^{2+} ion positions relative to the protein is more marked for *Sa*$NsrF_{WT}$ dimer (Fig. S3). Interestingly, this is not happening in the *Sa*$NsrF_{H202A}$ variant, where the interface seems to be more stable.

In terms of structural mobility, the central region of *Sa*$NsrF_{WT}$ and *Sa*$NsrF_{H202A}$ (residues ~ 50–150) shows a different profile in monomers and dimers (Fig. 4). In monomers (Fig. 4A,B), this region is less mobile than in dimers (Fig. 4C,D), with RMSF values lower than 2 Å and up to 4 Å, respectively. Moreover, in the dimeric *Sa*$NsrF_{H202A}$ variant, this region is slightly less mobile than in *Sa*$NsrF_{WT}$. The residues of the central region are oriented towards the TM region of the transporter (Fig. 4E,D). In addition, after the alignment of *Sa*NsrF with NBDs of structures containing the TMD (PDB ID 5XU1, Fig. 4G), most of the residues of this central region are located at < 5 Å distance from the coupling helices (CH1, between TM2 and TM3, and C-terminal CH2) of the transporter, suggesting that this central region is involved in NBD-TMD communication (Fig. 4H). A similar result was found for the HlyB transporter[50], where the X-loop motif (corresponding to residues 137–142 in *Sa*NsrF, located in the central region) has been proposed to be an important part of the NBD-TMD communication. Even though we are considering an ATP-bound pre-hydrolysis state, *Sa*NsrF in the dimer seems to be generally more mobile than in the monomer, in agreement with the idea that a dimeric assembly is needed in order to perform its function.

H-bond analysis in *Sa*$NsrF_{WT}$ and *Sa*$NsrF_{H202A}$ dimers reveals that the number of H-bond interactions between *Sa*NsrF and the ligands (ATP molecules and magnesium ions) is on average higher in the case of the *Sa*$NsrF_{H202A}$ variant (Fig. 5A). This is due to the higher structural stability compared to *Sa*$NsrF_{WT}$. Besides the three residues used as restraints for protein–protein docking (S43–R152–D176), other residues contribute to the stability of the dimer with H-bond occupancies up to 70%, such as R13, T14, R15, E42, E144, and R178 (Fig. 5B,C). Surprisingly, the residue-wise H-bond occupancy in *Sa*$NsrF_{WT}$ is significantly higher ($p < 0.01$) for two specific H-bonds involving both side chains and backbone atoms (D136–R15 and R133–R15), although the interface of the *Sa*$NsrF_{WT}$ dimer is less structurally stable (see above). Indeed, in the initial dimeric model, these interactions are not present, but require the movement of one monomer to the other for them to form.

To conclude, the generated models show a high structural stability over the simulation lengths. In the dimers, the central region is more mobile than in the monomers; in *Sa*$NsrF_{WT}$, the interface between subunits is structurally less stable than in the *Sa*$NsrF_{H202A}$ variant. Since a shift of one monomer to the other is necessary for NDBs to perform their function, these results together suggest that the mutation *Sa*$NsrF_{H202A}$ impacts the structural dynamics at the *Sa*NsrF interface and not only the catalytic mechanism.

Small angle X-ray scattering. Unfortunately, we were not able to crystalize the *Sa*NsrF protein, although extensively tried. In order to experimentally validate this new model, we choose Small Angle X-Ray Scattering (SAXS) to compare the theoretical model with the experimental scattering (Fig. 6A) measured with the Xenocs Xeuss 2. Based on the experimental data, we calculated an ab initio model for *Sa*$NsrF_{WT}$ with the program GASBOR[51] and obtained a χ^2 value of 0.97. Superimposing the ab initio and the TopModel model reveals that the structure and the envelope obtained by the SAXS experiment overlap, but also a density tail at the C-terminus of *Sa*$NsrF_{WT}$ (Fig. 6B) that is not occupied by the model. Scrutinizing the templates used by TopModel[52] shows that this helical part (Fig. 6B, orange helix) is rather unstructured or even missing. This finding indicated that this region might be highly flexible in solution, thereby covering the available free space in the SAXS envelope (Fig. 6B, red helix). With the program CRYSOL[53] we compared the theoretical scattering curve obtained from the TopModel model against the experimental data. The resulting χ^2 value of 1.16 indicates a good agreement between the prediction and the experiment. We uploaded the SAXS data and the corresponding model of *Sa*NsrF to the Small Angle Scattering Biological Data Bank (SASBDB)[54,55] with the accession code SASDJR3.

Molecular docking of other NTPs. In order to rationalize the hydrolysis preference for ATP over other NTPs, we predicted the binding mode of these molecules in complex with the *Sa*$NsrF_{WT}$ dimer. Ten different pocket conformations, obtained from five equilibrated structures used also for MD simulations times two pockets each, were considered. When focusing on the configurations with lowest Coulomb (ecoul) and van der Waals (evdw) energies, ATP is slightly enriched compared to the other NTP (3 × ATP, 2 × UTP, 1 × CTP and 1 × GTP), suggesting that ATP binding is preferred due to enthalpic contributions to binding (Fig. 7A). Residues giving rise to this preference are those interacting with the nucleobase, namely F12, T49, A23 of one subunit and F143′ and

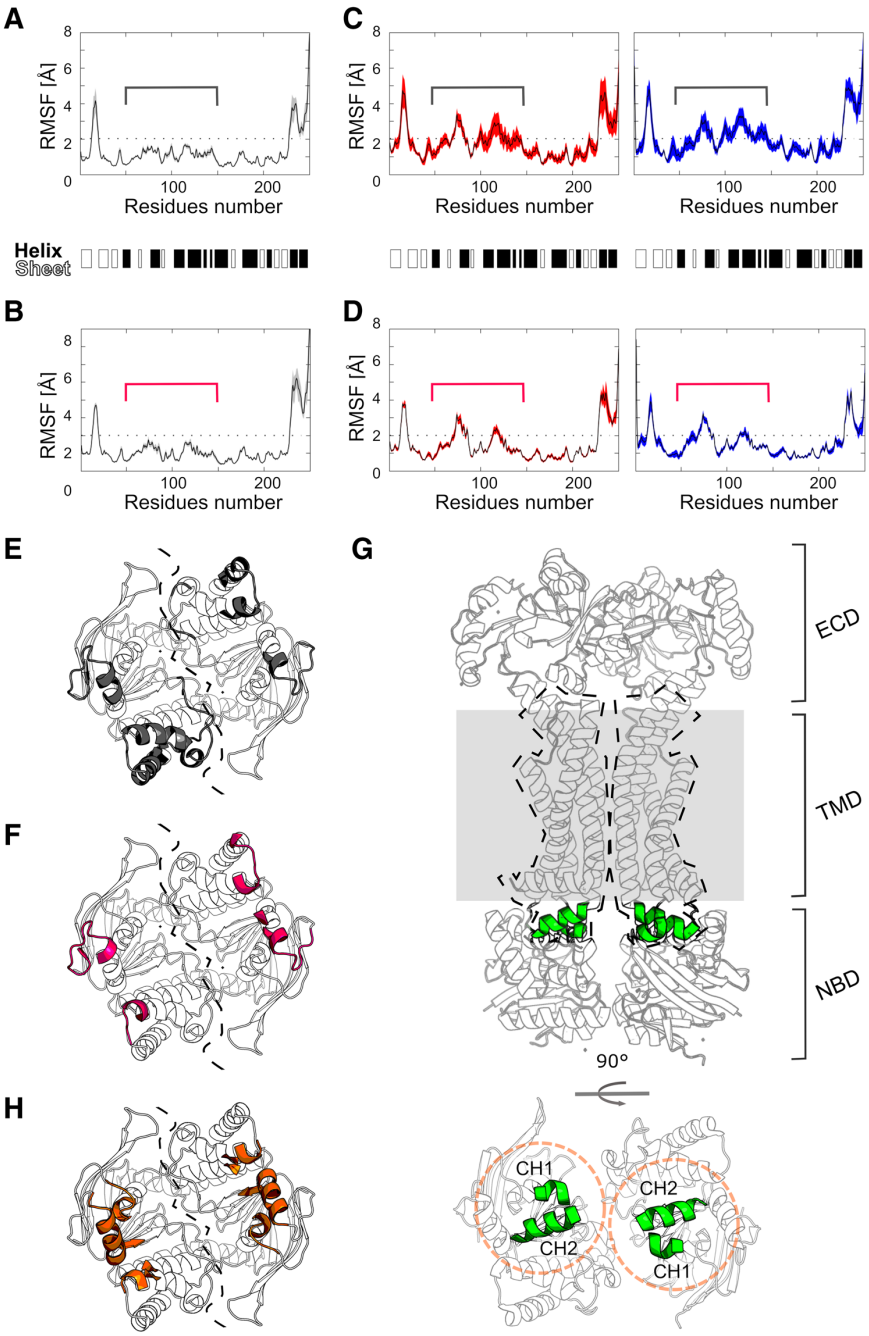

Figure 4. Structural mobility of the *Sa*NsrF$_{WT}$ and *Sa*NsrF$_{H202A}$ systems expressed as RMSF of Cα atoms. Before RMSF calculation, the structures were fitted onto the 15% least mobile residues, averaged over five MD simulation replicas. The variability between replicas is expressed as SEM and shown as colored area (grey for the monomers, red for chain A and blue for chain B). (**A**) *Sa*NsrF$_{WT}$ monomer. (**B**) *Sa*NsrF$_{H202}$ variant monomer. (**C**) *Sa*NsrF$_{WT}$ dimer. (**D**) *Sa*NsrF$_{H202}$ variant dimer. The secondary structure elements of the initial model are shown as black and white bands. The central region of *Sa*NsrF$_{H202}$ (residues ~ 50–150) is highlighted with brackets. Residues of the central region with RMSF > 2 Å are mapped onto the dimer structures. (**E**) For *Sa*NsrF$_{WT}$ (in grey) and (**F**) for *Sa*NsrF$_{H202}$ variant (in pink). The other two regions with RMSF > 2 Å (hairpin of the antiparallel β subdomain and the C-term) are not shown for clarity. The dashed line highlights the interface between subunits. (**G**) Structure of the MacAB-like transporter from *Streptococcus pneumoniae* (PDB ID 5XU1[45]) reported as comparison to highlight the expected orientation of the NBD to the TMD (shown as dashed shape), its coupling helices (CH1 and CH2, highlighted in green) and the membrane (as grey area). (**H**) After superimposition of the NBDs, regions of *Sa*NsrF located at < 5 Å from the coupling helices of the MacAB-like structure, and therefore likely involved in NBD-TMD communication, are highlighted in orange.

A

System	Replica	*Sa*NsrF$_A$-*Sa*NsrF$_B$	*Sa*NsrF-(ATP-Mg^{2+})
*Sa*NsrF$_{wt}$	I	6.29 (2.10)	15.54 (2.21)
	II	10.70 (3.12)	13.94 (2.05)
	III	8.07 (2.35)	15.19 (2.14)
	IV	9.02 (2.90)	13.24 (2.93)
	V	12.62 (3.20)	12.54 (2.05)
	All ± SEM	**9.34 ± 1.57**	**14.09 ± 1.15**
*Sa*NsrF$_{H202A}$	I	8.65 (2.39)	15.33 (2.05)
	II	9.51 (3.01)	14.64 (2.57)
	III	10.95 (2.85)	13.17 (2.41)
	IV	8.39 (2.34)	18.05 (2.39)
	V	18.05 (2.39)	18.66 (2.61)
	All ± SEM	**9.25 ± 1.30**	**15.97 ± 1.42**

**

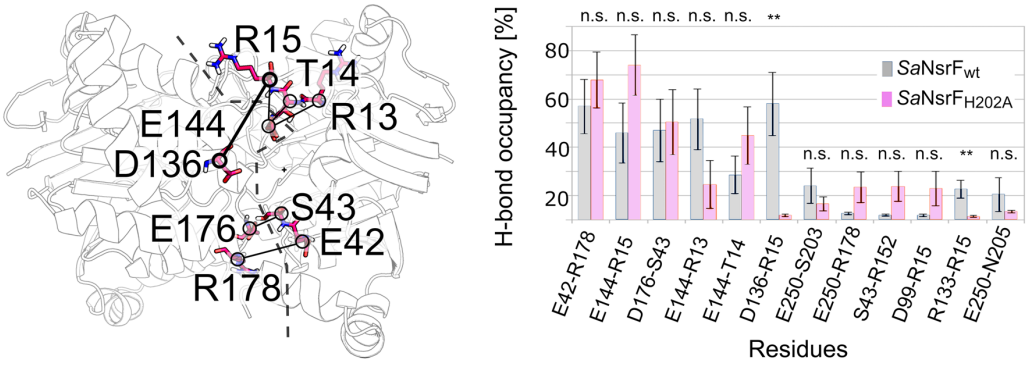

Figure 5. H-bond analysis in *Sa*NsrF$_{WT}$ and *Sa*NsrF$_{H202A}$ dimers. (**A**) The average number of H-bonds between the two proteins and between the protein and the ligands per MD replica. Standard deviations are reported in parentheses. For the numbers in bold, the SEM was computed according to $n = 5$. $^{**}p < 0.01$ according to a two-tailed *t*-test. (**B**) Residues in the interface that predominantly form H-bonds (occupancy > 20%). H-bonds are shown as lines connecting the Cα atoms of these residues. The dashed line highlights the interface between subunits. (**C**) H-bond occupancy for the most prevalent interactions (occupancy in at least one of the systems > 10%). Error bars are showing the SEM. $^{**}p < 0.01$ according to a two-tailed *t*-test for the comparison of *Sa*NsrF$_{WT}$ and *Sa*NsrF$_{H202A}$ variant; n.s.: not significant.

E144′ of the other (Fig. 7B). In particular, the phenylalanines are interacting with the nucleobase by π-π stacking interactions, and the amino groups of CTP and GTP form H-bonds with the backbone oxygen of F143′ and the carboxylate group of E144′, respectively. Since in ATP the amino group has the same orientation as in CTP, a similar kind of H-bond pattern can be expected.

Over respective pockets 1 or 2, which are not symmetric as described above, ATP shows the largest sums of Coulomb and van der Waals energies compared to the other NTPs (Fig. 7C), indicating strongest binding based on enthalpic components, which is in line with the biochemical data where ATP shows the lowest k_{half} value (Fig. 2 and Table 1).

Discussion

A rather novel family of ABC-transporters, the Bacitracin efflux (Bce) type transporters, have been identified to confer high-level resistance against bacitracin as well as against lantibiotics such as nisin and gallidermin in *Bacillus subtilis, Staphylococcus aureus,* and *Streptococcus agalactiae*[8,14,16,57–60]. These transporters have been rudimentarily characterized in vitro. We set out to characterize the NBD of the transporter *Sa*NsrFP; this transporter has been shown to be involved in lantibiotic resistance[8].

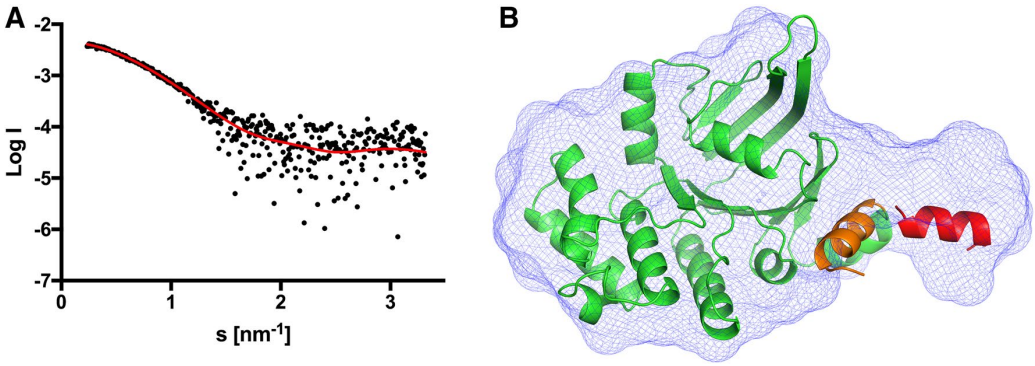

Figure 6. Comparison of the ab initio model with the homology model. (**A**) Experimental scattering data are shown as black dots and the ab initio model fit as red line. The intensity is displayed as a function of momentum transfer *s*. (**B**) Ab initio model of the *Sa*NsrF$_{WT}$. The volumetric envelope from *Sa*NsrF$_{WT}$, calculated from the scattering data using GASBOR[51], is shown by the blue mesh. The homology model of the *Sa*NsrF$_{WT}$ monomer (shown in green) was docked into the volumetric envelope using SUPCOMB[56]. Concerning the flexibility of the C-terminal helix (shown in orange), we show a possible, changed orientation of this helix in red.

We have purified and characterized the *Sa*NsrF$_{WT}$ and *Sa*NsrF$_{H202A}$ proteins regarding their ability of ATP hydrolysis. The results revealed that inorganic phosphate is only released in a pH range of 6–8, where an HEPES buffer at pH 7 was found to yield maximal ATPase activity. Interestingly, 20% difference could be found in a TRIS buffer system at the same pH (Fig S1A). Similar results were obtained by Zaitseva et al. examining the HlyB-NBD[36]. In that study, a correlation between the pH of 6 and the pK$_a$ values of the glutamate residue and/or the γ-phosphate of the nucleotide and between the pH of 8 and the pK$_a$ value of the conserved histidine bound in a salt bridge with the γ-phosphate was made. On that basis, the nucleophilic attack on the γ-phosphate is preceded, originating from a hydrolytic water molecule, which results in the cleavage of the γ-phosphate moiety[26,36,61]. Moreover, the importance of the conserved histidine could be confirmed since the *Sa*NsrF$_{H202A}$ variant was shown to be incapable of hydrolysing ATP. Here, the 'linchpin'-role during ATP-hydrolysis is conducted by the H-loop[22,36,38,62]. Also, this allows a possible explanation for the observed decrease of activity with increasing concentrations of NaCl (Fig. S1B). Since the conserved histidine is in contact with the γ-phosphate of the nucleotide by forming a salt bridge, rising salt concentration could disrupt this existing interaction. In contrast, a buffer system containing 300 mM of NaCl was used for protein storage, which indicates an inverse correlation between protein stability and activity at rising NaCl concentrations[63]. The incapability of *Sa*NsrF$_{H202A}$ to hydrolyse ATP supports in vivo studies where a loss of resistance against the lantibiotic nisin was observed when expressed in *L. lactis* bacterial cells[8].

Like many other NBDs, *Sa*NsrF was observed to be strictly dependent on its cofactor Mg^{2+}[39,64,65], because this is required as a Lewis acid in the catalytic cycle. Mg^{2+} is involved in proton abstraction from the nucleotide and the nucleophilic attack of the catalytic water, which results in the hydrolytic cleavage of its γ-phosphate[36].

Finally, we conducted kinetic measurements including all optimized parameters and the preference of *Sa*NsrF$_{WT}$ and *Sa*NsrF$_{H202A}$ for hydrolysing different NTPs. We propose that the main interaction of the nucleoside triphosphate and the protein occurs by π–π-stacking between the adenine moiety and F12 downstream of the Walker A motif (Fig. 3B,C) as also observed for other NBD's[22,24,25,30]. Also, Mg^{2+}, anchored to the protein through Asp and Glu residues of the Walker B motif, interacts with the phosphate region of ATP. The Walker A motif binds to the other side of the phosphate region (Fig. 3B).

Based on a comparison of docked binding poses of other NTPs, additional interacting residues were predicted (Fig. 7B). Amino group-containing NTPs (ATP, CTP and GTP) can form H-bonds with the backbone oxygen of F143′ and the carboxylate group of E144′, whereas purines in ATP and GTP form more extended π–π stacking interactions with F12 and F143′. ATP shows the largest sums of Coulomb and van der Waals energies compared to the other NTPs in either pocket of the NBD, in line with the biochemical data where ATP displayed the lowest k_{half} value (Fig. 2 and Table 1).

By comparing the measured kinetic parameters of each examined NTP, it becomes obvious that the reactions including UTP or CTP resulted in a significantly higher reaction velocity, respectively, when compared to ATP. Nevertheless, the CTPase and UTPase activities revealed noticeably high kinetic constants (k_{half}) as well. With regards to the substrate affinity represented by the k_{half} value, a minimum of 0.41 ± 0.05 mM was reached using ATP as a substrate, which signifies ATP as the most favoured of all four tested NTPs for *Sa*NsrF$_{WT}$. Hence, ATP has the highest affinity to *Sa*NsrF$_{WT}$ compared to the other examined NTPs, which corresponds with the physiological appearance in vivo of each NTP ([ATP] > [GTP] > [UTP] > [CTP]), which underlines that ATP is the preferred substrate for the protein[32,66–68]. Considering the physiology of purine (ATP, GTP) and pyrimidine (UTP, CTP) nucleotides, we concluded that the involved aromatic ring systems play a major role concerning the substrate affinity and stability of the protein-substrate-complex. Here, pyrimidine bases exhibit a smaller electron density that can be involved in π–π-stacking. Thus, dissociation of pyrimidine nucleotides from the enzyme occurs faster than purine nucleotides. By contrast, the stabilized protein–purine-complex is less liable

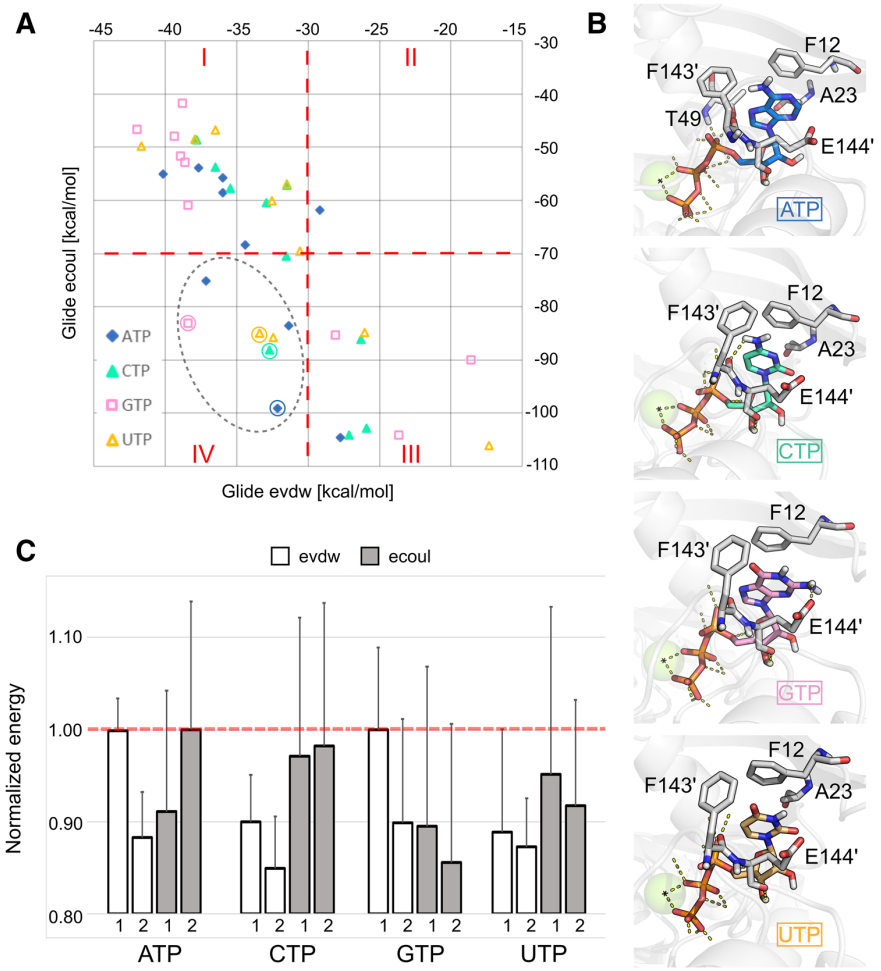

Figure 7. Molecular docking of other NTPs. (**A**) Scatterplot representing the Coulomb (ecoul) versus the van der Waals (evdw) energy terms of the docking score. Each data point represents an NTP configuration inside the two pockets of five different, equilibrated *Sa*NsrF structures. In quadrant IV, NTP configurations with respective lowest energies are circled. (**B**) Representative binding modes of NTPs, referring to the circled data points in section A. Residues at ≤ 4 Å from the nucleobases are shown in sticks and labelled. The Mg^{2+} ion is shown as a green sphere (**C**) Normalized average energy terms for pockets 1 and 2 of each SaNsrF complex. The error is reported as normalized SEM ($n = 5$).

to dissociation. Together, this may explain the small k_{half} values found for ATP and GTP and the high reaction velocities caused by a high turnover of CTP and UTP.

NBDs are assumed to share a large number of properties due to highly conserved sequences and specific motifs (see Fig. 3B,C and Table S2)[22–26,30]. The presence of a certain substrate such as ATP is supposed to induce a dimerization of the two NBD monomers in a typical head-to-tail formation, resulting in two ATP molecules in the dimer interface, sandwiched by the Walker A motif of one monomer and the signature motif of the other one as a cooperative process[22,24,25].

NBDs hydrolyse ATP, which drives substrate translocation by conformational changes of the TMD. In the case of the BceAB-type ABC transporter *Sa*NsrFP, the energy supply is provided by the BceA-domain *Sa*NsrF[16]. By employing SEC-MALS-coupled analysis we were able to confirm a monomeric state of $SaNsrF_{WT}$ and its variant $SaNsrF_{H202A}$ in solution since the measured molecular masses corresponded with the calculated values for each monomer. This agrees with the oligomeric state of other NBDs from other ABC transporter families in the absence of nucleotide[34–36].

Furthermore, this is in line with our SAXS data that allowed the construction of a volumetric envelope of the $SaNsrF_{WT}$ monomer. The experimental structure of *Sa*NsrF has not been published yet. Here, we generated a structural model using TopModel[52] based on five main templates 1F3O_A, 5XU1_B, 2PCL_A, 5GKO_A, 2OLJ_A (Fig. 3A, 6B). We compared this model with the volumetric envelope obtained from SAXS data, showing high

reliability and agreement with experimental data. It is striking that the density of the protein model is partly not occupied. A flexible C-terminus could be the reason, which would make a temporary fit of the versatile C-terminal helix to the proposed model possible. As for well-studied NBDs such as HisP, the modeled *Sa*NsrF dimer exhibits the typical head-to-tail formation including two sandwiched ATP molecules in the dimer interface between the Walker A motif of the first monomer and the C-loop of the second one[22,24,25,30]. Therefore, the *Sa*NsrF protein shares many structural similarities with other known NBDs. As the γ-phosphate moiety of ATP was predicted to be in close proximity of the conserved histidine (H-loop) and the cofactor Mg^{2+}, one can deduce a consensus with the hypothesis of the H-loop acting as a sensor, whereas the cofactor is involved in hydrolytic cleavage while being coordinated by the Walker B motif (Fig. 3B,C)[22,23,26,28]. Furthermore, in *Sa*NsrF$_{WT}$, the interface between subunits is structurally less stable than in *Sa*NsrF$_{H202A}$. Since a shift of one monomer to the other is necessary for NDBs to perform their function, these results suggest that the substitution *Sa*NsrF$_{H202A}$ impacts the structural dynamics at the *Sa*NsrF interface and not only the catalytic mechanism.

Clearly, the *Sa*NsrF protein represent an isolated NBD and we do not know if the kinetic correspond to the ATP hydrolysis that will occur in the presence of the transmembrane protein *Sa*NsrP. However, when comparing the data with known NBDs which has been described before in the presence and absence of the transmembrane segment it can be observed that v_{max} might be changed, the k_m values however remains very similar. For example the ATP hydrolysis kinetics have been described for the HlyB NBD as well as for the purified full length transporter in detergent solution[26,36,38,43,69]. Here the NBD showed a v_{max} of 200 nmol min^{-1} mg^{-1} with a k_m value of 0.31 where as the full length transporter displayed a lower v_{max} of 8.1 nmol min^{-1} mg^{-1} with a k_m value of 0.36. This reduction is likely due to the detergent, which is present to keep the HlyB transporter in solution. Important, however is that in both cases the kinetic displayed cooperativity (Hill coefficient > 1) as in the case of *Sa*NsrF and the corresponding histidine mutation also resulted in an inactive protein. This shows that our NTP analysis of the *Sa*NsrF will likely be similar even when the TMD *Sa*NsrP is present. The same observations were found for the nisin transporter NisT from *L. lactis*[70] and the nukacin ISK-1 transporter NukT from *Staphylococcus arneri* ISK-1[71] albeit in detergent solution.

In summary, the experiments revealed the first detailed insights into biochemical properties of the BceA domain of the BceAB-type ABC transporter *Sa*NsrFP. We showed that *Sa*NsrF$_{WT}$ and its variant *Sa*NsrF$_{H202A}$ exist as monomers in solution and determined several physiological and structural properties of the protein by evaluating its ATPase activity in comprehensive in vitro studies and molecular modelling and simulations. Hence, this study contributes to the mechanistic and structural understanding of the BceAB-type ABC transporter family, which opens up the possibility to pharmacologically target this family in order to combat multidrug-resistant species in the long run. It further confirms in vivo data where the H202A variant of *Sa*NsrF displayed a loss in the activity, which now can be pinpointed to a lack of ATP hydrolysis, and shows that this variant can well serve as a negative control in studies concerning BceAB type transporters since the histidine is conserved throughout the sequence of this family.

Materials and methods

Expression of SaNsrF$_{WT}$ and SaNsrF$_{H202A}$. *E. coli* BL21 (DE3) strains were transformed via heat shock method[72] with pET-16b-NHis$_{10}$-*Sa*NsrF$_{WT}$ or pET-16b-NHis$_{10}$-*Sa*NsrF$_{H202A}$, respectively. Precultures were selectively grown with 20 µg mL^{-1} ampicillin at 37 °C and 180 rpm overnight. Lysogeny Broth (LB) medium was pre-incubated with 20 µg mL^{-1} ampicillin and inoculated with the respective preculture to an OD_{600} of 0.1. The cultures were grown to an OD_{600} of 0.4 at 37 °C and 180 rpm whereupon the temperature was reduced to 18 °C. Protein expression was induced by the addition of 1 mM IPTG at an OD_{600} of 0.8 and the cultures were further grown overnight.

Protein purification. *Sa*NsrF$_{WT}$ and *Sa*NsrF$_{H202A}$ were purified using Immobilized Metal Ion Chromatography (IMAC). Therefore, a 5 mL HiTrap Chelating HP column, loaded with Zn^{2+}, was equilibrated with low IMAC-buffer (100 mM HEPES at pH 8, 300 mM NaCl, 20% glycerol). Protein elution was undertaken with the high IMAC-buffer (low IMAC-buffer plus 125 mM histidine). A washing step of 40-percent high IMAC-buffer was introduced before. The concentrated eluted proteins were then injected onto a Superdex 75 16/60 size exclusion column at a flow rate of 0.5 mL min^{-1}, pre-equilibrated with SEC buffer (100 mM HEPES at pH 8, 300 mM NaCl, 20% glycerol). Protein eluates were collected and stored at 4 °C.

ATPase activity assay. The ATPase activity of *Sa*NsrF$_{WT}$ and *Sa*NsrF$_{H202A}$ (diluted in 100 mM HEPES at pH 8, 100 mM NaCl) was examined by the Malachite Green Phosphate Assay at a protein concentration of 0.1 mg mL^{-1} that was initially undertaken at room temperature (20 °C). Several parameters were screened to determine the optimal buffer and temperature conditions for the protein activity (see Supplementary Information).

Kinetic measurements for *Sa*NsrF$_{WT}$ and *Sa*NsrF$_{H202A}$ were performed under the influence of NTP (ATP, GTP, CTP, UTP) with concentrations ranging from 0 to 5 mM.

Therefore, the kinetics were fitted using the Hill equation:

$$Y = \frac{v_{max} \times X^h}{\left(k_{half}^h + X^h\right)}.$$

Y: ATPase activity [nmol min^{-1} mg^{-1}], X: substrate concentration [mM], k_{half}: substrate concentration at half-maximal reaction velocity [mM], h: Hill coefficient.

All shown data are representing the average of a triple evaluation at least, with the standard deviation reported as errors.

Small angle X-ray scattering (SAXS). We collected all SAXS data on our Xeuss 2.0 Q-Xoom system from Xenocs, equipped with a PILATUS 3 R 300 K detector (Dectris) and a GENIX 3D CU Ultra Low Divergence x-ray beam delivery system (Xenocs). The chosen sample to detector distance for the experiment was 0.55 m, results in an achievable q-range of 0.18–6 nm^{-1}. All measurements were performed at 15 °C with protein concentrations between 0.5 and 4.2 mg mL^{-1}. Samples were injected in the Low Noise Flow Cell (Xenocs) via autosampler. For each sample, twelve frames with an exposer time of ten minutes were collected. By comparing these frames, we excluded the possibility of aggregation and radiation damage during the measurement. Data were scaled to absolute intensity against water. All used programs for data processing were part of the ATSAS Software package (Version 3.0.1), available on the EMBL website[73]. Primary data reduction was performed with the program PRIMUS[74]. With the Guinier approximation we determined the forward scattering $I(0)$ and the radius of gyration (Rg)[75]. The program GNOM was used to estimate the maximum particle dimension (D_{max}) with the pair distribution function $p(r)$[76]. Low resolution ab initio models were calculated using GASBOR[51]. The superposition of a predicted *Sa*NsrF model (see below) was done using the program SUPCOMB[56].

Structural models of SaNsrF complexes. As an experimental *Sa*NsrF structure is not available, a homology model was constructed using the template-based protein structure prediction program TopModel[52] and the $SaNsrF_{WT}$ sequence as input (NCBI Reference Sequence: WP_000923535.1). In order to build a *Sa*NsrF model arranged in a dimeric assembly with substrate (ATP) and cofactor (Mg^{2+}) bound, starting from the $SaNsrF_{WT}$ monomer in the *apo* state, a search for sequence similarity and structural properties was performed on the Protein Data Bank. The results were filtered according to the following criteria: sequence identity ≥ 33% and E-value cutoff 0.001 as determined by BLAST[77]; oligomeric state equals 2; sequence length of 250 ± 50 residues; resolution ≤ 2 Å. Out of six results, only one (PDB ID: 1L2T[28]) is crystallized as a functionally active "ATP sandwich" symmetrical dimer and was therefore used as a reference. Since ATP is bound at the interface of the dimer and its binding is influenced by both protein subunits, both protein–ligand and protein–protein docking would be particularly challenging in this case. Hence, we constructed first the $SaNsrF_{WT}$ dimer in the *apo* form and the ATP/Mg^{2+}-bound form subsequently.

To do so, protein–protein docking was performed with the program HADDOCK[78,79], using distances between respective three residues that bridge the two subunits together with H-bond interactions as restraints (S40/S43, R153/R152 and D177/D176, for PDB ID 1L2T/$SaNsrF_{WT}$ sequences, respectively). The most similar docking solution to the reference PDB ID 1L2T was used for further modeling steps.

Both, $SaNsrF_{WT}$ monomer and dimer structures were preprocessed with the Protein Preparation Wizard[80] of Schrödinger's Maestro Suite. Since the residues at the binding sites are highly conserved, ATP and Mg^{2+} are considered to bind in a very similar way as in PDB ID 1L2T. Thus, their coordinates were copied from the reference into the $SaNsrF_{WT}$ model after alignment to one protein subunit. Residues located ≤ 5 Å away from the ATP molecules were energy-minimized using the OPLS 2005 force field[81] with standard cutoff values for van der Waals, electrostatic, and H-bond interactions, until the average RMSD of non-hydrogen atoms reaches 0.30 Å. Bond orders as well as missing hydrogen atoms were assigned, and the H-bond network was optimized. Finally, residue 202 was substituted to construct the $SaNsrF_{H202A}$ variant of the monomer and dimer.

Molecular dynamics simulations. In order to validate the modeled protein–protein interface and the ATP binding mode, and to investigate the impact of the $SaNsrF_{H202A}$ substitution on structural dynamics, a set of MD simulations was performed using Amber 2019[82]. Four different ATP/Mg^{2+}-bound *Sa*NsrF systems were prepared for this with the LEaP program[83]: monomer and dimer, both for $SaNsrF_{WT}$ and $SaNsrF_{H202A}$.

After establishing charge neutrality by adding sodium counter ions, each system was placed in a truncated octahedral box of TIP3P[84] water with a distance of the nearest atom to the border of the box of ≥ 11 Å. Structural relaxation, thermalization, and production runs of MD simulations were conducted with pmemd.cuda[85] using the ff14SB force field[86] for the protein, Joung-Cheatham parameters[87] for ions, and available ATP parameters[88]. For each starting complex, five independent replicas of 500 ns length each were performed, resulting in a cumulative simulation time of 10 µs. In order to set up independent replicas and obtain slightly different starting structures, the target temperature was set to different values during thermalization (299.8 K, 299.9 K, 300.0 K, 300.1 K, 300.2 K and 300.3 K). A detailed description of the thermalization protocol can be found elsewhere[89]. The analysis of the MD trajectories was carried out with cpptraj[90] on snapshots extracted every 1 ns. All the MD-generated conformations were clustered applying a hierarchical agglomerative approach and an RMSD cutoff value of 4 Å. The representative structure of the $SaNsrF_{WT}$ monomer was compared to the experimentally determined SAXS density.

The representative structure of the most populated cluster for the $SaNsrF_{WT}$ dimer was used to calculate the electrostatic potential with the Adaptive Poisson-Boltzmann Solver (APBS) software package[49] as implemented in PyMOL[91]. Dielectric constants (ε) of 2.0 and 78.0 were used, respectively, for the protein and for water, and the concentration of monovalent cations and anions was set to 0.15 M.

To measure structural mobility, we computed the residue-wise root-mean-square fluctuation (RMSF) of backbone atoms. Structural changes over time, both for the *apo* *Sa*NsrF proteins and the ATP/Mg^{2+}-bound form, were detected calculating the root-mean-square deviation of atomic positions (RMSD) compared to the initial structure. To describe the changes occurring at the level of the interface, we performed two analyses: (I) measurement of the distance between the center of mass of two residues located in opposite subunits at the center of the interface (S43 and S146); (II) H-bond analysis (i) in terms of the total number of interactions between

two subunits ($SaNsrF_A$–$SaNsrF_B$) and between protein and ligands ($SaNsrF$-(ATP-Mg^{2+})) and ii) residue-wise H-bound occupancy between residues of the two subunits ($SaNsrF_A$–$SaNsrF_B$), allowing to identify which residues perform more frequent H-bonds throughout the simulations. For this analysis, only H-bonds with the following criteria were considered: occupancy between specific donor and acceptor > 1%; H-bond present in at least two replicas of the same system; H-bonds between two residues with residue-wise occupancy > 10% in at least one system.

Molecular docking of other NTPs. To predict the binding mode of other NTPs in complex with the $SaNsrF_{WT}$ dimer, molecular docking was performed. The starting points for these calculations were the five structures resulting from thermalization and equilibration steps, then used also for independent MD simulations replicas (production).

First, for each binding site a cubic grid of 20 Å length centered on the respective ATP molecule was built in the Maestro platform[92], for a total of 10 different grids. Then, starting from the ATP structures, other NTPs were built (GTP, CTP and UTP) by modifying the nucleobase. The generated conformations were refined and scored with the Glide-Extra precision (XP) mode of Glide[93]. Only the best solution for each NTP in each grid was considered. The Coulomb interaction energy (ecoul) and the van der Waals energy (evdw), components of the XP GlideScore scoring function, were computed, and used to describe the enthalpic contribution of binding.

Data availability

We upload the SAXS data and the corresponding model of *Sa*NsrF to the Small Angle Scattering Biological Data Bank (SASBDB)[54,55], with the accession code SASDJR3.

Received: 19 July 2020; Accepted: 27 August 2020
Published online: 16 September 2020

References

1. Gould, K. Antibiotics: from prehistory to the present day. *J. Antimicrob. Chemother.* **71**, 572–575. https://doi.org/10.1093/jac/dkv484 (2016).
2. Meade, E., Slattery, M. A. & Garvey, M. Bacteriocins, potent antimicrobial peptides and the fight against multi drug resistant species: resistance is futile?. *Antibiotics* https://doi.org/10.3390/antibiotics9010032 (2020).
3. Cotter, P. D., Hill, C. & Ross, R. P. Bacterial lantibiotics: strategies to improve therapeutic potential. *Curr. Protein Pept. Sci.* **6**, 61–75. https://doi.org/10.2174/1389203053027584 (2005).
4. Clemens, R., Zaschke-Kriesche, J., Khosa, S. & Smits, S. H. J. Insight into two ABC transporter Families involved in lantibiotic resistance. *Front. Mol. Biosci.* **4**, 91. https://doi.org/10.3389/fmolb.2017.00091 (2017).
5. Bierbaum, G. & Sahl, H. G. Lantibiotics: mode of action, biosynthesis and bioengineering. *Curr. Pharm. Biotechnol.* **10**, 2–18. https://doi.org/10.2174/138920109787048616 (2009).
6. Chatterjee, C., Paul, M., Xie, L. & van der Donk, W. A. Biosynthesis and mode of action of lantibiotics. *Chem. Rev.* **105**, 633–684. https://doi.org/10.1021/cr030105v (2005).
7. Jabes, D. *et al.* Efficacy of the new lantibiotic NAI-107 in experimental infections induced by multidrug-resistant Gram-positive pathogens. *Antimicrob. Agents Chemother.* **55**, 1671–1676. https://doi.org/10.1128/AAC.01288-10 (2011).
8. Reiners, J. *et al.* The N-terminal region of nisin is important for the BceAB-type ABC transporter NsrFP from *Streptococcus agalactiae* COH1. *Front. Microbiol.* **8**, 1643. https://doi.org/10.3389/fmicb.2017.01643 (2017).
9. Malin, J. J. & de Leeuw, E. Therapeutic compounds targeting Lipid II for antibacterial purposes. *Infect. Drug Resist.* **12**, 2613–2625. https://doi.org/10.2147/IDR.S215070 (2019).
10. Breukink, E. *et al.* Use of the cell wall precursor lipid II by a pore-forming peptide antibiotic. *Science* **286**, 2361–2364. https://doi.org/10.1126/science.286.5448.2361 (1999).
11. Hasper, H. E., de Kruijff, B. & Breukink, E. Assembly and stability of nisin-lipid II pores. *Biochemistry* **43**, 11567–11575. https://doi.org/10.1021/bi049476b (2004).
12. AlKhatib, Z. *et al.* The C-terminus of nisin is important for the ABC transporter NisFEG to confer immunity in *Lactococcus lactis*. *Microbiologyopen* **3**, 752–763. https://doi.org/10.1002/mbo3.205 (2014).
13. Draper, L. A., Cotter, P. D., Hill, C. & Ross, R. P. Lantibiotic resistance. *Microbiol. Mol. Biol. Rev.* **79**, 171–191. https://doi.org/10.1128/MMBR.00051-14 (2015).
14. Ohki, R. *et al.* The BceRS two-component regulatory system induces expression of the bacitracin transporter, BceAB, Bacillus subtilis. *Mol. Microbiol.* **49**, 1135–1144. https://doi.org/10.1046/j.1365-2958.2003.03653.x (2003).
15. Podlesek, Z. *et al. Bacillus licheniformis* bacitracin-resistance ABC transporter: relationship to mammalian multidrug resistance. *Mol. Microbiol.* **16**, 969–976. https://doi.org/10.1111/j.1365-2958.1995.tb02322.x (1995).
16. Khosa, S., AlKhatib, Z. & Smits, S. H. NSR from *Streptococcus agalactiae* confers resistance against nisin and is encoded by a conserved nsr operon. *Biol. Chem.* **394**, 1543–1549. https://doi.org/10.1515/hsz-2013-0167 (2013).
17. Khosa, S. *et al.* Structural basis of lantibiotic recognition by the nisin resistance protein from *Streptococcus agalactiae*. *Sci. Rep.* **6**, 18679. https://doi.org/10.1038/srep18679 (2016).
18. Khosa, S., Hoeppner, A., Gohlke, H., Schmitt, L. & Smits, S. H. Structure of the response regulator NsrR from *Streptococcus agalactiae*, which is involved in lantibiotic resistance. *PLoS ONE* **11**, e0149903. https://doi.org/10.1371/journal.pone.0149903 (2016).
19. Kerr, I. D. Structure and association of ATP-binding cassette transporter nucleotide-binding domains. *Biochim. Biophys. Acta* **1561**, 47–64. https://doi.org/10.1016/s0304-4157(01)00008-9 (2002).
20. Lawson, J., O'Mara, M. L. & Kerr, I. D. Structure-based interpretation of the mutagenesis database for the nucleotide binding domains of P-glycoprotein. *Biochim. Biophys. Acta* **1778**, 376–391. https://doi.org/10.1016/j.bbamem.2007.10.021 (2008).
21. Walker, J. E., Saraste, M., Runswick, M. J. & Gay, N. J. Distantly related sequences in the alpha- and beta-subunits of ATP synthase, myosin, kinases and other ATP-requiring enzymes and a common nucleotide binding fold. *EMBO J.* **1**, 945–951 (1982).
22. Szollosi, D., Rose-Sperling, D., Hellmich, U. A. & Stockner, T. Comparison of mechanistic transport cycle models of ABC exporters. *Biochim. Biophys. Acta Biomembr.* **818–832**, 2018. https://doi.org/10.1016/j.bbamem.2017.10.028 (1860).
23. Schmitt, L., Benabdelhak, H., Blight, M. A., Holland, I. B. & Stubbs, M. T. Crystal structure of the nucleotide-binding domain of the ABC-transporter haemolysin B: identification of a variable region within ABC helical domains. *J. Mol. Biol.* **330**, 333–342. https://doi.org/10.1016/s0022-2836(03)00592-8 (2003).
24. Schmitt, L. & Tampe, R. Structure and mechanism of ABC transporters. *Curr. Opin. Struct. Biol.* **12**, 754–760. https://doi.org/10.1016/s0959-440x(02)00399-8 (2002).
25. Wilkens, S. Structure and mechanism of ABC transporters. *F1000Prime Rep* **7**, 14. https://doi.org/10.12703/P7-14 (2015).

26. Hanekop, N., Zaitseva, J., Jenewein, S., Holland, I. B. & Schmitt, L. Molecular insights into the mechanism of ATP-hydrolysis by the NBD of the ABC-transporter HlyB. *FEBS Lett.* **580**, 1036–1041. https://doi.org/10.1016/j.febslet.2005.11.012 (2006).
27. Schmees, G., Stein, A., Hunke, S., Landmesser, H. & Schneider, E. Functional consequences of mutations in the conserved "signature sequence" of the ATP-binding-cassette protein MalK. *Eur J. Biochem.* **266**, 420–430. https://doi.org/10.1046/j.1432-1327.1999.00871.x (1999).
28. Smith, P. C. *et al.* ATP binding to the motor domain from an ABC transporter drives formation of a nucleotide sandwich dimer. *Mol. Cell.* **10**, 139–149 (2002).
29. Chen, J., Lu, G., Lin, J., Davidson, A. L. & Quiocho, F. A. A tweezers-like motion of the ATP-binding cassette dimer in an ABC transport cycle. *Mol. Cell.* **12**, 651–661. https://doi.org/10.1016/j.molcel.2003.08.004 (2003).
30. Locher, K. P. Structure and mechanism of ABC transporters. *Curr. Opin. Struct. Biol.* **14**, 426–431. https://doi.org/10.1016/j.sbi.2004.06.005 (2004).
31. Szollosi, D., Szakacs, G., Chiba, P. & Stockner, T. Dissecting the forces that dominate dimerization of the nucleotide binding domains of ABCB1. *Biophys. J.* **114**, 331–342. https://doi.org/10.1016/j.bpj.2017.11.022 (2018).
32. Wagner, M., Smits, S. H. J. & Schmitt, L. In vitro NTPase activity of highly purified Pdr5, a major yeast ABC multidrug transporter. *Sci. Rep.* **9**, 7761. https://doi.org/10.1038/s41598-019-44327-8 (2019).
33. Sahin, E. & Roberts, C. J. Size-exclusion chromatography with multi-angle light scattering for elucidating protein aggregation mechanisms. *Methods Mol. Biol.* **899**, 403–423. https://doi.org/10.1007/978-1-61779-921-1_25 (2012).
34. Greller, G., Horlacher, R., DiRuggiero, J. & Boos, W. Molecular and biochemical analysis of MalK, the ATP-hydrolyzing subunit of the trehalose/maltose transport system of the hyperthermophilic archaeon *Thermococcus litoralis*. *J. Biol. Chem.* **274**, 20259–20264. https://doi.org/10.1074/jbc.274.29.20259 (1999).
35. Nikaido, K., Liu, P. Q. & Ames, G. F. Purification and characterization of HisP, the ATP-binding subunit of a traffic ATPase (ABC transporter), the histidine permease of *Salmonella typhimurium*. Solubility, dimerization, and ATPase activity. *J. Biol. Chem.* **272**, 27745–27752. https://doi.org/10.1074/jbc.272.44.27745 (1997).
36. Zaitseva, J. *et al.* Functional characterization and ATP-induced dimerization of the isolated ABC-domain of the haemolysin B transporter. *Biochemistry* **44**, 9680–9690. https://doi.org/10.1021/bi0506122 (2005).
37. Kolaczkowski, M., Sroda-Pomianek, K., Kolaczkowska, A. & Michalak, K. A conserved interdomain communication pathway of pseudosymmetrically distributed residues affects substrate specificity of the fungal multidrug transporter Cdr1p. *Biochim Biophys Acta* **479–490**, 2013. https://doi.org/10.1016/j.bbamem.2012.10.024 (1828).
38. Zaitseva, J., Jenewein, S., Jumpertz, T., Holland, I. B. & Schmitt, L. H662 is the linchpin of ATP hydrolysis in the nucleotide-binding domain of the ABC transporter HlyB. *EMBO J.* **24**, 1901–1910. https://doi.org/10.1038/sj.emboj.7600657 (2005).
39. Zhou, Y., Ojeda-May, P. & Pu, J. H-loop histidine catalyzes ATP hydrolysis in the *E. coli* ABC-transporter HlyB. *Phys Chem Chem Phys* **15**, 15811–15815. https://doi.org/10.1039/c3cp50965f (2013).
40. Lagedroste, M., Reiners, J., Smits, S. H. J. & Schmitt, L. Systematic characterization of position one variants within the lantibiotic nisin. *Sci. Rep.* **9**, 935. https://doi.org/10.1038/s41598-018-37532-4 (2019).
41. Davidson, A. L., Laghaeian, S. S. & Mannering, D. E. The maltose transport system of *Escherichia coli* displays positive cooperativity in ATP hydrolysis. *J. Biol. Chem.* **271**, 4858–4863 (1996).
42. Senior, A. E. & Bhagat, S. P-glycoprotein shows strong catalytic cooperativity between the two nucleotide sites. *Biochemistry* **37**, 831–836. https://doi.org/10.1021/bi9719962 (1998).
43. Zaitseva, J. *et al.* A structural analysis of asymmetry required for catalytic activity of an ABC-ATPase domain dimer. *EMBO J.* **25**, 3432–3443. https://doi.org/10.1038/sj.emboj.7601208 (2006).
44. Okada, U. *et al.* Crystal structure of tripartite-type ABC transporter MacB from *Acinetobacter baumannii*. *Nat. Commun.* **8**, 1336. https://doi.org/10.1038/s41467-017-01399-2 (2017).
45. Yang, H. B. *et al.* Structure of a MacAB-like efflux pump from *Streptococcus pneumoniae*. *Nat. Commun.* **9**, 196. https://doi.org/10.1038/s41467-017-02741-4 (2018).
46. Mulnaes, D. & Gohlke, H. TopScore: using deep neural networks and large diverse data sets for accurate protein model quality assessment. *J. Chem. Theory. Comput.* **14**, 6117–6126. https://doi.org/10.1021/acs.jctc.8b00690 (2018).
47. Mariani, V., Biasini, M., Barbato, A. & Schwede, T. lDDT: a local superposition-free score for comparing protein structures and models using distance difference tests. *Bioinformatics* **29**, 2722–2728. https://doi.org/10.1093/bioinformatics/btt473 (2013).
48. Ishii, S., Yano, T., Okamoto, A., Murakawa, T. & Hayashi, H. Boundary of the nucleotide-binding domain of *Streptococcus* ComA based on functional and structural analysis. *Biochemistry* **52**, 2545–2555. https://doi.org/10.1021/bi3017069 (2013).
49. Baker, N. A., Sept, D., Joseph, S., Holst, M. J. & McCammon, J. A. Electrostatics of nanosystems: application to microtubules and the ribosome. *Proc. Natl. Acad. Sci. USA* **98**, 10037–10041. https://doi.org/10.1073/pnas.181342398 (2001).
50. Damas, J. M., Oliveira, A. S., Baptista, A. M. & Soares, C. M. Structural consequences of ATP hydrolysis on the ABC transporter NBD dimer: molecular dynamics studies of HlyB. *Protein Sci.* **20**, 1220–1230. https://doi.org/10.1002/pro.650 (2011).
51. Svergun, D. I., Petoukhov, M. V. & Koch, M. H. Determination of domain structure of proteins from X-ray solution scattering. *Biophys J* **80**, 2946–2953. https://doi.org/10.1016/S0006-3495(01)76260-1 (2001).
52. Mulnaes, D. *et al.* TopModel: template-based protein structure prediction at low sequence identity using top-down consensus and deep neural networks. *J. Chem. Theory Comput.* **16**, 1953–1967. https://doi.org/10.1021/acs.jctc.9b00825 (2020).
53. Svergun, D., Barberato, C. & Koch, M. H. J. CRYSOL: a program to evaluate x-ray solution scattering of biological macromolecules from atomic coordinates. *J. Appl. Crystallogr.* **28**, 768–773. https://doi.org/10.1107/S0021889895007047 (1995).
54. Valentini, E., Kikhney, A. G., Previtali, G., Jeffries, C. M. & Svergun, D. I. SASBDB, a repository for biological small-angle scattering data. *Nucleic Acids Res.* **43**, D357-363. https://doi.org/10.1093/nar/gku1047 (2015).
55. Kikhney, A. G., Borges, C. R., Molodenskiy, D. S., Jeffries, C. M. & Svergun, D. I. SASBDB: towards an automatically curated and validated repository for biological scattering data. *Protein Sci.* **29**, 66–75. https://doi.org/10.1002/pro.3731 (2020).
56. Kozin, M. B. & Svergun, D. I. Automated matching of high- and low-resolution structural models. *J. Appl. Crystallogr.* **34**, 33–41. https://doi.org/10.1107/S0021889800014126 (2001).
57. Collins, B., Curtis, N., Cotter, P. D., Hill, C. & Ross, R. P. The ABC transporter AnrAB contributes to the innate resistance of *Listeria monocytogenes* to nisin, bacitracin, and various beta-lactam antibiotics. *Antimicrob. Agents Chemother.* **54**, 4416–4423. https://doi.org/10.1128/AAC.00503-10 (2010).
58. Hiron, A., Falord, M., Valle, J., Debarbouille, M. & Msadek, T. Bacitracin and nisin resistance in *Staphylococcus aureus*: a novel pathway involving the BraS/BraR two-component system (SA2417/SA2418) and both the BraD/BraE and VraD/VraE ABC transporters. *Mol. Microbiol.* **81**, 602–622. https://doi.org/10.1111/j.1365-2958.2011.07735.x (2011).
59. Popella, P. *et al.* VraH is the third component of the *Staphylococcus aureus* VraDEH system involved in gallidermin and daptomycin resistance and pathogenicity. *Antimicrob. Agents Chemother.* **60**, 2391–2401. https://doi.org/10.1128/AAC.02865-15 (2016).
60. Staron, A., Finkeisen, D. E. & Mascher, T. Peptide antibiotic sensing and detoxification modules of *Bacillus subtilis*. *Antimicrob. Agents Chemother.* **55**, 515–525. https://doi.org/10.1128/AAC.00352-10 (2011).
61. Yang, J., Yu, M., Jan, Y. N. & Jan, L. Y. Stabilization of ion selectivity filter by pore loop ion pairs in an inwardly rectifying potassium channel. *Proc. Natl. Acad. Sci. USA* **94**, 1568–1572. https://doi.org/10.1073/pnas.94.4.1568 (1997).
62. Ramaen, O. *et al.* Structure of the human multidrug resistance protein 1 nucleotide binding domain 1 bound to Mg2+/ATP reveals a non-productive catalytic site. *J. Mol. Biol.* **359**, 940–949. https://doi.org/10.1016/j.jmb.2006.04.005 (2006).

63. Benabdelhak, H. *et al.* Positive co-operative activity and dimerization of the isolated ABC ATPase domain of HlyB from *Escherichia coli*. *Biochem. J.* **386**, 489–495. https://doi.org/10.1042/BJ20041282 (2005).
64. Ramaen, O., Sizun, C., Pamlard, O., Jacquet, E. & Lallemand, J. Y. Attempts to characterize the NBD heterodimer of MRP1: transient complex formation involves Gly771 of the ABC signature sequence but does not enhance the intrinsic ATPase activity. *Biochem. J.* **391**, 481–490. https://doi.org/10.1042/BJ20050897 (2005).
65. Schultz, K. M., Merten, J. A. & Klug, C. S. Characterization of the E506Q and H537A dysfunctional mutants in the *E. coli* ABC transporter MsbA. *Biochemistry* **50**, 3599–3608. https://doi.org/10.1021/bi101666p (2011).
66. Osorio, H. *et al.* H2O2, but not menadione, provokes a decrease in the ATP and an increase in the inosine levels in *Saccharomyces cerevisiae*: an experimental and theoretical approach. *Eur. J. Biochem.* **270**, 1578–1589. https://doi.org/10.1046/j.1432-1033.2003.03529.x (2003).
67. Buckstein, M. H., He, J. & Rubin, H. Characterization of nucleotide pools as a function of physiological state in *Escherichia coli*. *J. Bacteriol.* **190**, 718–726. https://doi.org/10.1128/JB.01020-07 (2008).
68. Bochner, B. R. & Ames, B. N. Complete analysis of cellular nucleotides by two-dimensional thin layer chromatography. *J. Biol. Chem.* **257**, 9759–9769 (1982).
69. Reimann, S. *et al.* Interdomain regulation of the ATPase activity of the ABC transporter haemolysin B from *Escherichia coli*. *Biochem. J.* **473**, 2471–2483. https://doi.org/10.1042/BCJ20160154 (2016).
70. Lagedroste, M., Reiners, J., Smits, S. H. J. & Schmitt, L. Impact of the nisin modification machinery on the transport kinetics of NisT. *Sci. Rep.* **10**, 12295. https://doi.org/10.1038/s41598-020-69225-2 (2020).
71. Zheng, S., Nagao, J. I., Nishie, M., Zendo, T. & Sonomoto, K. ATPase activity regulation by leader peptide processing of ABC transporter maturation and secretion protein, NukT, for lantibiotic nukacin ISK-1. *Appl. Microbiol. Biotechnol.* **102**, 763–772. https://doi.org/10.1007/s00253-017-8645-2 (2018).
72. Hanahan, D. Studies on transformation of *Escherichia coli* with plasmids. *J. Mol. Biol.* **166**, 557–580. https://doi.org/10.1016/s0022-2836(83)80284-8 (1983).
73. Franke, D. *et al.* ATSAS 2.8: a comprehensive data analysis suite for small-angle scattering from macromolecular solutions. *J. Appl. Crystallogr.* **50**, 1212–1225. https://doi.org/10.1107/S1600576717007786 (2017).
74. Konarev, P. V., Volkov, V. V., Sokolova, A. V., Koch, M. H. J. & Svergun, D. I. PRIMUS: a Windows PC-based system for small-angle scattering data analysis. *J. Appl. Crystallogr.* **36**, 1277–1282. https://doi.org/10.1107/S0021889803012779 (2003).
75. Guinier, A. Diffraction of x-rays of very small angles-application to the study of ultramicroscopic phenomenon. *Ann. Phys.* **12**, 161–237 (1939).
76. Svergun, D. I. Determination of the regularization parameter in indirect-transform methods using perceptual criteria. *J. Appl. Crystallogr.* **25**, 495–503. https://doi.org/10.1107/S0021889892001663 (1992).
77. Altschul, S. F., Gish, W., Miller, W., Myers, E. W. & Lipman, D. J. Basic local alignment search tool. *J. Mol. Biol.* **215**, 403–410. https://doi.org/10.1016/S0022-2836(05)80360-2 (1990).
78. Dominguez, C., Boelens, R. & Bonvin, A. M. HADDOCK: a protein-protein docking approach based on biochemical or biophysical information. *J. Am. Chem. Soc.* **125**, 1731–1737. https://doi.org/10.1021/ja026939x (2003).
79. van Zundert, G. C. P. *et al.* The HADDOCK2.2 web server: user-friendly integrative modeling of biomolecular complexes. *J. Mol. Biol.* **428**, 720–725. https://doi.org/10.1016/j.jmb.2015.09.014 (2016).
80. Schrödinger Release 2017-1: Schrödinger Suite 2017-1 Protein Preparation Wizard, Schrödinger, LLC, New York, NY, 2017.
81. Banks, J. L. *et al.* Integrated modeling program, applied chemical theory (IMPACT). *J. Comput. Chem.* **26**, 1752–1780. https://doi.org/10.1002/jcc.20292 (2005).
82. Case, D. A. *et al. Amber* (University of California, San Francisco, 2019).
83. Schafmeister Ceaf, R. W. & Romanovski, V. *LEaP* (University of California, San Francisco, 1995).
84. Jorgensen, W. L., Chandrasekhar, J., Madura, J. D., Impey, R. W. & Klein, M. L. Comparison of simple potential functions for simulating liquid water. *J. Chem. Phys.* **79**, 926–935. https://doi.org/10.1063/1.445869 (1983).
85. Salomon-Ferrer, R., Gotz, A. W., Poole, D., Le Grand, S. & Walker, R. C. Routine microsecond molecular dynamics simulations with AMBER on GPUs 2 explicit solvent particle mesh ewald. *J. Chem. Theory Comput.* **9**, 3878–3888. https://doi.org/10.1021/ct400314y (2013).
86. Maier, J. A. *et al.* ff14SB: improving the accuracy of protein side chain and backbone parameters from ff99SB. *J. Chem. Theory. Comput.* **11**, 3696–3713. https://doi.org/10.1021/acs.jctc.5b00255 (2015).
87. Joung, I. S. & Cheatham, T. E. 3rd. Determination of alkali and halide monovalent ion parameters for use in explicitly solvated biomolecular simulations. *J. Phys. Chem. B* **112**, 9020–9041. https://doi.org/10.1021/jp8001614 (2008).
88. Meagher, K. L., Redman, L. T. & Carlson, H. A. Development of polyphosphate parameters for use with the AMBER force field. *J. Comput. Chem.* **24**, 1016–1025. https://doi.org/10.1002/jcc.10262 (2003).
89. Frieg, B. *et al.* Molecular mechanisms of glutamine synthetase mutations that lead to clinically relevant pathologies. *PLoS Comput. Biol.* **12**, e1004693. https://doi.org/10.1371/journal.pcbi.1004693 (2016).
90. Roe, D. R. & Cheatham, T. E. 3rd. PTRAJ and CPPTRAJ: SOFTWARE for processing and analysis of molecular dynamics trajectory data. *J. Chem. Theory Comput.* **9**, 3084–3095. https://doi.org/10.1021/ct400341p (2013).
91. The PyMOL Molecular Graphics System, Version 2.0 Schrödinger, LLC.
92. Schrödinger Release 2020-2: Maestro, Schrödinger, LLC, New York (2020).
93. Schrödinger Release 2020-2: Schrödinger Suite 2020-2 Glide, Schrödinger, LLC, New York (2020).

Acknowledgements

We thank Lutz Schmitt for his continuous support and the members of the Institute of Biochemistry for valuable discussions. This work has been funded by the Deutsche Forschungsgemeinschaft (DFG, German Research Foundation)—Project number 270650915 (Research Training Group GRK2158, TP4a to H.G. and TP4b to S.S.). The Center for Structural studies is funded by the DFG (Grant Number 417919780 and INST 208/761-1 FUGG to S.S.). H.G. is grateful for computational support by the "Zentrum für Informations und Medientechnologie" at the Heinrich-Heine-Universität Düsseldorf and the computing time provided by the John von Neumann Institute for Computing (NIC) to H.G. on the supercomputer JUWELS at Jülich Supercomputing Centre (JSC) (user IDs: HKF7).

Author contributions

S.H.J.S. conceived and coordinated the study and evaluated all data; F.F performed overexpression, purification and functional characterization of the *Sa*NsrF enzymes and contributed to the writing; J.R. performed the SAXS and data analysis, and contributed to the writing; D.T.H., J.S. and J.G. did the cloning and established the purification protocol; H.G. conceptualized and supervised molecular modeling and simulation, analyzed the

data, and contributed to the writing; N.P. performed molecular modeling and simulation, analyzed the data, and contributed to the writing.

Funding

This work has been funded by the Deutsche Forschungsgemeinschaft (DFG, German Research Foundation)—Project Number 270650915 (Research Training Group GRK2158, TP4a to H.G. and TP4b to S.S.). The Center for Structural studies is funded by the DFG (Grant Number 417919780 and INST 208/761-1 FUGG to S.S.). H.G. is grateful for computational support by the "Zentrum für Informations und Medientechnologie" at the Heinrich-Heine-Universität Düsseldorf and the computing time provided by the John von Neumann Institute for Computing (NIC) to H.G. on the supercomputer JUWELS at Jülich Supercomputing Centre (JSC) (user IDs: HKF7). Open Access funding provided by Projekt DEAL.

Competing interests

The authors declare no competing interests.

Additional information

Supplementary information is available for this paper at https://doi.org/10.1038/s41598-020-72237-7.

Correspondence and requests for materials should be addressed to S.H.J.S.

Reprints and permissions information is available at www.nature.com/reprints.

Publisher's note Springer Nature remains neutral with regard to jurisdictional claims in published maps and institutional affiliations.

Supporting information

Characterization of the Nucleotide-Binding Domain NsrF from the BceAB-type ABC-Transporter NsrFP from the Human Pathogen *Streptococcus agalactiae*

Fabia Furtmann[1*], Nicola Porta[2*], Dai Tri Hoang[1], Jens Reiners[3], Julia Schumacher[1], Julia Gottstein[1], Holger Gohlke[2,4], Sander H. J. Smits[1,3#]

[1]Institute of Biochemistry, Heinrich-Heine-Universität Düsseldorf, Universitätsstraße 1, 40225 Düsseldorf, Germany

[2]Institute for Pharmaceutical and Medicinal Chemistry, Heinrich-Heine-Universität Düsseldorf, Universitätsstraße 1, 40225 Düsseldorf, Germany.

[3]Center for Structural Studies, Heinrich-Heine-Universität Düsseldorf, Universitätsstraße 1, 40225 Düsseldorf, Germany

[4]John von Neumann Institute for Computing (NIC), Jülich Supercomputing Centre (JSC), Institute of Biological Information Processing (IBI-7: Structural Biochemistry), Forschungszentrum Jülich GmbH, Wilhelm-Johnen-Straße, 52425 Jülich, Germany.

*These authors contributed equally

Keywords: antibiotic resistance, lantibiotics, nisin, ABC transporter, molecular dynamics simulations, structural model

Author ORCID
Nicola Porta: 0000-0002-6005-4372
Holger Gohlke: 0000-0001-8613-1447
Sander Smits: 0000-0003-0780-9251

[#] Corresponding author: Sander Smits
Address: Universitätsstr. 1, 40225 Düsseldorf, Germany.
Phone: (+49) 211 81 12647; Fax: (+49) 211 81 15037
E-mail: sander.smits@hhu.de

Materials and Methods

Multiangle Light Scattering (MALS)

To determine the protein's stoichiometry, Multiangle Light Scattering (MALS) was employed. Each protein was diluted in 100 mM HEPES at pH 8 and 300 mM NaCl. An Agilent 1260 HPLC system was used in combination with a triple-angle light scatter detector (miniDAWN TREOS II) and a differential refractive index detector (Optilab T-rEX) (both Wyatt Technology). *Sa*NsrF$_{WT}$ at a concentration of 3 mg/mL were injected onto a Superdex 75 16/300 increase column with a flowrate of 0.6 mL/min. For analysis the ASTRA software package (Astra 7.1) (Wyatt Technology) was used (Fig. 1B).

ATPase Activity Assay

The ATPase activity of *Sa*NsrF$_{WT}$ and *Sa*NsrF$_{H202A}$ (diluted in 100 mM HEPES at pH 8, 100 mM NaCl) was examined by the Malachite Green Phosphate Assay at a protein concentration of 0.1 mg/mL that was initially undertaken at room temperature (20 °C). The initial conditions required a final Mg^{2+}-concentration of 10 mM and an ATP concentration from 0 – 5 mM that was used for the reaction start.

Changes in protein's activity were detected in a time range from 4 – 26 min by stopping a part of the reaction every two minutes, whereupon 18 min were chosen as an optimal time of incubation. An ATP (or NTP) concentration was set at 3 mM for following ATPase screenings. By the addition of EDTA (final concentration: 50 mM) a control was implemented in order to observe the process of autohydrolysis in a Mg^{2+}-free solution.

To determine the maximal possible hydrolysis activity of *Sa*NsrF$_{WT}$, the protein was exposed to various buffer systems including a citrate buffer for pH 4 and 5, MES for pH 6, HEPES for pH 7 and 8, TRIS for pH 7, 8, 9 and CAPS for pH 10 and 11 (100 mM for each). Moreover, the influence of the NaCl concentration on the ATPase-buffer was analysed by determining the ATP hydrolysis of the *Sa*NsrF$_{WT}$ proteins in a buffer with 0, 100, 200, 300, 400, 500 and 1000 mM NaCl. Investigations were made concerning the cofactor choice of *Sa*NsrF$_{WT}$ by introducing Ca^{2+}, Mn^{2+}, Zn^{2+}, Fe^{2+} and Cu^{2+} instead of Mg^{2+} at a final concentration of 10 mM. An identical setup was performed without the addition of protein, which was used as a blank to encounter for autohydrolysis. The reaction including the optimized parameters was performed at 20 °C, 25 °C, 30 °C and 37 °C.

Results

Activity of SaNsrF$_{WT}$

After successful purification, we functionally characterized *Sa*NsrF$_{WT}$. To do so, we screened the following parameters on their influence on the ATP hydrolysis velocity: I) pH, II) salt concentration, III) nature of the divalent ion, and IV) temperature. This allowed us to obtain optimal conditions for our kinetic measurements

pH dependency of SaNsrF$_{WT}$

We assayed the ATP hydrolysis of the *Sa*NsrF$_{WT}$ protein at different pH conditions in order to determine the optimal buffer composition. Therefore, we used 100 mM of the following buffers: citrate at pH 4.0 – 5.0, MES at pH 6.0, HEPES at pH 7.0 – 8.0, TRIS at pH 7.0 – 9.0 and CAPS at pH 10.0 – 11.0.

We observed a large dependence on the pH of the buffer system (Figure 2A). ATP hydrolysis mediated by *Sa*NsrF$_{WT}$ can only be observed in a pH range from 6.0 – 8.0, and the highest ATPase activity was reached in a HEPES buffer at pH 7.0. Interestingly, a reduction in activity of about 20 – 30 % is observed between HEPES (zwitterionic sulphonic acid) and TRIS (cationic primary amine) buffer systems although the pH was very similar (7.0 and 8.0, respectively).

Influence of salt concentration on the activity of SaNsrF$_{WT}$

Next, we tested the influence of the ionic strengh on the activity of the *Sa*NsrF$_{WT}$ protein. We used 100 mM HEPES at pH 7.0 as the optimal conditions for protein activity and varied the NaCl concentration ranging from 0 – 1 M in steps of 0.1 M (Figure 2B).

With increasing NaCl concentration, the hydrolytic activity strongly decreased. At a concentration of 1 M NaCl, 20% residual activity was recorded when compared to the maximum reached at 0 mM NaCl.

Choice of Cofactor

As a third optimization step, we examined the influence of the cofactor of *Sa*NsrF$_{WT}$ on ATP hydrolysis. We replaced the 10 mM Mg^{2+} used so far with 10 mM Ca^{2+}, Mn^{2+}, Zn^{2+}, Fe^{2+} or Cu^{2+}, respectively. This revealed a clear dependency on the nature of the divalent ion where only for Mg^{2+} a reasonable hydrolytic activity was detected. Besides Mg^{2+}, also Mn^{2+} was taken up as cofactor, with an ATPase activity of about a fourth of the maximally measured value. The other tested divalent ions did not significantly (e.g. Cu^{2+} caused about 15 % of the activity maximum) contribute to the ATPase activity of *Sa*NsrF$_{WT}$ (Fig. S1C).

Temperature dependence

We assayed the ATPase activity of *Sa*NsrF$_{WT}$ within a temperature range from 20 °C – 37 °C including the optimized parameters of 100 mM HEPES assay buffer at pH 7 with no added NaCl (see above). 10 mM Mg^{2+} were used to provide the protein with its cofactor. As illustrated in Figure 2D, the ATPase activity of *Sa*NsrF$_{WT}$ was maximal at 30 °C. Further increase in the temperature resulted in a significant loss of activity as observed for 37 °C.

In summary, we varied several parameters of the ATPase activity assay in order to obtain the maximal hydrolytic activity for the *Sa*NsrF$_{WT}$ protein. As a result, the optimized conditions were found to be 100 mM HEPES at pH 7 with 0 mM NaCl as an assay buffer. The reaction approach included the addition of 10 mM Mg^{2+} and was finally performed at a temperature of 30 °C. The reaction with the respective NTP was followed for an incubation time of 18 min, then stopped and measured. These optimized conditions were applied in all following experiments.

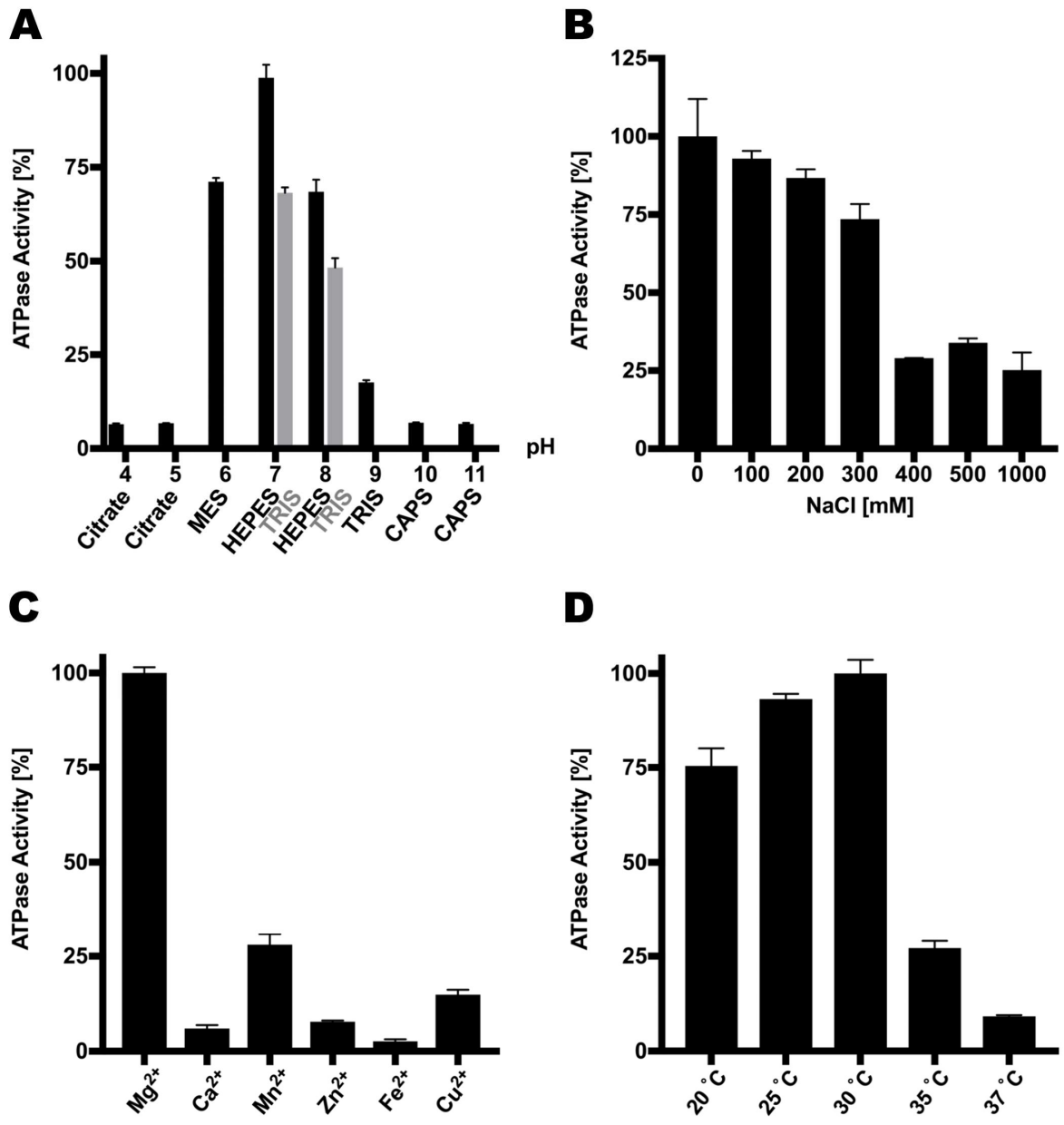

Figure S1. Influence of ATPase activity of *Sa*NsrF$_{WT}$ by parameter variations. (A) ATPase activity [%] of *Sa*NsrF$_{WT}$ dependent on pH and buffer system. 100 mM of citrate, MES, HEPES, TRIS and CAPS were diluted in ddH2O and adjusted to the respective pH. At pH 7 and 8 HEPES as well as TRIS were tested. **(B)** ATPase activity [%] of *Sa*NsrF$_{WT}$ dependent on concentrations of 0 mM to 1 M NaCl. *Sa*NsrF$_{WT}$ was diluted in 100 mM HEPES at pH 7 (0.1 mg/mL). **(C)** ATPase activity [%] of *Sa*NsrF$_{WT}$ dependent on twofold metal ions. *Sa*NsrF$_{WT}$ was exposed to 10 mM of Mg^{2+}, Ca^{2+}, Mn^{2+}, Zn^{2+}, Fe^{2+} or Cu^{2+}. *Sa*NsrF$_{WT}$ was diluted in 100 mM HEPES at pH 7 (0.1 mg/mL). **(D)** ATPase activity [%] of *Sa*NsrF$_{WT}$ dependent on temperature (triple evaluation). A concentration of 3 mM ATP was applied on *Sa*NsrF$_{WT}$ (0.1 mg/mL; diluted in 100 mM HEPES at pH 7). The reaction was incubated at temperatures of 20 °C, 25 °C, 30 °C, 35°C and 37 °C and was stopped after 18 min and dyed as described in ATPase Activity Assay for 7 min. All experiments have been performed in at least three biological replicates and are represented as means ± s.d..

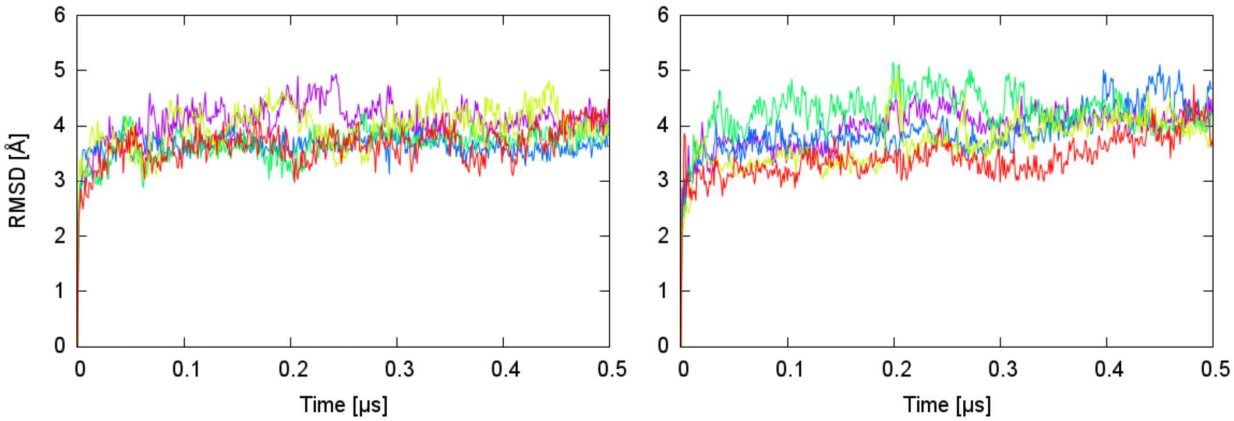

Figure S2: Structural variability of *Sa*NsrF monomers. The RMSD of backbone atoms was calculated after fitting the structures onto the 15% least mobile residues for each replica for *Sa*NsrF$_{WT}$ (left) and for the *Sa*NsrF$_{H202A}$ variant (right). The profiles are reported in a different color for each replica.

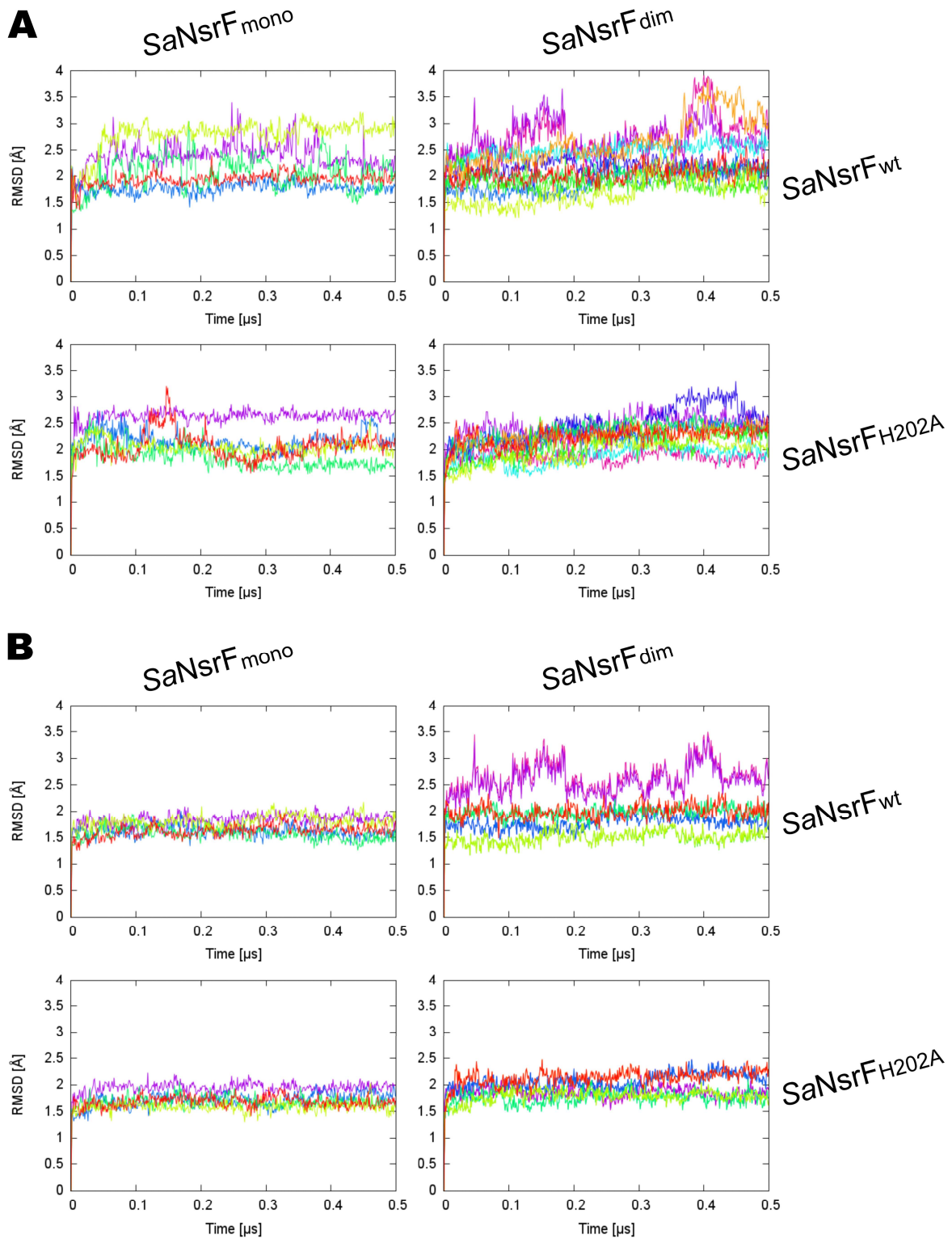

Figure S3: Change of ATP molecule and Mg^{2+} ion positions with respect to the protein for different *Sa*NsrF systems. (A) RMSD of ATP molecules; **(B)** RMSD of Mg^{2+} ions. The RMSD was calculated after fitting the structures onto the 15% least mobile protein residues for each replica. The profiles are shown in a different color for each molecule in each replica.

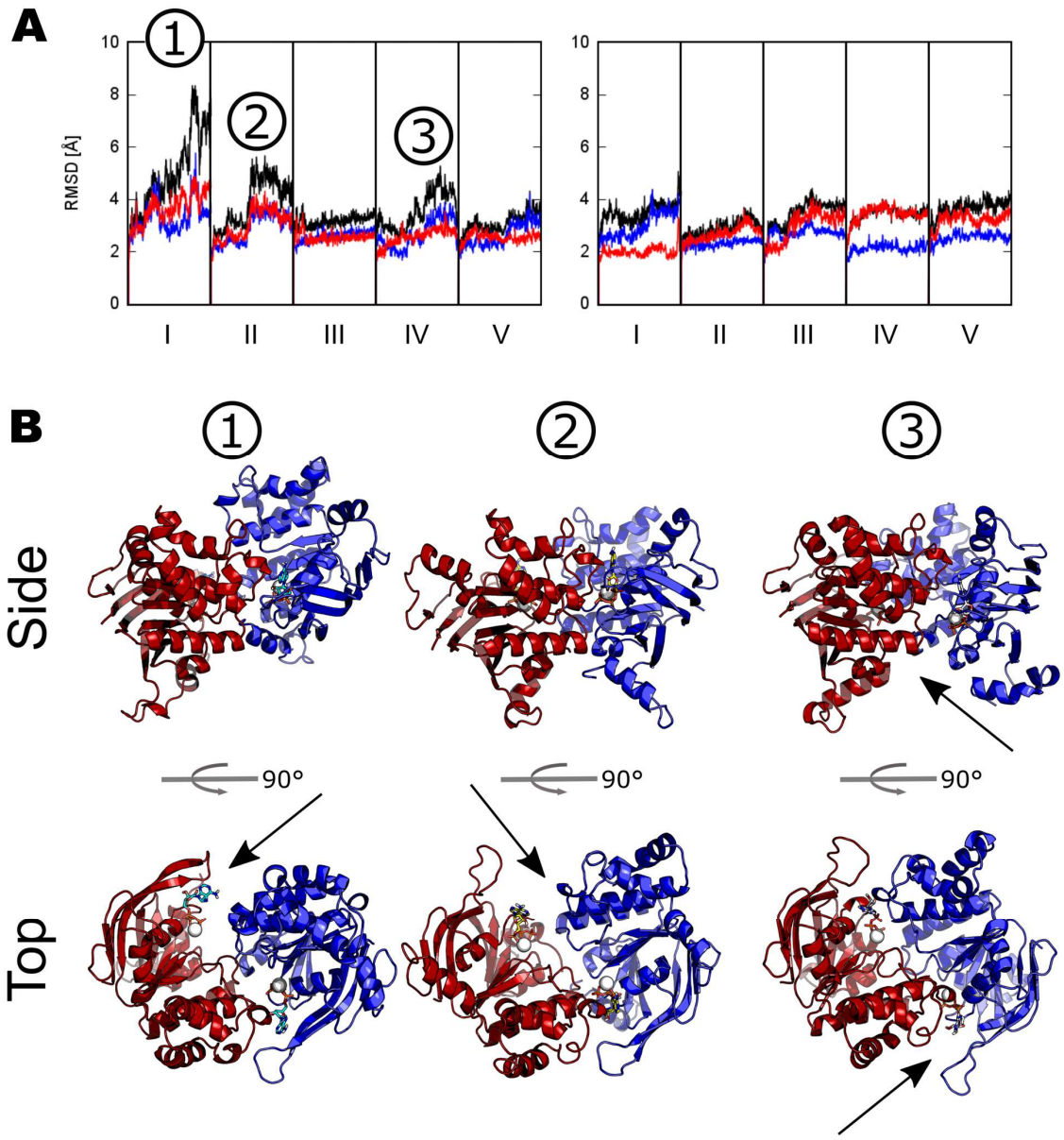

Figure S4: Structural variability of *Sa*NsrF$_{WT}$ and *Sa*NsrF$_{H202A}$ dimers. (A) The RMSD of backbone atoms was calculated for *Sa*NsrF$_{WT}$ (left) and for the *Sa*NsrF$_{H202A}$ variant (right) after fitting the structures onto the 15% least mobile residues for the whole dimer (black) and separately for either subunit A (red) or B (blue). Each box represents a replica of 0.5 µs simulation length (roman numbers). **(B)** Three representative structures of *Sa*NsrF$_{WT}$ with higher RMSD values are displayed from two orientations. Arrows highlight the partial opening of the dimer interface.

A

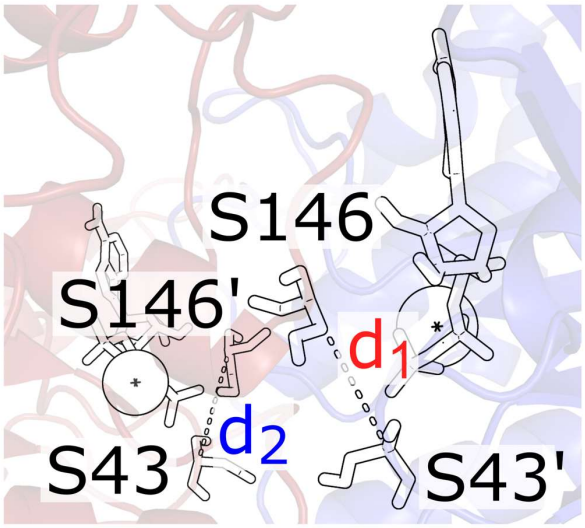

B

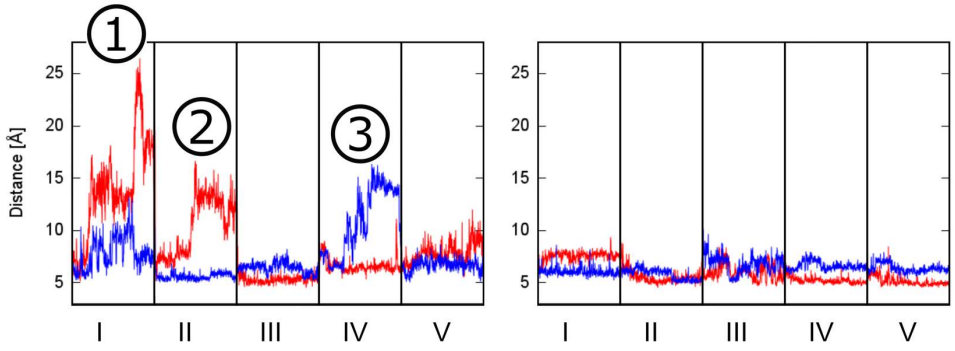

C

Structure$_{time}$ (replica), label	d_1 [Å]	d_2 [Å]
t_0 (I)	6.17	6.72
t_{400} (I), 1	<u>25.13</u>	7.63
t_0 (II)	7.22	7.92
t_{300} (II), 2	<u>13.62</u>	5.58
t_0 (IV)	8.24	7.29
t_{380} (IV), 3	7.06	<u>13.89</u>

Figure S5: Structural variability of dimers, expressed as distance between residues. (A) Representation of the distances *d1* and *d2* between the residues S43 and S146 (centers of mass) located on different monomers. **(B)** Distances for *Sa*NsrF$_{WT}$ dimer (left) and the *Sa*NsrF$_{H202A}$ variant (right). Each box represents a replica of 0.5 µs simulation length (roman numbers). **(C)** Distances for three representative structures with higher RMSD values are reported; these structures are identical to the ones shown in Figure S4. The largest distance values, indicating the separation of the subunits, are underlined.

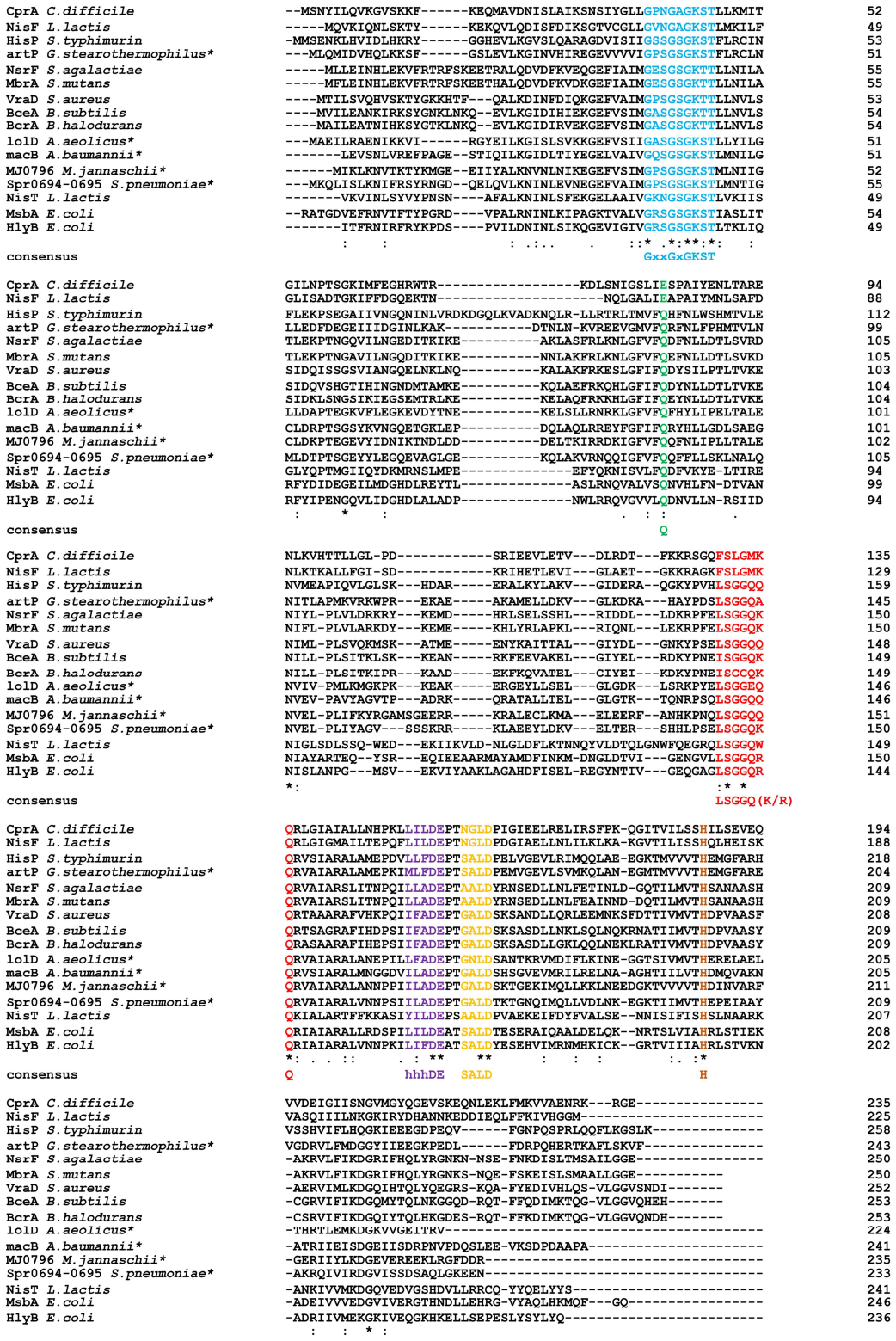

Figure S6: Sequence alignment of different NBDs. The sequence aligment was done with Clustal Omega [1]. TopModel templates are marked with an asterix (*). The conserved motives are labeled in cyan (Walker A), green (Q-loop), red (C-loop), purple (Walker B), orange (D-loop) and brown (H-loop).

Table S1: Five main templates used by the TopModel software for modeling of *Sa*NsrF.

PDB ID:	Identity [%]	Similarity [%]	Coverage [%]	TM-Score [%]	Note
1F3O [a]	37.7	88.4	88.0	91.9	ADP/Mg^{2+}-bound dimer, not functionally active assembly
5XU1 [b]	39.5	89.4	88.0	90.9	Mg^{2+}-bound dimer with TM domain
2PCL [c]	40.5	84.1	88.8	90.6	Mg^{2+}-bound dimer, not functionally active assembly
5GKO [d]	35.5	83.6	93.6	90.3	Apo dimer with TM domain
2OLI [e]	30.9	76.1	93.2	89.2	α-helical domain only

[a] [2]; [b] [3]; [c] According to RCSB: "To be published"; [d] [4]; [e] According to RCSB: "To be published".

Table S2: Consensus sequence of conserved motifs in the NBDs listed according to their occurrence from N- to C-terminus [5]. For a graphical representation see Fig. 3B.

Motif	Consensus sequence	*Sa*NsrF
A-loop	(F/K)xY	10-KV<u>F</u>-12
Walker A or P-loop	GxxGxGK(S/T)	41-<u>G</u>ES<u>G</u>S<u>GKT</u>-48
Q-loop	hV(S/P)Q	90-F<u>V</u>F<u>Q</u>-93
X-loop	TRVGDKGTQ	137-LL<u>DK</u>RP-142
Signature motif or C-loop	LSGGQ(K/R)Q	145-<u>LSGGQKQ</u>-151
Walker B	hhhhDE	165-ILLA<u>DE</u>-170
D-loop	SALD	173-A<u>ALD</u>-176
H-loop	hAHRL	200-VT<u>H</u>^{202}SA-204

Table S3: Overall SAXS Data

SAXS Device	Xenocs Xeuss 2.0 with Q-Xoom
Data collection parameters	
Detector	PILATUS 3 R 300K windowless
Detector distance (m)	0.550
Beam size (mm x mm)	0.8 x 0.8
Wavelength (Å)	1.54 (Cu Source)
Sample environment	Low Noise Flow Cell, 1 mm ø
s range (nm^{-1})‡	0.18 – 6.0
Temperature (K)	288
Exposure time per frame (min)	10
Sample	***Sa*NsrF$_{WT}$**
Mode of measurement	static
Protein concentration (mg/ml)	0.5 – 4.2
Structural parameters	
I(0) from P(r)	0.023
R_g (real-space from P(r)) (nm)	2.46
I(0) from Guinier fit	0.023
s-range for Guinier fit (nm^{-1})	0.23 – 0.54
R_g (from Guinier fit) (nm)	2.40
D_{max} (nm)	7.90
POROD volume estimate (nm^3)	64.37
Molecular mass (kDa)	
From I(0)	31.85
From MoW2 [6]	33.36
From Vc [7]	38.51
From POROD	40.23
From sequence	30.86
Structure Evaluation	
Ambimeter score	0.6990
Crysol χ^2	1.16
Software	
ATSAS Software Version [8]	3.0.1
Primary data reduction	PRIMUS [9]
Data processing	GNOM [10]
Ab initio modelling	GASBOR [11]
Superimposing	SUPCOMB [12]
Structure evaluation	AMBIMETER [13] / CRYSOL [14]
Model visualization	PyMOL [15]

‡s = $4\pi \sin(\theta)/\lambda$, 2θ – scattering angle

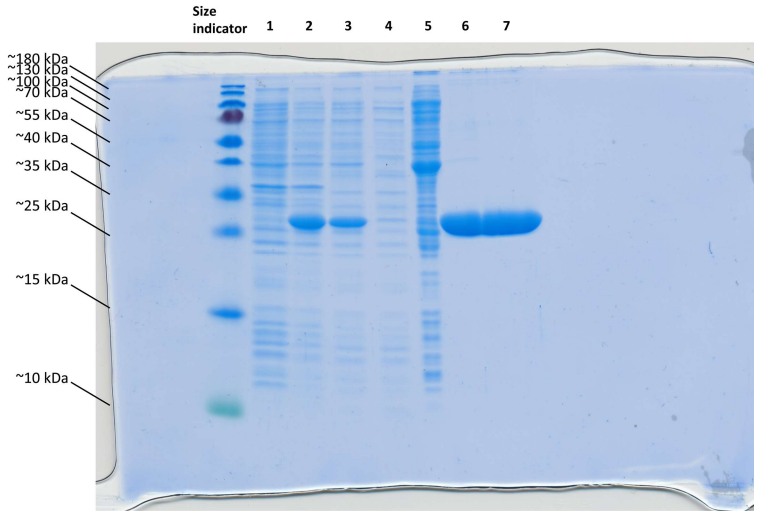

Original Figure 1. Purification and SEC-MALS of *Sa*NsrF$_{WT}$. (A) SDS-PAGE of the *Sa*NsrF$_{WT}$ purification progress. PageRuler Prestained Protein Ladder (size indicator; 10 to 180 kDa), *E. coli* strain before IPTG induction (1), *E. coli* strain after IPTG induction (2), IMAC load (3), IMAC flow-through (4), IMAC wash-fraction (5), IMAC eluate (6), SEC eluate (7).

References:

1 Madeira, F. *et al.* The EMBL-EBI search and sequence analysis tools APIs in 2019. *Nucleic Acids Res* **47**, W636-W641, doi:10.1093/nar/gkz268 (2019).

2 Yuan, Y. R. *et al.* The crystal structure of the MJ0796 ATP-binding cassette. Implications for the structural consequences of ATP hydrolysis in the active site of an ABC transporter. *J Biol Chem* **276**, 32313-32321, doi:10.1074/jbc.M100758200 (2001).

3 Yang, H. B. *et al.* Structure of a MacAB-like efflux pump from *Streptococcus pneumoniae*. *Nat Commun* **9**, 196, doi:10.1038/s41467-017-02741-4 (2018).

4 Okada, U. *et al.* Crystal structure of tripartite-type ABC transporter MacB from *Acinetobacter baumannii*. *Nat Commun* **8**, 1336, doi:10.1038/s41467-017-01399-2 (2017).

5 Szollosi, D., Rose-Sperling, D., Hellmich, U. A. & Stockner, T. Comparison of mechanistic transport cycle models of ABC exporters. *Biochim Biophys Acta Biomembr* **1860**, 818-832, doi:10.1016/j.bbamem.2017.10.028 (2018).

6 Fischer, H., Neto, M. D., Napolitano, H. B., Polikarpov, I. & Craievich, A. F. Determination of the molecular weight of proteins in solution from a single small-angle X-ray scattering measurement on a relative scale. *J Appl Crystallogr* **43**, 101-109, doi:10.1107/S0021889809043076 (2010).

7 Rambo, R. P. & Tainer, J. A. Accurate assessment of mass, models and resolution by small-angle scattering. *Nature* **496**, 477-481, doi:10.1038/nature12070 (2013).

8 Franke, D. *et al.* ATSAS 2.8: a comprehensive data analysis suite for small-angle scattering from macromolecular solutions. *J Appl Crystallogr* **50**, 1212-1225, doi:10.1107/S1600576717007786 (2017).

9 Konarev, P. V., Volkov, V. V., Sokolova, A. V., Koch, M. H. J. & Svergun, D. I. PRIMUS: a Windows PC-based system for small-angle scattering data analysis. *J Appl Crystallogr* **36**, 1277-1282, doi:10.1107/S0021889803012779 (2003).

10 Svergun, D. I. Determination of the Regularization Parameter in Indirect-Transform Methods Using Perceptual Criteria. *J Appl Crystallogr* **25**, 495-503, doi:Doi 10.1107/S0021889892001663 (1992).

11 Svergun, D. I., Petoukhov, M. V. & Koch, M. H. Determination of domain structure of proteins from X-ray solution scattering. *Biophys J* **80**, 2946-2953, doi:10.1016/S0006-3495(01)76260-1 (2001).

12 Kozin, M. B. & Svergun, D. I. Automated matching of high- and low-resolution structural models. *J Appl Crystallogr* **34**, 33-41, doi:Doi 10.1107/S0021889800014126 (2001).

13 Petoukhov, M. V. & Svergun, D. I. Ambiguity assessment of small-angle scattering curves from monodisperse systems. *Acta Crystallogr D Biol Crystallogr* **71**, 1051-1058, doi:10.1107/S1399004715002576 (2015).

14 Svergun, D., Barberato, C. & Koch, M. H. J. CRYSOL - A program to evaluate x-ray solution scattering of biological macromolecules from atomic coordinates. *J Appl Crystallogr* **28**, 768-773, doi:Doi 10.1107/S0021889895007047 (1995).

15 The PyMOL Molecular Graphics System, Version 2.0 Schrödinger, LLC.

3.9 Chapter IX

Title: The N-terminal Region of Nisin Is Important for the BceAB-Type ABC Transporter NsrFP from *Streptococcus agalactiae* COH1

Authors: **Jens Reiners**[#], Marcel Lagedroste[#], Katja Ehlen, Selina Leusch, Julia Zaschke-Kriesche and Sander H. J. Smits

[#]Authors contributed equally

Published in: Frontiers in Microbiology (2017)

Impact factor: 4.02

Own proportion of this work: 40%

- Design of experiments
- Expression and purification of pre-nisin A variants
- Performing biological and biochemical assays
- Data analysis
- Writing the manuscript

frontiers in Microbiology

ORIGINAL RESEARCH
published: 29 August 2017
doi: 10.3389/fmicb.2017.01643

The N-terminal Region of Nisin Is Important for the BceAB-Type ABC Transporter NsrFP from *Streptococcus agalactiae* COH1

*Jens Reiners†, Marcel Lagedroste†, Katja Ehlen, Selina Leusch, Julia Zaschke-Kriesche and Sander H. J. Smits**

Institute of Biochemistry, Heinrich Heine University Düsseldorf, Düsseldorf, Germany

Lantibiotics are (methyl)-lanthionine-containing antimicrobial peptides produced by several Gram-positive bacteria. Some human pathogenic bacteria express specific resistance proteins that counteract this antimicrobial activity of lantibiotics. In *Streptococcus agalactiae* COH1 resistance against the well-known lantibiotic nisin is conferred by, the nisin resistance protein (NSR), a two-component system (NsrRK) and a BceAB-type ATP-binding cassette (ABC) transporter (NsrFP). The present study focuses on elucidating the function of NsrFP via its heterologous expression in *Lactococcus lactis*. NsrFP is able to confer a 16-fold resistance against wild type nisin as determined by growth inhibition experiments and functions as a lantibiotic exporter. Several C-terminal nisin mutants indicated that NsrFP recognizes the N-terminal region of nisin. The N-terminus harbors three (methyl)-lanthionine rings, which are conserved in other lantibiotics.

Keywords: ABC transporter, lanthionine ring, lantibiotic, nisin, resistance

OPEN ACCESS

Edited by:
Helen Zgurskaya,
University of Oklahoma, United States

Reviewed by:
Rajeev Misra,
Arizona State University, United States
Karl Hassan,
Macquarie University, Australia

****Correspondence:***
Sander H. J. Smits
sander.smits@hhu.de

†These authors have contributed equally to this work.

Specialty section:
This article was submitted to Antimicrobials, Resistance and Chemotherapy, a section of the journal Frontiers in Microbiology

Received: *26 April 2017*
Accepted: *15 August 2017*
Published: *29 August 2017*

Citation:
Reiners J, Lagedroste M, Ehlen K, Leusch S, Zaschke-Kriesche J and Smits SHJ (2017) The N-terminal Region of Nisin Is Important for the BceAB-Type ABC Transporter NsrFP from Streptococcus agalactiae COH1. Front. Microbiol. 8:1643. doi: 10.3389/fmicb.2017.01643

INTRODUCTION

Lantibiotics are ribosomally synthesized antimicrobial peptides of approximately 19–38 amino acids, which are mainly produced by Gram-positive bacteria (Klaenhammer, 1993). They are characterized by extensive post-translational modifications, which result in the presence of dehydrated amino acids, lanthionine and methyl-lanthionine rings (Chatterjee et al., 2005). Lantibiotics are considered to be promising candidates as antibiotic alternatives due to their capability to inhibit various multidrug-resistant pathogenic bacteria such as Staphylococci, Enterococci, Streptococci and Clostridia species (Dischinger et al., 2014). Several lantibiotics are also effective against Gram-negative bacteria like species of the *Neisseria* and *Helicobacter* genus (Mota-Meira et al., 2000). The pharmaceutical potential of lantibiotics has been extensively studied and some are already in the preclinical and clinical phases of development (Yang et al., 2014). Lantibiotics exhibit different modes of action including binding to the cell wall, which results in growth inhibition, as well as subsequent pore formation leading to immediate cell death (Brötz et al., 1998a; Hasper et al., 2004, 2006; Islam et al., 2012).

Some bacteria, however, are inherently resistant against lantibiotics due to the expression of various protein systems that can detect and subsequently respond to the presence of lantibiotics in the extracellular medium (reviewed in Draper et al., 2015). These broad range resistance systems can either be unspecific such as changes in bacterial cell wall and membrane (Nawrocki et al., 2014;

de Freire Bastos et al., 2015; Draper et al., 2015) or more specific by proteolytic degradation of the lantibiotic itself (Sun et al., 2009).

In the present study, we focused on the lantibiotic nisin, which is produced by some *Lactococcus lactis* and *Streptococcus uberis* strains (Klaenhammer, 1993; Chatterjee et al., 2005). Nisin has a broad antimicrobial spectrum against a wide range of Gram-positive bacteria and exhibits several different modes of action (Ruhr and Sahl, 1985; Brötz et al., 1998b; Hsu et al., 2004; Hasper et al., 2006). One dominant activity is the binding to lipid II, a precursor molecule of peptidoglycan, thereby inhibiting cell wall synthesis (Wiedemann et al., 2001). Secondly, nisin is able to insert into the membrane to form pores (Hasper et al., 2004), which leads to the efflux of ions, nutrients, and subsequently to cell death. This last activity is a very rapid process and occurs almost instantly. Nisin can be structurally dissected in the N-terminus (containing the (methyl)-lanthionine rings A–C), a hinge region with the amino acids NMK and the C-terminus containing rings D and E (Van de Ven et al., 1991) (**Figure 1**). These rings are crucial for the nM activity and deletion of for example only ring E reduces the activity about eightfold (Alkhatib et al., 2014b).

Within the human pathogen *Streptococcus agalactiae* COH1 the expression of a proteogenous resistance system comprising of NSR (nisin resistance protein; a serine protease), an ATP-binding cassette (ABC) transporter (NsrFP) and a two-component system (TCS) (NsrRK) confers resistance against nisin (Khosa et al., 2013). Recently, this NSR operon has been characterized biochemically and structurally. *In vitro* studies showed that NSR expressed in *L. lactis* confers 20-fold resistance against nisin. This is mediated by cleaving off the last six amino acids from nisin, thereby lowering its activity (Sun et al., 2009; Khosa et al., 2013, 2016a). Another component of this nisin resistance operon is the BceAB-type ABC transporter NsrFP. BceAB-type ABC transporters, are putatively involved in antimicrobial peptide (like lantibiotics) removal from the lipid membrane (Gebhard and Mascher, 2011). They have been named after the BceAB transporter system from *Bacillus subtilis* conferring resistance against the antimicrobial peptide bacitracin (Ohki et al., 2003; Rietkötter et al., 2008). Interestingly, within the genomes the lantibiotic BceAB-type ABC transporter are encoded in close proximity to a TCS (Khosa et al., 2013) which senses the presence of the lantibiotic and subsequently up-regulates the expression of the ABC transporter (Dintner et al., 2011). The BceAB from *B. subtilis* has been shown to form a multicomponent complex with its designated TCS BceRS upon binding of bacitracin (Dintner et al., 2014). This highlights that the BceAB transporter from *B. subtilis* is directly involved in bacitracin sensing and consequently triggering the up-regulation of its own gene by the TCS BceRS.

Within NsrFP from *S. agalactiae* COH1, the transmembrane domain NsrP contains 10 predicted transmembrane helices and harbors a 212 amino acid large extracellular domain (ECD) in between helices VII and VIII (Khosa et al., 2013; **Figure 2**). NsrF is the nucleotide-binding domain delivering the energy for the transport by ATP hydrolysis.

In this study, we determined the function of NsrFP from *S. agalactiae* COH1 in conferring nisin resistance. We expressed only the NsrFP transporter without the corresponding NsrR/NsrK TCS and observe that NsrFP can confer resistance up to 80 nM nisin. In comparison to this, a strain lacking this transporter can only survive a nisin concentration of 5 nM. Above this concentration the cells are suffering from pore formation mediated by nisin. Furthermore, we could show that NsrFP works as a lantibiotic exporter by a peptide release assay. Additionally several mutants of nisin were used to investigate the substrate specificity, which highlights that NsrFP recognizes the N-terminal region of nisin. This was confirmed by the observed resistance against nisin H (O'Connor et al., 2015) and gallidermin (Kellner et al., 1988), which both contain a similar N-terminus but differ in the C-terminal part of the peptide.

MATERIALS AND METHODS

Cloning of *nsrfp*

The *nsrfp* gene from *S. agalactiae* COH1 was amplified from the chromosomal DNA using two primers (NsrFP_for 5′-CA TCACCACCACCACTTATTAGAAATCAATCACTTAG-3′ and NsrFP_rev 5′-GTGGTGGTGGTGGTGCATATAATTCTCCTTTA TTTATTATAC-3) and ligated into *pIL-SV* (*E. coli–L. lactis* shuttle vector) (Alkhatib et al., 2014b). The point mutation $NsrF_{H202A}$ was introduced by a standard mutagenesis protocol using the following primers: forward: 5′-GATGGT AACCGCTTCAGCAAATGCTG-3′; reverse: 5′-CAGCATTTGC TGAAGCGGTTACCATC-3′. The resulting plasmid was verified by sequencing and transformed into the *L. lactis* strain NZ9000 for expression (Holo and Nes, 1989) and the corresponding strains were termed NZ9000NsrFP and NZ9000$NsrF_{H202A}$P. An empty vector *pIL-SVCm* was also transformed into the NZ9000 strain and was used as a control (that excludes any possible effect of induction of the plasmid), and this strain was called NZ9000Cm. The expression of the *nsrfp* gene is regulated by the TCS NisR/NisK present in the NZ9000 strain genome.

Expression of NsrFP and $NsrF_{H202A}$P

The NZ9000NsrFP and NZ9000$NsrF_{H202A}$P strains were grown in GM17 media supplemented with 5 μg/ml chloramphenicol. By the addition of nisin (final concentration of 1 ng/ml, which is equivalent to 0.3 nM), the expression was induced and the culture was further grown overnight. To analyze the expression, the cells were harvested at OD_{600} of 2.0 by centrifuging at 5000 × *g* for 30 min. The resulting pellet was resuspended with R-buffer [50 mM HEPES pH 8.0, 150 mM NaCl, 10% (w/v) glycerol] to an OD_{600} of 200. Then 1/3 (w/v) glass beads (0.3 mm) were added and cells were lysed. A cycle of 1 min disruption and 2 min cooling on ice was repeated five to six times. A low centrifugation step at 10,000 × *g* to collect the cytoplasmic part was performed. Followed by a high spin step (100,000 × *g*) to harvest the membranes. To collected cytoplasmic and membrane fractions SDS-loading dye [0.2 M Tris–HCl, pH 6.8, 10% (w/v) SDS, 40% (v/v) glycerol, 0.02% (w/v) bromophenol and β-mercaptoethanol] was added, samples were

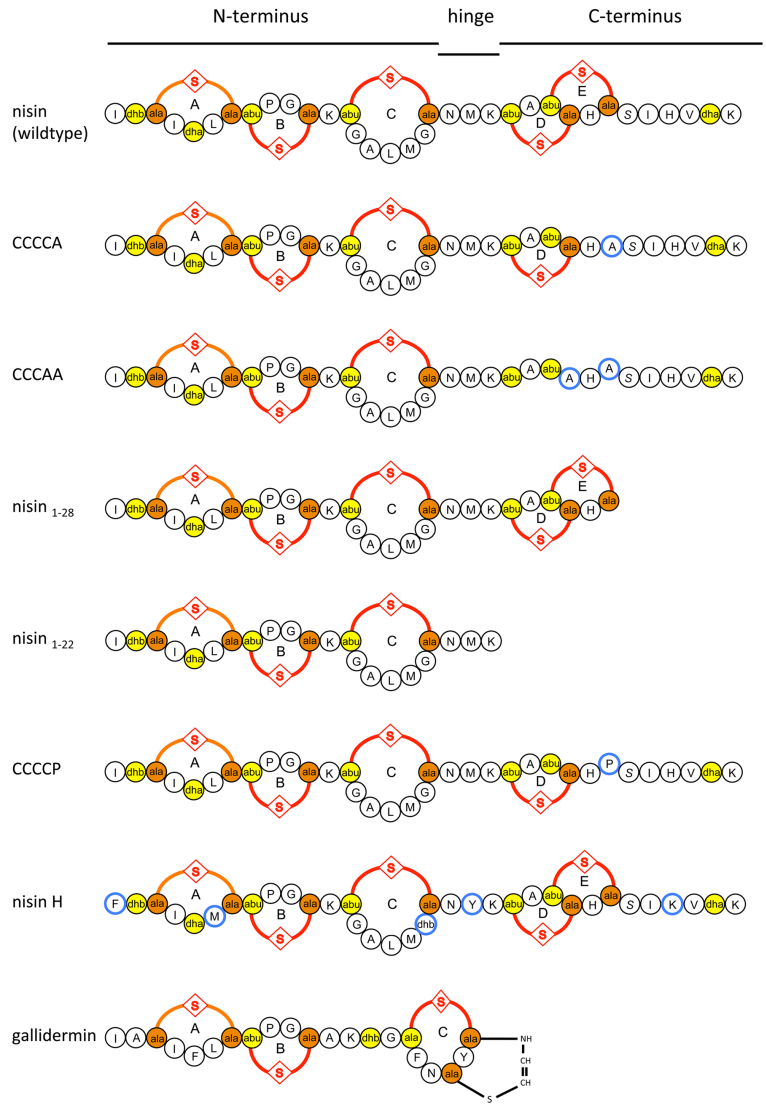

FIGURE 1 | Schematic overview of nisin, the variants of nisin, nisin H, and gallidermin used in this study. Introduced mutations in CCCCA, CCCAA, CCCCP, and the natural variants in nisin H are highlighted in blue. The (methyl)-lanthionine rings (labeled with A, B, C, D, and E) are formed by a dehydrated amino acid residue and a cysteine residue side chain (orange and yellow).

further used for SDS-PAGE and Western blot analysis (20 µl loaded). To detect NsrFP and $NsrF_{H202A}P$ a polyclonal antibody against the large extracellular loop of NsrP was used (Davids Biotechnologie, Regensburg, Germany).

Cloning of the Nisin H and CCCCP Variant

The used variants (CCCCA, CCCAA, $nisin_{1-28}$ and $nisin_{1-22}$) were previously described in Alkhatib et al. (2014b). Nisin H (O'Connor et al., 2015) was created by introducing five point mutations into the *pNZ-SV-nisA* vector (Alkhatib et al., 2014b). For the I_1F-L_6M point mutations we used the following primers (forward: 5′-GTG CATCACCACGCTTTACAAGTATTTCGATGTGTACACCCGG TTG-3′; reverse: 5′-CAACCGGGTGTACACATCGAAATACTT GTAAAGCGTGGTGATGCAC-3′). The $G_{18}T$-$M_{21}Y$ mutations were introduced with the primers (forward: 5′-GTAAAAC AGGAGCTCTGATGACATGTAACTATAAAACAGCAACTTGT CATTG-3′; reverse: 5′-CAATGACAAGTTGCTGTTTTATAGTT ACATGTCATCAGAGCTCCTGTTTTAC-3′) and the last mutation $H_{31}K$ with the primers (forward: 5′-CTTGTCATTG

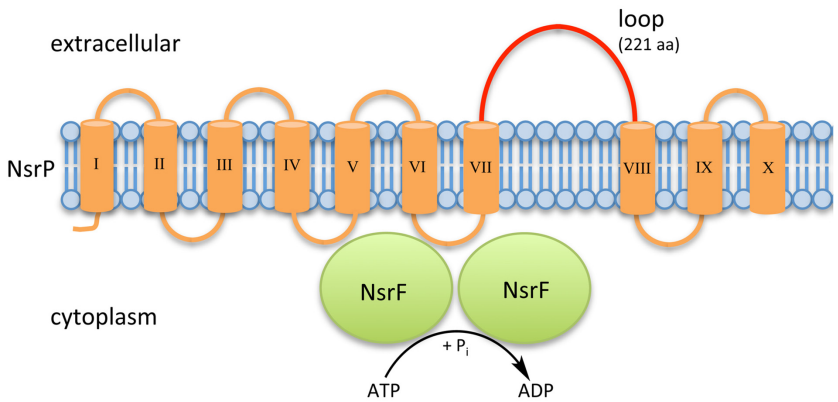

FIGURE 2 | Schematic representation of NsrFP from *S. agalactiae* COH1. NsrFP is an ABC transporter consisting of NsrF (highlighted in green), which hydrolyses ATP and NsrP (highlighted in orange). NsrP is a membrane protein consisting of 10 predicted transmembrane helices with an extracellular domain (depicted in red), which is a characteristic for the BceAB-type of lantibiotic resistance transporters.

TAGTATTAAAGTAAGCAAATAAGCTTTC-3′; reverse: 5′-GAAAGCTTATTTGCTTACTTTAATACTACAATGACAAG-3′). The CCCCP variant, were the last cysteine was exchanged by a proline was created into the *pNZ-SV-nisA* vector with the primers (forward: 5′-CAGCAACTTGTCATCCAAGTATTCACGTAAG-3′; reverse: 5′-CTTACGTGAATACTTGGATGACAAGTTGCTG-3′).

The resulting plasmids were verified by sequencing and transformed into the *L. lactis* strain NZ9000 (already containing the *pIL3-BTC* vector; Rink et al., 2005) for expression by electroporation as described above.

Expression, Purification of Prenisin Variants

Prenisin was purified as described in Alkhatib et al. (2014b). Activation of purified prenisin was done by overnight cleavage at 8°C with purified NisP (Abts et al., 2013). The efficiency of the reaction was monitored and the concentration of active nisin was determined by RP-HPLC as previously described (Abts et al., 2013). The activated nisin variants were then directly used for IC_{50} assays. Gallidermin is commercially available (Enzo Life Sciences).

Purification of Nisin

Nisin was purified as described in Abts et al. (2011). The concentration of nisin was measured by using RP-HPLC as previously described (Abts et al., 2013).

Determination the Activity of Nisin by Growth Inhibition (IC_{50})

Cells from the different expressing strains were grown overnight in GM17 supplemented with 5 μg/ml chloramphenicol in presence of 1 ng/ml nisin. The diluted cells (final OD_{584} was 0.1) were incubated with a serial dilution of nisin in a 96-well plate. The total volume in each well was 200 μl, consisting of 50 μl nisin and 150 μl GM17 containing the corresponding *L. lactis* strain. The highest concentration of nisin used was adapted to the corresponding maximum resistance displayed by each strain.

The plate was incubated at 30°C. After 5 h, the optical density was measured at 584 nm via 96-well plate reader BMG. The normalized optical density was plotted against the logarithm of the nisin concentration in order to calculate the IC_{50} of nisin and the data was evaluated using the following equation (Eq. 1):

$$y = \mathrm{OD}_{\min} + \frac{\mathrm{OD}_{\max} - \mathrm{OD}_{\min}}{1 + 10^{(\log(\mathrm{IC}_{50}) - x) \times p}}$$

The OD_{max} value describes the normalized optical density value where no nisin was added, while the OD_{min} value corresponds to the normalized optical density of the cells grown in the highest nisin concentrations. The y represents the resulted normalized optical density value and x represents the logarithmic of the nisin concentration added. The IC_{50} value is the concentration of nisin where the growth of the *L. lactis* strain is inhibited by 50% (Abts et al., 2011).

Calculation of the Fold of Resistance

We determined the IC_{50} value of nisin against the NZ9000Cm sensitive strain as well as the strain NZ9000NsrFP and NZ9000$NsrF_{H202A}$P. By dividing these two values the fold of resistance is obtained. For example wild type nisin displayed an IC_{50} of 4.9 nM against NZ9000Cm and 82.2 nM against NZ9000NsrFP. Dividing these two values results in a fold of resistance of 16.7. We used this fold of resistance to obtain a quantitative, comparable value for the nisin variants.

Dependency of Nisin Variants on Induced Expression of NsrFP

We verified the expression level of NsrFP in the corresponding strain NZ9000NsrFP by inducing expression with the different nisin variants. Here, we used half the IC_{50} value, which

was determined for each nisin variant against the sensitive NZ9000Cm strain, to exclude an effect on the expression level of NsrFP. The initial OD_{600} of the NZ9000NsrFP strain was 0.1 and we induced each sample with the half IC_{50} value of the corresponding nisin variants. The strains were further grown for 5 h at 30°C. After harvesting the cells, SDS-PAGE samples were prepared as describe above. The expression of NsrFP was analyzed by Western blot using a polyclonal antibody directed against the extracellular loop.

SYTOX Green Nucleic Acids Binding Assay

SYTOX green nucleic acids binding dye possesses a high binding affinity toward nucleic acids. It enters cells, which contain a pore in the plasma membrane and never crosses the intact membranes of living cells (Roth et al., 1997). The cells of NZ9000NsrFP were grown overnight in GM17 supplemented with 5 μg/ml chloramphenicol in presence of 1 ng/ml nisin. The next day, the overnight culture was diluted to an OD_{600} of 0.1 in fresh media supplemented with 5 μg/ml chloramphenicol. The cultures were grown until the OD_{600} reaches 0.5, the SYTOX green dye was added at a final concentration of 2.5 μM and incubated for 5 min according to the manual of the manufacturer (Invitrogen). The fluorescence signal, which was measured at an excitation and emission wavelength of 504 and 523 nm, respectively, was monitored. After a stable baseline is reached, nisin was added and the fluorescence was monitored over an additional time period.

Nisin Transport Assay

To answer the question whether NsrFP is an importer or exporter we performed a well-known nisin transport assay (Stein et al., 2003, 2005).

We grew the cells of NZ9000NsrFP, NZ9000$NsrF_{H202A}$P, and NZ9000Cm in GM17 supplemented with 5 μg/ml chloramphenicol in presence of 1 ng/ml nisin. We harvested the cells and washed them with 50 mM HEPES, pH 7, 500 mM NaCl, 10 % (v/v) glycerol. The cell density was adjusted to an OD_{600} of 10 in 1 ml of the corresponding strain and incubated with 8 μg nisin at 30°C for 30 min under gently shaking. After centrifugation at 10,000 × *g* for 10 min the supernatant was collected and applied to RP-HPLC for the quantification of nisin as described above.

RESULTS

IC_{50} Determination of NZ9000NsrFP and NZ9000$NsrF_{H202A}$P

We cloned NsrFP and $NsrF_{H202A}$P in a *pIL-SVCm* shuttle vector and induced the expression with a sublethal amount of nisin (0.3 nM). To ensure, that there were no side effects from induction with nisin, we compared all experiments with a control strain. This strain was transformed with an empty plasmid and was treated exactly the same. We observed that the induction using 0.3 nM had no influence on the morphology or growth behavior of the *L. lactis* strains. This expression system has been used in the past for several proteins involved in nisin modification as well as immunity and resistance (Kuipers et al., 2004; Plat et al., 2011; AlKhatib et al., 2014a; Khosa et al., 2016a). Nisin was purified as previously described (**Figure 3**; Abts et al., 2011). To address the activity of nisin against the NZ9000Cm, NZ9000NsrFP, and NZ9000$NsrF_{H202A}$P strains, growth experiments were performed using an increasing concentration of nisin. From these the IC_{50} values were determined, which reflects the growth inhibition of the corresponding strain by 50% using Eq. 1.

Nisin is highly active against the NZ9000Cm strain, as observed by the IC_{50} value of 4.9 ± 0.4 nM (**Figure 4** and **Table 1**). The NZ9000NsrFP strain exhibited a higher IC_{50} value of 82.2 ± 6.7 nM (**Figure 4** and **Table 1**). By dividing the two values a 16.7-fold of resistance was calculated (see Materials and Methods). This highlights that NsrFP expressed in *L. lactis* confers resistance against nisin. We cloned a variant of NsrFP termed $NsrF_{H202A}$P, where the histidine at position 202 of NsrF is mutated to an alanine. By sequence alignments this histidine residue was identified as the catalytically important residue for ATP hydrolysis, generally termed as H-loop (Zaitseva et al., 2005). The corresponding NZ9000$NsrF_{H202A}$P strain displayed a lower IC_{50} value of 5.1 ± 0.8 nM, which within experimental error represents the same value as obtained for the NZ9000Cm strain (**Figure 4** and **Table 1**). This suggests that NsrFP relies on ATP hydrolysis to confer resistance against nisin. Here, we have to note that the expression of $NsrF_{H202A}$P led to a reduced final OD (0.8 compared to 1.1 for the wild type strain) in our growth experiments. The observed difference does not rise from different expression levels of NsrFP and the $NsrF_{H202A}$P variant as shown by Western blot analysis using a polyclonal antibody directed against the large ECD of NsrP (Davids Biotechnology, Regensburg, Germany) (**Figure 3A**).

Pore Formation of Nisin in the NZ9000NsrFP Strain

Nisin is able to form pores in the membrane of Gram-positive bacteria initiated by the initial binding to lipid II and subsequently reorientation of the C-terminal part of nisin into the membrane (Hasper et al., 2004). This leads to membrane leakage and rapid cell death. We monitored this pore formation using a SYTOX green nucleic acid dye (Roth et al., 1997). When pores are formed in the membrane the SYTOX dye enters the cells and binds to the DNA, resulting in an increased fluorescence signal. This is an almost instant effect, which can be monitored in real time. We monitored the pore forming action of nisin against the NZ9000NsrFP, using different nisin concentrations, which were based on the IC_{50} values of the corresponding strains determined above. As a control, we added only buffer without nisin, which resulted in no increase of the fluorescence signal as observed by the black line in **Figure 5**. This control indicates that no cells are spontaneously lysed under this experimental setup.

When 40 nM nisin (corresponding to half the IC_{50} value determined for the NZ9000NsrFP strain) was added to the

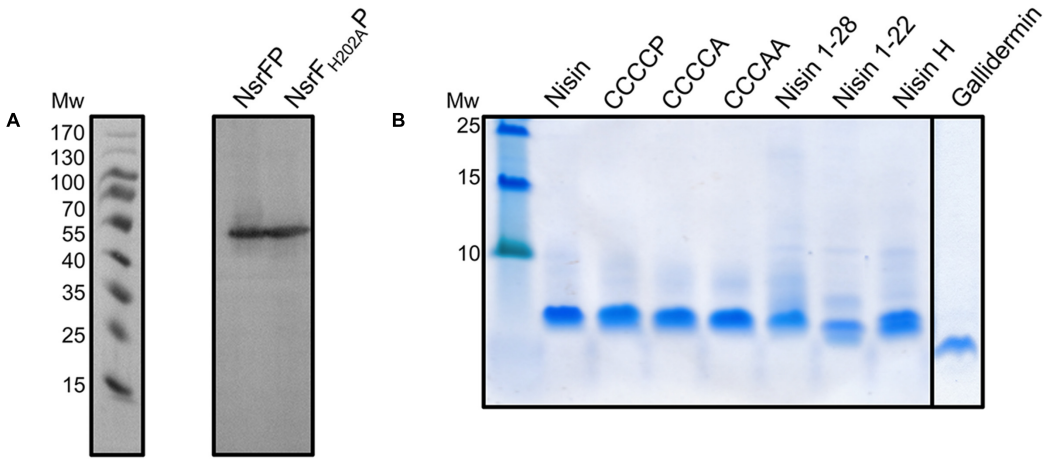

FIGURE 3 | Expression of NsrFP and $NsrF_{H202A}P$ in *L. lactis* and purification of nisin variants. **(A)** The expression of NsrFP and $NsrF_{H202A}P$ was monitored by Western blot using a polyclonal antibody against the extracellular domain. As observed both proteins are expressed at a similar level in *L. lactis* NZ9000. **(B)** Nisin and its variants were purified and activated by using a standard procedure (see Materials and Methods). All substrates display a similar purity, judged by a 20% Tricine-SDS-PAGE.

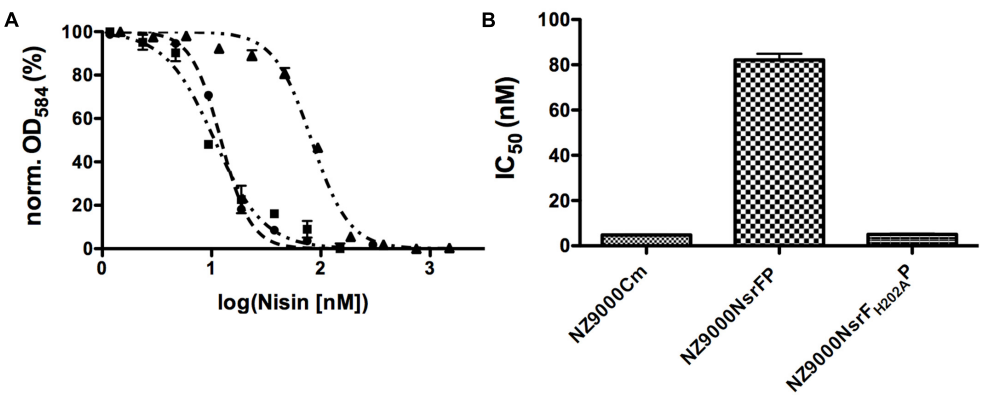

FIGURE 4 | Activity of nisin against the NZ9000Cm, NZ9000NsrFP, and $NZ9000NsrF_{H202A}P$ strains. **(A)** The IC_{50} of nisin against the NZ9000Cm (●), NZ9000NsrFP (▲), and strain $NZ9000NsrF_{H202A}P$ (■) was determined. As observed the curve shifted to higher nisin concentration indicating that the NZ9000NsrFP strain is more resistant toward nisin. **(B)** The calculated IC_{50} values of nisin against the NZ9000Cm, NZ9000NsrFP, and the $NZ9000NsrF_{H202A}P$ strain are highlighted.

NZ9000NsrFP strain, no increase of the fluorescence signal was observed (**Figure 5**, green line). This indicates that the NZ9000NsrFP strain can survive a nisin concentration of 40 nM. Only a small linear increase was visible after 400 s, which reflects to a less extent cell lysis after some time. A nisin concentration equivalent to the IC_{50} value (80 nM) resulted in a slightly stronger increase of the signal after a delay time (**Figure 5**, blue line). Finally, after adding a nisin concentration of two-times the IC_{50} value (e.g., 160 nM to the NZ9000NsrFP strain) a rapid increase of the fluorescence signal was observed and reaches a stable plateau already after a couple of seconds. This shows that NsrFP is not able to confer resistance above the determined IC_{50} concentration (**Figure 5**, red line).

Nisin Transport Assay–Peptide Release Assay

We performed a peptide release assay to verify the transport direction of NsrFP. Previously, the same assay was used to characterize NisFEG and SpaFEG, two exporting systems from lantibiotic producing strains (Stein et al., 2003, 2005). Here, we incubated the NsrFP expressing strain with 8 μg nisin for 30 min. After centrifugation of the cell, the supernatant was analyzed via RP-HPLC to determine the amount of nisin. From 8 μg nisin, 4.3 μg nisin was recovered from the supernatant (**Figure 6**). As a control, we used the $NsrF_{H202A}P$ and the sensitive NZ9000Cm strain. There only ∼2 μg nisin was recovered from the supernatant (**Figure 6**). This shows that NsrFP is able to

TABLE 1 | IC_{50} values of nisin and its variants against the NZ9000Cm, NZ9000NsrFP, and NZ9000$NsrF_{H202A}$P strains.

	NZ9000Cm	NZ9000NsrFP		NZ9000$NsrF_{H202A}$P	
Nisin variant	**IC_{50} (nM)**	**IC_{50} (nM)**	**Fold of resistance**	**IC_{50} (nM)**	**Fold of resistance**
Wild type	4.9 ± 0.4	82.2 ± 6.7	16.7	5.1 ± 0.8	1.1
CCCCP	39.7 ± 1.5	238.4 ± 11.7	6.0	37.8 ± 3.9	0.9
CCCCA	64.4 ± 8.4	2023 ± 143	31.4	38.9 ± 5.9	0.6
CCCAA	278.6 ± 18.8	36346 ± 3632	130.5	154.6 ± 30.8	0.5
$Nisin_{1-28}$	157.0 ± 8.7	5243 ± 1225	33.4	65.3 ± 11.4	0.4
$Nisin_{1-22}$	309.9 ± 51.4	12220 ± 804	39.4	209.0 ± 39.9	0.7
Nisin H	7.0 ± 0.4	86.5 ± 3.7	12.3	7.5 ± 0.8	1.1
Gallidermin	67.1 ± 9.1	840 ± 87.0	12.5	59.7 ± 7.3	0.9

Besides the IC_{50} values also the fold of resistance against the nisin variants mediated by NsrFP are shown. The fold of resistance is calculated by the division of the IC_{50} value obtained of the NZ9000NsrFP by the value for the NZ9000Cm strain. The values represent the average and standard deviation of at least four different experiments.

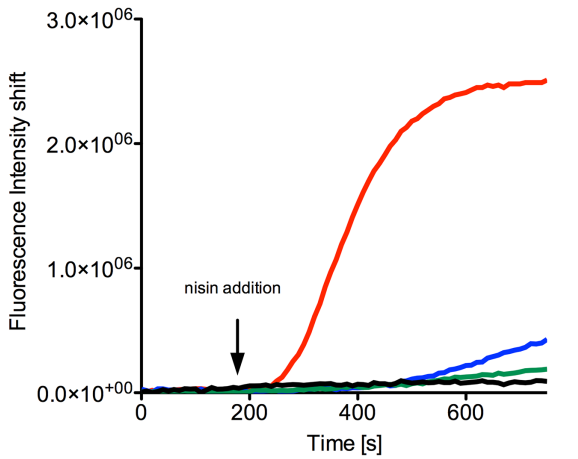

FIGURE 5 | SYTOX green assay to visualize pore formation mediated by nisin. The NZ9000NsrFP strain was grown until OD_{600} of 0.5 and then incubated with the SYTOX dye. After a stable baseline was reached nisin (indicated with an arrow) was added at various concentrations: 40 nM (green line), 80 nM (blue line), and 160 nM (red line). As a control only buffer was added (black line). The fluorescence signal was monitored online using a fluorolog (Horiba III) and the rapid increase indicates pore formation. The curves are representatives of at least four biological replicates.

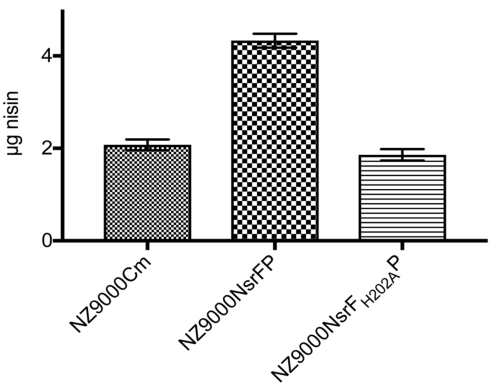

FIGURE 6 | Nisin transport assay. The NZ9000Cm, NZ9000NsrFP, and NZ9000$NsrF_{H202A}$P strain were incubated with 8 µg nisin. After incubation for 30 min the cells were spun down and the amount of nisin in the supernatant was determined using RP-HPLC. The NZ9000Cm and NZ9000$NsrF_{H202A}$P strain showed similar nisin amounts. The NZ9000NsrFP strain revealed a ~2-fold increased nisin amount, highlighting that NsrFP exports nisin from the *L lactis* membrane.

export nisin from the cellular membrane. Our results are similar to the results found for the NisFEG and SpaFEG transporters leading to the same conclusion that NsrFP is exporting nisin from the cellular membrane as well.

Substrate Specificity of NsrFP

In order to investigate the substrate specificity of NsrFP we used a set of nisin variants. Here, the nisin variants CCCCA, CCCAA, $nisin_{1-28}$, and $nisin_{1-22}$ were used (Khosa et al., 2016a). These variants are lacking the last or last two lanthionine rings or display deletions at the C-terminus of nisin, respectively. CCCCP is a variant, where the cysteine at position 28 (important for ring E formation) is exchanged to a proline (for a schematic view see **Figure 1**).

Expression and purification were performed as previously described (Alkhatib et al., 2014b), resulting in high purity (**Figure 3B**). The activities of these variants were determined against the nisin sensitive NZ9000Cm strain and the strains expressing NsrFP or $NsrF_{H202A}$P, respectively (**Table 1**). By comparing these values the fold of resistance was obtained (**Figure 7**) as determined for the wild type nisin (see above and Materials and Methods).

For CCCCP, the fold of resistance was determined to be 6.0 (IC_{50} against NZ9000Cm was 39.7 ± 1.5 nM and against NZ9000NsrFP was 238.4 ± 11.7 nM). For CCCCA, the fold of resistance was determined to be 31.4 (IC_{50} against NZ9000Cm was 64.4 ± 8.4 nM and against NZ9000NsrFP 2023 ± 143 nM). The CCCAA variants displayed a 130.5-fold of resistance (IC_{50} against NZ9000Cm was 278.6 ± 18.8 nM and against NZ9000NsrFP 36346 ± 3632 nM). The two deletion mutants displayed a 33.4 ($nisin_{1-28}$) and 39.4 ($nisin_{1-22}$) fold

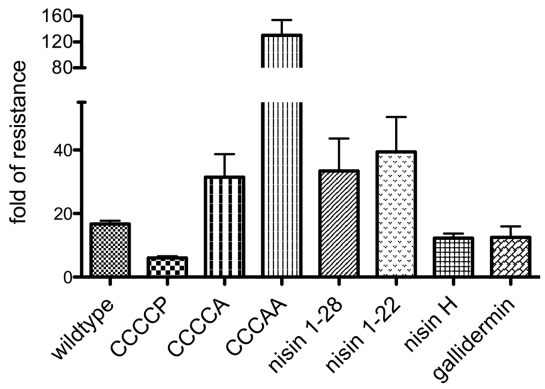

FIGURE 7 | Substrate specificity of NsrFP. Graphical representation of the fold of resistance exhibited by NsrFP with nisin and different nisin variants (CCCCA, CCCAA, CCCCP, $nisin_{1-22}$ and $nisin_{1-28}$) as well as nisin H and gallidermin. The NZ9000Cm and NZ9000NsrFP strains were used to determine the activity of all tested lantibiotics. The error bars indicate the standard error of at least three independent experiments.

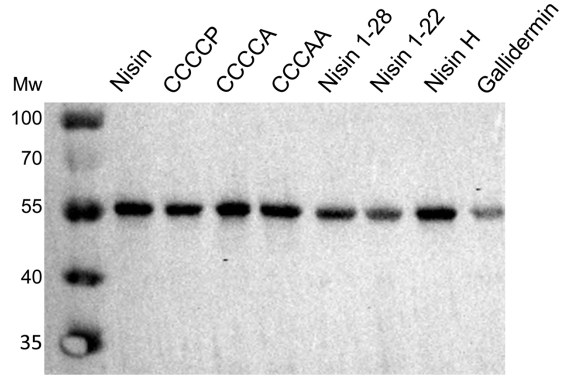

FIGURE 8 | Dependency of nisin variants on induced expression of NsrFP. The expression of NsrFP was monitored by Western blot using a polyclonal antibody against the extracellular domain. As observed, the expression of NsrFP was similar in all cases, independent of the used nisin variant.

of resistance, almost five times higher when compared to wild type. Here IC_{50} were determined to be 157 ± 8.7 nM against NZ9000Cm and 5243 ± 1225 nM against NZ9000NsrFP strain for $nisin_{1-28}$ and 309.9 ± 51.4 nM against NZ9000Cm and 12,220 ± 804 nM against NZ9000NsrFP for $nisin_{1-22}$, respectively.

These results revealed that NsrFP is able to be active as long as the N-terminal region of nisin is present, and since this part is highly conserved in several other lantibiotics, we hypothesized that the NsrFP transporter can besides nisin also recognize other lantibiotics. To test this, we used two other lantibiotics: nisin H (O'Connor et al., 2015) and gallidermin which is produced by *Staphylococcus gallinarum* Tü3928 (Kellner et al., 1988) (schematically shown in **Figure 1**). The latter contains a similar N-terminal part but has in comparison to nisin a structurally non-related C-terminus.

We determined the fold of resistance mediated by NsrFP for these lantibiotics (**Table 1** and **Figure 7**). Here, it was observed that nisin H as well as gallidermin are also recognized and NsrFP confers resistance to these lantibiotics. Our calculated fold of resistance is 12.3 for nisin H and 12.5 for gallidermin (**Table 1**). This strengthens the observation that the N-terminal region plays a predominant role in substrate recognition, since nisin H and gallidermin are recognized as well with similar efficiencies.

We were wondering whether the effect of a higher fold of resistance actually was a result of an increased expression of NsrFP in the membrane. Therefore, we incubated NZ9000NsrFP cells with the corresponding nisin variants (note: the concentration is 1/2 IC_{50} value of each nisin variant) and visualized the expression of NsrFP by Western blot. Here, we observed that the expression levels of NsrFP were similar for each strain and thereby cannot be the reason for the higher increased fold of resistance (**Figure 8**).

DISCUSSION

Lantibiotics possess antimicrobial activity against various bacteria including the well known MRSA, VISA, and VRE strains (Piper et al., 2009). However, various bacteria, especially human pathogens are actually inherently resistant against lantibiotics, which they do not produce themselves. Interestingly, this resistance is often arising from the expression of one or two membrane embedded proteins. Here, one belongs to the BceAB-type ABC transporter family and confer resistance against antimicrobial peptides including lantibiotics (Kallenberg et al., 2013; Kingston et al., 2014). Genetically the BceAB-type transporters are often located next to a TCS in the genome, which regulates the expression of the genes encoded (Dintner et al., 2011). It is thought that especially the ECD, which is a hallmark of BceAB-type ABC transporters is involved in lantibiotic sensing and transferring the signal to the corresponding histidine kinase (Staroń et al., 2011; Kallenberg et al., 2013). We focused on the nisin resistance operon from the *S. agalactiae* COH1, more specifically the BceAB-type ABC transporter NsrFP (Khosa et al., 2013). This transporter is localized on a gene operon together with the membrane associated protease NSR and the TCS NsrR and NsrK (Khosa et al., 2013, 2016b). We heterologously expressed the transporter in *L. lactis*, which lacks the NsrR/NsrK TCS and observed that NsrFP is able to confer resistance by itself. The fold of resistance, which we used as a measure of the activity, revealed that the *L. lactis* cells are able to deal with a 16-fold higher nisin concentration when compared to the same strain lacking NsrFP. The fold of resistance of an ATP hydrolysis deficient mutant of NsrFP is reduced to levels observed for the nisin sensitive NZ9000Cm strain. Like NisFEG (Stein et al., 2003) and SpaFEG (Stein et al., 2005), NsrFP acts as an lantibiotic exporter, which so far has not been conclusively shown for an lantibiotic resistance ABC transporter.

Intriguing is the observation that the N-terminal part of nisin appears to be important for NsrFP. By using C-terminal

variants and deletions of nisin the fold of resistance increased in comparison to the wild type nisin. Only the variant CCCCP displayed a reduced fold of resistance. The recognition of the N-terminal region was further underlined by the observation that nisin H as well as gallidermin were also recognized as substrates. Here, especially the latter is containing a similar N-terminal region but differs structurally completely at the C-terminus (**Figure 1**).

Previously, the recognition of ring A and B was observed for the lantibiotic resistance ABC transporter CprABC from *Clostridium difficile*, which recognizes multiple lantibiotics: for example, nisin, gallidermin, subtilin, and mutacin 1140 (McBride and Sonenshein, 2011; Suárez et al., 2013).

Within the nisin resistance operon in *S. agalactiae* COH1 two proteins, namely the membrane associated protease NSR and NsrFP, are present (Khosa et al., 2013, 2016b). NSR is cleaving off the last six amino acids of nisin resulting in $nisin_{1-28}$, which has a 32-fold lower activity. This product of NSR ($nisin_{1-28}$), however, is still well recognized by NsrFP, as shown by an even increased fold of resistance. This suggests that both proteins are working together to obtain full resistance in *S. agalactiae*. The first line of defense would be NSR and the resulting processed product $nisin_{1-28}$, is transported by NsrFP, once it reaches the membrane with high efficiency. This type of cooperativity would be similar to the natural immunity system observed in the nisin and subtilin (auto)immunity systems from *L. lactis* and *B. subtilis*, respectively. There, a cooperative mode of action of the immunity proteins LanI and LanFEG have been observed by which only full immunity was displayed when both protein are simultaneously expressed (Stein et al., 2003, 2005). Therefore, we suggest that NsrFP and NSR have a similar cooperative mode of action and only when both proteins are expressed simultaneously within the membrane of *S. agalactiae* COH1 full resistance is occurring.

AUTHOR CONTRIBUTIONS

SS conceived and directed this study. JR, ML, SL, and KE conducted the experiments. JZ-K established the mutants of nisin and created the figures. JR, ML, and SS wrote the manuscript with input of all authors. All authors read and approved the manuscript.

FUNDING

This work has been supported by the Graduate School 2158, which is funded by the Deutsche Forschungsgemeinschaft (DFG).

ACKNOWLEDGMENTS

We thank Diana Kleinschrodt and Iris Fey of the Protein Production Facility for excellent support during the initial stages of this project. We thank all members of the Institute of Biochemistry for fruitful discussions. The students of the master course "Fascination Biochemistry" for their initial experiments during their bachelor studies.

REFERENCES

Abts, A., Mavaro, A., Stindt, J., Bakkes, P. J., Metzger, S., Driessen, A. J., et al. (2011). Easy and rapid purification of highly active nisin. *Int. J. Pept.* 2011:175145. doi: 10.1155/2011/175145

Abts, A., Montalban-Lopez, M., Kuipers, O. P., Smits, S. H., and Schmitt, L. (2013). NisC binds the FxLx motif of the nisin leader peptide. *Biochemistry* 52, 5387–5395. doi: 10.1021/bi4008116

AlKhatib, Z., Lagedroste, M., Fey, I., Kleinschrodt, D., Abts, A., and Smits, S. H. (2014a). Lantibiotic immunity: inhibition of nisin mediated pore formation by NisI. *PLoS ONE* 9:e102246. doi: 10.1371/journal.pone.0102246

Alkhatib, Z., Lagedroste, M., Zaschke, J., Wagner, M., Abts, A., Fey, I., et al. (2014b). The C-terminus of nisin is important for the ABC transporter NisFEG to confer immunity in *Lactococcus lactis*. *MicrobiologyOpen* 3, 752–763. doi: 10.1002/mbo3.205

Brötz, H., Bierbaum, G., Leopold, K., Reynolds, P. E., and Sahl, H. G. (1998a). The lantibiotic mersacidin inhibits peptidoglycan synthesis by targeting lipid II. *Antimicrob. Agents Chemother.* 42, 154–160.

Brötz, H., Josten, M., Wiedemann, I., Schneider, U., Götz, F., Bierbaum, G., et al. (1998b). Role of lipid-bound peptidoglycan precursors in the formation of pores by nisin, epidermin and other lantibiotics. *Mol. Microbiol.* 30, 317–327.

Chatterjee, C., Paul, M., Xie, L., and van der Donk, W. A. (2005). Biosynthesis and mode of action of lantibiotics. *Chem. Rev.* 105, 633–684. doi: 10.1021/cr030105v

de Freire Bastos, M. D. C., Coelho, M. L. V., and da Silva Santos, O. C. (2015). Resistance to bacteriocins produced by Gram-positive bacteria. *Microbiology* 161, 683–700. doi: 10.1099/mic.0.082289-0

Dintner, S., Heermann, R., Fang, C., Jung, K., and Gebhard, S. (2014). A sensory complex consisting of an ATP-binding cassette transporter and a two-component regulatory system controls bacitracin resistance in *Bacillus subtilis*. *J. Biol. Chem.* 289, 27899–27910. doi: 10.1074/jbc.M114.596221

Dintner, S., Staroń, A., Berchtold, E., Petri, T., Mascher, T., and Gebhard, S. (2011). Coevolution of ABC transporters and two-component regulatory systems as resistance modules against antimicrobial peptides in Firmicutes bacteria. *J. Bacteriol.* 193, 3851–3862. doi: 10.1128/JB.05175-11

Dischinger, J., Chipalu, S. B., and Bierbaum, G. (2014). Lantibiotics: promising candidates for future applications in health care. *Int. J. Med. Microbiol.* 304, 51–62. doi: 10.1016/j.ijmm.2013.09.003

Draper, L. A., Cotter, P. D., Hill, C., and Ross, R. P. (2015). Lantibiotic resistance. *Microbiol. Mol. Biol. Rev.* 79, 171–191. doi: 10.1128/MMBR.00051-14

Gebhard, S., and Mascher, T. (2011). Antimicrobial peptide sensing and detoxification modules: unravelling the regulatory circuitry of *Staphylococcus aureus*. *Mol. Microbiol.* 81, 581–587. doi: 10.1111/j.1365-2958.2011.07747.x

Hasper, H. E., de Kruijff, B., and Breukink, E. (2004). Assembly and stability of nisin-lipid II pores. *Biochemistry* 43, 11567–11575. doi: 10.1021/bi049476b

Hasper, H. E., Kramer, N. E., Smith, J. L., Hillman, J. D., Zachariah, C., Kuipers, O. P., et al. (2006). An alternative bactericidal mechanism of action for lantibiotic peptides that target lipid II. *Science* 313, 1636–1637. doi: 10.1126/science.1129818

Holo, H., and Nes, I. F. (1989). High-frequency transformation, by electroporation, of *Lactococcus lactis* subsp. *cremoris* grown with glycine in osmotically stabilized media. *Appl. Environ. Microbiol.* 55, 3119–3123.

Hsu, S.-T. D., Breukink, E., Tischenko, E., Lutters, M. A. G., de Kruijff, B., Kaptein, R., et al. (2004). The nisin-lipid II complex reveals a pyrophosphate cage that provides a blueprint for novel antibiotics. *Nat. Struct. Mol. Biol.* 11, 963–967. doi: 10.1038/nsmb830

Islam, M. R., Nishie, M., Nagao, J., Zendo, T., Keller, S., Nakayama, J., et al. (2012). Ring A of nukacin ISK-1: a lipid II-binding motif for type-A(II) lantibiotic. *J. Am. Chem. Soc.* 134, 3687–3690. doi: 10.1021/ja300007h

Kallenberg, F., Dintner, S., Schmitz, R., and Gebhard, S. (2013). Identification of regions important for resistance and signalling within the antimicrobial

peptide transporter BceAB of *Bacillus subtilis*. *J. Bacteriol.* 195, 3287–3297. doi: 10.1128/JB.00419-13

Kellner, R., Jung, G., Horner, T., Zahner, H., Schnell, N., Entian, K. D., et al. (1988). Gallidermin: a new lanthionine-containing polypeptide antibiotic. *Eur. J. Biochem.* 177, 53–59. doi: 10.1111/j.1432-1033.1988.tb14344.x

Khosa, S., Alkhatib, Z., and Smits, S. H. (2013). NSR from *Streptococcus agalactiae* confers resistance against nisin and is encoded by a conserved NSR operon. *Biol. Chem.* 394, 1543–1549. doi: 10.1515/hsz-2013-0167

Khosa, S., Frieg, B., Mulnaes, D., Kleinschrodt, D., Hoeppner, A., Gohlke, H., et al. (2016a). Structural basis of lantibiotic recognition by the nisin resistance protein from *Streptococcus agalactiae*. *Sci. Rep.* 6:18679. doi: 10.1038/srep18679

Khosa, S., Lagedroste, M., and Smits, S. H. (2016b). Protein defense systems against the lantibiotic nisin: function of the immunity protein NisI and the resistance protein NSR. *Front. Microbiol.* 7:504. doi: 10.3389/fmicb.2016.00504

Kingston, A. W., Zhao, H., Cook, G. M., and Helmann, J. D. (2014). Accumulation of heptaprenyl diphosphate sensitizes *Bacillus subtilis* to bacitracin: implications for the mechanism of resistance mediated by the BceAB transporter. *Mol. Microbiol.* 93, 37–49. doi: 10.1111/mmi.12637

Klaenhammer, T. R. (1993). Genetics of bacteriocins produced by lactic acid bacteria. *FEMS Microbiol. Rev* 12, 39–85. doi: 10.1111/j.1574-6976.1993.tb00012.x

Kuipers, A., de Boef, E., Rink, R., Fekken, S., Kluskens, L. D., Driessen, A. J., et al. (2004). NisT, the transporter of the lantibiotic nisin, can transport fully modified, dehydrated, and unmodified prenisin and fusions of the leader peptide with non-lantibiotic peptides. *J. Biol. Chem.* 279, 22176–22182. doi: 10.1074/jbc.M312789200

McBride, S. M., and Sonenshein, A. L. (2011). Identification of a genetic locus responsible for antimicrobial peptide resistance in *Clostridium difficile*. *Infect. Immun.* 79, 167–176. doi: 10.1128/IAI.00731-10

Mota-Meira, M., Lapointe, G., Lacroix, C., and Lavoie, M. C. (2000). MICs of mutacin B-Ny266, nisin A, vancomycin, and oxacillin against bacterial pathogens. *Antimicrob. Agents Chemother.* 44, 24–29. doi: 10.1128/AAC.44.1.24-29.2000

Nawrocki, K. L., Crispell, E. K., and McBride, S. M. (2014). Antimicrobial peptide resistance mechanisms of Gram-positive bacteria. *Antibiotics* 3, 461–492. doi: 10.3390/antibiotics3040461

O'Connor, P. M., O'Shea, E. F., Guinane, C. M., O'Sullivan, O., Cotter, P. D., Ross, R. P., et al. (2015). Nisin H is a new nisin variant produced by the gut-derived strain *Streptococcus hyointestinalis* DPC6484. *Appl. Environ. Microbiol.* 81, 3953–3960. doi: 10.1128/AEM.00212-15

Ohki, R., Giyanto, Tateno, K., Masuyama, W., Moriya, S., Kobayashi, K., et al. (2003). The BceRS two-component regulatory system induces expression of the bacitracin transporter, BceAB, in *Bacillus subtilis*. *Mol. Microbiol.* 49, 1135–1144. doi: 10.1046/j.1365-2958.2003.03653.x

Piper, C., Cotter, P. D., Ross, R. P., and Hill, C. (2009). Discovery of medically significant lantibiotics. *Curr. Drug Discov. Technol.* 6, 1–18. doi: 10.2174/157016309787581075

Plat, A., Kluskens, L. D., Kuipers, A., Rink, R., and Moll, G. N. (2011). Requirements of the engineered leader peptide of nisin for inducing modification, export, and cleavage. *Appl. Environ. Microbiol.* 77, 604–611. doi: 10.1128/AEM.01503-10

Rietkötter, E., Hoyer, D., and Mascher, T. (2008). Bacitracin sensing in *Bacillus subtilis*. *Mol. Microbiol.* 68, 768–785. doi: 10.1111/j.1365-2958.2008.06194.x

Rink, R., Kuipers, A., de Boef, E., Leenhouts, K. J., Driessen, A. J., Moll, G. N., et al. (2005). Lantibiotic structures as guidelines for the design of peptides that can be modified by lantibiotic enzymes. *Biochemistry* 44, 8873–8882. doi: 10.1021/bi050081h

Roth, B. L., Poot, M., Yue, S. T., and Millard, P. J. (1997). Bacterial viability and antibiotic susceptibility testing with SYTOX green nucleic acid stain. *Appl. Environ. Microbiol.* 63, 2421–2431.

Ruhr, E., and Sahl, H.-G. (1985). Mode of action of the peptide antibiotic nisin and influence on the membrane potential of whole cells and on cytoplasmic and artificial membrane vesicles. *Antimicrob. Agents Chemother.* 27, 841–845. doi: 10.1128/AAC.27.5.841

Staroń, A., Finkeisen, D. E., and Mascher, T. (2011). Peptide antibiotic sensing and detoxification modules of *Bacillus subtilis*. *Antimicrob. Agents Chemother.* 55, 515–525. doi: 10.1128/AAC.00352-10

Stein, T., Heinzmann, S., Düsterhus, S., Borchert, S., and Entian, K.-D. (2005). Expression and functional analysis of the subtilin immunity genes spaIFEG in the subtilin-sensitive host *Bacillus subtilis* MO1099. *J. Bacteriol.* 187, 822–828. doi: 10.1128/JB.187.3.822-828.2005

Stein, T., Heinzmann, S., Solovieva, I., and Entian, K.-D. (2003). Function of *Lactococcus lactis* nisin immunity genes nisI and nisFEG after coordinated expression in the surrogate host *Bacillus subtilis*. *J. Biol. Chem.* 278, 89–94. doi: 10.1074/jbc.M207237200

Suárez, J. M., Edwards, A. N., and McBride, S. M. (2013). The *Clostridium difficile cpr* locus is regulated by a noncontiguous two-component system in response to type A and B lantibiotics. *J. Bacteriol.* 195, 2621–2631. doi: 10.1128/JB.00166-13

Sun, Z., Zhong, J., Liang, X., Liu, J., Chen, X., and Huan, L. (2009). Novel mechanism for nisin resistance via proteolytic degradation of nisin by the nisin resistance protein NSR. *Antimicrob. Agents Chemother.* 53, 1964–1973. doi: 10.1128/AAC.01382-08

Van de Ven, F., Van den Hooven, H., Konings, R., and Hilbers, C. (1991). "The spatial structure of nisin in aqueous solution," in *Nisin and Novel Lantibiotics*, eds G. Jung and H.-G. Sahl (Leiden: ESCOM Publishers), 35–42.

Wiedemann, I., Breukink, E., Van Kraaij, C., Kuipers, O. P., Bierbaum, G., De Kruijff, B., et al. (2001). Specific binding of nisin to the peptidoglycan precursor lipid II combines pore formation and inhibition of cell wall biosynthesis for potent antibiotic activity. *J. Biol. Chem.* 276, 1772–1779. doi: 10.1074/jbc.M006770200

Yang, S.-C., Lin, C.-H., Sung, C. T., and Fang, J.-Y. (2014). Antibacterial activities of bacteriocins: application in foods and pharmaceuticals. *Front. Microbiol.* 5:241. doi: 10.3389/fmicb.2014.00241

Zaitseva, J., Jenewein, S., Jumpertz, T., Holland, I. B., and Schmitt, L. (2005). H662 is the linchpin of ATP hydrolysis in the nucleotide-binding domain of the ABC transporter HlyB. *EMBO J.* 24, 1901–1910. doi: 10.1038/sj.emboj.7600657

Conflict of Interest Statement: The authors declare that the research was conducted in the absence of any commercial or financial relationships that could be construed as a potential conflict of interest.

4 Discussion

Within this thesis, several topics concerning lantibiotics were presented and addressed, providing various useful insights in lantibiotics themselves and their mechanism of resistance. Chapter I comprised an overview about the different classes of lantibiotics and their modification machinery, which is responsible for the installation of the post-translationally modifications. Furthermore, the binding of the maturation enzymes NisB and NisC with their substrate nisin A was shown, revealing the interplay between the proteins and the stoichiometry of the modification complex (Chapter II). These modification enzymes also have the capability to influence the ABC transporter NisT as shown in Chapter III. Several nisin variants were created and produced; and the effect of the mutations on the whole maturation machinery as well on the antimicrobial activity was analyzed. This included screening of position one of nisin A (Chapter IV), followed by analysis of the natural variant, nisin H (Chapter V). Special regions of nisin A, concerning the C-terminal part of nisin A or the important hinge region were analyzed as well (Chapters VI – VII, IX). A detailed introspection of the BceAB-type ABC-transporter NsrFP from nisin resistance operon and its corresponding NBD NsrF were presented in Chapters VIII and IX.

4.1 Lanthipeptides and their machinery, a story of success

In the history of mankind, bacterial infections are responsible for millions of deaths and until the 20th century, no effective treatment was found. The first antimicrobial substance, penicillin was discovered in 1928 by Alexander Flemming (Fleming, 1929). Since this discovery, hundreds of antimicrobial substances have been found and one promising group is the lanthionine-containing antibiotic (lantibiotics) with the best characterized lantibiotic nisin A (Ingram, 1969; Kellner et al., 1988; Knerr & van der Donk, 2012; Newton et al., 1953; Schnell et al., 1988; Xie & van der Donk, 2004). The (methyl-) lanthionine rings present in nisin are characteristic of lantibiotics and responsible for their high thermostability, antimicrobial activity in nanomolar concentrations and resistance against proteolytic digestions (Chan et al., 1996; Gross & Morell, 1967; Lu et al., 2010; Oppedijk et al., 2016). With the increased need of highly active antimicrobial peptides, other natural nisin variants were also found and so far, nine natural variants of nisin have been identified (Figure 3). Although, most natural lantibiotics are only effective against Gram-positive bacteria and lack Gram-negative activity

(Kordel et al., 1988; Stevens et al., 1991); lantibiotics are used in the fields of veterinary medicine, food industry and pharmaceutical applications. Nisin A, for example, is used in the food industry since decades as an additive (E234) in cheese or milk (Delves-Broughton et al., 1996) or used in the veterinary medicine to treat mastitis in cows (Cao et al., 2007). The class I lantibiotic, NAI-107, for example, is in pre-clinical trials and might be a good candidate in the treatment of multidrug-resistant strains such as MRSA or similar Gram-positive strains (Brunati et al., 2018; Jabes et al., 2011). However, some lanthipeptides also show antifungal, antiviral, morphogenetic, or antinociceptive activities (Ferir et al., 2013; Iorio et al., 2014; Kodani et al., 2004; Kodani et al., 2005; Mohr et al., 2015); making them an excellent alternative candidate to antibiotics in the pharmaceutical industry. Even the lantibiotic gene clusters have been extensively used in the biotechnological industry. For example, parts of the nisin gene cluster are used for biotechnology applications in the so called nisin-controlled expression (NICE) system. This is an established platform containing the TCS system NisRK (nisin inducer) and the corresponding *nisA* promoter, for the expression of the target peptide or protein (Kuipers et al., 1997; Kuipers et al., 1998; Mierau & Kleerebezem, 2005). Furthermore, enzymes of the nisin A maturation e.g. NisBTC were successfully used for the installation of PTMs and the secretion of therapeutic peptides, like angiotensin or vasopressin (Khusainov et al., 2013; Kluskens et al., 2005; Kluskens et al., 2009; Plat et al., 2011; Rink et al., 2005).

4.2 The nisin maturation machinery

The proteins responsible for the installation of PTMs and thereby resulting in mature precursor peptide are the dehydratase NisB (responsible for the dehydration of serine and threonine residues in the core peptide) and the cyclase NisC (catalyzing the Michael-type condensation and forming the (methyl-) lanthionine rings) (Karakas Sen et al., 1999; Koponen et al., 2002; Okeley et al., 2003). Both these proteins were purified and based on SPR or ITC experiments, the binding affinities of these proteins for the precursor peptide of nisin A were determined (Abts et al., 2013; Mavaro et al., 2011). It was shown that both the NisB dimer and the NisC monomer bind nisin A in a 1:1 stoichiometry. Furthermore, it could be shown that the affinity of NisC is independent of the modification state of the substrate, whereas the modification state is crucial for NisB. NisC has a K_D of ~2 µM for the substrate (Abts et al., 2013), but the K_D of NisB varied depending on the modification state of the substrate: 1.05 µM for the unmodified core, 0.31 µM for the dehydrated substrate and 10.5 µM for the modified core (Mavaro et al.,

2011). Additionally, the importance of the -FNLD-box for substrate binding could be shown *in vitro* and an exchange against -AAAA- resulted in no binding at all (Abts et al., 2013; Khusainov et al., 2011; Khusainov et al., 2013; Mavaro et al., 2011; Plat et al., 2011; Plat et al., 2013). Nevertheless, mutational studies of the substrate e.g. leaderless nisin or *in trans* expression of the leader peptide resulted in partial modification of the substrate *in vivo*, but full modification was only observed when the leader peptide was attached to the core peptide. This led to the conclusion that the leader peptide is not crucial for the PTM installation, but for the efficiency (Khusainov & Kuipers, 2012). The interplay of NisB and NisC was extensively analyzed *in vivo* and it could be shown that dehydration and ring formation acted in cooperation, resulting in the protection of potential dehydration positions within the core peptide during maturation (for example Ser_{29} in nisin A) (Garg et al., 2013; Karakas Sen et al., 1999; Khusainov & Kuipers, 2012; Khusainov et al., 2013; Koponen et al., 2002; Li & van der Donk, 2007; Li et al., 2006; Lubelski et al., 2009; Oman & van der Donk, 2010; Ortega et al., 2015; Plat et al., 2011; Plat et al., 2013; Rink et al., 2007). Based on these findings, it was proposed that the modification process has a strict N- to C-terminal directional orientation in an intertwined process (Ortega et al., 2015). Nevertheless, this is strictly not the case for all classes of lanthipeptides and not even for the whole class I. As an example, the class I lantibiotic NAI-107 has a C- to N terminal direction (Ortega et al., 2016).

In the Chapters IV-VII and IX, several nisin variants were expressed and secreted in the presence of NisB and NisC. The analysis of these variants via mass spectrometry (MS) showed that all variants were dehydrated and (methyl-) lanthionine rings were installed. Nevertheless, it should be mentioned that sub-populations of minor dehydrations were also detected. One exception is the variant Ile_1Cys, where the introduced cysteine was not involved in a (methyl-) lanthionine ring, likely due to the lack of availability of a N-terminal dehydrated amino acid. Additionally, it was shown that for the Ile_1Trp variant of nisin Z, Thr_2 partially escaped the dehydration (Breukink et al., 1998). Similar results were also obtained for Ile_1Phe and Ile_1Tyr, were the main species having seven-fold dehydrated residues instead of eight (Chapter IV) and we could also observe these phenomena in nisin H (Chapter V). This is in line with the statistical analyses that aromatic residues could influence the dehydration activity of NisB (Rink et al., 2005). Interestingly, the Ile_1Ser or Ile_1Thr variants showed no or minor additional dehydrations in the MS spectra (Chapter IV). An explanation for this could be the lack of amino acid at the N-terminus. Another possibility would be that this position is somehow inaccessible

for NisB due to its position in the core peptide. The only nisin variant with a Thr at position one is nisin O4, however MS data confirming that this Thr is dehydrated are missing (Hatziioanou et al., 2017). Additionally, no other nisin variant is known with three potential dehydration positions in a row.

4.3 The nisin modification complex

The interplay between NisB and NisC, as well as the transporter NisT was already studied in the early days based on co-immunoprecipitations and yeast-two-hybrid experiments. A potential complex consisting of NisB, NisC, NisT and nisin A was proposed with a stoichiometry of 1:2:2:1 (Lubelski et al., 2009; Siegers et al., 1996). However, contradictory studies on the homolog subtilin proposed a composition of SpaB, SpaC, SpaT and subtilin with a stoichiometry of 2:2:2:1 (Kiesau et al., 1997). Within this thesis, via size exclusion chromatography coupled with multi-angle-light scattering (SEC-MALS), it could be shown that at least the modification complex (NisB, NisC and nisin A) comprises of a dimer of NisB, a monomer of NisC and a single nisin A molecule. Furthermore, it could be shown that both NisB and NisC individually have a 1:1 stoichiometry with their substrate (Chapter II). Moreover, via small-angle X-ray scattering (SAXS) analysis the orientation of NisC and NisB could be determined within the NisBCA complex (shown in Figure 16 and Chapter II).

The analysis of the modification complex assemblies clearly showed a dependency on the modification state of nisin A core peptide. The fully modified core peptide did not induce the assembly in a significant way (Chapter II). With (methyl-) lanthionine ring deficient mutants (Cys to Ala exchange), it could be further shown that the complex assembles until the last ring E is installed, clearly indicating that this is the trigger factor for release of the modified precursor peptide to NisT.

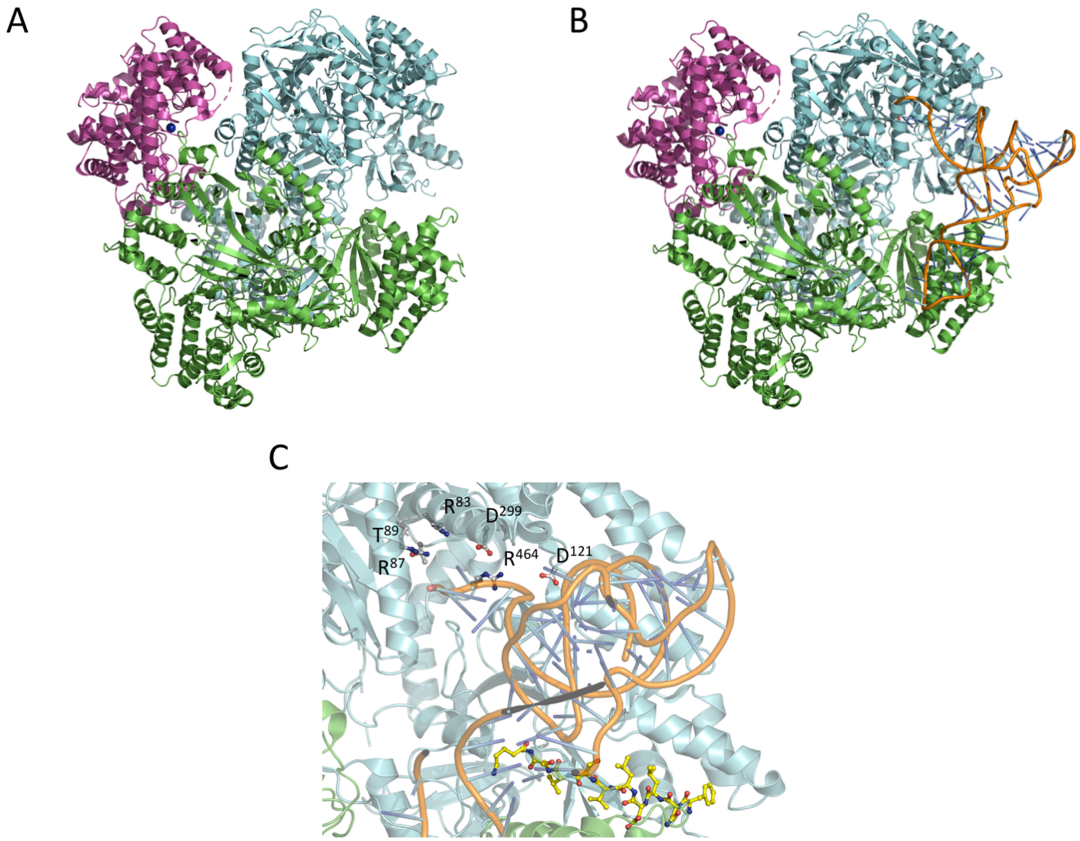

Figure 16: The nisin maturation complex. A: The NisC (PDB ID: 2G0D) and NisB (PDB ID: 4WD9) crystal structures were used as template for the docking of the ensembled complex using collected SAXS data (details in Chapter 2). Protomers of dimeric NisB are shown as cartoon representation in green and cyan and monomeric NisC in magenta. **B:** Docking of $tRNA^{Glu}$ into the nisin A maturation complex. **C:** Zoom-in into the tip region of bound $tRNA^{Glu}$. Residues of NisB which resulted in abolished dehydration upon mutation (Arg_{87}, Thr_{89}, Asp_{121}, Asp_{299}, and Arg_{464}), are highlighted in ball-and-stick representation as well as the leader peptide bound to NisB(Garg et al., 2013; Khusainov et al., 2013; Ortega et al., 2015). Figure taken from Chapter I.

In 2015, the crystal structure of NisB co-expressed with the leader peptide of nisin was solved and regions of the leader peptide, most importantly the -FNDL-box which is responsible for binding, were visible in the electron density. The structure showed a 2:2 stoichiometry of NisB: nisin leader which is in clear contrast to the *in vitro* data from SPR or SEC-MALS experiments (shown in Chapter 2 and (Mavaro et al., 2011)). However, the observed differences might be a result from the simultaneous overexpression of both, NisB and the leader peptide of nisin. Additional co-crystallization experiments were performed with a non-reactive substrate (NisB-Val_{169}Cys with nisin A-Ser_3Dap^{Glu}-Ser(-12)Cys) which revealed a stoichiometry of 2:2 (Bothwell et al., 2019). However, the reason for this difference is still an open question.

The dehydration reaction of serine and threonine residues requires the delivery of a glutamate by a $tRNA^{Glu}$. In Figure 16 B (and Chapter I) a docking approach is presented where the $tRNA^{Glu}$ (PDB ID: 1N78) is docked into the dimeric NisB. The docking results show a binding mapped around with crucial amino acids resides known to be important for functionality (Garg et al., 2013; Khusainov et al., 2013; Ortega et al., 2015), supporting the significance of the docking results, but obviously requires experimental verification.

The structural availability of PTM enzymes is very limited. There are only two structures available in apo state, namely, class I LanB called MibB from *Microbispora* sp. 107891 and class II LanM enzyme CylM from *Enterococcus faecalis* (Dong et al., 2015; Ortega et al., 2016; Ortega et al., 2015). However, NisB from *Lactococcus lactis* is the only LanB enzyme in substrate bound state with regions of leader peptide partially visible. Structural information about other classes such as III-V are completely lacking. By superposition of the substrate bound NisB and the apo MibB it was shown that the glutamylation domains undergo a translational and rotational motion, resulting in a more compact shape (Chapter I). This would result in a conformational selection which is also a proposed mechanism for class II LanM enzymes, where the equilibrium between inactive (open conformation) and active (closed conformation) is shifted towards the active form in the presence of leader peptide (Levengood et al., 2007; Oman et al., 2012; Thibodeaux et al., 2015).

The crystal structure of NisC (PDB ID: 2G0D), a LanC enzyme, is only solved in apo state and no information about the binding motif of the leader peptide or the structure of a trapped core in the active center is available (Li & van der Donk, 2007; Li et al., 2006). With further computational improvements, an AlphaFold2 (Jumper et al., 2021) model of the precursor peptide nisin A bound to NisC (Figure 17) was created. The predicted model showed that the leader is orientated between α-helix 3 and α-helix 5 from the outer layer (Figure 17 A). Nevertheless, there is no predicted binding motif for this region and no experimental evidence is available to support that this position is correct.

However, ITC experiments revealed that the binding affinity of NisC towards the precursor peptide is a due to the leader peptide and not the core peptide, indicating that a consistent binding side must be present (Abts et al., 2013). Intriguingly, residues Thr_3 and ´Cys_7 align in close proximity to the zinc ion in the active center (Figure 17 B), which is required for a cyclization reaction. The rest of the C-terminal core peptide after Cys_7 remains flexible in the models (not shown for clarity in the Figure 17).

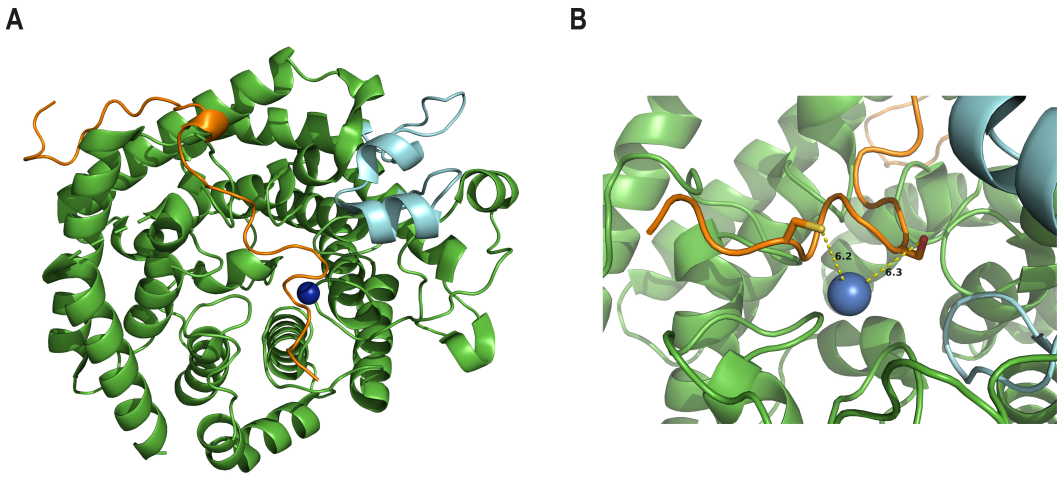

Figure 17: Nisin A precursor binding. Until now, no structural information about a bound state LanC are available. A: The structure of NisC (PDB ID: 2G0D) is shown in green with the SH2 domain in cyan and the zinc ion in blue. An AlphaFold2 prediction of the precursor peptide nisin A is shown in orange. For clarity, only amino acids 1- 31 of the precursor peptide are shown. B: Zoom-in of the active site of NisC showed that the Thr4 and Cys8 from the core peptide are in close proximity to the zinc ion. Created with PyMOL 2.5 (Schrodinger, 2022), nisin A bound NisC model was created using AlphaFold2 (Jumper et al., 2021).

Although this model is also speculative, a superposition of the predicted model and the determined NisBCA complex from SAXS analysis (as determined in chapter II) is shown in Figure 18.

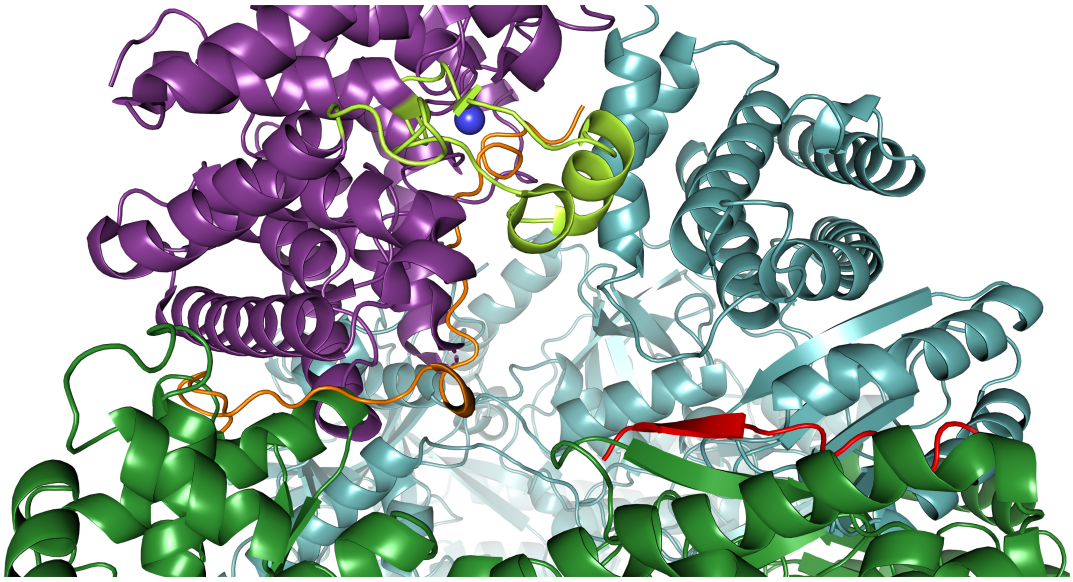

Figure 18: Superposition of predicted nisin A precursor peptide within the NisBCA complex. The protomers of dimeric NisB are shown in cyan and green and the partial visible leader fragment in the crystal structure in red. The cyclase NisC is shown in magenta with the SH2 domain in yellow and the zinc ion in blue. The predicted nisin A precursor peptide from AlphaFold2 is shown in orange. Created with PyMOL 2.5 (Schrodinger, 2022).

The predicted leader peptide from the AlphaFold2 prediction (Figure 18, orange) is on the opposite side of the partially-solved leader peptide from the bound NisB structure (Figure 18, red). This makes sense because the leader needs to flip between NisB and NisC during the maturation process. Moreover, when we twist this L-shape leader to the predicted site in NisB, the distance of the core peptide to the zinc ions remains identical, strongly suggesting that this could be a possible orientation of the core peptide which is further supported by the position of NisC determined via small angle X-ray scattering (SAXS). Interestingly, in between of this region is the SH2 domain from NisC. Although its direct function is not clear and the functional role of the SH2 domains in the complex of NisB and NisC remains unclear but it is potentially involved in substrate binding or in the flipping process between NisB and NisC (based on this superposition).

4.4 The interplay between NisT and the modification enzymes NisB and NisC

As stated above the interplay between NisB and NisC, as well as the transporter NisT was already studied in the early days and a potential complex consisting of NisB, NisC, NisT and nisin A was proposed with a stoichiometry of 1:2:2:1 (Lubelski et al., 2009; Siegers et al., 1996). However, contradictory studies on the homolog subtilin proposed a composition of SpaB, SpaC, SpaT and subtilin with a stoichiometry of 2:2:2:1 (Kiesau et al., 1997). The interplay between the modification enzymes NisB and NisC (installing the PTMs) and ABC transporter NisT (responsible for the secretion of the fully modified precursor peptide into the extracellular space) is an important question. For the nisin system, it was shown that the ABC transporter NisT is able to transport the substrate nisin A independent of the modification state, but with reduced efficiency (Kuipers et al., 2004). However, if the modification enzymes NisB and NisC are present, only fully modified and neither dehydrated nor unmodified precursor peptide was secreted via NisT in the extracellular space (Lubelski et al., 2009; van den Berg van Saparoea et al., 2008). In Chapter III, the secretion rate of precursor nisin A of different strains contains combinations of the NisBTC or inactive variants. It was shown that there is a clear correlation between the secretion efficiency and the presence of the modification enzymes (NZ9000BTC > NZ9000BT > NZ9000T) and every aberration of the secretion system reduced the secretion rate by a factor of ~2. This supports the proposed channeling mechanism by the modification enzymes NisBC (Khusainov et al., 2013; Lubelski et al., 2009; van den Berg van Saparoea et al., 2008). Additionally, the ABC transporter is not stimulated *in vitro* by its

substrate independent form the modification state or the leader peptide alone nor the modification enzymes NisB and NisC. In the Chapters IV–VII and IX, several variants of nisin were expressed, modified and secreted in the presence of NisBTC, but interestingly, nearly no substrate reached similar secretion levels like wild type nisin A. A potential explanation is that most of the variants contain minor species of partly modified precursor peptide. Based on our findings in Chapter II, the modification complex is stable when the core peptide is not fully modified and the transfer of the substrate to the ABC transporter NisT is thereby interfered and slows down the secretion process, which would be in line with the stated channeling mechanism (van den Berg van Saparoea et al., 2008).

4.4 The multimeric membrane-associated lanthionine synthetase complex

The presence of multimeric membrane-associated lanthionine synthetase complex was already proposed in the early days, based on co-immunoprecipitations and yeast-two-hybrid experiments for the nisin and the subtilin system (Kiesau et al., 1997; Siegers et al., 1996).

Recent studies on the subcellular localization showed that NisB is localized at the pole of a bacterial membrane and act as a “recruiter”. Additionally, it was also shown that NisC and the precursor peptide nisin A are co-localized at the old pole as well, whereas the ABC transporter NisT was uniformly distributed in the cell periphery. The precursor peptide, NisC and NisT travel to the poles, bind to NisB and form the NisABTC modification complex (Figure 19) (Chen et al., 2020). This is in line with previous findings that NisB is the lead component of the NisABTC complex (Chapter III and (van den Berg van Saparoea et al., 2008)). These observations of a membrane-associated modification complex were also supported with recent co-purification/ pull down assays and Western blot analyses of the proteins (Chapter III and (Chen & Kuipers, 2021).

Nevertheless, the structure of the whole assembled complex to complete the picture of the interplay is still missing. Especially, the information regarding the release of the modified precursor peptide from the NisBC machinery and the hand-over of the peptide to the ABC transporter NisT for secretion remains still unclear.

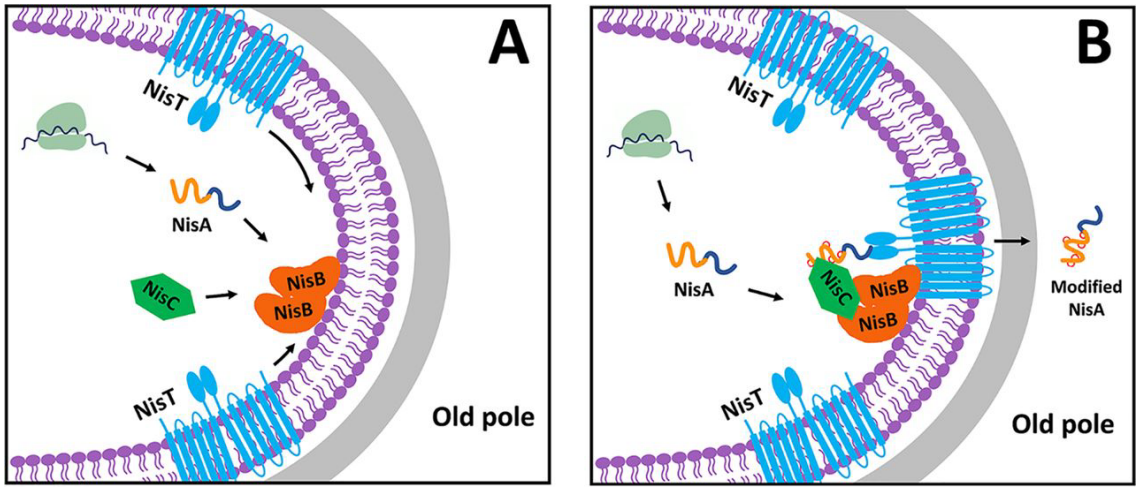

Figure 19: Assembly process and subcellular localization of nisin biosynthesis machinery. A: NisB is localized at the old pole and recruits the precursor peptide nisin A, NiC and NisT. **B:** Fully assembled complex and transport of fully modified nisin A into the extracellular space after PTM installation from NisBC. Taken from (Chen et al., 2020)

4.5 Leader cleavage, the final step of maturation

After the secretion of the modified precursor peptide via the ABC transporter NisT into the extracellular space, the last step of maturation is to cleave off the leader peptide releasing biologically active nisin A (van der Meer et al., 1993). This step is performed by a membrane-anchored subtilisin-like serine protease NisP, which recognizes the cleavage site in the leader peptide with the motif -GASPR- and cleaves after the arginine residue, thereby, releasing mature active nisin A (Lagedroste et al., 2017; Montalban-Lopez et al., 2018; Plat et al., 2011; van der Meer et al., 1993). Although NisP is membrane-anchored in nature, it could be shown that the cleavage reaction is independent of the location (Kuipers et al., 2004) and a purified soluble version of NisP was used (Abts et al., 2013) in the corresponding Chapters II-VII, IX. An important point of the cleavage reaction is that no “leftover” amino acids remains at the core peptide after the -GASPR- motif. However, this motif can be exchanged against the motif of the thrombine cleavage site (-AVPR-), the Factor Xa cleavage site (-IEGR-) as well as the NisP auto-cleavage site (-VSLR-), without any loss of function (Montalban-Lopez et al., 2018). Initially, it was stated that the cleavage of the nisin A precursor is dependent on at least one (methyl-) lanthionine ring, but recent experiments showed that although NisP is independent but its catalytic activity is dependent on the modification state (Kuipers et al., 2004; Lagedroste et al., 2017; Montalban-Lopez et al., 2018; Plat et al., 2011; van der Meer et al., 1993). In Chapters IV-VII and IX, NisP was used to cleave off the leader peptide from the different nisin

variants. Here, it was observed that in line with previously findings, the cleavage efficiency is not consistent and favored small hydrophobic amino acids at position one of the core peptide whereas bulky or charged amino acids reduced the efficiency drastically (Chapters IV-VII, IX and (Siezen et al., 1995)). Interestingly, the presence of a proline at position one completely abolished the cleavage reaction, likely due to an unfavorable orientation of the precursor peptide (Chapter IV). This could be a potential drawback for the use of NisP in the future as the analyses in Chapters IV and V showed that especially aromatic residues at position one showed high antimicrobial potential. Some natural nisin variants like nisin H from *Streptococcus hyointestinalis* (O'Connor et al., 2015) or nisin O1-3 from *Blautia obeum* A2-162 (Hatziioanou et al., 2017) have a phenylalanine or a tyrosine, respectively, at position one. Computational analysis identified genes of the nisin O1-4 operon (*nsoFEGIRKABTC*) (GenBank: FP929054), but no probable gene for protease was found (Hatziioanou et al., 2017). The structural model analysis of the nisin H protease NshP (GenBank: AKB95123.1) from *Streptococcus hyointestinalis* revealed only a minor positional orientational change from Asp_{178} in the active center, which is maybe responsible for better access of bulky amino acids (Figure 20 and Chapter V). Experimental evidence whether NshP could cleave other variants like Ile_1Trp or Ile_1Phe from nisin A with a better efficiency and remains highly active even with small hydrophobic amino acids at position one, are lacking so far.

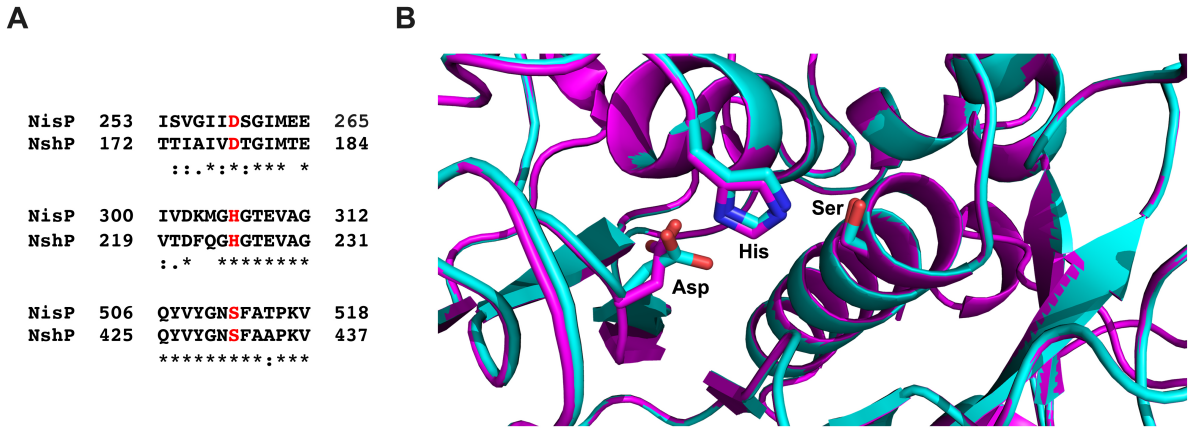

Figure 20: Alignment of NisP from *Lactococcus lactis* and NshP from *Streptococcus hyointestinalis*. A: The important residues from the active site (Asp_{259}, His_{306}, and Ser_{512} for NisP and Asp_{178}, His_{225}, and Ser_{431} for NshP) are marked in red, shown together with the close neighborhood residues. The sequence alignment was done with Clustal Omega (Sievers et al., 2011). **B:** Zoom-in into the active sites of NshP (magenta) and NisP (cyan). The important residues for the catalytic activity (Asp_{259}, His_{306}, and Ser_{512} for NisP and Asp_{178}, His_{225}, and Ser_{431} for NshP) are shown in stick representation. Created with PyMOL 2.5 (Schrodinger, 2022). Modified from Chapter V.

A commonly used alternative for the nisin A leader cleavage *in vitro* is trypsin, which cleaves after the arginine in the NisP -GASPR- cleavage motif (Cheng et al., 2007). Noteworthy, that nisin A contains two additional cleavage positions (Lys_{12} and Lys_{22}), which are shielded from the (methyl-) lanthionine rings in mature nisin. A lack of the (methyl-) lanthionine ring, or a longer distance would result in an accessible cleavage site for trypsin, ending in a degraded product. Thus, additional/accessible cleavage sites need to be considered when using trypsin *in vitro*.

4.6 Resistance is futile

Lantibiotics are highly effective against various bacteria. However, the nisin producer strains contain an innate immunity system (comprising of NisI and NisFEG) to survive the antimicrobial activity of their own produced lantibiotic. On the contrary, some non-lantibiotic producer strains established a resistance mechanism against lantibiotics (de Ruyter et al., 1996; Draper et al., 2015; Engelke et al., 1994; Hacker et al., 2015; Kuipers et al., 1993; Siegers & Entian, 1995; Stein et al., 2003). One such example is the Nisin resistance system from *S. agalactiae* COH1, containing *Sa*NsrFP which encodes for a BceAB-type ABC transporter and a nisin resistance protein NSR (Khosa et al., 2013; Khosa, Frieg, et al., 2016; Khosa, Hoeppner, et al., 2016; Khosa, Lagedroste, et al., 2016). In Chapters IV-VII and IX, several nisin variants were analyzed regarding the effects on the immunity- (NisI and NisFEG) as well as on the resistance- (NSR and *Sa*NsrFP) systems. In general, it could be shown that hydrophobic or aromatic residues at position one are required for a high antimicrobial activity (Chapters IV and V).

Analysis of the ABC transporter *Sa*NsrFP in Chapter IX showed that the N-terminal part of nisin A is important for recognition. Interestingly, for the NSR cleaved product $nisin_{1-28}$, the determined fold of resistance was even higher, indicating that the resistance system NSR and *Sa*NsrFP are working together (Chapter IX). This cooperativity phenomena was also observed for immunity systems like NisI and NisFEG, and SpaI and SpaFEG (Stein et al., 2005; Stein et al., 2003). Based on the results in Chapter IX, *Sa*NsrFP acts as an exporter. However, recent studies indicate that *Sa*NsrFP is involved in shielding of membrane-localized targets for these antimicrobial peptides (Gottstein et al., 2022) and nisin resistance is more of a side effect of

bacterial cell wall modification rather than a direct transport of the nisin A molecule, but this remains to be elucidated (Draper et al., 2015; Gottstein et al., 2022).

In Chapter VII, variations of the nisin A hinge region were analyzed. This hinge region was shown to be important for antimicrobial activity because it is the flexible linker for the C-terminus to insert into the membrane (Healy et al., 2013; Yuan et al., 2004; Zhou et al., 2015). Variations in the length or the amino acid composition has a strong effect on the biological activity as well on the spectra of the target organisms. In Nisin Z, for example, the $Asn_{20}Lys$ and $Met_{21}Lys$ variants showed an antimicrobial effect against Gram-negative strains like *Shigella*, *Pseudomonas* and *Salmonella,* which are normally not effected by wild type nisin Z treatment (Yuan et al., 2004). In Chapter V, a nisin variant where Ile and Val were introduced after the hinge regain ($_{20}NMKIV_{24}$) was identified to be a promising candidate for future applications, because this variant was less recognized by all the tested immunity and resistance proteins.

The NSR protein cleaves off the last six amino acids of nisin, lowering the antimicrobial potential of nisin (Liang et al., 2010; Sun et al., 2009). In Chapter VI, it was shown that the nisin variant $Cys_{29}Pro$, could still bind to NSR but the efficiency of the cleavage reaction is drastically reduced. In screening assays, another mutation, $Ser_{29}Pro$, was found to be very efficient in inhibition of the NSR activity (Field et al., 2019), here the Ser_{29} was mutated against all other amino acid variants and their effect on NSR protein was analyzed. Intriguingly, this inhibitory effect also holds true for $Ser_{29}Pro$ variants of nisin F, nisin Z and nisin Q (Field et al., 2019). In addition to nisin variants which inhibit the activity of NSR, recent studies identified a compound (e.g. NPG9) which reduced the NSR activity as well (Porta et al., 2019).

Taken together, many mutational studies as well as genome mining approaches delivery new and better lantibiotics, which could counteract against established resistance mechanisms as well as the extent of the antimicrobial spectra in the future to Gram-negative strains (Field et al., 2019; Field et al., 2008; Healy et al., 2013; van Heel et al., 2016; van Heel et al., 2011; Yuan et al., 2004; Zhou et al., 2015).

5 Literature

Abts, A., Mavaro, A., Stindt, J., Bakkes, P. J., Metzger, S., Driessen, A. J., Smits, S. H., & Schmitt, L. (2011). Easy and rapid purification of highly active nisin. *Int J Pept*, *2011*, 175145.

Abts, A., Montalban-Lopez, M., Kuipers, O. P., Smits, S. H., & Schmitt, L. (2013). NisC binds the FxLx motif of the nisin leader peptide. *Biochemistry*, *52*(32), 5387-5395.

Agrawal, P., Khater, S., Gupta, M., Sain, N., & Mohanty, D. (2017). RiPPMiner: a bioinformatics resource for deciphering chemical structures of RiPPs based on prediction of cleavage and cross-links. *Nucleic Acids Research*, *45*(W1), W80-W88.

AlKhatib, Z., Lagedroste, M., Fey, I., Kleinschrodt, D., Abts, A., & Smits, S. H. (2014a). Lantibiotic immunity: inhibition of nisin mediated pore formation by NisI. *PLoS ONE*, *9*(7), e102246.

AlKhatib, Z., Lagedroste, M., Zaschke, J., Wagner, M., Abts, A., Fey, I., Kleinschrodt, D., & Smits, S. H. (2014b). The C-terminus of nisin is important for the ABC transporter NisFEG to confer immunity in Lactococcus lactis. *MicrobiologyOpen*, *3*(5), 752-763.

Arnison, P. G., Bibb, M. J., Bierbaum, G., Bowers, A. A., Bugni, T. S., Bulaj, G., Camarero, J. A., Campopiano, D. J., Challis, G. L., Clardy, J., Cotter, P. D., Craik, D. J., Dawson, M., Dittmann, E., Donadio, S., Dorrestein, P. C., Entian, K. D., Fischbach, M. A., Garavelli, J. S., van der Donk, W. A. (2013). Ribosomally synthesized and post-translationally modified peptide natural products: overview and recommendations for a universal nomenclature. *Nat Prod Rep*, *30*(1), 108-160.

Bahar, A. A., & Ren, D. (2013). Antimicrobial peptides. *Pharmaceuticals (Basel)*, *6*(12), 1543-1575.

Barber, M., Elliot, G. J., Bordoli, R. S., Green, B. N., & Bycroft, B. W. (1988). Confirmation of the structure of nisin and its major degradation product by FAB-MS and FAB-MS/MS. *Experientia*, *44*(3), 266-270.

Bastos Mdo, C., Coelho, M. L., & Santos, O. C. (2015). Resistance to bacteriocins produced by Gram-positive bacteria. *Microbiology (Reading)*, *161*(Pt 4), 683-700.

Bbosa, G. S., Mwebaza, N., Odda, J., Kyegombe, D. B., & Ntale, M. (2014). Antibiotics/antibacterial drug use, their marketing and promotion during the post-antibiotic golden age and their role in emergence of bacterial resistance. *Health*, *2014*.

Bernard, R., Guiseppi, A., Chippaux, M., Foglino, M., & Denizot, F. (2007). Resistance to bacitracin in Bacillus subtilis: unexpected requirement of the BceAB ABC transporter in the control of expression of its own structural genes. *J Bacteriol*, *189*(23), 8636-8642.

Blin, K., Medema, M. H., Kottmann, R., Lee, S. Y., & Weber, T. (2017). The antiSMASH database, a comprehensive database of microbial secondary metabolite biosynthetic gene clusters. *Nucleic Acids Research*, *45*(D1), D555-D559.

Bothwell, I. R., Cogan, D. P., Kim, T., Reinhardt, C. J., van der Donk, W. A., & Nair, S. K. (2019). Characterization of glutamyl-tRNA-dependent dehydratases using nonreactive substrate mimics. *Proc Natl Acad Sci U S A*, *116*(35), 17245-17250.

Bradshaw, J. M., & Waksman, G. (2002). Molecular recognition by SH2 domains. *Adv Protein Chem*, *61*, 161-210.

Breukink, E., & de Kruijff, B. (2006). Lipid II as a target for antibiotics. *Nature Reviews Drug Discovery*, *5*(4), 321-332.

Breukink, E., van Kraaij, C., van Dalen, A., Demel, R. A., Siezen, R. J., de Kruijff, B., & Kuipers, O. P. (1998). The orientation of nisin in membranes. *Biochemistry*, *37*(22), 8153-8162.

Brunati, C., Thomsen, T. T., Gaspari, E., Maffioli, S., Sosio, M., Jabes, D., Lobner-Olesen, A., & Donadio, S. (2018). Expanding the potential of NAI-107 for treating serious ESKAPE pathogens: synergistic combinations against Gram-negatives and bactericidal activity against non-dividing cells. *J Antimicrob Chemother*, *73*(2), 414-424.

Buchman, G. W., Banerjee, S., & Hansen, J. N. (1988). Structure, expression, and evolution of a gene encoding the precursor of nisin, a small protein antibiotic. *Journal of Biological Chemistry*, *263*(31), 16260-16266.

Burkhart, B. J., Hudson, G. A., Dunbar, K. L., & Mitchell, D. A. (2015). A prevalent peptide-binding domain guides ribosomal natural product biosynthesis. *Nature chemical biology*, *11*(8), 564-570.

Burkhart, B. J., Kakkar, N., Hudson, G. A., van der Donk, W. A., & Mitchell, D. A. (2017). Chimeric Leader Peptides for the Generation of Non-Natural Hybrid RiPP Products. *ACS Central Science*, *3*(6), 629-638.

Burrage, S., Raynham, T., Williams, G., Essex, J. W., Allen, C., Cardno, M., Swali, V., & Bradley, M. (2000). Biomimetic synthesis of lantibiotics. *Chemistry*, *6*(8), 1455-1466.

Cao, L. T., Wu, J. Q., Xie, F., Hu, S. H., & Mo, Y. (2007). Efficacy of nisin in treatment of clinical mastitis in lactating dairy cows. *J Dairy Sci*, *90*(8), 3980-3985.

Chan, W. C., Leyland, M., Clark, J., Dodd, H. M., Lian, L. Y., Gasson, M. J., Bycroft, B. W., & Roberts, G. C. (1996). Structure-activity relationships in the peptide antibiotic nisin: antibacterial activity of fragments of nisin. *FEBS Lett*, *390*(2), 129-132.

Chatterjee, C., Paul, M., Xie, L., & van der Donk, W. A. (2005). Biosynthesis and mode of action of lantibiotics. *Chem Rev*, *105*(2), 633-684.

Chen, J., & Kuipers, O. P. (2021). Isolation and Analysis of the Nisin Biosynthesis Complex NisBTC: further Insights into Their Cooperative Action. *mBio*, *12*(5), e0258521.

Chen, J., van Heel, A. J., & Kuipers, O. P. (2020). Subcellular Localization and Assembly Process of the Nisin Biosynthesis Machinery in Lactococcus lactis. *mBio*, *11*(6).

Cheng, F., Takala, T. M., & Saris, P. E. (2007). Nisin biosynthesis in vitro. *J Mol Microbiol Biotechnol*, *13*(4), 248-254.

Clemens, R., Zaschke-Kriesche, J., Khosa, S., & Smits, S. H. J. (2017). Insight into Two ABC Transporter Families Involved in Lantibiotic Resistance. *Front Mol Biosci*, *4*, 91.

Crowther, G. S., Baines, S. D., Todhunter, S. L., Freeman, J., Chilton, C. H., & Wilcox, M. H. (2013). Evaluation of NVB302 versus vancomycin activity in an in vitro human gut model of Clostridium difficile infection. *J Antimicrob Chemother*, *68*(1), 168-176.

Dawson, M. J., & Scott, R. W. (2012). New horizons for host defense peptides and lantibiotics. *Curr Opin Pharmacol*, *12*(5), 545-550.

de Kwaadsteniet, M., Ten Doeschate, K., & Dicks, L. M. (2008). Characterization of the structural gene encoding nisin F, a new lantibiotic produced by a Lactococcus lactis subsp. lactis isolate from freshwater catfish (Clarias gariepinus). *Appl Environ Microbiol*, *74*(2), 547-549.

de Ruyter, P. G., Kuipers, O. P., Beerthuyzen, M. M., van Alen-Boerrigter, I., & de Vos, W. M. (1996). Functional analysis of promoters in the nisin gene cluster of Lactococcus lactis. *J Bacteriol*, *178*(12), 3434-3439.

Delves-Broughton, J., Blackburn, P., Evans, R. J., & Hugenholtz, J. (1996). Applications of the bacteriocin, nisin. *Antonie van Leeuwenhoek*, *69*(2), 193-202.

Dieye, Y., Oxaran, V., Ledue-Clier, F., Alkhalaf, W., Buist, G., Juillard, V., Lee, C. W., & Piard, J. C. (2010). Functionality of sortase A in Lactococcus lactis. *Appl Environ Microbiol*, *76*(21), 7332-7337.

Dintner, S., Heermann, R., Fang, C., Jung, K., & Gebhard, S. (2014). A sensory complex consisting of an ATP-binding cassette transporter and a two-component regulatory system controls bacitracin resistance in Bacillus subtilis. *Journal of Biological Chemistry*, *289*(40), 27899-27910.

Dintner, S., Staron, A., Berchtold, E., Petri, T., Mascher, T., & Gebhard, S. (2011). Coevolution of ABC transporters and two-component regulatory systems as resistance modules against antimicrobial peptides in Firmicutes Bacteria. *J Bacteriol*, *193*(15), 3851-3862.

Dischinger, J., Basi Chipalu, S., & Bierbaum, G. (2014). Lantibiotics: promising candidates for future applications in health care. *Int J Med Microbiol*, *304*(1), 51-62.

Dong, S. H., Tang, W., Lukk, T., Yu, Y., Nair, S. K., & van der Donk, W. A. (2015). The enterococcal cytolysin synthetase has an unanticipated lipid kinase fold. *Elife*, *4*.

Draper, L. A., Cotter, P. D., Hill, C., & Ross, R. P. (2015). Lantibiotic resistance. *Microbiol Mol Biol Rev*, *79*(2), 171-191.

Engelke, G., Gutowski-Eckel, Z., Hammelmann, M., & Entian, K. D. (1992). Biosynthesis of the lantibiotic nisin: genomic organization and membrane localization of the NisB protein. *Appl Environ Microbiol*, *58*(11), 3730-3743.

Engelke, G., Gutowski-Eckel, Z., Kiesau, P., Siegers, K., Hammelmann, M., & Entian, K. D. (1994). Regulation of nisin biosynthesis and immunity in Lactococcus lactis 6F3. *Appl Environ Microbiol*, *60*(3), 814-825.

Ferir, G., Petrova, M. I., Andrei, G., Huskens, D., Hoorelbeke, B., Snoeck, R., Vanderleyden, J., Balzarini, J., Bartoschek, S., Bronstrup, M., Sussmuth, R. D., & Schols, D. (2013). The lantibiotic peptide labyrinthopeptin A1 demonstrates broad anti-HIV and anti-HSV activity with potential for microbicidal applications. *PLoS ONE*, *8*(5), e64010.

Field, D., Blake, T., Mathur, H., PM, O. C., Cotter, P. D., Paul Ross, R., & Hill, C. (2019). Bioengineering nisin to overcome the nisin resistance protein. *Mol Microbiol*, *111*(3), 717-731.

Field, D., Connor, P. M., Cotter, P. D., Hill, C., & Ross, R. P. (2008). The generation of nisin variants with enhanced activity against specific gram-positive pathogens. *Mol Microbiol*, *69*(1), 218-230.

Fleming, A. (1929). On the Antibacterial Action of Cultures of a Penicillium, with Special Reference to their Use in the Isolation of B. influenzæ. *British journal of experimental pathology*, *10*(3), 226-236.

Froseth, B. R., & McKay, L. L. (1991). Molecular characterization of the nisin resistance region of Lactococcus lactis subsp. lactis biovar diacetylactis DRC3. *Appl Environ Microbiol*, *57*(3), 804-811.

Furgerson Ihnken, L. A., Chatterjee, C., & van der Donk, W. A. (2008). In vitro reconstitution and substrate specificity of a lantibiotic protease. *Biochemistry*, *47*(28), 7352-7363.

Garg, N., Salazar-Ocampo, L. M., & van der Donk, W. A. (2013). In vitro activity of the nisin dehydratase NisB. *Proc Natl Acad Sci U S A*, *110*(18), 7258-7263.

Gebhard, S. (2012). ABC transporters of antimicrobial peptides in Firmicutes bacteria - phylogeny, function and regulation. *Mol Microbiol*, *86*(6), 1295-1317.

Gebhard, S., & Mascher, T. (2011). Antimicrobial peptide sensing and detoxification modules: unravelling the regulatory circuitry of Staphylococcus aureus. *Mol Microbiol*, *81*(3), 581-587.

Geiger, C., Korn, S. M., Hasler, M., Peetz, O., Martin, J., Kotter, P., Morgner, N., & Entian, K. D. (2019). LanI-Mediated Lantibiotic Immunity in Bacillus subtilis: Functional Analysis. *Appl Environ Microbiol*, *85*(11).

George, N. L., Schilmiller, A. L., & Orlando, B. J. (2022). Conformational snapshots of the bacitracin sensing and resistance transporter BceAB. *Proc Natl Acad Sci U S A*, *119*(14), e2123268119.

Goto, Y., Li, B., Claesen, J., Shi, Y., Bibb, M. J., & van der Donk, W. A. (2010). Discovery of unique lanthionine synthetases reveals new mechanistic and evolutionary insights. *PLoS Biol*, *8*(3), e1000339.

Gottstein, J., Zaschke-Kriesche, J., Unsleber, S., Voitsekhovskaia, I., Kulik, A., Behrmann, L. V., Overbeck, N., Stuhler, K., Stegmann, E., & Smits, S. H. J. (2022). New insights into the resistance mechanism for the BceAB-type transporter SaNsrFP. *Sci Rep*, *12*(1), 4232.

Gross, E., & Morell, J. L. (1967). The presence of dehydroalanine in the antibiotic nisin and its relationship to activity. *J Am Chem Soc*, *89*(11), 2791-2792.

Gross, E., & Morell, J. L. (1971). The structure of nisin. *J Am Chem Soc*, *93*(18), 4634-4635.

Gross, E., Morell, J. L., & Craig, L. C. (1969). Dehydroalanyllysine: identical COOH-terminal structures in the peptide antibiotics nisin and subtilin. *Proc Natl Acad Sci U S A*, *62*(3), 952-956.

Hacker, C., Christ, N. A., Duchardt-Ferner, E., Korn, S., Gobl, C., Berninger, L., Dusterhus, S., Hellmich, U. A., Madl, T., Kotter, P., Entian, K. D., & Wohnert, J. (2015). The Solution Structure of the Lantibiotic Immunity Protein NisI and Its Interactions with Nisin. *Journal of Biological Chemistry*, *290*(48), 28869-28886.

Hancock, R. E., & Lehrer, R. (1998). Cationic peptides: a new source of antibiotics. *Trends Biotechnol*, *16*(2), 82-88.

Hasper, H. E., de Kruijff, B., & Breukink, E. (2004). Assembly and stability of nisin-lipid II pores. *Biochemistry*, *43*(36), 11567-11575.

Hatziioanou, D., Gherghisan-Filip, C., Saalbach, G., Horn, N., Wegmann, U., Duncan, S. H., Flint, H. J., Mayer, M. J., & Narbad, A. (2017). Discovery of a novel lantibiotic nisin O from Blautia obeum A2-162, isolated from the human gastrointestinal tract. *Microbiology*, *163*(9), 1292-1305.

Healy, B., Field, D., O'Connor, P. M., Hill, C., Cotter, P. D., & Ross, R. P. (2013). Intensive mutagenesis of the nisin hinge leads to the rational design of enhanced derivatives. *PLoS ONE*, *8*(11), e79563.

Heng, N. C. K., & Tagg, J. R. (2006). What's in a name? Class distinction for bacteriocins. *Nature Reviews Microbiology*, *4*(2), 160-160.

Hsu, S. T. D., Breukink, E., Tischenko, E., Lutters, M. A. G., de Kruijff, B., Kaptein, R., Bonvin, A. M. J. J., & van Nuland, N. A. J. (2004). The nisin-lipid II complex reveals a pyrophosphate cage that provides a blueprint for novel antibiotics. *Nature Structural & Molecular Biology*, *11*(10), 963-967.

Ingram, L. C. (1969). Synthesis of the antibiotic nisin: formation of lanthionine and beta-methyl-lanthionine. *Biochim Biophys Acta*, *184*(1), 216-219.

Iorio, M., Sasso, O., Maffioli, S. I., Bertorelli, R., Monciardini, P., Sosio, M., Bonezzi, F., Summa, M., Brunati, C., Bordoni, R., Corti, G., Tarozzo, G., Piomelli, D., Reggiani, A., & Donadio, S. (2014). A glycosylated, labionin-containing lanthipeptide with marked antinociceptive activity. *ACS Chem Biol*, *9*(2), 398-404.

Jabes, D., Brunati, C., Candiani, G., Riva, S., Romano, G., & Donadio, S. (2011). Efficacy of the new lantibiotic NAI-107 in experimental infections induced by multidrug-resistant Gram-positive pathogens. *Antimicrob Agents Chemother*, *55*(4), 1671-1676.

Jeong, J. H., & Ha, S. C. (2018). Crystal Structure of NisI in a Lipid-Free Form, the Nisin Immunity Protein, from Lactococcus lactis. *Antimicrob Agents Chemother*, *62*(3).

Jumper, J., Evans, R., Pritzel, A., Green, T., Figurnov, M., Ronneberger, O., Tunyasuvunakool, K., Bates, R., Zidek, A., Potapenko, A., Bridgland, A., Meyer, C., Kohl, S. A. A., Ballard, A. J., Cowie, A., Romera-Paredes, B., Nikolov, S., Jain, R., Adler, J., . . . Hassabis, D. (2021). Highly accurate protein structure prediction with AlphaFold. *Nature*, *596*(7873), 583-589.

Jung, G. (1991). Lantibiotics—Ribosomally Synthesized Biologically Active Polypeptides containing Sulfide Bridges and α,β-Didehydroamino Acids. *Angewandte Chemie International Edition in English*, *30*(9), 1051-1068.

Kaletta, C., & Entian, K. D. (1989). Nisin, a peptide antibiotic: cloning and sequencing of the nisA gene and posttranslational processing of its peptide product. *J Bacteriol*, *171*(3), 1597-1601.

Karakas Sen, A., Narbad, A., Horn, N., Dodd, H. M., Parr, A. J., Colquhoun, I., & Gasson, M. J. (1999). Post-translational modification of nisin. The involvement of NisB in the dehydration process. *Eur J Biochem*, *261*(2), 524-532.

Kellner, R., Jung, G., Horner, T., Zahner, H., Schnell, N., Entian, K. D., & Gotz, F. (1988). Gallidermin: a new lanthionine-containing polypeptide antibiotic. *Eur J Biochem*, *177*(1), 53-59.

Khosa, S., AlKhatib, Z., & Smits, S. H. (2013). NSR from Streptococcus agalactiae confers resistance against nisin and is encoded by a conserved nsr operon. *Biol Chem*, *394*(11), 1543-1549.

Khosa, S., Frieg, B., Mulnaes, D., Kleinschrodt, D., Hoeppner, A., Gohlke, H., & Smits, S. H. (2016). Structural basis of lantibiotic recognition by the nisin resistance protein from Streptococcus agalactiae. *Sci Rep*, *6*, 18679.

Khosa, S., Hoeppner, A., Gohlke, H., Schmitt, L., & Smits, S. H. (2016). Structure of the Response Regulator NsrR from Streptococcus agalactiae, Which Is Involved in Lantibiotic Resistance. *PLoS ONE*, *11*(3), e0149903.

Khosa, S., Lagedroste, M., & Smits, S. H. (2016). Protein Defense Systems against the Lantibiotic Nisin: Function of the Immunity Protein NisI and the Resistance Protein NSR. *Front Microbiol*, *7*, 504.

Khusainov, R., Heils, R., Lubelski, J., Moll, G. N., & Kuipers, O. P. (2011). Determining sites of interaction between prenisin and its modification enzymes NisB and NisC. *Mol Microbiol*, *82*(3), 706-718.

Khusainov, R., & Kuipers, O. P. (2012). When the leader gets loose: in vivo biosynthesis of a leaderless prenisin is stimulated by a trans-acting leader peptide. *Chembiochem*, *13*(16), 2433-2438.

Khusainov, R., Moll, G. N., & Kuipers, O. P. (2013). Identification of distinct nisin leader peptide regions that determine interactions with the modification enzymes NisB and NisC. *FEBS open bio*, *3*, 237-242.

Khusainov, R., van Heel, A. J., Lubelski, J., Moll, G. N., & Kuipers, O. P. (2015). Identification of essential amino acid residues in the nisin dehydratase NisB. *Front Microbiol*, *6*, 102.

Kiesau, P., Eikmanns, U., Gutowski-Eckel, Z., Weber, S., Hammelmann, M., & Entian, K. D. (1997). Evidence for a multimeric subtilin synthetase complex. *J Bacteriol*, *179*(5), 1475-1481.

Kingston, A. W., Zhao, H., Cook, G. M., & Helmann, J. D. (2014). Accumulation of heptaprenyl diphosphate sensitizes Bacillus subtilis to bacitracin: implications for the mechanism of resistance mediated by the BceAB transporter. *Mol Microbiol*, *93*(1), 37-49.

Klaenhammer, T. R. (1993). Genetics of bacteriocins produced by lactic acid bacteria. *FEMS Microbiol Rev*, *12*(1-3), 39-85.

Kluskens, L. D., Kuipers, A., Rink, R., de Boef, E., Fekken, S., Driessen, A. J., Kuipers, O. P., & Moll, G. N. (2005). Post-translational modification of therapeutic peptides by NisB, the dehydratase of the lantibiotic nisin. *Biochemistry*, *44*(38), 12827-12834.

Kluskens, L. D., Nelemans, S. A., Rink, R., de Vries, L., Meter-Arkema, A., Wang, Y., Walther, T., Kuipers, A., Moll, G. N., & Haas, M. (2009). Angiotensin-(1-7) with thioether bridge: an angiotensin-converting enzyme-resistant, potent angiotensin-(1-7) analog. *J Pharmacol Exp Ther*, *328*(3), 849-854.

Knerr, P. J., & van der Donk, W. A. (2012). Discovery, biosynthesis, and engineering of lantipeptides. *Annual Review of Biochemistry, Vol 81*, *81*, 479-505.

Kobras, C. M., Piepenbreier, H., Emenegger, J., Sim, A., Fritz, G., & Gebhard, S. (2020). BceAB-Type Antibiotic Resistance Transporters Appear To Act by Target Protection of Cell Wall Synthesis. *Antimicrob Agents Chemother*, *64*(3).

Kodani, S., Hudson, M. E., Durrant, M. C., Buttner, M. J., Nodwell, J. R., & Willey, J. M. (2004). The SapB morphogen is a lantibiotic-like peptide derived from the product of the developmental gene ramS in Streptomyces coelicolor. *Proc Natl Acad Sci U S A*, *101*(31), 11448-11453.

Kodani, S., Lodato, M. A., Durrant, M. C., Picart, F., & Willey, J. M. (2005). SapT, a lanthionine-containing peptide involved in aerial hyphae formation in the streptomycetes. *Mol Microbiol*, *58*(5), 1368-1380.

Koponen, O., Takala, T. M., Saarela, U., Qiao, M., & Saris, P. E. (2004). Distribution of the NisI immunity protein and enhancement of nisin activity by the lipid-free NisI. *FEMS Microbiol Lett*, *231*(1), 85-90.

Koponen, O., Tolonen, M., Qiao, M., Wahlstrom, G., Helin, J., & Saris, P. E. (2002). NisB is required for the dehydration and NisC for the lanthionine formation in the post-translational modification of nisin. *Microbiology*, *148*(Pt 11), 3561-3568.

Kordel, M., Benz, R., & Sahl, H. G. (1988). Mode of action of the staphylococcinlike peptide Pep 5: voltage-dependent depolarization of bacterial and artificial membranes. *J Bacteriol*, *170*(1), 84-88.

Kuipers, A., de Boef, E., Rink, R., Fekken, S., Kluskens, L. D., Driessen, A. J., Leenhouts, K., Kuipers, O. P., & Moll, G. N. (2004). NisT, the transporter of the lantibiotic nisin, can transport fully modified, dehydrated, and unmodified prenisin and fusions of the leader peptide with non-lantibiotic peptides. *Journal of Biological Chemistry*, *279*(21), 22176-22182.

Kuipers, O. P., Beerthuyzen, M. M., de Ruyter, P. G., Luesink, E. J., & de Vos, W. M. (1995). Autoregulation of nisin biosynthesis in Lactococcus lactis by signal transduction. *Journal of Biological Chemistry*, *270*(45), 27299-27304.

Kuipers, O. P., Beerthuyzen, M. M., Siezen, R. J., & De Vos, W. M. (1993). Characterization of the nisin gene cluster nisABTCIPR of Lactococcus lactis. Requirement of expression of the nisA and nisI genes for development of immunity. *Eur J Biochem*, *216*(1), 281-291.

Kuipers, O. P., de Ruyter, P. G., Kleerebezem, M., & de Vos, W. M. (1997). Controlled overproduction of proteins by lactic acid bacteria. *Trends Biotechnol*, *15*(4), 135-140.

Kuipers, O. P., de Ruyter, P. G. G. A., Kleerebezem, M., & de Vos, W. M. (1998). Quorum sensing-controlled gene expression in lactic acid bacteria. *Journal of biotechnology*, *64*(1), 15-21.

Lagedroste, M., Reiners, J., Knospe, C. V., Smits, S. H. J., & Schmitt, L. (2020). A Structural View on the Maturation of Lanthipeptides. *Front Microbiol*, *11*, 1183.

Lagedroste, M., Smits, S. H. J., & Schmitt, L. (2017). Substrate Specificity of the Secreted Nisin Leader Peptidase NisP. *Biochemistry*, *56*(30), 4005-4014.

Lee, H., & van der Donk, W. A. (2022). Macrocyclization and Backbone Modification in RiPP Biosynthesis. *Annual Review of Biochemistry, Vol 81*, *91*, 269-294.

Levengood, M. R., Patton, G. C., & van der Donk, W. A. (2007). The leader peptide is not required for post-translational modification by lacticin 481 synthetase. *J Am Chem Soc*, *129*(34), 10314-10315.

Li, B., & van der Donk, W. A. (2007). Identification of essential catalytic residues of the cyclase NisC involved in the biosynthesis of nisin. *Journal of Biological Chemistry*, *282*(29), 21169-21175.

Li, B., Yu, J. P., Brunzelle, J. S., Moll, G. N., van der Donk, W. A., & Nair, S. K. (2006). Structure and mechanism of the lantibiotic cyclase involved in nisin biosynthesis. *Science*, *311*(5766), 1464-1467.

Liang, X., Sun, Z., Zhong, J., Zhang, Q., & Huan, L. (2010). Adverse effect of nisin resistance protein on nisin-induced expression system in Lactococcus lactis. *Microbiol Res*, *165*(6), 458-465.

Lu, Y., Jiang, L., Chen, M., Huan, L., & Zhong, J. (2010). [Improving heat and pH stability of nisin by site-directed mutagenesis]. *Wei Sheng Wu Xue Bao*, *50*(11), 1481-1487.

Lubelski, J., Khusainov, R., & Kuipers, O. P. (2009). Directionality and coordination of dehydration and ring formation during biosynthesis of the lantibiotic nisin. *Journal of Biological Chemistry*, *284*(38), 25962-25972.

Malmsten, M. (2014). Antimicrobial peptides. *Ups J Med Sci*, *119*(2), 199-204.

Mascher, T. (2006). Intramembrane-sensing histidine kinases: a new family of cell envelope stress sensors in Firmicutes bacteria. *FEMS Microbiol Lett*, *264*(2), 133-144.

Mavaro, A., Abts, A., Bakkes, P. J., Moll, G. N., Driessen, A. J. M., Smits, S. H. J., & Schmitt, L. (2011). Substrate recognition and specificity of the NisB protein, the lantibiotic dehydratase involved in nisin biosynthesis. *Journal of Biological Chemistry*, *286*(35), 30552-30560.

McAuliffe, O., Ross, R. P., & Hill, C. (2001). Lantibiotics: structure, biosynthesis and mode of action. *FEMS Microbiol Rev*, *25*(3), 285-308.

McIntosh, J. A., Donia, M. S., & Schmidt, E. W. (2009). Ribosomal peptide natural products: bridging the ribosomal and nonribosomal worlds. *Nat Prod Rep*, *26*(4), 537-559.

Medeiros-Silva, J., Jekhmane, S., Paioni, A. L., Gawarecka, K., Baldus, M., Swiezewska, E., Breukink, E., & Weingarth, M. (2018). High-resolution NMR studies of antibiotics in cellular membranes. *Nat Commun*, *9*(1), 3963.

Mierau, I., & Kleerebezem, M. (2005). 10 years of the nisin-controlled gene expression system (NICE) in Lactococcus lactis. *Appl Microbiol Biotechnol*, *68*(6), 705-717.

Mohr, K. I., Volz, C., Jansen, R., Wray, V., Hoffmann, J., Bernecker, S., Wink, J., Gerth, K., Stadler, M., & Muller, R. (2015). Pinensins: the first antifungal lantibiotics. *Angew Chem Int Ed Engl*, *54*(38), 11254-11258.

Montalban-Lopez, M., Deng, J., van Heel, A. J., & Kuipers, O. P. (2018). Specificity and Application of the Lantibiotic Protease NisP. *Front Microbiol*, *9*, 160.

Montalban-Lopez, M., Scott, T. A., Ramesh, S., Rahman, I. R., van Heel, A. J., Viel, J. H., Bandarian, V., Dittmann, E., Genilloud, O., Goto, Y., Grande Burgos, M. J., Hill, C., Kim, S., Koehnke, J., Latham, J. A., Link, A. J., Martinez, B., Nair, S. K., Nicolet, Y., van der Donk, W. A. (2021). New developments in RiPP discovery, enzymology and engineering. *Nat Prod Rep*, *38*(1), 130-239.

Mota-Meira, M., LaPointe, G., Lacroix, C., & Lavoie, M. C. (2000). MICs of mutacin B-Ny266, nisin A, vancomycin, and oxacillin against bacterial pathogens. *Antimicrob Agents Chemother*, *44*(1), 24-29.

Mulders, J. W., Boerrigter, I. J., Rollema, H. S., Siezen, R. J., & de Vos, W. M. (1991). Identification and characterization of the lantibiotic nisin Z, a natural nisin variant. *Eur J Biochem*, *201*(3), 581-584.

Nawrocki, K. L., Crispell, E. K., & McBride, S. M. (2014). Antimicrobial Peptide Resistance Mechanisms of Gram-Positive Bacteria. *Antibiotics (Basel)*, *3*(4), 461-492.

Newton, G. G., Abraham, E. P., & Berridge, N. J. (1953). Sulphur-containing amino-acids of nisin. *Nature*, *171*(4353), 606.

Nishie, M., Sasaki, M., Nagao, J., Zendo, T., Nakayama, J., & Sonomoto, K. (2011). Lantibiotic transporter requires cooperative functioning of the peptidase domain and the ATP binding domain. *Journal of Biological Chemistry*, *286*(13), 11163-11169.

O'Connor, P. M., O'Shea, E. F., Guinane, C. M., O'Sullivan, O., Cotter, P. D., Ross, R. P., & Hill, C. (2015). Nisin H Is a New Nisin Variant Produced by the Gut-Derived Strain Streptococcus hyointestinalis DPC6484. *Appl Environ Microbiol*, *81*(12), 3953-3960.

O'Sullivan, J. N., O'Connor, P. M., Rea, M. C., O'Sullivan, O., Walsh, C. J., Healy, B., Mathur, H., Field, D., Hill, C., & Ross, R. P. (2020). Nisin J, a Novel Natural Nisin Variant, Is Produced by Staphylococcus capitis Sourced from the Human Skin Microbiota. *J Bacteriol*, *202*(3).

Ohki, R., Giyanto, Tateno, K., Masuyama, W., Moriya, S., Kobayashi, K., & Ogasawara, N. (2003). The BceRS two-component regulatory system induces expression of the bacitracin transporter, BceAB, in Bacillus subtilis. *Mol Microbiol*, *49*(4), 1135-1144.

Okeley, N. M., Paul, M., Stasser, J. P., Blackburn, N., & van der Donk, W. A. (2003). SpaC and NisC, the cyclases involved in subtilin and nisin biosynthesis, are zinc proteins. *Biochemistry*, *42*(46), 13613-13624.

Okeley, N. M., Zhu, Y., & van Der Donk, W. A. (2000). Facile chemoselective synthesis of dehydroalanine-containing peptides. *Org Lett*, *2*(23), 3603-3606.

Okuda, K., Yanagihara, S., Sugayama, T., Zendo, T., Nakayama, J., & Sonomoto, K. (2010). Functional significance of the E loop, a novel motif conserved in the lantibiotic immunity ATP-binding cassette transport systems. *J Bacteriol*, *192*(11), 2801-2808.

Oman, T. J., Knerr, P. J., Bindman, N. A., Velasquez, J. E., & van der Donk, W. A. (2012). An engineered lantibiotic synthetase that does not require a leader peptide on its substrate. *J Am Chem Soc*, *134*(16), 6952-6955.

Oman, T. J., & van der Donk, W. A. (2010). Follow the leader: the use of leader peptides to guide natural product biosynthesis. *Nature chemical biology*, *6*(1), 9-18.

Ongey, E. L., Yassi, H., Pflugmacher, S., & Neubauer, P. (2017). Pharmacological and pharmacokinetic properties of lanthipeptides undergoing clinical studies. *Biotechnol Lett*, *39*(4), 473-482.

Oppedijk, S. F., Martin, N. I., & Breukink, E. (2016). Hit 'em where it hurts: The growing and structurally diverse family of peptides that target lipid-II. *Biochim Biophys Acta*, *1858*(5), 947-957.

Ortega, M. A., Hao, Y., Walker, M. C., Donadio, S., Sosio, M., Nair, S. K., & van der Donk, W. A. (2016). Structure and tRNA Specificity of MibB, a Lantibiotic Dehydratase from Actinobacteria Involved in NAI-107 Biosynthesis. *Cell Chem Biol*, *23*(3), 370-380.

Ortega, M. A., Hao, Y., Zhang, Q., Walker, M. C., van der Donk, W. A., & Nair, S. K. (2015). Structure and mechanism of the tRNA-dependent lantibiotic dehydratase NisB. *Nature*, *517*(7535), 509-512.

Ortega, M. A., Velasquez, J. E., Garg, N., Zhang, Q., Joyce, R. E., Nair, S. K., & van der Donk, W. A. (2014). Substrate specificity of the lanthipeptide peptidase ElxP and the oxidoreductase ElxO. *ACS Chem Biol*, *9*(8), 1718-1725.

Patton, G. C., Paul, M., Cooper, L. E., Chatterjee, C., & van der Donk, W. A. (2008). The importance of the leader sequence for directing lanthionine formation in lacticin 481. *Biochemistry*, *47*(28), 7342-7351.

Pei, Z. F., Zhu, L., Sarksian, R., van der Donk, W. A., & Nair, S. K. (2022). Class V Lanthipeptide Cyclase Directs the Biosynthesis of a Stapled Peptide Natural Product. *J Am Chem Soc*.

Plat, A., Kluskens, L. D., Kuipers, A., Rink, R., & Moll, G. N. (2011). Requirements of the engineered leader peptide of nisin for inducing modification, export, and cleavage. *Appl Environ Microbiol*, *77*(2), 604-611.

Plat, A., Kuipers, A., Rink, R., & Moll, G. N. (2013). Mechanistic aspects of lanthipeptide leaders. *Curr Protein Pept Sci*, *14*(2), 85-96.

Porta, N., Zaschke-Kriesche, J., Frieg, B., Gopalswamy, M., Zivkovic, A., Etzkorn, M., Stark, H., Smits, S. H. J., & Gohlke, H. (2019). Small-molecule inhibitors of nisin resistance protein NSR from the human pathogen Streptococcus agalactiae. *Bioorg Med Chem*, *27*(20), 115079.

Powers, J. H. (2004). Antimicrobial drug development--the past, the present, and the future. *Clin Microbiol Infect*, *10 Suppl 4*, 23-31.

Qiao, M., Immonen, T., Koponen, O., & Saris, P. E. (1995). The cellular location and effect on nisin immunity of the NisI protein from Lactococcus lactis N8 expressed in Escherichia coli and L. lactis. *FEMS Microbiol Lett*, *131*(1), 75-80.

Qiao, M., & Saris, P. E. (1996). Evidence for a role of NisT in transport of the lantibiotic nisin produced by Lactococcus lactis N8. *FEMS Microbiol Lett*, *144*(1), 89-93.

Qiao, M., Ye, S., Koponen, O., Ra, R., Usabiaga, M., Immonen, T., & Saris, P. E. (1996). Regulation of the nisin operons in Lactococcus lactis N8. *J Appl Bacteriol*, *80*(6), 626-634.

Ra, R., Beerthuyzen, M. M., de Vos, W. M., Saris, P. E. J., & Kuipers, O. P. (1999). Effects of gene disruptions in the nisin gene cluster of Lactococcus lactis on nisin production and producer immunity. *Microbiology (Reading)*, *145 (Pt 5)*, 1227-1233.

Rawlings, N. D., & Barrett, A. J. (1993). Evolutionary families of peptidases. *Biochem J*, *290 (Pt 1)*, 205-218.

Repka, L. M., Chekan, J. R., Nair, S. K., & van der Donk, W. A. (2017). Mechanistic Understanding of Lanthipeptide Biosynthetic Enzymes. *Chemical reviews*, *117*(8), 5457-5520.

Rietkotter, E., Hoyer, D., & Mascher, T. (2008). Bacitracin sensing in Bacillus subtilis. *Mol Microbiol*, *68*(3), 768-785.

Rink, R., Kuipers, A., de Boef, E., Leenhouts, K. J., Driessen, A. J., Moll, G. N., & Kuipers, O. P. (2005). Lantibiotic structures as guidelines for the design of peptides that can be modified by lantibiotic enzymes. *Biochemistry*, *44*(24), 8873-8882.

Rink, R., Wierenga, J., Kuipers, A., Kluskens, L. D., Driessen, A. J., Kuipers, O. P., & Moll, G. N. (2007). Production of dehydroamino acid-containing peptides by Lactococcus lactis. *Appl Environ Microbiol*, *73*(6), 1792-1796.

Rodnina, M. V., Beringer, M., & Wintermeyer, W. (2007). How ribosomes make peptide bonds. *Trends Biochem Sci*, *32*(1), 20-26.

Rogers, L. A. (1928). The Inhibiting Effect of Streptococcus Lactis on Lactobacillus Bulgaricus. *J Bacteriol*, *16*(5), 321-325.

Rogers, L. A., & Whittier, E. O. (1928). Limiting Factors in the Lactic Fermentation. *J Bacteriol*, *16*(4), 211-229.

Sahl, H. G., & Bierbaum, G. (1998). Lantibiotics: biosynthesis and biological activities of uniquely modified peptides from gram-positive bacteria. *Annu Rev Microbiol*, *52*, 41-79.

Sandiford, S. K. (2019). Current developments in lantibiotic discovery for treating Clostridium difficile infection. *Expert Opin Drug Discov*, *14*(1), 71-79.

Schneewind, O., Fowler, A., & Faull, K. F. (1995). Structure of the cell wall anchor of surface proteins in Staphylococcus aureus. *Science*, *268*(5207), 103-106.
Schneewind, O., & Missiakas, D. (2014). Sec-secretion and sortase-mediated anchoring of proteins in Gram-positive bacteria. *Biochim Biophys Acta*, *1843*(8), 1687-1697.
Schnell, N., Entian, K. D., Schneider, U., Gotz, F., Zahner, H., Kellner, R., & Jung, G. (1988). Prepeptide sequence of epidermin, a ribosomally synthesized antibiotic with four sulphide-rings. *Nature*, *333*(6170), 276-278.
Schrodinger, LLC. (2022). *The PyMOL Molecular Graphics System, Version 2.5*.
Schwarzer, D., Finking, R., & Marahiel, M. A. (2003). Nonribosomal peptides: from genes to products. *Nat Prod Rep*, *20*(3), 275-287.
Siegers, K., & Entian, K. D. (1995). Genes involved in immunity to the lantibiotic nisin produced by Lactococcus lactis 6F3. *Appl Environ Microbiol*, *61*(3), 1082-1089.
Siegers, K., Heinzmann, S., & Entian, K. D. (1996). Biosynthesis of lantibiotic nisin. Posttranslational modification of its prepeptide occurs at a multimeric membrane-associated lanthionine synthetase complex. *Journal of Biological Chemistry*, *271*(21), 12294-12301.
Sievers, F., Wilm, A., Dineen, D., Gibson, T. J., Karplus, K., Li, W., Lopez, R., McWilliam, H., Remmert, M., Soding, J., Thompson, J. D., & Higgins, D. G. (2011). Fast, scalable generation of high-quality protein multiple sequence alignments using Clustal Omega. *Mol Syst Biol*, *7*, 539.
Siezen, R. J., Rollema, H. S., Kuipers, O. P., & de Vos, W. M. (1995). Homology modelling of the Lactococcus lactis leader peptidase NisP and its interaction with the precursor of the lantibiotic nisin. *Protein Eng*, *8*(2), 117-125.
Stein, T., Heinzmann, S., Dusterhus, S., Borchert, S., & Entian, K. D. (2005). Expression and functional analysis of the subtilin immunity genes spaIFEG in the subtilin-sensitive host Bacillus subtilis MO1099. *J Bacteriol*, *187*(3), 822-828.
Stein, T., Heinzmann, S., Solovieva, I., & Entian, K. D. (2003). Function of Lactococcus lactis nisin immunity genes nisI and nisFEG after coordinated expression in the surrogate host Bacillus subtilis. *Journal of Biological Chemistry*, *278*(1), 89-94.
Stevens, K. A., Sheldon, B. W., Klapes, N. A., & Klaenhammer, T. R. (1991). Nisin treatment for inactivation of Salmonella species and other gram-negative bacteria. *Appl Environ Microbiol*, *57*(12), 3613-3615.
Strieker, M., Tanovic, A., & Marahiel, M. A. (2010). Nonribosomal peptide synthetases: structures and dynamics. *Curr Opin Struct Biol*, *20*(2), 234-240.
Sun, Z., Zhong, J., Liang, X., Liu, J., Chen, X., & Huan, L. (2009). Novel mechanism for nisin resistance via proteolytic degradation of nisin by the nisin resistance protein NSR. *Antimicrob Agents Chemother*, *53*(5), 1964-1973.
Takala, T. M., Koponen, O., Qiao, M., & Saris, P. E. J. (2004). Lipid-free NisI: interaction with nisin and contribution to nisin immunity via secretion. *FEMS microbiology letters*, *237*(1), 171-177.
Takala, T. M., & Saris, P. E. J. (2006). C terminus of NisI provides specificity to nisin. *Microbiology (Reading)*, *152*(Pt 12), 3543-3549.
Taylor, W. R. (1997). Residual colours: a proposal for aminochromography. *Protein Eng*, *10*(7), 743-746.
Thibodeaux, G. N., McClerren, A. L., Ma, Y., Gancayco, M. R., & van der Donk, W. A. (2015). Synergistic binding of the leader and core peptides by the lantibiotic synthetase HalM2. *ACS Chem Biol*, *10*(4), 970-977.
Trabi, M., Mylne, J. S., Sando, L., & Craik, D. J. (2009). Circular proteins from Melicytus (Violaceae) refine the conserved protein and gene architecture of cyclotides. *Org Biomol Chem*, *7*(11), 2378-2388.

Tracanna, V., de Jong, A., Medema, M. H., & Kuipers, O. P. (2017). Mining prokaryotes for antimicrobial compounds: from diversity to function. *FEMS Microbiol Rev*, *41*(3), 417-429.

Van de Ven, F. J., Van den Hooven, H. W., Konings, R. N., & Hilbers, C. W. (1991). NMR studies of lantibiotics. The structure of nisin in aqueous solution. *Eur J Biochem*, *202*(3), 1181-1188.

van den Berg van Saparoea, H. B., Bakkes, P. J., Moll, G. N., & Driessen, A. J. (2008). Distinct contributions of the nisin biosynthesis enzymes NisB and NisC and transporter NisT to prenisin production by Lactococcus lactis. *Appl Environ Microbiol*, *74*(17), 5541-5548.

van der Meer, J. R., Polman, J., Beerthuyzen, M. M., Siezen, R. J., Kuipers, O. P., & De Vos, W. M. (1993). Characterization of the Lactococcus lactis nisin A operon genes nisP, encoding a subtilisin-like serine protease involved in precursor processing, and nisR, encoding a regulatory protein involved in nisin biosynthesis. *J Bacteriol*, *175*(9), 2578-2588.

van der Meer, J. R., Rollema, H. S., Siezen, R. J., Beerthuyzen, M. M., Kuipers, O. P., & de Vos, W. M. (1994). Influence of amino acid substitutions in the nisin leader peptide on biosynthesis and secretion of nisin by Lactococcus lactis. *Journal of Biological Chemistry*, *269*(5), 3555-3562.

van Heel, A. J., de Jong, A., Song, C., Viel, J. H., Kok, J., & Kuipers, O. P. (2018). BAGEL4: a user-friendly web server to thoroughly mine RiPPs and bacteriocins. *Nucleic Acids Research*, *46*(W1), W278-W281.

van Heel, A. J., Kloosterman, T. G., Montalban-Lopez, M., Deng, J., Plat, A., Baudu, B., Hendriks, D., Moll, G. N., & Kuipers, O. P. (2016). Discovery, Production and Modification of Five Novel Lantibiotics Using the Promiscuous Nisin Modification Machinery. *ACS Synth Biol*, *5*(10), 1146-1154.

van Heel, A. J., Montalban-Lopez, M., & Kuipers, O. P. (2011). Evaluating the feasibility of lantibiotics as an alternative therapy against bacterial infections in humans. *Expert Opin Drug Metab Toxicol*, *7*(6), 675-680.

van Heusden, H. E., de Kruijff, B., & Breukink, E. (2002). Lipid II induces a transmembrane orientation of the pore-forming peptide lantibiotic nisin. *Biochemistry*, *41*(40), 12171-12178.

van Hoek, A. H., Mevius, D., Guerra, B., Mullany, P., Roberts, A. P., & Aarts, H. J. (2011). Acquired antibiotic resistance genes: an overview. *Front Microbiol*, *2*, 203.

van Wageningen, A. M., Kirkpatrick, P. N., Williams, D. H., Harris, B. R., Kershaw, J. K., Lennard, N. J., Jones, M., Jones, S. J., & Solenberg, P. J. (1998). Sequencing and analysis of genes involved in the biosynthesis of a vancomycin group antibiotic. *Chem Biol*, *5*(3), 155-162.

Waterhouse, A. M., Procter, J. B., Martin, D. M., Clamp, M., & Barton, G. J. (2009). Jalview Version 2--a multiple sequence alignment editor and analysis workbench. *Bioinformatics*, *25*(9), 1189-1191.

Wiedemann, I., Benz, R., & Sahl, H. G. (2004). Lipid II-mediated pore formation by the peptide antibiotic nisin: a black lipid membrane study. *J Bacteriol*, *186*(10), 3259-3261.

Willey, J. M., & van der Donk, W. A. (2007). Lantibiotics: peptides of diverse structure and function. *Annu Rev Microbiol*, *61*, 477-501.

Wirawan, R. E., Klesse, N. A., Jack, R. W., & Tagg, J. R. (2006). Molecular and genetic characterization of a novel nisin variant produced by Streptococcus uberis. *Appl Environ Microbiol*, *72*(2), 1148-1156.

Wu, Z., Wang, W., Tang, M., Shao, J., Dai, C., Zhang, W., Fan, H., Yao, H., Zong, J., Chen, D., Wang, J., & Lu, C. (2014). Comparative genomic analysis shows that Streptococcus suis meningitis isolate SC070731 contains a unique 105K genomic island. *Gene*, *535*(2), 156-164.

Xie, L., & van der Donk, W. A. (2004). Post-translational modifications during lantibiotic biosynthesis. *Curr Opin Chem Biol*, *8*(5), 498-507.

Xu, M., Zhang, F., Cheng, Z., Bashiri, G., Wang, J., Hong, J., Wang, Y., Xu, L., Chen, X., Huang, S. X., Lin, S., Deng, Z., & Tao, M. (2020). Functional Genome Mining Reveals a Class V Lanthipeptide Containing a d-Amino Acid Introduced by an F420 H2 - Dependent Reductase. *Angew Chem Int Ed Engl*, *59*(41), 18029-18035.

Xu, Y., Li, X., Li, R., Li, S., Ni, H., Wang, H., Xu, H., Zhou, W., Saris, P. E., Yang, W., Qiao, M., & Rao, Z. (2014). Structure of the nisin leader peptidase NisP revealing a C-terminal autocleavage activity. *Acta Crystallogr D Biol Crystallogr*, *70*(Pt 6), 1499-1505.

Yuan, J., Zhang, Z. Z., Chen, X. Z., Yang, W., & Huan, L. D. (2004). Site-directed mutagenesis of the hinge region of nisinZ and properties of nisinZ mutants. *Appl Microbiol Biotechnol*, *64*(6), 806-815.

Zendo, T., Fukao, M., Ueda, K., Higuchi, T., Nakayama, J., & Sonomoto, K. (2003). Identification of the lantibiotic nisin Q, a new natural nisin variant produced by Lactococcus lactis 61-14 isolated from a river in Japan. *Biosci Biotechnol Biochem*, *67*(7), 1616-1619.

Zhang, Q., Yu, Y., Velasquez, J. E., & van der Donk, W. A. (2012). Evolution of lanthipeptide synthetases. *Proc Natl Acad Sci U S A*, *109*(45), 18361-18366.

Zhou, L., van Heel, A. J., & Kuipers, O. P. (2015). The length of a lantibiotic hinge region has profound influence on antimicrobial activity and host specificity. *Front Microbiol*, *6*, 11.

6 Curriculum Vitae

Personal Data

Name:	Jens Reiners
Date of birth:	15. June 1984 (Heinsberg)
Nationality:	German

Working experience, Studies & School Education

Since 07/2019	Member of the Center of Structural Studies (CSS) Responsible for Small-Angle-X-ray-Scattering (SAXS) Heinrich-Heine University Duesseldorf
Since 10/2013	Ph.D. student at the Institute of Biochemistry Heinrich-Heine University Duesseldorf Supervisor: Prof. Dr. Lutz Schmitt
09/2011 – 09/2013	Master of Science (M.Sc.): Biochemistry (Overall grade:1,4) Heinrich-Heine University Duesseldorf Title: Analysis of the Nisin modifications process
10/2008 – 09/2011	Bachelor of Science (B.Sc.): Biochemistry (Overall grade:1,9) Heinrich-Heine University Duesseldorf Title: Characterization of the Cyclase NisC
08/2006 – 06/2008	Training for Biological Technical Assistant (BTA), Berufskolleg Hilden
09/2002 – 06/2005	Abitur, Euregio Kolleg Wuerselen

Workshops and Conferences

06/2022	NRW BAG Meeting
06/2022	CBMS workbenches on Solution Scattering (SAXS/WAXS) and Macromolecular Crystallography (MX), Brookhaven National Laboratory, USA
05/2022	3rd Hands-On Computational Enzyme Design Course, Loschmidt Laboratories, Brno, Czech Republic
05/2022	Workshop “The database of small-angle scattering data and models for biology and soft matter”, EMBL Hamburg
11/2021	P12 Virtual User Meeting, EMBL Hamburg
11/2021	Biophysical Society’s virtual symposium, "Protein Data Bank (PDB) Celebrates 50 Years"
06/2021	NRW BAG Meeting
11/2020	P12 Virtual User Meeting, EMBL Hamburg
09/2019	EMBO Practical Course “Small angle neutron and X-ray scattering from biomacromolecules in solution”, Grenoble, France
06/2018	6th International Symposium on Antimicrobial Peptides (AMP), Poitiers, France
08/2016	Agilent Protein Analytics Seminar, Duesseldorf
06/2016	23th Workshop “Micro Methods in Protein Chemistry”, Dortmund
02/2016	Agilent Seminar „New Ways in LC-MS”, Bochum
06/2015	22th Workshop “Micro Methods in Protein Chemistry”, Dortmund
06/2015	Chrom Forum, Bonn
03/2015	Seminar for “Sample Preparation and HPLC”, Duesseldorf
10/2014	VAAM Annual Meeting 2014, Dresden
06/2013	GE Healthcare Biacore & MicroCal User Meeting, Weimar

7 List of publications

Publications which are part of this Thesis

9. **Reiners J.**, Lagedroste M., Gottstein J., Adeniyi E.T., Kalscheuer R., Poschmann G., Stühler K., Smits S.H.J., Schmitt L. (2020). Insights in the antimicrobial potential of the natural nisin variant nisin H. *Frontiers in Microbiology* 11:573614.

8. Furtmann F., Porta N., Hoang D.T., **Reiners J.**, Schumacher J., Gottstein J., Gohlke H., Smits S.H.J. (2020). Characterization of the Nucleotide-Binding Domain NsrF from the BceAB-type ABC-Transporter NsrFP from the Human Pathogen *Streptococcus agalactiae*. *Scientific Reports* 10(1):15208.

7. Lagedroste M., **Reiners J.**, Smits S.H.J., Schmitt L. (2020). Impact of the nisin modification machinery on the transport kinetics of NisT. *Scientific Reports* 10(1):12295.

6. Lagedroste, M., **Reiners J.**, Knospe V., Smits S.H.J., Schmitt L. (2020). The maturation of lanthipeptides: A structural view on the maturation of lanthipeptides. *Frontiers in Microbiology* 11:1183.

5. Zaschke-Kriesche J., **Reiners J.**, Lagedroste M., Smits S. H. J. (2019). Influence of nisin hinge-region variants on lantibiotic immunity and resistance proteins. *Bioorganic & Medicinal Chemistry* 27(17) 3947-3953.

4. Zaschke-Kriesche J., Behrmann L.V., **Reiners J.**, Lagedroste M., Gröner Y., Kalscheuer R., Smits S.H.J. (2019). Bypassing lantibiotic resistance by an effective nisin derivative. *Bioorganic & Medicinal Chemistry* 27(15):3454-3462.

3. Lagedroste M., **Reiners J**., Smits S.H.J., Schmitt L. (2019). Systematic characterization of position one variants within the lantibiotic nisin. *Scientific Reports* 9: 935

2. **Reiners J.**, Lagedroste M., Ehlen K., Leusch S., Zaschke-Kriesche J., Smits S.H.J. (2017). The N-terminal Region of Nisin Is Important for the BceAB-Type ABC Transporter NsrFP from *Streptococcus agalactiae COH1*. *Frontiers in Microbiology* 8:1643.

1. **Reiners J.**, Abts A., Clemens R., Smits S.H.J., Schmitt L. (2017). Stoichiometry and structure of a lantibiotic maturation complex. *Scientific Reports* 7**,** 42163.

Additional publications

10. Papadopoulos A., Busch M., **Reiners J.**, Hachani E., Baeumers M., Schmitt L., Jaeger K.-E., Kovacic F., Smits S.H.J., Kedrov A. (2022). The periplasmic chaperone Skp prevents misfolding of the secretory lipase A from Pseudomonas aeruginosa. *Frontiers in Molecular Biosciences* 9:1026724

9. Gopalswamy M., Kroeger T., Bickel D., Frieg B., Akter S., Schott-Verdugo S., Viegas A., Pauly T., Mayer M., Przibilla J., **Reiners J.**, Nagel-Steger L., Smits S.H.J., Groth G., Etzkorn M., Gohlke H. (2022). Biophysical and pharmacokinetic characterization of a small-molecule inhibitor of RUNX1/ETO tetramerization with anti-leukemic effects. *Scientific Reports* 12, 14158.

8. Devan S.-K., Schott-Verdugo S., Muentjes K., Bismar L., **Reiners J.**, Hachani E., Schmitt L., Hoeppner A., Smits S.H.J., Gohlke H., Feldbruegge M. (2022). A MademoiseLLE domain binding platform links the key RNA transporter to endosomes. *PLOS Genetics* 18(6): e1010269

7. Bhatia S., Spanier L., Bickel D., Dienstbier N., Woloschin V., Vogt M., Pols M. Lungerich B., **Reiners J.**, Aghaallaei N., Diedrich D., Frieg B., Ahlert H., Bopp B., Lang F., Loschwitz J.., Bajohgli B., Borkhardt A., Hauer J., Hansen F.K., Smits S.H.J, Jose J., Gohlke H., Kurz T. (2022). Development of a First-in-Class Small Molecule Inhibitor of the C-terminal Hsp90 Dimerization, *ACS Central Science* 8, 636−655

6. Huber M., Wagner A., **Reiners J.**, Seyfert C., Eric M., Sharpe T., Smits S.H.J., Schirmer T., Dehio C. (2022). Full-Length Structure of the Host Targeted Bacterial Effector Bep1 Reveals a Novel Structural Domain Conserved in FIC Effector Proteins From Bartonella. Available at SSRN: https://ssrn.com/abstract=4109528

5. Spitz O., Erenburg I.N., Kannonenberg K., Peherstorfer S., Lenders M.H.H., **Reiners J.**, Ma M., Luisi B.F., Smits S.H.J., Schmitt L. (2022). Identity determinants of the translocation signal for a Type 1 secretion system. *Frontiers in Physiology* 12:804646.

4. Gottstein J., Klose H., Knospe C.V., **Reiners J.**, Smits S.H.J, Schmitt L. (2021). Lantibiotika – hoffnungsvolle Alternative gegen Antibiotikaresistenz? *BIOspektrum*-Ausgabe 5/21.

3. Mulnaes D., Porta N., Clemens R., Apanasenko I., **Reiners J.**, Gremer L., Neudecker P., Smits S.H.J., Gohlke H. (2020). TopModel: Template-based protein structure prediction at low sequence identity using top-down consensus and deep neural networks. *Journal of Chemical Theory and Computation* 16(3):1953-1967.

2. Heilers J-H., **Reiners J.**, Heller E.M., Smits S.H.J., van der Does C. (2019). DNA processing by the MOBH family relaxase TraI encoded within the gonococcal genetic island. *Nucleic Acids Research* 47(15): 8136–8153.

1. Meyer Zu Hörste G., **Reiners J.**, Lehmann H. C., Airas L., Kieseier B. C., (2009). CD73 is expressed on invading T lymphocytes in the inflamed peripheral nerve. *Muscle Nerve* 40: 287-289.

8 Acknowledgements

Es war ein langer Weg bis zu diesem Punkt. Manch einer hat schon nicht mehr daran geglaubt, doch es ist geschafft. Viele haben mich auf dem Weg unterstützt, denen ich hiermit meinen Dank aussprechen möchte.

Zuerst möchte ich natürlich Prof. Dr. Lutz Schmitt danken für das Vertrauen und die Möglichkeit in seinem Institut meine Promotion beginnen zu dürfen. Danke für das spannende Thema und die Freiheiten, die du deinen Leuten im Labor gewährst. Sollte man sich doch einmal auf dem Holzweg befinden, war deine Tür stets offen. Du hast mit deiner Kompetenz (eines Lutzerators würdig) und der nötigen Ruhe immer eine gute Idee gehabt. Es gab jedoch auch Ausnahmen, wo die innere Ruhe stark beansprucht wurde. Mir fällt hier spontan die mögliche Fehlinterpretation der Abkürzung SFB ein, oder wenn wir uns über Auswahl von Farben oder die Ausrichtung von Abbildungen uneinig waren, gerade wenn es sich um Proof Versionen handelt. Aber allen Gerüchten zum Trotz, nein ich bin für kein graues Haar verantwortlich. Ich danke dir für diese besondere Zeit in deinem Institut.

Sander, ich kenne wohl niemand anderen, der mit seiner lockeren holländischen Art jeden noch so schlechten Tag retten kann. Egal, ob fehlgeschlagenes Experiment, chaotische Datenlage, oder einfach nur weil es montags morgens vorm Kaffee war, du hast gute Laune verteilt. Ok, solange die Kaffeemaschine funktioniert hat. Dein Optimismus und deine Zuversicht, auch wenn es mal nicht so lief, haben mich wohl gerettet und dafür gesorgt, dass ich das Ziel nicht aus den Augen verliere. Ich danke dir für die Hilfe während der Promotion, aber auch auf persönlicher Ebene. Es hat mir sehr geholfen, auch wenn es sicherlich manchmal nicht einfach für dich war. Auch hier kann ich aber mit gutem Gewissen behaupten, dass ich für kein graues Haar verantwortlich bin (aber vielleicht für ein paar fehlende Haare…). Ich danke dir für das Vertrauen, dass du in mich hast.

Mein ganz herzlicher Dank geht auch an PD Dr. Ulrich Schulte. Du warst als Ansprechpartner für uns Studenten im Biochemie Studium immer geschätzt und als Betreuer im Praktikum gefürchtet. Ich kenne persönlich niemanden, der mit so einer intrinsischen Genauigkeit weiß, welche Fragen man im Kolloquium nicht beantworten kann. Auch während der Promotion warst du als „wandelndes Lehrbuch“ immer da, um uns Fragen zu beantworten, deren Antwort

wir eigentlich selbst wissen sollten… Ich danke dir, dass du die Hoffnung für uns Studenten trotz diverser Wissenslücken nie aufgegeben hast.

Für die freundliche Übernahme des Koreferats möchte ich Prof. Dr. Georg Groth danken.

Den ehemaligen Sekretärinnen der Biochemie, Mathilde Blum und Tatjana Platz, möchte ich dafür danken, dass sie jede bürokratische Hürde für uns meistern konnten.

Martina, Iris und Silke, euch kann man eigentlich nicht genug danken. Ich weiß persönlich nicht, wie ihr das Chaos, das wir regelmäßig in Bestelllisten oder in den Laboren fabrizierten, meistern konntet. Danke, dass ihr trotz allem immer geholfen habt, wenn Not am Mann war. Ohne euch läuft der Laden halt nicht.

„Und ich weiß bis heute nicht, wie er es in unserem Büro mit all den verrückten Hühnern ausgehalten hat.“ (Rebecca Clemens, Promotion 2018). Ja, so richtig weiß ich das auch nicht. Aber was soll ich sagen, es war einfach eine schöne Mischung. Eine kölsche Frohnatur Julia, eine ordnungsliebende Katja, eine Schokoladenqueen Alex, eine Gleichstellungsbeauftragte Isa und meine persönliche Lieblingshexe Rebecca. Ja, das war schon etwas. Der Ruhepol war wohl in all der Zeit Martina, die es stets mit Humor verfolgt hat. Ich danke euch für die schöne gemeinsame Zeit. Es bleiben viele Erinnerungen an so manch tollen Moment im Büro. Aber auch die SAXS Trips nach Grenoble, mit Isa und Rebecca, werden in Erinnerung bleiben, wo fehlender Schlaf oder ein abhanden gekommener Stressball für den ein oder anderen lustigen Momente gesorgt haben. Besonders dir Rebecca, möchte ich für die schöne Zeit als du meine Masterstudentin warst und nachher als Kollegin danken. Du hattest es schon nicht immer leicht mit mir, vor allem mein Taschenrechnerverbot war ja sehr beliebt bei dir. Aber auch Julia war ein wichtiger Ankerpunkt. Als kölsche Frohnatur hast du immer für gute Laune gesorgt, selbst wenn ein Experiment mal fehlgeschlagen ist, danke dafür.

Kerstin, dein Kaffee-, Schokolade- und Burgerkonsum war ja schon vor mir legendär, aber zusammen haben wir das schon auf eine neue Stufe gehoben. Gerne erinnere ich mich an die abendlichen Ausflüge zum Scotti‘s, wo nach eintausend und drei ATPasen endlich mal Feierabend für dich war. Ebenso an das „KAFFFEEEEE“, mit einem nachfolgenden „K K KALT!!!“, wenn man wieder bei sommerlichen Temperaturen ohne Jacke im Schnee auf der Dachterrasse war. Einfach legendär. Genau wie deine sportlichen Aktivitäten, die zwar keiner

so richtig verstehen konnte, aber auch da hast du ja einen rechtlich sauberen Weg beim Lutz gefunden (die, die es wissen, werden es verstehen). Ich danke dir für die schöne gemeinsame Zeit im Institut, für die vielen tollen tiefsinnigen und manchmal weniger tiefsinnigen Gespräche und für die fortlaufende Unterstützung von dir. Du bist zwar ein kleiner „Chaot", aber einer meiner liebsten! Ich danke dir und bleib so wie du bist.

Sakshi, da du ja fleißig Deutsch lernen wolltest unterstütze ich das natürlich indem ich auf Deutsch schreibe. Ich danke dir für alle die Hilfe. Gerade in der Anfangszeit, wo ich noch Masterstudent bei André war. Sicherlich war es auch für dich nicht einfach all die neuen Eindrücke von uns Chaoten zu verarbeiten. Das nennt man dann wohl Kulturschock. Trotz allem hast du dich nicht unterkriegen lassen, auch wenn wir (ok, primär ich) dich gerne erschreckt haben. Du warst immer hilfsbereit, wenn Not am Mann war und hast dies, auch jetzt, wo du nach längerer Abstinenz wieder zurück bist, beibehalten. Ich danke dir für den unermüdlichen Willen einen zu motivieren. Bleib so wie du bist, und lass dich von komischen Western Blots oder tonnenweise EM daten nicht aus der Ruhe bringen. Es war und wird super.

Tim, es war mir immer ein besonderes Vergnügen mit dir im Labor zu fachsimpeln, um dann festzustellen, dass wir doch wieder Uli brauchen, um unsere Fragen zu beantworten. Auch die restlichen Gespräche waren immer sehr lustig, es liegt wohl an deiner Art, das ein oder andere „Fettnäpfchen" mitzunehmen. Der „Faster Tim, Faster" ist halt ein echtes Original. Danke dir für die tolle Zeit.

Unserer kreativen Seele Oli möchte ich für die schöne Zeit danken. Deine offene und ehrliche Art bei Gesprächen über „Gott und die Welt" bei einem Kaffee war immer toll. Auch wenn es wieder an Kreativität bei Bildern oder Geschichten für Promotionen mangelte, warst du immer die erste Adresse. Dass Labronomicon war ein echtes Meisterwerk.

Ebenso möchte ich den restlichen Leidensgenossen vom Labor 30, Steffi, Martin und Manuel, für die schöne Zeit und Unterstützung danken: Martin für die MALS Experimente, Steffi für die Hilfe bei ATPasen und Manuel für die fachlichen Diskussionen. Danke euch.

Unseren „Plant Ladies", Katharina und Kalpana, möchte ich für die schöne Zeit und die tollen Gespräche im Labor danken. Die Tanz- und Gesangseinlagen von Katharina im Labor waren

legendär. Vor allem da du nie bemerkt hat, wenn noch andere ins Labor gekommen sind („Wie lange stehst du schon da, was hast du mitbekommen?“).

Der neuen „Nisin Gang“ bestehend aus der ordnungsliebenden Julia G., dem immer wiederkehrenden Hans und einer budgetfreundlichen Vivien, möchte ich danken für die schöne Zeit im Labor. Ihr seid schon eine coole Truppe und es wird nie langweilig mit euch. Bleibt am Ball und viele Paper werden folgen.

Beim Thema Nisin muss ich natürlich auch direkt an den „dunklen Lord“ Marcel denken. Wir haben gemeinsam das Studium der Biochemie begonnen und so manch lustige Zeit in den Praktika gehabt. In der Nisin Gruppe ging dann unsere Reise der Promotion los und ich danke dir für die tolle Zusammenarbeit und die fachlichen Gespräche. Aber auch abseits von der Arbeit habe ich die Gespräche über Whisky und „Gott und die Welt“, sehr genossen, egal ob abends im Institut oder in der Altstadt. Es war eine tolle Zeit.

Bei Whisky und Gespräche über „Gott und die Welt“ kommt man an einer Person nicht vorbei. Tobi „Master of Coins“ und unumstrittener Meister des „unnützen Wissens“. Diese Titel hast du dir redlich verdient. Du warst eine Bereicherung bei jeder Diskussion, auch wenn es manchmal in einem dozierenden Monolog endete. Keine Gnade für Unwissende! Besonders die abendlichen Sitzungen mit Marcel, Sven und vielen anderen bei einem guten „Wasser des Lebens“ bleiben in Erinnerung. Danke für die tolle Zeit.

Dem „Hofstab des Lutzerators“, bestehend aus Manuel A., Florestan, Feby, Eymen und Zohreh wünsche ich viel Erfolg in ihren Projekten. Ihr habt es euch nicht einfach gemacht beim Thema Hämolysin. Aber für euch gibt es halt keine Probleme, sondern nur Herausforderungen. Mit dieser Einstellung werdet ihr eure Projekte meistern. Ein spezieller Dank geht an Manuel und Florestan, dass ihr das Erbe des „dunklen Lords“ angetreten habt und das Abenteuer Äktas bisher gut gemeistert habt. Viel Erfolg und danke für die schöne Zeit. Wenn es um Hämolysin geht, darf man natürlich auch unsere beiden Originale Sven und Michael nicht vergessen. Es war eine super Zeit mit euch beiden. Wir haben viel gelacht und Michaels „ruhige“ Art wird mir stehts in Erinnerung bleiben. Ihr beiden seid schon ein Herz und eine Seele, was zu diversen Motiven für Doktorwagen geführt hat. Danke euch.

Dem neuen Außenposten der Biochemie, unter der Kommandantur vom „Lord of the Order“ Alexej, samt seinen treuen „Glorious Knights“, Maryna, Michael und Athanasios, wünsche ich viel Glück und Erfolg für die Zukunft. Besonders Athanasios möchte ich für die gute Zusammenarbeit und die tiefgründigen Gespräche danken. Du wirst deinen Weg schon machen, die richtige Einstellung und dein Talent lassen keine Zweifel.

Auch meinen Studenten Dominik Daniels, Katja Ehlen, Selina Leusch, Dai Tri Hoang und Fabia Furtmann möchte ich danken. Ihr habt euren Teil dazu beigetragen, ich danke euch für euren Einsatz. Einen besonderen Dank gilt auch der „alten Garde“, die mich zur Bachelor/Masterarbeit herzlichst aufgenommen haben, rund um Dr. Christian Schwarz, Dr. Patrick Bakkes, Dr. André Abts, Dr. Phillip Ellinger, Dr. Miroslav Kirov, Dr. Ricarda Moseler, Dr. Zainab Alkhatib, Dr. Marianne Kluth, Dr. Rakeshkumar Gupta, Dr. Nils Hanekopp, Dr. Jan Stindt, Dr. Iris Gawarzeski, Dr. Susanne Prybylla, Dr. Sabrina Thomas und Dr. Nacera Infeld. Besonders Andr möchte ich danken, dass du mir als Betreuer in Bachelor- und Masterarbeit immer mit Rat und Tat zur Seite standest und mir all dein Wissen über das Nisin System vermittelt hast. Danke!

Neben unserer kölschen Frohnatur Julia, möchte ich natürlich auch meinen neuen Kollegen im CSS, den „drei Engeln für Sander“ Astrid, Violetta und Steffi, aber auch Christoph und Elisa für die schöne Zeit danken. Astrid, du bist immer organisiert und findest für jedes Problem eine Lösung, auch wenn es dir die Uni manchmal schwer macht. Steffi und Violetta, danke für die lustigen Momente im Büro. Möge euch das Glück holt bleiben, dass ihr immer schöne „Klunker“ findet.

Besonders möchte ich natürlich allen Freunden danken, die mich auf dem langen Weg unterstütz, ertragen und motiviert haben. Es war steinig, aber ihr hattet stets Verständnis, wenn man mal keine Zeit hatte oder man länger brauchte als ursprünglich geplant war. Ich danke euch!

Nicht genug danken kann ich meinen Eltern. Ich danke euch für die Unterstützung und, dass ihr mir diesen Weg überhaupt ermöglicht habt. Der Weg war steinig, aber ihr habt geholfen jedes Hindernis zu beseitigen, egal wie groß es auch war. Auch danke ich meinen Brüdern, die ihren Teil dazu beigetragen haben, dass ich derjenigen bin, der ich heute bin. Ich danke euch allen für euren unermüdlichen Einsatz. Familie ist eben alles! DANKE!

9 Declaration

Ich, Jens Reiners, versichere an Eides statt, dass die vorliegende Dissertation von mir selbstständig und ohne unzulässige fremde Hilfe unter Beachtung der „Grundsätze zur Sicherung guter wissenschaftlicher Praxis an der Heinrich-Heine-Universität Düsseldorf“ erstellt worden ist.
Diese Dissertation wurde in der vorgelegten oder in ähnlicher Form noch bei keiner anderen Institution eingereicht. Ich habe bisher keine erfolglosen Promotionsversuche unternommen.

_____ _____

Ort, Datum Unterschrift